

**TRANSITION METAL CATALYZED REACTIONS OF
PYRIDINIUM AND IMINIUM IONS**

by

Jennie Liao

A dissertation submitted to the Faculty of the University of Delaware in partial fulfillment of the requirements for the degree of Doctor of Philosophy in Chemistry and Biochemistry

Winter 2019

© 2019 Jennie Liao
All Rights Reserved

**TRANSITION METAL CATALYZED REACTIONS OF
PYRIDINIUM AND IMINIUM IONS**

by

Jennie Liao

Approved: _____

Brian J. Bahnson, Ph.D.

Chair of the Department of Chemistry and Biochemistry

Approved: _____

John Pelesko, Ph.D.

Interim Dean of the College of Arts and Sciences

Approved: _____

Douglas Doren, Ph.D.

Interim Vice Provost for Graduate and Professional Education

I certify that I have read this dissertation and that in my opinion it meets the academic and professional standard required by the University as a dissertation for the degree of Doctor of Philosophy.

Signed:

Mary P. Watson, Ph.D.
Professor in charge of dissertation

I certify that I have read this dissertation and that in my opinion it meets the academic and professional standard required by the University as a dissertation for the degree of Doctor of Philosophy.

Signed:

Donald A. Watson, Ph.D.
Member of dissertation committee

I certify that I have read this dissertation and that in my opinion it meets the academic and professional standard required by the University as a dissertation for the degree of Doctor of Philosophy.

Signed:

Klaus H. Theopold, Ph.D.
Member of dissertation committee

I certify that I have read this dissertation and that in my opinion it meets the academic and professional standard required by the University as a dissertation for the degree of Doctor of Philosophy.

Signed:

Christopher J. Kloxin, Ph.D.
Member of dissertation committee

ACKNOWLEDGMENTS

Grad school has been one of the most memorable times of my life. Here I have had the pleasure of meeting some of the most interesting and extraordinary people in the world. I would not be who I am today without the help and support from everyone who has been a part of this journey. Thank you all from the bottom of my heart!

To my advisor Mary: You are one of the most inspiring people I have ever met. Thank you for all your support and guidance throughout this journey. I may have made some regrettable decisions in my life, but the decision to join your lab is one I will never regret. Thank you for taking me under your wing and for making me a better chemist and a better person. You have taught me so much both on and off the bench. It has truly been an honor to work with you over the past four years. Thank you so much for your encouragement and for believing that I can achieve so much more. You have opened up a world I never thought was possible. I will never forget all that you have done for me. I am sure I will never find anyone like you: a boss, a colleague, and more importantly a friend!

To my committee members, Professor Donald Watson, Professor Klaus Theopold, and Professor Christopher Kloxin: Thank you for your guidance and support throughout my PhD career. You have molded me into a better chemist and prepared me to tackle any problem the real world has to offer. Words cannot express my gratitude for all that you have done.

To my collaborators at Pfizer, Michelle Garnsey, Brian Boscoe, and Joseph Tucker: It has truly been a wonderful and eye-opening experience working with you.

Thank you for all your wonderful suggestions and for sparking my interest in the pharmaceutical industry.

To the wonderful members of the MPW group: You have all been indispensable in my graduate school career. I am so grateful to have been able to call you my friends. You make coming into lab every day all the more enjoyable. Thank you for putting up with me and accepting me into your lives. It has been a pleasure working with you over the past four years. I have learned so much from you and I hope you have done the same. A special thanks to my colleagues Javon, Weiye, Jianyu, Megan, Kristen, and Shane. Thank you for all the wonderful times both in and out of the lab. You have made my mundane life so much more exciting and entertaining. I will forever cherish these memories. I will miss you all!

To all the friends I've made along the way: Thank you for being a part of this journey. From strangers to comrades, you have been there every step of the way. To Klare, Sina, Will, Max, and Tianyu – you have made this road less lonely and your support has led me to the finish line. Thank you for never allowing me to give up and for encouraging me to continue fighting this uphill battle. This is not the end of our adventures, but the start of many new ones.

To my loving family, Mom, Dad, Connie, and Vinson: Thank you for your unwavering love and support throughout this journey. It has always been great to have someone believe in you more than you believe in yourself. Thank you for accepting my flaws and for never giving up on me. You have always encouraged me to follow my dreams and have always been there when I needed you. I am so fortunate to have you in my life. I hope I have made you proud. I love you all so much!

TABLE OF CONTENTS

LIST OF TABLES.....	x
LIST OF SCHEMES.....	xi
ABSTRACT.....	xv

Chapter

1	SUZUKI-MIYAURA CROSS-COUPPLING OF ALKYL PYRIDINIUM SALTS WITH ARYLBORONIC ACIDS.....	1
1.1	Introduction.....	1
1.2	Results and Discussion.....	8
1.2.1	Synthesis of Katritzky Pyridinium Salts.....	8
1.2.2	Reaction Optimization.....	9
1.2.3	Reaction Scope.....	10
1.2.4	Mechanistic Studies.....	14
1.3	Conclusion.....	18
1.4	Experimental.....	18
1.4.1	General Information.....	18
1.4.2	Suzuki-Miyaura Cross-Coupling of Alkyl Pyridinium Salts.....	20
1.4.2.1	General Procedure A: Cross-Coupling with Non-Pyridyl Aryl Boronic Acids.....	20
1.4.2.2	General Procedure B: Cross-Coupling with Pyridyl Boronic Acids.....	33
1.4.3	Preparation of Pyridinium Salts.....	40
1.4.3.1	General Procedure C: Conversion of Amines to Pyridinium Salts.....	40
1.4.4	Mechanistic Experiments.....	53
1.4.4.1	Test for Stereospecificity.....	53
1.4.4.2	Radical-Clock Experiment.....	54

1.4.4.3	Radical Trap Experiment	55
	REFERENCES	56
2	SUZUKI–MIYAURA CROSS-COUPLING OF BENZYLIC PYRIDINIUM SALTS WITH ARYLBORONIC ACIDS	60
2.1	Introduction.....	60
2.2	Results and Discussion	69
2.2.1	Synthesis of Benzylic Pyridinium Salts.....	69
2.2.2	Reaction Optimization	72
2.2.3	Reaction Scope.....	74
2.2.4	Mechanistic Studies	80
2.3	Conclusion	81
2.4	Experimental.....	82
2.4.1	General Information.....	82
2.4.2	Preparation of PhenNi(OAc) ₂ ·xH ₂ O (2-66).....	83
2.4.3	Cross-Coupling of Pyridinium Salts to Give Diarylmethanes.....	84
2.4.3.1	General Procedure A: Cross-Coupling of Pyridinium Salts with Boronic Acids	84
2.4.3.2	One-pot Cross-Coupling of Benzylamine with Boronic Acid.....	98
2.4.3.3	Cross-Coupling of Secondary Benzylic Pyridinium Salt with Boronic Acid.....	99
2.4.4	Preparation of Pyridinium Salts.....	100
2.4.4.1	General Procedure B: Conversion of Electron-poor (Hetero)Arylamines to Pyridinium Salts	100
2.4.4.2	General Procedure C: Conversion of Electron-rich (Hetero)Arylamines to Pyridinium Salts	105
2.4.5	Mechanistic Experiment	112
2.4.5.1	Radical Trap Experiment	112
	REFERENCES	113
3	SUZUKI–MIYAURA CROSS-COUPLING OF BENZYLIC PYRIDINIUM SALTS WITH VINYLBORONIC ACIDS	118

3.1	Introduction.....	118
3.2	Results and Discussion	121
3.3	Conclusion	126
3.4	Experimental.....	127
3.4.1	General Information.....	127
3.4.2	Cross-Coupling of Pyridinium Salts	128
3.4.2.1	General Procedure A: Cross-Coupling of Pyridinium Salts with Boronic Acids	128
3.4.2.2	General Procedure B: Cross-Coupling of Pyridinium Salts with Boronic Acid Pinacol Ester.....	129
	REFERENCES	138
4	REDUCTIVE CROSS-ELECTROPHILE COUPLING OF ALKYL PYRIDINIUM SALTS WITH ARYL BROMIDES	142
4.1	Introduction.....	142
4.2	Results and Discussion	154
4.2.1	Reaction Optimization: Primary Alkyl Pyridinium Salts	154
4.2.2	Reaction Optimization: Secondary Alkyl Pyridinium Salts	156
4.2.3	Reaction Scope.....	159
4.2.4	Mechanism Studies	163
4.3	Conclusion	167
4.4	Experimental.....	167
4.4.1	General Information.....	167
4.4.2	General Optimization Procedure.....	168
4.4.3	Reductive Cross-Electrophile Coupling of Alkyl Pyridinium Salts with Aryl Bromides.....	169
4.4.3.1	General Procedure A: Cross-Coupling of Primary Alkyl Pyridinium Salts.....	169
4.4.3.2	General Procedure B: Cross-Coupling of Secondary Alkyl Pyridinium Salts.....	170
	REFERENCES	185
5	COPPER-CATALYZED ENANTIOSELECTIVE ALKYNYLATION OF IMINIUM IONS TO FORM α -DIARYL TETRASUBSTITUTED STEREOCENTERS.....	188

5.1	Introduction.....	188
5.2	Results and Discussion	195
5.3	Conclusion	205
5.4	Experimental.....	206
5.4.1	Enantioselective Alkynylation of Iminium Ions.....	206
5.4.1.1	General Procedure A: Reaction Optimization of <i>N</i> -sulfonyl Ketimines.....	206
5.4.1.2	General Procedure B: Reaction Optimization of Benzisoxazole 5-53.....	207
5.4.2	Preparation of Substrates	208
5.4.3	Preparation of PHOX Ligands.....	210
	REFERENCES	212

Appendix

A	SPECTRAL AND CHROMATOGRAPHY DATA FOR CHAPTER 1	215
B	SPECTRAL AND CHROMATOGRAPHY DATA FOR CHAPTER 2	329
C	SPECTRAL AND CHROMATOGRAPHY DATA FOR CHAPTER 3	427
D	SPECTRAL AND CHROMATOGRAPHY DATA FOR CHAPTER 4	458
E	SPECTRAL AND CHROMATOGRAPHY DATA FOR CHAPTER 5	508
F	PERMISSION LETTERS.....	521

LIST OF TABLES

Table 1.1	Reaction optimization of the Suzuki–Miyaura cross-coupling of alkyl pyridinium salts with arylboronic acids.....	9
Table 2.1	Reaction optimization of the Suzuki–Miyaura cross-coupling of benzylic pyridinium salts with arylboronic acids	73
Table 2.2	Wide solvent tolerance.....	78
Table 3.1	Reaction optimization of the Suzuki–Miyaura cross-coupling of benzylic pyridinium salts with vinylboronic acids	122
Table 4.1	Reaction optimization of the reductive cross-electrophile coupling primary alkyl pyridinium salts with aryl bromides.....	155
Table 4.2	Reaction optimization of the reductive cross-electrophile coupling secondary alkyl pyridinium salts with aryl bromides	159
Table 5.1	Temperature dependence of the alkynylation reaction	202
Table 5.2	Decomposition of alkynylated product 5-54	204

LIST OF SCHEMES

Scheme 1.1	Examples of natural or synthetic bioactive alkyl primary amines.....	2
Scheme 1.2	C _{sp3} -N electrophiles used in transition metal-catalyzed cross-couplings	2
Scheme 1.3	Reagents for installing unactivated alkyl groups via cross-couplings	3
Scheme 1.4	Fu's Negishi cross-coupling of alkyl halides.....	4
Scheme 1.5	MacMillan's metallaphotoredox cross-coupling of alkyl oxalates.....	5
Scheme 1.6	Doyle and MacMillan's decarboxylative metallaphotoredox cross- coupling of α -amino carboxylic acids.....	5
Scheme 1.7	Nickel-catalyzed cross-couplings of redox-active esters.....	6
Scheme 1.8	Proposed cross-coupling of alkyl amine derived pyridinium salts	7
Scheme 1.9	Selected examples of alkyl pyridinium salts formed	8
Scheme 1.10	Scope of non-pyridyl boronic acid.....	11
Scheme 1.11	Scope of pyridyl boronic acid.....	14
Scheme 1.12	Katritzky's alkylation of nitronate anions with alkyl pyridinium salts.	15
Scheme 1.13	Mechanistic support for radical intermediate	16
Scheme 1.14	Proposed catalytic cycle.....	17
Scheme 2.1	Examples of medicinally relevant diarylmethanes	61
Scheme 2.2	Metal-catalyzed arylations of benzylic halides.....	62
Scheme 2.3	Metal-catalyzed arylations of benzyl alcohols and their derivatives	64
Scheme 2.4	Arylations of benzylic organometallic nucleophiles.....	66
Scheme 2.5	Metal-catalyzed arylations of benzylic amine derivatives.....	67

Scheme 2.6	Proposed cross-coupling of benzylic amine derived pyridinium salts..	69
Scheme 2.7	Selected examples of electron-poor benzylic pyridinium salts formed	70
Scheme 2.8	Synthesis of electron-rich benzylic pyridinium salts	71
Scheme 2.9	Selected examples of electron-rich benzylic pyridinium salts formed .	72
Scheme 2.10	Preparation of metal-ligand complex PhenNi(OAc) ₂ ·xH ₂ O 2-66	74
Scheme 2.11	Reaction scope of Suzuki arylation of benzylic pyridinium salts.....	75
Scheme 2.12	One-pot transformation.....	79
Scheme 2.13	Radical trapping experiment.....	80
Scheme 2.14	Proposed catalytic cycle for cross-coupling of benzylic pyridinium salts	81
Scheme 3.1	Synthetic versatility of 1,3-disubstituted allylic molecules	119
Scheme 3.2	Strategies for the synthesis of 1,3-diaryl allylic compounds	119
Scheme 3.3	Cross-couplings of allylic electrophiles.....	120
Scheme 3.4	Cross-couplings of benzylic substrates.....	121
Scheme 3.5	Proposed vinylation of benzylic pyridinium salts.....	121
Scheme 3.6	Comparison of reactions with and without the nickel catalyst	124
Scheme 3.7	Reaction scope of vinylation reaction.....	125
Scheme 4.1	Synthesis of alkylarenes.....	143
Scheme 4.2	Conventional cross-coupling vs reductive cross electrophile-coupling	144
Scheme 4.3	Strategies for obtaining high yields in reductive cross-couplings	145
Scheme 4.4	Weix's reductive coupling of alkyl halides with aryl halides.....	147
Scheme 4.5	Weix's reductive coupling of redox-active esters with aryl iodides...	147
Scheme 4.6	Weix's proposed radical-chain bimetallic pathway.....	148

Scheme 4.7	Gong's coupling of secondary alkyl bromides	149
Scheme 4.8	Molander's coupling of heterocyclic alkyl bromides	149
Scheme 4.9	Gong's reductive coupling of tertiary alkyl halides.....	149
Scheme 4.10	MacMillan's metallaphotoredox reductive coupling.....	150
Scheme 4.11	Metal-catalyzed reductive cross-couplings.....	151
Scheme 4.12	Gong's nickel-catalyzed reductive alkyl-alkyl coupling	152
Scheme 4.13	Fu and Liu's cobalt-catalyzed reductive alkyl-alkyl/aryl coupling	153
Scheme 4.14	Challenging substrates under Suzuki conditions	153
Scheme 4.15	Cross-coupling of secondary alkyl pyridinium salt 4-33	156
Scheme 4.16	Proposed radical-chain mechanism for reductive coupling.....	157
Scheme 4.17	Reaction scope of reductive coupling.....	160
Scheme 4.18	Cross-coupling of substrates derived from pharmaceutical drugs.....	163
Scheme 4.19	Mechanistic experiments	164
Scheme 4.20	Two possible mechanisms for the reductive coupling of alkyl pyridinium salts with aryl bromides	165
Scheme 4.21	Stoichiometric Ni ⁰ study.....	166
Scheme 5.1	Examples of bioactive amines containing an α -diaryl tetrasubstitued stereocenter	188
Scheme 5.2	Synthetic utility of alkynylated products	189
Scheme 5.3	Enantioselective additions to diaryl ketimines	190
Scheme 5.4	Watson's copper-catalyzed enantioselective alkynylations.....	191
Scheme 5.5	Proposed strategy towards enantioselective synthesis of acyclic amines	192
Scheme 5.6	Substrates containing a removable tether	193
Scheme 5.7	Enantioselective additions to cyclic <i>N</i> -sulfonyl imines.....	193

Scheme 5.8	Enantioselective alkynylations of cyclic <i>N</i> -sulfonyl imines.....	194
Scheme 5.9	Synthesis of cyclic <i>N</i> -sulfonyl ketimines 5-40 and 5-42	195
Scheme 5.10	Methylation and alkynylation of sulfonyl ketimine 5-40	196
Scheme 5.11	Enantioselective alkynylations of sulfonyl ketimines 5-40 and 5-42 .	197
Scheme 5.12	Synthesis of 5-53	198
Scheme 5.13	Representative HTE plate	199
Scheme 5.14	Synthesis of PHOX ligands	200
Scheme 5.15	Screening of various PHOX ligands.....	201

ABSTRACT

This dissertation focuses primarily on the development of novel methods for the transition metal-catalyzed cross-couplings of alkyl amine derivatives via carbon-nitrogen (C–N) bond activation. Chapters 1–4 focus on the use of Katritzky pyridinium salts, which can easily be obtained in a single step from primary amines. These redox-active amine derivatives can then serve as non-traditional electrophiles in a variety of nickel-catalyzed cross-coupling reactions. This work allows one to consider alkyl amines as substrates in cross-couplings for the first time and may have applications in late-stage derivatization of pharmaceutical targets. Chapter 5 focuses on the development of a copper-catalyzed enantioselective alkynylation of iminium ions to afford α -tetrasubstituted amines, an important motif in a variety of biologically active molecules.

Chapter 1 describes a nickel-catalyzed Suzuki–Miyaura cross-coupling of alkyl pyridinium salts with arylboronic acids. The combination of air- and moisture-stable $\text{Ni}(\text{OAc})_2 \cdot 4\text{H}_2\text{O}$ and redox non-innocent bathophenanthroline (BPhen) ligand was found to promote the desired cross-coupling. Both primary and secondary alkyl groups participated smoothly under the optimized reaction conditions with excellent functional group tolerance. Excitingly, we have demonstrated the amenability of this method to pharmaceutical intermediates and amino acid derivatives. Notably, this is the first example of a metal-catalyzed cross-coupling of an amine derivative bearing *unactivated* alkyl groups. Preliminary mechanistic experiments suggest the

intermediacy of alkyl radical species, and the reaction is proposed to proceed via a $\text{Ni}^{\text{I/III}}$ catalytic cycle.

Chapter 2 describes a nickel-catalyzed Suzuki–Miyaura cross-coupling of benzylic pyridinium salts with arylboronic acids. This method enables the synthesis of diarylmethanes, a pharmaceutically relevant motif, from widely abundant benzylic amines. The use of a benzylic pyridinium intermediate allows for the incorporation of heteroaryl substitution, an important facet which is largely overlooked in other cross-couplings to deliver diarylmethanes. Metal-ligand complex $\text{PhenNi}(\text{OAc})_2 \cdot 4\text{H}_2\text{O}$ was synthesized to enable facile reaction set-up and a wide solvent tolerance was demonstrated to facilitate the use of this chemistry in synthesis. A one-pot procedure was also developed for the direct conversion of a primary amine into the desired diarylmethane. This work was performed in collaboration with Michelle Garnsey, Brian Boscoe, and Joseph Tucker at Pfizer, Inc.

Chapter 3 describes a nickel-catalyzed Suzuki–Miyaura cross-coupling of benzylic pyridinium salts with vinylboronic acids and esters. This method allows for the rapid construction of 1,3-disubstituted allylic motifs. This chemistry is tolerant of heteroaryl substitution and can employ either the vinylboronic acid or pinacol ester as the coupling partner. Notably, this approach allows for control of the regioselectivity of the alkene.

Chapter 4 describes a nickel-catalyzed reductive cross-electrophile coupling of alkyl pyridinium salts with aryl bromides. This reaction leverages the wide availability of alkyl amines and aryl halides to deliver highly valuable alkylarenes. The optimized reaction conditions employ a catalyst system comprised of $\text{NiCl}_2 \cdot \text{DME}$ and 4,4'-diOMeBipy in conjunction with manganese as a stoichiometric reductant. Primary,

secondary, and benzylic pyridinium salts are all amenable to this chemistry. Importantly, this method is tolerant of acidic protons and epimerizable stereocenters. We have shown the applicability of this chemistry to amino acid derivatives, pharmaceuticals, and pharmaceutical intermediates. Preliminary mechanistic experiments suggest that a radical-chain bimetallic pathway may be operative. This work was performed in collaboration with Michelle Garnsey, Brian Boscoe, and Joseph Tucker at Pfizer, Inc.

Chapter 5 describes my efforts towards a copper-catalyzed enantioselective alkynylation of iminium ions to form α -diaryl tetrasubstituted amines. The use of cyclic imines containing a removable tether allow for downstream cleavage to reveal enantioenriched acyclic amine products. Preliminary efforts on cyclic *N*-sulfonyl ketimine substrates have lead to good yields and modest ee's. Further optimization of this reaction is ongoing. Additionally, unique conditions have been identified that can achieve kinetic resolution of a related benzisoxazoles.

Chapter 1

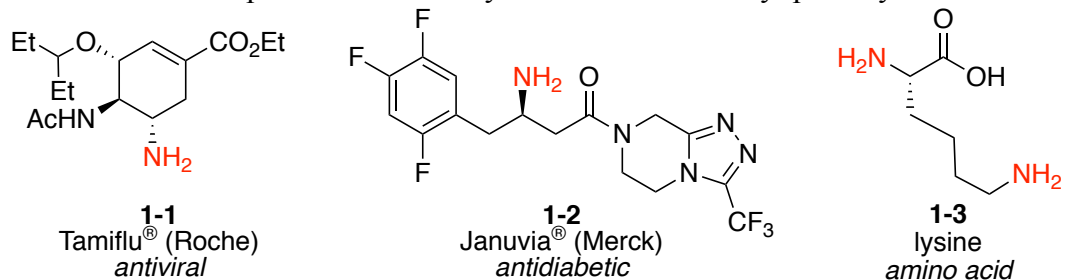
SUZUKI–MIYAURA CROSS-COUPLING OF ALKYL PYRIDINIUM SALTS WITH ARYLBORONIC ACIDS

Work described here has already been published (Basch, C. H.; Liao, J.; Xu, J.; Piane, J. J.; Watson, M. P. *J. Am. Chem. Soc.* **2017**, *139* (15), 5313-5316.). It is reprinted in this chapter with permission of the *Journal of the American Chemical Society* (Copyright © 2017, American Chemical Society).

1.1 Introduction

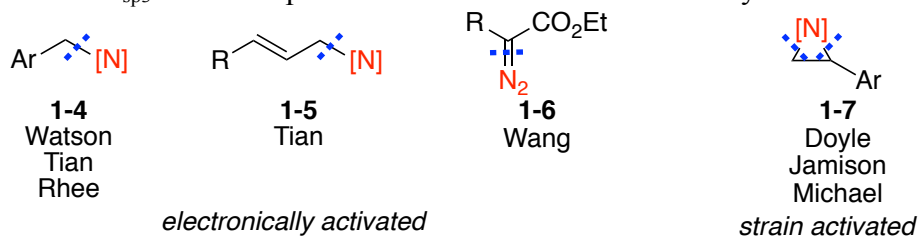
Alkyl primary amines are prevalent amongst a wide range of natural and synthetic biologically active molecules, as well as building blocks of various complexities (Scheme 1.1).¹ The amino (NH₂) group possesses many attractive features such as ease of installation, straightforward purification, and the ability to be carried through multi- step syntheses in protected form. The advantages of alkylamines have been well recognized in the synthesis of many nitrogen containing compounds. In contrast, alkylamines have yet to be broadly utilized as alkylating agents in metal-catalyzed cross-coupling reactions. This would allow for rapid construction of new carbon-carbon bonds from inexpensive, widely available primary amine precursors. This would also enable the use of the amine (NH₂) moiety as a synthetic handle for structure-activity relationship (SAR) studies, along with late-stage functionalization of complex bioactive molecules.

Scheme 1.1 Examples of natural or synthetic bioactive alkyl primary amines



Cross-couplings have been achieved via cleavage of various C_{sp^2} -N bonds, including those of aniline,^{2, 3} enamine,⁴ and amide derivatives.⁵⁻⁹ In contrast, methods to harness C_{sp^3} -N bonds have been limited to electronically activated benzylic (**1-4**),¹⁰⁻¹⁴ allylic (**1-5**),¹⁵ or α -keto amine derivatives (**1-6**),^{16, 17} as well as strain-activated aziridines (**1-7**)¹⁸⁻²⁰ (Scheme 1.2). Recognizing the potential of unactivated C_{sp^3} -N bonds, we set out to develop methodologies that would allow for the use of alkylamine derivatives as non-traditional electrophiles in nickel-catalyzed cross-couplings via C-N bond activation. Prior to our work, there were no examples of utilizing an alkylamine derivative bearing *unactivated* alkyl groups in transition metal-catalyzed cross-coupling reactions.

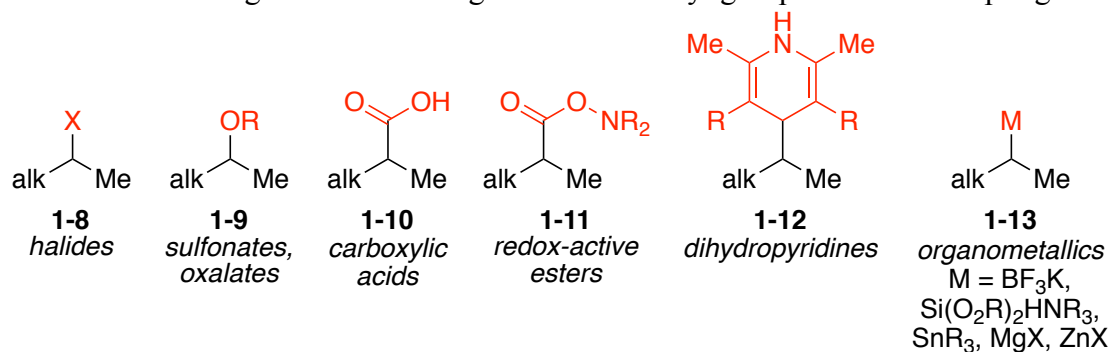
Scheme 1.2 C_{sp^3} -N electrophiles used in transition metal-catalyzed cross-couplings



Historically, the use of alkyl C_{sp^3} coupling partners (both electrophilic and nucleophilic) have proven challenging. Potential issues include slow oxidative

addition or transmetalation as well as slow reductive elimination. Additionally, the alkylmetallic intermediates are prone to decomposition pathways such as β -hydride elimination and protodemetalation. Nonetheless, intense efforts have identified a variety of reagents suitable for the installation of alkyl groups lacking electronic or strain activation (Scheme 1.3). Conditions have been developed for metal-catalyzed cross-couplings of alkyl halides, pseudohalides, redox-active esters, and organometallic nucleophiles. Moreover, dual photoredox/nickel catalysis has enabled the use of oxalates, carboxylic acids, 1,4-dihydropyridines, organoboronates, and organosilicates. Seminal reports in this area are detailed below.

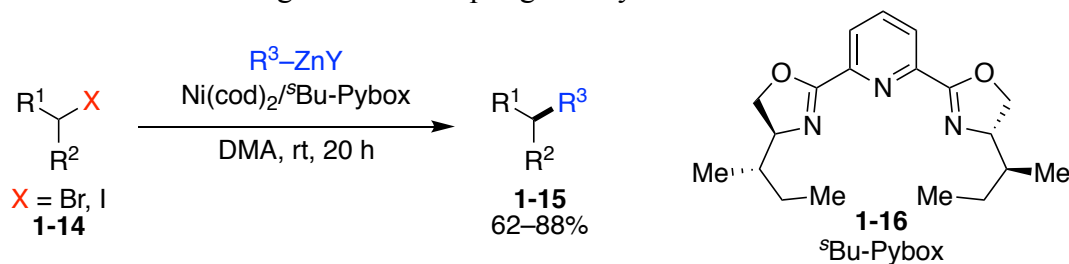
Scheme 1.3 Reagents for installing unactivated alkyl groups via cross-couplings



In 2003, Fu reported his seminal publication on the nickel-catalyzed Negishi cross-coupling of unactivated alkyl bromides and iodides (**1-14**) (Scheme 1.4).²¹ Notably, this was the first example of a nickel- or palladium-catalyzed cross-coupling of unactivated, β -hydrogen-containing, secondary alkyl halides. Mechanistic studies have revealed that alkyl halides can undergo single-electron transfer (SET) oxidative addition to generate the corresponding alkyl radicals.²² This finding set the stage for a number of subsequent accounts expanding upon this chemistry for the construction of

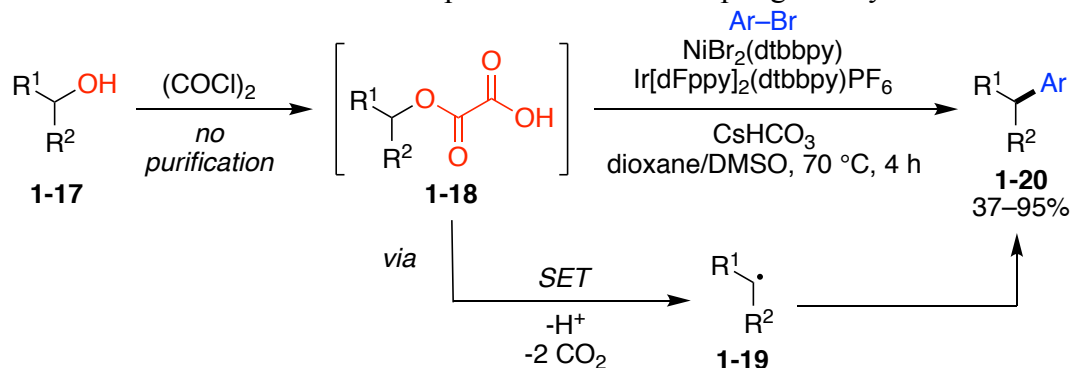
new C–C and C–X bonds.²³⁻²⁶ In fact, alkyl halides remain an active area of research for the installation of alkyl groups via metal-catalyzed cross-coupling reactions.

Scheme 1.4 Fu's Negishi cross-coupling of alkyl halides



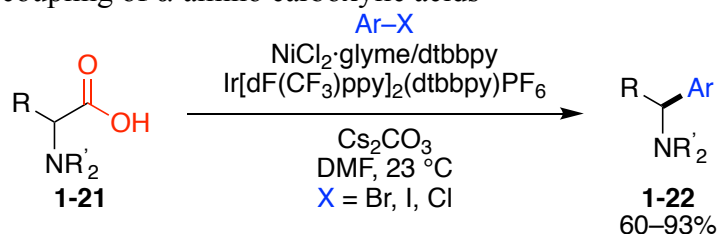
Within the last decade, interest has expanded towards the identification of other readily available alkylating agents such as alcohols and carboxylic acids. The MacMillan group has demonstrated that by combining photoredox and nickel catalysis, cross-coupling of alkyl oxalates (**1-18**) and aryl halides can be achieved (Scheme 1.5).²⁷ In this case, **1-18** is formed from the corresponding alcohol (**1-17**) and oxalyl chloride, and used without further purification. The iridium photocatalyst is used to generate carbon-centered radical **1-19** via successive loss of two equivalents of CO₂. This alkyl radical can then intercept the nickel cycle to deliver cross-coupled product **1-20**. This method highlights the feasibility of alcohols to serve as latent C_{sp3}-nucleophiles.

Scheme 1.5 MacMillan's metallaphotoredox cross-coupling of alkyl oxalates



Similarly, carboxylic acids can also serve as alkyl nucleophiles. The Doyle and MacMillan groups have shown that α -amino carboxylic acids (**1-21**) can undergo cross-couplings with aryl halides by merging photoredox and nickel catalysis (Scheme 1.6).²⁸ Again, the iridium photocatalyst is used to generate the α -amino radical via loss of CO_2 . This can then engage in the nickel cycle with an aryl halide to give arylated product **1-22**. Additionally, the Molander group has demonstrated a variety of dual photoredox/nickel-catalyzed cross-couplings using alkyl trifluoroborate salts, silicates, and dihydropyridines.²⁹⁻³¹

Scheme 1.6 Doyle and MacMillan's decarboxylative metallaphotoredox cross-coupling of α -amino carboxylic acids

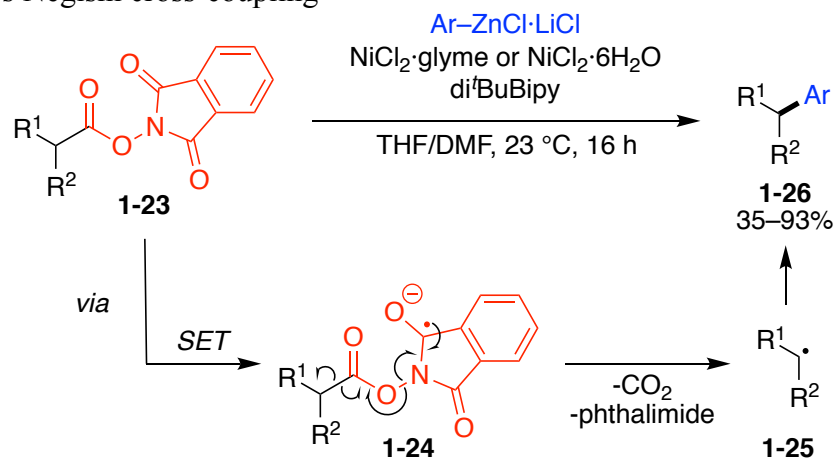


The umpolung approach utilizing carboxylic acids as alkyl electrophiles has also been investigated. Alkyl carboxylic acids can be converted into the corresponding *N*-hydroxyphthalimide esters (**1-23**). These redox-active esters have been demonstrated to participate in a number of cross-coupling reactions. For example, in his seminal publication, Baran has shown that these substrates can undergo Negishi cross-couplings to form arylated products **1-26** (Scheme 1.7A).³² The proposed mechanism for this transformation involves a Ni^{I/III} catalytic cycle. Radical anion **1-24** is generated via single electron-transfer from a Ni^I species into the redox-active ester. Fragmentation of **1-24** leads to extrusion of CO₂ and loss of the phthalimide anion, forming alkyl radical **1-25**. Additionally, Weix has demonstrated that these redox-active esters (**1-27**) can participate in a reductive cross-electrophile coupling with aryl iodides using Zn as a stoichiometric reductant (Scheme 1.7B).³³ However, unlike Baran's chemistry, a radical-chain bimetallic pathway is proposed. Since then, a number of different cross-couplings utilizing redox-active esters have been reported.³⁴⁻

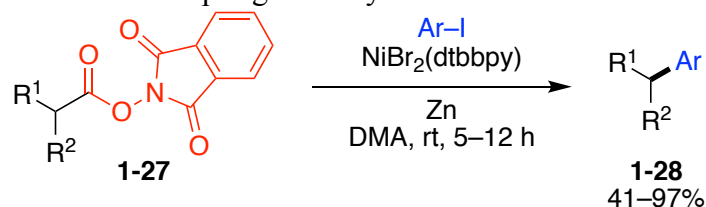
36

Scheme 1.7 Nickel-catalyzed cross-couplings of redox-active esters

A. Baran's Negishi cross-coupling

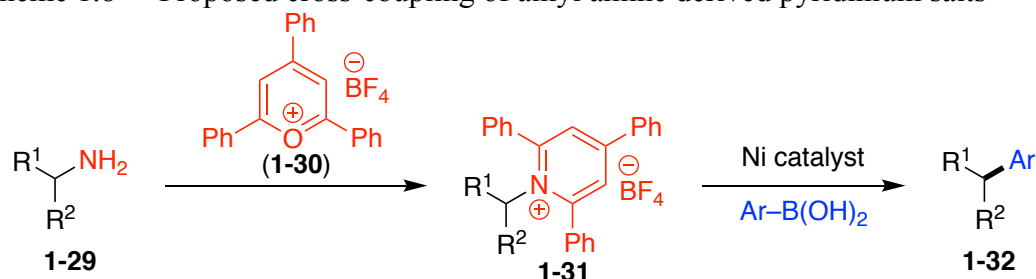


B. Weix's reductive cross-coupling with aryl iodides



Alkyl amines are inexpensive, widely available feedstock chemicals. The cross-coupling of an alkyl amine derivative would offer an exciting complementary approach for installing unactivated alkyl groups. Towards this end, we identified Katritzky pyridinium salts (**1-31**) as potential electrophiles for nickel-catalyzed cross-couplings (Scheme 1.8).³⁷ This unique approach hinges on the redox-active nature of these pyridinium salts and their ability to serve as alkyl radical precursors via C_{sp3}-N bond cleavage. Historically, these salts have primarily been employed in a variety of two-electron nucleophilic substitution reactions.³⁸ Herein, we disclose the first example of a metal-catalyzed cross-coupling of an amine derivative bearing *unactivated* alkyl groups.

Scheme 1.8 Proposed cross-coupling of alkyl amine derived pyridinium salts

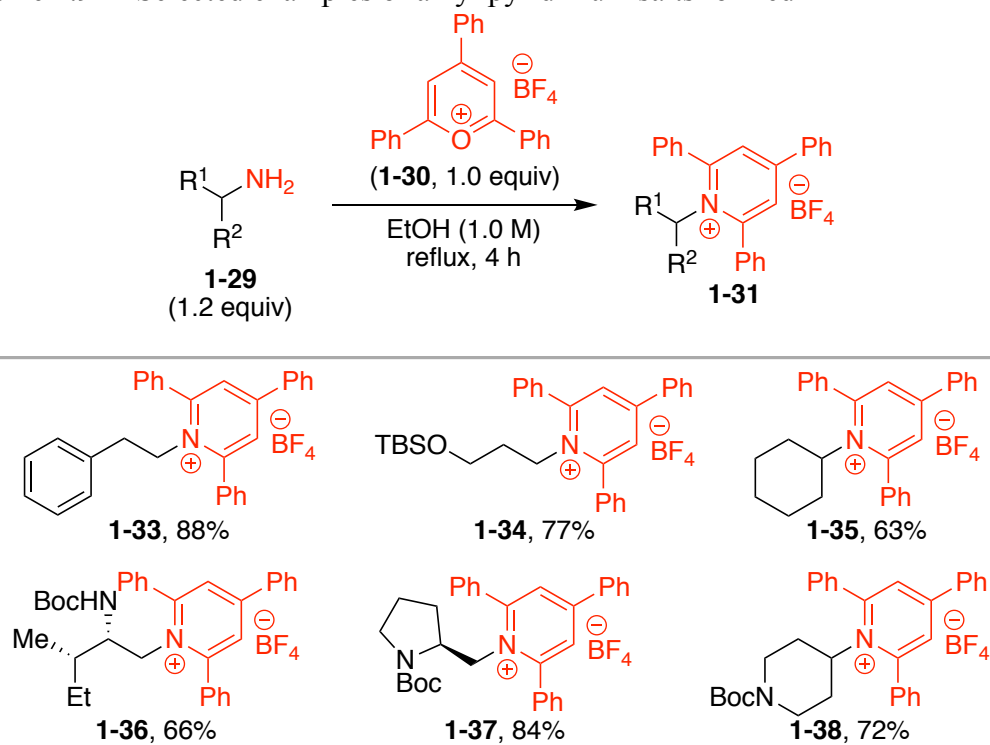


1.2 Results and Discussion

1.2.1 Synthesis of Katritzky Pyridinium Salts

The Katritzky pyridinium salts (**1-31**) can be prepared in a single step via condensation of an alkyl primary amine (**1-29**) with commercially available 2,4,6-triphenylpyrylium tetrafluoroborate (**1-30**). Excitingly, this method is chemoselective for primary amines and allows for the incorporation of other nitrogen containing functionalities within the organic framework. Moreover, these salts often require no chromatography as they precipitate upon trituration with ether to afford **1-31** as an air- and moisture-stable solid. A variety of alkyl pyridinium salts can be prepared via this method (Scheme 1.9). Notably, both primary and secondary alkyl groups can be incorporated, as well as protected secondary (**1-36**) and tertiary (**1-37** & **1-38**) amines.

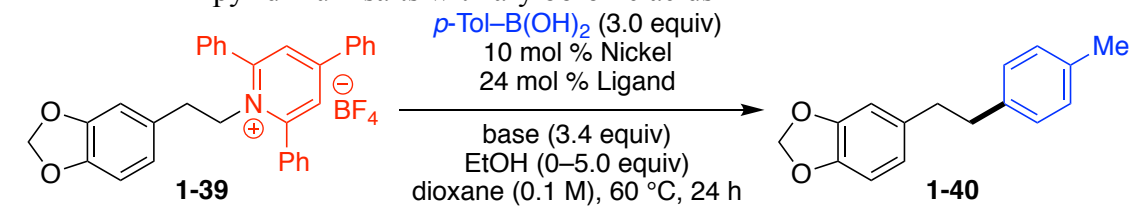
Scheme 1.9 Selected examples of alkyl pyridinium salts formed



1.2.2 Reaction Optimization

My colleague Corey Basch chose pyridinium salt **1-39** for the preliminary investigation of the Suzuki–Miyaura cross-coupling with bench-stable arylboronic acids. Optimization began with the first-generation conditions our group had previously identified for the activation of benzylic trimethylammonium salts.¹¹ Disappointingly, the formation of only a trace amount of **1-40** was observed (Table 1.1, entry 1). A brief ligand screen revealed that redox non-innocent phenanthroline-based ligands, specifically bathophenanthroline (BPhen, **1-41**), were the most effective in promoting the desired cross-coupling (entry 2). Switching to an alkoxide base as well as from a Ni⁰ source to a Ni^{II} salt further improved the yield (entries 3 & 4). By pre-mixing the nickel and ligand separately from the rest of the reagents, further improvement was observed (entry 5). Finally, the addition of ethanol was found to increase the yield of the reaction substantially (entry 6). We hypothesize that this additive likely improves the solubility of the base and/or boronic acid.

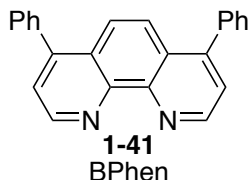
Table 1.1 Reaction optimization of the Suzuki–Miyaura cross-coupling of alkyl pyridinium salts with arylboronic acids^a



Entry	Ni Source	Ligand	Base	Additive	Yield (%) ^b
1	Ni(cod) ₂	PPh ₂ Cy	K ₃ PO ₄	none	6
2	Ni(cod) ₂	BPhen	K ₃ PO ₄	none	21
3	Ni(cod) ₂	BPhen	KO ^t Bu	none	24

4	Ni(OAc) ₂ ·4H ₂ O	BPhen	KO ^t Bu	none	39
5 ^c	Ni(OAc) ₂ ·4H ₂ O	BPhen	KO ^t Bu	none	52
6 ^c	Ni(OAc) ₂ ·4H ₂ O	BPhen	KO ^t Bu	EtOH ^d	81

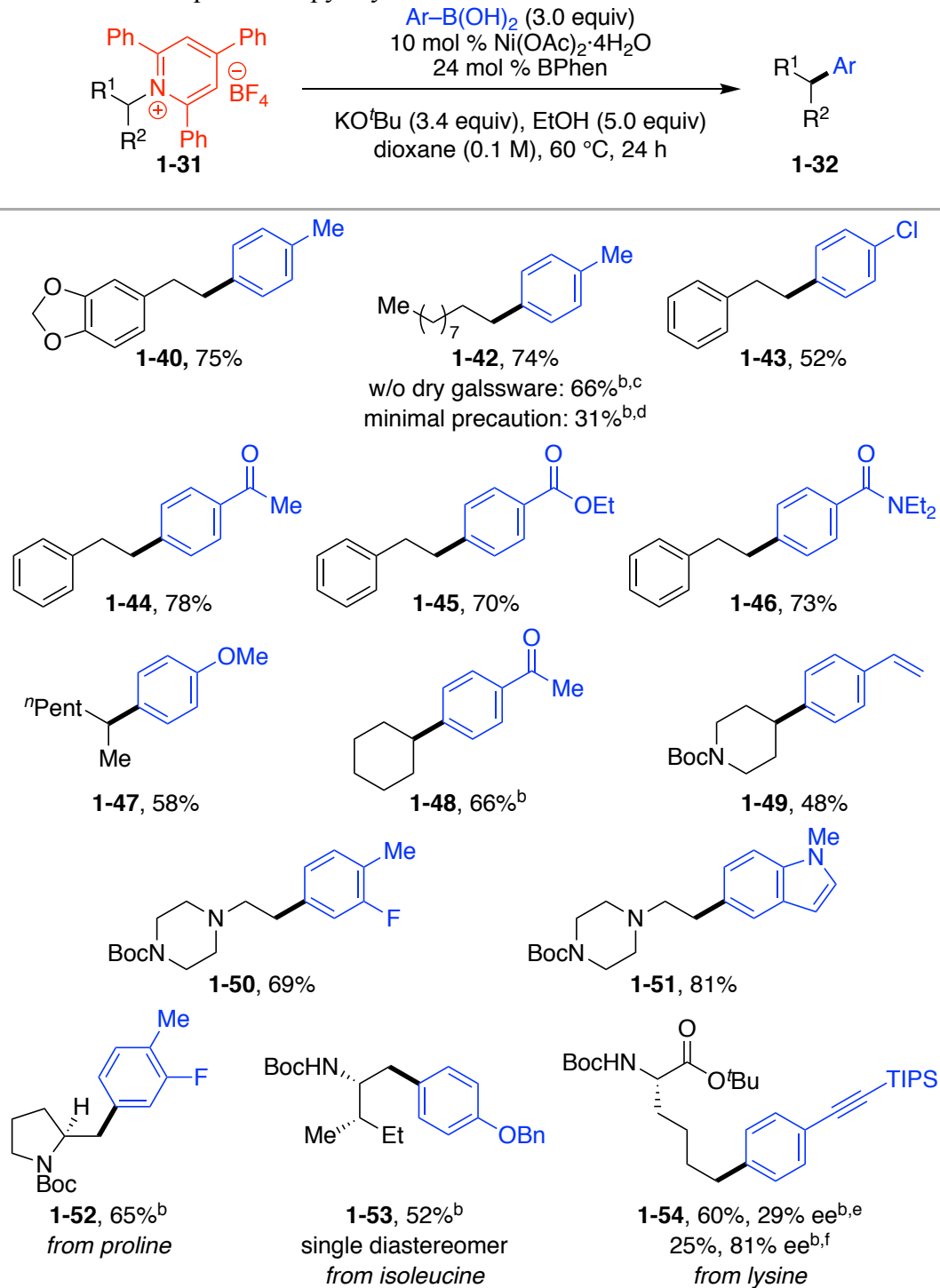
^aConditions: pyridinium salt **1-39** (0.10 mmol), *p*-Tol-B(OH)₂ (3.0 equiv), [Ni] (10 mol %), ligand (24 mol %), base (3.4 equiv), dioxane (0.1 M), 60 °C, 24 h, unless noted otherwise. ^bDetermined by ¹H NMR analysis using 1,3,5-trimethoxybenzene as internal standard. ^cTwo mixtures (Vial 1: [Ni], Ligand, dioxane. Vial 2: pyridinium salt **1-39**, *p*-Tol-B(OH)₂, Base, EtOH, dioxane.) were stirred for 1 h before combining. ^dEtOH (5.0 equiv) added.

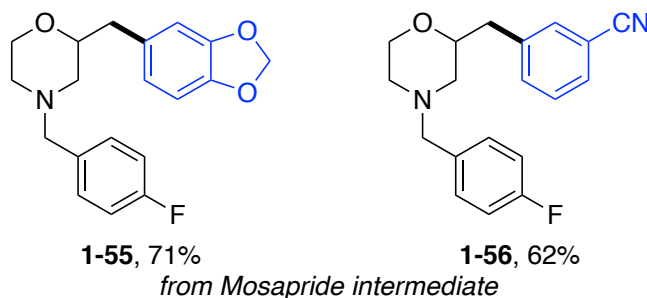


1.2.3 Reaction Scope

With optimized conditions in hand, I, along with Jianyu Xu and Jacob Piane, joined the project to demonstrate the scope of this transformation (Scheme 1.10). We were very delighted to find that a number of primary and secondary (cyclic and acyclic) alkyl groups participated smoothly under these reaction conditions. The model reaction afforded **1-40** in 75% isolated yield on a 1.0-mmol scale. We have also shown that the reaction is somewhat tolerant of moisture, as a similar yield was observed in the absence of oven-dried glassware for the formation of cross-coupled product **1-42**. However, a significant drop in yield (31%) was observed when minimal precaution was taken to exclude air or moisture (solvents and glassware were not dried and the reaction was set up under air).

Scheme 1.10 Scope of non-pyridyl boronic acid^a





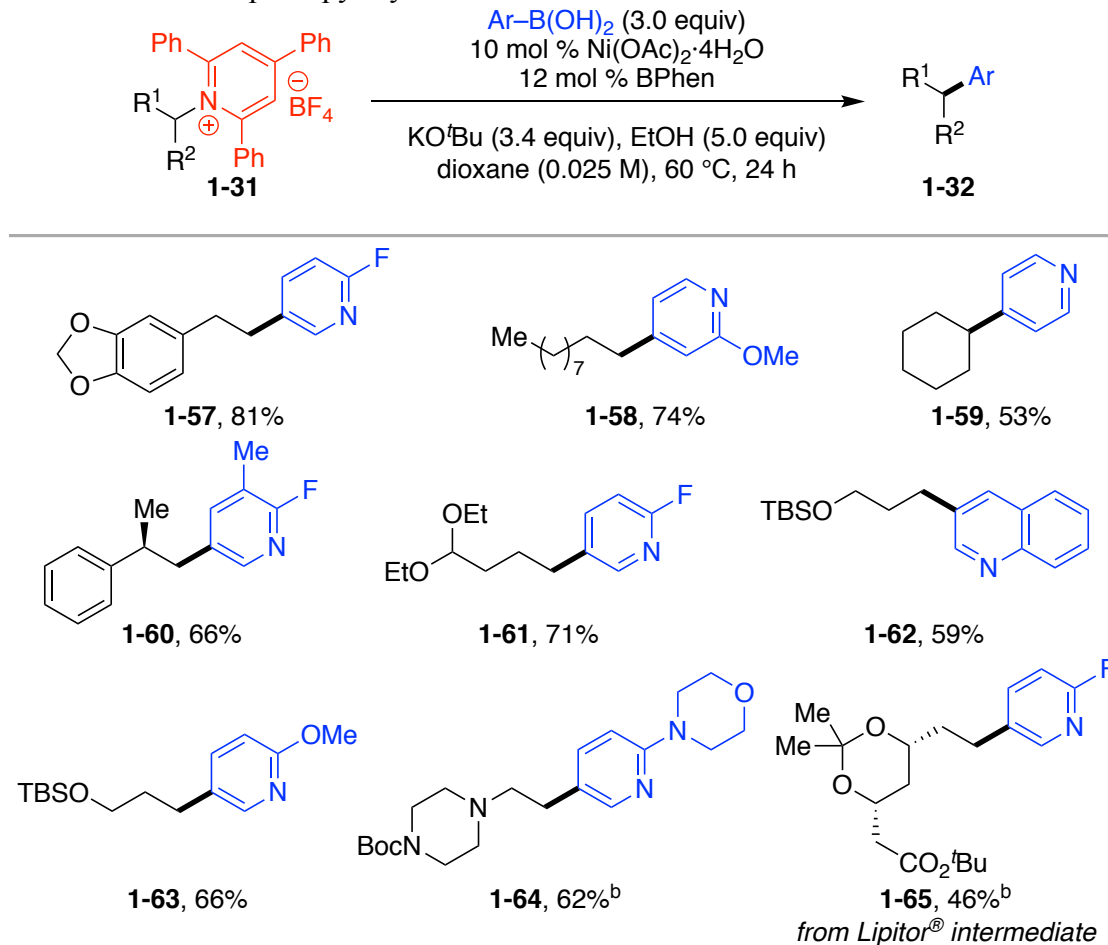
^aConditions: pyridinium salt **1-31** (1.0 mmol), Ni(OAc)₂·4H₂O (10 mol %), BPhen (24 mol %), ArB(OH)₂ (3.0 equiv), KO^tBu (3.4 equiv), EtOH (5 equiv), dioxane (0.1 M), 60 °C, 24 h. Average isolated yields (±6%) from duplicate experiments. ^bSingle experiment. ^cGlassware not oven-dried before use. ^dMinimal precautions to protect from air and moisture. ^e0.5-mmol scale. ^f0.05-mmol scale. *p*-(CF₃)C₆H₄OH (2 equiv) added. Yield determined by ¹H NMR using 1,3,5-trimethoxybenzene as internal standard.

Many functional groups on the alkyl coupling partner were well tolerated, including ethers, silyl ethers, acetals, and esters. In addition, tertiary and Boc-protected amines as well as heterocycles, such as piperidines, piperazines, and morpholine, can be used. We have also coupled substrates derived from amino acids. Products **1-52** and **1-53** are derived from proline and isoleucine, respectively. Notably, **1-53** is formed as a single diastereomer, indicating that non-acidic stereocenters are preserved under these conditions. Cross-coupling of the amino side chain of *N*-Boc lysine also proceeded in good yield, albeit with poor conservation of enantiomeric excess (*ee*) (**1-54**). However, a much higher *ee*, but lower yield, was observed with the use of an acidic additive (i.e., *p*-(CF₃)C₆H₄OH), suggesting conditions can be identified to solve this problem. Moreover, we have demonstrated the synthetic utility

of this chemistry for late-stage functionalization of intermediates in the synthesis of bioactive molecules. For example, products **1-55** and **1-56** are derived from an amine intermediate in the synthesis of Mosapride, a treatment for gastrointestinal disorders.³⁹

Broad scope was also achieved with the arylboronic acid. Various functionalities were tolerated, including aryl chlorides (**1-43**) and fluorides (**1-50**, **1-52**), methyl ketones (**1-44**, **1-48**), esters (**1-45**), amides (**1-46**), ethers (**1-47**, **1-52**), alkenes (**1-49**), silyl-protected alkynes (**1-54**), acetals (**1-55**), and nitriles (**1-56**). Given the prevalence of heterocycles in bioactive molecules, we prioritized the incorporation of heteroarylboronic acids in the cross-coupling. *N*-Methylindole was easily installed (**1-51**). Pyridyl boronic acids can also be used under slightly modified conditions. By utilizing a lower ligand loading (12 mol %) and more dilute conditions (0.025 M), a variety of heteroarenes can be incorporated (Scheme 1.11). Both 3- and 4-pyridyl groups work, including those with fluoride (**1-57**, **1-60**, **1-61**, & **1-65**), ether (**1-58** & **1-63**), and morpholino (**1-64**) substituents. Notably, 2-fluoropyridines are primed for elaboration via S_NAr chemistry. Unsubstituted pyridyl (**1-59**) and quinoline (**1-62**) were also successful. Moreover, product **1-65** is derived from an amine intermediate used in the synthesis of Lipitor[®] (Pfizer, Inc.), an anti-cholesterol drug.⁴⁰

Scheme 1.11 Scope of pyridyl boronic acid^a



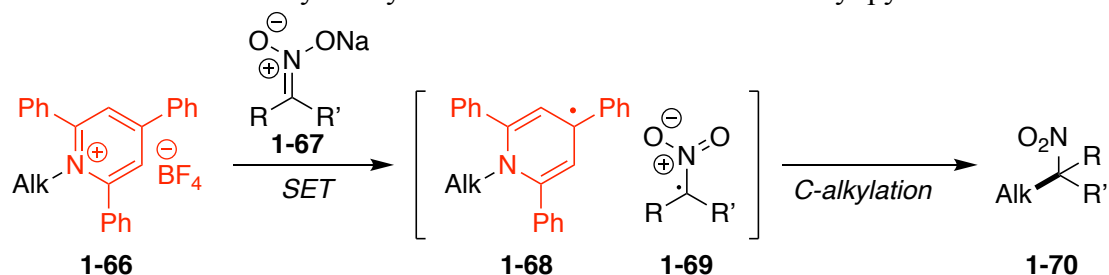
^aConditions: pyridinium salt **1-31** (1.0 mmol), $\text{Ni(OAc)}_2 \cdot 4\text{H}_2\text{O}$ (10 mol %), BPhen (12 mol %), ArB(OH)_2 (3.0 equiv), KO^tBu (3.4 equiv), EtOH (5 equiv), dioxane (0.025 M), 60 °C, 24 h. Average isolated yields ($\pm 6\%$) from duplicate experiments. ^bSingle experiment.

1.2.4 Mechanistic Studies

We reckoned that the cross-coupling could proceed via a $\text{Ni}^{\text{I/III}}$ or $\text{Ni}^{\text{0/II}}$ catalytic cycle. A $\text{Ni}^{\text{0/II}}$ mechanism would involve two-electron oxidative addition

(S_N1 or S_N2), whereas a Ni^{I/III} cycle would proceed via single-electron transfer (SET) from a Ni^I intermediate to the pyridinium salt. Although, pyridinium salts have been preceded to participate in S_N2 chemistry,⁴¹ Katritzky has also shown that these salts can act as single-electron acceptors. For instance, they have been used in the C-alkylation of nitronate anions (Scheme 1.12).⁴² Pyridinium salts have also shown to be effective photosensitizers⁴³ and sources of nitrogen-centered radicals.⁴⁴

Scheme 1.12 Katritzky's alkylation of nitronate anions with alkyl pyridinium salts

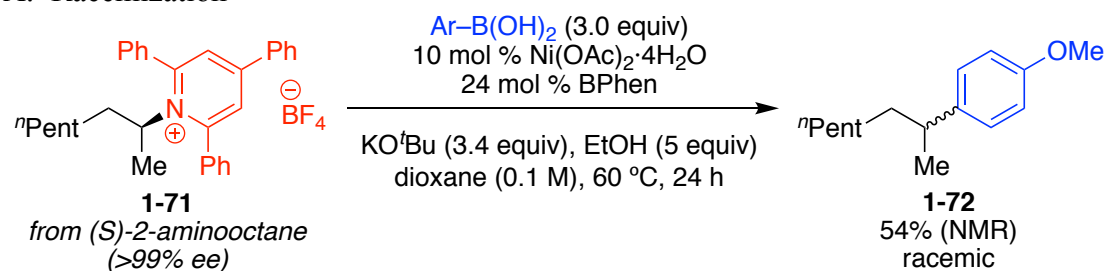


The superiority of bipyridyl ligands, which are often employed in Ni^{I/III} catalysis, and the fact that Ni^{II} precursors outcompete Ni⁰ pre-catalysts further allude to a SET mechanism (See Table 1.1, entries 3 & 4). This mechanism would lead to the formation of an alkyl radical intermediate. With that in mind, I performed several mechanistic experiments to probe the intermediacy of this alkyl radical species. Given the rapid interconversion of alkyl radicals, we proposed that erosion of stereochemical information through the course of the reaction would be observed. In fact, cross-coupling of pyridinium salt **1-71**, which was prepared from enantiopure (*S*)-2-aminoctane, led to the formation of racemic arylated product **1-72** in 54% yield (Scheme 1.13A). Moreover, cross-coupling of radical-clock cyclopropane **1-73** resulted in ring-opened product **1-74** (Scheme 1.13B). The addition of TEMPO shut

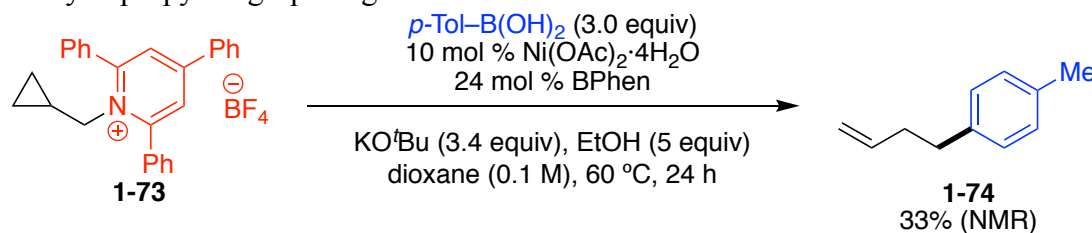
down the cross-coupling reaction and provided only TEMPO-trapped adduct **1-76** in 20% yield (Scheme 1.13C). These results are in support of an alkyl radical intermediate.

Scheme 1.13 Mechanistic support for radical intermediate

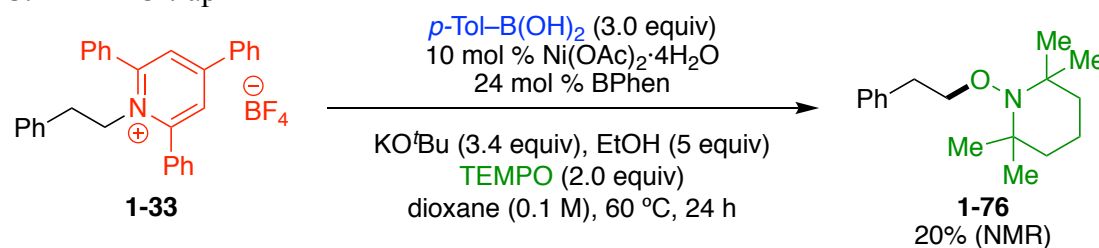
A. Racemization



B. Cyclopropyl ring-opening



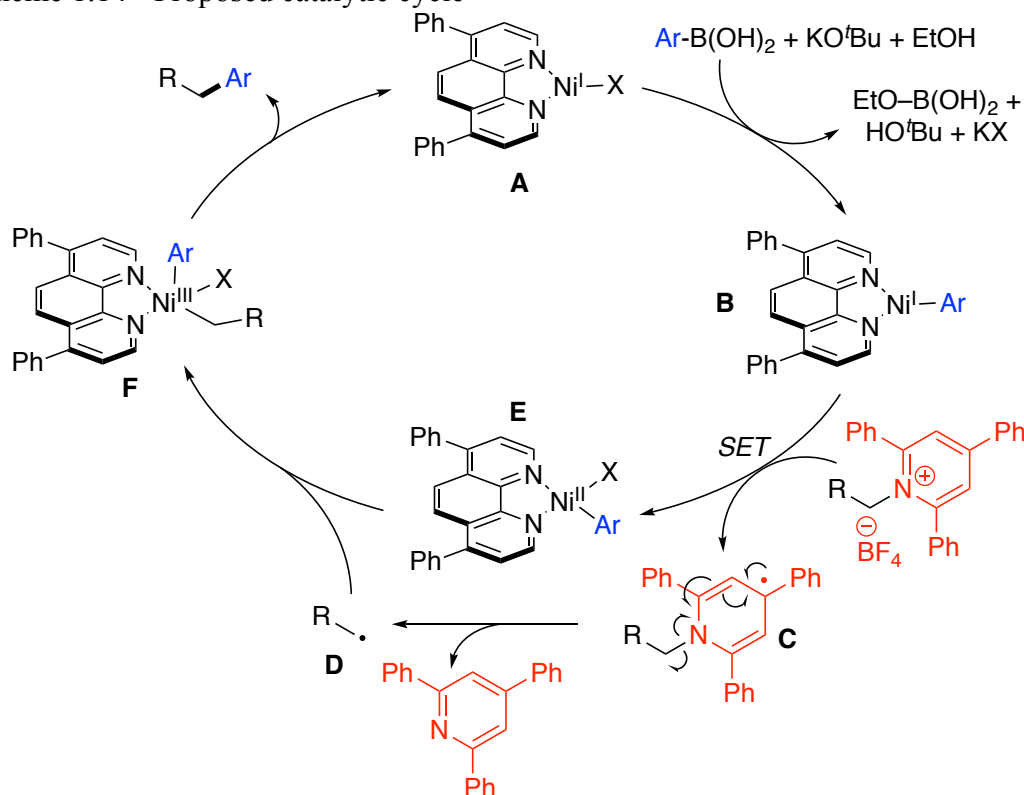
C. TEMPO trap



In light of this data, we have proposed the following $\text{Ni}^{\text{I/III}}$ catalytic cycle (Scheme 1.14). In this scheme, I have assigned redox events only to the nickel center for simplicity, but certainly the BPhen ligand may also be undergoing redox events. Ni^{I} species **A** undergoes transmetalation with the activated boronate to generate aryl- Ni^{I} species **B**. Single-electron transfer (SET) from **B** into the pyridinium ring leads to

the formation of radical species **C**. This then induces homolytic C–N bond cleavage to generate alkyl radical **D** as well as 2,4,6-triphenylpyridine as byproduct. Alkyl radical **D** can then recombine with Ni^{II}-arene **E** via a radical-rebound pathway to generate Ni^{III} species **F**. This intermediate is then prone to reductive elimination to deliver the desired cross-coupled product and regenerate active catalyst **A**. This monometallic “transmetalation-first” type mechanism is analogous to that proposed by Vicic for Fu’s Negishi cross-coupling of alkyl halides.²² We are cognizant that alternative pathways are possible such as a radical chain bimetallic SET oxidative addition⁴⁵ and cannot distinguish these possibilities with the current data. Future efforts in the group are focused on elucidating the elementary steps of this catalytic process.

Scheme 1.14 Proposed catalytic cycle



1.3 Conclusion

In summary, we have developed a nickel-catalyzed cross coupling of alkyl pyridinium salts with arylboronic acids. We have demonstrated broad substrate scope in both coupling partners, particularly with the incorporation of nitrogen containing functionalities. We have also shown the amenability of this method to a number of amino acid derivatives and drug intermediates. These examples highlight the potential of the amine (NH₂) moiety to serve as a handle for elaboration and late-stage functionalization, especially within the context of drug discovery efforts. Moreover, this method allows inexpensive primary amine precursors to be converted into complex, high value compounds. Notably, this is the first example of a metal-catalyzed cross-coupling of an amine derivative bearing unactivated alkyl groups. This work was published in the *Journal of the American Chemical Society*.⁴⁶

1.4 Experimental

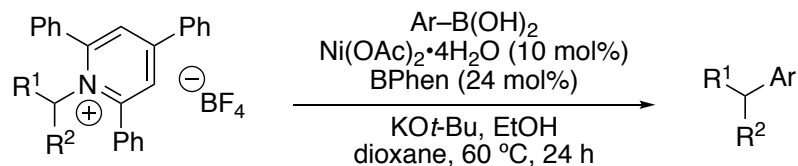
1.4.1 General Information

Reactions were performed in oven-dried Schlenk flasks or in oven-dried round-bottomed flasks unless otherwise noted. Round-bottomed flasks were fitted with rubber septa, and reactions were conducted under a positive pressure of N₂. Stainless steel syringes or cannulae were used to transfer air- and moisture-sensitive liquids. Silica gel chromatography was performed on silica gel 60 (40-63 μm, 60Å) unless otherwise noted. Commercial reagents, including 2,4,6-triphenylpyrylium tetrafluoroborate and the primary and secondary alkyl amines (or corresponding

hydrochloride salts), were purchased from Sigma Aldrich, Acros, Fisher, Strem, TCI, Combi Blocks, Alfa Aesar, AK Scientific, Oakwood, or Cambridge Isotopes Laboratories and used as received with the following exceptions: anhydrous ethanol was degassed by sparging with N₂ for 20-30 minutes prior to use in the cross-coupling reactions; dioxane was dried by passing through drying columns, then degassed by sparging with N₂.⁴⁷ In some instances oven-dried potassium carbonate was added to CDCl₃ to remove trace acid. Proton nuclear magnetic resonance (¹H NMR) spectra, carbon nuclear magnetic resonance (¹³C NMR) spectra, fluorine nuclear magnetic resonance spectra (¹⁹F NMR), and silicon nuclear magnetic resonance spectra (²⁹Si NMR) were recorded on both 400 MHz and 600 MHz spectrometers. Chemical shifts for protons are reported in parts per million downfield from tetramethylsilane and are referenced to residual protium in the NMR solvent (CHCl₃ = δ 7.26). Chemical shifts for carbon are reported in parts per million downfield from tetramethylsilane and are referenced to the carbon resonances of the solvent (CDCl₃ = δ 77.16). Chemical shifts for fluorine were externally referenced to CFCl₃ in CDCl₃ (CFCl₃ = δ 0). Data are represented as follows: chemical shift, multiplicity (br = broad, s = singlet, d = doublet, t = triplet, q = quartet, p = pentet, m = multiplet, dd = doublet of doublets, h = heptet), coupling constants in Hertz (Hz), integration. Infrared (IR) spectra were obtained using FTIR spectrophotometers with material loaded onto a KBr plate. The mass spectral data was obtained at the University of Delaware mass spectrometry facility. Optical rotations were measured using a 2.5 mL cell with a 0.1 dm path length. Melting points were taken on a Thomas-Hoover Uni-Melt Capillary Melting Point Apparatus.

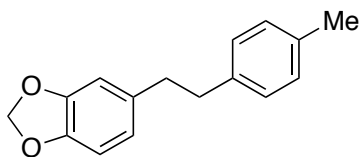
1.4.2 Suzuki–Miyaura Cross-Coupling of Alkyl Pyridinium Salts

1.4.2.1 General Procedure A: Cross-Coupling with Non-Pyridyl Aryl Boronic Acids

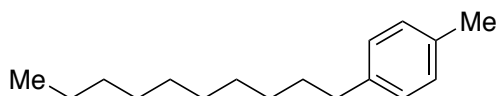


To an oven-dried, 25-mL pear-shaped flask, was added $\text{Ni(OAc)}_2 \cdot 4\text{H}_2\text{O}$ (25 mg, 0.10 mmol, 10 mol %) and bathophenanthroline (BPhen, 80 mg, 0.24 mmol, 24 mol %). The flask was fitted with a rubber septum, sealed with parafilm, and then evacuated and refilled with N_2 (x 3). To an oven-dried, 50-mL Schlenk flask was added the alkyl pyridinium salt (1.0 mmol, 1.0 equiv), arylboronic acid (3.0 equiv, 3.0 mmol), and $\text{KO}t\text{-Bu}$ (382 mg, 3.4 mmol, 3.4 equiv). The flask was fitted with a rubber septum, sealed with parafilm, and then evacuated and refilled with N_2 (x 3). To the pear-shaped flask containing $\text{Ni(OAc)}_2 \cdot 4\text{H}_2\text{O}$ and BPhen was added dioxane (sparged, anhydrous; 2.5 mL). To the Schlenk flask containing the pyridinium salt, boronic acid, and $\text{KO}t\text{-Bu}$ was added dioxane (sparged, anhydrous; 2.5 mL), followed by EtOH (sparged, anhydrous; 0.29 mL, 5.0 mmol, 5.0 equiv). After vigorously stirring of the resulting mixtures for 1 h at room temperature, the heterogeneous mixture containing the catalyst was transferred via cannula to the mixture containing the pyridinium salt and activated boronate complex. The pear-shaped flask was rinsed multiple times with dioxane (totaling 5 mL; each rinse was transferred via cannula to the reaction mixture) to bring the total volume of dioxane in the reaction flask to 10 mL (0.1 M). The resulting reaction mixture was stirred at 60 °C for 24 h. The mixture was allowed to cool to room temperature. EtOAc (10 mL) was added. The mixture was stirred for 2–5 min, and then filtered through a small plug of silica gel. The filter cake was washed

with EtOAc (4 x 20 mL), and the resulting solution was concentrated. The cross-coupled product was then purified via silica gel chromatography.



5-(4-Methylphenethyl)benzo[*d*][1,3]dioxole (1-40). Prepared via General Procedure A using pyridinium salt **1-39**. The crude mixture was purified by silica gel chromatography (step gradient: 1→5→10→20% toluene/hexanes) to give **1-40** (run 1: 183 mg, 76%; run 2: 177 mg, 74%) as a white solid (mp 81–82 °C): ¹H NMR (600 MHz, CDCl₃) δ 7.12-7.03 (m, 4H), 6.72 (d, *J* = 7.9 Hz, 1H), 6.69 (d, *J* = 1.5 Hz, 1H), 6.62 (dd, *J* = 7.9, 1.5 Hz, 1H), 5.92 (s, 2H), 2.87 – 2.78 (m, 4H), 2.32 (s, 3H); ¹³C NMR (151 MHz, CDCl₃) δ 147.6, 145.8, 138.7, 135.9, 135.5, 129.2, 128.4, 121.3, 109.1, 108.2, 100.9, 37.9, 37.9, 21.2; FTIR (neat) 2940, 1490, 1246, 1038, 927, 815, 741 cm⁻¹; HRMS (ESI⁺) calculated for C₁₆H₁₇O₂: 241.1223, found 241.1222.



1-Decyl-4-methylbenzene (1-42). Prepared via General Procedure A using pyridinium salt **1-77**. The crude mixture was purified by silica gel chromatography (100% pentane) to give **1-42** (run 1: 172 mg, 74%) as a clear oil (Note: This product is slightly volatile. Care should be used when drying under high vacuum.): ¹H NMR (400 MHz, CDCl₃) δ 7.14 – 7.02 (m, 4H), 2.59 – 2.52 (m, 2H), 2.32 (s, 3H), 1.63 – 1.54 (m, 2H), 1.45 – 1.07 (m, 14H), 0.92 – 0.83 (m, 3H); ¹³C NMR (101 MHz, CDCl₃)

δ 140.0, 135.1, 129.0, 128.4, 35.7, 32.1, 31.8, 29.79, 29.76, 29.7, 29.5, 22.9, 21.2, 14.3. The spectral data matches that of the literature.⁴⁸

Reaction without Oven-dried Glassware

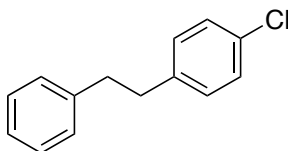
Product **1-42** also prepared via General Procedure A, except that the Schlenk flask, pear-shaped flask, stir bars, and cannula were not oven-dried prior to use. The crude mixture was purified by silica gel chromatography (100% pentane) to give **1-42** (154 mg, 66%).

Reaction with “Minimal Precaution” Set-up

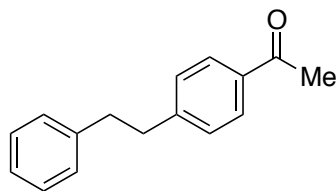
Product **1-42** was also prepared via a procedure similar to General Procedure A, except that minimal precautions were taken to protect the reaction from air and moisture. No precautions were taken to either dry or degass dioxane and EtOH. Neither the round-bottomed flask nor the pear-shaped flask were oven-dried prior to use. The volume of dioxane was measured with a graduated cylinder and added directly into each flask, open to air. Transfer of the catalyst mixture was performed with a non-oven-dried pipet directly from the pear-shaped flask into the round-bottomed flask. The reaction was set-up under air (no N₂).

To a round-bottomed flask equipped with a stir bar was added *p*-TolB(OH)₂ (408 mg, 3.0 mmol, 3.0 equiv), pyridinium salt **1-77** (536 mg, 1.0 mmol, 1.0 equiv), and KO*t*-Bu (382 mg, 3.4 mmol, 3.4 equiv). The flask was capped with a septum. To a pear-shaped flask equipped with a stir bar was added Ni(OAc)₂·4H₂O (25 mg, 0.10 equiv, 0.10 mmol) and BPhen (80 mg, 0.24 mmol, 0.24 equiv), followed by dioxane (2.5 mL). Dioxane (2.5 mL) was added to the round-bottomed flask containing the boronic acid, pyridinium salt, and KO*t*-Bu, followed by EtOH (0.29 mL, 5.0 mmol, 5 equiv) via syringe. The septum was replaced, and the pear-shaped flask was also fitted

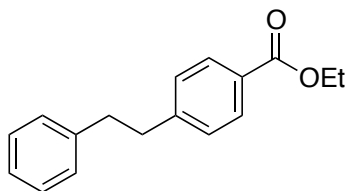
with a septum. After stirring both mixtures vigorously for 1 h, both septa were removed, and the catalyst mixture was transferred via pipet to the flask containing the “activated-boronate” mixture. Additional dioxane (5 mL total) was used to rinse the pear-shaped flask in order to ensure complete transfer of the catalyst mixture, thus bringing the total volume of dioxane in the reaction to 10 mL (0.1 M). The reaction flask was fitted with a septum, which was then wrapped in parafilm and secured with a copper wire. The reaction mixture was stirred at 60 °C for 24 h. After cooling to room temperature, EtOAc (10 mL) was added, and the mixture was filtered through a short plug of silica gel. The filter cake was rinsed with EtOAc (4 x 20 mL), and the resulting filtrate solution was concentrated. The residue was purified by silica gel chromatography (100% pentane) to afford **1-42** (73 mg, 31%) as a clear oil.



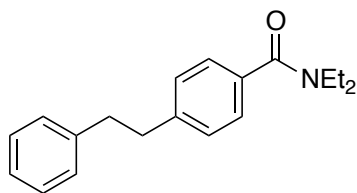
1-Chloro-4-phenethylbenzene (1-43). Prepared via General Procedure A using pyridinium salt **1-33**. The crude mixture was purified by silica gel chromatography (100% pentanes) to give **1-43** (run 1: 109 mg, 50%; run 2: 114 mg, 53%) as a white solid: ^1H NMR (600 MHz, CDCl_3) δ 7.30 – 7.26 (m, 2H), 7.25 – 7.22 (m, 2H), 7.22 – 7.18 (m, 1H), 7.17 – 7.13 (m, 2H), 7.11 – 7.05 (m, 2H), 2.89 (s, 4H); ^{13}C NMR (151 MHz, CDCl_3) δ 141.4, 140.3, 131.8, 130.0, 128.6, 128.54, 128.52, 126.2, 37.9, 37.3. The spectral data matches that of the literature.⁴⁹



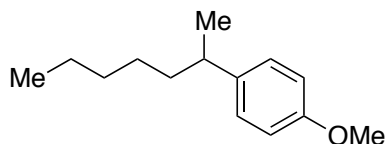
1-(4-Phenethylphenyl)ethanone (1-44). Prepared via General Procedure A using pyridinium salt **1-33**. The crude mixture was purified by silica gel chromatography (5% EtOAc/hexanes) to give **1-44** (run 1: 175 mg, 78%; run 2: 172 mg 77%) as a white solid: ^1H NMR (600 MHz, CDCl_3) δ 7.90 – 7.85 (m, 2H), 7.30 – 7.26 (m, 2H), 7.26 – 7.23 (m, 2H), 7.22 – 7.18 (m, 1H), 7.17 – 7.13 (m, 2H), 3.01 – 2.96 (m, 2H), 2.96 – 2.91 (m, 2H), 2.59 (s, 3H); ^{13}C NMR (151 MHz, CDCl_3) δ 197.9, 147.6, 141.2, 135.4, 128.9, 128.7, 128.58, 128.55, 126.3, 38.0, 37.6, 26.7. The spectral data matches that of the literature.⁵⁰



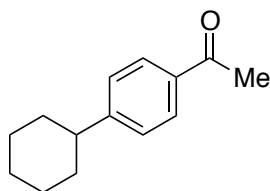
Ethyl 4-phenethylbenzoate (1-45). Prepared via General Procedure A using pyridinium salt **1-33**. The crude mixture was purified by silica gel chromatography (50% toluene/hexanes) to give **1-45** (run 1: 178 mg, 70%; run 2: 176 mg, 69%) as an off-white solid: ^1H NMR (400 MHz, CDCl_3) δ 7.98 – 7.92 (m, 2H), 7.30 – 7.26 (m, 2H), 7.24 – 7.18 (m, 3H), 7.15 (d, $J = 7.15$ Hz, 2H), 4.37 (q, $J = 7.1$ Hz, 2H), 3.00 – 2.96 (m, 2H), 2.95 – 2.91 (m, 2H), 1.39 (t, $J = 7.1$ Hz, 3H); ^{13}C NMR (101 MHz, CDCl_3) δ 166.8, 147.2, 141.3, 129.8, 128.63, 128.58, 128.5, 128.4, 126.2, 61.0, 38.0, 37.6, 14.5. The spectral data matches that of the literature.⁵¹



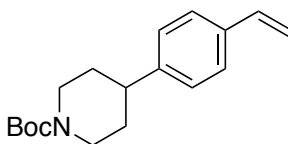
***N,N*-Diethyl-4-phenethylbenzamide (1-46).** Prepared via General Procedure A using pyridinium salt **1-33**. The crude mixture was purified by silica gel chromatography (50% EtOAc/hexanes) to give **1-46** (run 1: 211 mg, 75%; run 2: 200 mg, 71%) as a yellow oil: ^1H NMR (600 MHz, CDCl_3) δ 7.32 – 7.26 (m, 4H), 7.23 – 7.14 (m, 5H), 3.62 – 3.41 (m, br, 2H), 3.37 – 3.16 (m, br, 2H), 2.97 – 2.88 (m, 4H), 1.34 – 1.18 (m, br, 3H), 1.18 – 1.02 (m, br, 3H); ^{13}C NMR (101 MHz, CDCl_3) δ 171.5, 143.0, 141.6, 135.0, 128.59, 128.58, 128.5, 126.5, 126.1, 43.4, 39.4, 37.87, 37.85, 14.4, 13.0; FTIR (neat) 2972, 1630, 1426, 1287, 1095, 700 cm^{-1} ; HRMS (ESI+) $[\text{M}+\text{H}]^+$ calculated for $\text{C}_{19}\text{H}_{24}\text{NO}$: 282.1852, found 282.1852.



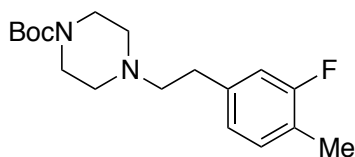
1-(Heptan-2-yl)-4-methoxybenzene (1-47). Prepared via General Procedure A using pyridinium salt **1-78**. The crude mixture was purified by silica gel chromatography (step gradient: 0→2→5% toluene/hexanes) to give **1-47** (run 1: 119 mg, 58%; run 2: 118 mg, 57%) as a colorless oil: ^1H NMR (600 MHz, CDCl_3) δ 7.14 – 7.04 (m, 2H), 6.89 – 6.78 (m, 2H), 3.79 (s, 3H), 2.63 (h, $J = 7.1$ Hz, 1H), 1.56 – 1.48 (m, 2H), 1.31 – 1.12 (m, 9H), 0.90 – 0.81 (m, 3H); ^{13}C NMR (151 MHz, CDCl_3) δ 157.8, 140.3, 127.9, 113.8, 55.4, 39.2, 38.7, 32.1, 27.5, 22.75, 22.67, 14.2; FTIR (neat) 2956, 2926, 1513, 1247, 828 cm^{-1} ; HRMS (ESI+) $[\text{M}+\text{H}]^+$ calculated for $\text{C}_{14}\text{H}_{23}\text{O}$: 207.1743, found 207.1741.



1-(4-Cyclohexylphenyl)ethanone (1-48). Prepared via General Procedure A using pyridinium salt **1-35**. The crude mixture was purified by silica gel chromatography (step gradient: 50→75% toluene/hexanes) to give **1-48** (run 1: 134 mg, 66%) as a pale yellow solid: ^1H NMR (600 MHz, CDCl_3) δ 7.94 – 7.83 (m, 2H), 7.33 – 7.27 (m, 2H), 2.63 – 2.49 (m, 4H), 1.93 – 1.80 (m, 4H), 1.80 – 1.73 (m, 1H), 1.48 – 1.35 (m, 4H), 1.31 – 1.23 (m, 1H); ^{13}C NMR (151 MHz, CDCl_3) δ 198.0, 153.9, 135.2, 128.7, 127.2, 44.8, 34.3, 26.9, 26.7, 26.2. The spectral data matches that of the literature.⁵²

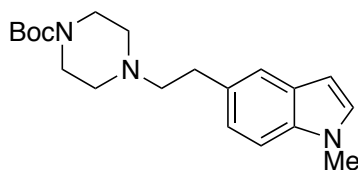


tert-Butyl 4-(4-vinylphenyl)piperidine-1-carboxylate (1-49). Prepared via General Procedure A using pyridinium salt **1-38**. The crude mixture was purified by silica gel chromatography (3% EtOAc/hexanes) to give **1-49** (run 1: 148 mg, 51%; run 2: 130 mg, 45%) as a clear oil: ^1H NMR (600 MHz, CDCl_3) δ 7.38 – 7.33 (m, 2H), 7.19 – 7.14 (m, 2H), 6.69 (dd, $J = 17.6, 10.9$ Hz, 1H), 5.72 (dd, $J = 17.6, 0.9$ Hz, 1H), 5.21 (dd, $J = 10.9, 0.8$ Hz, 1H), 4.42 – 4.08 (m, br, 2H), 2.88 – 2.70 (m, 2H), 2.63 (tt, $J = 12.1, 3.5$ Hz, 1H), 1.85 – 1.76 (m, br, 2H), 1.67 – 1.55 (m, 2H), 1.48 (s, 9H); ^{13}C NMR (151 MHz, CDCl_3) δ 155.0, 145.7, 136.6, 135.9, 127.1, 126.5, 113.5, 79.6, 44.5 (br), 42.6, 33.3, 28.6; FTIR (neat) 2933, 1693, 1424, 1170, 840 cm^{-1} ; HRMS (ESI+) $[\text{M}+\text{H}]^+$ calculated for $\text{C}_{18}\text{H}_{26}\text{NO}_2$: 288.1958, found 288.1956.



***tert*-Butyl 4-(3-fluoro-4-methylphenethyl)piperazine-1-carboxylate (1-50).**

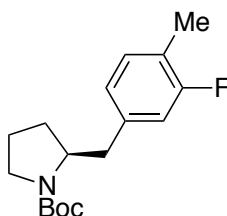
Prepared via General Procedure A using pyridinium salt **1-79**. The crude mixture was purified by silica gel chromatography (step gradient: 0→10→20→40% EtOAc/hexanes) to give **1-50** (run 1: 214 mg, 66%; run 2: 228 mg, 71%) as a yellow semi-solid; ^1H NMR (600 MHz, CDCl_3) δ 7.07 (t, $J = 8.0$ Hz, 1H), 6.89 – 6.81 (m, 2H), 3.50 – 3.41 (m, 4H), 2.79 – 2.72 (m, 2H), 2.61 – 2.55 (m, 2H), 2.50 – 2.40 (m, br, 4H), 2.23 (s, 3H), 1.46 (s, 9H); ^{13}C NMR (151 MHz, CDCl_3) δ 161.4 (d, $J_{\text{C-F}} = 244.6$ Hz), 154.9, 139.9 (d, $J_{\text{C-F}} = 9.1$ Hz), 131.4 (d, $J_{\text{C-F}} = 6.0$ Hz), 124.1 (d, $J_{\text{C-F}} = 3.0$ Hz), 122.5 (d, $J_{\text{C-F}} = 16.6$ Hz), 115.3 (d, $J_{\text{C-F}} = 22.7$ Hz), 79.8, 60.3, 53.1, 43.3 (br), 33.0, 28.6, 14.3; ^{19}F NMR (565 MHz, CDCl_3) δ -118.0; FTIR (neat) 2930, 2809, 1698, 1422, 1249, 1173, 1123, 1004; HRMS (ESI+) $[\text{M}+\text{H}]^+$ calculated for $\text{C}_{18}\text{H}_{28}\text{FN}_2\text{O}_2$: 323.2129, found 323.2128.



***tert*-Butyl 4-(2-(1-methyl-1H-indol-5-yl)ethyl)piperazine-1-carboxylate (1-51).**

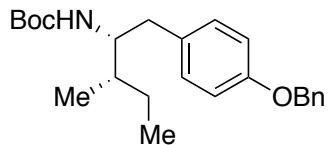
Prepared via General Procedure A using pyridinium salt **1-79**. The crude mixture was purified by silica gel chromatography (step gradient: 30→70% EtOAc/hexanes) to give **1-51** (run 1: 272 mg, 79%; run 2: 282 mg, 82%) as a light orange/yellow solid (mp 80–83 °C): ^1H NMR (600 MHz, CDCl_3) δ 7.46 – 7.41 (m, 1H), 7.26 – 7.23 (m, 1H), 7.10 – 7.05 (m, 1H), 7.03 (d, $J = 3.1$ Hz, 1H), 6.43 – 6.39 (m, 1H), 3.77 (m, br,

3H), 3.59 – 3.41 (m, br, 4H), 2.91 (m, br, 2H), 2.66 (m, br, 2H), 2.50 (s, 4H), 1.47 (s, 9H); ^{13}C NMR (101 MHz, CDCl_3) δ 154.9, 135.6, 130.9, 129.2, 128.8, 122.7, 120.5, 109.2, 100.5, 79.7, 61.6, 53.2, 43.7, 33.7, 33.0, 28.6; FTIR (neat) 2929, 2808, 1694, 1422, 1247, 1171, 1002, 718 cm^{-1} ; HRMS (ESI+) $[\text{M}+\text{H}]^+$ calculated for $\text{C}_{20}\text{H}_{30}\text{N}_3\text{O}_2$: 344.2333, found 344.2331.

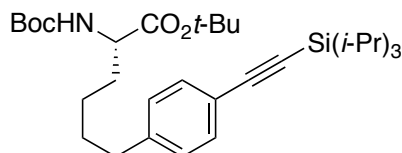


(S)-tert-Butyl 2-(3-fluoro-4-methylbenzyl)pyrrolidine-1-carboxylate (1-52).

Prepared via General Procedure A using pyridinium salt **1-37**. The crude mixture was purified by silica gel chromatography (5% Et_2O /toluene) to give **1-52** (189 mg, 65%) as a yellow oil (mixture of rotamers): ^1H NMR (600 MHz, CDCl_3) δ 7.13 – 7.02 (m, br, 1H), 6.92 – 6.76 (m, br, 2H), 4.05 – 3.85 (m, br, 1H), 3.45 – 3.18 (m, br, 2H), 3.16 – 2.95 (m, br, 1H), 2.59 – 2.41 (m, br, 1H), 2.23 (s, br, 3H), 1.84 – 1.64 (m, br, 4H), 1.57 – 1.44 (s, br, 9H); ^{13}C NMR (151 MHz, CDCl_3) δ 161.3 (d, $J_{\text{C-F}} = 245.1$ Hz), 154.6, 138.9 (d, $J_{\text{C-F}} = 7.4$ Hz), 131.4 (d, $J_{\text{C-F}} = 4.9$ Hz, major), 131.2 (d, $J_{\text{C-F}} = 4.4$ Hz, minor), 125.0 (minor), 124.8 (major), 122.6 (d, $J_{\text{C-F}} = 17.6$ Hz, minor), 122.4 (d, $J_{\text{C-F}} = 16.4$ Hz, major), 116.1 (d, $J_{\text{C-F}} = 20.3$ Hz, minor), 115.8 (d, $J_{\text{C-F}} = 22.2$ Hz, major), 79.5 (major), 79.2 (minor), 58.9 (major), 58.6 (minor), 47.0 (minor), 46.4 (major), 40.2 (major), 39.1 (minor), 29.8 (major), 29.1 (minor), 28.7, 23.6 (minor), 22.8 (major), 14.33, 14.31; ^{19}F NMR (565 MHz, CDCl_3) δ -118.0 (major), -118.4 (minor); FTIR (neat) 2973, 2875, 1694, 1394, 1172, 1114, 771 cm^{-1} ; HRMS (ESI+) $[\text{M}+\text{H}]^+$ calculated for $\text{C}_{17}\text{H}_{25}\text{FNO}_2$: 294.1864, found 294.1862.



tert-butyl ((2R,3S)-1-(4-(benzyloxy)phenyl)-3-methylpentan-2-yl)carbamate (1-53). Prepared via General Procedure A using pyridinium salt **1-36**. The crude mixture was purified by silica gel chromatography (gradient: 1→2% EtOAc/toluene) to give **1-53** (201 mg, 52%) as an off-white solid (mp 121–123 °C): ^1H NMR (600 MHz, CDCl_3) δ 7.44 – 7.40 (m, 2H), 7.40 – 7.35 (m, 2H), 7.34 – 7.29 (m, 1 H), 7.12 – 7.05 (m, 2H), 6.92–6.86 (m, 2H), 5.03 (s, 2H), 4.36 – 4.24 (m, 1H), 3.80 – 3.68 (m, br, 1H), 2.79 – 2.73 (m, 1H), 2.57 – 2.53 (m, 1H), 1.55–1.47 (m, 2H), 1.35 (s, br, 9H), 1.15 – 1.05 (m, br, 1H), 0.97–0.86 (m, 6H); ^{13}C NMR (101 MHz, CDCl_3) δ 157.4, 155.7, 137.3, 131.3, 130.3, 128.7, 128.0, 127.6, 114.8, 79.0, 70.1, 56.1, 37.7, 37.0, 28.5, 24.8, 15.8, 11.9; FTIR (neat) 3384, 2962, 1684, 1518, 1240, 744 cm^{-1} ; HRMS (ESI+) $[\text{M}+\text{H}]^+$ calculated for $\text{C}_{24}\text{H}_{34}\text{NO}_3$: 384.2533, found 384.2526.

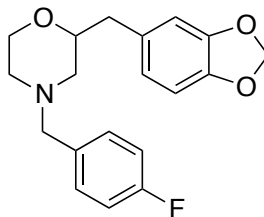


(S)-tert-Butyl 2-((tert-butoxycarbonyl)amino)-6-(4-((triisopropylsilyl)ethynyl)phenyl)hexanoate (1-54). Prepared via General Procedure A using pyridinium salt **1-80** and (4-((triisopropylsilyl)ethynyl)phenyl)boronic acid⁵³ with the following exceptions: the reaction was run on a 0.5 mmol scale and pyridinium salt **1-80** was pre-stirred with $\text{Ni}(\text{OAc})_2 \cdot 4\text{H}_2\text{O}$ and BPhen instead of with the boronic acid, $\text{KO}t\text{-Bu}$, and EtOH. The crude mixture was purified by silica gel chromatography (5% EtOAc/hexanes) to give **1-54** (165 mg, 60%) as a clear oil. The enantiomeric excess was determined to be 29%

by chiral HPLC analysis (CHIRALPAK IA, 1.0 mL/min, 2% *i*-PrOH/hexanes, $\lambda=254$ nm); $t_R(\text{major}) = 14.52$ min, $t_R(\text{minor}) = 9.78$ min. $[\alpha]_D^{26} = +40.1^\circ$ (c 1.6, CHCl_3): ^1H NMR (600 MHz, CDCl_3) δ 7.38 (d, $J = 8.0$ Hz, 2H), 7.09 (d, $J = 8.1$ Hz, 2H), 4.98 (d, $J = 7.8$ Hz, 1H), 4.23 – 4.07 (m, 1H), 2.59 (t, $J = 7.6$ Hz, 2H), 1.81 – 1.72 (m, 1H), 1.68 – 1.57 (m, 3H), 1.44 (s, 9H), 1.43 (s, 9H), 1.40 – 1.35 (m, 1H), 1.35 – 1.29 (m, 1H), 1.12 (s, 21H); ^{13}C NMR (151 MHz, CDCl_3) δ 172.1, 155.5, 142.9, 132.2, 128.4, 121.1, 107.4, 89.8, 81.9, 79.7, 54.0, 35.7, 33.0, 30.9, 28.5, 28.1, 24.7, 18.8, 11.5; ^{29}Si NMR (119 MHz, CDCl_3) δ -2.0; FTIR (neat) 3358, 2942, 2865, 2155, 1717, 1504, 1367, 1155, 677 cm^{-1} ; HRMS (ESI+) $[\text{M}+\text{H}]^+$ calculated for $\text{C}_{32}\text{H}_{54}\text{NO}_4\text{Si}$: 544.3817, found 544.3811.

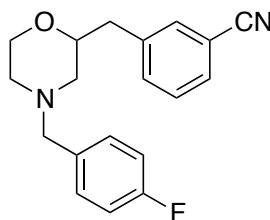
The arylation of pyridinium salt **1-80** was also performed in the presence of 4-(trifluoromethyl)phenol. In a N_2 -atmosphere glovebox: $\text{Ni}(\text{OAc})_2 \cdot 4\text{H}_2\text{O}$ (1.2 mg, 0.005 mmol, 10 mol %), BPhen (4.0 mg, 0.0012 mmol, 24 mol %), 4-(trifluoromethyl)phenol (16 mg, 0.1 mmol, 2.0 equiv), and pyridinium salt **1-80** (34 mg, 0.05 mmol, 1.0 equiv) were added to an oven-dried 1-dram vial. To a separate oven-dried 1-dram vial was added $\text{KO}t\text{-Bu}$ (19 mg, 0.17 mmol, 3.4 equiv) and 4-((triisopropylsilyl)ethynyl)phenyl)boronic acid (45 mg, 0.15 mmol, 3.0 equiv). Dioxane (125 μL) was added to each vial. Each vial was then equipped with a micro stir bar, capped with a pierceable Teflon-coated cap, and removed from the glovebox. To the vial containing the boronic acid and $\text{KO}t\text{-Bu}$ was added EtOH (15 μL) via a N_2 -purged syringe. Both mixtures were stirred for 1 h at rt. After pre-stirring was complete, the catalyst mixture containing the pyridinium salt and 4-(trifluoromethyl)phenol was transferred to the “activated- boronate” mixture via a N_2 -purged syringe. Dioxane (250 μL total) was used to insure complete transfer of the

catalyst mixture and bring the total concentration of the reaction to 0.1 M. The resulting reaction mixture was heated to 60 °C and stirred vigorously for 24 h. Upon completion, the mixture was diluted with EtOAc (approx. 1.5 mL) and filtered through a short plug of silica gel. The filter cake was washed with EtOAc (5 x 1.5 mL) and the resulting solution was concentrated. The yield of the crude product was determined to be 25% and was obtained by integration by ¹H-NMR with 1,3,5-trimethoxybenzene as an internal standard. A small sample of the product was purified via preparatory thin-layer chromatography (5% EtOAc/hexanes) and the enantiomeric excess was determined to be 81% by chiral HPLC analysis (CHIRALPAK IA, 1.0 mL/min, 2% *i*-PrOH/hexanes, λ=254 nm); t_R(major) = 14.57 min, t_R(minor) = 9.84 min.



2-(Benzo[*d*][1,3]dioxol-5-ylmethyl)-4-(4-fluorobenzyl)morpholine (1-55). Prepared via General Procedure A using pyridinium salt **1-81**. After the silica gel filtration, the crude mixture was dissolved in Et₂O (20 mL) and washed with HCl (1 N, 4 x 25 mL). The combined aqueous layers were extracted with Et₂O (4 x 50 mL, these organic layers were discarded), basified to pH ≥ 12 with NaOH (4 N), and then extracted with Et₂O (4 x 50 mL). The combined organic layers were dried (MgSO₄), filtered, and concentrated. The residue was then purified by silica gel chromatography (step gradient: 10→20% EtOAc/hexanes) to give **1-55** (run 1: 224 mg, 68%; run 2: 240 mg, 73%) as a yellow oil: ¹H NMR (600 MHz, CDCl₃) δ 7.28 – 7.23 (m, 2H, *overlaps with CHCl₃*), 7.04 – 6.94 (m, 2H), 6.76 – 6.67 (m, 2H), 6.65 – 6.60 (m, 1H), 5.92 (s, 2H),

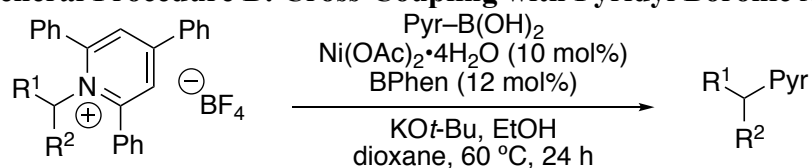
3.87 – 3.81 (m, 1H), 3.74 – 3.66 (m, 1H), 3.64 – 3.57 (m, 1H), 3.52 – 3.46 (m, 1H), 3.41 – 3.34 (m, 1H), 2.78 – 2.67 (m, 2H), 2.62 – 2.55 (m, 2H), 2.16 – 2.08 (m, 1H), 1.96 – 1.87 (m, 1H); ^{13}C NMR (151 MHz, CDCl_3) δ 162.2 (d, $J_{\text{C-F}} = 245.1$ Hz), 147.6, 146.1, 133.6, 131.9, 130.7 (d, $J_{\text{C-F}} = 7.7$ Hz), 122.2, 115.2 (d, $J_{\text{C-F}} = 21.3$ Hz), 109.8, 108.2, 100.9, 76.7, 66.9, 62.6, 58.4, 52.8, 40.0; ^{19}F NMR (565 MHz, CDCl_3) δ -115.8; FTIR (neat) 2859, 2804, 1604, 1508, 1247, 1114, 1040, 810 cm^{-1} ; HRMS (ESI+) $[\text{M}+\text{H}]^+$ calculated for $\text{C}_{19}\text{H}_{21}\text{FNO}_3$: 330.1500, found 330.1491.



3-((4-(4-Fluorobenzyl)morpholin-2-yl)methyl)benzonitrile (1-56). Prepared via General Procedure A using pyridinium salt **1-81**. After the silica gel filtration, the crude mixture was dissolved in Et_2O (20 mL) and washed with HCl (1 N, 4 x 25 mL). The combined aqueous layers were extracted with Et_2O (4 x 50 mL, these organic layers were discarded), basified to $\text{pH} \geq 12$ with NaOH (4 N), and then extracted with Et_2O (4 x 50 mL). The combined organic layers were dried (MgSO_4), filtered, and concentrated. The residue was then purified by silica gel chromatography (20% EtOAc /hexanes) to give **1-56** (run 1: 201 mg, 65%; run 2: 180 mg, 58%) as a yellow oil: ^1H NMR (600 MHz, CDCl_3) δ 7.51 – 7.50 (m, 2H), 7.44 – 7.43 (m, 1H), 7.39 – 7.36 (m, 1H), 7.28 – 7.25 (m, 2H, overlaps with CHCl_3), 7.02– 6.99 (m, 2H), 3.82 – 3.84 (m, 1H), 3.72 (m, 1H), 3.61 – 3.57 (m, 1H), 3.48-3.41 (m, 2H), 2.82 – 2.79 (m, 1H), 2.72 – 2.69 (m, 2H), 2.63 – 2.61 (m, 1H), 2.16 – 2.12 (m, 1H), 1.94 – 1.90 (m, 1H); ^{13}C NMR (151 MHz, CDCl_3) δ 162.2 (d, $J_{\text{C-F}} = 245.4$ Hz), 139.9, 134.0, 133.4,

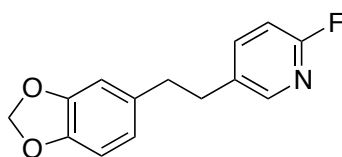
133.0, 130.7 (d, $J_{C-F} = 7.6$ Hz), 130.2, 129.1, 119.1, 115.3 (d, $J_{C-F} = 21.1$ Hz), 112.4, 75.9, 66.9, 62.5, 58.2, 52.9, 39.7; ^{19}F NMR (376 MHz, CDCl_3) δ -115.6; FTIR (neat) 2933, 2807, 2229, 1508, 1221, 1114, 693 cm^{-1} ; HRMS (ESI+) $[\text{M}+\text{H}]^+$ calculated for $\text{C}_{19}\text{H}_{20}\text{FN}_2\text{O}$: 311.1554, found 311.1551.

1.4.2.2 General Procedure B: Cross-Coupling with Pyridyl Boronic Acids

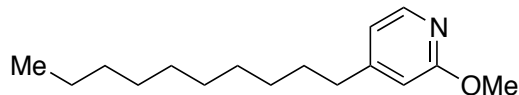


To an oven-dried, 25-mL pear-shaped flask was added $\text{Ni(OAc)}_2 \cdot 4\text{H}_2\text{O}$ (25 mg, 0.10 mmol, 10 mol %), bathophenanthroline (BPhen, 40 mg, 0.12 mmol, 12 mol %), and the alkyl pyridinium salt (1.0 mmol, 1.0 equiv). The flask was fitted with a rubber septum, sealed with parafilm, and then evacuated and refilled with N_2 (x 3). To an oven-dried, 100-mL Schlenk flask was added the arylboronic acid (3.0 equiv, 3.0 mmol) and $\text{KO}t\text{-Bu}$ (382 mg, 3.4 mmol, 3.4 equiv). The flask was fitted with a rubber septum, sealed with parafilm, and then evacuated and refilled with N_2 (x 3). To the pear-shaped flask containing $\text{Ni(OAc)}_2 \cdot 4\text{H}_2\text{O}$ and BPhen was added dioxane (sparged, anhydrous; 10 mL). To the Schlenk flask containing the boronic acid and $\text{KO}t\text{-Bu}$ was added dioxane (sparged, anhydrous; 10 mL), followed by EtOH (sparged, anhydrous; 0.29 mL, 5.0 mmol, 5.0 equiv). After vigorously stirring the resulting mixtures for 2 h at room temperature, the mixture (heterogeneous in some cases) of catalyst and pyridinium salt was transferred via large-gauge cannula to the mixture containing the activated boronate complex. The pear-shaped flask was rinsed multiple times with dioxane (totaling 20 mL; each rinse was transferred via cannula to the reaction

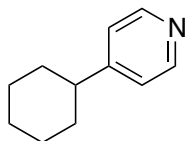
mixture) to bring the total volume of dioxane in the reaction to 40 mL (0.025 M). The resulting reaction mixture was stirred at 60 °C for 24 h. The mixture was allowed to cool to room temperature. EtOAc (10 mL) was added. The mixture was stirred 2–5 min, and then filtered through a small plug of silica gel. The filter cake was washed with EtOAc (4 x 20 mL), and the resulting solution was concentrated. The cross-coupled product was then purified via silica gel chromatography.



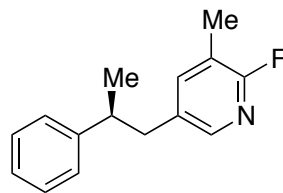
5-(2-(Benzo[*d*][1,3]dioxol-5-yl)ethyl)-2-fluoropyridine (1-57). Prepared via General Procedure B using pyridinium salt **1-39**. The crude mixture was purified by silica gel chromatography (4% EtOAc/hexanes) to give **1-57** (run 1: 201 mg, 82%; run 2: 193 mg, 79%) as a yellow oil: ^1H NMR (600 MHz, CDCl_3) δ 7.98 – 7.92 (m, 1H), 7.50 (td, $J = 8.1, 2.6$ Hz, 1H), 6.82 (dd, $J = 8.3, 2.9$ Hz, 1H), 6.71 (d, $J = 7.9$ Hz, 1H), 6.62 (d, $J = 1.7$ Hz, 1H), 6.54 (dd, $J = 7.8, 1.7$ Hz, 1H), 5.93 (s, 2H), 2.90 – 2.85 (m, 2H), 2.85 – 2.80 (m, 2H); ^{13}C NMR (101 MHz, CDCl_3) δ 162.4 (d, $J_{\text{C-F}} = 238.0$ Hz), 147.8, 147.3 (d, $J_{\text{C-F}} = 14.3$ Hz), 146.0, 141.3 (d, $J_{\text{C-F}} = 7.7$ Hz), 134.324, 134.319 (d, $J_{\text{C-F}} = 4.4$ Hz), 121.5, 109.1 (d, $J_{\text{C-F}} = 37.5$ Hz), 109.0, 108.3, 101.0, 37.4, 34.2; ^{19}F NMR (376 MHz, CDCl_3) δ -71.9; FTIR (neat) 2925, 1596, 1486, 1246, 1040, 932, 811 cm^{-1} ; HRMS (ESI+) $[\text{M}+\text{H}]^+$ calculated for $\text{C}_{14}\text{H}_{13}\text{FNO}_2$: 246.0925, found 246.0925.



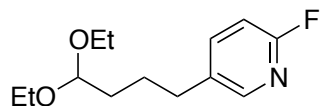
4-Decyl-2-methoxypyridine (1-58). Prepared via General Procedure B using pyridinium salt **1-77**. The crude mixture was purified by silica gel chromatography (step gradient: 100% toluene→2% EtOAc/hexanes) to give **1-58** (run 1: 195 mg, 78%; run 2: 175 mg, 70%) as a yellow oil: ^1H NMR (600 MHz, CDCl_3) δ 8.03 (d, $J = 5.3$ Hz, 1H), 6.72 – 6.67 (m, 1H), 6.58 – 6.51 (m, 1H), 3.92 (s, 3H), 2.59 – 2.49 (m, 2H), 1.62 – 1.56 (m, 2H), 1.35 – 1.19 (m, 14H), 0.88 (t, $J = 6.9$ Hz, 3H); ^{13}C NMR (151 MHz, CDCl_3) δ 164.7, 154.8, 146.6, 117.7, 110.4, 53.4, 35.3, 32.0, 30.3, 29.74, 29.68, 29.6, 29.5, 29.3, 22.8, 14.2; FTIR (neat) 2926, 1613, 1398, 1157, 1044, 820; HRMS (ESI+) $[\text{M}+\text{H}]^+$ calculated for $\text{C}_{16}\text{H}_{27}\text{NO}$: 250.2165, found 250.2157.



4-Cyclohexylpyridine (1-59). Prepared via General Procedure B using pyridinium salt **1-35**. The crude mixture was purified by silica gel chromatography (50% EtOAc/hexanes) to give **1-59** (run 1: 81 mg, 50%; run 2: 91 mg, 56%) as an orange oil: ^1H NMR (400 MHz, CDCl_3) δ 8.49 – 8.47 (m, 2H), 7.13 – 7.11 (m, 2H), 2.53 – 2.45 (m, 1H), 1.91 – 1.67 (m, 5H), 1.46 – 1.19 (m, 5H); ^{13}C NMR (101 MHz, CDCl_3) δ 156.7, 149.9, 122.5, 43.9, 33.6, 26.7, 26.1. The spectral data matches that of the literature.⁵⁴

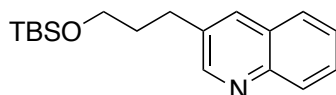


(S)-2-Fluoro-3-methyl-5-(2-phenylpropyl)pyridine (1-60). Prepared via General Procedure B using pyridinium salt **1-82**. The crude mixture was purified by silica gel chromatography (gradient: 10→20→30→50→70% toluene/hexanes→100% toluene) to give **1-60** (run 1: 151 mg, 66%; run 2: 152 mg, 66%) as a dark orange oil: ^1H NMR (400 MHz, CDCl_3) δ 7.67 (s, br, 1H), 7.32 – 7.26 (m, 2H), 7.24 – 7.15 (m, 2H), 7.15 – 7.07 (m, 2H), 2.94 (h, $J = 7.0$ Hz, 1H), 2.87 – 2.72 (m, 2H), 2.22 – 2.15 (s, 3H), 1.27 (d, $J = 6.9$ Hz, 3H); ^{13}C NMR (101 MHz, CDCl_3) δ 161.1 (d, $J_{\text{C-F}} = 237.0$ Hz), 145.8, 144.8 (d, $J_{\text{C-F}} = 14.2$ Hz), 142.4 (d, $J_{\text{C-F}} = 5.9$ Hz), 133.7 (d, $J_{\text{C-F}} = 4.6$ Hz), 128.6, 127.2, 126.5, 118.8 (d, $J_{\text{C-F}} = 32.8$ Hz), 41.8, 41.1 (d, $J_{\text{C-F}} = 0.9$ Hz), 21.3, 14.6 (d, $J_{\text{C-F}} = 1.5$ Hz); ^{19}F NMR (376 MHz, CDCl_3) δ -76.6; FTIR (neat) 2962, 1591, 1471, 1246, 1143, 700 cm^{-1} ; HRMS (ESI+) $[\text{M}+\text{H}]^+$ calculated for $\text{C}_{15}\text{H}_{16}\text{FN}$: 230.1340, found 230.1334.

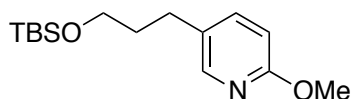


5-(4,4-Diethoxybutyl)-2-fluoropyridine (1-61). Prepared via General Procedure B using pyridinium salt **1-83**. The crude mixture was purified by silica gel chromatography (5% EtOAc/hexanes) to give **1-61** (run 1: 176 mg, 73%; run 2: 164 mg, 68%) as a yellow oil: ^1H NMR (600 MHz, CDCl_3) δ 8.02 (s, 1H), 7.59 (td, $J = 8.1, 2.5$ Hz, 1H), 6.84 (dd, $J = 8.3, 2.9$ Hz, 1H), 4.49 (t, $J = 5.3$ Hz, 1H), 3.63 (dq, $J = 9.4, 7.1$ Hz, 2H), 3.48 (dq, $J = 9.4, 7.1$ Hz, 2H), 2.63 (t, $J = 7.3$ Hz, 2H), 1.72 – 1.61

(m, 4H), 1.20 (t, $J = 7.1$ Hz, 6H); ^{13}C NMR (151 MHz, CDCl_3) δ 162.5 (d, $J_{\text{C-F}} = 236.8$ Hz), 147.2 (d, $J_{\text{C-F}} = 14.3$ Hz), 141.1 (d, $J_{\text{C-F}} = 7.6$ Hz), 135.2 (d, $J_{\text{C-F}} = 4.5$ Hz), 109.1 (d, $J_{\text{C-F}} = 37.4$ Hz), 102.8, 61.3, 33.2, 31.94, 31.93, 26.4, 15.5; ^{19}F NMR (565 MHz, CDCl_3) δ -72.3; FTIR (neat) 2975, 2872, 1593, 1485, 1249, 1126, 1065, 831 cm^{-1} ; HRMS (ESI+) $[\text{M}+\text{H}]^+$ calculated for $\text{C}_{13}\text{H}_{21}\text{FNO}_2$: 242.1551, found 242.1548.

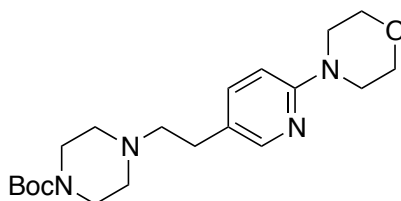


3-(3-((*tert*-Butyldimethylsilyloxy)propyl)quinoline (1-62). Prepared via General Procedure B using pyridinium salt **1-34**. The crude mixture was purified by silica gel chromatography (5% EtOAc/hexanes) to give **1-62** (run 1: 160 mg, 53%; run 2: 195 mg, 65%) as a yellow oil: ^1H NMR (600 MHz, CDCl_3) δ 8.80 (d, $J = 2.2$ Hz, 1H), 8.08 (d, $J = 8.4$ Hz, 1H), 7.94 (s, 1H), 7.76 (d, $J = 8.1$ Hz, 1H), 7.66 (t, $J = 7.2$ Hz, 1H), 7.52 (t, $J = 7.5$ Hz, 1H), 3.68 (t, $J = 6.1$ Hz, 2H), 2.92 – 2.87 (m, 2H), 1.96 – 1.90 (m, 2H), 0.92 (s, 9H), 0.07 (s, 6H); ^{13}C NMR (151 MHz, CDCl_3) δ 152.2, 146.9, 135.0, 134.5, 129.3, 128.7, 128.3, 127.4, 126.7, 62.0, 34.1, 29.6, 26.1, 18.5, -5.1; FTIR (neat) 2929, 2857, 1471, 1255, 1102, 836 cm^{-1} ; HRMS (ESI+) $[\text{M}+\text{H}]^+$ calculated for $\text{C}_{18}\text{H}_{28}\text{NOSi}$: 302.1935, found 302.1934.



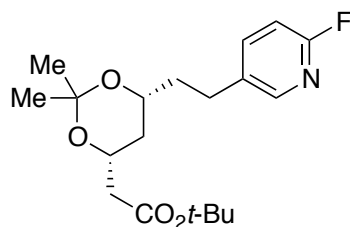
5-(3-((*tert*-butyldimethylsilyloxy)propyl)-2-methoxypyridine (1-63). Prepared via General Procedure B using pyridinium salt **1-34**. The crude mixture was purified by silica gel chromatography (gradient: 50→75% toluene/hexanes→100% toluene→5% EtOAc/toluene) to give **1-63** (run 1: 196 mg, 70%; run 2: 176 mg, 62%) as a yellow

oil: ^1H NMR (400 MHz, CDCl_3) δ 7.97 (d, $J = 2.1$ Hz, 1H), 7.41 (dd, $J = 8.5, 2.5$ Hz, 1H), 6.67 (d, $J = 8.4$ Hz, 1H), 3.91 (s, 3H), 3.62 (t, $J = 6.2$ Hz, 1H), 2.63 – 2.55 (m, 2H), 1.83 – 1.73 (m, 2H), 0.90 (s, 9H), 0.05 (s, 6H); ^{13}C NMR (101 MHz, CDCl_3) δ 162.7, 146.2, 139.2, 130.1, 110.5, 62.1, 53.4, 34.5, 28.3, 26.1, 18.5, –5.1; FTIR (neat) 2929, 2857, 1608, 1493, 1256, 1102, 835 cm^{-1} ; HRMS (ESI+) $[\text{M}+\text{H}]^+$ calculated for $\text{C}_{15}\text{H}_{27}\text{NO}_2\text{Si}$: 282.1884, found 282.1874.



***tert*-Butyl 4-(2-(6-morpholinopyridin-3-yl)ethyl)piperazine-1-carboxylate (1-64).**

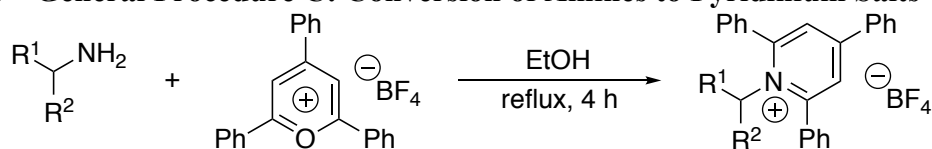
Prepared via General Procedure B using pyridinium salt **1-79**. The crude mixture was purified by silica gel chromatography (100% EtOAc) to give **1-64** (233 mg, 62%) as a yellow solid (mp 125–127 °C): ^1H NMR (400 MHz, CDCl_3) δ 8.05 (d, $J = 2.3$ Hz, 1H), 7.37 (dd, $J = 8.6, 2.4$ Hz, 1H), 6.59 (d, $J = 8.6$ Hz, 1H), 3.91 – 3.75 (m, 4H), 3.58 – 3.32 (m, 8H), 2.73 – 2.64 (m, 2H), 2.58 – 2.51 (m, 2H), 2.50 – 2.35 (m, 4H), 1.46 (s, 9H); ^{13}C NMR (101 MHz, CDCl_3) δ 158.6, 154.9, 147.8, 138.2, 125.3, 107.0, 79.8, 66.9, 60.4, 53.1, 46.0, 43.7 (br), 29.8, 28.6; FTIR (neat) 2971, 2860, 1694, 1499, 1265, 1126, 810 cm^{-1} ; HRMS (ESI+) $[\text{M}+\text{H}]^+$ calculated for $\text{C}_{20}\text{H}_{33}\text{N}_4\text{O}_3$: 377.2547, found 377.2544.



tert-Butyl 2-((4R,6R)-6-(2-(6-fluoropyridin-3-yl)ethyl)-2,2-dimethyl-1,3-dioxan-4-yl)acetate (1-65). Prepared via General Procedure B using pyridinium salt **1-84**. The crude mixture was purified by silica gel chromatography (5% EtOAc/hexanes) to give **1-65** (161 mg, 46%) as a dark pink oil: ^1H NMR (400 MHz, CDCl_3) δ 8.02 – 8.01 (m, 1H), 7.59 (td, $J = 8.1, 2.6$ Hz, 1H), 6.85 (dd, $J = 8.4, 2.9$ Hz, 1H), 4.21 (dtd, $J = 11.6, 6.6, 2.4$ Hz, 1H), 3.83 – 3.72 (m, 1H), 2.79 – 2.61 (m, 2H), 2.43 (dd, $J = 15.2, 6.9$ Hz, 1H), 2.29 (dd, $J = 15.2, 6.2$ Hz, 1H), 1.85 – 1.73 (m, 1H), 1.73 – 1.61 (m, 1H), 1.53 (dt, $J = 12.7, 2.5$ Hz, 1H), 1.43 (s, 9H), 1.41 (s, 3H), 1.38 (s, 3H), 1.27 – 1.17 (m, 1H); ^{13}C NMR (101 MHz, CDCl_3) δ 170.4, 162.4 (d, $J_{\text{C-F}} = 237.8$ Hz), 147.2 (d, $J_{\text{C-F}} = 14.2$ Hz), 141.3 (d, $J_{\text{C-F}} = 7.7$ Hz), 134.9 (d, $J_{\text{C-F}} = 4.5$ Hz), 109.2 (d, $J_{\text{C-F}} = 37.5$ Hz), 98.9, 80.8, 67.5, 66.3, 42.8, 37.6, 36.6, 30.2, 28.2, 27.4, 19.9; ^{19}F NMR (376 MHz, CDCl_3) δ -72.2; FTIR (neat) 2981, 2940, 1730, 1484, 1249, 1159, 951, 840 cm^{-1} ; HRMS (ESI+) $[\text{M}+\text{H}]^+$ calculated for $\text{C}_{19}\text{H}_{29}\text{FNO}_4$: 354.2075, found 354.2072.

1.4.3 Preparation of Pyridinium Salts

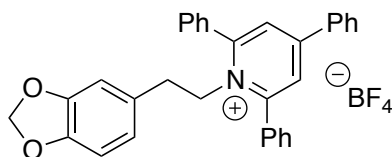
1.4.3.1 General Procedure C: Conversion of Amines to Pyridinium Salts



Primary amine (1.2 equiv) was added to a suspension of 2,4,6-triphenylpyrylium tetrafluoroborate (1.0 equiv) and EtOH (1.0 M) in a round-bottomed flask. The flask was fitted with a reflux condenser. The mixture was stirred and heated at reflux in an oil bath at 80–85 °C for 4 h. The mixture was then allowed to cool to room temperature. If product precipitation occurred during reflux, the solid was filtered, washed with EtOH (3 x 25 mL) and then Et₂O (3 x 25 mL), and dried under high vacuum. If product precipitation did not occur during reflux, the solution was diluted with Et₂O (2–3x volume of EtOH used) and vigorously stirred for 1 h to induce trituration. The resulting solid pyridinium salt was filtered and washed with Et₂O (3 x 25 mL). If the pyridinium salt failed to precipitate at this point, the flask containing the reaction mixture and Et₂O was sealed with parafilm and stored in a –27 °C freezer for 1–3 days (or until precipitation occurred). The cold mixture was quickly filtered and washed with Et₂O (3 x 25 mL) to give the corresponding analytically pure pyridinium salt. If the salt still did not precipitate, it was subjected to silica gel chromatography with acetone/DCM.

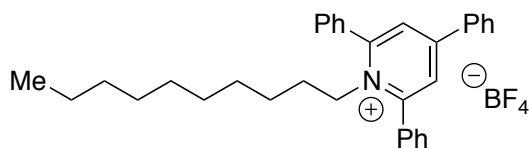
The corresponding amine hydrochloride salts can also be used (see synthesis of pyridinium salt **1-82**) using the following modified procedure: Et₃N (1.2 equiv) was added to a mixture of the corresponding alkyl ammonium hydrochloride salt (1.2 equiv) and EtOH (1.0 M). After stirring the mixture for 30 min at room temperature, 2,4,6-triphenylpyrylium tetrafluoroborate (1 equiv) was added. From this point

forward, the same procedure was followed as for alkyl amines described above; however prior to washing the solid product with EtOH and/or Et₂O, the mixture was washed with water (3 x 25 mL) to remove Et₃N·HCl.



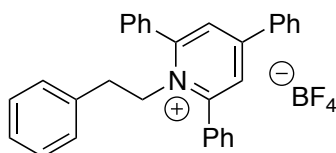
1-(2-(Benzo[*d*][1,3]dioxol-5-yl)ethyl)-2,4,6-triphenylpyridin-1-ium

tetrafluoroborate (1-39). Prepared via General Procedure C on a 7.5 mmol scale with commercially available 2-(benzo[*d*][1,3]dioxol-5-yl)ethanamine (9.0 mmol) to give **1-39** (3.64 g, 89%) as an off-white solid (mp 234–235 °C): ¹H NMR (600 MHz, CDCl₃) δ 7.91 (s, 2H), 7.83 – 7.77 (m, 6H), 7.68 – 7.62 (m, 6H), 7.59 – 7.55 (m, 1H), 7.55 – 7.51 (m, 2H), 6.48 (d, *J* = 7.9 Hz, 1H), 5.85 (s, 2H), 5.77 – 5.74 (m, 1H), 5.69 – 5.66 (m, 1H), 4.61 – 4.55 (m, 2H), 2.65 – 2.58 (m, 2H); ¹³C NMR (151 MHz, CDCl₃) δ 156.7, 156.3, 148.0, 146.9, 134.2, 132.9, 132.3, 131.4, 129.9, 129.6, 129.3, 128.9, 128.3, 126.9, 121.4, 108.61, 108.57, 101.2, 56.1, 35.7; ¹⁹F NMR (565 MHz, CDCl₃) δ –153.27 (minor, ¹¹BF₄), –153.32 (major, ¹⁰BF₄); FTIR (neat) 3060, 2903, 1624, 1489, 1053, 699 cm⁻¹; HRMS (ESI+) [M–BF₄]⁺ calculated for C₃₂H₂₆NO₄: 456.1958, found 456.1961.

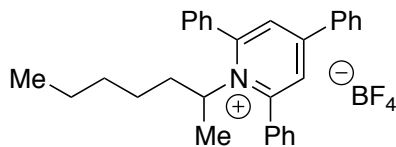


1-Decyl-2,4,6-triphenylpyridin-1-ium tetrafluoroborate (1-77). Prepared via General Procedure C on a 4.17 mmol scale with commercially available decan-1-amine (5.0 mmol) to give **1-77** (1.56 g, 58%) as a white solid (mp 98–100 °C): ¹H

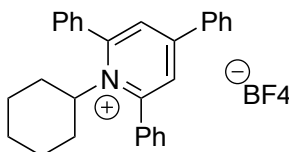
NMR (600 MHz, CDCl₃) δ 7.84 (s, 1H), 7.82 – 7.76 (m, 4H), 7.76 – 7.72 (m, 2H), 7.64 – 7.56 (m, 6H), 7.56 – 7.52 (m, 1H), 7.52 – 7.47 (m, 2H), 4.45 – 4.34 (m, 2H), 1.48 – 1.38 (m, 2H), 1.25 (p, $J = 7.1$ Hz, 2H), 1.20 – 1.08 (m, 4H), 1.05 – 0.97 (m, 2H), 0.95 – 0.81 (m, 5H), 0.79 – 0.69 (m, 4H); ¹³C NMR (151 MHz, CDCl₃) δ 156.6, 155.8, 134.2, 132.9, 132.1, 131.1, 129.8, 129.4, 129.2, 128.2, 126.8, 54.9, 31.9, 29.8, 29.3, 29.2, 29.0, 28.0, 26.1, 22.8, 14.2; ¹⁹F NMR (376 MHz, CDCl₃) δ –153.4 (minor, ¹¹BF₄), –153.5 (major, ¹⁰BF₄); FTIR (neat) 2926, 1625, 1566, 1056, 704 cm⁻¹; HRMS (ESI+) [M–BF₄]⁺ calculated for C₃₃H₃₈N: 448.2999, found 448.3004.



1-Phenethyl-2,4,6-triphenylpyridin-1-ium tetrafluoroborate (1-33). Prepared via General Procedure C on a 10 mmol scale with commercially available 2-phenylethanamine to give **1-33** (4.40 g, 88%) as a white solid (mp >260 °C): ¹H NMR (400 MHz, CDCl₃) δ 7.92 (s, 2H), 7.89 – 7.73 (m, 6H), 7.73 – 7.48 (m, 9H), 7.15 – 7.09 (m, 1H), 7.09 – 7.03 (m, 2H), 6.32 – 6.26 (m, 2H), 4.69 – 4.62 (m, 2H), 2.73 – 2.66 (m, 2H); ¹³C NMR (101 MHz, CDCl₃) δ 156.8, 156.2, 135.3, 134.1, 132.8, 132.3, 131.3, 129.9, 129.5, 129.3, 128.9, 128.33, 128.30, 127.4, 126.9, 56.0, 35.8; ¹⁹F NMR (376 MHz, CDCl₃) δ –153.26 (minor, ¹¹BF₄), –153.32 (major, ¹⁰BF₄); FTIR (neat) 3068, 1624, 1494, 1055, 699 cm⁻¹; HRMS (ESI+) [M–BF₄]⁺ calculated for C₃₁H₂₆N: 412.2060, found 412.2048.

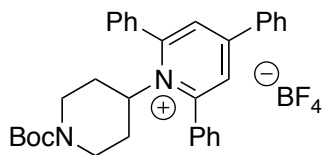


1-(Heptan-2-yl)-2,4,6-triphenylpyridin-1-ium tetrafluoroborate (1-78). Prepared via General Procedure C on a 5.0 mmol scale with commercially available heptan-2-amine to give **1-78** (1.21 g, 49%) as a pale yellow solid (mp 157–158 °C): ^1H NMR (400 MHz, CDCl_3) δ 87.99 – 7.44 (m, 17H), 4.96 – 4.84 (m, 1H), 1.84 – 1.70 (m, 1H), 1.49 – 1.36 (m, 4H), 1.20 – 1.08 (m, 2H), 1.07 – 0.93 (m, 3H), 0.89 – 0.73 (m, 4H); ^{13}C NMR (151 MHz, acetone- d_6) δ 158.7, 155.3, 135.1, 134.4, 133.3, 131.9, 130.6, 130.4, 129.7, 129.4, 128.6, 68.4, 37.2, 31.7, 26.7, 22.8, 22.5, 14.1; ^{19}F NMR (376 MHz, CDCl_3) δ –153.3 (minor, $^{11}\text{BF}_4$), –153.4 (major, $^{10}\text{BF}_4$); FTIR (neat) 2956, 1621, 1412, 1056, 765 cm^{-1} ; HRMS (ESI+) $[\text{M}-\text{BF}_4]^+$ calculated for $\text{C}_{30}\text{H}_{32}\text{N}$: 406.2529, found 406.2516.



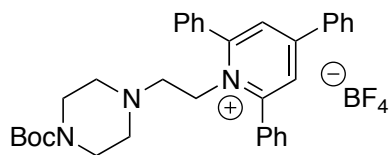
1-Cyclohexyl-2,4,6-triphenylpyridin-1-ium tetrafluoroborate (1-35). Prepared via General Procedure C on a 10 mmol scale with commercially available cyclohexanamine (12 mmol) to give **1-35** (2.99 g, 63%) as pale yellow solid (mp 181–182 °C): ^1H NMR (400 MHz, CDCl_3) δ 7.83 – 7.76 (m, 2H), 7.76 – 7.69 (m, 6H), 7.64 – 7.54 (m, 6H), 7.54 – 7.48 (m, 1H), 7.48 – 7.42 (m, 2H), 4.61 (tt, $J = 12.2, 2.9$ Hz, 1H), 2.12 (m, 2H), 1.64 – 1.40 (m, 4H), 1.34 (d, $J = 13.3$ Hz, 1H), 0.74 (m, 2H), 0.61 (tt, $J = 13.1, 3.5$ Hz, 1H); ^{13}C NMR (101 MHz, CDCl_3) δ 157.1, 155.1, 134.2, 134.1, 131.9, 130.9, 129.7, 129.4, 128.9, 128.4, 128.2, 72.0, 33.7, 26.6, 24.7; ^{19}F NMR (376 MHz, CDCl_3) δ –152.36 (minor, $^{11}\text{BF}_4$), –153.41 (major, $^{10}\text{BF}_4$); FTIR (neat) 3061,

2934, 1621, 1055, 705 cm^{-1} ; HRMS (ESI+) $[\text{M}-\text{BF}_4]^+$ calculated for $\text{C}_{29}\text{H}_{28}\text{N}$: 390.2216, found 390.2199.



1-(1-(*tert*-Butoxycarbonyl)piperidin-4-yl)-2,4,6-triphenylpyridin-1-ium

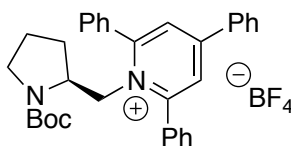
tetrafluoroborate (1-38). Prepared via General Procedure C on a 5.0 mmol scale with commercially available *tert*-butyl 4-aminopiperidine-1-carboxylate to give **1-38** (2.08 g, 72%) as an off-white solid (mp 165–166 °C): ^1H NMR (600 MHz, CDCl_3) δ 7.86 – 7.69 (m, 6H), 7.67 (d, $J = 7.2$ Hz, 2H), 7.64 – 7.52 (m, 6H), 7.52 – 7.46 (m, 1H), 7.46 – 7.36 (m, 2H), 4.82 – 4.69 (m, 1H), 4.04 – 3.75 (m, 2H), 2.27 – 1.95 (m, 4H), 1.74 – 1.51 (m, 2H), 1.30 (s, 9H); ^{13}C NMR (101 MHz, CDCl_3) δ 157.2, 155.5, 154.3, 134.0, 133.8, 132.1, 131.2, 129.7, 129.4, 129.1, 128.4, 128.3, 80.2, 70.0, 44.3 (br), 32.8 (br), 28.3; ^{19}F NMR (565 MHz, CDCl_3) δ –153.07 (minor, $^{11}\text{BF}_4$), –153.13 (major, $^{10}\text{BF}_4$); FTIR (neat) 2977, 1692, 1621, 1057, 706 cm^{-1} ; HRMS (ESI+) $[\text{M}-\text{BF}_4]^+$ calculated for $\text{C}_{33}\text{H}_{35}\text{N}_2\text{O}_2$: 491.2693, found 491.2686.



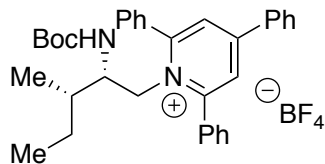
1-(2-(4-(*tert*-Butoxycarbonyl)piperazin-1-yl)ethyl)-2,4,6-triphenylpyridin-1-ium

tetrafluoroborate (1-79). Prepared via General Procedure C on a 1.67 mmol scale with commercially available *tert*-butyl 4-(2-aminoethyl)piperazine-1-carboxylate to give **1-79** (0.82 g, 81%) as an off-white solid (mp 133–135 °C): ^1H NMR (600 MHz,

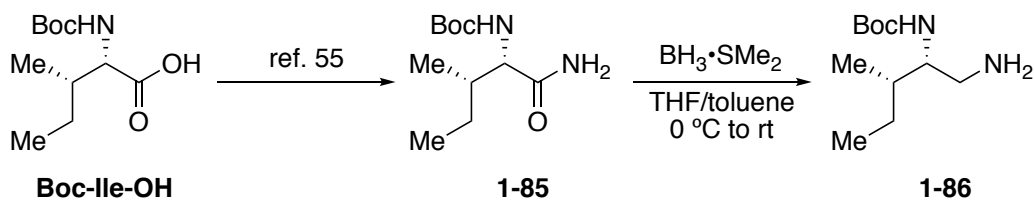
CDCl₃) δ 7.88 – 7.75 (m, 6H), 7.74 – 7.69 (m, 2H), 7.65 – 7.56 (m, 6H), 7.55 – 7.50 (m, 1H), 7.50 – 7.44 (m, 2H), 4.66 – 4.57 (m, 2H), 3.13 – 3.00 (m, 4H), 2.41 – 2.31 (m, 2H), 1.82 – 1.73 (m, br, 4H), 1.39 (s, 9H); ¹³C NMR (151 MHz, CDCl₃) δ 157.0, 156.1, 154.6, 134.1, 133.0, 132.3, 131.3, 129.8, 129.51, 129.46, 128.3, 126.8, 79.9, 56.4, 52.4, 51.8, 43.2 (br), 28.5; ¹⁹F NMR (565 MHz, CDCl₃) δ –152.96 (minor, ¹¹BF₄), –153.01 (major, ¹⁰BF₄); FTIR (neat) 2976, 1690, 1623, 1169, 1056, 703 cm⁻¹; HRMS (ESI+) [M–BF₄]⁺ calculated for C₃₄H₃₈N₃O₂: 520.2959, found 520.2950.



(S)-1-((1-(*tert*-Butoxycarbonyl)pyrrolidin-2-yl)methyl)-2,4,6-triphenylpyridin-1-ium tetrafluoroborate (1-37). Prepared via General Procedure C on a 4.17 mmol scale with commercially available (*S*)-*tert*-butyl 2-(aminomethyl)pyrrolidine-1-carboxylate to give **1-37** (2.08 g, 84%) as a white solid (mp 180–181 °C): ¹H NMR (600 MHz, CDCl₃) δ 8.31 – 7.84 (m, br, 3H), 7.80 (s, 2H), 7.72 (d, *J* = 7.4 Hz, 2H), 7.70 – 7.38 (m, 10H), 4.89 – 4.74 (m, 1H), 4.71 – 4.55 (m, 1H), 3.98 – 3.83 (m, 1H), 2.91 (td, *J* = 10.7, 6.5 Hz, 1H), 2.66 (t, *J* = 9.3 Hz, 1H), 1.58 – 1.43 (m, 2H), 1.32 (s, 9H), 1.28 – 1.22 (m, 1H), 0.88 – 0.74 (m, 1H); ¹³C NMR (151 MHz, CDCl₃) δ 158.0 (br), 155.6, 155.4, 134.3, 133.5, 132.1, 131.0, 130.4, 129.8, 129.4, 128.0, 126.3, 80.1, 57.5, 55.1, 47.3, 28.5, 28.4, 23.4; ¹⁹F NMR (565 MHz, CDCl₃) δ –153.08 (minor, ¹¹BF₄), –153.13 (major, ¹⁰BF₄); FTIR (neat) 2975, 1687, 1622, 1383, 1058, 704 cm⁻¹; HRMS (ESI+) [M–BF₄]⁺ calculated for C₃₃H₃₅N₂O₂: 491.2693, found 491.2672.



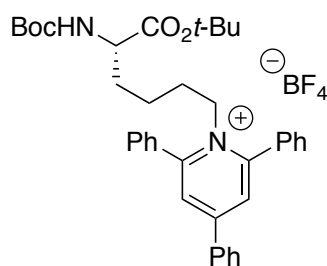
1-((2*S*,3*S*)-2-((*tert*-Butoxycarbonyl)amino)-3-methylpentyl)-2,4,6-triphenylpyridin-1-ium tetrafluoroborate (1-36). Prepared via General Procedure C; however a 1:1 ratio of 2,4,6-triphenylpyrylium tetrafluoroborate (1.9 mmol) to *tert*-butyl ((2*S*,3*S*)-1-amino-3-methylpentan-2-yl)carbamate **1-86** (see synthesis below) was used. After stirring for the 4 h period, the reaction mixture was concentrated. The crude residue was purified via column chromatography (5% acetone/CH₂Cl₂) to give pyridinium salt (**1-36**) (0.74 g, 66%) as a pale yellow solid (mp 107–109 °C): ¹H NMR (600 MHz, CDCl₃) δ 8.42 – 8.12 (m, 2H), 7.96 – 7.50 (m, 15H), 4.98 (dd, *J* = 14.6, 3.4 Hz, 1H), 4.59 (dd, *J* = 14.6, 11.7 Hz, 1H), 3.91 (d, *J* = 10.1 Hz, 1H), 3.61 – 3.54 (m, 1H), 1.31 (s, 9H), 1.09 – 1.01 (m, 1H), 0.85 – 0.72 (m, 2H), 0.49 (t, *J* = 7.4 Hz, 3H), 0.31 (d, *J* = 6.8 Hz, 3H); ¹³C NMR (151 MHz, CDCl₃) δ 158.3, 155.9, 155.1, 134.2, 133.5, 132.3, 131.2, 130.4, 129.9, 129.4, 128.0, 126.5, 80.3, 56.4, 53.6, 37.1, 28.5, 25.2, 14.2, 10.6; ¹⁹F NMR (565 MHz, CDCl₃) δ –153.0 (minor, ¹¹BF₄), –153.1 (major, ¹⁰BF₄); FTIR (neat) 3442, 3357, 2968, 1707, 1621, 1057, 703 cm⁻¹; HRMS (ESI+) [M–BF₄]⁺ calculated for C₃₄H₃₉N₂O₂: 507.3006, found 507.2995.



***tert*-Butyl ((2*S*,3*S*)-1-amino-3-methyl-1-oxopent-2-yl)carbamate (1-85).**

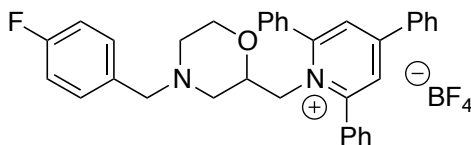
Prepared according to the literature procedure.⁵⁵

tert-Butyl ((2S,3S)-1-amino-3-methylpentan-2-yl)carbamate (1-86). Prepared according to a procedure adapted from the literature⁵⁶ (note: these reduction conditions are *unoptimized* for Boc-Ile-NH₂ **1-85**): In a round-bottomed flask, a solution of amide **1-85** (1.5 g, 6.5 mmol, 1.0 equiv) in THF (21.7 mL, 0.30 M) was cooled to 0 °C. BH₃·SMe₂ (2.0 M in toluene, 32.6 mL, 65.1 mmol, 10.0 equiv) was added portionwise (approx. 6-7 mL/min). After the addition was complete, the solution was stirred for 5 min at 0 °C, allowed to warm room temperature, and stirred for 24 h. The solution was then concentrated, and MeOH (36 mL, 5.6 mL/mmol) was slowly added (CAUTION: add slowly to prevent violent evolution of gas!). The solution was stirred briefly and then concentrated. This dilution/concentration protocol was repeated two more times. The resulting residue was then dissolved in Et₂O (50 mL) and extracted with HCl (1 N, 4 x 50 mL). The combined aqueous layers were washed with Et₂O (4 x 50 mL) and then basified with KOH (4 N) to pH \geq 12. The basic aqueous layer was then extracted with Et₂O (4 x 100 mL). The combined organic layers were washed with sat. NaCl (100 mL), dried (MgSO₄), filtered through a cotton plug, and concentrated to afford amine **1-86** (0.464 g, 33%) as a white solid which was used without further purification.



(S)-1-(6-(tert-Butoxy)-5-((tert-butoxycarbonyl)amino)-6-oxohexyl)-2,4,6-triphenylpyridin-1-ium tetrafluoroborate (1-80). Prepared via General Procedure C

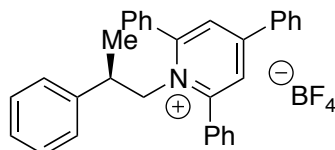
on a 4.91 mmol scale with Boc-Lys-O^tBu.⁵⁷ Attempts to triturate the product failed; the crude residue was purified via column chromatography (5→20% acetone/CH₂Cl₂) to give pyridinium salt **1-80** as a tan solid (mp 96–100 °C): ¹H NMR (600 MHz, CDCl₃) δ 7.91 (s, 2H), 7.85 – 7.77 (m, 6H), 7.67 – 7.61 (m, 6H), 7.61 – 7.57 (m, 1H), 7.57 – 7.53 (m, 2H), 4.84 (d, br, *J* = 7.7 Hz, 1H), 4.49 – 4.38 (m, 2H), 3.90 – 3.78 (m, 1H), 1.55 – 1.46 (m, 2H), 1.42 (s, 9H), 1.40 (s, 9H), 1.33 – 1.26 (m, 1H), 1.11 – 1.03 (m, 1H), 0.94 – 0.76 (m, 1H); ¹³C NMR (151 MHz, CDCl₃) δ 171.3, 156.6, 156.0, 155.4, 134.2, 132.8, 132.2, 131.2, 129.8, 129.5, 129.2, 128.3, 126.9, 82.2, 79.9, 54.5, 53.5, 31.8, 29.5, 28.4, 28.1, 22.1; ¹⁹F NMR (376 MHz, CDCl₃) δ –153.3 (minor, ¹¹BF₄), –153.4 (major, ¹⁰BF₄); FTIR (neat) 3374, 2978, 1711, 1624, 1155, 1057, 704 cm⁻¹; HRMS (ESI+) [M–BF₄]⁺ calculated for C₃₈H₄₅N₂O₄: 593.3374, found 593.3366.



1-((4-(4-Fluorobenzyl)morpholin-2-yl)methyl)-2,4,6-triphenylpyridin-1-ium

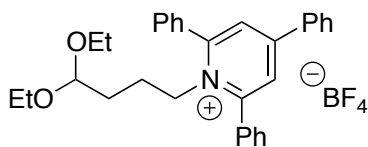
tetrafluoroborate (1-81). Prepared via General Procedure C (refluxed for 22 h) on a 5 mmol scale with commercially available (4-(4-fluorobenzyl)morpholin-2-yl)methanamine (6.0 mmol) to give **1-81** (2.67 g, 89%) as a tan solid (mp 170–172 °C): ¹H NMR (400 MHz, CDCl₃) δ 7.89 (s, 2H), 7.87 – 7.67 (m, 6H), 7.64 – 7.51 (m, 9H), 7.09 – 7.03 (m, 2H), 6.98 – 6.91 (m, 2H), 4.73 (dd, *J* = 14.9, 4.1 Hz, 1H), 4.55 (dd, *J* = 14.9, 9.7 Hz, 1H), 3.67 – 3.58 (m, 1H), 3.33 – 3.16 (m, 4H), 2.47 – 2.39 (m, 1H), 2.13 – 2.04 (m, 1H), 1.89 (td, *J* = 11.4, 3.3 Hz, 1H), 1.33 – 1.24 (m, 1H); ¹³C NMR (151 MHz, CDCl₃) δ 162.2 (d, *J*_{C-F} = 245.7 Hz), 157.8, 155.7, 134.0, 133.2, 132.6, 132.4, 131.1, 130.7 (d, *J*_{C-F} = 7.9 Hz), 129.9, 129.6, 129.3, 128.2, 126.3, 115.2

(d, $J_{C-F} = 21.4$ Hz), 72.5, 66.6, 61.9, 56.3, 55.6, 52.2; ^{19}F NMR (376 MHz, CDCl_3) δ – 115.3, –153.2 (minor, $^{11}\text{BF}_4$), –153.3 (major, $^{10}\text{BF}_4$); FTIR (neat) 3065, 2815, 1622, 1058, 703 cm^{-1} ; HRMS (ESI+) $[\text{M}-\text{BF}_4]^+$ calculated for $\text{C}_{35}\text{H}_{32}\text{FN}_2\text{O}$: 515.2493, found 515.2486.



(*R*)-2,4,6-Triphenyl-1-(2-phenylpropyl)pyridin-1-ium tetrafluoroborate (1-82).

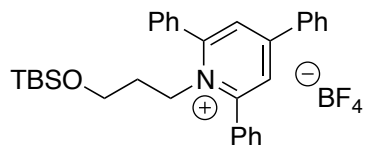
Prepared via General Procedure C on a 5.0 mmol scale with commercially available (*R*)-2-phenylpropan-1-aminium chloride to give **1-82** (2.27 g, 88%) as a white solid (mp 206–207 °C): ^1H NMR (400 MHz, CDCl_3) δ 8.44 – 7.30 (m, 17H), 7.23 – 7.16 (m, 1H), 7.08 (t, $J = 7.5$ Hz, 2H), 6.49 – 6.37 (m, 2H), 5.03 (dd, $J = 14.3, 5.5$ Hz, 1H), 4.81 (dd, $J = 14.3, 9.4$ Hz, 1H), 2.80 – 2.63 (m, 1H), 0.82 (d, $J = 7.0$ Hz, 3H); ^{13}C NMR (101 MHz, CDCl_3) δ 157.6, 155.8, 140.4, 133.8, 133.2, 132.5, 131.2, 129.9, 129.65, 129.59, 129.1, 128.2, 127.7, 126.9, 126.6, 61.3, 39.8, 17.9; ^{19}F NMR (565 MHz, CDCl_3) δ –153.1 (minor, $^{11}\text{BF}_4$), –153.2 (major, $^{10}\text{BF}_4$); FTIR (neat) 3062, 1620, 1562, 1057, 702 cm^{-1} ; HRMS (ESI+) $[\text{M}-\text{BF}_4]^+$ calculated for $\text{C}_{32}\text{H}_{28}\text{N}$: 426.2216, found 426.2220.



1-(4,4-Diethoxybutyl)-2,4,6-triphenylpyridin-1-ium tetrafluoroborate (1-83).

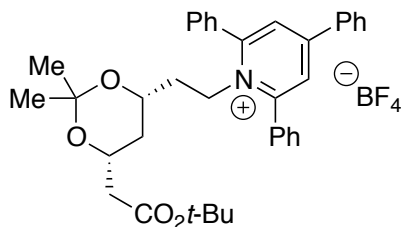
Prepared via General Procedure C on a 4.0 mmol scale with commercially available 4,4-diethoxybutan-1-amine (4.8 mmol) to give **1-83** (1.86 g, 86%) as a fluffy white

solid (mp 139–140 °C): ^1H NMR (600 MHz, CDCl_3) δ 7.87 (s, 2H), 7.83 – 7.78 (m, 4H), 7.78 – 7.74 (m, 2H), 7.63 – 7.58 (m, 6H), 7.58 – 7.54 (m, 1H), 7.54 – 7.48 (m, 2H), 4.49 – 4.42 (m, 2H), 4.01 (t, $J = 5.2$ Hz, 1H), 3.36 (dq, $J = 9.0, 7.0$ Hz, 2H), 3.18 (dq, $J = 9.1, 7.0$ Hz, 2H), 1.60 – 1.52 (m, 2H), 1.10 – 0.98 (m, 8H); ^{13}C NMR (101 MHz, CDCl_3) δ 156.5, 155.8, 134.0, 132.8, 132.1, 131.0, 129.7, 129.3, 129.0, 128.1, 126.8, 101.5, 61.6, 54.7, 30.5, 25.1, 15.2; ^{19}F NMR (376 MHz, CDCl_3) δ –153.4 (minor, $^{11}\text{BF}_4$), –153.5 (major, $^{10}\text{BF}_4$); FTIR (neat) 2975, 2880, 1624, 1566, 1056, 703 cm^{-1} ; HRMS (ESI+) $[\text{M}-\text{BF}_4]^+$ calculated for $\text{C}_{31}\text{H}_{34}\text{NO}_2$: 452.2584, found 452.2589.

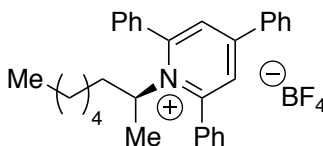


1-(3-((*tert*-Butyldimethylsilyloxy)propyl)-2,4,6-triphenylpyridin-1-ium

tetrafluoroborate (1-34). Prepared via General Procedure C on a 1.67 mmol scale with 3-((*tert*-butyldimethylsilyloxy)propan-1-amine⁵⁸ (2.0 mmol) to give **1-34** (0.73 g, 77%) as a white solid (mp 170–171 °C): ^1H NMR (600 MHz, CDCl_3) δ 7.89 (s, 2H), 7.84 – 7.75 (m, 6H), 7.65 – 7.58 (m, 6H), 7.58 – 7.49 (m, 3H), 4.58 – 4.52 (m, 2H), 3.13 (t, $J = 5.6$ Hz, 2H), 1.74 – 1.65 (m, 2H), 0.67 (s, 9H), –0.21 (s, 6H); ^{13}C NMR (101 MHz, CDCl_3) δ 156.7, 156.0, 134.3, 133.0, 132.1, 131.2, 129.8, 129.5, 129.1, 128.3, 127.1, 60.1, 53.4, 32.8, 25.9, 18.2, –5.5; ^{19}F NMR (376 MHz, CDCl_3) δ –153.4 (minor, $^{11}\text{BF}_4$), –153.5 (major, $^{10}\text{BF}_4$); FTIR (neat) 2954, 2855, 1622, 1054, 837, 771, 703 cm^{-1} ; HRMS (ESI+) $[\text{M}-\text{BF}_4]^+$ calculated for $\text{C}_{32}\text{H}_{38}\text{NO}_4$: 480.2717, found 480.2716.

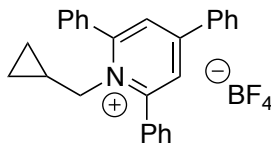


1-(2-((4R,6R)-6-(2-(*tert*-Butoxy)-2-oxoethyl)-2,2-dimethyl-1,3-dioxan-4-yl)ethyl)-2,4,6-triphenylpyridin-1-ium tetrafluoroborate (1-84). Prepared via General Procedure C on a 5.0 mmol scale with commercially available *tert*-Butyl 2-((4R,6R)-6-(2-aminoethyl)-2,2-dimethyl-1,3-dioxan-4-yl)acetate (6.0 mmol) to give **1-84** (1.44 g, 44%) as a white solid (mp 128–130 °C): ^1H NMR (600 MHz, CDCl_3) δ 7.90 (s, 2H), 7.87 – 7.72 (m, 6H), 7.70 – 7.60 (m, 6H), 7.60 – 7.56 (m, 1H), 7.56 – 7.50 (m, 2H), 4.71 – 4.63 (m, 1H), 4.55 – 4.47 (m, 1H), 4.02 – 3.96 (m, 1H), 3.33 – 3.27 (m, 1H), 2.26 (dd, $J = 15.3, 7.2$ Hz, 1H), 2.14 (dd, $J = 15.3, 5.9$ Hz, 1H), 1.65 – 1.54 (m, 2H), 1.42 (s, 9H), 1.16 (s, 3H), 1.13 (dt, $J = 12.6, 2.2$ Hz, 1H), 1.03 (s, 3H), 0.72 (q, $J = 11.7$ Hz, 1H); ^{13}C NMR (101 MHz, CDCl_3) δ 170.1, 156.9, 156.0, 134.2, 132.9, 132.2, 131.2, 129.8, 129.5, 129.2, 128.2, 126.9, 98.6, 80.9, 66.1, 65.7, 51.9, 42.4, 35.9, 35.4, 29.9, 28.2, 19.6; ^{19}F NMR (376 MHz, CDCl_3) δ –153.3 (minor, $^{11}\text{BF}_4$), –153.4 (major, $^{10}\text{BF}_4$); FTIR (neat) 2990, 1726, 1624, 1160, 1057, 703 cm^{-1} ; HRMS (ESI+) $[\text{M}-\text{BF}_4]^+$ calculated for $\text{C}_{37}\text{H}_{42}\text{NO}_4$: 564.3108, found 564.3099.



(S)-1-(Octan-2-yl)-2,4,6-triphenylpyridin-1-ium tetrafluoroborate (1-71). Prepared via General Procedure C; however a 1:1 ratio of 2,4,6-triphenylpyrylium tetrafluoroborate (5.0 mmol) to commercially available (*S*)-octan-2-amine was used.

After refluxing overnight with stirring, the reaction mixture was concentrated. The crude residue was purified via silica gel chromatography (10% acetone/CH₂Cl₂) to give **1-71** (1.55 g, 61%) as an orange solid (mp 67–69 °C): ¹H NMR (400 MHz, CDCl₃) δ 7.93 – 7.38 (m, 17H), 4.94 – 4.82 (m, 1H), 1.82 – 1.71 (m, 1H), 1.48 – 1.32 (m, 4H), 1.21 – 1.11 (m, 2H), 1.11 – 0.91 (m, 5H), 0.88 – 0.72 (m, 4H); ¹³C NMR (101 MHz, CDCl₃) δ 157.2 (br), 155.1, 134.0, 133.9, 132.0, 131.0, 129.7, 129.3 (br), 128.9 (br), 128.8 (br), 128.4, 67.1, 36.9, 31.5, 28.5, 26.6, 22.5, 21.7, 14.1; ¹⁹F NMR (376 MHz, CDCl₃) δ –153.25 (minor, ¹¹BF₄), –153.31 (major, ¹⁰BF₄); FTIR (neat) 2927, 2857, 1621, 1564, 1055, 765, 703 cm⁻¹; HRMS (ESI+) [M–BF₄]⁺ calculated for C₃₁H₃₄N: 420.2686, found 420.2685.

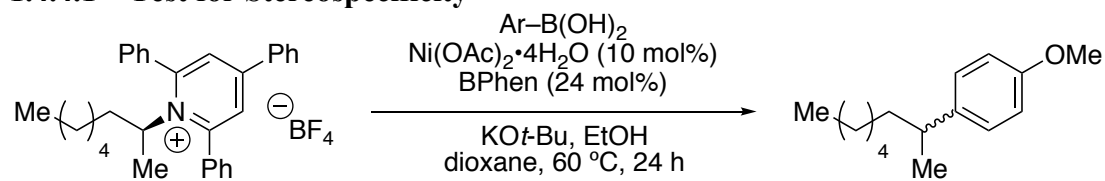


1-(cyclopropylmethyl)-2,4,6-triphenylpyridin-1-ium tetrafluoroborate (1-73).

Prepared via General Procedure C on a 5.0 mmol scale with commercially available cyclopropylmethanamine (6.0 mmol) to give **1-73** (1.64 g, 71%) as a white solid (mp 178–180 °C): ¹H NMR (400 MHz, CDCl₃) δ 7.86 (s, 2H), 7.84 – 7.78 (m, 4H), 7.78 – 7.71 (m, 2H), 7.66 – 7.56 (m, 6H), 7.56 – 7.45 (m, 3H), 4.51 (d, *J* = 6.8 Hz, 2H), 0.72 – 0.61 (m, 1H), 0.34 – 0.20 (m, 2H), –0.38 (q, *J* = 5.1 Hz, 2H); ¹³C NMR (101 MHz, CDCl₃) δ 157.0, 155.7, 133.9, 133.3, 132.3, 131.2, 129.9, 129.54, 129.46, 128.2, 126.8, 59.2, 10.8, 5.1; ¹⁹F NMR (376 MHz, CDCl₃) δ –153.2 (minor, ¹¹BF₄), –153.3 (major, ¹⁰BF₄); FTIR (neat) 3064, 1621, 1566, 1057, 703 cm⁻¹; HRMS (ESI+) [M–BF₄]⁺ calculated for C₂₇H₂₄N: 362.1903, found 362.1898.

1.4.4 Mechanistic Experiments

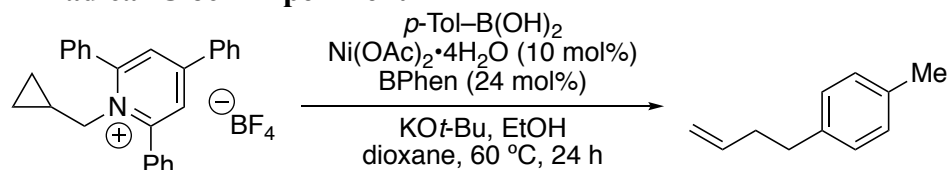
1.4.4.1 Test for Stereospecificity



In a N_2 -filled glovebox: To an oven-dried 1-dram vial was added $\text{Ni(OAc)}_2 \cdot 4\text{H}_2\text{O}$ (2.5 mg, 0.01 mmol, 10 mol %) and BPhen (8.0 mg, 0.024 mmol, 24 mol %). To a separate oven-dried 1-dram vial was added $\text{KO}t\text{-Bu}$ (38 mg, 0.17 mmol, 3.4 equiv), 4-methoxyphenylboronic acid (46 mg, 0.30 mmol, 3.0 equiv), and pyridinium salt **1-71** (51 mg, 0.10 mmol, 1.0 equiv). Dioxane (250 μL) was added to each vial. Each vial was then equipped with a micro stir bar, capped with a pierceable Teflon-coated cap, and removed from the glovebox. To the vial containing the boronic acid, $\text{KO}t\text{-Bu}$, and pyridinium salt **1-71**, was added EtOH (29 μL) via a N_2 -purged syringe. Both mixtures were stirred for 1 h at rt. The catalyst mixture was then transferred to the “activated-boronate” and pyridinium salt mixture via a N_2 -purged syringe. Dioxane (500 μL total) was used to ensure complete transfer of the catalyst mixture and bring the total concentration of the reaction to 0.1 M. The resulting reaction mixture was stirred vigorously at $60\text{ }^\circ\text{C}$ for 24 h. The mixture was diluted with Et_2O (approx. 1.5 mL) and filtered through a short plug of silica gel. The filter cake was washed with Et_2O (5 x 1.5 mL), and the resulting solution was concentrated. The yield of the crude product **1-72** was determined to be 54% by $^1\text{H-NMR}$ analysis with 1,3,5-trimethoxybenzene as an internal standard. A small sample of the product was purified via preparatory thin-layer chromatography (10% toluene/hexanes), and the enantiomeric excess was determined to be 0% by chiral HPLC analysis.

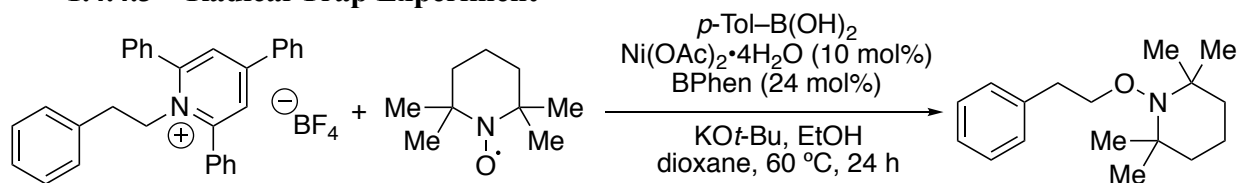
(CHIRALPAK IF, 0.2 mL/min, 100% hexanes, $\lambda=254$ nm); t_R (enantiomer A) = 31.32 min, t_R (enantiomer B) = 32.85 min.

1.4.4.2 Radical-Clock Experiment



In a N₂-filled glovebox: To an oven-dried 1-dram vial was added Ni(OAc)₂·4H₂O (2.5 mg, 0.01 mmol, 10 mol %) and BPhen (8.0 mg, 0.024 mmol, 24 mol %). To a separate oven-dried 1-dram vial was added KO*t*-Bu (38 mg, 0.17 mmol, 3.4 equiv), 4-methylphenylboronic acid (41 mg, 0.30 mmol, 3.0 equiv) and pyridinium salt **1-73** (45 mg, 0.10 mmol, 1.0 equiv). Dioxane (250 μL) was added to each vial. Each vial was then equipped with a micro stir bar, capped with a pierceable Teflon-coated cap, and removed from the glovebox. To the vial containing the boronic acid, KO*t*-Bu, and pyridinium salt **1-73**, was added EtOH (29 μL) via a N₂-purged syringe. Both mixtures were stirred for 1 h at rt. The catalyst mixture was then transferred to the “activated-boronate” and pyridinium salt mixture via a N₂-purged syringe. Dioxane (500 μL total) was used to insure complete transfer of the catalyst mixture and bring the total concentration of the reaction to 0.1 M. The resulting reaction mixture was stirred vigorously at 60 °C for 24 h. The mixture was then diluted with Et₂O (approx. 1.5 mL) and filtered through a short plug of silica gel. The filter cake was washed with Et₂O (5 x 1.5 mL), and the resulting solution was concentrated. The yield of the crude ring-opened product **1-74** was determined to be 33% by ¹H-NMR analysis with 1,3,5-trimethoxybenzene as an internal standard.

1.4.4.3 Radical Trap Experiment



In a N_2 -filled glovebox: To an oven-dried 1-dram vial was added $\text{Ni(OAc)}_2 \cdot 4\text{H}_2\text{O}$ (2.5 mg, 0.01 mmol, 10 mol %) and BPhen (8.0 mg, 0.024 mmol, 24 mol %). To a separate oven-dried 1-dram vial was added $\text{KO}t\text{-Bu}$ (38 mg, 0.17 mmol, 3.4 equiv), 4-methylphenylboronic acid (41 mg, 0.30 mmol, 3.0 equiv), 2,2,6,6-tetramethylpiperidine-*N*-oxyl (TEMPO; 31 mg, 0.20 mmol, 2.0 equiv), and pyridinium salt **1-33** (50 mg, 0.10 mmol, 1.0 equiv). Dioxane (250 μL) was added to each vial. Each vial was then equipped with a micro stir bar, capped with a pierceable Teflon-coated cap, and removed from the glovebox. To the vial containing the boronic acid, $\text{KO}t\text{-Bu}$, TEMPO, and pyridinium salt **1-33**, was added EtOH (30 μL) via a N_2 -purged syringe. Both mixtures were stirred for 1 h at rt. After pre-stirring was complete, the catalyst mixture was transferred to the “activated-boronate” and TEMPO/pyridinium salt mixture via a N_2 -purged syringe. Dioxane (500 μL total) was used to ensure complete transfer of the catalyst mixture and bring the total concentration of the reaction to 0.1 M. The resulting reaction mixture was heated to $60\text{ }^\circ\text{C}$ and stirred vigorously for 24 h. The mixture was diluted with Et_2O (approx. 1.5 mL) and filtered through a short plug of silica gel. The filter cake was washed with Et_2O (5 x 1.5 mL), and the resulting solution was concentrated. 1,3,5-trimethoxybenzene (7.2 mg, 0.043 mmol, 0.43 equiv) was added as an internal standard. The yield of known TEMPO adduct **1-76**⁵⁹ was determined to be 20% by analysis of the $^1\text{H-NMR}$ spectrum of the crude reaction mixture. No cross-coupled product was observed.

REFERENCES

1. Ruiz-Castillo, P.; Buchwald, S. L., *Chemical Reviews* **2016**, *116*, 12564-12649.
2. Blakey, S. B.; MacMillan, D. W. C., *J. Am. Chem. Soc.* **2003**, *125*, 6046-6047.
3. Tobisu, M.; Nakamura, K.; Chatani, N., *J. Am. Chem. Soc.* **2014**, *136*, 5587-5590.
4. Buszek, K. R.; Brown, N., *Org. Lett.* **2007**, *9*, 707-710.
5. Hie, L.; Baker, E. L.; Anthony, S. M.; Desrosiers, J.-N.; Senanayake, C.; Garg, N. K., *Angewandte Chemie International Edition* **2016**, *55*, 15129-15132.
6. Meng, G.; Szostak, M., *Org. Lett.* **2016**, *18*, 796-799.
7. Shi, S.; Meng, G.; Szostak, M., *Angewandte Chemie International Edition* **2016**, *55*, 6959-6963.
8. Simmons, B. J.; Weires, N. A.; Dander, J. E.; Garg, N. K., *ACS Catalysis* **2016**, *6*, 3176-3179.
9. Weires, N. A.; Baker, E. L.; Garg, N. K., *Nature Chemistry* **2015**, *8*, 75.
10. Maity, P.; Shacklady-McAtee, D. M.; Yap, G. P. A.; Sirianni, E. R.; Watson, M. P., *J. Am. Chem. Soc.* **2013**, *135*, 280-285.
11. Shacklady-McAtee, D. M.; Roberts, K. M.; Basch, C. H.; Song, Y.-G.; Watson, M. P., *Tetrahedron* **2014**, *70*, 4257-4263.
12. Basch, C. H.; Cobb, K. M.; Watson, M. P., *Org. Lett.* **2016**, *18*, 136-139.
13. Li, M.-B.; Tang, X.-L.; Tian, S.-K., *Adv. Synth. Catal.* **2011**, *353*, 1980-1984.
14. Yoon, S.; Hong, M. C.; Rhee, H., *The Journal of Organic Chemistry* **2014**, *79*, 4206-4211.
15. Li, M.-B.; Wang, Y.; Tian, S.-K., *Angewandte Chemie International Edition* **2012**, *51*, 2968-2971.

16. Peng, C.; Wang, Y.; Wang, J., *J. Am. Chem. Soc.* **2008**, *130*, 1566-1567.
17. Wu, G.; Deng, Y.; Wu, C.; Zhang, Y.; Wang, J., *Angewandte Chemie International Edition* **2014**, *53*, 10510-10514.
18. Huang, C.-Y.; Doyle, A. G., *J. Am. Chem. Soc.* **2012**, *134*, 9541-9544.
19. Jensen, K. L.; Standley, E. A.; Jamison, T. F., *J. Am. Chem. Soc.* **2014**, *136*, 11145-11152.
20. Duda, M. L.; Michael, F. E., *J. Am. Chem. Soc.* **2013**, *135*, 18347-18349.
21. Zhou, J.; Fu, G. C., *J. Am. Chem. Soc.* **2003**, *125*, 14726-14727.
22. Jones, G. D.; Martin, J. L.; McFarland, C.; Allen, O. R.; Hall, R. E.; Haley, A. D.; Brandon, R. J.; Konovalova, T.; Desrochers, P. J.; Pulay, P.; Vicic, D. A., *J. Am. Chem. Soc.* **2006**, *128*, 13175-13183.
23. González-Bobes, F.; Fu, G. C., *J. Am. Chem. Soc.* **2006**, *128*, 5360-5361.
24. Saito, B.; Fu, G. C., *J. Am. Chem. Soc.* **2007**, *129*, 9602-9603.
25. Dudnik, A. S.; Fu, G. C., *J. Am. Chem. Soc.* **2012**, *134*, 10693-10697.
26. Zultanski, S. L.; Fu, G. C., *J. Am. Chem. Soc.* **2013**, *135*, 624-627.
27. Zhang, X.; MacMillan, D. W. C., *J. Am. Chem. Soc.* **2016**, *138*, 13862-13865.
28. Zuo, Z.; Ahneman, D. T.; Chu, L.; Terrett, J. A.; Doyle, A. G.; MacMillan, D. W. C., *Science* **2014**, *345*, 437.
29. Tellis, J. C.; Primer, D. N.; Molander, G. A., *Science* **2014**, *345*, 433.
30. Jouffroy, M.; Primer, D. N.; Molander, G. A., *J. Am. Chem. Soc.* **2016**, *138*, 475-478.
31. Gutiérrez-Bonet, Á.; Tellis, J. C.; Matsui, J. K.; Vara, B. A.; Molander, G. A., *ACS Catalysis* **2016**, *6*, 8004-8008.
32. Cornella, J.; Edwards, J. T.; Qin, T.; Kawamura, S.; Wang, J.; Pan, C.-M.; Gianatassio, R.; Schmidt, M.; Eastgate, M. D.; Baran, P. S., *J. Am. Chem. Soc.* **2016**, *138*, 2174-2177.
33. Huihui, K. M. M.; Caputo, J. A.; Melchor, Z.; Olivares, A. M.; Spiewak, A. M.; Johnson, K. A.; DiBenedetto, T. A.; Kim, S.; Ackerman, L. K. G.; Weix, D. J., *J. Am. Chem. Soc.* **2016**, *138*, 5016-5019.

34. Qin, T.; Cornella, J.; Li, C.; Malins, L. R.; Edwards, J. T.; Kawamura, S.; Maxwell, B. D.; Eastgate, M. D.; Baran, P. S., *Science* **2016**, 352, 801.
35. Toriyama, F.; Cornella, J.; Wimmer, L.; Chen, T.-G.; Dixon, D. D.; Creech, G.; Baran, P. S., *J. Am. Chem. Soc.* **2016**, 138, 11132-11135.
36. Wang, J.; Qin, T.; Chen, T.-G.; Wimmer, L.; Edwards, J. T.; Cornella, J.; Vokits, B.; Shaw, S. A.; Baran, P. S., *Angewandte Chemie International Edition* **2016**, 55, 9676-9679.
37. Bapat, J. B.; Blade, R. J.; Boulton, A. J.; Epszajn, J.; Katritzky, A. R.; Lewis, J.; Molina-Buendia, P.; Nie, P.-L.; Ramsden, C. A., *Tetrahedron Letters* **1976**, 17, 2691-2694.
38. Katritzky, A. R.; Marson, C. M., *Angewandte Chemie International Edition in English* **1984**, 23, 420-429.
39. Kato, S.; Morie, T.; Yoshida, N., *CHEMICAL & PHARMACEUTICAL BULLETIN* **1995**, 43, 699-702.
40. Roth, B. D., US4681893A, 1987/07/21/, 1987.
41. Said, S. A.; Fiksdahl, A., *Tetrahedron: Asymmetry* **2001**, 12, 1947-1951.
42. Katritzky, A. R.; De Ville, G.; Patel, R. C., *Tetrahedron* **1981**, 37, 25-30.
43. Álvaro, M.; Formentín, P.; García, H.; Palomares, E.; Sabater, M. J., *The Journal of Organic Chemistry* **2002**, 67, 5184-5189.
44. Greulich, T. W.; Daniliuc, C. G.; Studer, A., *Org. Lett.* **2015**, 17, 254-257.
45. Biswas, S.; Weix, D. J., *J. Am. Chem. Soc.* **2013**, 135, 16192-16197.
46. Basch, C. H.; Liao, J.; Xu, J.; Pian, J. J.; Watson, M. P., *J. Am. Chem. Soc.* **2017**, 139, 5313-5316.
47. Pangborn, A. B.; Giardello, M. A.; Grubbs, R. H.; Rosen, R. K.; Timmers, F. J., *Organometallics* **1996**, 15, 1518-1520.
48. Ghorai, S. K.; Jin, M.; Hatakeyama, T.; Nakamura, M., *Org. Lett.* **2012**, 14, 1066-1069.
49. Jin, L.; Zhao, Y.; Zhu, L.; Zhang, H.; Lei, A., *Adv. Synth. Catal.* **2009**, 351, 630-634.

50. St. Denis, J. D.; Scully, C. C. G.; Lee, C. F.; Yudin, A. K., *Org. Lett.* **2014**, *16*, 1338-1341.
51. Krasovskiy, A.; Duplais, C.; Lipshutz, B. H., *J. Am. Chem. Soc.* **2009**, *131*, 15592-15593.
52. Patel, N. R.; Molander, G. A., *The Journal of Organic Chemistry* **2016**, *81*, 7271-7275.
53. Godt, A.; Ünsal, Ö.; Roos, M., *The Journal of Organic Chemistry* **2000**, *65*, 2837-2842.
54. Molander, G. A.; Argintaru, O. A.; Aron, I.; Dreher, S. D., *Org. Lett.* **2010**, *12*, 5783-5785.
55. Toumi, M.; Couty, F.; Evano, G., *The Journal of Organic Chemistry* **2008**, *73*, 1270-1281.
56. Bagley, M. C.; Dwyer, J. E.; Molina, M. D. B.; Rand, A. W.; Rand, H. L.; Tomkinson, N. C. O., *Organic & Biomolecular Chemistry* **2015**, *13*, 6814-6824.
57. Fekner, T.; Li, X.; Lee, M. M.; Chan, M. K., *Angewandte Chemie International Edition* **2009**, *48*, 1633-1635.
58. Padwa, A.; Rashatasakhon, P.; Ozdemir, A. D.; Willis, J., *The Journal of Organic Chemistry* **2005**, *70*, 519-528.
59. Thuy-Boun, P. S.; Villa, G.; Dang, D.; Richardson, P.; Su, S.; Yu, J.-Q., *J. Am. Chem. Soc.* **2013**, *135*, 17508-17513.

Chapter 2

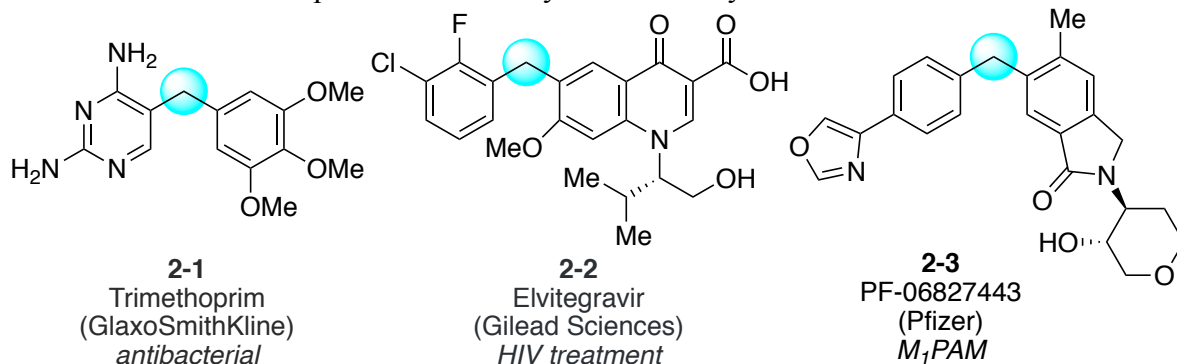
SUZUKI–MIYAURA CROSS-COUPLED OF BENZYLIC PYRIDINIUM SALTS WITH ARYLBORONIC ACIDS

Work described here has already been published (Liao, J.; Guan, W.; Boscoe, B. P.; Tucker, J. W.; Garnsey, M. R.; Watson, M. P. *Org. Lett.*, **2018**, *20* (10), 3030–3033). It is reprinted in this chapter with permission of *Organic Letters* (Copyright © 2018, American Chemical Society). This work was performed in collaboration with Michelle Garnsey, Brian Boscoe, and Joseph Tucker at Pfizer, Inc.

2.1 Introduction

Diarylmethanes are an important motif in a number of medicinally relevant molecules including anti-bacterial, anti-HIV, and antitumor agents (Scheme 2.1).¹⁻⁴ In particular, heteroaryl substitution is commonly found in these bioactive molecules but largely overlooked in conventional methods to furnish these targets. In fact, our collaborator at Pfizer, Dr. Michelle Garnsey, has identified diarylmethanes such as **2-3** as subtype-selective positive allosteric modulators (PAMs) of the muscarinic M₁ receptor.^{5,6} With the growing abundance of diarylmethanes as bioactive molecules, we recognized the importance of developing methods to enable the rapid synthesis of these motifs from readily available precursors. As discussed in Chapter 1, we were attracted to amines as starting materials because of their wide availability and ease of synthesis.

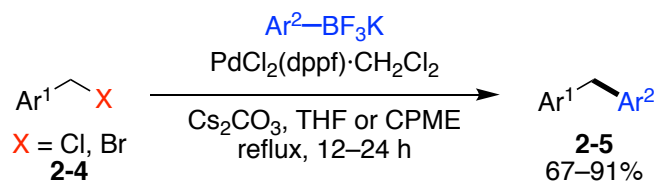
Scheme 2.1 Examples of medicinally relevant diarylmethanes



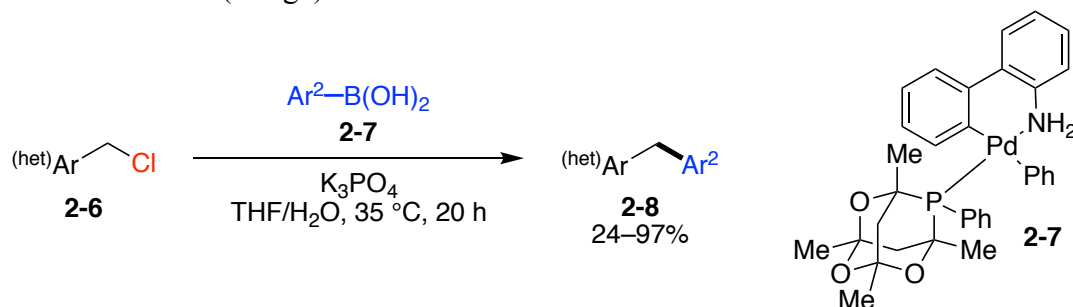
Traditionally, the diarylmethane motif can be synthesized via transition-metal catalyzed cross-couplings of a benzylic electrophile with an aryl nucleophile. One of the most common approaches focuses on the use of benzylic halides. In particular, Suzuki–Miyaura cross-couplings are the method of choice. For example, the Molander group has shown the palladium-catalyzed coupling of potassium aryltrifluoroborates with benzylic halides (**2-4**) to form diarylmethanes (**2-5**) (Scheme 2.2A).⁷ Similarly, Tudge et al. at Merck have demonstrated the use of palladium catalyst **2-7** to affect cross-coupling of benzylic chlorides (**2-6**) with (hetero)arylboronic acids for the preparation of highly-functionalized nitrogen-bearing diarylmethanes (**2-8**) (Scheme 2.2B).⁸ Other organometallic nucleophiles such as aryl Grignard reagents (Scheme 2.2C)⁹ and diaryl zinc reagents (Scheme 2.2D)¹⁰ have also been shown to cross-couple with benzylic halides to access this motif. Alternatively, a reductive approach cross-coupling benzyl chlorides (**2-14**) with aryl chlorides and fluorides using nickel catalyst **2-15** has been demonstrated by the Sun group (Scheme 2.2E).¹¹

Scheme 2.2 Metal-catalyzed arylations of benzylic halides

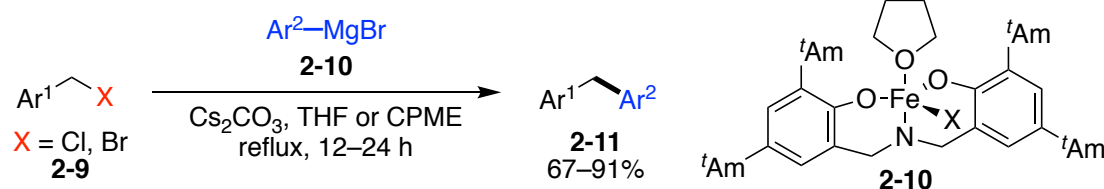
A. Aryltrifluoroborates (Molander)



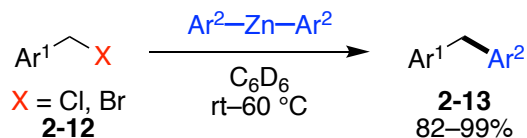
B. Boronic acids (Tudge)



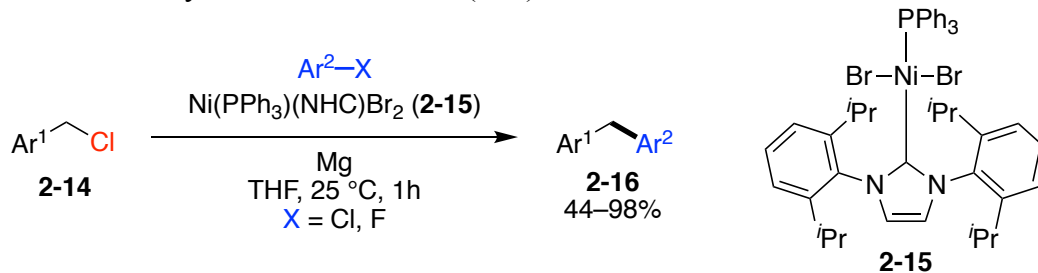
C. Aryl Grignard reagents (Kozak)



D. Diaryl zinc reagents (Ingleson)



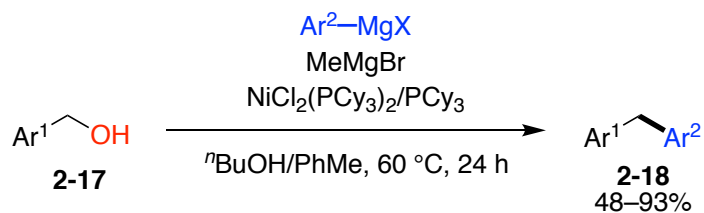
E. Reductive aryl chlorides/fluorides (Sun)



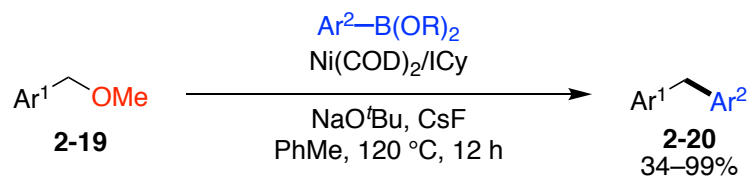
Benzylic alcohols can also serve as common precursors in the synthesis of diarylmethanes. The Shi group has demonstrated the direct arylation of benzyl alcohols (**2-17**) with Grignard reagents via nickel-catalyzed C–O bond activation (Scheme 2.3A).¹² In addition, a number of benzyl alcohol derivatives have been utilized as electrophiles in metal-catalyzed arylation reactions. The Tobisu and Chatani group have shown that benzyl methyl ethers (**2-19**) can be cross-coupled with arylboronic esters under nickel-catalysis to form diarylmethanes (**2-20**) (Scheme 2.3B).¹³ Similarly, Stewart and Maligres et al. at Merck have demonstrated an approach to di(hetero)arylmethanes (**2-22**) via a Suzuki cross-coupling of heterobenzylic acetates (**2-21**) with heteroarylboronic acids under nickel-catalyzed conditions (Scheme 2.3C).¹⁴ Kuwano has shown that benzylic carbonates (**2-23**) can undergo analogous Suzuki cross-couplings under palladium catalysis (Scheme 2.3D).^{15, 16} McLaughlin has also published on the Suzuki arylation of benzylic phosphates (**2-25**) (Scheme 2.3E).^{17, 18} Additionally, our group and others have identified benzylic alcohol derivatives as electrophiles in a variety of stereospecific transformations.¹⁹⁻²⁵

Scheme 2.3 Metal-catalyzed arylations of benzyl alcohols and their derivatives

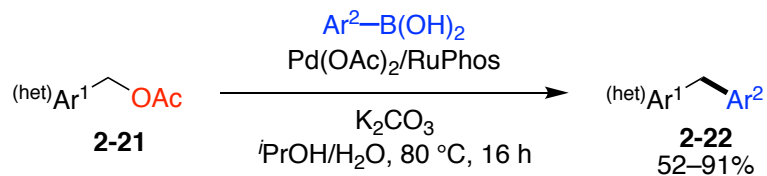
A. Benzyl alcohols (Shi)



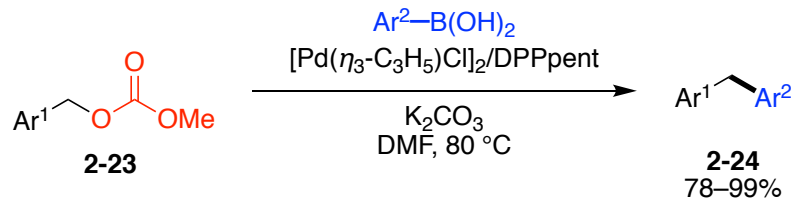
B. Benzylic ethers (Tobisu and Chatani)



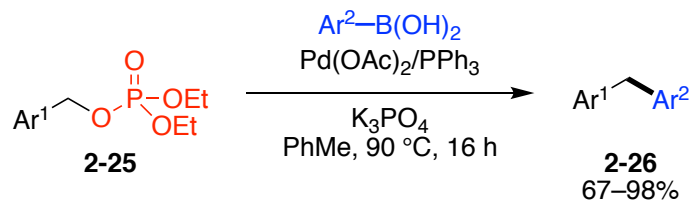
C. Benzylic acetates (Stewart and Maligres)



D. Benzylic carbonates (Kuwano)



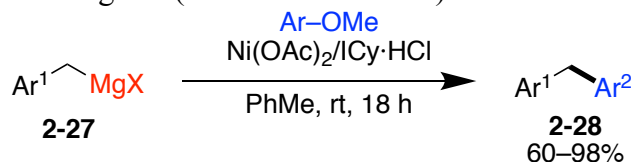
E. Benzylic phosphates (McLaughlin)



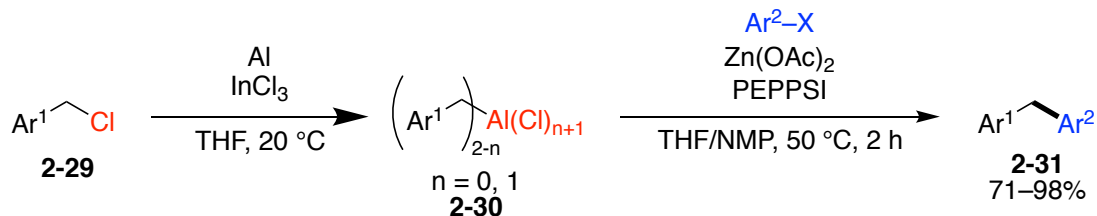
The umpolung approach using metal-based benzylic nucleophiles has also been explored for the construction of diarylmethanes. For example, the Tobisu and Chatani group have shown that benzylic Grignard reagents (**2-27**) can react with anisoles under nickel-catalyzed conditions to form diarylmethanes (**2-28**) via C–O bond cleavage (Scheme 2.4A).²⁶ The Knochel group has demonstrated that benzylic aluminum organometallic reagents (**2-30**) can be formed from insertion of aluminum powder into the benzylic C–X bond of benzylic chlorides (**2-29**). These can then undergo palladium-catalyzed cross-couplings with various electrophiles such as arylhalides to deliver diarylmethanes (**2-31**) (Scheme 2.4B).²⁷ Knochel has also shown that $\text{TMPZnCl}\cdot\text{LiCl}$ (TMP= 2,2,6,6-tetramethylpiperidyl) can afford directed zincation of methyl-substituted *N*-heterocycles (**2-32**) to generate **2-33**. These nucleophiles can then participate in Negishi cross-couplings to afford diarylmethane **2-34** (Scheme 2.4C).²⁸ Moreover, benzylic boronates have also been employed as nucleophiles, although mostly in the context of stereospecific cross-couplings. For example, the Crudden group has demonstrated palladium-catalyzed cross-coupling of chiral secondary boronic esters (**2-35**) with aryl halides to form enantioenriched 1,1-diarylethanes (**2-36**) (Scheme 2.4D).²⁹

Scheme 2.4 Arylations of benzylic organometallic nucleophiles

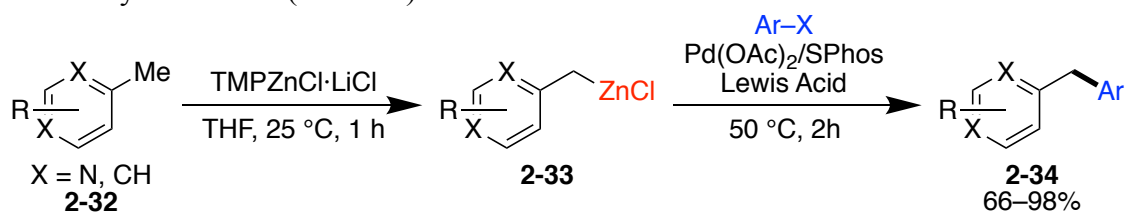
A. Benzylic Grignard reagents (Tobisu and Chatani)



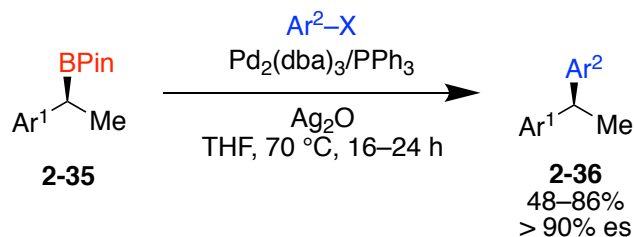
B. Benzylic aluminum sesquichlorides (Knochel)



C. Benzylic zincates (Knochel)



D. Stereospecific cross-coupling of secondary benzylic boronic esters (Crudden)

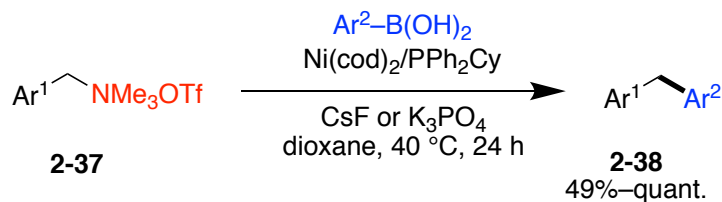


In contrast to benzylic halides and alcohol derivatives, benzylic amine derivatives have only sparingly been investigated as electrophiles for the construction of diarylmethanes. Our group has demonstrated that benzylic trimethylammonium salts (**2-37**) can participate in nickel-catalyzed Suzuki cross-couplings with arylboronic acids to deliver diarylmethanes (**2-38**) (Scheme 2.5A).^{30, 31} More recently,

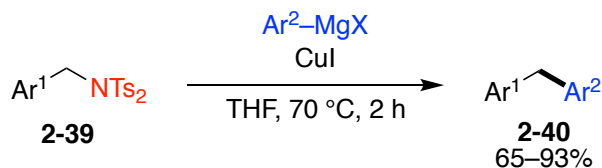
Zhao has reported an analogous cross-coupling using palladium.³² The benzylic C–N bond can also be activated via conversion to the corresponding benzylic sulfonimides. The Tian group has investigated the copper(I)-catalyzed arylation of **2-39** with Grignard reagents (Scheme 2.5B).³³ In addition, the Rhee group has shown that benzylic sulfonimides (**2-41**) can be coupled with arylboronic acids under palladium catalysis (Scheme 2.5C).³⁴ Notably, however, conversion of benzylic primary amines to ammonium salts or sulfonimides requires two steps and can limit the inclusion of basic heteroatoms elsewhere in the substrate. These constraints restrict the utility of these cross-couplings, particularly in the context of drug discovery which often requires basic heteroatoms in the final structure.

Scheme 2.5 Metal-catalyzed arylations of benzylic amine derivatives

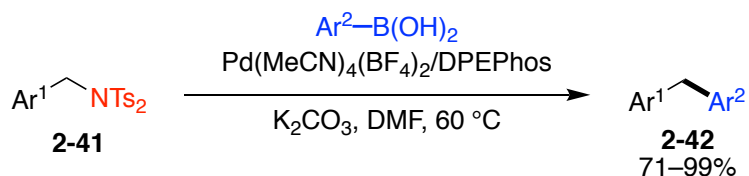
A. Watson's cross-coupling of benzylic ammonium salts with arylboronic acids



B. Tian's cross-coupling of benzylic sulfonimides with aryl Grignards



C. Rhee's cross-coupling of benzylic sulfonimides with arylboronic acids

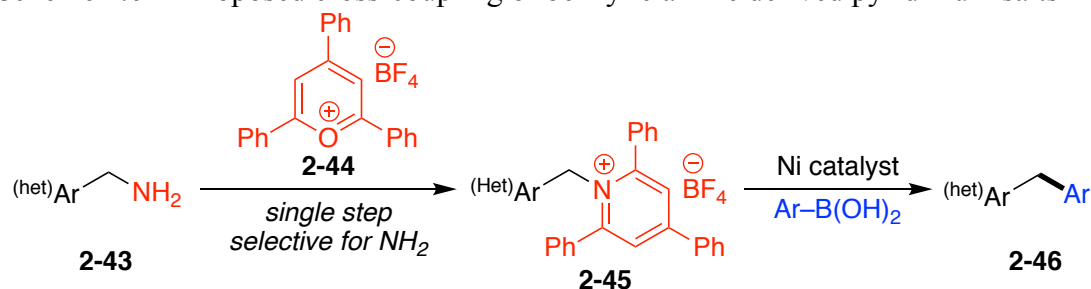


We believe that the lack of methods to harness benzylic amines in cross-couplings is a missed opportunity in the toolbox of reactions for drug discovery. Benzylic amines are generally inexpensive and widely available. They can be easily synthesized³⁵⁻³⁹ and can often be purified without chromatography. As a case study for their availability versus more common substrates for cross-couplings, our collaborator Dr. Michelle Garnsey queried the internal Pfizer chemical store in mid-2018. She found that 5,208 benzylic primary amines are present in the internal chemical store, in contrast to only 1,843 benzylic chlorides and 1,020 benzylic bromides. Moreover, we recognized that benzylic halides can serve as genotoxic impurities (GTIs), and benzylic amines would be superior in that regard. Additionally, a benzylic amine can easily be brought through a multi-step synthesis in protected form, providing opportunities for late-stage functionalization.

In Chapter 1, I discussed our development of nickel-catalyzed cross-couplings of Katritzky pyridinium salts bearing unactivated alkyl groups with arylboronic acids. Initial studies suggested that these reactions likely proceed via an alkyl radical formed via single-electron transfer (SET) from a Ni^I intermediate to the pyridinium ring, initiating C–N bond fragmentation.⁴⁰ Based on this mechanistic hypothesis, cross-coupling of a benzylic pyridinium salt (**2-45**) should also be feasible, given that a stabilized benzylic radical will be formed in this key step. Thus, we envisioned that benzylic amines could be converted to diarylmethanes in a 2-step process. First, benzylic amine **2-43** could be converted into the corresponding benzylic pyridinium salt **2-45**. Pyridinium salt **2-45** can then participate in nickel-catalyzed Suzuki–Miyaura cross-coupling with arylboronic acids to deliver diarylmethane **2-46** (Scheme 2.6). In particular, I focused on developing this method to enable access to

diarylmethanes with heteroaryl substitution, as these motifs are prevalent in pharmaceuticals and largely overlooked in other cross-couplings to deliver diarylmethanes. Because pyridinium formation is chemoselective for primary amines, other nitrogen containing functionalities such as secondary or tertiary amines as well as other heterocycles can be tolerated using this unique mode of activation.

Scheme 2.6 Proposed cross-coupling of benzylic amine derived pyridinium salts

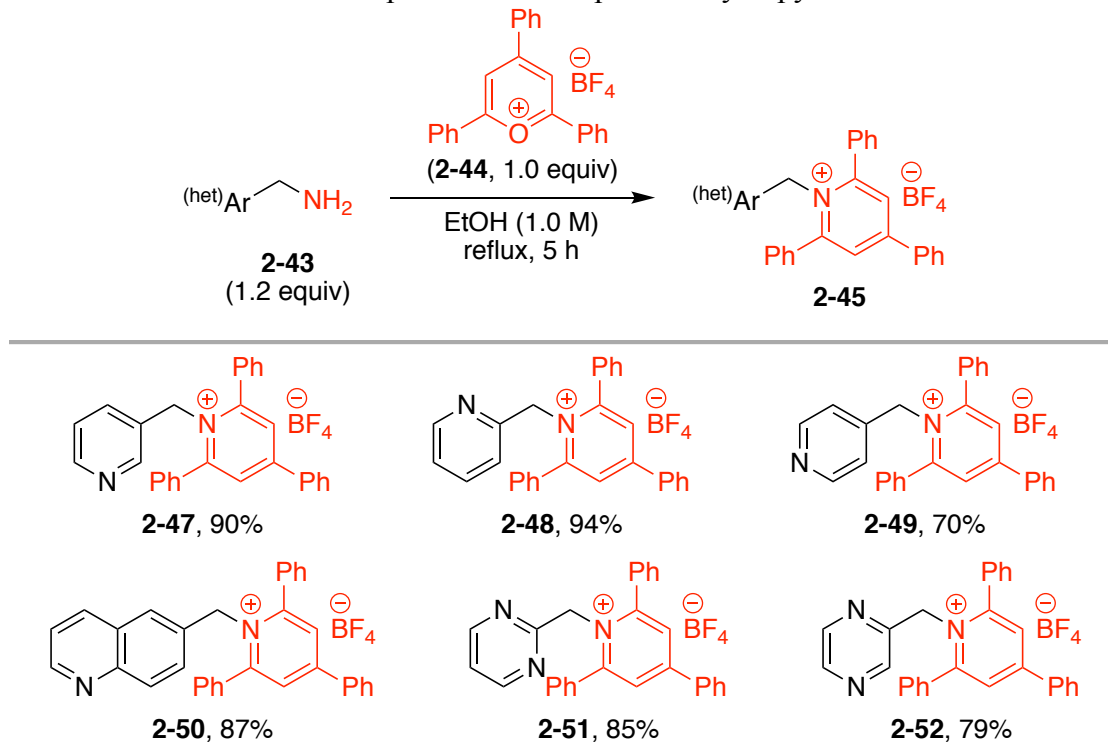


2.2 Results and Discussion

2.2.1 Synthesis of Benzylic Pyridinium Salts

The benzylic pyridinium salts were prepared following the procedure previously used for the synthesis of alkyl pyridinium salts.⁴⁰ The benzylic amine precursors were obtained commercially or via reduction of the corresponding benzonitriles. Treatment of the benzylic amine (2-43) with commercially available 2,4,6-triphenylpyrylium tetrafluoroborate (2-44) in ethanol afforded the electron-poor benzylic pyridinium salts in excellent yields with no chromatography upon precipitation with ether (Scheme 2.7). A variety of heteroaromatic substrates can be incorporated via this method including pyridines (2-47, 2-48, 2-49), quinoline (2-50), pyrimidine (2-51), and pyrazine (2-52).

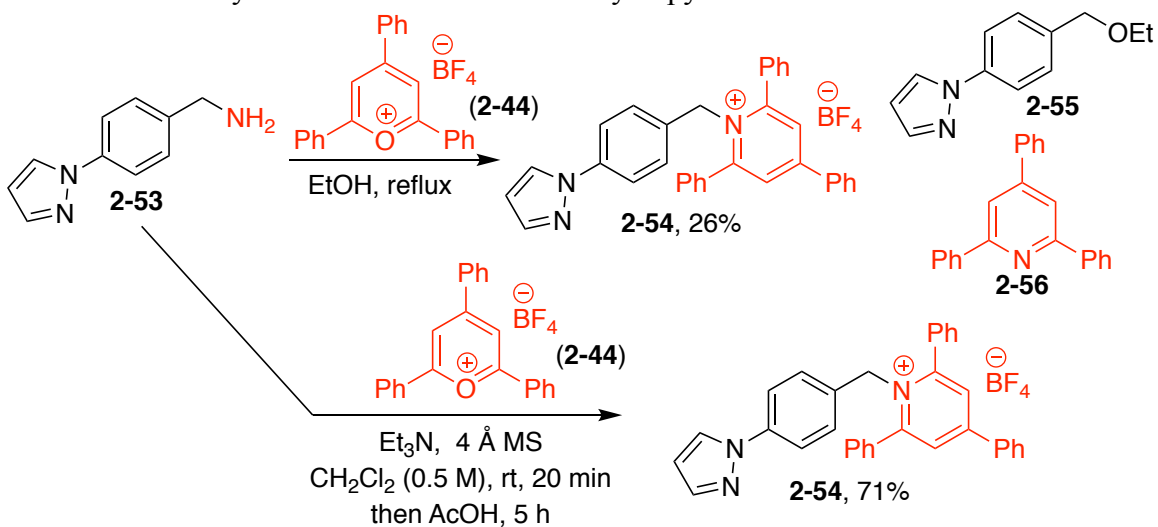
Scheme 2.7 Selected examples of electron-poor benzylic pyridinium salts formed



However, utilization of more electron-rich benzylic amine substrates, such as **2-53**, resulted in low desired product yield (**2-54**, 26%). Formation of the undesired benzylic ether byproduct (**2-55**) was observed, likely arising from a nucleophilic substitution reaction of ethanol to cleave the labile C–N bond of the desired pyridinium salt under these elevated temperatures (Scheme 2.8, top). Triphenylpyridine (**2-56**) is also formed as result of this reaction. In an effort to suppress the formation of benzylic ether byproduct **2-55**, the reaction was performed using a non-nucleophilic solvent (CH_2Cl_2) under much milder conditions (Scheme 2.8, bottom). Excitingly, the desired pyridinium salt was obtained in a much higher yield (71%). It has been shown that the use of acetic acid can help to accelerate the rate of pyridinium ring closure.⁴¹ Moreover, silica gel chromatography can be avoided with

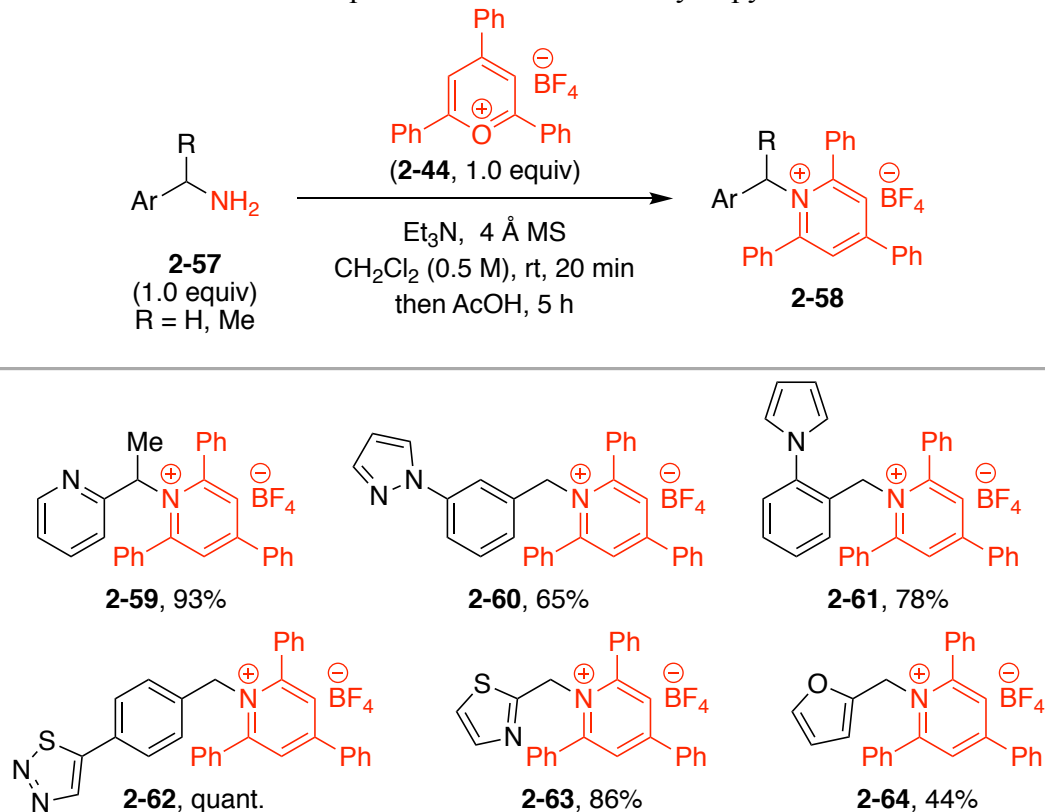
the use of an aqueous work-up, and the target pyridinium salts can then be precipitated with ether.

Scheme 2.8 Synthesis of electron-rich benzylic pyridinium salts



With this procedure, a number of electron-rich benzylic amines (**2-57**) were converted into the corresponding benzylic pyridinium salts (**2-58**) in good to excellent yields, often without the need for chromatographic purifications (Scheme 2.9). Interestingly, secondary benzylic pyridinium salt **2-59** can be formed via this method. Note that a deactivating electron-poor aryl substituent is required for pyridinium formation from secondary benzylic amines; the pyridinium salt of α -methylbenzylamine could not be isolated. I hypothesize that the desired pyridinium salt is relatively unstable and rapidly hydrolyzes to form the corresponding benzylic alcohol. Electron-rich 5-membered heterocycles pendent off the phenyl ring (**2-60**, **2-61**, **2-62**) as well as directly bound to the benzylic carbon (**2-63**, **2-64**) worked well under these conditions.

Scheme 2.9 Selected examples of electron-rich benzylic pyridinium salts formed

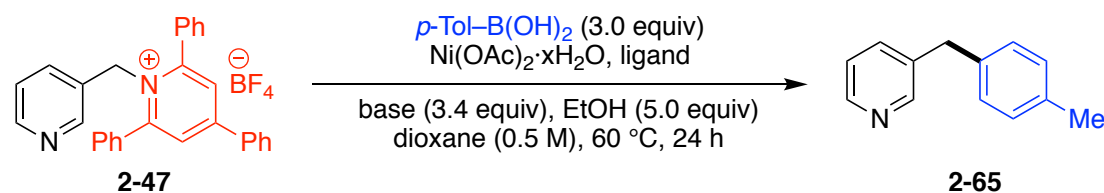


2.2.2 Reaction Optimization

My optimization began with examining the conditions previously identified for the Suzuki–Miyaura cross-coupling of alkyl pyridinium salts. I chose pyridinium salt **2-47** for the model reaction. Excitingly, the desired product (**2-65**) was afforded in 66% yield under these conditions (Table 2.1, entry 1). Switching ligands from the exotic bathophenanthroline (BPhen) to the much simpler and cheaper phenanthroline (Phen) provided a comparable yield (entry 2). On the basis of commercial availability and cost, I decided to continue optimizing with phenanthroline as ligand. I hypothesized that the use of a harsh alkoxide base may lead to the formation of the

undesired ylide,⁴² especially given the increased acidity of the benzylic proton. Indeed, switching to a milder phosphate base led to a dramatic increase in yield (entry 3).

Table 2.1 Reaction optimization of the Suzuki–Miyaura cross-coupling of benzylic pyridinium salts with arylboronic acids^a

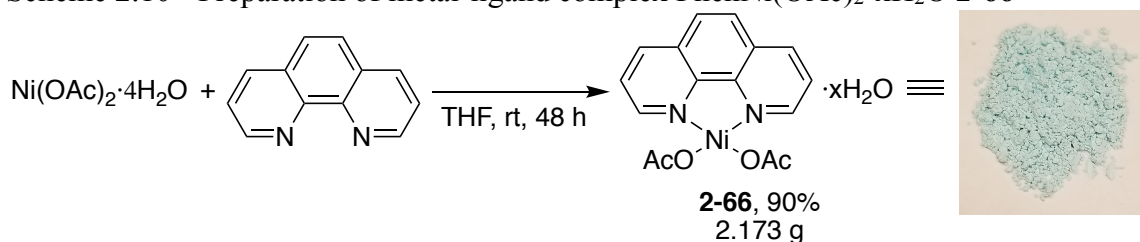


Entry	Catalyst (mol %)	Base	Yield (%) ^b
1 ^c	Ni(OAc) ₂ ·4H ₂ O (10)/ BPhen (24)	KO ^t Bu	66
2 ^c	Ni(OAc) ₂ ·4H ₂ O (10)/ Phen (12)	KO ^t Bu	59
3 ^c	Ni(OAc) ₂ ·4H ₂ O (10)/ Phen (12)	K ₃ PO ₄	90
4	Ni(OAc) ₂ ·4H ₂ O (10)/ Phen (12)	K ₃ PO ₄	75
5	PhenNi(OAc) ₂ ·xH ₂ O (10)	K ₃ PO ₄	93
6 ^d	PhenNi(OAc) ₂ ·xH ₂ O (5)	K ₃ PO ₄	93
7 ^{d,e}	PhenNi(OAc) ₂ ·xH ₂ O (5)	K ₃ PO ₄	98

^aConditions: pyridinium salt **2-47** (0.10 mmol), *p*-Tol–B(OH)₂ (3.0 equiv), [Ni], ligand, base (3.4 equiv), EtOH (5.0 equiv), dioxane (0.1 M), 60 °C, 24 h, unless noted otherwise. ^bDetermined by ¹H NMR analysis using 1,3,5-trimethoxybenzene as internal standard. ^cTwo mixtures (Vial 1: [Ni], Ligand, dioxane. Vial 2: pyridinium salt **2-47**, *p*-Tol–B(OH)₂, Base, EtOH, dioxane.) were stirred for 1 h before combining. ^d5 h. ^e0.5 M.

Unfortunately, one of the mechanical issues associated with this reaction was the need to pre-stir $\text{Ni}(\text{OAc})_2 \cdot 4\text{H}_2\text{O}$ and Phen for 1 h before combining with the other reagents. In the absence of this protocol, wherein the reaction was set up in a single pot, the desired product **2-65** was obtained in only 75% yield (entry 4). I theorized that pre-ligation of the nickel-ligand complex may be critical, so I decided to synthesize the single-component catalyst **2-66** (Scheme 2.10). This catalyst can easily be made in multi-gram quantities as an air- and moisture-stable solid. Gratifyingly, the utilization of **2-66** enabled the reaction to be set up under a one-pot procedure and eliminated the need for a prestir (Table 2.1, entry 5). With this operationally simplified set-up, much better reproducibility was also observed. Furthermore, this improvement allowed for lower catalyst loadings and shortened reaction times (entry 6). Finally, by increasing the overall concentration of the reaction to 0.5 M, the yield of **2-65** was increased to 98% (entry 7).

Scheme 2.10 Preparation of metal-ligand complex $\text{PhenNi}(\text{OAc})_2 \cdot x\text{H}_2\text{O}$ **2-66**

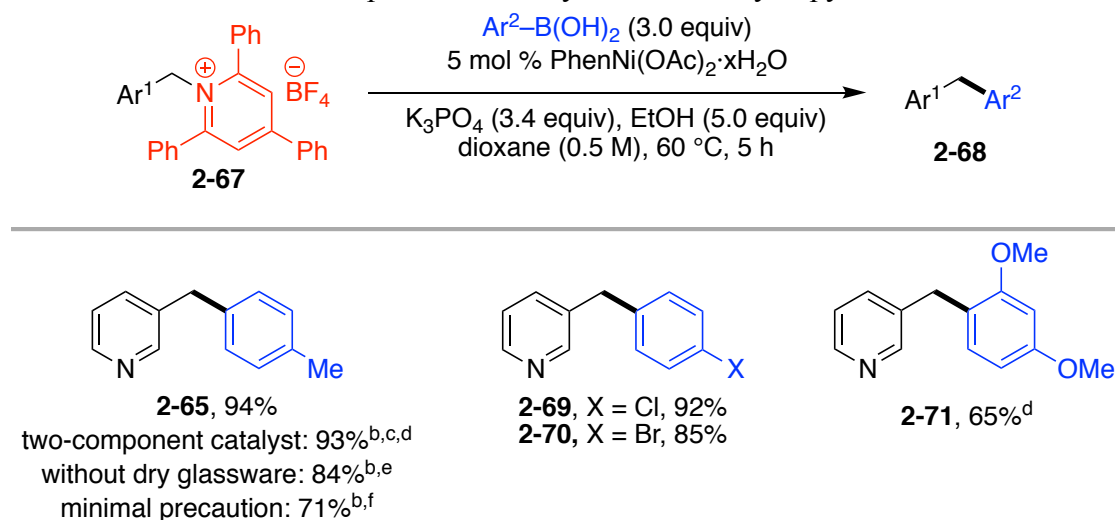


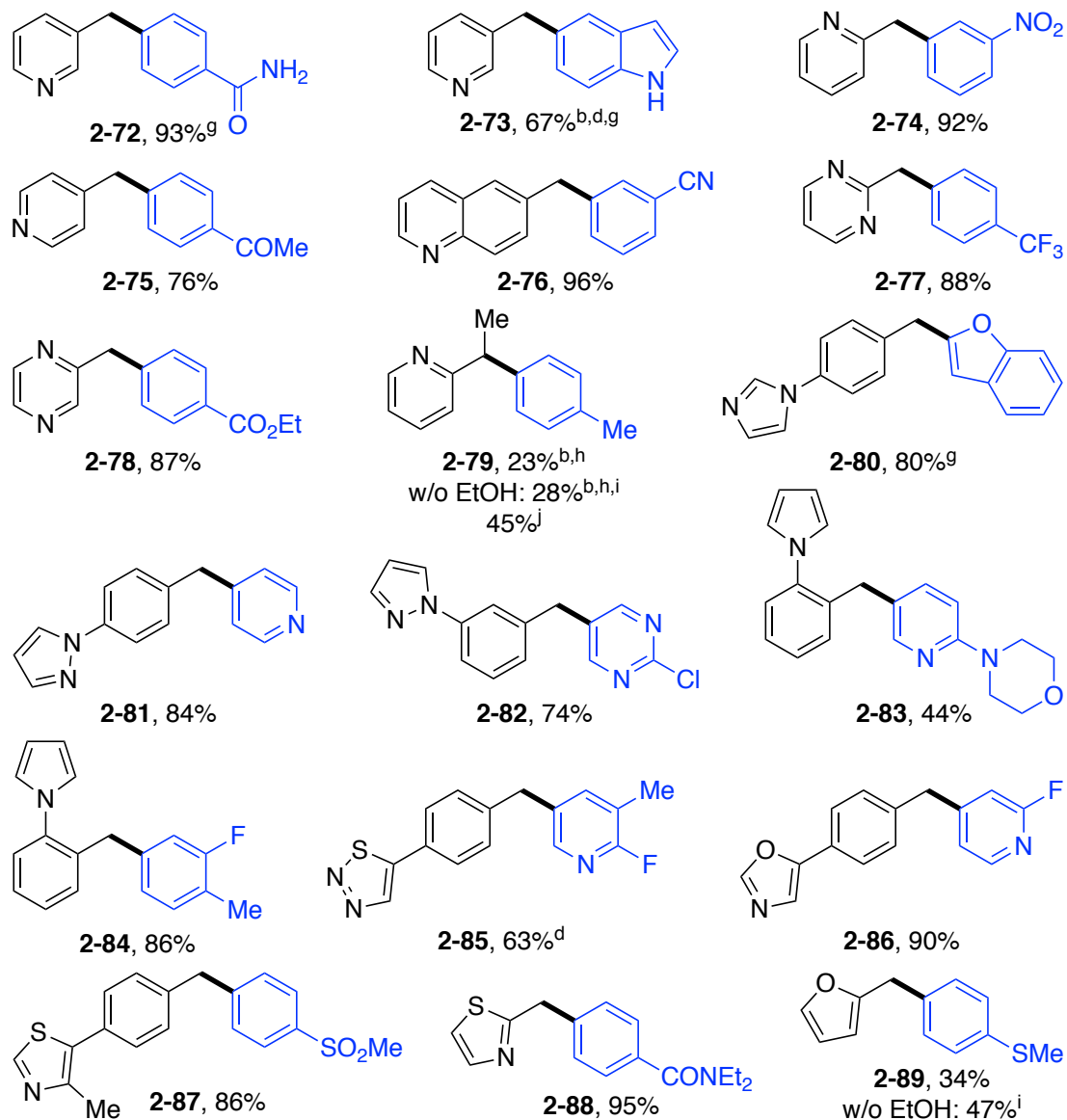
2.2.3 Reaction Scope

With optimized conditions in hand, my colleague Weiye Guan and I investigated the scope of this transformation. A wide range of benzylic pyridinium salts successfully underwent the desired cross-coupling reaction (Scheme 2.11). Model

product **2-65** was isolated in 94% yield on a 1.0-mmol scale. I have also demonstrated that the two-component catalyst system is viable using 10 mol % Ni and 12 mol % Phen, and can be used when preparation of the single-component nickel-ligand complex is less convenient. To test the sensitivity of the reaction, it was performed without oven-dried glassware and without precautions against air or moisture. In both cases, good yields were still obtained, highlighting the robustness of the reaction. Other electron-poor heteroaryl pyridinium salts were well-tolerated, including 2-, 3-, and 4-pyridine (**2-74**, **2-65**, **2-75**), quinoline (**2-76**), pyrimidine (**2-77**), and pyrazine (**2-78**). Various electron-rich heteroaryls were also tolerated, including imidazole (**2-80**), pyrazole (**2-81**, **2-82**), pyrrole (**2-83**, **2-84**), thiadiazole (**2-85**), oxazole (**2-86**), and thiazole (**2-87**, **2-88**). Furan-derived pyridinium salts were competent as well, providing **2-89** in 34% yield, along with undesired ethyl ether byproduct. By eliminating EtOH, the yield improved to 47%. When solubility of the pyridinium salt or boronic acid was low, 3:1 dioxane/DMSO was used as solvent.

Scheme 2.11 Reaction scope of Suzuki arylation of benzylic pyridinium salts^a





^aConditions: pyridinium salt **2-67** (1.0 mmol), PhenNi(OAc)₂·xH₂O (5 mol %), ArB(OH)₂ (3.0 equiv), K₃PO₄ (3.4 equiv), EtOH (5 equiv), dioxane (0.5 M), 60 °C, 5 h. Average isolated yields (±5%) from duplicate experiments. ^bSingle experiment. ^c10 mol % Ni(OAc)₂·4H₂O, 12 mol % Phen. ^d24 h. ^eGlassware was not oven-dried. ^fMinimal precautions to protect from air and moisture. ^g3:1 dioxane:DMSO. ^h0.1 mmol scale. Yield determined by ¹H NMR analysis using 1,3,5-trimethoxybenzene as internal standard. ⁱEtOH omitted. ^jConditions: pyridinium salt **2-59** (1.0 mmol),

Ni(OAc)₂·4H₂O (10 mol %), 4,4'-di^tBuBipy (12 mol %), *p*-Tol-B(OH)₂ (3.0 equiv), K₃PO₄ (3.4 equiv), dioxane (0.1 M), 60 °C, 24 h.

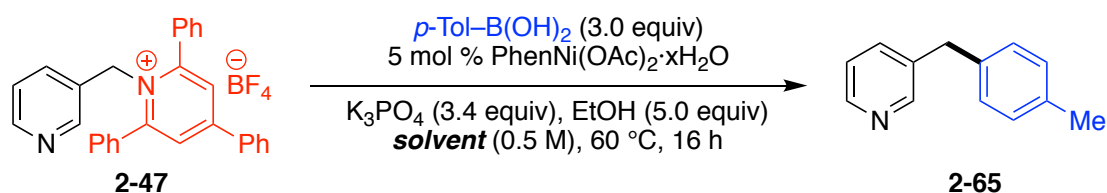
Secondary benzylic pyridinium salts were also examined. However, diarylethane **2-79** was formed in only 23% yield. Omission of EtOH only slightly increased the yield. A brief screen of ligands revealed that the use of 4,4'-di^tBuBipy increased the yield to 45%. Triphenylpyridine was only formed in ~60% in this reaction, suggesting that C–N bond cleavage was sluggish.

For the aryl boronic acid, broad tolerance for functional groups and heteroaryls was observed, including aryl chlorides (**2-69**, **2-74**), fluorides (**2-85**, **2-86**) and even bromides (**2-70**), ethers (**2-71**, **2-83**), amides (**2-72**, **2-88**), nitroarenes (**2-74**), ketones (**2-75**), nitriles (**2-76**), trifluoromethyls (**2-77**), esters (**2-78**), tertiary amines (**2-83**), sulfones (**2-87**), and thioethers (**2-89**). Both electron-rich and electron-poor heteroaryls can be used, including unprotected indole (**2-73**), benzofuran (**2-80**), pyridine (**2-81**, **2-83**, **2-85**, **2-86**), and pyrazine (**2-82**). Notably, many of these pyridines are poised for further elaboration via S_NAr chemistry. Moreover, aryl groups containing acidic protons can be used without the need for any excess base (**2-72**, **2-73**).

Cognizant that poor solubility can be limiting for some substrates, I tested the tolerance of this reaction to a variety of solvents (Table 2.2). Excitingly, a wide range of solvents can be used. Etheral solvents provided excellent yields of **2-65** (entries 1–3). Lower yields were observed when very polar solvents such as DMSO or DMF were used (entries 7 & 8), but these yields were still of high synthetic utility. In fact, the reaction can be run in neat ethanol to afford **2-65** in 77% isolated yield (entry 9). Notably, however, this can only be used for pyridinium salts with electron-poor heteroaryls, which do not undergo substitution with EtOH. These results highlight the

feasibility of finding a solvent mixture that would be compatible with any given substrate.

Table 2.2 Wide solvent tolerance^a

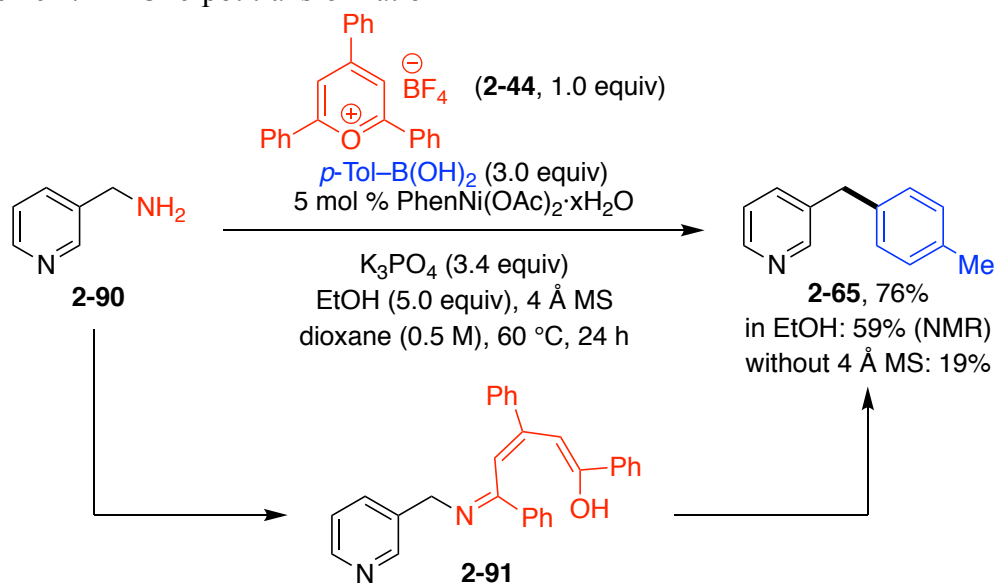


Entry	Solvent	Yield (%) ^b
1	2-Me-THF	96
2	CPME	96
3	Et ₂ O	90
4	PhMe	94
5	MeCN	91
6	CH ₂ Cl ₂	83
7	DMSO	62
8	DMF	61
9 ^c	EtOH	77 ^d

^aConditions: pyridinium salt **2-47** (0.10 mmol), PhenNi(OAc)₂·xH₂O (5 mol %), ArB(OH)₂ (3.0 equiv), K₃PO₄ (3.4 equiv), EtOH (5 equiv), solvent (0.5 M), 60 °C, 16 h. ^bDetermined by ¹H NMR analysis using 1,3,5-trimethoxybenzene as internal standard. ^c24 h. ^dIsolated yield.

The robustness of the cross-coupling reaction as well as tolerance for various solvents presented the opportunity to combine the pyridinium formation and cross-coupling in a one-pot operation. By forming the pyridinium salt *in-situ*, cross-coupled product **2-65** can be obtained directly from benzylic amine **2-90** (Scheme 2.12). The addition of 4 Å molecular sieves proved critical in this transformation. In the absence of sieves, **2-65** was obtained in only 19% yield. I believe that the desiccant may aid in pyridinium formation by preventing undesired hydrolysis of intermediate **2-91**, as well as by eliminating water that may be problematic in the cross-coupling. Notably, this is not a two-step, one-pot procedure; all reagents were added simultaneously at the beginning of the reaction. We believe that this approach can enable rapid screening to access a variety of diarylmethanes.

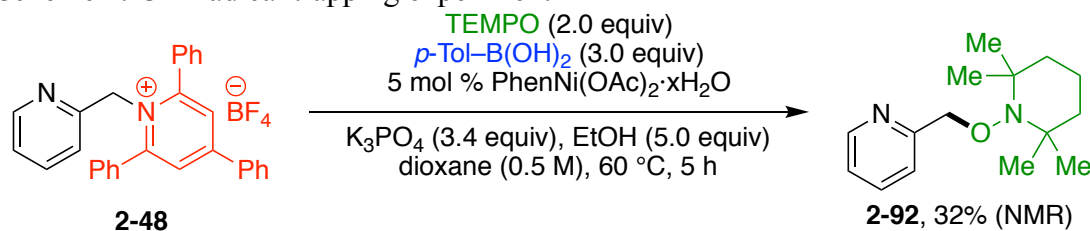
Scheme 2.12 One-pot transformation



2.2.4 Mechanistic Studies

We theorize that this reaction proceeds via a $\text{Ni}^{\text{I/III}}$ catalytic cycle, analogous to that of the Suzuki–Miyaura cross-coupling of alkyl pyridinium salts (Chapter 1). The identity of the ligand, redox non-innocent phenanthroline, suggests that the oxidative addition likely proceeds through a single-electron transfer (SET) pathway. Although further experiments are needed to confirm the active nickel species, a radical trapping experiment supports the intermediacy of a benzylic radical.⁴³ When TEMPO was added to the cross-coupling of pyridinium **2-48**, known TEMPO adduct **2-92** was produced in 32% yield (Scheme 2.13). No desired cross-coupled product was observed.

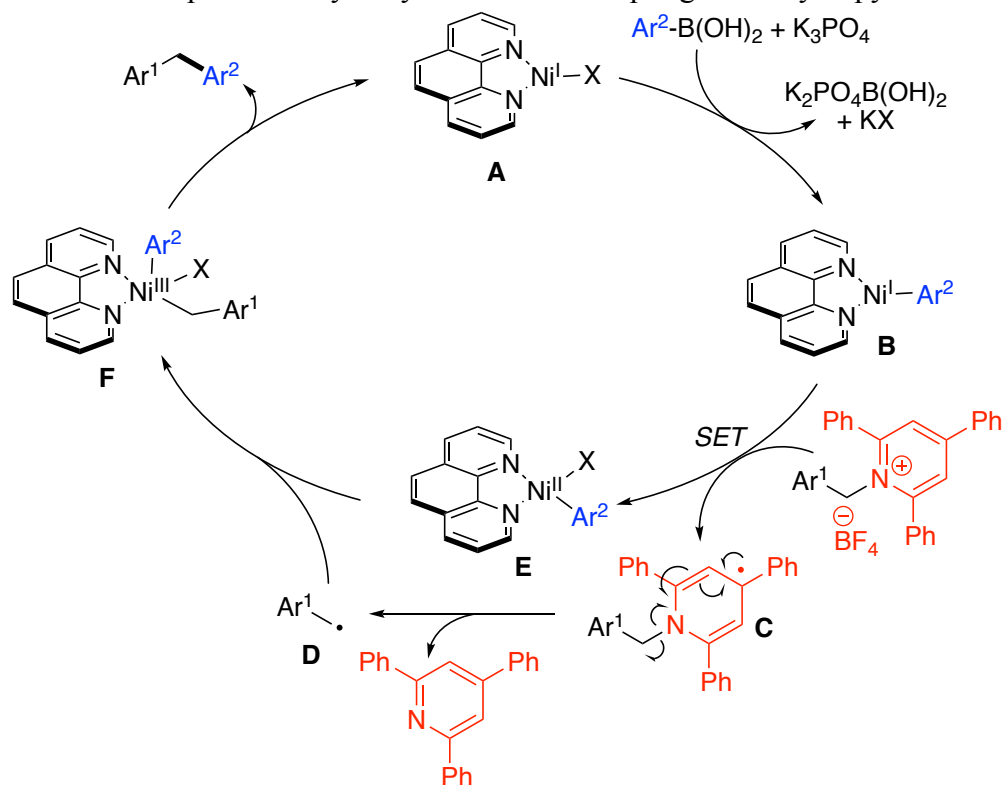
Scheme 2.13 Radical trapping experiment



We believe that the following $\text{Ni}^{\text{I/III}}$ catalytic cycle may be operative (Scheme 2.14). This mechanism is analogous to that of Fu's Negishi cross-coupling of alkyl halides.⁴⁴ Ni^{I} species **A** can undergo transmetalation with the activated aryl boronate to generate Ni^{I} -arene species **B**. This species can then perform single-electron transfer into the benzylic pyridinium salt to generate **C**, which fragments to give stabilized benzylic radical **D**. This radical can then recombine with Ni^{II} species **E** to afford Ni^{III} species **F**. Reductive elimination from **F** delivers the diarylmethane product and regenerates the active Ni^{I} catalyst **A**. Another possible mechanism is a radical-chain

bimetallic pathway, which has been observed in Weix's reductive cross-electrophile couplings.⁴⁵ With our current data, we cannot rule out this possibility.

Scheme 2.14 Proposed catalytic cycle for cross-coupling of benzylic pyridinium salts



2.3 Conclusion

In summary, I have developed a nickel-catalyzed Suzuki–Miyaura cross-coupling of benzylic pyridinium salts with aryl boronic acids. This reaction enables efficient conversion of widely available benzylic amines to diarylmethanes, a prevalent motif in pharmaceuticals and other bioactive molecules. Notably, the use of a pyridinium salt enables broad scope of heteroaromatic substituents, including those that would not be amenable to activation via a trimethylammonium triflate. Broad

solvent tolerance was also demonstrated, providing viable alternatives when solubility becomes problematic. Finally, for benzylic pyridinium salts with electron-poor aryl groups, a one-pot procedure was developed to facilitate the use of this chemistry in synthesis. This work was published in *Organic Letters* and highlighted in *Synfacts*.⁴⁶

47

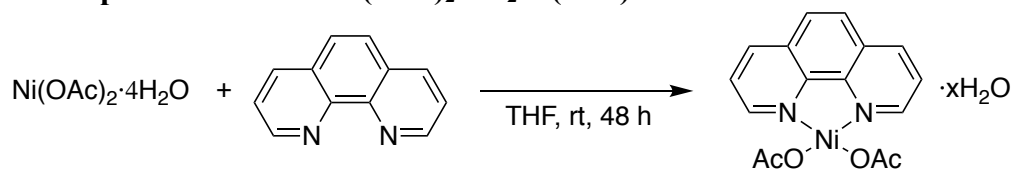
2.4 Experimental

2.4.1 General Information

Reactions were performed in oven-dried Schlenk flasks or in oven-dried round-bottomed flasks unless otherwise noted. Round-bottomed flasks were fitted with rubber septa, and reactions were conducted under a positive pressure of N₂. Stainless steel syringes were used to transfer air- and moisture-sensitive liquids. Silica gel chromatography was performed on silica gel 60 (40-63 μm, 60Å) unless otherwise noted. Commercial reagents were purchased from Sigma Aldrich, Acros, Fisher, Strem, TCI, Combi Blocks, Alfa Aesar, AK Scientific, Oakwood, or Cambridge Isotopes Laboratories and used as received with the following exceptions: anhydrous ethanol and DMSO were degassed by sparging with N₂ for 20–30 minutes prior to use in the cross-coupling reactions; THF and CH₂Cl₂ were dried by passing through drying columns; dioxane was dried by passing through drying columns, then degassed by sparging with N₂.⁴⁸ Powdered, activated 4Å molecular sieves were prepared by heating sieves to ~200°C under high vacuum overnight and then crushing to achieve a fine powder. In some instances oven-dried potassium carbonate was added to CDCl₃ to remove trace acid. Proton nuclear magnetic resonance (¹H NMR) spectra, carbon

nuclear magnetic resonance (^{13}C NMR) spectra, and fluorine nuclear magnetic resonance spectra (^{19}F NMR) were recorded on both 400 MHz and 600 MHz spectrometers. Chemical shifts for protons are reported in parts per million downfield from tetramethylsilane and are referenced to residual protium in the NMR solvent ($\text{CHCl}_3 = \delta$ 7.26). Chemical shifts for carbon are reported in parts per million downfield from tetramethylsilane and are referenced to the carbon resonances of the solvent ($\text{CDCl}_3 = \delta$ 77.16). Chemical shifts for fluorine were externally referenced to CFCl_3 in CDCl_3 ($\text{CFCl}_3 = \delta$ 0). Data are represented as follows: chemical shift, multiplicity (br = broad, s = singlet, d = doublet, t = triplet, q = quartet, p = pentet, m = multiplet, dd = doublet of doublets, h = heptet), coupling constants in Hertz (Hz), integration. Infrared (IR) spectra were obtained using FTIR spectrophotometers with material loaded onto a KBr plate. The mass spectral data were obtained at the University of Delaware mass spectrometry facility. Melting points were taken on a Thomas-Hoover Uni-Melt Capillary Melting Point Apparatus.

2.4.2 Preparation of $\text{PhenNi}(\text{OAc})_2 \cdot x\text{H}_2\text{O}$ (2-66)

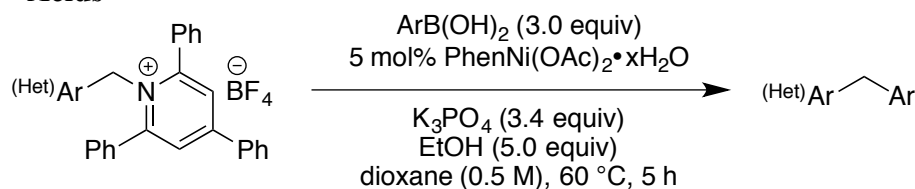


The following was adapted from a literature procedure.⁴⁹ To an oven-dried, 100-mL round-bottomed flask was added $\text{Ni}(\text{OAc})_2 \cdot 4\text{H}_2\text{O}$ (1.49 g, 6.0 mmol, 1.0 equiv) and phenanthroline (1.08 g, 6.0 mmol, 1.0 equiv). The flask was fitted with a septum, and THF (35 mL) was added. The reaction mixture was stirred at room temperature for 48 h. The resulting pale blue suspension was filtered. The solid was

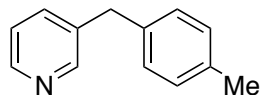
washed with Et₂O (3 x 20 mL) and dried under high vacuum. The solid was used as is without further purification: ¹H NMR (400 MHz, DMSO-*d*₆) δ 47.32 – 41.84 (m, 8H), 22.88 (s, 3H), 18.03 (s, 3H); HRMS (LIFDI) [M]⁺ calculated for C₁₆H₁₄N₂O₄Ni: 356.0307, found 356.0290.

2.4.3 Cross-Coupling of Pyridinium Salts to Give Diarylmethanes

2.4.3.1 General Procedure A: Cross-Coupling of Pyridinium Salts with Boronic Acids



To an oven-dried, 25-mL Schlenk flask was added PhenNi(OAc)₂·xH₂O (20 mg, 0.050 mmol, 5 mol %), pyridinium salt (1.0 mmol, 1.0 equiv), arylboronic acid (3.0 mmol, 3.0 equiv), and K₃PO₄ (722 mg, 3.4 mmol, 3.4 equiv). The flask was fitted with a rubber septum, sealed with parafilm, and then evacuated and refilled with N₂ (x 3). Dioxane (2.0 mL) was added, followed by EtOH (0.29 mL, 5.0 mmol, 5.0 equiv). The flask was sealed and resulting mixture was stirred at 60 °C for 5 h. The mixture was allowed to cool to room temperature, and then filtered through a small pad of Celite. The filter cake was washed with CH₂Cl₂ (4 x 25 mL), and the filtrate was concentrated. The cross-coupled product was then purified via silica gel chromatography.



3-(4-Methylbenzyl)pyridine (2-65). Prepared via General Procedure A using pyridinium salt **2-47**. The crude mixture was purified by silica gel chromatography (50% ether/hexanes) to give **2-65** (run 1: 170 mg, 93%; run 2: 172 mg, 94%) as pale yellow oil: ^1H NMR (600 MHz, CDCl_3) δ 8.50 (s, 1H), 8.47 – 8.43 (m, 1H), 7.48 – 7.43 (m, 1H), 7.21 – 7.16 (m, 1H), 7.11 (d, $J = 7.9$ Hz, 2H), 7.07 (d, $J = 8.0$ Hz, 2H), 3.94 (s, 2H), 2.32 (s, 3H); ^{13}C NMR (151 MHz, CDCl_3) δ 150.2, 147.6, 136.8, 136.7, 136.2, 136.0, 129.4, 128.7, 123.4, 38.7, 21.0. The spectral data matches that reported in the literature.⁵⁰

Reaction without Oven-dried Glassware

Product **2-65** also prepared via General Procedure A, except that the Schlenk flask and stir bar were not oven-dried prior to use. The crude mixture was purified by silica gel chromatography (50% ether/hexanes) to give **2-65** (155 mg, 84%).

Reaction with “Minimal Precaution” Set-up

Product **2-65** was also prepared via a procedure similar to General Procedure A, except that minimal precautions were taken to protect the reaction from air and moisture. Dioxane (ACS grade) and EtOH (absolute) were used as received; they were not dried or degassed. The round-bottomed flask and stir bar were not oven-dried prior to use. Reagents were added directly into the flask, open to air. The reaction was set up under air (no N_2).

To a 25-mL round-bottomed flask equipped with a stir bar was added $\text{PhenNi}(\text{OAc})_2 \cdot x\text{H}_2\text{O}$ (20 mg, 0.050 mmol, 5 mol %), pyridinium salt **2-47** (486 mg, 1.0 mmol, 1.0 equiv), *p*-tolylboronic acid (408 mg, 3.0 mmol, 3.0 equiv), and K_3PO_4 (722 mg, 3.4 mmol, 3.4 equiv). Dioxane (2.0 mL) was added, followed by EtOH (0.29

mL, 5.0 mmol, 5.0 equiv). The flask was fitted with a rubber septum and sealed with parafilm (no N₂ inlet). The resulting mixture was stirred at 60 °C for 5 h. The mixture was allowed to cool to room temperature, and then filtered through a small pad of Celite. The filter cake was washed with CH₂Cl₂ (4 x 25 mL), and the filtrate was concentrated. The crude mixture was purified by silica gel chromatography (50% ether/hexanes) to give **2-65** (131 mg, 71%).

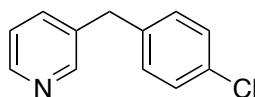
Reaction with Ethanol as Solvent

Product **2-65** was also prepared via a procedure similar to General Procedure A, except that EtOH was used as the solvent. To an oven-dried, 25-mL Schlenk flask, was added PhenNi(OAc)₂·xH₂O (20 mg, 0.050 mmol, 5 mol %), pyridinium salt **2-47** (486 mg, 1.0 mmol, 1.0 equiv), *p*-tolylboronic acid (408 mg, 3.0 equiv, 3.0 mmol), and K₃PO₄ (722 mg, 3.4 mmol, 3.4 equiv). The flask was fitted with a rubber septum, sealed with parafilm, and then evacuated and refilled with N₂ (x 3). EtOH (2.0 mL) was added. The resulting mixture was stirred at 60 °C for 24 h. The mixture was allowed to cool to room temperature, and then filtered through a small pad of Celite. The filter cake was washed with CH₂Cl₂ (4 x 25 mL), and the filtrate was concentrated. The crude mixture was purified by silica gel chromatography (50% ether/hexanes) to give **2-65** (141 mg, 77%).

Reaction with Two-component Catalyst

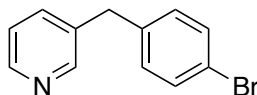
Product **2-65** was also prepared using a two-component catalyst system. To an oven-dried, 25-mL pear-shaped flask, was added Ni(OAc)₂·4H₂O (25 mg, 0.10 mmol, 10 mol %) and phenanthroline (22 mg, 0.12 mmol, 12 mol %). The flask was fitted with a rubber septum, sealed with parafilm, and then evacuated and refilled with N₂ (x 3). To an oven-dried, 25-mL Schlenk flask was added pyridinium salt **2-47** (486 mg,

1.0 mmol, 1.0 equiv), *p*-tolylboronic acid (408 mg, 3.0 equiv, 3.0 mmol), and K₃PO₄ (722 mg, 3.4 mmol, 3.4 equiv). The flask was fitted with a rubber septum, sealed with parafilm, and then evacuated and refilled with N₂ (x 3). To the pear-shaped flask containing Ni(OAc)₂·4H₂O and Phen was added dioxane (sparged, anhydrous; 2.5 mL). To the Schlenk flask containing the pyridinium salt, boronic acid, and K₃PO₄ was added dioxane (sparged, anhydrous; 2.5 mL), followed by EtOH (sparged, anhydrous; 0.29 mL, 5.0 mmol, 5.0 equiv). After vigorously stirring of the resulting mixtures for 1 h at room temperature, the heterogeneous mixture containing the catalyst was transferred via cannula to the mixture containing the pyridinium salt and activated boronate complex. The pear-shaped flask was rinsed multiple times with dioxane (totaling 5 mL; each rinse was transferred via cannula to the reaction mixture) to bring the total volume of dioxane in the reaction flask to 10 mL (0.1 M). The resulting reaction mixture was stirred at 60 °C for 24 h. The mixture was allowed to cool to room temperature, and then filtered through a small pad of Celite. The filter cake was washed with CH₂Cl₂ (4 x 25 mL), and the resulting solution was concentrated. The crude mixture was purified by silica gel chromatography (50% ether/hexanes) to give **2-65** (171 mg, 93%).

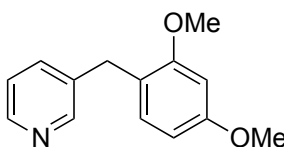


3-(4-Chlorobenzyl)pyridine (2-69). Prepared via General Procedure A using pyridinium salt **2-47**. The crude mixture was purified by silica gel chromatography (50% ether/hexanes) to give **2-69** (run 1: 182 mg, 90%; run 2: 190 mg, 93%) as a clear oil: ¹H NMR (600 MHz, CDCl₃) δ 8.53 – 8.48 (m, 2H), 7.49 – 7.43 (m, 1H), 7.32 – 7.27 (m, 2H), 7.26 – 7.21 (m, 1H), 7.15 – 7.11 (m, 2H), 3.97 (s, 2H); ¹³C NMR (151

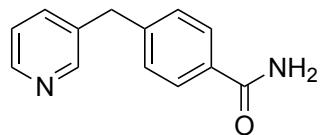
MHz, CDCl₃) δ 150.2, 147.9, 138.3, 136.2, 135.9, 132.4, 130.2, 128.8, 123.5, 38.4. The spectral data matches that reported in the literature.⁵¹



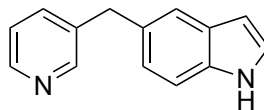
3-(4-Bromobenzyl)pyridine (2-70). Prepared via General Procedure A using pyridinium salt **2-47**. The crude mixture was purified by silica gel chromatography (60% ether/hexanes) to give **2-70** (run 1: 222 mg, 89%; run 2: 199 mg, 80%) as a pale yellow oil: ¹H NMR (600 MHz, CDCl₃) δ 8.50 – 8.45 (m, 2H), 7.46 – 7.40 (m, 3H), 7.23 – 7.18 (m, 1H), 7.07 – 7.02 (m, 2H), 3.93 (s, 2H); ¹³C NMR (151 MHz, CDCl₃) δ 150.1, 147.9, 138.8, 136.2, 135.8, 131.8, 130.6, 123.5, 120.4, 38.5. The spectral data matches that reported in the literature.⁵²



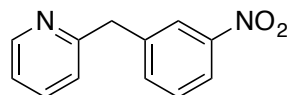
3-(2,4-Dimethoxybenzyl)pyridine (2-71). Prepared via General Procedure A using pyridinium salt **2-47**, except that the reaction mixture was heated for 24 h. The crude mixture was purified by silica gel chromatography (30% ethyl acetate/hexanes) to give **2-71** (run 1: 168 mg, 68%; run 2: 154 mg, 62%) as pale yellow oil: ¹H NMR (400 MHz, CDCl₃) δ 8.53 – 8.47 (m, 1H), 8.44 – 8.37 (m, 1H), 7.50 – 7.42 (m, 1H), 7.20 – 7.12 (m, 1H), 7.03 – 6.96 (m, 1H), 6.48 – 6.38 (m, 2H), 3.87 (s, 2H), 3.79 (s, 3H), 3.77 (s, 3H); ¹³C NMR (151 MHz, CDCl₃) δ 159.8, 158.2, 150.3, 147.2, 136.9, 136.1, 130.5, 123.2, 120.9, 104.1, 98.7, 55.4, 55.3, 32.8; FTIR (neat) 2936, 2835, 1612, 1507, 1209, 1035, 713 cm⁻¹; HRMS (ESI+) [M+H]⁺ calculated for C₁₄H₁₆NO₂: 230.1181, found 230.1178.



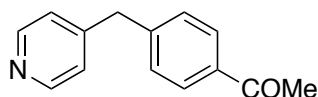
4-(Pyridin-3-ylmethyl)benzamide (2-72). Prepared via General Procedure A using pyridinium salt **2-47**, except that a 3:1 mixture of dioxane (1.5 mL) and DMSO (0.5 mL) was used as the solvent. The crude mixture was purified by silica gel chromatography (5–10 MeOH/CH₂Cl₂) to give **2-72** (run 1: 186 mg, 88%; run 2: 208 mg, 98%) as an off-white solid (mp 152–154 °C): ¹H NMR (600 MHz, CDCl₃) δ 8.53 – 8.46 (m, 2H), 7.78 – 7.73 (m, 2H), 7.48 – 7.42 (m, 1H), 7.28 – 7.25 (m, 2H, *overlaps with CHCl₃*), 7.25 – 7.19 (m, 1H), 6.01 (s, br, 1H), 5.57 (s, br, 1H), 4.03 (s, 2H); ¹³C NMR (151 MHz, CDCl₃) δ 168.8, 150.2, 148.0, 144.2, 136.3, 135.6, 131.6, 129.1, 127.8, 123.5, 38.9; FTIR (neat) 3393, 3172, 1652, 1616, 1416, 1394, 1030, 712 cm⁻¹; HRMS (ESI+) [M+H]⁺ calculated for C₁₃H₁₃N₂O: 213.1022, found 213.1019.



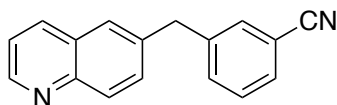
5-(Pyridin-3-ylmethyl)-1H-indole (2-73). Prepared via General Procedure A using pyridinium salt **2-47**, except that a 3:1 mixture of dioxane (1.5 mL) and DMSO (0.5 mL) was used as the solvent and the reaction mixture was heated for 24 h. The crude mixture was purified by silica gel chromatography (50% ethyl acetate/hexanes) to give **2-73** (140 mg, 67%) as an off-white solid: ¹H NMR (600 MHz, CDCl₃) δ 8.57 – 8.53 (m, 1H), 8.46 – 8.42 (m, 1H), 8.18 (s, br, 1H), 7.52 – 7.47 (m, 1H), 7.47 – 7.43 (m, 1H), 7.35 – 7.30 (m, 1H), 7.22 – 7.19 (m, 1H), 7.19 – 7.15 (m, 1H), 7.04 – 6.99 (m, 1H), 6.52 – 6.48 (m, 1H), 4.08 (s, 2H); ¹³C NMR (151 MHz, CDCl₃) δ 150.2, 147.4, 137.6, 136.3, 134.6, 131.3, 128.2, 124.6, 123.3, 123.3, 120.6, 111.2, 102.5, 39.2. The spectral data matches that reported in the literature.¹⁴



2-(3-Nitrobenzyl)pyridine (2-74). Prepared via General Procedure A using pyridinium salt **2-48**. The crude mixture was purified by silica gel chromatography (50% ether/hexanes) to give **2-74** (run 1: 196 mg, 91%; run 2: 200 mg, 93%) as an orange oil: ^1H NMR (600 MHz, CDCl_3) δ 8.59 – 8.55 (m, 1H), 8.13 (s, 1H), 8.11 – 8.06 (m, 1H), 7.66 – 7.59 (m, 2H), 7.50 – 7.45 (m, 1H), 7.19 – 7.14 (m, 2H), 4.25 (s, 2H); ^{13}C NMR (151 MHz, CDCl_3) δ 159.2, 149.8, 148.4, 141.5, 136.9, 135.3, 129.4, 123.9, 123.2, 121.8, 121.6, 44.1. The spectral data matches that reported in the literature.⁵³

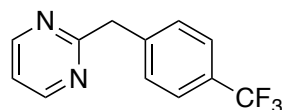


1-(4-(Pyridin-4-ylmethyl)phenyl)ethan-1-one (2-75). Prepared via General Procedure A using pyridinium salt **2-49**. The crude mixture was purified by silica gel chromatography (50% ethyl acetate/hexanes) to give **2-75** (run 1: 163 mg, 77%; run 2: 159 mg, 75%) as a yellow oil: ^1H NMR (600 MHz, CDCl_3) δ 8.52 (d, $J = 5.9$ Hz, 2H), 7.91 (d, $J = 8.2$ Hz, 2H), 7.27 (d, $J = 8.2$ Hz, 2H), 7.09 (d, $J = 5.9$ Hz, 2H), 4.02 (s, 2H), 2.59 (s, 3H); ^{13}C NMR (151 MHz, CDCl_3) δ 197.6, 150.1, 148.8, 144.4, 135.8, 129.2, 128.8, 124.2, 41.2, 26.6; FTIR (neat) 3029, 2921, 1681, 1597, 1414, 1268, 609 cm^{-1} ; HRMS (ESI+) $[\text{M}+\text{H}]^+$ calculated for $\text{C}_{14}\text{H}_{14}\text{NO}$: 212.1075, found 212.1071.

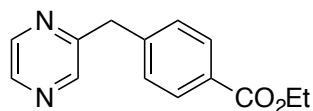


3-(Quinolin-6-ylmethyl)benzonitrile (2-76). Prepared via General Procedure A using pyridinium salt **2-50**. The crude mixture was purified by silica gel chromatography

(50–80% ether/hexanes) to give **2-76** (run 1: 231 mg, 94%; run 2: 238 mg, 98%) as a pale yellow solid (mp 79–81 °C): ^1H NMR (400 MHz, CDCl_3) δ 8.93 – 8.87 (m, 1H), 8.14 – 8.02 (m, 2H), 7.61 – 7.56 (m, 1H), 7.56 – 7.45 (m, 4H), 7.45 – 7.38 (m, 2H), 4.20 (s, 2H); ^{13}C NMR (101 MHz, CDCl_3) δ 150.3, 147.3, 141.9, 137.8, 135.7, 133.5, 132.5, 130.8, 130.3, 130.1, 129.4, 128.4, 127.1, 121.5, 118.8, 112.7, 41.4; FTIR (neat) 3032, 2920, 2229, 1594, 1501, 838, 688 cm^{-1} ; HRMS (ESI+) $[\text{M}+\text{H}]^+$ calculated for $\text{C}_{17}\text{H}_{13}\text{N}_2$: 245.1079, found 245.1074.

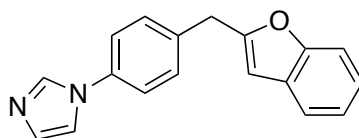


2-(4-(Trifluoromethyl)benzyl)pyrimidine (2-77). Prepared via General Procedure A using pyridinium salt **2-51**. The crude mixture was purified by silica gel chromatography (50% ether/hexanes) to give **2-77** (run 1: 212 mg, 89%; run 2: 208 mg, 87%) as a yellow oil: ^1H NMR (600 MHz, CDCl_3) δ 8.69 (d, $J = 4.9$ Hz, 2H), 7.56 (d, $J = 8.0$ Hz, 2H), 7.48 (d, $J = 8.0$ Hz, 2H), 7.16 (t, $J = 4.9$ Hz, 1H), 4.35 (s, 2H); ^{13}C NMR (101 MHz, CDCl_3) δ 169.2, 157.5, 142.2 (q, $J_{\text{C-F}} = 1.5$ Hz), 129.5, 128.9 (q, $J_{\text{C-F}} = 32.4$ Hz), 125.5 (q, $J_{\text{C-F}} = 3.8$ Hz), 124.2 (q, $J_{\text{C-F}} = 271.9$ Hz), 119.0, 45.8; ^{19}F NMR (565 MHz, CDCl_3) δ -62.49; FTIR (neat) 3043, 2929, 1563, 1418, 1327, 1067, 633 cm^{-1} ; HRMS (ESI+) $[\text{M}+\text{H}]^+$ calculated for $\text{C}_{12}\text{H}_{10}\text{F}_3\text{N}_2$: 239.0796, found 239.0791.

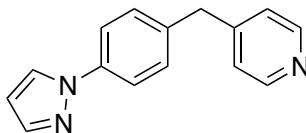


Ethyl 4-(pyrazin-2-ylmethyl)benzoate (2-78). Prepared via General Procedure A using pyridinium salt **2-52**. The crude mixture was purified by silica gel chromatography (50% ether/hexanes) to give **2-78** (run 1: 210 mg, 87%; run 2: 209

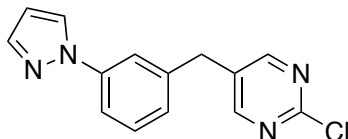
mg, 86%) as an orange solid (mp 62–65 °C): ¹H NMR (600 MHz, CDCl₃) δ 8.53 – 8.49 (m, 1H), 8.49 – 8.46 (m, 1H), 8.45 – 8.41 (m, 1H), 7.99 (d, *J* = 8.2 Hz, 2H), 7.34 (d, *J* = 8.2 Hz, 2H), 4.36 (q, *J* = 7.1 Hz, 2H), 4.22 (s, 2H), 1.37 (t, *J* = 7.1 Hz, 3H); ¹³C NMR (151 MHz, CDCl₃) δ 166.3, 155.7, 144.7, 144.2, 143.2, 142.7, 130.0, 129.2, 129.0, 60.9, 41.9, 14.3; FTIR (neat) 2981, 2924, 1713, 1276, 1100, 1019, 758 cm⁻¹; HRMS (ESI+) [*M*+H]⁺ calculated for C₁₄H₁₅N₂O₂: 243.1134, found 243.1129.



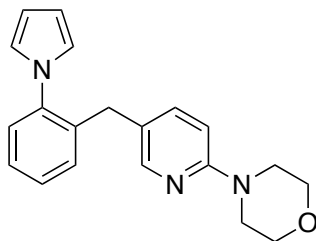
1-(4-(Benzofuran-2-ylmethyl)phenyl)-1H-imidazole (2-80). Prepared via General Procedure A using pyridinium salt **2-93**, except that a 3:1 mixture of dioxane (1.5 mL) and DMSO (0.5 mL) was used as the solvent. The crude mixture was purified by silica gel chromatography (70% ethyl acetate/hexanes) to give **2-80** (run 1: 216 mg, 79%; run 2: 221 mg, 81%) as a pale yellow solid (mp 76–78 °C): ¹H NMR (600 MHz, CDCl₃) δ 7.88 – 7.84 (m, 1H), 7.54 – 7.50 (m, 1H), 7.47 – 7.42 (m, 3H), 7.41 – 7.35 (m, 2H), 7.30 – 7.29 (m, 1H), 7.27 – 7.20 (m, 3H), 6.49 – 6.45 (m, 1H), 4.19 (s, 2H); ¹³C NMR (151 MHz, CDCl₃) δ 156.8, 155.0, 136.8, 136.2, 135.6, 130.5, 130.3, 128.6, 123.7, 122.7, 121.8, 120.5, 118.3, 111.0, 103.7, 34.5; FTIR (neat) 3111, 1522, 1303, 1252, 1056, 752 cm⁻¹; HRMS (ESI+) [*M*+H]⁺ calculated for C₁₈H₁₅N₂O: 275.1184, found 275.1180.



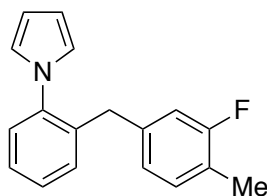
4-(4-(1H-Pyrazol-1-yl)benzyl)pyridine (2-81). Prepared via General Procedure A using pyridinium salt **2-54**. The crude mixture was purified by silica gel chromatography (50% ethyl acetate/hexanes) to give **2-81** (run 1: 189 mg, 80%; run 2: 205 mg, 87%) as a tan solid (mp 51–53 °C): ^1H NMR (600 MHz, CDCl_3) δ 8.52 (d, J = 6.0 Hz, 2H), 7.90 (d, J = 2.0 Hz, 1H), 7.72 (d, J = 1.5 Hz, 1H), 7.65 (d, J = 8.5 Hz, 2H), 7.26 (d, J = 8.5 Hz, 2H, overlaps with CHCl_3), 7.11 (d, J = 6.0 Hz, 2H), 6.46 (dd, J = 2.0, 1.5 Hz, 1H), 4.00 (s, 2H); ^{13}C NMR (151 MHz, CDCl_3) δ 150.0, 149.6, 141.1, 139.0, 137.1, 130.0, 126.7, 124.1, 119.5, 107.6, 40.6; FTIR (neat) 3026, 2921, 1599, 1524, 1394, 936, 785 cm^{-1} ; HRMS (ESI+) $[\text{M}+\text{H}]^+$ calculated for $\text{C}_{15}\text{H}_{14}\text{N}_3$: 236.1188, found 236.1183.



5-(3-(1H-Pyrazol-1-yl)benzyl)-2-chloropyrimidine (2-82). Prepared via General Procedure A using pyridinium salt **2-60**. The crude mixture was purified by silica gel chromatography (25–50% ether/hexanes) to give **2-82** (run 1: 188 mg, 70%; run 2: 208 mg, 77%) as an orange solid (mp 71–73 °C): ^1H NMR (600 MHz, CDCl_3) δ 8.49 (s, 2H), 7.93 – 7.89 (m, 1H), 7.73 – 7.70 (m, 1H), 7.64 – 7.60 (m, 1H), 7.57 – 7.52 (m, 1H), 7.45 – 7.39 (m, 1H), 7.09 – 7.05 (m, 1H), 6.49 – 6.45 (m, 1H), 4.02 (s, 2H); ^{13}C NMR (151 MHz, CDCl_3) δ 159.8, 159.6, 141.3, 140.8, 139.4, 132.4, 130.2, 126.7, 126.6, 119.7, 117.6, 107.9, 35.7; FTIR (neat) 2922, 1548, 1393, 1153, 1044, 753; HRMS (ESI+) $[\text{M}+\text{H}]^+$ calculated for $\text{C}_{14}\text{H}_{12}\text{ClN}_4$: 271.0750, found 271.0745.

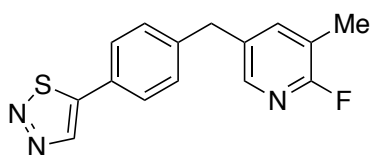


4-(5-(2-(1H-Pyrrol-1-yl)benzyl)pyridin-2-yl)morpholine (2-83). Prepared via General Procedure A using pyridinium salt **2-61**. The crude mixture was purified by silica gel chromatography (20% ethyl acetate/hexanes) to give **2-83** (run 1: 135 mg, 42%; run 2: 141 mg, 44%) as a white solid (mp 119–121 °C): ^1H NMR (400 MHz, CDCl_3) δ 7.89 (d, $J = 2.1$ Hz, 1H), 7.35 – 7.19 (m, 4H, *overlaps with CHCl₃*), 7.08 (dd, $J = 8.7, 2.5$ Hz, 1H), 6.74 (t, $J = 2.1$ Hz, 2H), 6.53 (d, $J = 8.7$ Hz, 1H), 6.31 (t, $J = 2.1$ Hz, 2H), 3.85 – 3.77 (m, 4H), 3.73 (s, 2H), 3.47 – 3.40 (m, 4H); ^{13}C NMR (101 MHz, CDCl_3) δ 158.3, 147.8, 140.3, 138.1, 136.9, 130.6, 128.0, 127.3, 127.1, 125.5, 122.3, 109.0, 106.8, 66.8, 45.8, 33.3; FTIR (neat) 2959, 2852, 1606, 1493, 1244, 1120, 494, 729 cm^{-1} ; HRMS (ESI+) $[\text{M}+\text{H}]^+$ calculated for $\text{C}_{20}\text{H}_{22}\text{N}_3\text{O}$: 320.1763, found 320.1749.



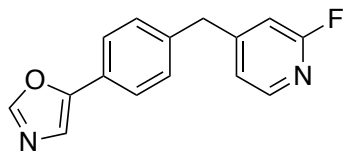
1-(2-(3-Fluoro-4-methylbenzyl)phenyl)-1H-pyrrole (2-84). Prepared via General Procedure A using pyridinium salt **2-61**. The crude mixture was purified by silica gel chromatography (25% toluene/hexanes) to give **2-84** (run 1: 220 mg, 83%; run 2: 236 mg, 89%) as a clear oil: ^1H NMR (400 MHz, CDCl_3) δ 7.35 – 7.27 (m, 3H), 7.26 – 7.21 (m, 1H), 7.07 – 6.98 (m, 1H), 6.72 (t, $J = 2.1$ Hz, 2H), 6.70 – 6.58 (m, 2H), 6.29 (t, $J = 2.1$ Hz, 2H), 3.81 (s, 2H), 2.21 (d, $J_{\text{H-F}} = 1.8$ Hz, 3H); ^{13}C NMR (101 MHz,

CDCl₃) δ 161.2 (d, J_{C-F} = 244.4 Hz), 140.4, 140.0 (d, J_{C-F} = 7.2 Hz), 136.5, 131.2 (d, J_{C-F} = 5.6 Hz), 130.9, 128.0, 127.3 (d, J_{C-F} = 6.7 Hz), 124.1 (d, J_{C-F} = 3.2 Hz), 122.5, 122.31, 122.28, 115.2 (d, J_{C-F} = 22.3 Hz), 108.9, 36.3 (d, J_{C-F} = 1.7 Hz), 14.2 (d, J_{C-F} = 3.4 Hz); ¹⁹F NMR (565 MHz, CDCl₃) δ -117.88; FTIR (neat) 3030, 2927, 2860, 1503, 1328, 1113, 728 cm⁻¹; HRMS (ESI+) [M+H]⁺ calculated for C₁₈H₁₇FN: 266.1345, found 266.1341.

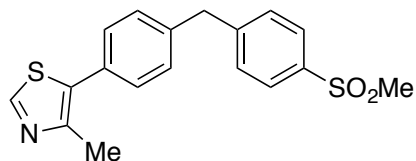


5-(4-((6-Fluoro-5-methylpyridin-3-yl)methyl)phenyl)-1,2,3-thiadiazole (2-85).

Prepared via General Procedure A using pyridinium salt **2-62**, except that the reaction mixture was heated for 24 h. The crude mixture was purified by silica gel chromatography (30–50% ether/hexanes) to give **2-85** (run 1: 172 mg, 60%; run 2: 188 mg, 66%) as a yellow solid (mp 141–143 °C): ¹H NMR (600 MHz, CDCl₃) δ 8.62 (s, 1H), 8.00 (d, J = 8.2 Hz, 2H), 7.93 (s, 1H), 7.42 – 7.36 (m, 1H), 7.32 (d, J = 8.2 Hz, 2H), 4.00 (s, 2H), 2.24 (s, 3H); ¹³C NMR (151 MHz, CDCl₃) δ 162.5, 161.2 (d_{C-F}, J = 237.3 Hz), 144.4 (d, J_{C-F} = 14.3 Hz), 142.0 (d, J_{C-F} = 6.0 Hz), 141.3, 133.7 (d, J_{C-F} = 4.7 Hz), 129.7, 129.6, 129.3, 127.8, 119.5 (d, J_{C-F} = 32.8 Hz), 37.8, 14.5 (d, J_{C-F} = 1.2 Hz); ¹⁹F NMR (565 MHz, CDCl₃) δ -75.62; FTIR (neat) 3091, 2923, 2851, 1590, 1464, 1244, 804, 544 cm⁻¹; HRMS (ESI+) [M+H]⁺ calculated for C₁₅H₁₃FN₃S: 286.0814, found 286.0810.

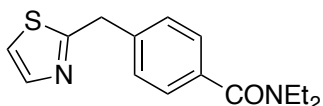


5-(4-((2-Fluoropyridin-4-yl)methyl)phenyl)oxazole (2-86). Prepared via General Procedure A using pyridinium salt **2-94**. The crude mixture was purified by silica gel chromatography (30% ethyl acetate/hexanes) to give **2-86** (run 1: 231 mg, 91%; run 2: 224 mg, 88%) as a pale yellow solid (mp 68–71 °C): ^1H NMR (400 MHz, CDCl_3) δ 8.18 – 8.12 (m, 1H), 7.94 (s, 1H), 7.69 – 7.62 (m, 2H), 7.37 (s, 1H), 7.27 (d, $J = 8.3$ Hz, 2H), 7.06 – 6.99 (m, 1H), 6.79 – 6.73 (m, 1H), 4.05 (s, 2H); ^{13}C NMR (101 MHz, CDCl_3) δ 164.2 (d, $J_{\text{C-F}} = 238.9$ Hz), 155.5 (d, $J_{\text{C-F}} = 7.7$ Hz), 151.2, 150.5, 147.7 (d, $J_{\text{C-F}} = 15.3$ Hz), 138.6, 129.7, 126.6, 124.9, 121.9 (d, $J_{\text{C-F}} = 4.0$ Hz), 121.6, 109.6 (d, $J_{\text{C-F}} = 37.2$ Hz), 40.8 (d, $J_{\text{C-F}} = 3.0$ Hz); ^{19}F NMR (376 MHz, CDCl_3) δ –68.31 ; FTIR (neat) 3124, 1611, 1410, 941, 819, 640 cm^{-1} ; HRMS (ESI+) $[\text{M}+\text{H}]^+$ calculated for $\text{C}_{15}\text{H}_{12}\text{FN}_2\text{O}$: 255.0934, found 255.0930.

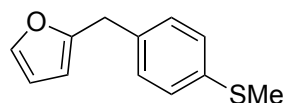


4-Methyl-5-(4-(4-(methylsulfonyl)benzyl)phenyl)thiazole (2-87). Prepared via General Procedure A using pyridinium salt **2-95**. The crude mixture was purified by silica gel chromatography (50% ethyl acetate/hexanes) to give **2-87** (run 1: 296 mg, 86%; run 2: 280 mg, 81%) as a pale yellow solid (mp 123–125 °C): ^1H NMR (600 MHz, CDCl_3) δ 8.67 (s, 1H), 7.91 – 7.86 (m, 2H), 7.44 – 7.37 (m, 4H), 7.26 – 7.21 (m, 2H), 4.11 (s, 2H), 3.05 (s, 3H), 2.53 (s, 3H); ^{13}C NMR (151 MHz, CDCl_3) δ 150.2, 148.6, 147.1, 139.2, 138.7, 131.5, 130.5, 129.8, 129.7, 129.3, 127.8, 44.6, 41.5, 16.1;

FTIR (neat) 2922, 1408, 1304, 1149, 759, 533 cm^{-1} ; HRMS (ESI+) $[\text{M}+\text{H}]^+$ calculated for $\text{C}_{18}\text{H}_{18}\text{NO}_2\text{S}_2$: 344.0779, found 344.0775.



N,N-Diethyl-4-(thiazol-2-ylmethyl)benzamide (2-88). Prepared via General Procedure A using pyridinium salt **2-63**. The crude mixture was purified by silica gel chromatography (50–80% ethyl acetate/hexanes) to give **2-88** (run 1: 264 mg, 96%; run 2: 259 mg, 94%) as a dark orange oil: ^1H NMR (400 MHz, CDCl_3) δ 7.71 (d, $J = 3.3$ Hz, 1H), 7.36 – 7.31 (m, 4H), 7.22 (d, $J = 3.3$ Hz, 1H), 4.36 (s, 2H), 3.66 – 3.39 (m, br, 2H), 3.39 – 3.09 (m, br, 2H), 1.35 – 1.17 (m, br, 3H), 1.17 – 0.95 (m, br, 3H); ^{13}C NMR (101 MHz, CDCl_3) δ 171.0, 169.5, 142.6, 138.9, 136.0, 129.0, 126.9, 119.2, 43.3, 39.3 (2C), 14.3, 12.9; FTIR (neat) 3077, 2972, 2933, 1627, 1427, 1427, 1288, 1095 cm^{-1} ; HRMS (ESI+) $[\text{M}+\text{H}]^+$ calculated for $\text{C}_{15}\text{H}_{19}\text{N}_2\text{OS}$: 275.1218, found 275.1212.



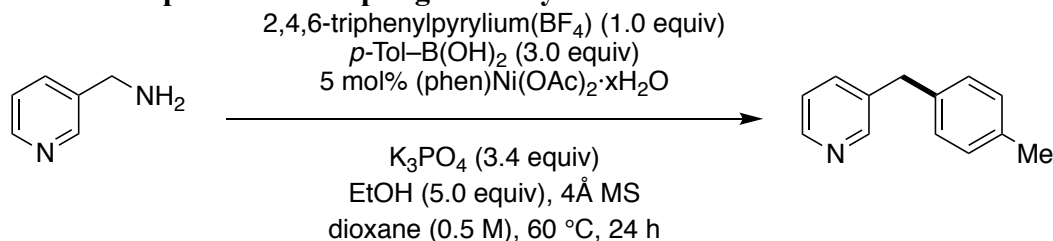
2-(4-(Methylthio)benzyl)furan (2-89). Prepared via General Procedure A using pyridinium salt **2-64**. The crude mixture was purified by silica gel chromatography (10–20% toluene/hexanes) to give **2-89** (run 1: 69 mg, 34%; run 2: 70 mg, 34%) as an orange oil: ^1H NMR (600 MHz, CDCl_3) δ 7.34 – 7.30 (m, 1H), 7.24 – 7.19 (m, 2H), 7.18 – 7.13 (m, 2H), 6.31 – 6.27 (m, 1H), 6.02 – 5.98 (m, 1H), 3.93 (s, 2H), 2.47 (s, 3H); ^{13}C NMR (151 MHz, CDCl_3) δ 154.4, 141.5, 136.3, 135.2, 129.2, 127.1, 110.2,

106.2, 34.0, 16.2; FTIR (neat) 3115, 3021, 2919, 1494, 1009, 799, 732 cm^{-1} ; HRMS (ESI+) $[\text{M}+\text{H}]^+$ calculated for $\text{C}_{12}\text{H}_{13}\text{OS}$: 205.0687, found 205.0677.

Reaction of Pyridinium Salt **2-64** without Ethanol

Product **2-89** also prepared via General Procedure A, except that no EtOH was added to the reaction mixture. The crude mixture was purified by silica gel chromatography (10–20% toluene/hexanes) to give **2-89** (95 mg, 47%).

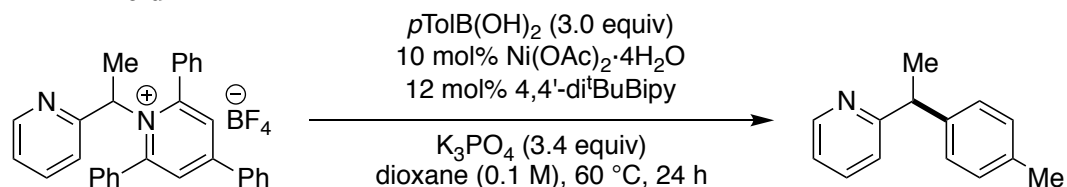
2.4.3.2 One-pot Cross-Coupling of Benzylamine with Boronic Acid



Product **2-65** was formed via a procedure adapted from General Procedure A, except that the pyridinium salt was formed in situ. To an oven-dried, 25-mL Schlenk flask was added PhenNi(OAc) $_2 \cdot x\text{H}_2\text{O}$ (20 mg, 0.050 mmol, 5 mol %), *p*-tolylboronic acid (408 mg, 3.0 equiv, 3.0 mmol), K_3PO_4 (722 mg, 3.4 mmol, 3.4 equiv), 2,4,6-triphenylpyrylium tetrafluoroborate (396 mg, 1.0 mmol, 1.0 equiv), and powered, activated 4Å molecular sieves (500 mg, 500 mg/mmol). The flask was fitted with a rubber septum, sealed with parafilm, and then evacuated and refilled with N_2 (x 3). Commercially available 3-(aminomethyl)pyridine (**2-90**) (sparged; 0.10 mL, 1.0 mmol, 1.0 equiv) was added, followed by dioxane (sparged, anhydrous; 2.0 mL) and EtOH (sparged, anhydrous; 0.29 mL, 5.0 mmol, 5.0 equiv). The resulting mixture was stirred at 60 °C for 24 h. The mixture was allowed to cool to room temperature, and then filtered through a small pad of Celite. The filter cake was washed with CH_2Cl_2 (4

x 25 mL), and the filtrate was concentrated. The crude mixture was purified by silica gel chromatography (50% ether/hexanes) to give **2-65** (140 mg, 76%).

2.4.3.3 Cross-Coupling of Secondary Benzylic Pyridinium Salt with Boronic Acid

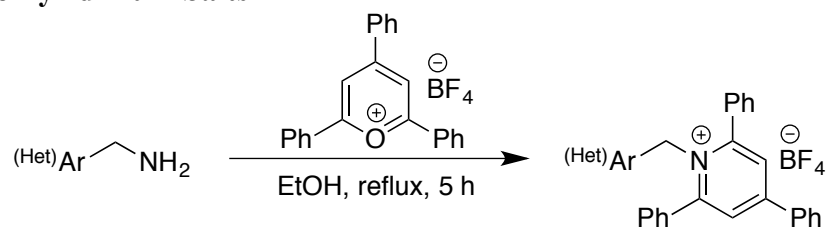


2-(1-(*p*-Tolyl)ethyl)pyridine (2-79). To an oven-dried, 25-mL pear-shaped flask, was added $\text{Ni(OAc)}_2 \cdot 4\text{H}_2\text{O}$ (25 mg, 0.10 mmol, 10 mol %) and 4,4'-di^tBuBipy (32 mg, 0.012 mmol, 12 mol %). The flask was fitted with a rubber septum, sealed with parafilm, and then evacuated and refilled with N_2 (x 3). To an oven-dried, 25-mL Schlenk flask was added pyridinium salt **2-59** (500 mg, 1.0 mmol, 1.0 equiv), *p*-tolylboronic acid (408 mg, 3.0 equiv, 3.0 mmol), and K_3PO_4 (722 mg, 3.4 mmol, 3.4 equiv). The flask was fitted with a rubber septum, sealed with parafilm, and then evacuated and refilled with N_2 (x 3). To the pear-shaped flask containing $\text{Ni(OAc)}_2 \cdot 4\text{H}_2\text{O}$ and 4,4'-di^tBuBipy was added dioxane (sparged, anhydrous; 2.5 mL). To the Schlenk flask containing the pyridinium salt, boronic acid, and K_3PO_4 was added dioxane (sparged, anhydrous; 2.5 mL). After vigorously stirring of the resulting mixtures for 1 h at room temperature, the heterogeneous mixture containing the catalyst was transferred via cannula to the mixture containing the pyridinium salt and activated boronate complex. The pear-shaped flask was rinsed multiple times with dioxane (totaling 5 mL; each rinse was transferred via cannula to the reaction mixture) to bring the total volume of dioxane in the reaction flask to 10 mL (0.1 M). The flask

was sealed off and resulting mixture was stirred at 60 °C for 24 h. The mixture was allowed to cool to room temperature, and then filtered through a small pad of Celite. The filter cake was washed with CH₂Cl₂ (4 x 25 mL), and the filtrate was concentrated. The cross-coupled product was then purified via silica gel chromatography (25% ether/hexanes) to give **2-79** (run 1: 92 mg, 47%; run 2: 85 mg, 43%): ¹H NMR (600 MHz, CDCl₃) δ 8.58 – 8.53 (m, 1H), 7.58 – 7.52 (m, 1H), 7.21 – 7.17 (m, 2H), 7.13 – 7.09 (m, 3H), 7.09 – 7.06 (m, 1H), 4.26 (q, *J* = 7.2 Hz, 1H), 2.31 (s, 3H), 1.69 (d, *J* = 7.2 Hz, 3H); ¹³C NMR (151 MHz, CDCl₃) δ 165.3, 149.1, 142.1, 136.3, 135.8, 129.2, 127.5, 122.0, 121.1, 47.0, 21.0, 20.8; FTIR (neat) 3048, 3006, 2968, 2927, 2871, 1588, 1432, 748, 549 cm⁻¹; HRMS (ESI+) [M+H]⁺ calculated for C₁₄H₁₆N: 198.1277, found 198.1272.

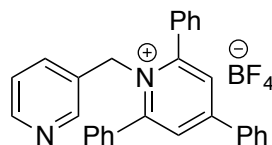
2.4.4 Preparation of Pyridinium Salts

2.4.4.1 General Procedure B: Conversion of Electron-poor (Hetero)Arylamines to Pyridinium Salts



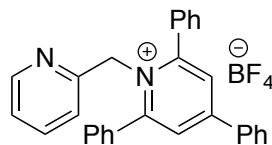
The following reaction was run open to air without oven-dried flasks. To a 25-mL, round-bottomed flask was added 2,4,6-triphenylpyridinium tetrafluoroborate (1.98 g, 5.0 mmol, 1.0 equiv) followed by EtOH (5 mL). Amine (6.0 mmol, 1.2 equiv) was added to the resulting suspension. The flask was fitted with a reflux condenser and heated in an oil bath at 80–85 °C for 5 h. The mixture was then allowed to cool to

room temperature. If product precipitation occurred during reflux or upon cooling, the solid was filtered, washed with EtOH (3 x 25 mL) and then Et₂O (3 x 25 mL), and dried under vacuum. If product precipitation did not occur, the solution was diluted with Et₂O (15 mL) and vigorously stirred for 1 h to induce precipitation. The resulting solid pyridinium salt was filtered and washed with Et₂O (3 x 25 mL). If the pyridinium salt failed to precipitate at this point, the flask containing the reaction mixture and Et₂O was sealed with parafilm and stored in a -27 °C freezer for 1–3 days (or until precipitation occurred). The cold mixture was quickly filtered and washed with Et₂O (3 x 25 mL) to give the corresponding analytically pure pyridinium salt. If the salt still did not precipitate, it was subjected to silica gel chromatography with acetone/CH₂Cl₂.



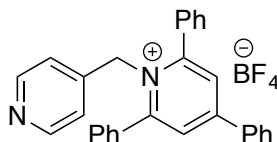
2,4,6-Triphenyl-1-(pyridin-3-ylmethyl)pyridin-1-ium tetrafluoroborate (2-47).

Prepared via General Procedure B on a 10 mmol scale with commercially available 3-(aminomethyl)pyridine to give **2-47** (4.37 g, 90%) as a white solid (mp 174–176 °C): ¹H NMR (600 MHz, CDCl₃) δ 8.42 – 8.37 (m, 1H), 7.97 (s, 2H), 7.83 – 7.78 (m, 2H), 7.75 – 7.71 (m, 1H), 7.70 – 7.66 (m, 4H), 7.63 – 7.58 (m, 1H), 7.57 – 7.48 (m, 8H), 7.07 – 7.01 (m, 1H), 6.88 – 6.82 (m, 1H), 5.84 (s, 2H); ¹³C NMR (151 MHz, CDCl₃) δ 157.5, 156.9, 149.6, 147.4, 134.5, 133.7, 132.6, 132.5, 131.3, 130.0, 129.9, 129.5, 129.1, 128.2, 126.8, 123.6, 56.0; ¹⁹F NMR (376 MHz, CDCl₃) δ -152.63 (minor, ¹¹BF₄), -152.68 (major, ¹⁰BF₄); FTIR (neat) 3063, 1622, 1599, 1057, 703 cm⁻¹; HRMS (ESI+) [M-BF₄]⁺ calculated for C₂₉H₂₃N₂: 399.1856, found 399.1855.



2,4,6-Triphenyl-1-(pyridin-2-ylmethyl)pyridin-1-ium tetrafluoroborate (2-48).

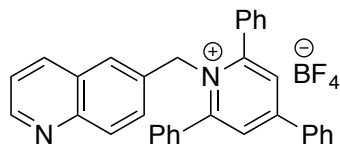
Prepared via General Procedure B on a 5.0 mmol scale with commercially available 2-(aminomethyl)pyridine to give **2-48** (2.28 g, 94%) as a white solid (mp 170–173 °C): ¹H NMR (600 MHz, CDCl₃) δ 8.46 – 8.42 (m, 1H), 7.94 (s, 2H), 7.85 – 7.80 (m, 2H), 7.66 – 7.52 (m, 7H), 7.49 – 7.42 (m, 2H), 7.42 – 7.34 (m, 5H), 7.16 – 7.11 (m, 1H), 6.52 (d, *J* = 7.8 Hz, 1H), 5.78 (s, 2H); ¹³C NMR (151 MHz, CDCl₃) δ 157.5, 155.9, 153.3, 149.2, 136.7, 134.1, 133.0, 132.1, 130.7, 129.7, 128.88, 128.85, 128.1, 126.1, 123.0, 121.8, 59.0; ¹⁹F NMR (565 MHz, CDCl₃) δ –153.30 (minor, ¹¹BF₄), –153.35 (major, ¹⁰BF₄); FTIR (neat) 3061, 1622, 1598, 1056, 764, 701 cm⁻¹; HRMS (ESI+) [M–BF₄]⁺ calculated for C₂₉H₂₃N₂: 399.1856, found 399.1859.



2,4,6-Triphenyl-1-(pyridin-4-ylmethyl)pyridin-1-ium tetrafluoroborate (2-49).

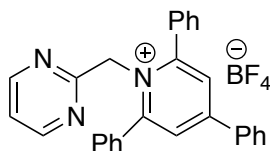
Prepared via General Procedure B on a 5.0 mmol scale with commercially available 4-(aminomethyl)pyridine to give **2-49** (1.70 g, 70%) as an orange solid (mp 168–172 °C): ¹H NMR (600 MHz, CDCl₃) δ 8.40 – 8.36 (m, 2H), 8.00 (s, 2H), 7.85 – 7.80 (m, 2H), 7.67 – 7.59 (m, 5H), 7.58 – 7.50 (m, 4H), 7.50 – 7.44 (m, 4H), 6.52 – 6.47 (m, 2H), 5.79 (s, 2H); ¹³C NMR (151 MHz, CDCl₃) δ 157.6, 157.0, 150.2, 143.0, 133.6, 132.7, 132.3, 131.3, 129.9, 129.4, 129.0, 128.2, 126.7, 120.9, 57.0; ¹⁹F NMR (565 MHz, CDCl₃) δ –152.85 (minor, ¹¹BF₄), –152.90 (major, ¹⁰BF₄); FTIR (neat) 3061,

1622, 1560, 1055, 702 cm^{-1} ; HRMS (ESI+) $[\text{M}-\text{BF}_4]^+$ calculated for $\text{C}_{29}\text{H}_{23}\text{N}_2$: 399.1856, found 399.1860.



2,4,6-Triphenyl-1-(quinolin-6-ylmethyl)pyridin-1-ium tetrafluoroborate (2-50).

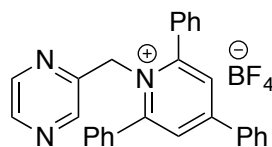
Prepared via General Procedure B on a 5.0 mmol scale with commercially available 6-aminomethylquinoline to give **2-50** (2.32 g, 87%) as a white solid (mp 207–210 °C): ^1H NMR (400 MHz, CDCl_3) δ 8.90 – 8.84 (m, 1H), 8.04 – 7.93 (m, 3H), 7.87 – 7.77 (m, 3H), 7.69 – 7.62 (m, 4H), 7.60 – 7.46 (m, 5H), 7.44 – 7.33 (m, 5H), 6.99 – 6.94 (m, 1H), 6.86 – 6.78 (m, 1H), 5.95 (s, 2H); ^{13}C NMR (101 MHz, CDCl_3) δ 157.5, 156.7, 151.3, 147.4, 136.2, 133.7, 132.7, 132.5, 132.0, 131.1, 130.3, 129.8, 129.3, 129.1, 128.2, 127.8, 126.8, 126.7, 126.3, 122.1, 58.1; ^{19}F NMR (376 MHz, CDCl_3) δ –152.50 (minor, $^{11}\text{BF}_4$), –152.55 (major, $^{10}\text{BF}_4$); FTIR (neat) 3062, 1622, 1564, 1057, 702 cm^{-1} ; HRMS (ESI+) $[\text{M}-\text{BF}_4]^+$ calculated for $\text{C}_{33}\text{H}_{25}\text{N}_2$: 449.2012, found 449.2018.



2,4,6-Triphenyl-1-(pyrimidin-2-ylmethyl)pyridin-1-ium tetrafluoroborate (2-51).

Prepared via General Procedure B on a 5.0 mmol scale with commercially available 2-aminomethylpyrimidine hydrochloride to give **2-51** (2.06 g, 85%) as an orange solid (mp 110–118 °C): ^1H NMR (600 MHz, CDCl_3) δ 8.52 (d, $J = 4.9$ Hz, 2H), 7.95 (s, 2H), 7.84 – 7.79 (m, 2H), 7.70 – 7.50 (m, 6H), 7.48 – 7.31 (m, 7H), 7.22 (t, $J = 4.9$

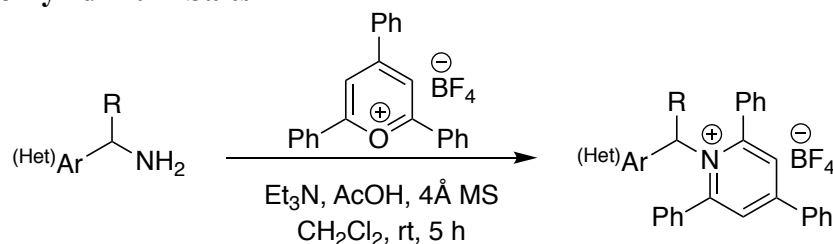
Hz, 1H), 5.79 (s, 2H); ^{13}C NMR (151 MHz, CDCl_3) δ 157.4, 157.3, 156.5, 134.1, 132.7, 132.2, 130.9, 129.7, 129.0, 128.7, 128.2, 126.3, 120.3, 120.2, 59.5; ^{19}F NMR (565 MHz, CDCl_3) δ -153.43 (minor, $^{11}\text{BF}_4$), -153.48 (major, $^{10}\text{BF}_4$); FTIR (neat) 3061, 1622, 1599, 1055, 702 cm^{-1} ; HRMS (ESI+) $[\text{M}-\text{BF}_4]^+$ calculated for $\text{C}_{28}\text{H}_{22}\text{N}_3$: 400.1808, found 400.1812.



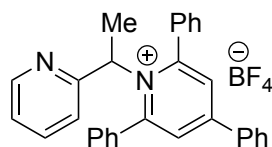
2,4,6-Triphenyl-1-(pyrazin-2-ylmethyl)pyridin-1-ium tetrafluoroborate (2-52).

Prepared via General Procedure B on a 5.0 mmol scale with commercially available 2-aminomethylpyrazine. The crude residue was purified via silica gel chromatography (10% acetone/dichloromethane) to give **2-52** (1.93 g, 79%) as an orange solid (mp 95–99 °C): ^1H NMR (600 MHz, CDCl_3) δ 8.44 – 8.40 (m, 2H), 7.97 (s, 2H), 7.86 – 7.81 (m, 2H), 7.76 – 7.72 (m, 1H), 7.65 – 7.53 (m, 7H), 7.53 – 7.47 (m, 2H), 7.47 – 7.41 (m, 4H), 5.87 (s, 2H); ^{13}C NMR (151 MHz, CDCl_3) δ 157.5, 156.4, 149.4, 144.1, 143.7, 143.5, 133.9, 132.7, 132.4, 131.2, 129.8, 129.1, 128.8, 128.1, 126.1, 56.8; ^{19}F NMR (565 MHz, CDCl_3) δ -152.94 (minor, $^{11}\text{BF}_4$), -152.99 (major, $^{10}\text{BF}_4$); FTIR (neat) 3063, 1624, 1569, 1418, 1057, 702 cm^{-1} ; HRMS (ESI+) $[\text{M}-\text{BF}_4]^+$ calculated for $\text{C}_{28}\text{H}_{22}\text{N}_3$: 400.1808, found 400.1811.

2.4.4.2 General Procedure C: Conversion of Electron-rich (Hetero)Arylamines to Pyridinium Salts



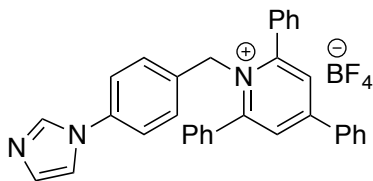
To a 50-mL round-bottomed flask was added 2,4,6-triphenylpyrillium tetrafluoroborate (1.98 g, 5.0 mmol, 1.0 equiv), amine (5.0 mmol, 1.0 equiv), and powered, activated 4Å molecular sieves (2.5 g, 0.5 g/mmol). The flask was fitted with a rubber septum. To the flask was added CH₂Cl₂ (anhydrous; 10 mL) followed by Et₃N (0.70 mL, 5.0 mmol, 1.0 equiv). The reaction mixture was stirred for 20 min at room temperature. To the flask was added AcOH (0.57 mL, 10.0 mmol, 2.0 equiv), and the resultant mixture was stirred for 5 h at room temperature. The mixture was filtered through a small pad of Celite, and the filter cake was washed with CH₂Cl₂ (4 x 15 mL). The resulting solution was washed with water (2 x 30 mL) and brine (1 x 30 mL). The organic extract was dried (MgSO₄), filtered, and concentrated. The residue was suspended in Et₂O (25 mL) and vigorously stirred for 1 h to induce precipitation. The resulting solid pyridinium salt was filtered and washed with Et₂O (3 x 25 mL). If the solid contained impurities, it was subjected to silica gel chromatography with acetone/CH₂Cl₂.



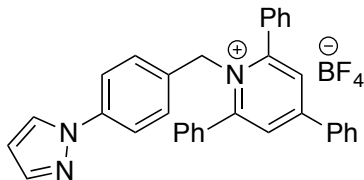
2,4,6-Triphenyl-1-(1-(pyridin-2-yl)ethyl)pyridin-1-ium tetrafluoroborate (2-59).

Prepared via General Procedure C on a 5.0 mmol scale with commercially available 1-

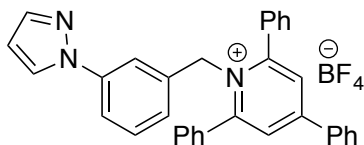
(pyridin-2-yl)ethan-1-amine to give **2-59** (2.31 g, 93%) as an orange solid (mp 119–123 °C): ^1H NMR (600 MHz, CDCl_3) δ 8.57 – 8.52 (m, 1H), 7.91 – 7.84 (m, 4H), 7.83 – 7.78 (m, 2H), 7.56 – 7.40 (m, 9H), 7.29 – 7.15 (m, 4H), 6.69 (d, $J = 8.0$ Hz, 1H), 6.22 (q, $J = 7.2$ Hz, 1H), 1.85 (d, $J = 7.2$ Hz, 3H); ^{13}C NMR (151 MHz, CDCl_3) δ 157.3, 157.2, 155.7, 149.3, 137.2, 134.2, 133.6, 131.9, 130.5, 129.6, 128.7, 128.5, 128.3, 127.9, 123.3, 120.5, 66.8, 18.4; ^{19}F NMR (565 MHz, CDCl_3) δ –153.26 (minor, $^{11}\text{BF}_4$), –153.31 (major, $^{10}\text{BF}_4$); FTIR (neat) 3061, 1621, 1564, 1055, 762, 699 cm^{-1} ; HRMS (ESI+) $[\text{M}-\text{BF}_4]^+$ calculated for $\text{C}_{30}\text{H}_{25}\text{N}_2$: 413.2012, found 413.2019.



1-(4-(1H-Imidazol-1-yl)benzyl)-2,4,6-triphenylpyridin-1-ium tetrafluoroborate (2-93). Prepared via General Procedure C on a 6.7 mmol scale with (4-(1H-imidazol-1-yl)phenyl)methanamine.⁵⁴ The crude residue was purified via silica gel chromatography (30% acetone/ CH_2Cl_2) to give **2-93** (1.69 g, 55%) as a yellow solid (mp 109–114 °C): ^1H NMR (600 MHz, CDCl_3) δ 8.01 (s, 2H), 7.89 – 7.83 (m, 2H), 7.82 – 7.78 (m, 1H), 7.73 – 7.66 (m, 4H), 7.65 – 7.50 (m, 9H), 7.24 – 7.15 (m, 4H), 6.68 – 6.62 (m, 2H), 5.87 (s, 2H); ^{13}C NMR (151 MHz, CDCl_3) δ 157.5, 156.7, 137.1, 135.2, 133.7, 133.2, 132.7, 132.6, 131.2, 130.8, 129.9, 129.4, 129.1, 128.2, 128.1, 126.8, 121.3, 117.8, 57.6; ^{19}F NMR (565 MHz, CDCl_3) δ –152.40 (minor, $^{11}\text{BF}_4$), –152.45 (major, $^{10}\text{BF}_4$); FTIR (neat) 3062, 1621, 1524, 1058, 701 cm^{-1} ; HRMS (ESI+) $[\text{M}-\text{BF}_4]^+$ calculated for $\text{C}_{33}\text{H}_{26}\text{N}_3$: 464.2121, found 464.2118.

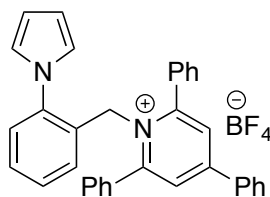


1-(4-(1H-Pyrazol-1-yl)benzyl)-2,4,6-triphenylpyridin-1-ium tetrafluoroborate (2-54). Prepared via General Procedure C on a 4.8 mmol scale with [4-(1H-pyrazol-1-yl)phenyl]methylamine.⁵⁵ The crude residue was purified via silica gel chromatography (10% acetone/CH₂Cl₂) to give **2-54** (1.87 g, 71%) as a yellow solid (mp 111–115 °C): ¹H NMR (600 MHz, CDCl₃) δ 7.97 (s, 2H), 7.86 – 7.84 (m, 1H), 7.84 – 7.80 (m, 2H), 7.70 – 7.64 (m, 5H), 7.60 – 7.46 (m, 11H), 6.57 (d, *J* = 8.3 Hz, 2H), 6.48 – 6.41 (m, 1H), 5.80 (s, 2H); ¹³C NMR (151 MHz, CDCl₃) δ 157.6, 156.6, 141.4, 139.9, 133.8, 132.7, 132.5, 132.0, 131.1, 129.8, 129.3, 129.1, 128.2, 127.5, 126.7, 126.7, 119.1, 108.1, 57.7; ¹⁹F NMR (565 MHz, CDCl₃) δ –152.83 (minor, ¹¹BF₄), –152.89 (major, ¹⁰BF₄); FTIR (neat) 3061, 1621, 1526, 1395, 1057, 701 cm⁻¹; HRMS (ESI+) [M–BF₄]⁺ calculated for C₃₃H₂₆N₃: 464.2121, found 464.2125.

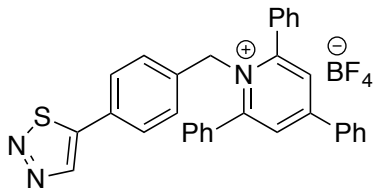


1-(3-(1H-Pyrazol-1-yl)benzyl)-2,4,6-triphenylpyridin-1-ium tetrafluoroborate (2-60). Prepared via General Procedure C on a 5.0 mmol scale with commercially available [3-(1H-pyrazol-1-yl)phenyl]methylamine. The crude residue was purified via silica gel chromatography (10% acetone/CH₂Cl₂) to give **2-60** (1.80 g, 65%) as a tan solid (mp 109–114 °C): ¹H NMR (600 MHz, CDCl₃) δ 7.96 (s, 2H), 7.83 – 7.78 (m, 2H), 7.77 – 7.73 (m, 1H), 7.71 – 7.62 (m, 5H), 7.60 – 7.44 (m, 10H), 7.19 (t, *J* = 7.9 Hz, 1H), 6.92 – 6.88 (m, 1H), 6.45 – 6.41 (m, 1H), 6.39 (d, *J* = 7.7 Hz, 1H), 5.82

(s, 2H); ^{13}C NMR (151 MHz, CDCl_3) δ 157.6, 156.5, 141.4, 140.4, 135.5, 133.7, 132.7, 132.5, 131.1, 130.0, 129.8, 129.3, 129.1, 128.2, 126.7, 126.6, 124.0, 118.5, 117.0, 108.1, 57.9; ^{19}F NMR (565 MHz, CDCl_3) δ -152.75 (minor, $^{11}\text{BF}_4$), -152.80 (major, $^{10}\text{BF}_4$); FTIR (neat) 3064, 1621, 1057, 765, 701 cm^{-1} ; HRMS (ESI+) $[\text{M}-\text{BF}_4]^+$ calculated for $\text{C}_{33}\text{H}_{26}\text{N}_3$: 464.2121, found 464.2129.

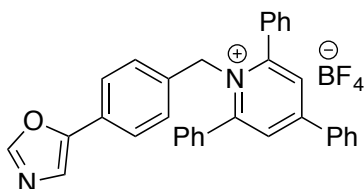


1-(2-(1H-Pyrrol-1-yl)benzyl)-2,4,6-triphenylpyridin-1-ium tetrafluoroborate (2-61). Prepared via General Procedure C on a 5.0 mmol scale with commercially available [2-(1H-pyrrol-1-yl)phenyl]methylamine to give **2-61** (2.16 g 78%) as a tan solid (mp 183–188 °C): ^1H NMR (600 MHz, CDCl_3) δ 7.86 (s, 2H), 7.82 – 7.77 (m, 2H), 7.60 – 7.55 (m, 5H), 7.54 – 7.50 (m, 4H), 7.47 – 7.41 (m, 4H), 7.30 – 7.24 (m, 2H, overlaps with CHCl_3), 6.99 – 6.95 (m, 1H), 6.79 – 6.74 (m, 1H), 6.14 (t, $J = 2.1$ Hz, 2H), 5.97 (t, $J = 2.1$ Hz, 2H), 5.64 (s, 2H); ^{13}C NMR (101 MHz, $(\text{CD}_3)_2\text{CO}$) δ 157.6, 156.3, 138.9, 133.7, 133.0, 132.6, 131.1, 130.2, 129.7, 129.3, 129.11, 129.09, 128.7, 128.2, 128.1, 127.0, 126.7, 121.8, 109.5, 55.8; ^{19}F NMR (565 MHz, CDCl_3) δ -153.04 (minor, $^{11}\text{BF}_4$), -153.09 (major, $^{10}\text{BF}_4$); FTIR (neat) 3063, 1620, 1503, 1056, 701 cm^{-1} ; HRMS (ESI+) $[\text{M}-\text{BF}_4]^+$ calculated for $\text{C}_{34}\text{H}_{27}\text{N}_2$: 463.2169, found 463.2176.



1-(4-(1,2,3-Thiadiazol-5-yl)benzyl)-2,4,6-triphenylpyridin-1-ium

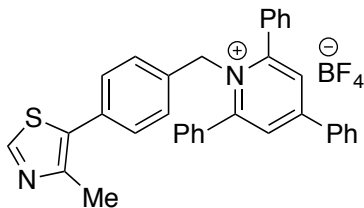
tetrafluoroborate (2-62). Prepared via General Procedure C on a 4.4 mmol scale with commercially available 4-(1,2,3-thiadiazol-5-yl)benzylamine to give **2-62** (2.53 g, quant.) as a yellow solid (mp 119–122 °C): ^1H NMR (600 MHz, CDCl_3) δ 8.68 (s, 1H), 7.98 (s, 2H), 7.85 – 7.80 (m, 4H), 7.74 – 7.70 (m, 3H), 7.63 – 7.42 (m, 10H), 6.63 (d, $J = 8.1$ Hz, 2H), 5.86 (s, 2H); ^{13}C NMR (151 MHz, CDCl_3) δ 161.6, 157.6, 156.6, 135.1, 133.7, 132.7, 132.5, 131.1, 130.89, 130.85, 129.8, 129.3, 129.1, 128.2, 127.7, 127.0, 126.7, 58.1; ^{19}F NMR (565 MHz, CDCl_3) δ –152.81 (minor, $^{11}\text{BF}_4$), –152.86 (major, $^{10}\text{BF}_4$); FTIR (neat) 3062, 1621, 1560, 1057, 701 cm^{-1} ; HRMS (ESI+) $[\text{M}-\text{BF}_4]^+$ calculated for $\text{C}_{32}\text{H}_{24}\text{N}_3\text{S}$: 482.1685, found 482.1693.



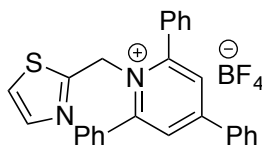
1-(4-(Oxazol-5-yl)benzyl)-2,4,6-triphenylpyridin-1-ium tetrafluoroborate (2-94).

Prepared via General Procedure C on a 2.8 mmol scale with [4-(1,3-oxazol-5-yl)phenyl]methanamine.⁵⁶ The crude residue was purified via silica gel chromatography (10% acetone/ CH_2Cl_2) to give **2-94** (0.680 g, 44%) as a yellow solid (mp 118–123 °C): ^1H NMR (600 MHz, CDCl_3) δ 7.98 (s, 2H), 7.89 (s, 1H), 7.86 – 7.82 (m, 2H), 7.69 – 7.66 (m, 3H), 7.63 – 7.45 (m, 10H), 7.42 – 7.38 (m, 2H), 7.31 (s, 1H), 6.58 – 6.54 (m, 2H), 5.81 (s, 2H); ^{13}C NMR (151 MHz, CDCl_3) δ 157.6, 156.6,

150.7, 150.4, 134.5, 133.8, 132.7, 132.5, 131.1, 129.8, 129.3, 129.1, 128.2, 127.7, 126.9, 126.7, 124.6, 122.3, 57.9; ^{19}F NMR (565 MHz, CDCl_3) δ -153.01 (minor, $^{11}\text{BF}_4$), -153.07 (major, $^{10}\text{BF}_4$); FTIR (neat) 3063, 1622, 1559, 1056, 701 cm^{-1} ; HRMS (ESI+) $[\text{M}-\text{BF}_4]^+$ calculated for $\text{C}_{33}\text{H}_{25}\text{N}_2\text{O}$: 465.1961, found 465.1963.

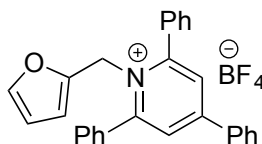


1-(4-(4-Methylthiazol-5-yl)benzyl)-2,4,6-triphenylpyridin-1-ium tetrafluoroborate (2-95). Prepared via General Procedure C on a 1.8 mmol scale with [4-(4-methyl-1,3-thiazol-5-yl)phenyl]methanamine.⁵⁷ The crude residue was purified via silica gel chromatography (10% acetone/ CH_2Cl_2) to give **2-95** (0.482 g, 46%) as a yellow solid (mp 89–108 °C): ^1H NMR (600 MHz, CDCl_3) δ 8.66 (s, 1H), 7.94 (s, 2H), 7.82 – 7.78 (m, 2H), 7.69 – 7.66 (m, 3H), 7.59 – 7.45 (m, 10H), 7.19 – 7.14 (m, 2H), 6.56 – 6.52 (m, 2H), 5.82 (s, 2H), 2.44 (s, 3H); ^{13}C NMR (151 MHz, $(\text{CD}_3)_2\text{CO}$) δ 158.2, 156.9, 151.5, 149.5, 134.7, 134.4, 133.9, 133.2, 132.60, 132.58, 131.7, 130.4, 130.0, 129.9, 129.8, 129.3, 127.7, 127.4, 58.9, 16.0; ^{19}F NMR (565 MHz, CDCl_3) δ -152.84 (minor, $^{11}\text{BF}_4$), -152.89 (major, $^{10}\text{BF}_4$); FTIR (neat) 3062, 1621, 1560, 1057, 701 cm^{-1} ; HRMS (ESI+) $[\text{M}-\text{BF}_4]^+$ calculated for $\text{C}_{34}\text{H}_{27}\text{N}_2\text{S}$: 495.1889, found 495.1890.



2,4,6-Triphenyl-1-(thiazol-2-ylmethyl)pyridin-1-ium tetrafluoroborate (2-63). Prepared via General Procedure C on a 5.0 mmol scale with commercially available 2-

(aminomethyl)thiazole to give **2-63** (2.12 g, 86%) as a tan solid (mp 209–215 °C): ^1H NMR (600 MHz, CDCl_3) δ 7.95 (s, 2H), 7.84 – 7.79 (m, 2H), 7.71 – 7.64 (m, 4H), 7.61 – 7.42 (m, 10H), 7.23 (d, $J = 3.2$ Hz, 1H), 5.93 (s, 2H); ^{13}C NMR (101 MHz, CDCl_3) δ 162.1, 157.3, 156.4, 142.4, 133.9, 132.6, 132.4, 131.0, 129.8, 129.0, 128.9, 128.2, 126.2, 121.2, 55.5; ^{19}F NMR (565 MHz, CDCl_3) δ –153.23 (minor, $^{11}\text{BF}_4$), –153.29 (major, $^{10}\text{BF}_4$); FTIR (neat) 3060, 1621, 1055, 767, 701 cm^{-1} ; HRMS (ESI+) $[\text{M}-\text{BF}_4]^+$ calculated for $\text{C}_{27}\text{H}_{21}\text{N}_2\text{S}$: 405.1420, found 405.1423.

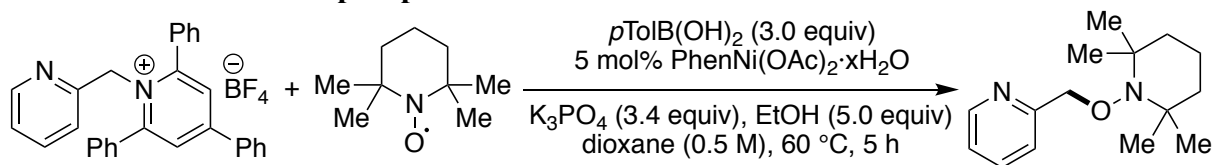


1-(Furan-2-ylmethyl)-2,4,6-triphenylpyridin-1-ium tetrafluoroborate (2-64).

Prepared via General Procedure C on a 5.0 mmol scale with commercially available 2-aminomethylfuran to give **2-64** (1.05 g, 44%) as a tan solid (mp 109–111 °C, decomp): ^1H NMR (600 MHz, CDCl_3) δ 7.91 (s, 2H), 7.81 – 7.77 (m, 2H), 7.75 – 7.70 (m, 4H), 7.59 – 7.51 (m, 9H), 7.23 (s, 1H), 6.11 – 6.07 (m, 1H), 5.71 (s, 2H), 5.37 – 5.33 (m, 1H); ^{13}C NMR (151 MHz, CDCl_3) δ 157.4, 156.3, 145.7, 143.1, 133.8, 132.7, 132.3, 131.0, 129.8, 129.2, 129.1, 128.1, 126.5, 110.9, 110.2, 51.9; ^{19}F NMR (565 MHz, CDCl_3) δ –152.98 (minor, $^{11}\text{BF}_4$), –153.03 (major, $^{10}\text{BF}_4$); FTIR (neat) 3063, 1621, 1056, 736, 701 cm^{-1} ; HRMS (ESI+) $[\text{M}-\text{BF}_4]^+$ calculated for $\text{C}_{28}\text{H}_{22}\text{NO}$: 388.1696, found 388.1682.

2.4.5 Mechanistic Experiment

2.4.5.1 Radical Trap Experiment



In a N_2 -filled glovebox, $\text{PhenNi(OAc)}_2 \cdot x\text{H}_2\text{O}$ (2.0 mg, 0.005 mmol, 5 mol %), 2,2,6,6-tetramethylpiperidine-*N*-oxyl (TEMPO; 31 mg, 0.20 mmol, 2.0 equiv), pyridinium salt **2-48** (49 mg, 0.1 mmol, 1.0 equiv), *p*-tolylboronic acid (41 mg, 0.3 mmol, 3.0 equiv), and K_3PO_4 (722 mg, 3.4 mmol, 3.4 equiv) were added to an oven-dried 1-dram vial. Dioxane (200 μL) was added to the vial. The vial was then equipped with a stir bar, capped with a pierceable Teflon-coated cap, and removed from the glovebox. To the vial was added EtOH (29 μL) via a N_2 -purged syringe. The resulting mixture was stirred vigorously at 60 °C for 5 h. The mixture was then diluted with EtOAc (1.5 mL) and filtered through a short plug of silica gel. The filter cake was washed with EtOAc (10 mL), and the filtrate was concentrated. 1,3,5-Trimethoxybenzene (internal standard) and CDCl_3 were added. The yield of known TEMPO adduct **2-92**⁵⁸ was determined to be 32% by analysis of the $^1\text{H-NMR}$ spectrum of the crude reaction mixture. No cross-coupled product was observed.

REFERENCES

1. Brogden, R. N.; Carmine, A. A.; Heel, R. C.; Speight, T. M.; Avery, G. S., *Drugs* **1982**, *23*, 405-430.
2. Shimura, K.; Kodama, E.; Sakagami, Y.; Matsuzaki, Y.; Watanabe, W.; Yamataka, K.; Watanabe, Y.; Ohata, Y.; Doi, S.; Sato, M.; Kano, M.; Ikeda, S.; Matsuoka, M., *Journal of Virology* **2008**, *82*, 764.
3. de Wit, R.; Kaye, S. B.; Roberts, J. T.; Stoter, G.; Scott, J.; Verweij, J., *British Journal Of Cancer* **1993**, *67*, 388.
4. Iyer, R.; Wehrmann, L.; Golden, R. L.; Naraparaju, K.; Croucher, J. L.; MacFarland, S. P.; Guan, P.; Kolla, V.; Wei, G.; Cam, N.; Li, G.; Hornby, Z.; Brodeur, G. M., *Cancer Letters* **2016**, *372*, 179-186.
5. Davoren, J. E.; Garnsey, M.; Pettersen, B.; Brodney, M. A.; Edgerton, J. R.; Fortin, J.-P.; Grimwood, S.; Harris, A. R.; Jenkinson, S.; Kenakin, T.; Lazzaro, J. T.; Lee, C.-W.; Lotarski, S. M.; Nottebaum, L.; O'Neil, S. V.; Popiolek, M.; Ramsey, S.; Steyn, S. J.; Thorn, C. A.; Zhang, L.; Webb, D., *Journal of Medicinal Chemistry* **2017**, *60*, 6649-6663.
6. Davoren, J. E.; Lee, C.-W.; Garnsey, M.; Brodney, M. A.; Cordes, J.; Dlugolenski, K.; Edgerton, J. R.; Harris, A. R.; Helal, C. J.; Jenkinson, S.; Kauffman, G. W.; Kenakin, T. P.; Lazzaro, J. T.; Lotarski, S. M.; Mao, Y.; Nason, D. M.; Northcott, C.; Nottebaum, L.; O'Neil, S. V.; Pettersen, B.; Popiolek, M.; Reinhart, V.; Salomon-Ferrer, R.; Steyn, S. J.; Webb, D.; Zhang, L.; Grimwood, S., *Journal of Medicinal Chemistry* **2016**, *59*, 6313-6328.
7. Molander, G. A.; Elia, M. D., *The Journal of Organic Chemistry* **2006**, *71*, 9198-9202.
8. Schmink, J. R.; Tudge, M. T., *Tetrahedron Letters* **2013**, *54*, 15-20.

9. Chard, E. F.; Dawe, L. N.; Kozak, C. M., *Journal of Organometallic Chemistry* **2013**, *737*, 32-39.
10. Dunsford, J. J.; Clark, E. R.; Ingleson, M. J., *Angewandte Chemie International Edition* **2015**, *54*, 5688-5692.
11. Zhang, J.; Lu, G.; Xu, J.; Sun, H.; Shen, Q., *Org. Lett.* **2016**, *18*, 2860-2863.
12. Yu, D.-G.; Wang, X.; Zhu, R.-Y.; Luo, S.; Zhang, X.-B.; Wang, B.-Q.; Wang, L.; Shi, Z.-J., *J. Am. Chem. Soc.* **2012**, *134*, 14638-14641.
13. Tobisu, M.; Yasutome, A.; Kinuta, H.; Nakamura, K.; Chatani, N., *Org. Lett.* **2014**, *16*, 5572-5575.
14. Stewart, G. W.; Maligres, P. E.; Baxter, C. A.; Junker, E. M.; Krska, S. W.; Scott, J. P., *Tetrahedron* **2016**, *72*, 3701-3706.
15. Kuwano, R.; Yokogi, M., *Org. Lett.* **2005**, *7*, 945-947.
16. Kuwano, R.; Yokogi, M., *Chemical Communications* **2005**, 5899-5901.
17. McLaughlin, M., *Org. Lett.* **2005**, *7*, 4875-4878.
18. Kofink, C. C.; Knochel, P., *Org. Lett.* **2006**, *8*, 4121-4124.
19. Zhou, Q.; Srinivas, H. D.; Dasgupta, S.; Watson, M. P., *J. Am. Chem. Soc.* **2013**, *135*, 3307-3310.
20. Zhou, Q.; Cobb, K. M.; Tan, T.; Watson, M. P., *J. Am. Chem. Soc.* **2016**, *138*, 12057-12060.
21. Taylor, B. L. H.; Swift, E. C.; Waetzig, J. D.; Jarvo, E. R., *J. Am. Chem. Soc.* **2011**, *133*, 389-391.
22. Taylor, B. L. H.; Harris, M. R.; Jarvo, E. R., *Angewandte Chemie International Edition* **2012**, *51*, 7790-7793.
23. Harris, M. R.; Hanna, L. E.; Greene, M. A.; Moore, C. E.; Jarvo, E. R., *J. Am. Chem. Soc.* **2013**, *135*, 3303-3306.
24. Wisniewska, H. M.; Swift, E. C.; Jarvo, E. R., *J. Am. Chem. Soc.* **2013**, *135*, 9083-9090.
25. Li, C.; Zhang, Y.; Sun, Q.; Gu, T.; Peng, H.; Tang, W., *J. Am. Chem. Soc.* **2016**, *138*, 10774-10777.

26. Tobisu, M.; Takahira, T.; Chatani, N., *Org. Lett.* **2015**, *17*, 4352-4355.
27. Blümke, T. D.; Groll, K.; Karaghiosoff, K.; Knochel, P., *Org. Lett.* **2011**, *13*, 6440-6443.
28. Duez, S.; Steib, A. K.; Manolikakes, S. M.; Knochel, P., *Angewandte Chemie International Edition* **2011**, *50*, 7686-7690.
29. Imao, D.; Glasspoole, B. W.; Laberge, V. S.; Crudden, C. M., *J. Am. Chem. Soc.* **2009**, *131*, 5024-5025.
30. Maity, P.; Shacklady-McAtee, D. M.; Yap, G. P. A.; Sirianni, E. R.; Watson, M. P., *J. Am. Chem. Soc.* **2013**, *135*, 280-285.
31. Shacklady-McAtee, D. M.; Roberts, K. M.; Basch, C. H.; Song, Y.-G.; Watson, M. P., *Tetrahedron* **2014**, *70*, 4257-4263.
32. Wang, T.; Yang, S.; Xu, S.; Han, C.; Guo, G.; Zhao, J., *RSC Advances* **2017**, *7*, 15805-15808.
33. Li, M.-B.; Tang, X.-L.; Tian, S.-K., *Adv. Synth. Catal.* **2011**, *353*, 1980-1984.
34. Yoon, S.; Hong, M. C.; Rhee, H., *The Journal of Organic Chemistry* **2014**, *79*, 4206-4211.
35. Nystrom, R. F.; Brown, W. G., *J. Am. Chem. Soc.* **1948**, *70*, 3738-3740.
36. Cha, J. S.; Brown, H. C., *The Journal of Organic Chemistry* **1993**, *58*, 3974-3979.
37. Gross, T.; Seayad, A. M.; Ahmad, M.; Beller, M., *Org. Lett.* **2002**, *4*, 2055-2058.
38. Bartoli, G.; Di Antonio, G.; Giovannini, R.; Giuli, S.; Lanari, S.; Paoletti, M.; Marcantoni, E., *The Journal of Organic Chemistry* **2008**, *73*, 1919-1924.
39. Laval, S.; Dayoub, W.; Pehlivan, L.; Métay, E.; Favre-Réguillon, A.; Delbrayelle, D.; Mignani, G.; Lemaire, M., *Tetrahedron Letters* **2011**, *52*, 4072-4075.
40. Basch, C. H.; Liao, J.; Xu, J.; Piane, J. J.; Watson, M. P., *J. Am. Chem. Soc.* **2017**, *139*, 5313-5316.
41. Katritzky, A. R.; Manzo, R. H., *Journal of the Chemical Society, Perkin Transactions 2* **1981**, 571-575.

42. Katritzky, A. R.; Rubio, O.; Aurrecochea, J. M.; Patel, R. C., *Journal of the Chemical Society, Perkin Transactions I* **1984**, 941-945.
43. Marquet, J.; Moreno-Mañas, M.; Pacheco, P.; Prat, M.; Katritzky, A. R.; Brycki, B., *Tetrahedron* **1990**, *46*, 5333-5346.
44. Jones, G. D.; Martin, J. L.; McFarland, C.; Allen, O. R.; Hall, R. E.; Haley, A. D.; Brandon, R. J.; Konovalova, T.; Desrochers, P. J.; Pulay, P.; Vivic, D. A., *J. Am. Chem. Soc.* **2006**, *128*, 13175-13183.
45. Biswas, S.; Weix, D. J., *J. Am. Chem. Soc.* **2013**, *135*, 16192-16197.
46. Liao, J.; Guan, W.; Boscoe, B. P.; Tucker, J. W.; Tomlin, J. W.; Garnsey, M. R.; Watson, M. P., *Org. Lett.* **2018**, *20*, 3030-3033.
47. Knochel, P.; Lutter, F. H., *Synfacts* **2018**, *14*, 0858.
48. Pangborn, A. B.; Giardello, M. A.; Grubbs, R. H.; Rosen, R. K.; Timmers, F. J., *Organometallics* **1996**, *15*, 1518-1520.
49. Ye, B.-H.; Chen, X.-M.; Xue, G.-Q.; Ji, L.-N., *Journal of the Chemical Society, Dalton Transactions* **1998**, 2827-2832.
50. Chen, X.; Zhou, L.; Li, Y.; Xie, T.; Zhou, S., *The Journal of Organic Chemistry* **2014**, *79*, 230-239.
51. Otohiko, T.; Shuji, K.; Toshio, N.; Junji, T., *Bulletin of the Chemical Society of Japan* **1987**, *60*, 1497-1504.
52. Tran, D. N.; Battilocchio, C.; Lou, S.-B.; Hawkins, J. M.; Ley, S. V., *Chemical Science* **2015**, *6*, 1120-1125.
53. De Houwer, J.; Abbaspour Tehrani, K.; Maes, B. U. W., *Angewandte Chemie International Edition* **2012**, *51*, 2745-2748.
54. Zhang, X., CN105254613 (A), 2016/01/20/, 2016.
55. Lewis, J. G.; Jacobs, J. W.; Reich, N.; Leadbetter, M. R.; Bell, N.; Chang, H.-T.; Chen, T.; Navre, M.; Charmot, D.; Carreras, C.; Labonte, E., US2015164876 (A1), 2015/06/18/, 2015.

56. Crews, C.; Buckley, D.; Ciulli, A.; Jorgensen, W.; Gareiss, P.; Molle, I.; Gustafson, J.; Tae, H.-S.; Michel, J.; Hoyer, D.; Roth, A.; Harling, J.; Smith, I. E.; Miah, A.; Campos, S.; Le, J., WO2013106643 (A2), 2013/07/18/, 2013.
57. Buckley, D. L.; Gustafson, J. L.; Van Molle, I.; Roth, A. G.; Tae, H. S.; Gareiss, P. C.; Jorgensen, W. L.; Ciulli, A.; Crews, C. M., *Angewandte Chemie International Edition* **2012**, *51*, 11463-11467.
58. Badsara, S. S.; Liu, Y.-C.; Hsieh, P.-A.; Zeng, J.-W.; Lu, S.-Y.; Liu, Y.-W.; Lee, C.-F., *Chemical Communications* **2014**, *50*, 11374-11377.

Chapter 3

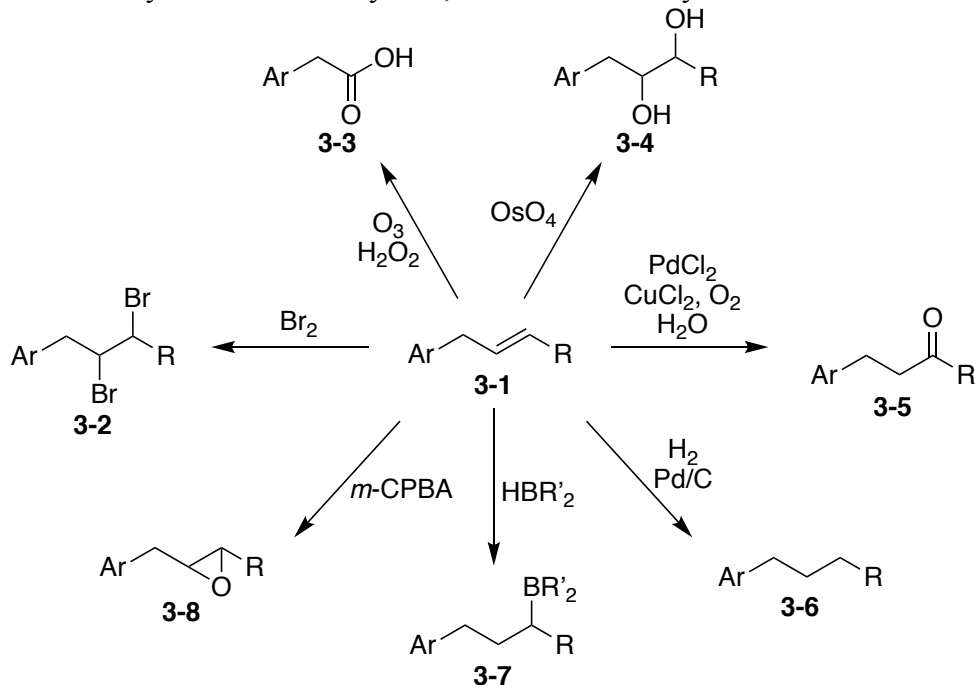
SUZUKI–MIYAURA CROSS-COUPLING OF BENZYLIC PYRIDINIUM SALTS WITH VINYLBORONIC ACIDS

Work described here has already been published (Guan, W.; Liao, J.; Watson, M. P. *Synthesis*, **2018**, 50 (16), 3231–3237). It is reprinted in this chapter with permission of *Synthesis* (Copyright © 2018, Georg Thieme Verlag KG). Weiye Guan and I are co-first authors.

3.1 Introduction

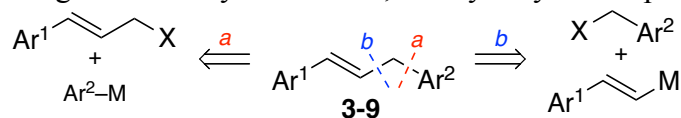
1,3-Disubstituted allylic molecules have proven to be versatile intermediates in the synthesis of complex organic molecules.¹⁻⁴ They can be elaborated via the functionalization of the alkene or reactive benzylic position (Scheme 3.1). Excitingly, these molecules can participate in a number of oxidation and reduction reactions as well as addition reactions. Moreover, 1,3-diaryl allylic molecules themselves can possess promising biological activity.⁵⁻⁸ Building on our success in cross-coupling benzylic pyridinium salts, we believed that an analogous approach would open a new avenue for the synthesis of these valuable molecules.

Scheme 3.1 Synthetic versatility of 1,3-disubstituted allylic molecules



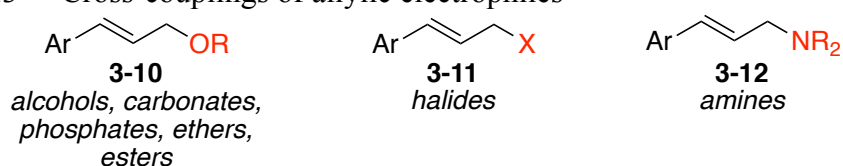
The importance of this motif has encouraged the development of efficient methods to access these targets (**3-9**), with transition metal-catalyzed cross-couplings being a predominant approach. A common strategy employs the cross-coupling of an allylic electrophile with an aryl nucleophile (Scheme 3.2, left). However, controlling regioselectivity and stereoselectivity of the alkene geometry can be challenging. An alternative disconnection relies on the cross-coupling of a benzylic electrophile with a vinyl nucleophile (Scheme 3.2, right). This approach mitigates many of the problematic isomerization issues.

Scheme 3.2 Strategies for the synthesis of 1,3-diaryl allylic compounds



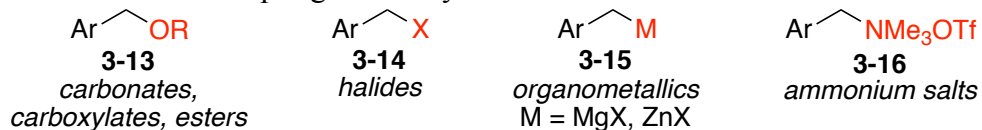
The former approach leverages the wide availability of allylic electrophiles (Scheme 3.3). Towards this end, allylic alcohols⁹⁻¹⁵, carbonates,^{16, 17} phosphates,¹⁸ ethers,¹⁹ and esters²⁰⁻²³ have been utilized as electrophiles in this type of chemistry. Additionally, allylic halides²⁴⁻²⁶ and amine derivatives^{27, 28} have also been demonstrated to be competent electrophiles. The ability to be cross-coupled with various organometallic aryl nucleophiles (e.g., Ar–BX₂, Ar–MgX) allows for rapid diversifications of these precursors. However, many of these reactions proceed via a π -allyl intermediate, which can lead to the formation of undesired regioisomers.

Scheme 3.3 Cross-couplings of allylic electrophiles



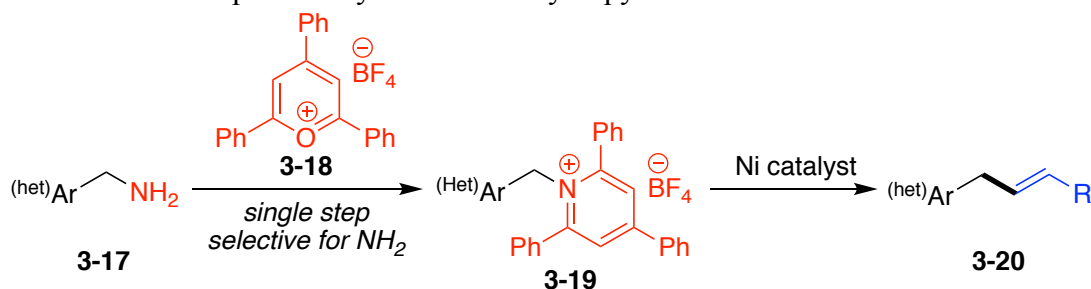
The latter approach utilizes benzylic electrophiles in conjunction with a vinyl nucleophile (Scheme 3.4). Benzylic alcohol derivatives (carbonates, carboxylates, esters)^{29, 30} and halides³¹⁻³⁵ are frequently employed. In addition, the umpolung approach of cross-coupling a benzylic nucleophile with a vinyl electrophile³⁶⁻³⁸ as well as reductive cross-electrophile couplings of benzylic and vinyl halides³⁹⁻⁴² have also been reported. In contrast, examples of cross-couplings of benzylic amine derivatives with vinyl nucleophiles are much more limited. In one of these examples, our group has shown that benzylic trimethylammonium salts (**3-16**) can participate in Suzuki–Miyaura cross-couplings with vinylboronic acids.⁴³⁻⁴⁶

Scheme 3.4 Cross-couplings of benzylic substrates



While these methods are highly efficient in the formation of 1,3-disubstituted allylic products, heteroaryl substitution is largely neglected. Given the importance of heteroaromatics in bioactive molecules as well as the abundance of benzylic amines, we envisioned that the cross-coupling of benzylic pyridinium salt **3-19** with vinyl boronic acids would afford vinylated product **3-20** bearing a useful alkene handle (Scheme 3.5). More importantly, this would allow for the incorporation of heteroaryl fragments from readily available benzylic amine precursors **3-17**.

Scheme 3.5 Proposed vinylation of benzylic pyridinium salts

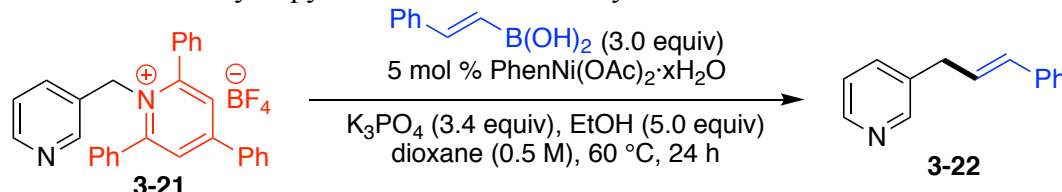


3.2 Results and Discussion

Given our success with nickel-catalyzed Suzuki–Miyaura arylation of benzylic pyridinium salts (Chapter 2), we wanted to extend these conditions to incorporate other nucleophiles such as vinylboronic acids. Gratifyingly, the desired vinylated product **3-22** was produced in 76% yield under the previously optimized conditions (Table 3.1, entry 1). Surprisingly, in the absence of nickel catalyst, the formation of **3-**

22 was also observed, albeit in slightly diminished yield (entry 2). Moreover, in an effort to improve the utility of this reaction, we found that only two equivalents of boronic acid were needed (entry 3). In this case, omission of nickel catalyst led to a greatly reduced yield (entry 4). The pinacol boronic ester could also be used, requiring only 2.5 equivalents of base (entry 5). The ability to cross-couple either a boronic acid or a boronic ester broadens the pool of commercially available reagents that can be used.

Table 3.1 Reaction optimization of the Suzuki–Miyaura cross-coupling of benzylic pyridinium salts with vinylboronic acids^a

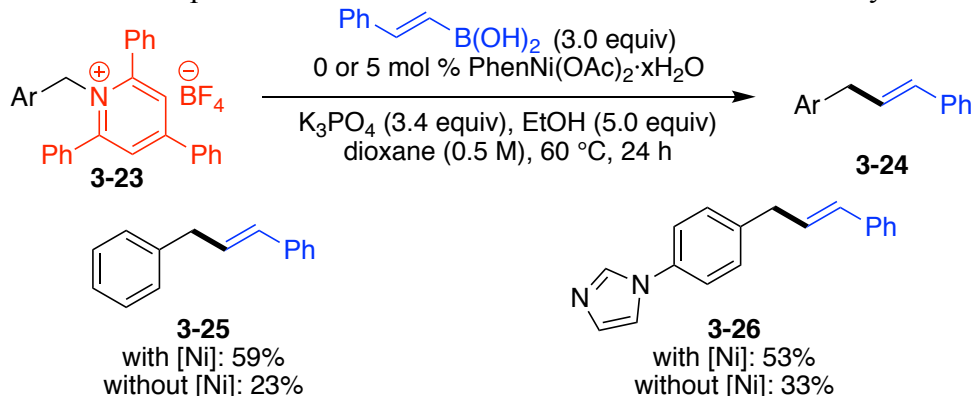


Entry	Modification from original conditions	Yield (%) ^b
1	none	76
2	no PhenNi(OAc) ₂ ·xH ₂ O	62
3	boronic acid (2 equiv)	74
4	no PhenNi(OAc) ₂ ·xH ₂ O, boronic acid (2 equiv)	46
5	boronic acid pinacol ester (2.0 equiv), K ₃ PO ₄ (2.5 equiv)	74

^aConditions: pyridinium salt **3-22** (0.10 mmol), PhenNi(OAc)₂·xH₂O (5 mol %), boronic acid (3.0 equiv), K₃PO₄ (3.4 equiv), EtOH (5 equiv), dioxane (0.5 M), 60 °C, 24 h. ^bDetermined by ¹H NMR analysis using 1,3,5-trimethoxybenzene as internal standard.

We were intrigued by the transition-metal-free results and wanted to probe this possibility further. In using only two equivalents of boronic acid, the nickel-catalyzed reaction, produced vinylated product **3-22** in 74% yield, while the metal-free reaction gave only 46% yield (Table 3.1, entries 3 & 4). Similarly, the metal-free conditions proved less effective for other substrates (Scheme 3.6). Phenyl-substituted product **3-25** and imidazole **3-26** were formed in only 23% and 33% yield, respectively, under these conditions. In all cases, a considerable drop in yield was observed when switching to the metal-free conditions. These results demonstrate that a metal-free reaction is feasible but not as efficient as the nickel-catalyzed pathway. There are a few reports of metal-free vinylation reactions.⁴⁷⁻⁴⁹ We believe that a similar pathway is operational in our case, whereby nucleophilic attack (likely S_N2) of a vinyl boronate to the benzylic pyridinium ion leads to the formation of desired product. However, in the presence of the nickel catalyst, a Ni^{I/III} (or Ni^{0/II}) catalytic cycle may also be at play. We are also cognizant of the possibility that nickel may act as a Lewis acid. Because higher yields are observed with all three substrates, we proceeded to investigate the scope of the reaction in the presence of the nickel catalyst. Notably, these conditions are also the less expensive choice. For a 1.0-mmol scale reaction, the cost of 5 mol % Ni(OAc)₂·4H₂O and 5 mol % Phen (approximately \$0.20 from Sigma-Aldrich) is less than an extra equivalent of phenylvinylboronic acid (approximately \$2.00) or pinacol ester (approximately \$10.40).

Scheme 3.6 Comparison of reactions with and without the nickel catalyst^a

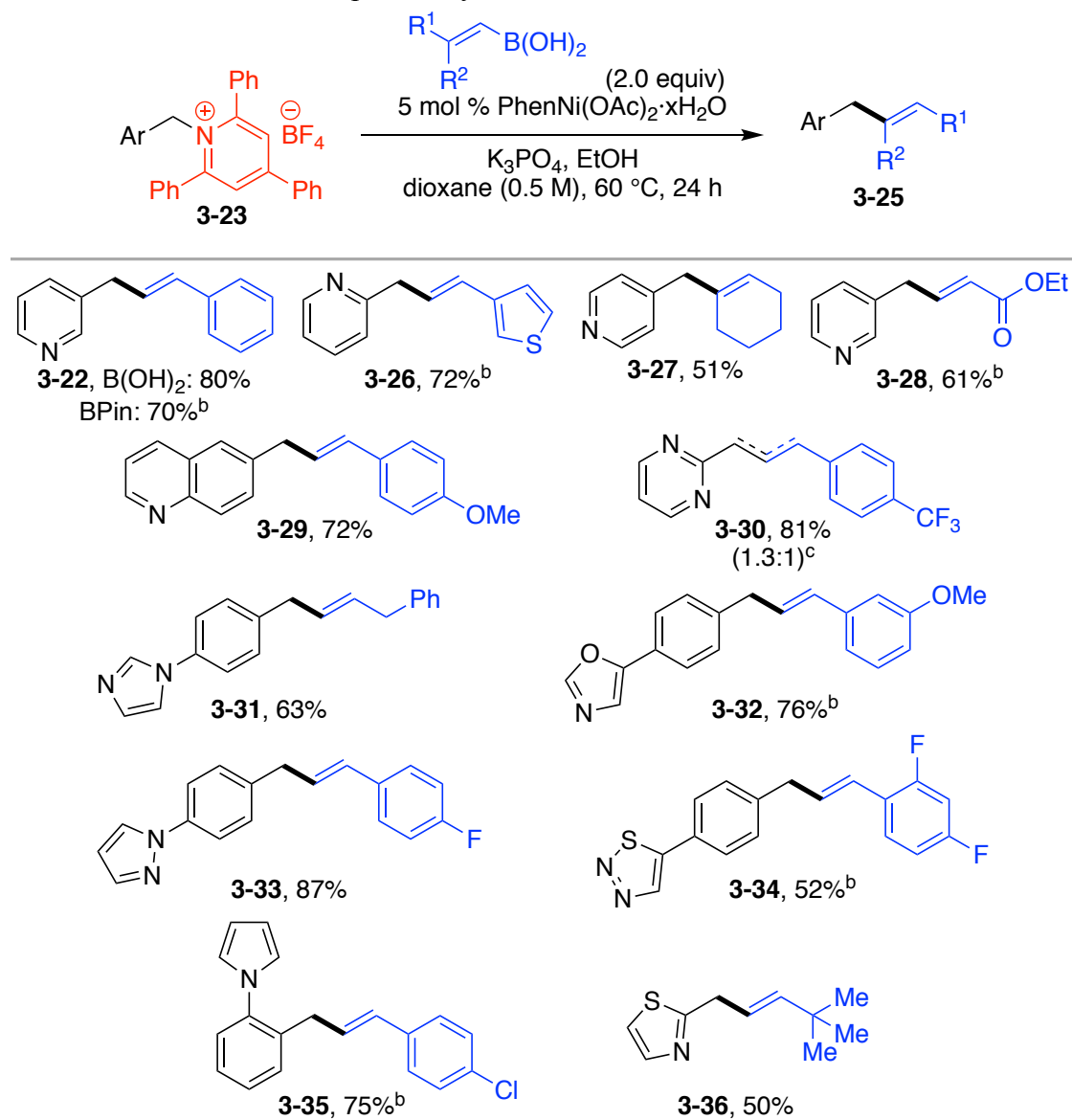


^aConditions: Salt **3-23** (0.1 mmol), $\text{PhenNi(OAc)}_2 \cdot x\text{H}_2\text{O}$ (0 or 5 mol %), boronic acid (2.0 equiv), K_3PO_4 (3.4 equiv), EtOH (5 equiv), dioxane (0.5 M), 60 °C, 24 h. Yields determined by ¹H NMR analysis using 1,3,5-trimethoxybenzene as internal standard.

With optimized conditions in hand, my colleague Weiye Guan and I demonstrated the broad scope of this transformation. In particular, we prioritized substrates with heteroaryl substituents. We were delighted to find that a variety of benzylic pyridinium salts cross-coupled effectively (Scheme 3.7). Model product **3-22** was obtained in 80% and 70% yield using the corresponding vinylboronic acid or pinacol boronic ester, respectively. Throughout our scope studies, we used either the boronic acid or ester, depending on which was commercially available. If both were available, the less expensive reagent was used. Electron-poor benzylic coupling partners such as 2-, 3-, and 4-pyridine (**3-22**, **3-26**, **3-27**, **4-28**), quinoline (**3-29**), and pyrimidine (**3-30**) were well tolerated. Substrates containing electron-rich heterocycles such as imidazole (**3-31**), oxazole (**3-32**), pyrazole (**3-33**), thiadiazole (**3-34**), pyrrole (**3-35**), and thiazole (**3-46**) also cross-coupled effectively. Notably, no isomerization of

the alkene double bond was observed except in the case of pyrimidine **3-34**, which gave a 1.3:1 ratio of alkene isomers.

Scheme 3.7 Reaction scope of vinylation reaction^a



^aConditions: pyridinium salt **3-23** (1.0 mmol), PhenNi(OAc)₂·xH₂O (5 mol %), boronic acid (2.0 equiv), K₃PO₄ (3.4 equiv), EtOH (5.0 equiv), dioxane (0.5 M), 60

°C, 24 h, unless noted otherwise. Isolated yields. ^bPinacol boronate ester (2.0 equiv), K₃PO₄ (2.5 equiv). ^cAlkene isomers readily separated via silica gel chromatography and isolated in 45% and 36% yield.

A wide range of vinyl groups can also be installed via this method. Both electron-rich (**3-29**) and electron-poor (**3-30**) phenyl substitution is well tolerated. Heteroaryls such as thiophene (**3-26**) can also be used. Additionally, aliphatic alkenes can be formed, including cyclic trisubstituted alkene **3-27**, benzyl-substituted alkene **3-31**, and *tert*-butyl-substituted alkene **3-36**, as well as electron-poor α,β -unsaturated ester **3-28**. In addition to the heteroaryl tolerance, multiple functional groups are compatible, including esters (**3-28**), ethers (**3-29**, **3-32**), trifluoromethyl (**3-30**), fluoride (**3-33**, **3-34**), and chloride (**3-35**). Unfortunately, more bulky vinyl groups, such as (3-methyl-2-buten-2-yl)boronic ester, 2-methylprop-1-enylboronic ester, or 1-phenylvinylboronic ester, resulted in less than 30% yield. Simple vinylboronic ester also resulted in a low yield (17% by ¹H NMR analysis).

Given the similarity in conditions between the arylation (Chapter 2) and vinylation reactions, we believe that this cross-coupling may proceed via an analogous Ni^{II/III} catalytic cycle involving a stabilized benzylic radical intermediate (See Scheme 2.14). The nickel free pathway may also be in operation and contribute to the observed product formation via a nucleophilic substitution event.

3.3 Conclusion

In summary, we have developed conditions for the Suzuki–Miyaura cross-coupling of benzylic pyridinium salts with vinyl boronic acids and esters. This method

allows for efficient access to valuable 1,3-disubstituted allylic molecules. This reaction is amenable to heteroaryl substitution on both coupling partners, as well as a wide range of functional groups. This work was published in *Synthesis* as part of the Special Topic: *Modern Coupling Approaches and their Strategic Applications in Synthesis*.⁵⁰

3.4 Experimental

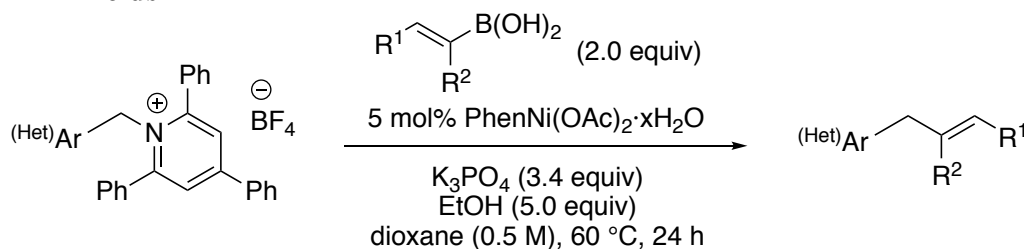
3.4.1 General Information

Reactions were performed in oven-dried Schlenk flasks or in oven-dried round-bottomed flasks unless otherwise noted. Round-bottomed flasks were fitted with rubber septa, and reactions were conducted under a positive pressure of N₂. Stainless steel syringes were used to transfer air- and moisture-sensitive liquids. Silica gel chromatography was performed on silica gel 60 (40-63 μm, 60Å) unless otherwise noted. Commercial reagents were purchased from Sigma Aldrich, Acros, Fisher, Strem, TCI, Combi Blocks, Alfa Aesar, AK Scientific, Oakwood, or Cambridge Isotopes Laboratories and used as received with the following exceptions: anhydrous ethanol was degassed by sparging with N₂ for 20–30 minutes prior to use in the cross-coupling reactions; dioxane was dried by passing through drying columns, then degassed by sparging with N₂.⁵¹ In some instances oven-dried potassium carbonate was added to CDCl₃ to remove trace acid. Proton nuclear magnetic resonance (¹H NMR) spectra, carbon nuclear magnetic resonance (¹³C NMR) spectra, and fluorine nuclear magnetic resonance spectra (¹⁹F NMR) were recorded on both 400 MHz and 600 MHz spectrometers. Chemical shifts for protons are reported in parts per million

downfield from tetramethylsilane and are referenced to residual protium in the NMR solvent ($\text{CHCl}_3 = \delta 7.26$). Chemical shifts for carbon are reported in parts per million downfield from tetramethylsilane and are referenced to the carbon resonances of the solvent ($\text{CDCl}_3 = \delta 77.16$). Chemical shifts for fluorine were externally referenced to CFCl_3 in CDCl_3 ($\text{CFCl}_3 = \delta 0$). Data are represented as follows: chemical shift, multiplicity (br = broad, s = singlet, d = doublet, t = triplet, q = quartet, p = pentet, m = multiplet, dd = doublet of doublets, h = heptet), coupling constants in Hertz (Hz), integration. Infrared (IR) spectra were obtained using FTIR spectrophotometers with material loaded onto a KBr plate. The mass spectral data were obtained at the University of Delaware mass spectrometry facility. Melting points were taken on a Thomas-Hoover Uni-Melt Capillary Melting Point Apparatus.

3.4.2 Cross-Coupling of Pyridinium Salts

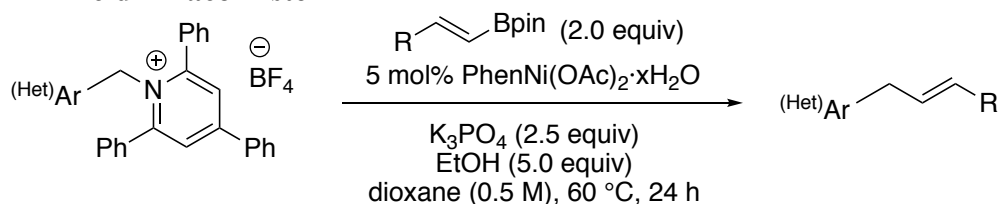
3.4.2.1 General Procedure A: Cross-Coupling of Pyridinium Salts with Boronic Acids



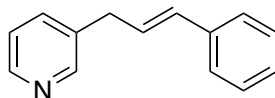
To an oven-dried, 25-mL Schlenk flask equipped with a stir bar was added $\text{PhenNi(OAc)}_2 \cdot x\text{H}_2\text{O}$ (20 mg, 0.050 mmol, 5 mol %), pyridinium salt (1.0 mmol, 1.0 equiv), vinylboronic acid (2.0 equiv, 2.0 mmol), and K_3PO_4 (722 mg, 3.4 mmol, 3.4 equiv). The flask was fitted with a rubber septum, sealed with parafilm, and then evacuated and refilled with N_2 (x 3). Dioxane (2.0 mL) was added, followed by EtOH

(0.29 mL, 5.0 mmol, 5.0 equiv). The flask was sealed off and resulting mixture was stirred at 60 °C for 24 h. The mixture was allowed to cool to room temperature, and then filtered through a small pad of Celite. The filter cake was washed with CH₂Cl₂ (4 x 25 mL), and the filtrate was concentrated. The cross-coupled product was then purified via silica gel chromatography.

3.4.2.2 General Procedure B: Cross-Coupling of Pyridinium Salts with Boronic Acid Pinacol Ester

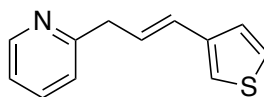


To an oven-dried, 10-mL round bottom flask equipped with a stir bar was added PhenNi(OAc)₂·xH₂O (20 mg, 0.050 mmol, 5 mol %), pyridinium salt (1.0 mmol, 1.0 equiv), vinylboronic acid pinacol ester (2.0 equiv, 2.0 mmol), and K₃PO₄ (531 mg, 2.5 mmol, 2.5 equiv). The flask was fitted with a rubber septum, sealed with parafilm, and then purged with a nitrogen line for 20 minutes. Dioxane (2.0 mL) was added, followed by EtOH (0.29 mL, 5.0 mmol, 5.0 equiv). The flask was sealed off and resulting mixture was stirred at 60 °C for 24 h. The mixture was allowed to cool to room temperature, and then filtered through a small pad of Celite. The filter cake was washed with CH₂Cl₂ (4 x 25 mL), and the filtrate was concentrated. The cross-coupled product was then purified via silica gel chromatography.

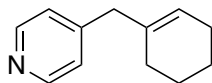


3-Cinnamylpyridine (3-22). Prepared via General Procedure A using 2,4,6-Triphenyl-1-(pyridin-3-ylmethyl)pyridin-1-ium tetrafluoroborate. The crude mixture was purified by silica gel chromatography (50% ether/hexanes) to give **3-22** (156 mg, 80%) as a pale yellow oil: ^1H NMR (600 MHz, CDCl_3) δ 8.54 – 8.46 (m, 2H), 7.58 – 7.53 (m, 1H), 7.37 – 7.33 (m, 2H), 7.33 – 7.28 (m, 2H), 7.25 – 7.20 (m, 2H), 6.47 (d, $J = 15.8$ Hz, 1H), 6.32 (dt, $J = 15.8, 6.8$ Hz, 1H), 3.56 (d, $J = 5.4$ Hz, 2H); ^{13}C NMR (151 MHz, CDCl_3) δ 150.3, 147.9, 137.2, 136.3, 135.6, 132.1, 128.7, 127.9, 127.6, 126.3, 123.5, 36.6. The spectral data matches that reported in the literature.⁵²

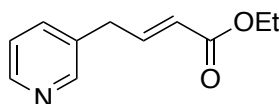
Product **3-22** was also prepared via General Procedure B. The crude mixture was purified by silica gel chromatography to give **3-22** (135 mg, 70%).



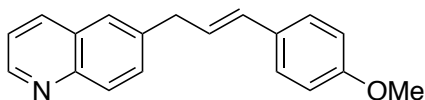
(E)-2-(3-(Thiophen-3-yl)allyl)pyridine (3-26). Prepared via General Procedure B using 2,4,6-Triphenyl-1-(pyridin-2-ylmethyl)pyridin-1-ium tetrafluoroborate. The crude mixture was purified by silica gel chromatography (50% ethyl acetate/hexanes) to give **3-26** (146 mg, 72%) as an orange oil: ^1H NMR (600 MHz, CDCl_3) δ 8.58 – 8.53 (m, 1H), 7.61 (td, $J = 7.7, 1.8$ Hz, 1H), 7.26 – 7.18 (m, 3H), 7.16 – 7.08 (m, 2H), 6.54 (d, $J = 15.8$ Hz, 1H), 6.30 (dt, $J = 15.7, 7.1$ Hz, 1H), 3.70 (dd, $J = 7.1, 1.4$ Hz, 2H); ^{13}C NMR (151 MHz, CDCl_3) δ 160.4, 149.6, 140.1, 136.7, 127.6, 126.3, 126.0, 125.2, 123.0, 121.5, 121.4, 42.1; FTIR (neat) 3078, 3007, 2923, 1590, 1472, 1434, 965, 766 cm^{-1} ; HRMS (ESI+) $[\text{M}+\text{H}]^+$ calculated for $\text{C}_{12}\text{H}_{12}\text{NS}$: 202.0690, found 202.0687.



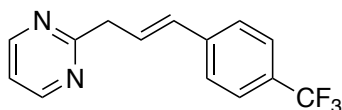
4-(Cyclohex-1-en-1-ylmethyl)pyridine (3-27). Prepared via General Procedure A using 2,4,6-Triphenyl-1-(pyridin-4-ylmethyl)pyridin-1-ium tetrafluoroborate. The crude mixture was purified by silica gel chromatography (step gradient: 20→100% EtOAc/hexanes) to give **3-27** (88 mg, 51%) as yellow oil: ^1H NMR (600 MHz, CDCl_3) δ 8.51 – 8.46 (m, 2H), 7.12 – 7.08 (m, 2H), 5.53 – 5.48 (m, 1H), 3.22 (s, 2H), 2.06 – 2.00 (m, 2H), 1.86 – 1.80 (m, 2H), 1.63 – 1.51 (m, 4H); ^{13}C NMR (151 MHz, CDCl_3) δ 149.8, 149.7, 135.6, 124.6, 124.4, 44.1, 28.2, 25.5, 23.0, 22.4; FTIR (neat) 3024, 2926, 2834, 1599, 1559, 1414 cm^{-1} ; HRMS (ESI+) $[\text{M}+\text{H}]^+$ calculated for $\text{C}_{12}\text{H}_{16}\text{N}$: 174.1283, found 174.1277.



Ethyl (E)-4-(pyridin-3-yl)but-2-enoate (2-28). Prepared via General Procedure B using 2,4,6-Triphenyl-1-(pyridin-3-ylmethyl)pyridin-1-ium tetrafluoroborate. The crude mixture was purified by silica gel chromatography (step gradient: 50→75% EtOAc/hexanes) to give **3-28** (117 mg, 61%) as pale yellow oil: ^1H NMR (400 MHz, CDCl_3) δ 8.61 – 8.55 (m, 1H), 8.50 – 8.43 (m, 1H), 7.74 – 7.66 (m, 1H), 7.26 – 7.21 (m, 1H), 6.48 (d, $J = 16.0$ Hz, 1H), 6.38 (dt, $J = 16.0, 6.8$ Hz, 1H), 4.18 (q, $J = 7.1$ Hz, 2H), 3.27 (dd, $J = 6.9, 1.2$ Hz, 2H), 1.29 (t, $J = 7.1$ Hz, 3H); ^{13}C NMR (151 MHz, CDCl_3) δ 171.3, 148.8, 148.4, 132.8, 132.6, 130.0, 124.5, 123.6, 61.1, 38.6, 14.4; FTIR (neat) 3030, 2982, 2937, 1734, 1160, 1025, 970, 709 cm^{-1} ; HRMS (ESI+) $[\text{M}+\text{H}]^+$ calculated for $\text{C}_{11}\text{H}_{14}\text{NO}_2$: 192.1025, found 192.1020.

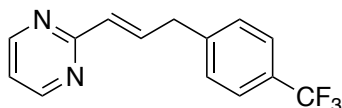


(E)-6-(3-(4-Methoxyphenyl)allyl)quinoline (3-29). Prepared via General Procedure A using 2,4,6-Triphenyl-1-(quinolin-6-ylmethyl)pyridin-1-ium tetrafluoroborate. The crude mixture was purified by silica gel chromatography (step gradient: 5→50% EtOAc/hexanes) to give **3-29** (197 mg, 72%) as yellow oil: ^1H NMR (600 MHz, CDCl_3) δ 8.88 (dd, $J = 4.2, 1.7$ Hz, 1H), 8.13 – 8.08 (m, 1H), 8.08 – 8.03 (m, 1H), 7.67 – 7.60 (m, 2H), 7.38 (dd, $J = 8.3, 4.2$ Hz, 1H), 7.34 – 7.29 (m, 2H), 6.87 – 6.83 (m, 2H), 6.47 (d, $J = 15.7$ Hz, 1H), 6.29 (dt, $J = 15.7, 6.9$ Hz, 1H), 3.80 (s, 3H), 3.72 (d, $J = 6.9$ Hz, 2H); ^{13}C NMR (151 MHz, CDCl_3) δ 159.2, 150.0, 147.5, 139.1, 135.8, 131.3, 131.3, 130.3, 129.7, 128.6, 127.5, 126.6, 126.4, 121.3, 114.2, 55.5, 39.4; FTIR (neat) 3030, 2956, 2834, 1606, 1511, 1247, 1175, 968, 835 cm^{-1} ; HRMS (ESI+) $[\text{M}+\text{H}]^+$ calculated for $\text{C}_{19}\text{H}_{18}\text{NO}$: 276.1388, found 276.1384.

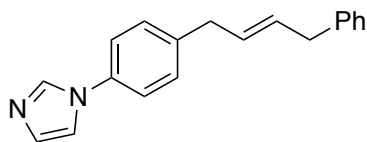


(E)-2-(3-(4-(Trifluoromethyl)phenyl)allyl)pyrimidine (3-30a). Prepared via General Procedure A using 2,4,6-Triphenyl-1-(pyrimidin-2-ylmethyl)pyridin-1-ium tetrafluoroborate. The crude mixture was purified by silica gel chromatography (step gradient: 8→70% EtOAc/hexanes) to give **3-30a** (119 mg, 45%) as yellow oil: ^1H NMR (600 MHz, CDCl_3) δ 8.71 (d, $J = 4.9$ Hz, 2H), 7.54 (d, $J = 8.2$ Hz, 2H), 7.47 (d, $J = 8.2$ Hz, 2H), 7.17 (t, $J = 4.9$ Hz, 1H), 6.72 – 6.58 (m, 2H), 3.94 (d, $J = 6.7$ Hz, 2H); ^{13}C NMR (151 MHz, CDCl_3) δ 169.4, 157.5, 140.9, 131.2, 129.2 (q, $J = 32.3$ Hz), 129.1, 126.6, 125.6 (q, $J = 3.8$ Hz), 124.5 (q, $J = 271.7$ Hz), 119.0, 43.4; ^{19}F NMR (565 MHz, CDCl_3) δ -62.48; FTIR (neat) 3041, 1563, 1422, 1327, 1164, 1122,

1068 cm^{-1} ; HRMS (ESI+) $[\text{M}+\text{H}]^+$ calculated for $\text{C}_{14}\text{H}_{12}\text{F}_3\text{N}_2$: 265.0953, found 265.0950.

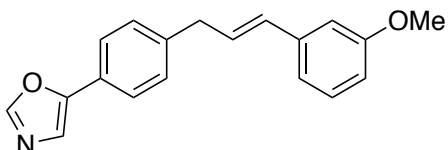


(E)-2-(3-(4-(Trifluoromethyl)phenyl)prop-1-en-1-yl)pyrimidine (3-30b). Prepared via General Procedure A using 2,4,6-Triphenyl-1-(pyrimidin-2-ylmethyl)pyridin-1-ium tetrafluoroborate. The crude mixture was purified by silica gel chromatography (step gradient: 8→70% EtOAc/hexanes) to give **3-30b** (94 mg, 36%) as yellow oil: ^1H NMR (600 MHz, CDCl_3) δ 8.66 (d, $J = 4.9$ Hz, 2H), 7.57 (d, $J = 8.0$ Hz, 2H), 7.37 (d, $J = 8.0$ Hz, 2H), 7.32 – 7.26 (m, 1H), 7.09 (t, $J = 4.8$ Hz, 1H), 6.61 – 6.55 (m, 1H), 3.69 (d, $J = 6.6$ Hz, 2H); ^{13}C NMR (151 MHz, CDCl_3) δ 164.4, 157.0, 143.0, 138.8, 131.3, 129.2, 128.9 (q, $J = 32.1$ Hz), 125.5 (q, $J = 3.8$ Hz), 124.3 (q, $J = 271.8$ Hz), 118.7, 38.7; ^{19}F NMR (565 MHz, CDCl_3) δ -62.43; FTIR (neat) 3037, 2918, 1557, 1421, 1332, 1161, 1105 cm^{-1} ; HRMS (ESI+) $[\text{M}+\text{H}]^+$ calculated for $\text{C}_{14}\text{H}_{12}\text{F}_3\text{N}_2$: 265.0953, found 265.0951.

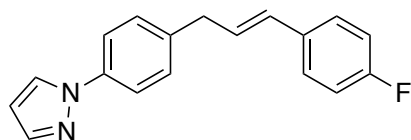


(E)-1-(4-(4-Phenylbut-2-en-1-yl)phenyl)-1H-imidazole (3-31). Prepared via General Procedure A using 1-(4-(1H-Imidazol-1-yl)benzyl)-2,4,6-triphenylpyridin-1-ium tetrafluoroborate. The crude mixture was purified by silica gel chromatography (step gradient: 20→100% EtOAc/hexanes) to give **3-31** (172 mg, 63%) as yellow oil: ^1H NMR (600 MHz, CDCl_3) δ 7.85 – 7.81 (m, 1H), 7.34 – 7.27 (m, 6H), 7.26 – 7.25 (m,

1H), 7.24 – 7.17 (m, 4H), 5.76 – 5.62 (m, 2H), 3.44 – 3.37 (m, 4H); ¹³C NMR (151 MHz, CDCl₃) δ 140.6, 140.4, 135.8, 135.7, 131.4, 130.5, 130.0, 129.8, 128.7, 128.6, 126.2, 121.8, 118.5, 39.1, 38.5; FTIR (neat) 3026, 2899, 1521, 1492, 1303, 1057, 965 cm⁻¹; HRMS (ESI+) [M+H]⁺ calculated for C₁₉H₁₉N₂: 275.1548, found 275.1543.

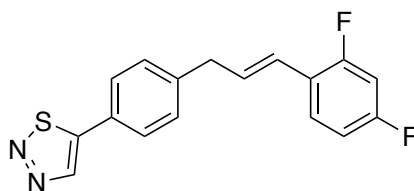


(E)-5-(4-(3-(3-Methoxyphenyl)allyl)phenyl)oxazole (3-32). Prepared via General Procedure B using 1-(4-(Oxazol-5-yl)benzyl)-2,4,6-triphenylpyridin-1-ium tetrafluoroborate. The crude mixture was purified by silica gel chromatography (step gradient: 10→50% EtOAc/hexanes) to give **3-32** (220 mg, 76%) as yellow solid (mp 60–63 °C): ¹H NMR (600 MHz, CDCl₃) δ 7.90 (s, 1H), 7.63 – 7.58 (m, 2H), 7.34 – 7.29 (m, 3H), 7.22 (t, *J* = 7.9 Hz, 1H), 6.99 – 6.94 (m, 1H), 6.92 – 6.88 (m, 1H), 6.80 – 6.75 (m, 1H), 6.48 – 6.41 (m, 1H), 6.35 (dt, *J* = 15.7, 6.8 Hz, 1H), 3.81 (s, 3H), 3.58 (d, *J* = 7.2 Hz, 2H); ¹³C NMR (151 MHz, CDCl₃) δ 160.0, 151.7, 150.4, 141.0, 138.9, 131.6, 129.7, 129.4, 129.0, 126.0, 124.8, 121.3, 119.0, 113.1, 111.6, 55.4, 39.2; FTIR (neat) 3027, 2937, 2833, 1598, 1579, 1490, 1267, 1043, 941 cm⁻¹; HRMS (ESI+) [M+H]⁺ calculated for C₁₉H₁₈NO₂: 292.1338, found 292.1331.



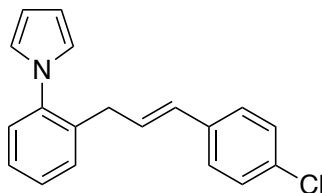
(E)-1-(4-(3-(4-Fluorophenyl)allyl)phenyl)-1H-pyrazole (3-33). Prepared via General Procedure A using 1-(4-(1H-Pyrazol-1-yl)benzyl)-2,4,6-triphenylpyridin-1-ium tetrafluoroborate. The crude mixture was purified by silica gel chromatography (step

gradient: 5→20% ether/hexanes) to give **3-33** (241 mg, 87%) as light yellow solid (mp 80–83 °C): ¹H NMR (600 MHz, CDCl₃) δ 7.90 (d, *J* = 2.4 Hz, 1H), 7.72 (d, *J* = 1.7 Hz, 1H), 7.66 – 7.61 (m, 2H), 7.35 – 7.29 (m, 4H), 7.02 – 6.96 (m, 2H), 6.48 – 6.39 (m, 2H), 6.28 (dt, *J* = 15.8, 6.8 Hz, 1H), 3.57 (dd, *J* = 6.8, 1.4 Hz, 2H); ¹³C NMR (151 MHz, CDCl₃) δ 162.3 (d, *J*_{C-F} = 246.1 Hz), 141.1, 138.8, 138.5, 133.6 (d, *J*_{C-F} = 3.4 Hz), 130.4, 129.8, 128.7 (d, *J*_{C-F} = 2.2 Hz), 127.7 (d, *J*_{C-F} = 8.0 Hz), 126.8, 119.6, 115.6 (d, *J* = 21.2 Hz), 107.6, 38.8; ¹⁹F NMR (565 MHz, CDCl₃) δ -115.13; FTIR (neat) 3037, 2922, 1524, 1507, 1394, 1225, 936, 838, 748 cm⁻¹; HRMS (ESI+) [M+H]⁺ calculated for C₁₈H₁₆FN₂: 279.1298, found 279.1292.

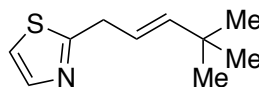


(E)-5-(4-(3-(2,4-Difluorophenyl)allyl)phenyl)-1,2,3-thiadiazole (3-34). Prepared via General Procedure B using 1-(4-(1,2,3-Thiadiazol-5-yl)benzyl)-2,4,6-triphenylpyridin-1-ium tetrafluoroborate. The crude mixture was purified by silica gel chromatography (step gradient: 1→10% ether/hexanes) to give **3-34** (163 mg, 52%) as yellow solid (mp 117–120 °C): ¹H NMR (600 MHz, CDCl₃) δ 8.62 (s, 1H), 8.03 – 7.98 (m, 2H), 7.43 – 7.37 (m, 3H), 6.85 – 6.75 (m, 2H), 6.62 – 6.55 (m, 1H), 6.39 (dt, *J* = 15.9, 6.9 Hz, 1H), 3.63 (d, *J* = 6.3 Hz, 2H); ¹³C NMR (101 MHz, CDCl₃) δ 162.88, 162.30 (dd, *J* = 196.6, 11.9 Hz), 159.81 (dd, *J* = 199.2, 11.9 Hz), 141.42, 131.01 (dd, *J* = 4.7, 2.3 Hz), 129.76, 129.60, 129.07, 128.10 (dd, *J* = 9.5, 5.5 Hz), 127.73, 123.16 (dd, *J* = 3.0, 1.4 Hz), 121.52 (dd, *J* = 12.5, 4.0 Hz), 111.51 (dd, *J* = 21.3, 3.7 Hz), 104.10 (t, *J* = 25.7 Hz), 39.60; ¹⁹F NMR (565 MHz, CDCl₃) δ -111.66 (d, *J*_{F-F} = 7.1 Hz), -114.30 (d,

$J_{F-F} = 7.1$ Hz); FTIR (neat) 3094, 2931, 1589, 1503, 1427, 1223, 970, 846, 809 cm^{-1} ; HRMS (ESI+) $[M+H]^+$ calculated for $\text{C}_{17}\text{H}_{13}\text{F}_2\text{N}_2\text{S}$: 315.0768, found 315.0759.



(E)-1-(2-(3-(4-Chlorophenyl)allyl)phenyl)-1H-pyrrole (3-35). Prepared via General Procedure B using 1-(2-(1H-Pyrrol-1-yl)benzyl)-2,4,6-triphenylpyridin-1-ium tetrafluoroborate. The crude mixture was purified by silica gel chromatography (step gradient: 1→10% toluene/hexanes) to give **3-35** (220 mg, 75%) as colorless oil: ^1H NMR (600 MHz, CDCl_3) δ 7.38 – 7.28 (m, 4H), 7.25 – 7.19 (m, 4H), 6.82 – 6.78 (m, 2H), 6.34 – 6.30 (m, 2H), 6.21 (d, $J = 15.9$ Hz, 1H), 6.14 (dt, $J = 15.8, 6.4$ Hz, 1H), 3.40 (d, $J = 6.4$ Hz, 2H); ^{13}C NMR (151 MHz, CDCl_3) δ 140.6, 136.1, 136.0, 132.9, 130.6, 130.4, 129.3, 128.8, 128.1, 127.5, 127.4, 127.3, 122.5, 109.1, 34.8; FTIR (neat) 3028, 1502, 1491, 1327, 1093, 764, 727 cm^{-1} ; HRMS (ESI+) $[M+H]^+$ calculated for $\text{C}_{19}\text{H}_{17}\text{ClN}$: 294.1050, found 294.1041.



(E)-2-(4,4-Dimethylpent-2-en-1-yl)thiazole (3-36). Prepared via General Procedure A using 2,4,6-Triphenyl-1-(thiazol-2-ylmethyl)pyridin-1-ium tetrafluoroborate. The crude mixture was purified by silica gel chromatography (step gradient: 2→20% EtOAc/hexanes) to give **3-36** (91 mg, 50%) as light yellow oil: ^1H NMR (600 MHz, CDCl_3) δ 7.69 (d, $J = 3.3$ Hz, 1H), 7.20 (d, $J = 3.3$ Hz, 1H), 5.75 – 5.69 (m, 1H), 5.58 (dt, $J = 15.5, 6.9$ Hz, 1H), 3.71 (dd, $J = 6.9, 1.3$ Hz, 2H), 1.04 (s, 9H); ^{13}C NMR (151

MHz, CDCl₃) δ 171.4, 145.9, 142.6, 120.5, 118.6, 36.9, 33.3, 29.6; FTIR (neat) 3081, 2959, 2902, 2866, 1501, 1363, 973, 720 cm⁻¹; HRMS (ESI+) [M+H]⁺ calculated for C₁₀H₁₆NS: 182.1003, found 182.0998.

REFERENCES

1. Yang, Z.; Tang, P.; Gauuan, J. F.; Molino, B. F., *The Journal of Organic Chemistry* **2009**, *74*, 9546-9549.
2. Yadav, J. S.; Rajendar, G.; Rao, R. S.; Pabbaraja, S., *The Journal of Organic Chemistry* **2013**, *78*, 8524-8530.
3. Butt, N. A.; Zhang, W., *Chemical Society Reviews* **2015**, *44*, 7929-7967.
4. Yuan, Q.; Yao, K.; Liu, D.; Zhang, W., *Chemical Communications* **2015**, *51*, 11834-11836.
5. Breault, G. A.; Oldfield, J.; Tucker, H.; Warner, P., US5811459A, 1998/09/22/, 1998.
6. Jacques, V.; Rusche, J. R.; Peet, N. P.; Singh, J., WO2012118782A1, 2012/09/07/, 2012.
7. Lubisch, W.; Moller, A.; Treiber, H.-J., US6103720A, 2000/08/15/, 2000.
8. Tempone, A. G.; Pompeu da Silva, A. C. M.; Brandt, C. A.; Martinez, F. S.; Treiger Borborema, S. E.; Barata da Silveira, M. A.; de Andrade, H. F., *Antimicrobial Agents and Chemotherapy* **2005**, *49*, 1076.
9. Kabalka, G. W.; Dong, G.; Venkataiah, B., *Org. Lett.* **2003**, *5*, 893-895.
10. Kayaki, Y.; Koda, T.; Ikariya, T., *European Journal of Organic Chemistry* **2004**, *2004*, 4989-4993.
11. Manabe, K.; Nakada, K.; Aoyama, N.; Kobayashi, S., *Adv. Synth. Catal.* **2005**, *347*, 1499-1503.
12. Tabélé, C.; Curti, C.; Primas, N.; Kabri, Y.; Remusat, V.; Vanelle, P., *Synthesis* **2015**, *47*, 3339-3346.
13. Tsukamoto, H.; Sato, M.; Kondo, Y., *Chemical Communications* **2004**, 1200-1201.

14. Tsukamoto, H.; Uchiyama, T.; Suzuki, T.; Kondo, Y., *Organic & Biomolecular Chemistry* **2008**, *6*, 3005-3013.
15. Zhang, Y.; Yin, S.-C.; Lu, J.-M., *Tetrahedron* **2015**, *71*, 544-549.
16. Lee, Y.; Shabbir, S.; Lee, S.; Ahn, H.; Rhee, H., *Green Chemistry* **2015**, *17*, 3579-3583.
17. Xu, J.; Zhai, X.; Wu, X.; Zhang, Y. J., *Tetrahedron* **2015**, *71*, 1712-1717.
18. Maslak, V.; Tokic-Vujosevic, Z.; Saicic, R. N., *Tetrahedron Letters* **2009**, *50*, 1858-1860.
19. Mino, T.; Kogure, T.; Abe, T.; Koizumi, T.; Fujita, T.; Sakamoto, M., *European Journal of Organic Chemistry* **2013**, *2013*, 1501-1505.
20. Bouyssi, D.; Gerusz, V.; Balme, G., *European Journal of Organic Chemistry* **2002**, *2002*, 2445-2448.
21. Hamasaka, G.; Sakurai, F.; Uozumi, Y., *Tetrahedron* **2015**, *71*, 6437-6441.
22. Hamasaka, G.; Sakurai, F.; Uozumi, Y., *Chemical Communications* **2015**, *51*, 3886-3888.
23. Poláčková, V.; Toma, Š.; Oliver Kappe, C., *Tetrahedron* **2007**, *63*, 8742-8745.
24. Moreno-Manas, M.; Pajuelo, F.; Pleixats, R., *The Journal of Organic Chemistry* **1995**, *60*, 2396-2397.
25. Singh, R.; Viciu, M. S.; Kramareva, N.; Navarro, O.; Nolan, S. P., *Org. Lett.* **2005**, *7*, 1829-1832.
26. Nájera, C.; Gil-Moltó, J.; Karlström, S., *Adv. Synth. Catal.* **2004**, *346*, 1798-1811.
27. Li, M.-B.; Wang, Y.; Tian, S.-K., *Angewandte Chemie International Edition* **2012**, *51*, 2968-2971.
28. Li, M.-B.; Tang, X.-L.; Tian, S.-K., *Adv. Synth. Catal.* **2011**, *353*, 1980-1984.
29. Narahashi, H.; Shimizu, I.; Yamamoto, A., *Journal of Organometallic Chemistry* **2008**, *693*, 283-296.
30. Kuwano, R.; Yokogi, M., *Org. Lett.* **2005**, *7*, 945-947.

31. Fernandez Reina, D.; Ruffoni, A.; Al-Faiyz, Y. S. S.; Douglas, J. J.; Sheikh, N. S.; Leonori, D., *ACS Catalysis* **2017**, *7*, 4126-4130.
32. Alacid, E.; Nájera, C., *The Journal of Organic Chemistry* **2009**, *74*, 2321-2327.
33. Anselmi, E.; Abarbri, M.; Duchêne, A.; Langle-Lamandé, S.; Thibonnet, J., *Synthesis* **2012**, *44*, 2023-2040.
34. Frye, E. C.; O' Connor, C. J.; Twigg, D. G.; Elbert, B.; Laraia, L.; Hulcoop, D. G.; Venkitaraman, A. R.; Spring, D. R., *Chemistry – A European Journal* **2012**, *18*, 8774-8779.
35. Ronson, T. O.; Carney, J. R.; Whitwood, A. C.; Taylor, R. J. K.; Fairlamb, I. J. S., *Chemical Communications* **2015**, *51*, 3466-3469.
36. Frlan, R.; Sova, M.; Gobec, S.; Stavber, G.; Časar, Z., *The Journal of Organic Chemistry* **2015**, *80*, 7803-7809.
37. Sova, M.; Frlan, R.; Gobec, S.; Stavber, G.; Časar, Z., *Applied Organometallic Chemistry* **2015**, *29*, 528-535.
38. Baba, Y.; Toshimitsu, A.; Matsubara, S., *Synlett* **2008**, *2008*, 2061-2063.
39. Cai, Y.; Benischke, A. D.; Knochel, P.; Gosmini, C., *Chemistry – A European Journal* **2016**, *23*, 250-253.
40. Johnson, K. A.; Biswas, S.; Weix, D. J., *Chemistry – A European Journal* **2016**, *22*, 7399-7402.
41. Cherney, A. H.; Reisman, S. E., *J. Am. Chem. Soc.* **2014**, *136*, 14365-14368.
42. Krasovskaya, V.; Krasovskiy, A.; Bhattacharjya, A.; Lipshutz, B. H., *Chemical Communications* **2011**, *47*, 5717-5719.
43. Maity, P.; Shacklady-McAtee, D. M.; Yap, G. P. A.; Sirianni, E. R.; Watson, M. P., *J. Am. Chem. Soc.* **2013**, *135*, 280-285.
44. Shacklady-McAtee, D. M.; Roberts, K. M.; Basch, C. H.; Song, Y.-G.; Watson, M. P., *Tetrahedron* **2014**, *70*, 4257-4263.
45. Basch, C. H.; Cobb, K. M.; Watson, M. P., *Org. Lett.* **2016**, *18*, 136-139.

46. Wang, T.; Yang, S.; Xu, S.; Han, C.; Guo, G.; Zhao, J., *RSC Advances* **2017**, *7*, 15805-15808.
47. Li, C.; Zhang, Y.; Sun, Q.; Gu, T.; Peng, H.; Tang, W., *J. Am. Chem. Soc.* **2016**, *138*, 10774-10777.
48. Li, G.; Wu, L.; Lv, G.; Liu, H.; Fu, Q.; Zhang, X.; Tang, Z., *Chemical Communications* **2014**, *50*, 6246-6248.
49. Ueda, M.; Nishimura, K.; Kashima, R.; Ryu, I., *Synlett* **2012**, *23*, 1085-1089.
50. Guan, W.; Liao, J.; Watson, M. P., *Synthesis* **2018**, *50*, 3231-3237.
51. Pangborn, A. B.; Giardello, M. A.; Grubbs, R. H.; Rosen, R. K.; Timmers, F. J., *Organometallics* **1996**, *15*, 1518-1520.
52. Ellwart, M.; Knochel, P., *Angewandte Chemie International Edition* **2015**, *54*, 10662-10665.

Chapter 4

REDUCTIVE CROSS-ELECTROPHILE COUPLING OF ALKYL PYRIDINIUM SALTS WITH ARYL BROMIDES

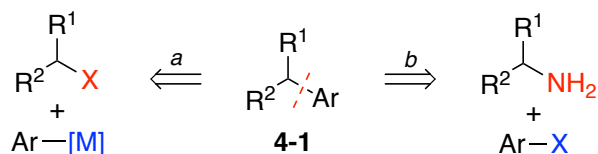
This work was performed in collaboration with Michelle Garnsey, Brian Boscoe, and Joseph Tucker at Pfizer, Inc.

4.1 Introduction

Over the last century, transition-metal catalysis has revolutionized our ability to form new carbon-carbon bonds. Notably, these advancements have enabled the rapid construction of a variety of C_{sp^3} - C_{sp^2} bonds. For example, alkylarene **4-1** can easily be obtained via the cross-coupling of an alkyl halide with an arylboronic acid or arylzinc halide (Scheme 4.1, left).¹ However, the generation of these aryl nucleophiles requires additional synthetic steps and can sometimes limit functional group tolerance and scope. Thus, intense efforts have focused on the identification of novel, inexpensive cross-coupling partners for synthesis. In particular, we were drawn towards aryl halides because of their wide abundance and ease of synthesis. As a case study for their availability versus more common aryl nucleophiles, our collaborator, Dr. Michelle Garnsey, performed a search of Pfizer's internal chemical store. Over 56,000 (hetero)aryl bromides are present in the internal chemical store, in contrast to only 6,200 boronic acids/esters. We have previously developed methods to utilize Katritzky pyridinium salts in nickel-catalyzed cross-coupling reactions as a means to

harness ubiquitous alkyl amines as electrophiles via C–N bond activation (Chapters 1–3). We envisioned that the cross-coupling of these two feedstock chemicals (i.e., an alkyl amine derivative with an aryl halide) would allow one to build complexity from inexpensive starting materials and greatly expand the pools of compounds available for such cross-coupling approaches (Scheme 4.1, right).

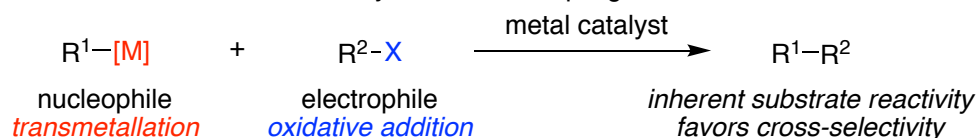
Scheme 4.1 Synthesis of alkylarenes



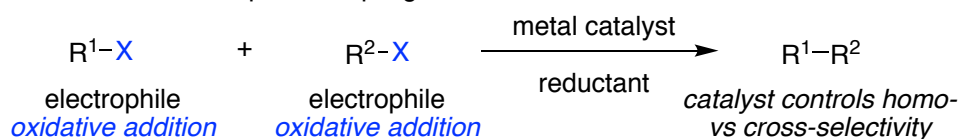
Most conventional approaches to cross-couplings require the use of a preformed organometallic nucleophile (e.g., R–BX₂, R–MgX, R–ZnX) in conjunction with an organic electrophile (e.g., R–X) (Scheme 4.2, top).¹ The inherent differences in reactivity between the nucleophile and electrophile allow these reactions to be cross-selective; the nucleophile reacts with the catalyst by transmetalation, and the electrophile reacts by oxidative addition. Nonetheless, the use of nucleophilic carbon reagents presents some shortcomings and challenges. Many organometallic reagents have limited commercial availability and are often synthesized from the corresponding organohalide, which adds steps to a synthetic sequence. Furthermore, some of these reagents have limited air and moisture stability, preventing their widespread use in industry. The intrinsic nucleophilicity of these organometallic reagents can limit the incorporation of electrophilic functional groups; the basic reagents required to facilitate transmetalation poses issues in substrates containing acidic protons. More importantly, these couplings often require a large excess of the organic nucleophile

due to competing side reactions such as protodemetalation, thereby decreasing the overall atom economy of these transformations.

Scheme 4.2 Conventional cross-coupling vs reductive cross electrophile-coupling
Conventional Transition Metal-Catalyzed Cross-Coupling



Reductive Cross-Electrophile Coupling



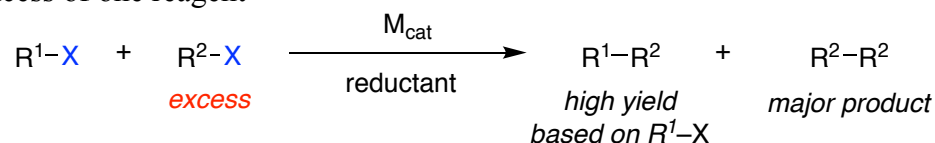
In contrast, a reductive cross-electrophile approach mitigates many of these issues by eliminating the need for preformed organometallic species (Scheme 4.2, bottom).² As a result, this area has garnered significant attention over the past decade. These couplings employ the use of commercially abundant organohalides, which are much more stable and easier to handle than their organometallic counterparts. More importantly, greater functional group compatibility can be observed due to the omission of stoichiometric strong bases and nucleophiles. This approach also provides a unique opportunity for synthetic orthogonality to traditional cross-couplings.

However, one of the ongoing challenges associated with cross-electrophile couplings is selectivity. The two coupling partners are both electrophilic in nature and tend to react with a metal catalyst via oxidative addition. This can lead to dimerization of either electrophile, as well as other byproducts such as protodehalogenation and β -hydride elimination. Intense efforts have identified several strategies to afford high

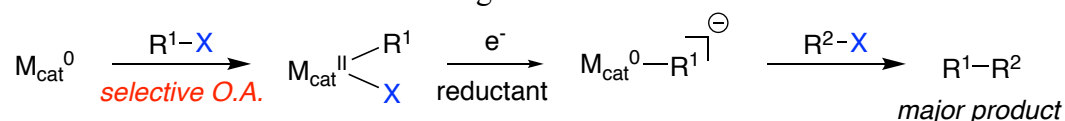
yields and/or cross-selectivity in these types of reductive cross-couplings (Scheme 4.3).³

Scheme 4.3 Strategies for obtaining high yields in reductive cross-couplings

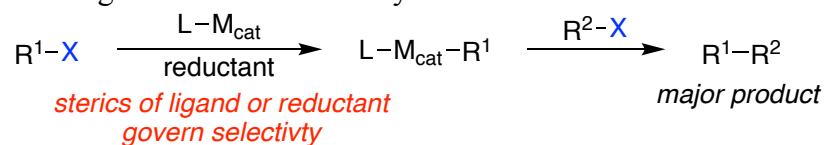
A. Excess of one reagent



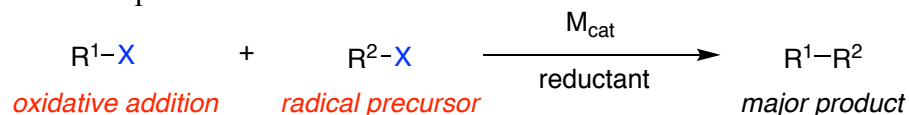
B. Electronic differentiation of starting materials



C. Steric matching of substrate and catalyst



D. Radical chain process

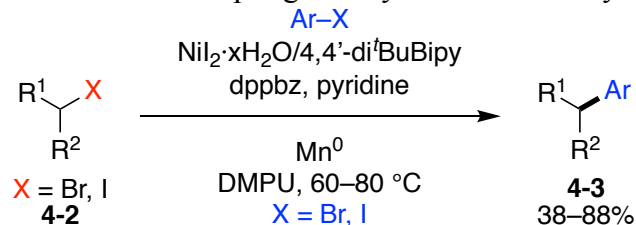


Employing an excess of one reagent leads to a statistical mixture of products and delivers the cross-coupled product in high yield (Scheme 4.3A). However, this sacrifices a large amount of one starting material, and the major product of this reaction is the dimer of the excess reagent. The second approach relies on the electronic differentiation of two unlike electrophiles through sequential oxidative addition (Scheme 4.3B). The catalytic cycle must have two different active, low-valent species that can each selectively react with one of the starting materials. If the

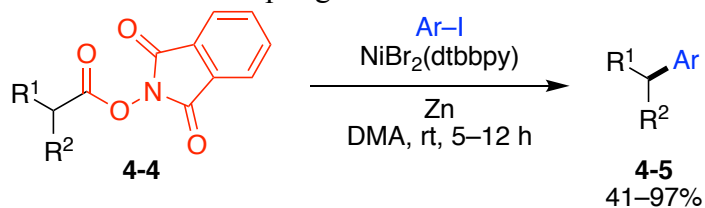
reactivities of the electrophiles are similar, sterics can be used to differentiate the two species (Scheme 4.3C). Steric matching between substrate and ligand or reductant can afford cross-selectivity. Finally, the native heterolytic versus homolytic reactivity patterns of the starting materials can be exploited to achieve selective cross-coupling (Scheme 4.3D). One electrophile is prone to undergo a two-electron oxidative addition, while the other proceeds through a SET mechanism to generate the corresponding radical intermediate. In this case, the catalyst must be capable of both single- and two-electron processes. We sought to utilize this strategy for our proposed reaction.

In 2010, Weix and coworkers disclosed a seminal report on the nickel-catalyzed reductive cross-coupling of primary and secondary alkyl halides (**4-3**) with aryl halides using manganese as a stoichiometric reductant (Scheme 4.4).⁴ In contrast to previously reported couplings of alkyl halides with aryl halides, this reaction does not go through an intermediate organometallic species. Instead, this approach relies on the ability of the aryl halide to undergo a two-electron oxidative addition, while the alkyl halide can serve as a radical precursor. Shortly after, Weix expanded on this initial finding and published more general conditions using zinc as the stoichiometric metal reductant.⁵ He demonstrated broad scope with over 40 examples including those containing nucleophilic and electrophilic groups as well as acidic protons. Additionally, vinyl halides were also amenable to this chemistry. More recently, Weix disclosed an analogous reductive cross-coupling of redox-active esters (**4-4**) with aryl iodides (Scheme 4.5).⁶

Scheme 4.4 Weix's reductive coupling of alkyl halides with aryl halides

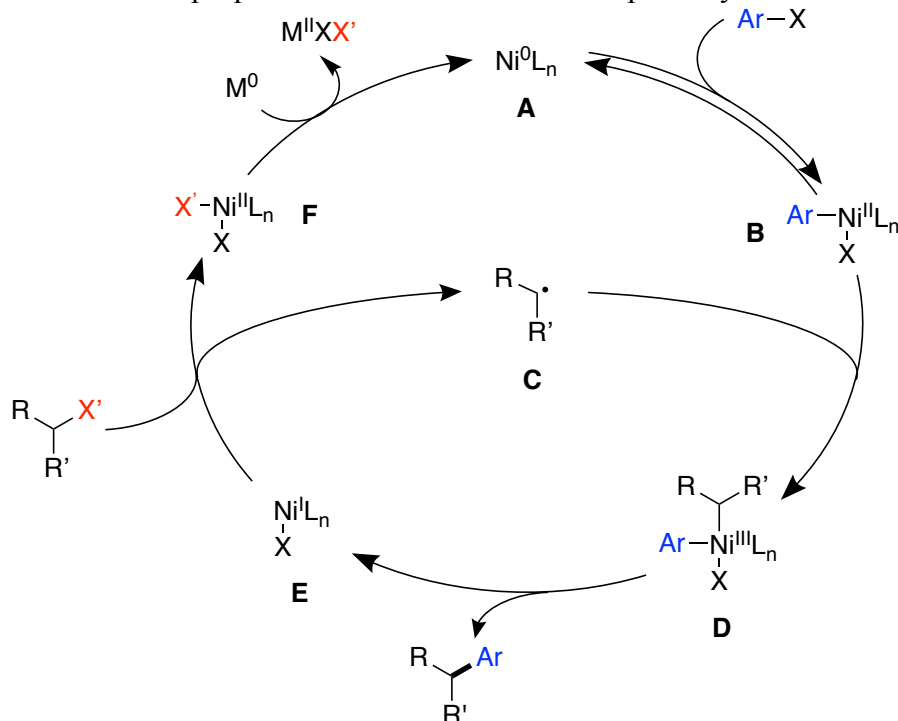


Scheme 4.5 Weix's reductive coupling of redox-active esters with aryl iodides



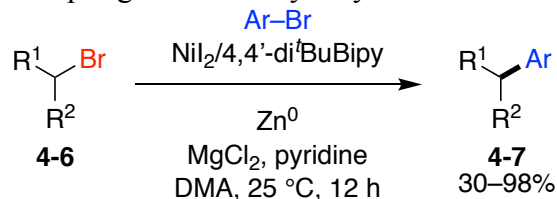
In a subsequent publication, the Weix group performed detailed mechanistic studies to elucidate the mechanism of his reductive cross-electrophile coupling of alkyl halides with aryl halides.^{2, 7} He proposed a radical-chain bimetallic pathway (Scheme 4.6). Notably, this is distinct from the traditional radical rebound mechanism in which the radical intermediate recombines with the same nickel complex that formed it. Starting from low-valent Ni⁰ species **A**, selective two-electron oxidative addition of the aryl halide generates Ni^{II}-arene **B**, which appears to be the catalyst resting state. This then reacts with a solvent cage escaped alkyl radical **C** to form diorgano-Ni^{III} species **D**. Reductive elimination of the cross-coupled product produces reactive Ni^I species **E** that can then undergo SET with the alkyl halide to generate the aforementioned alkyl radical **C** and Ni^{II} species **F**. Finally, the cycle can be turned-over via reduction of **F** back to the active Ni⁰ species **A** with a stoichiometric reductant such as manganese or zinc.

Scheme 4.6 Weix's proposed radical-chain bimetallic pathway

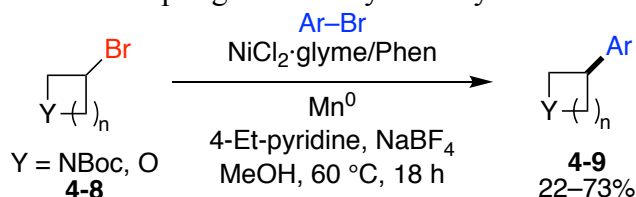


Although Weix focused primarily on primary alkyl halides, he demonstrated limited examples of cross-coupling secondary alkyl halides and only in modest yields (<70%). Gong later improved on this chemistry to affect cross-coupling of secondary alkyl bromides (**4-6**) with aryl bromides (Scheme 4.7).⁸ Notably, however, these methods lacked scope in heterocyclic alkyl electrophiles. Towards this end, the Molander group has optimized conditions for the cross-coupling of saturated heterocyclic bromides (**4-8**) with (hetero)aryl bromides (Scheme 4.8).⁹ A number of 4-, 5-, and 6-membered *O*- and *N*-heterocyclic alkyl bromides were well tolerated under these conditions. This chemistry was later extended to heterocyclic tosylates as well.¹⁰

Scheme 4.7 Gong's coupling of secondary alkyl bromides

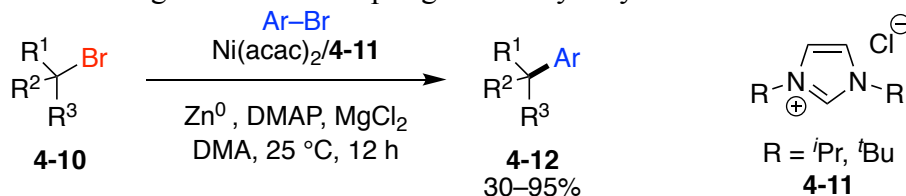


Scheme 4.8 Molander's coupling of heterocyclic alkyl bromides



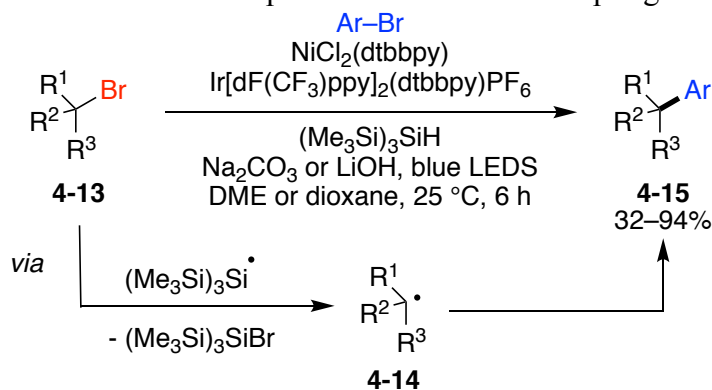
However, despite these advancements, tertiary alkyl halides remained a challenging class of substrates. In 2015, the Gong group disclosed conditions for the reductive cross-coupling of tertiary alkyl bromides (**4-10**) with aryl bromides to afford all-carbon quaternary centers (**4-12**) (Scheme 4.9).¹¹ Although pyridine-based bidentate and tridentate ligands were ineffective, the use of *N*-heterocyclic carbene precursors (**4-11**) resulted in the desired cross-coupling. Unfortunately, cross-couplings of electron-rich aryl halides were problematic under these original conditions. More recently, Gong modified these conditions to enable the coupling of electron-rich aryl iodides.¹²

Scheme 4.9 Gong's reductive coupling of tertiary alkyl halides



Reductive cross-couplings utilizing a metallaphotoredox approach have also been investigated. Unlike methods that employ a stoichiometric metal reductant, this approach allows for the cross-coupling to occur under much milder conditions by utilizing a photocatalyst. The MacMillan group has demonstrated that under Ni/Ir dual-photoredox conditions, alkyl bromides (**4-13**) can be coupled with aryl bromides at room temperature with blue LED irradiation (Scheme 4.10).¹³ This method relies on a photocatalytically generated silyl radical species, which can perform halogen-atom abstraction to generate the nucleophilic carbon-centered radical **4-14**. Notably a variety of heteroarenes can be incorporated as well as two examples of tertiary alkyl groups.

Scheme 4.10 MacMillan's metallaphotoredox reductive coupling

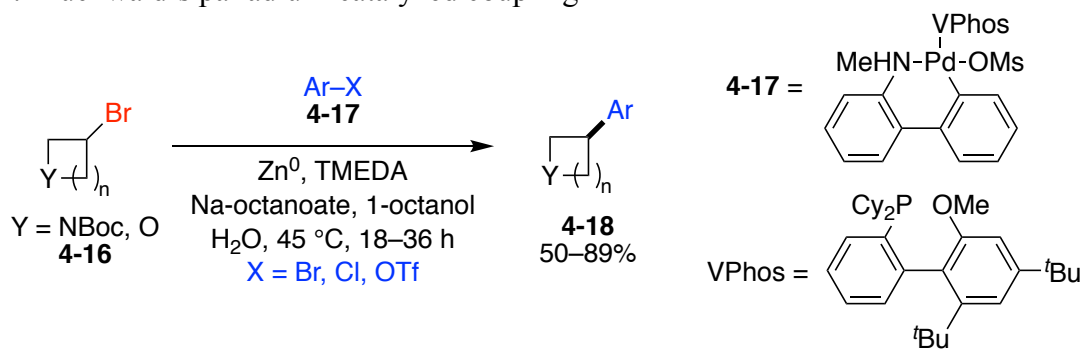


Although nickel-catalyzed reductive cross-couplings have exploded within the past decade, a number of other metals have also been found to effect analogous reactions. For example, the Buchwald group has found that palladium precatalyst **4-17** can promote the cross-coupling of heterocyclic alkyl bromides (**4-16**) with aryl halides and triflates under aqueous Lipshutz-Negishi conditions (Scheme 4.11A).¹⁴ In 2009, Jacobi von Wagelin published the first direct iron-catalyzed cross-coupling of alkyl

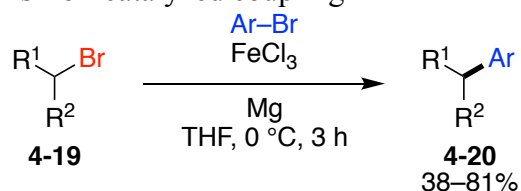
bromides (**4-19**) with aryl bromides (Scheme 4.11B).¹⁵ However, the functional group tolerance was much lower than manganese- or zinc-mediated reactions due to the formation of a Grignard reagent *in-situ*. Gosmini reported a cobalt-catalyzed coupling of alkyl bromides (**4-21**) with aryl bromides (Scheme 4.11C).¹⁶ Notably, however, the alkyl electrophile is generally used in excess (1.1–3 equiv).

Scheme 4.11 Metal-catalyzed reductive cross-couplings

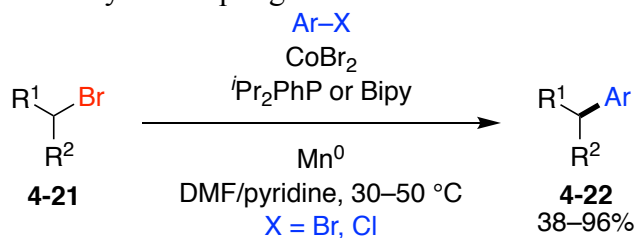
A. Buchwald's palladium-catalyzed coupling



B. Jacobi von Wagelin's iron-catalyzed coupling

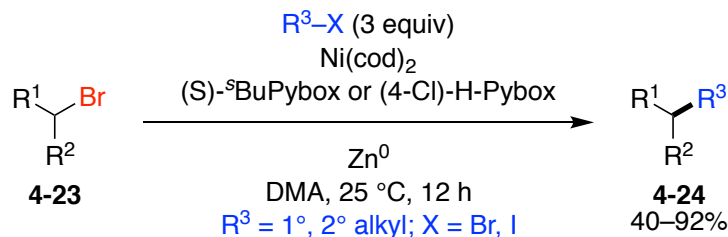


C. Gosmini's cobalt-catalyzed coupling

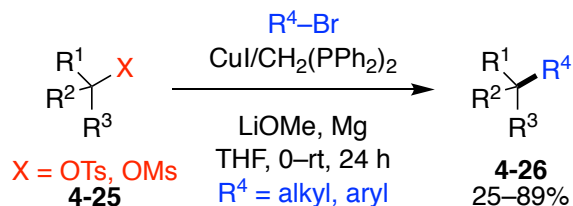


With the advancement of metal-catalyzed reductive cross-couplings, a variety of $C_{sp^3}-C_{sp^2}$ bonds can be forged via these types of approaches. However, examples of cross-selective couplings of two unactivated alkyl electrophiles to form new $C_{sp^3}-C_{sp^3}$ bonds have been much more limited. In 2011, Gong reported a nickel-catalyzed coupling of two unactivated alkyl halides (primary or secondary) (Scheme 4.12).¹⁷ Notably, a large excess of one alkyl halide (3 equiv) was required to achieve high selectivity and competing dimerization was a major side reaction. Gong later improved upon this chemistry and reported an analogous reaction using B_2Pin_2 as the terminal reductant in place of zinc.¹⁸ In this case, only a slight excess (1.5 equiv) of one of the alkyl halides can be used to achieve good yields. This method relies on the steric differentiation of the two alkyl electrophiles (*vide supra*, Scheme 4.3C) to enable selective sequential oxidative addition. More recently, the Fu and Liu groups disclosed the copper-catalyzed coupling of alkyl tosylates and mesylates with alkyl and aryl bromides (Scheme 4.13).¹⁹ Again, this method relies on an excess of the alkyl or aryl bromide (2–3 equiv). There is also one example of coupling *tert*-butyl bromide, albeit in poor yield (25%). To date, a general cross-selective reductive alkyl-alkyl cross-coupling remains an unsolved challenge.

Scheme 4.12 Gong's nickel-catalyzed reductive alkyl-alkyl coupling

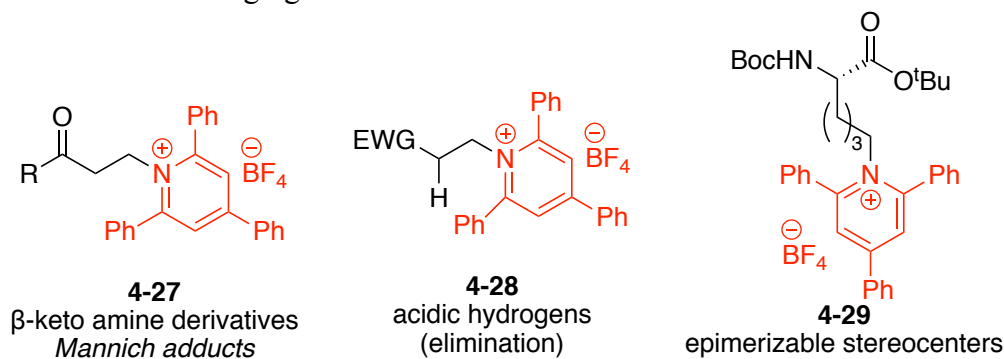


Scheme 4.13 Fu and Liu's cobalt-catalyzed reductive alkyl-alkyl/aryl coupling



Recognizing the advantages of a reductive cross-electrophile coupling as well as the lack of methods to utilize alkyl amine derivatives in this regard, I set out to develop a reductive coupling of alkyl pyridinium salts with aryl bromides. Unlike the previously discussed Suzuki–Miyaura cross-coupling (Chapter 1), this approach allows for a much broader scope under mild conditions. In particular, I hoped to successfully utilize substrates that were problematic under our basic Suzuki conditions (Scheme 4.14). Substrates such as **4-27** and **4-28** were prone to elimination under the basic conditions. Acidic protons as well as substrates susceptible to base-promoted epimerization events (**4-29**) are now tolerated and existing stereocenters are preserved under the new reductive conditions. More importantly, this approach allows for the use of more widely abundant aryl bromides in place of arylboronic acids and provides a complementary method to our existing chemistries.

Scheme 4.14 Challenging substrates under Suzuki conditions



4.2 Results and Discussion

4.2.1 Reaction Optimization: Primary Alkyl Pyridinium Salts

The optimization of this reductive cross-coupling began by coupling model pyridinium salt **4-30** with 3-bromoquinoline to afford desired arylated product **4-31**. Analogous to the competing dimerization of alkyl halides, one of the major byproducts (**4-32**) results from addition of the alkyl radical into the 4-position of another molecule of unreacted pyridinium salt. My colleague Corey Basch conducted preliminary experiments to demonstrate the feasibility of this reductive approach. Initial screens focused on the identification of a suitable reductant for this transformation. Common metal reductants such as zinc and manganese were tested (Table 4.1, entries 1 & 2). Excitingly, the arylated product **4-31** was observed in 26% yield using manganese. The addition of an additive, such as lithium chloride, was found to increase the yield considerably as well as suppress the formation of **4-32** (entry 3). Switching to *N*-methylpyrrolidone as solvent under slightly more dilute conditions further improved the yield of the reaction (entry 4). Upon investigating a variety of additives, I found that magnesium chloride was superior in giving high yields of **4-31** while suppressing the formation of **4-32** (entry 5). We propose that the magnesium chloride may serve a role in accelerating the rate of reduction of the Ni^{II} intermediates as well as help activate the surface of the metal reductant.^{20, 21} Decreasing the amount of metal reductant to two equivalents did not impact yield (entry 6). I screened a variety of ligands and found that the more electron-rich 4,4'-dimethoxy-2,2'-bipyridine ligand was unique in improving this reaction (entry 7). Finally, by employing a slight excess of pyridinium salt **4-30** (1.2 equiv) relative to the aryl bromide (1.0 equiv), **4-31** was observed in 85% isolated yield (entry 8).

Table 4.1 Reaction optimization of the reductive cross-electrophile coupling primary alkyl pyridinium salts with aryl bromides^a

Entry	M ⁰	Additive	Ligand	Solvent	Yield (%) ^b		
					4-31	4-32	Ar-Ar
1	Zn ⁰	none	4,4'-di ^t BuBipy	DMA (0.33 M)	9	24	5
2	Mn ⁰	none	4,4'-di ^t BuBipy	DMA (0.33 M)	26	25	4
3	Mn ⁰	LiCl	4,4'-di ^t BuBipy	DMA (0.33 M)	54	14	4
4	Mn ⁰	LiCl	4,4'-di ^t BuBipy	NMP (0.17 M)	62	10	10
5	Mn ⁰	MgCl ₂	4,4'-di ^t BuBipy	NMP (0.17M)	65	8	15
6 ^c	Mn ⁰	MgCl ₂	4,4'-di ^t BuBipy	NMP (0.17M)	67	6	17
7 ^c	Mn ⁰	MgCl ₂	4,4'-diOMeBipy	NMP (0.17M)	74	7	15
8 ^{c,d}	Mn ⁰	MgCl ₂	4,4'-diOMeBipy	NMP (0.17 M)	85 ^e	n.d.	n.d.

^aConditions: pyridinium salt **4-30** (0.10 mmol), 3-bromoquinoline (1.1 equiv), [Ni] (10 mol %), ligand (12 mol %), M⁰ (3.0 equiv), 80 °C, 24 h, unless noted otherwise.

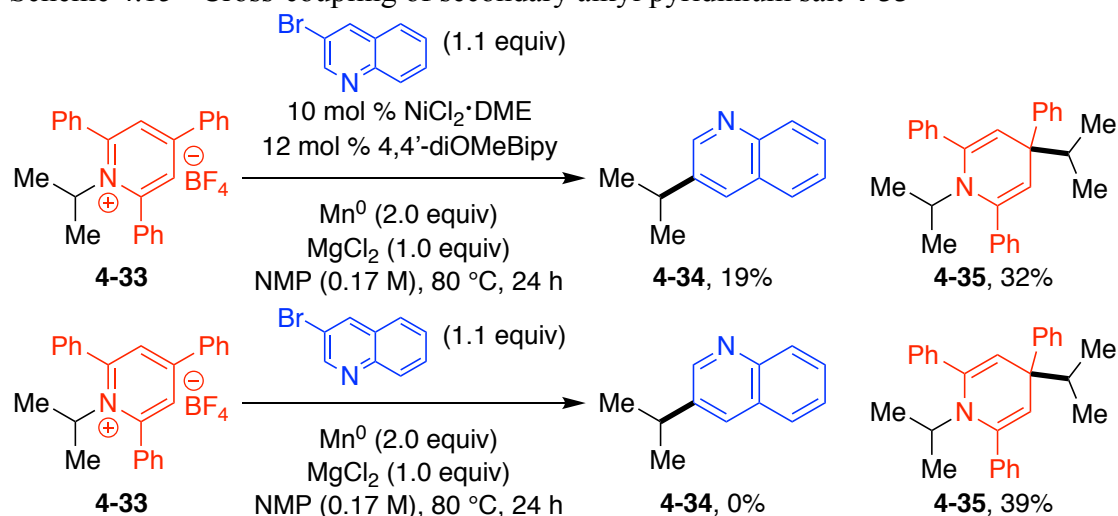
^bDetermined by ¹H NMR analysis using 1,3,5-trimethoxybenzene as internal standard.

^c2.0 equiv M⁰. ^d1.2 equiv **4-30**, 1.0 equiv ArBr. ^eIsolated yield.

4.2.2 Reaction Optimization: Secondary Alkyl Pyridinium Salts

With conditions optimized for the primary alkyl system, I wanted to see if the same conditions would be amenable to the corresponding secondary alkyl system. I chose pyridinium salt **4-33** to test for reactivity. Although the desired product (**4-34**) was formed in 19% yield, the unwanted 4-addition byproduct (**4-35**) was observed in 32% yield (Scheme 4.15, top). Notably for every molecule of **4-35** formed, two molecules of starting material **4-33** are consumed, making this a particularly detrimental competing reaction. I decided to run a series of control experiments to probe this competing pathway. In the absence of nickel and ligand, **4-35** was formed in a similar 39% yield (Scheme 4.15, bottom). Therefore, this byproduct can arise from an off-cycle non-nickel-catalyzed pathway at a rate that is competitive with cross-coupling. The major challenge here was to figure out how to use transition metal catalysis to accelerate the rate of productive cross-coupling while suppressing this unwanted off-cycle pathway.

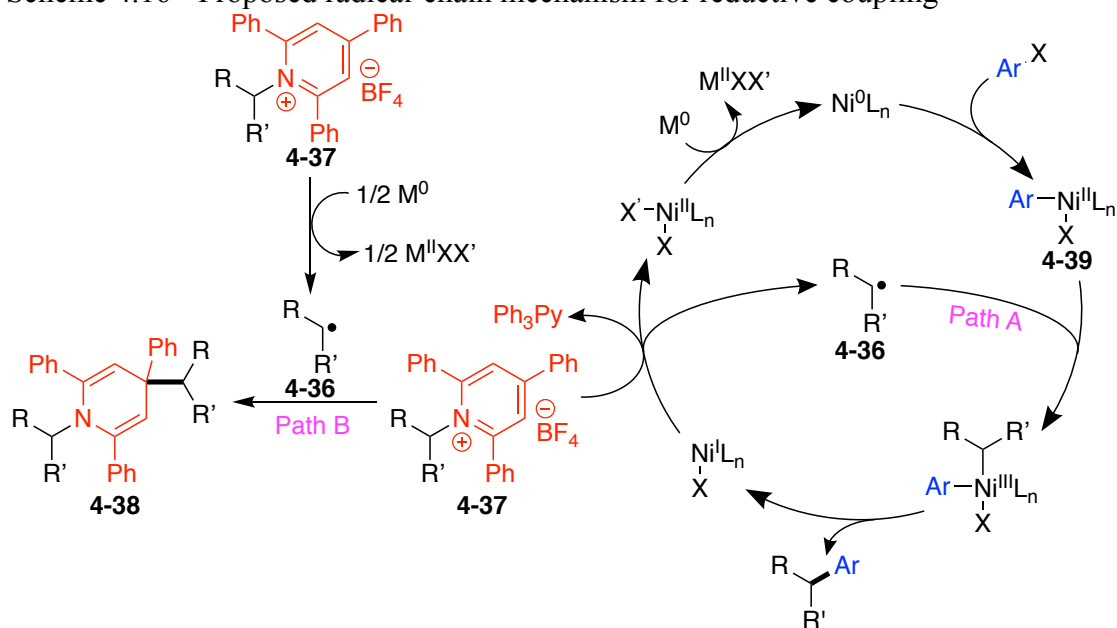
Scheme 4.15 Cross-coupling of secondary alkyl pyridinium salt **4-33**



Yields determined by ¹H NMR analysis using 1,3,5-trimethoxybenzene as internal standard.

To gain a deeper understanding of the reaction, I took a closer look at one possible mechanism. I proposed a radical-chain bimetallic pathway (Scheme 4.16), analogous to Weix's reductive coupling of alkyl halides with aryl halides (*vide supra*, Scheme 4.6).⁷ If the generated alkyl radical intermediate **4-36** proceeds via a productive on-cycle event (Path A), desired cross-coupling is observed. However, if instead it gets trapped by another molecule of unreacted pyridinium **4-37** (Path B), we observe the formation of 4-addition byproduct **4-38**. This is further complicated by the fact that manganese appears to be able to directly reduce the pyridinium to form alkyl radical **4-36**, and in turn lead to the formation of undesired **4-38**.

Scheme 4.16 Proposed radical-chain mechanism for reductive coupling



Thus, effectively controlling the reactivity of carbon-centered radical **4-36** is key in controlling the selectivity of this reaction. We need to limit the concentration of pyridinium salt **4-37** relative to radical **4-36** to suppress the competing dimerization

pathway (Path B), while having a relatively high concentration of Ni^{II}-arene **4-39** to intercept alkyl radical **4-36** and enable cross-coupling (Path A). I proposed performing a slow-addition of pyridinium salt **4-37**. This procedure would limit the concentration of **4-36** in solution and suppress the formation of unwanted **4-38**. Additionally, this would allow for build-up of Ni species **4-39** to enable rapid capture of alkyl radical **4-36** and feed back into the catalytic cycle.

I was delighted to find that a slow-addition of **4-33** over the course of two hours more than doubled the yield of desired cross-coupled product **4-34** (Table 4.2, entries 1 vs 3). Moreover, the formation of 4-addition **4-35** was greatly suppressed. Notably, however, the amount of biaryl (Ar–Ar) formed increased significantly. This dimer presumably arises from metathesis of the Ni^{II}-arene species **4-39** followed by reductive elimination. This tells us that the rate of oxidative addition of the aryl halide into the low valent Ni⁰ species is likely fast. Additionally, the overall mass balance for the alkyl portion of the molecule is quite poor, suggesting that the corresponding rate of radical formation is slower. In order to mitigate these issues, I performed a slow addition of a solution of both the alkyl pyridinium salt as well as the aryl halide. In doing so, the amount of biaryl formation was suppressed and a much better mass balance was observed (entry 4). Finally, good yield of cross-coupled product **4-34** was observed with a slow addition of pyridinium salt **4-33** and 3-bromoquinoline over six hours (entry 7). Excitingly, there is only minimal formation the 4-addition **4-35** and biaryl byproducts under these conditions.

Table 4.2 Reaction optimization of the reductive cross-electrophile coupling secondary alkyl pyridinium salts with aryl bromides^a

Entry	Reagents	Time (h)	Yield (%) ^b		
			4-34	4-35	Ar–Ar
1	none	none	19	32	12
2	4-33	1	24	28	28
3	4-33	2	50	3	20
4	4-33 + ArBr	2	50	14	12
5	4-33 + ArBr	3	68	9	11
6	4-33 + ArBr	4	76	8	6
7	4-33 + ArBr	6	84	2	4

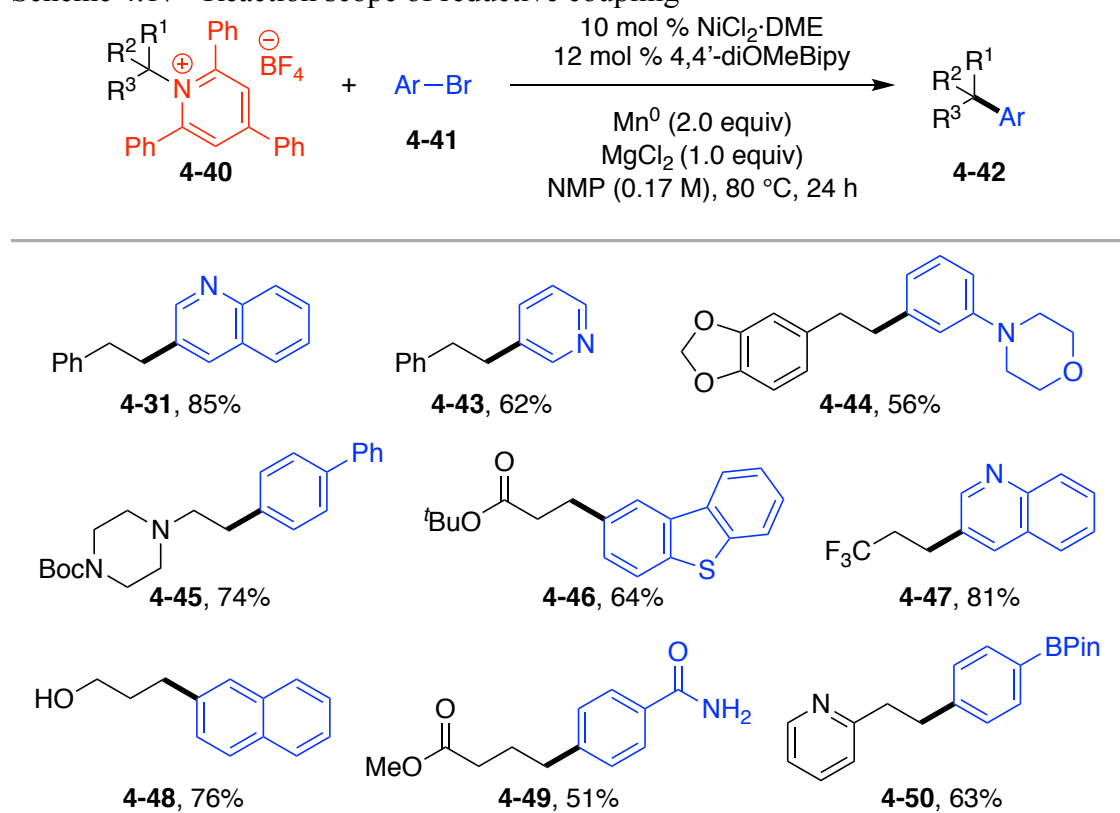
^aConditions: pyridinium salt **4-33** (0.5 mmol), 3-bromoquinoline (1.1 equiv), NiCl₂·DME (10 mol %), 4,4'-dimethoxy-2,2'-bipyridine (12 mol %), Mn⁰ (2.0 equiv), MgCl₂ (1.0 equiv), NMP (0.17 M), 80 °C, 24 h, unless noted otherwise. ^bDetermined by ¹H NMR analysis using 1,3,5-trimethoxybenzene as internal standard.

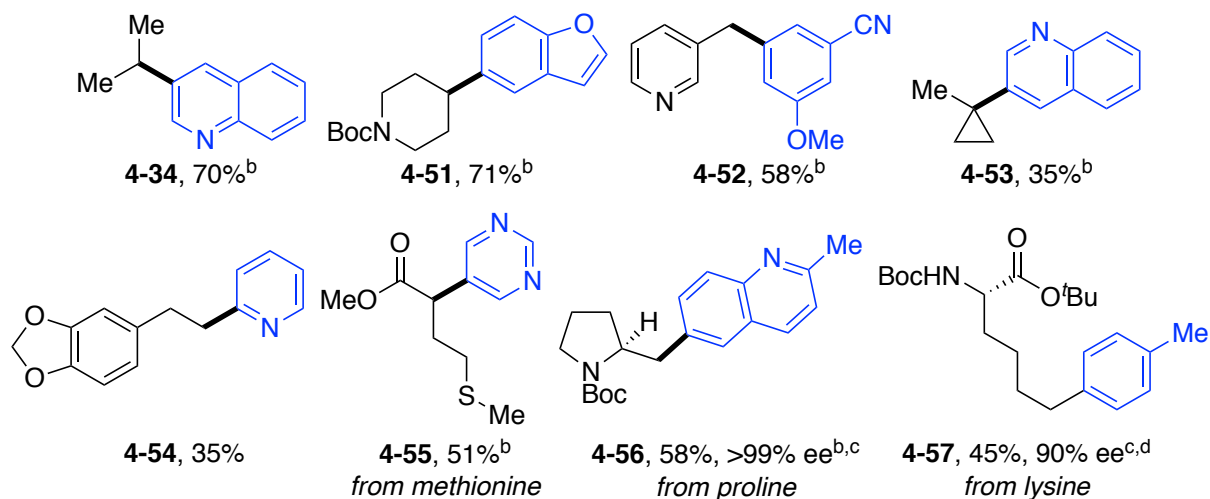
4.2.3 Reaction Scope

With conditions optimized for both the primary and secondary alkyl systems, I recruited my colleagues Megan Hoerrner and Mike Talley to help explore the scope of

this transformation. Overall, very broad substrate scope was realized (Scheme 4.17). Model product **4-31** was isolated in 85% yield on a 1.0-mmol scale. A variety of primary and secondary (cyclic and acyclic) alkyl groups coupled effectively. Excitingly, substrates containing heterocycles such as piperazine (**4-45**), piperidine (**4-51**), pyrrolidine (**4-56**), and pyridine (**4-50** & **4-52**) were amenable to this chemistry. Additionally, benzylic pyridinium salts were competent coupling partners (**4-52**). I have also demonstrated the cross-coupling of tertiary alkyl substrate **4-53**, albeit in low yield. Importantly, substrates that readily eliminate under the basic Suzuki conditions such as **4-46** and **4-47** proceeded smoothly under these reductive conditions. Additionally, unprotected alcohol **4-48** was well tolerated.

Scheme 4.17 Reaction scope of reductive coupling^a





^aConditions: pyridinium salt **4-40** (1.2 mmol), aryl bromide **4-41** (1.0 mmol), NiCl₂·DME (10 mol %), 4,4'-dimethoxy-2,2'-bipyridine (12 mol %), Mn⁰ (2.0 equiv), MgCl₂ (1.0 equiv), NMP (0.17 M) 80 °C, 24 h. Average isolated yields (±5%) from duplicate experiments. ^bPyridinium salt **4-40** (1.0 mmol), aryl bromide **4-41** (1.1 mmol). ^cEnantiomeric excess determined by chiral HPLC analysis. ^dSingle experiment. 0.1-mmol scale. Yield determined by ¹H NMR using 1,3,5-trimethoxybenzene as internal standard.

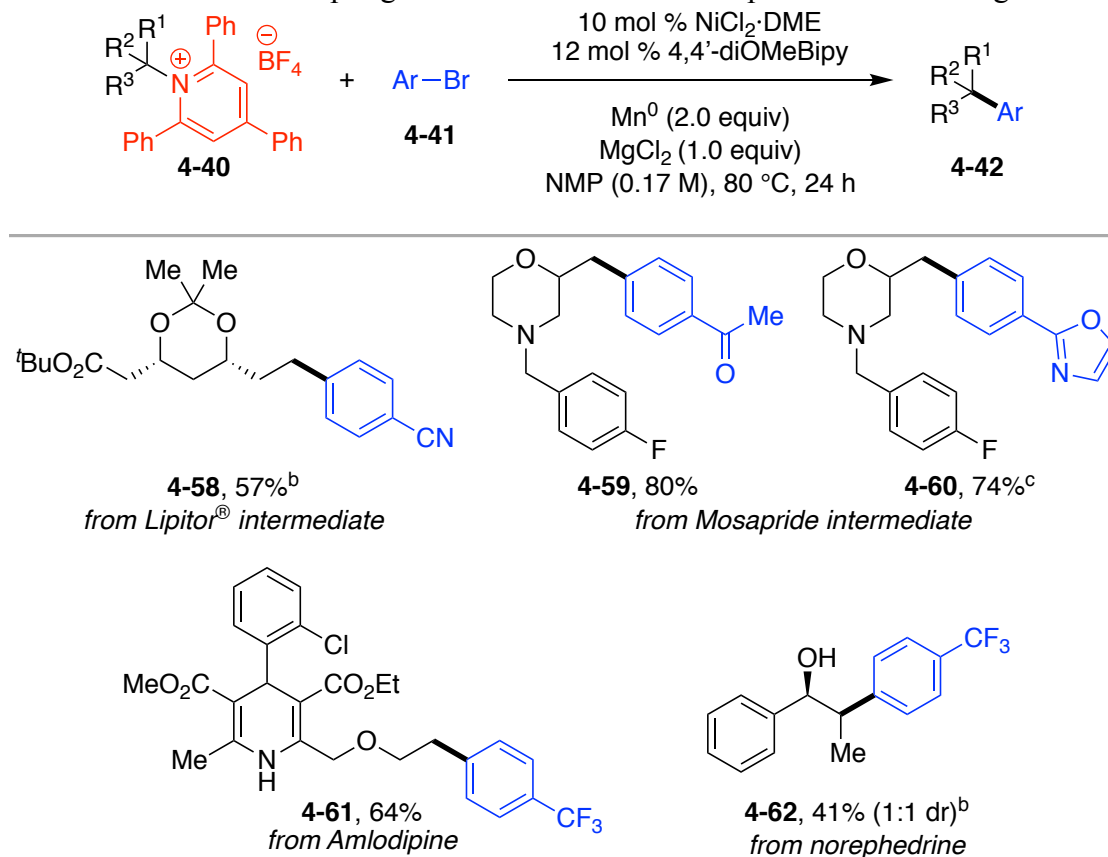
Substrates derived from amino acids were also competent coupling partners. Cross-coupling of the α -amino group of methionine methyl ester (**4-55**) and a proline derivative (**4-56**) proceeded smoothly. Moreover, cross-coupling of the amino side chain of *N*-Boc lysine produced **4-57** in 45% yield and 90% *ee*. Notably, the parent amine of *N*-Boc lysine *tert*-butyl ester was determined to be 90% *ee*. This example highlights the advantage of this reductive approach for the preservation of enantiomeric excess in substrates containing epimerizable stereocenters. Excitingly, this has implications for biological applications of this chemistry, particularly in the

context of peptide conjugation and the formation of cyclic peptides via cross couplings of the *N*-terminus or lysine side chain.

Broad scope was also observed in the aryl bromide coupling partner. Heteroarenes such as quinoline (**4-31**, **4-47**, **4-34**, **4-53** & **4-56**), 2- and 3-pyridine (**4-43** & **4-54**), pyrimidine (**4-55**), benzofuran (**4-51**), and dibenzothiophene (**4-46**) were well tolerated. Excitingly, unprotected benzamide (**4-49**) participated smoothly under the reaction conditions, demonstrating that functional groups containing acidic protons can be incorporated via this method. Aryl boronic ester (**4-50**) highlights the orthogonality of this approach to standard Suzuki–Miyaura cross-couplings.

Additionally, I wanted to demonstrate the advantage of utilizing an alkyl amine, as well as the utility of this chemistry for late-stage functionalization by cross-coupling substrates derived from pharmaceutical drugs and their intermediates (Scheme 4.18). Product **4-58** derives from an amine intermediate used in the synthesis of Lipitor[®] (Pfizer, Inc.), an anti-cholesterol drug.²² Products **4-59** and **4-60** are derived from an amine intermediate in the synthesis of Mosapride, a treatment for gastrointestinal disorders.²³ Notably, **4-60** was formed on a gram scale (1.04 g), highlighting the scalability of this reaction, even with the heterogeneous nature of the metal reductant. Moreover, we recognized that the amine (NH₂) moiety is present in a number of bioactive molecules and can be further derivatized via this approach. Amlodipine, a treatment for high blood pressure,²⁴ cross-coupled effectively under the standard reaction conditions to afford **4-61** in 64% yield. Norephedrine, a common decongestant,²⁵ afforded **4-62** in synthetically useful yield, albeit in poor diastereomeric ratio (dr). Excitingly, these examples demonstrate the advantage of harnessing the native amine (NH₂) moiety of these molecules in cross-couplings.

Scheme 4.18 Cross-coupling of substrates derived from pharmaceutical drugs^a



^aConditions: pyridinium salt **4-40** (1.2 mmol), aryl bromide **4-41** (1.0 mmol), NiCl₂·DME (10 mol %), 4,4'-dimethoxy-2,2'-bipyridine (12 mol %), Mn⁰ (2.0 equiv), MgCl₂ (1.0 equiv), NMP (0.17 M) 80 °C, 24 h. Average isolated yields (±5%) from duplicate experiments. ^bPyridinium salt **4-40** (1.0 mmol), aryl bromide **4-41** (1.1 mmol). ^cSingle experiment. 4.0-mmol scale.

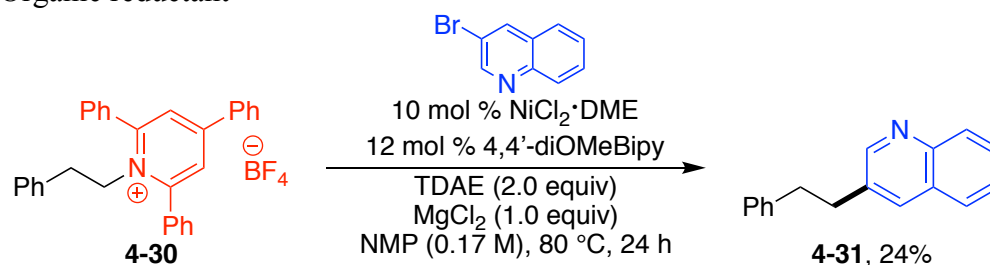
4.2.4 Mechanism Studies

A series of mechanistic experiments were conducted to elucidate the mechanism of this transformation (Scheme 4.19). In using an organic reductant such as tetra(dimethylamino)ethylene (TDAE) in place of manganese, arylated product **4-**

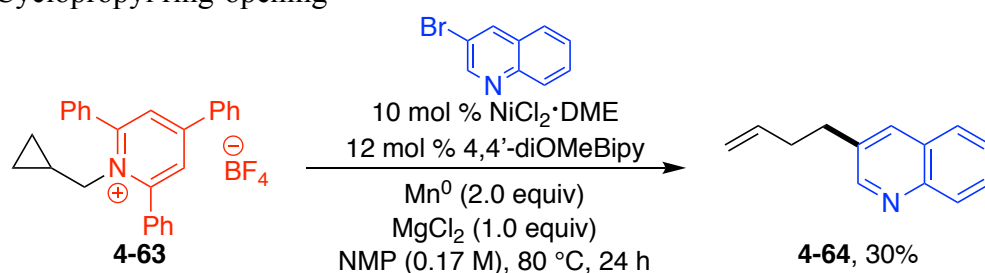
31 was observed in 24% yield (Scheme 4.19A). This result suggests that an organomanganese species is not an intermediate, because both arylated product **4-31** and catalyst turnover are observed in the absence of manganese. Furthermore, cyclopropyl ring-opening and TEMPO trapping experiments (Scheme 4.19B and C) support the formation of an alkyl radical intermediate from the alkyl pyridinium salt. This is evidence against mechanisms involving sequential two-electron oxidative additions.

Scheme 4.19 Mechanistic experiments

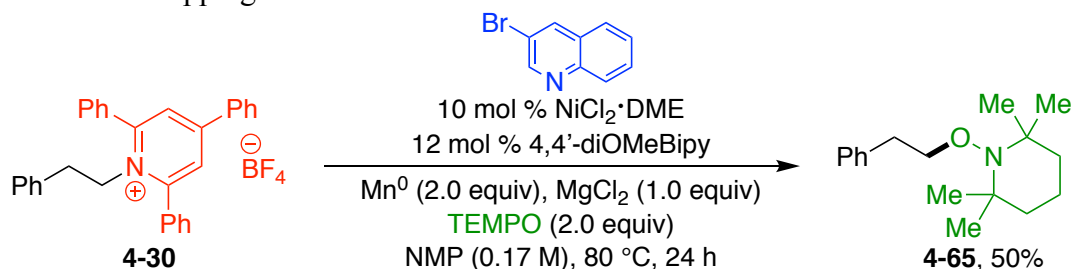
A. Organic reductant



B. Cyclopropyl ring-opening



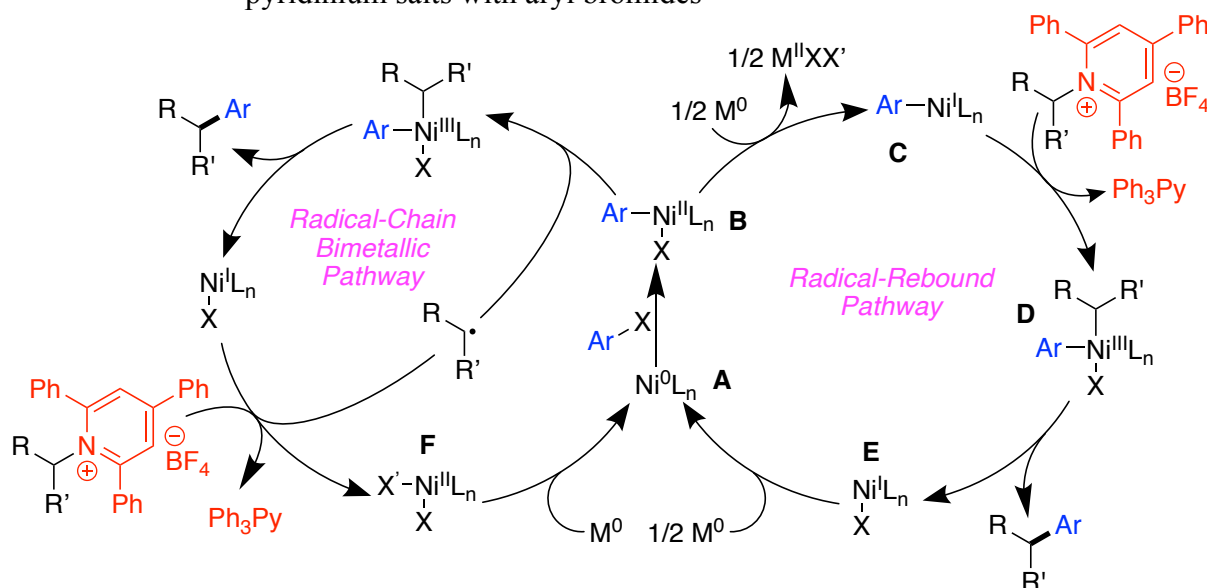
C. TEMPO trapping



Yields determined by ^1H NMR analysis using 1,3,5-trimethoxybenzene as internal standard.

Based on observations made in related cross-couplings of alkyl halides, the two most likely mechanistic pathways involving alkyl radical intermediates are shown in Scheme 4.20. The proposed radical-chain bimetallic pathway (*vide supra*) is shown on the left. The other major competing mechanism invokes a radical rebound pathway (Scheme 4.20, right). In this case, low valent Ni^0 species **A** undergoes oxidative addition into the aryl halide to form Ni^{II} -arene species **B**. This is followed by a single-electron reduction to generate Ni^{I} -arene **C**. Oxidative addition of the alkyl pyridinium salt via single electron transfer and recombination leads to diorgano- Ni^{III} species **D**, which is primed to undergo reductive elimination forming arylated product and Ni^{I} -X species **E**. Finally, the cycle is turned over via a single-electron reduction of **E** back to Ni^0 species **A** by manganese.

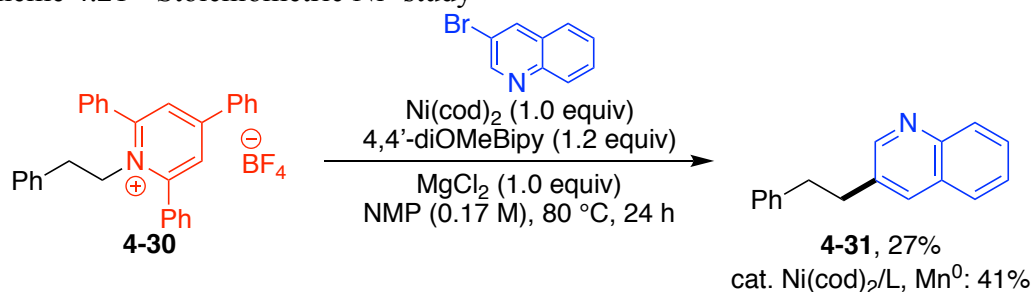
Scheme 4.20 Two possible mechanisms for the reductive coupling of alkyl pyridinium salts with aryl bromides



Notably, the role of manganese is unique in each pathway. In the radical-chain bimetallic pathway, manganese is required to reduce Ni^{II} species **F** back to Ni^0 species

A and turn over the catalytic cycle. However, in the radical-rebound pathway, manganese is involved in both reduction of Ni^{II}-arene **B** to Ni^I-arene **C** as well as reduction of Ni^I species **F** back to Ni⁰ species **A**. In this case, manganese is required for catalyst turnover and for one of the elementary steps of the catalytic cycle. A stoichiometric nickel study in the absence of manganese would help differentiate between the two mechanisms. In the case of the former mechanism, the lack of a reductant should have little or no effect on the reaction if it is only required for catalyst turnover. However, in the latter mechanism, the absence of manganese should prevent the desired pathway from proceeding, leading to little or no product formation. In utilizing a stoichiometric amount of Ni⁰, the desired product **4-31** was observed in substantial yield (Scheme 4.21). This is evidence against the radical-rebound pathway. Notably, however, there are other ways to get to Ni^I-arene species **C** such as comproportionation of **A** and **B**, and therefore we cannot currently rule out this possibility. Moreover, although initiation of this reaction has not been studied in detail, it may involve Mn⁰ or one of the Ni intermediates (on- or off-cycle). Further mechanistic studies are needed to confirm our proposed radical-chain bimetallic pathway.

Scheme 4.21 Stoichiometric Ni⁰ study



Yield determined by ¹H NMR analysis using 1,3,5-trimethoxybenzene as internal standard.

4.3 Conclusion

In summary, I have developed a reductive cross-electrophile coupling of alkyl pyridinium salts with aryl bromides. This approach leverages the wide availability of alkyl amines and aryl halides for the construction of new carbon-carbon bonds. Additionally, this method demonstrates increased scope compared to the initial Suzuki–Miyaura cross-coupling. Notably, substrates containing acidic protons, eliminatable hydrogens, or epimerizable stereocenters were well tolerated. We have also shown the applicability of this chemistry to amino acid derivatives, pharmaceuticals, and pharmaceutical intermediates. Preliminary mechanistic data supports a radical-chain bimetallic pathway.

4.4 Experimental

4.4.1 General Information

Reactions were performed in oven-dried Schlenk flasks or in oven-dried round-bottomed flasks unless otherwise noted. Round-bottomed flasks were fitted with rubber septa, and reactions were conducted under a positive pressure of N₂. Stainless steel syringes were used to transfer air- and moisture-sensitive liquids. Silica gel chromatography was performed on silica gel 60 (40-63 μm, 60Å) unless otherwise noted. Commercial reagents were purchased from Sigma Aldrich, Acros, Fisher, Strem, TCI, Combi Blocks, Alfa Aesar, AK Scientific, Oakwood, or Cambridge Isotopes Laboratories and used as received with the following exceptions: anhydrous NMP degassed by sparging with N₂ for 20–30 minutes prior to use in the cross-coupling reactions; CH₂Cl₂ was dried by passing through drying columns.²⁶ Powdered, activated 4Å molecular sieves were prepared by heating sieves to ~200°C under high

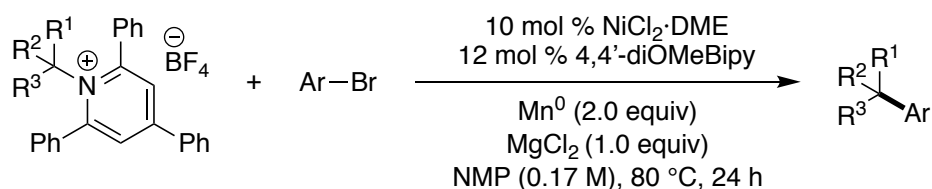
vacuum overnight and then crushing to achieve a fine powder. In some instances oven-dried potassium carbonate was added to CDCl_3 to remove trace acid. Proton nuclear magnetic resonance (^1H NMR) spectra, carbon nuclear magnetic resonance (^{13}C NMR) spectra, and fluorine nuclear magnetic resonance spectra (^{19}F NMR) were recorded on both 400 MHz and 600 MHz spectrometers. Chemical shifts for protons are reported in parts per million downfield from tetramethylsilane and are referenced to residual protium in the NMR solvent ($\text{CHCl}_3 = \delta$ 7.26). Chemical shifts for carbon are reported in parts per million downfield from tetramethylsilane and are referenced to the carbon resonances of the solvent ($\text{CDCl}_3 = \delta$ 77.16). Chemical shifts for fluorine were externally referenced to CFCl_3 in CDCl_3 ($\text{CFCl}_3 = \delta$ 0). Data are represented as follows: chemical shift, multiplicity (br = broad, s = singlet, d = doublet, t = triplet, q = quartet, p = pentet, m = multiplet, dd = doublet of doublets, hept = heptet), coupling constants in Hertz (Hz), integration. Infrared (IR) spectra were obtained using FTIR spectrophotometers with material loaded onto a KBr plate. The mass spectral data were obtained at the University of Delaware mass spectrometry facility. Melting points were taken on a Thomas-Hoover Uni-Melt Capillary Melting Point Apparatus.

4.4.2 General Optimization Procedure

In a N_2 -filled glovebox: To an oven-dried 1-dram vial was added nickel salt (0.010 mmol, 10 mol %), ligand (0.012 mmol, 12 mol %), additive (0.1 mmol, 1.0 equiv), reductant (0.3 mmol, 3.0 equiv), and pyridinium salt **4-30**. 3-Bromoquinoline (15 μL , 0.11 mmol, 1.1 equiv) was then added to the vial followed by solvent. The vial was then equipped with a stir bar, capped with a Teflon-coated cap, and removed from the glovebox. The resulting mixture was stirred vigorously at 80 $^\circ\text{C}$ for 24 h. The

mixture was then diluted with EtOAc (1.5 mL), filtered through a short plug of silica gel, and the filter cake was washed with EtOAc (10 mL). The filtrate was then washed with brine (2 x 5 mL), dried with MgSO₄, and concentrated. 1,3,5-Trimethoxybenzene (internal standard) and CDCl₃ were added, and the yield was determined by ¹H NMR analysis.

4.4.3 Reductive Cross-Electrophile Coupling of Alkyl Pyridinium Salts with Aryl Bromides



4.4.3.1 General Procedure A: Cross-Coupling of Primary Alkyl Pyridinium Salts

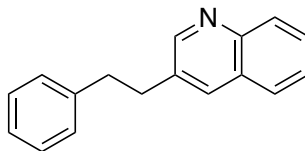
To an oven-dried, 25-mL Schlenk flask was added NiCl₂·DME (22 mg, 0.10 mmol, 10 mol %), 4,4'-dimethoxy-2,2'-bipyridine (26 mg, 0.12 mmol, 12 mol %), magnesium chloride (95 mg, 1.0 mmol, 1.0 equiv), manganese powder (110 mg, 2.0 mmol, 2.0 equiv), alkyl pyridinium salt (1.2 mmol, 1.2 equiv), and arylbromide (1.0 mmol, 1.0 equiv), if solid. The flask was fitted with a rubber septum, sealed with parafilm, and then evacuated and refilled with N₂ (x 3). If the arylbromide was a liquid, it was introduced via syringe at this point. *N*-Methyl-2-pyrrolidone (6.0 mL) was added, and the flask was sealed. The resulting mixture was stirred at 80 °C for 24 hours. The mixture was then allowed to cool to room temperature, filtered through a short plug of silica gel, and the filter cake washed with ethyl acetate (4 x 25 mL). The

filtrate was then washed with brine (4 x 25 mL). The combined aqueous layers were back-extracted with ethyl acetate (1 x 25 mL). The combined organic layers were dried with magnesium sulfate and concentrated. The cross-coupled product was then purified via silica gel chromatography.

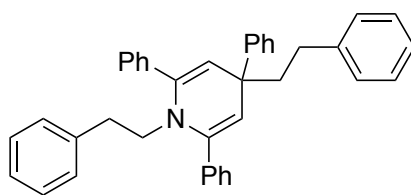
4.4.3.2 General Procedure B: Cross-Coupling of Secondary Alkyl Pyridinium Salts

To an oven-dried, 25-mL Schlenk flask was added NiCl₂·DME (22 mg, 0.10 mmol, 10 mol %), 4,4'-dimethoxy-2,2'-bipyridine (26 mg, 0.12 mmol, 12 mol %), magnesium chloride (95 mg, 1.0 mmol, 1.0 equiv), and manganese powder (110 mg, 2.0 mmol, 2.0 equiv). The flask was fitted with a rubber septum, sealed with parafilm, and then evacuated and refilled with N₂ (x 3). *N*-Methyl-2-pyrrolidone (4.0 mL) was added, and the resultant mixture was heated to 80 °C. To a separate oven-dried, 10-mL Schlenk flask was added alkyl pyridinium salt (1.0 mmol, 1.0 equiv) and arylbromide (1.1 mmol, 1.1 equiv), if solid. The flask was fitted with a rubber septum, sealed with parafilm, and then evacuated and refilled with N₂ (x 3). If the arylbromide was a liquid, it was introduced via syringe at this point. *N*-Methyl-2-pyrrolidone (2.0 mL) was added and the contents transferred into a 3-mL nitrogen-purged leur-lock syringe. The solution was added at a steady rate into the flask containing the catalyst mixture via syringe pump over a period of six hours. The resulting mixture was stirred at 80 °C for an additional 18 hours (24 hours total). The mixture was then allowed to cool to room temperature, filtered through a short plug of silica gel, and the filter cake washed with ethyl acetate (4 x 25 mL). The filtrate was then washed with brine (4 x 25 mL). The combined aqueous layers were back-extracted with ethyl acetate (1 x 25 mL). The

combined organic layers were dried with magnesium sulfate and concentrated. The cross-coupled product was then purified via silica gel chromatography.

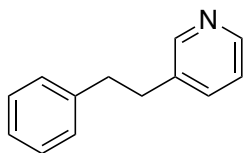


3-Phenethylquinoline (4-31). Prepared via General Procedure A using 1-phenethyl-2,4,6-triphenylpyridin-1-ium tetrafluoroborate. The crude mixture was purified by silica gel chromatography (10–50% ethyl acetate/hexanes) to give **4-31** (run 1: 201 mg, 86%; run 2: 195 mg, 84%) as a pale yellow oil: ^1H NMR (600 MHz, CDCl_3) δ 8.75 (d, $J = 2.2$ Hz, 1H), 8.08 (d, $J = 8.5$ Hz, 1H), 7.88 – 7.85 (m, 1H), 7.77 – 7.72 (m, 1H), 7.69 – 7.63 (m, 1H), 7.55 – 7.49 (m, 1H), 7.29 (t, $J = 7.5$ Hz, 2H), 7.23 – 7.14 (m, 3H), 3.13 (t, $J = 7.8$ Hz, 2H), 3.03 (t, $J = 7.8$ Hz, 2H); ^{13}C NMR (151 MHz, CDCl_3) δ 152.0, 146.9, 140.8, 134.4, 134.2, 129.2, 128.7, 128.5, 128.1, 127.3, 126.6, 126.2, 37.5, 35.1. The spectral data matches that reported in the literature.²⁷

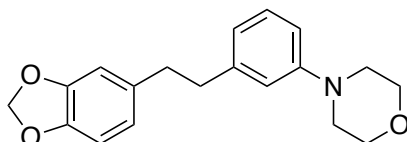


1,4-Diphenethyl-2,4,6-triphenyl-1,4-dihydropyridine (4-32): ^1H NMR (400 MHz, CDCl_3) δ 7.57 (s, 6H), 7.44 – 7.35 (m, 8H), 7.25 – 7.11 (m, 6H), 7.04 – 6.95 (m, 3H), 6.51 – 6.44 (m, 2H), 5.18 (s, 2H), 3.29 – 3.20 (m, 2H), 2.72 – 2.63 (m, 2H), 2.37 – 2.28 (m, 2H), 2.20 – 2.11 (m, 2H); ^{13}C NMR (101 MHz, CDCl_3) δ 151.4, 143.1, 143.0, 139.1, 138.0, 128.42, 128.39, 128.37, 128.35, 128.3, 128.11, 128.08, 128.00,

126.4, 125.8, 125.6, 125.5, 113.3, 50.0, 46.7, 43.8, 34.7, 32.7; HRMS (ESI+) $[M+H]^+$ calculated for $C_{39}H_{36}N$: 518.2842, found 518.2823.

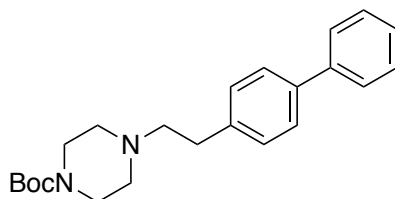


3-Phenethylpyridine (4-43). Prepared via General Procedure A using 1-phenethyl-2,4,6-triphenylpyridin-1-ium tetrafluoroborate. The crude mixture was purified by silica gel chromatography (5–60% ether/hexanes w/ 1% Et_3N) to give **4-43** (run 1: 115 mg, 63%; run 2: 110 mg, 60%) as a pale yellow oil: 1H NMR (400 MHz, $CDCl_3$) δ 8.45 (dd, $J = 4.8, 1.7$ Hz, 1H), 8.44 – 8.41 (m, 1H), 7.43 (dt, $J = 7.8, 2.0$ Hz, 1H), 7.31 – 7.26 (m, 2H), 7.23 – 7.13 (m, 4H), 2.93 (s, 4H); ^{13}C NMR (101 MHz, $CDCl_3$) δ 150.2, 147.6, 141.0, 136.9, 136.0, 128.59, 128.57, 126.3, 123.3, 37.6, 35.1. The spectral data matches that reported in the literature.²⁸



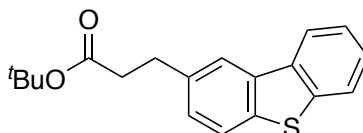
4-(3-(2-(Benzo[*d*][1,3]dioxol-5-yl)ethyl)phenyl)morpholine (4-44). Prepared via General Procedure A using 1-(2-(benzo[*d*][1,3]dioxol-5-yl)ethyl)-2,4,6-triphenylpyridin-1-ium tetrafluoroborate. The crude mixture was purified by silica gel chromatography (5–20% ethyl acetate/hexanes) to give **4-44** (run 1: 164 mg, 53%; run 2: 181 mg, 58%) as an off-white solid (mp 44–46 °C): 1H NMR (600 MHz, $CDCl_3$) δ 7.20 (t, $J = 7.8$ Hz, 1H), 6.76 (dd, $J = 8.1, 2.0$ Hz, 1H), 6.74 – 6.70 (m, 3H), 6.68 (d, $J = 1.6$ Hz, 1H), 6.63 (dd, $J = 7.9, 1.7$ Hz, 1H), 5.92 (s, 2H), 3.88 – 3.83 (m, 4H), 3.16 – 3.11 (m, 4H), 2.83 (s, 4H); ^{13}C NMR (151 MHz, $CDCl_3$) δ 151.4, 147.5, 145.6, 142.7,

135.7, 129.1, 121.2, 120.3, 116.1, 113.4, 109.0, 108.1, 100.8, 67.0, 49.5, 38.6, 37.7; FTIR (neat) 2853, 1600, 1489, 1443, 1242, 1121, 928, 696 cm^{-1} ; HRMS (ESI+) $[\text{M}+\text{H}]^+$ calculated for $\text{C}_{19}\text{H}_{22}\text{NO}_3$: 312.1594, found 312.1590.



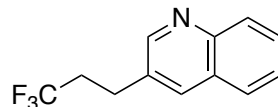
***tert*-Butyl 4-(2-([1,1'-biphenyl]-4-yl)ethyl)piperazine-1-carboxylate (4-45).**

Prepared via General Procedure A using 1-(2-(4-(*tert*-butoxycarbonyl)piperazin-1-yl)ethyl)-2,4,6-triphenylpyridin-1-ium tetrafluoroborate. The crude mixture was purified by silica gel chromatography (10–20% ethyl acetate/hexanes) to give **4-45** (run 1: 268 mg, 73%; run 2: 275 mg, 75%) as a white solid (mp 85–89 °C): ^1H NMR (400 MHz, CDCl_3) δ 7.61 – 7.55 (m, 2H), 7.55 – 7.48 (m, 2H), 7.48 – 7.39 (m, 2H), 7.38 – 7.31 (m, 1H), 7.31 – 7.27 (m, 2H), 3.52 – 3.44 (m, 4H), 2.90 – 2.81 (m, 2H), 2.69 – 2.60 (m, 2H), 2.52 – 2.46 (m, 4H), 1.47 (s, 9H); ^{13}C NMR (101 MHz, CDCl_3) δ 154.8, 141.0, 139.2, 139.1, 129.1, 128.8, 127.2, 127.1, 127.0, 79.7, 60.5, 53.0, 33.2, 28.5; FTIR (neat) 2929, 2807, 1695, 1420, 1247, 1171, 1003, 761 cm^{-1} ; HRMS (ESI+) $[\text{M}+\text{H}]^+$ calculated for $\text{C}_{23}\text{H}_{31}\text{N}_2\text{O}_2$: 367.2380, found 367.2376.

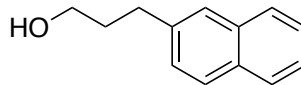


***tert*-Butyl 3-(dibenzo[*b,d*]thiophen-2-yl)propanoate (4-46).** Prepared via General Procedure A using 1-(3-(*tert*-butoxy)-3-oxopropyl)-2,4,6-triphenylpyridin-1-ium tetrafluoroborate. The crude mixture was purified by silica gel chromatography (2–

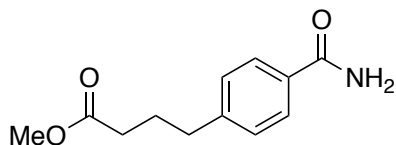
10% diethyl ether/hexanes) to give **4-46** (run 1: 200 mg, 64%; run 2: 199 mg, 64%) as a white solid (mp 53–55 °C): ^1H NMR (600 MHz, CDCl_3) δ 8.19 – 8.13 (m, 1H), 8.02 (s, 1H), 7.90 – 7.84 (m, 1H), 7.79 (d, $J = 8.2$ Hz, 1H), 7.50 – 7.44 (m, 2H), 7.37 – 7.32 (m, 1H), 3.12 (t, $J = 7.8$ Hz, 2H), 2.67 (t, $J = 7.8$ Hz, 2H), 1.45 (s, 9H); ^{13}C NMR (151 MHz, CDCl_3) δ 172.2, 139.8, 137.23, 137.21, 135.8, 135.4, 127.5, 126.6, 124.3, 122.9, 122.7, 121.5, 121.2, 80.5, 37.5, 31.2, 28.1; FTIR (neat) 2976, 2930, 1726, 1366, 1150, 764 cm^{-1} ; HRMS (ESI+) $[\text{M}+\text{H}]^+$ calculated for $\text{C}_{19}\text{H}_{21}\text{O}_2\text{S}$: 313.1257, found 313.1245.



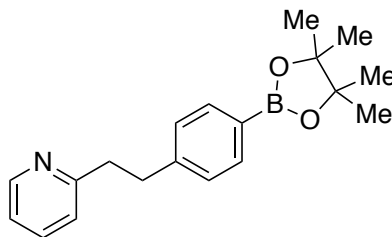
3-(3,3,3-Trifluoropropyl)quinoline (4-47). Prepared via General Procedure A using 2,4,6-triphenyl-1-(3,3,3-trifluoropropyl)pyridin-1-ium tetrafluoroborate. The crude mixture was purified by silica gel chromatography (10–40% ethyl acetate/hexanes) to give **4-47** (run 1: 188 mg, 84%; run 2: 173 mg, 77%) as a pale yellow solid (mp 54–55 °C): ^1H NMR (400 MHz, CDCl_3) δ 8.80 (d, $J = 2.3$ Hz, 1H), 8.10 (d, $J = 8.5$ Hz, 1H), 7.97 (d, $J = 1.3$ Hz, 1H), 7.83 – 7.75 (m, 1H), 7.75 – 7.66 (m, 1H), 7.60 – 7.51 (m, 1H), 3.14 – 3.05 (m, 2H), 2.60 – 2.43 (m, 2H); ^{13}C NMR (101 MHz, CDCl_3) δ 151.3, 147.2, 134.5, 131.5, 129.3, 129.2, 127.9, 127.4, 127.0, 126.4 (q, $J_{\text{C-F}} = 276.9$ Hz), 35.3 (q, $J_{\text{C-F}} = 28.8$ Hz), 25.7 (q, $J_{\text{C-F}} = 3.3$ Hz); ^{19}F NMR (376 MHz, CDCl_3) δ –66.43; FTIR (neat) 2955, 1496, 1235, 1143, 1097, 976, 756 cm^{-1} ; HRMS (ESI+) $[\text{M}+\text{H}]^+$ calculated for $\text{C}_{12}\text{H}_{11}\text{F}_3\text{N}$: 226.0838, found 226.0838.



3-(Naphthalen-2-yl)propan-1-ol (4-48). Prepared via General Procedure A using 1-(3-hydroxypropyl)-2,4,6-triphenylpyridin-1-ium tetrafluoroborate. The crude mixture was purified by silica gel chromatography (10–40% ethyl acetate/hexanes) to give 4-48 (run 1: 145 mg, 78%; run 2: 137 mg, 74%) as a white solid: ^1H NMR (600 MHz, CDCl_3) δ 7.73 (d, $J = 8.0$ Hz, 1H), 7.72 – 7.68 (m, 2H), 7.57 (s, 1H), 7.40 – 7.33 (m, 2H), 7.30 – 7.26 (m, 1H), 3.64 (t, $J = 6.4$ Hz, 2H), 2.84 – 2.78 (m, 2H), 1.96 – 1.88 (m, 2H); ^{13}C NMR (151 MHz, CDCl_3) δ 139.30, 133.64, 132.03, 127.97, 127.61, 127.40, 127.27, 126.43, 125.94, 125.18, 62.28, 34.10, 32.22. The spectral data matches that reported in the literature.²⁹

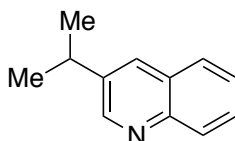


Methyl 4-(4-carbamoylphenyl)butanoate (4-49). Prepared via General Procedure A using 1-(4-methoxy-4-oxobutyl)-2,4,6-triphenylpyridin-1-ium tetrafluoroborate. The crude mixture was purified by silica gel chromatography (50–100% ethyl acetate/hexanes) to give 4-49 (run 1: 103 mg, 46%; run 2: 125 mg, 56%) as a light pink solid: ^1H NMR (400 MHz, CDCl_3) δ 7.74 (d, $J = 8.2$ Hz, 2H), 7.26 (d, $J = 8.0$ Hz, 2H, overlaps with CHCl_3), 6.06 (s, br, 1H), 5.69 (s, br, 1H), 3.67 (s, 3H), 2.70 (t, $J = 7.6$ Hz, 2H), 2.33 (t, $J = 7.4$ Hz, 2H), 1.97 (p, $J = 7.5$ Hz, 2H); ^{13}C NMR (101 MHz, CDCl_3) δ 173.7, 169.2, 145.9, 131.1, 128.8, 127.6, 51.6, 35.0, 33.3, 26.2; HRMS (ESI+) $[\text{M}+\text{H}]^+$ calculated for $\text{C}_{12}\text{H}_{16}\text{NO}_3$: 222.1125, found 222.1124.



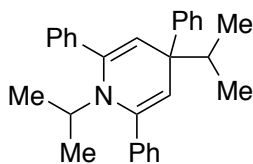
2-(4-(4,4,5,5-Tetramethyl-1,3,2-dioxaborolan-2-yl)phenethyl)pyridine (4-50).

Prepared via General Procedure A using 2,4,6-triphenyl-1-(2-(pyridin-2-yl)ethyl)pyridin-1-ium tetrafluoroborate. The crude mixture was purified by silica gel chromatography (2–10% ethyl acetate/hexanes) to give **4-50** (run 1: 183 mg, 59%; run 2: 203 mg, 66%) as a white solid: ^1H NMR (400 MHz, CDCl_3) δ 8.59 – 8.52 (m, 1H), 7.72 (d, $J = 8.0$ Hz, 2H), 7.55 (td, $J = 7.7, 1.9$ Hz, 1H), 7.21 (d, $J = 7.9$ Hz, 2H), 7.13 – 7.08 (m, 1H), 7.08 – 7.01 (m, 1H), 3.13 – 3.02 (m, 4H), 1.33 (s, 12H); ^{13}C NMR (101 MHz, $(\text{CD}_3)_2\text{CO}$) δ 161.9, 150.13, 150.11, 146.2, 137.0, 135.6, 128.8, 123.7, 122.0, 84.4, 40.5, 36.5, 25.2; HRMS (ESI+) $[\text{M}+\text{H}]^+$ calculated for $\text{C}_{19}\text{H}_{25}\text{BNO}_2$: 310.1973, found 310.1972.

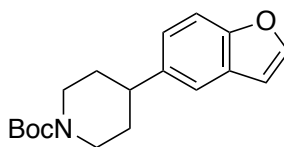


3-Isopropylquinoline (4-34). Prepared via General Procedure B using 1-isopropyl-2,4,6-triphenylpyridin-1-ium tetrafluoroborate. The crude mixture was purified by silica gel chromatography (5–15% ethyl acetate/hexanes) to give **4-34** (run 1: 119 mg, 70%; run 2: 118 mg, 69%) as a yellow oil: ^1H NMR (400 MHz, CDCl_3) δ 8.84 (d, $J = 2.3$ Hz, 1H), 8.07 (d, $J = 8.5$ Hz, 1H), 7.93 (d, $J = 2.2$ Hz, 1H), 7.82 – 7.75 (m, 1H), 7.70 – 7.61 (m, 1H), 7.56 – 7.47 (m, 1H), 3.14 (hept, $J = 7.0$ Hz, 1H), 1.38 (d, $J = 6.9$ Hz, 6H); ^{13}C NMR (101 MHz, CDCl_3) δ 151.3, 146.9, 141.1, 131.8, 129.1, 128.5,

128.2, 127.5, 126.5, 31.9, 23.7. The spectral data matches that reported in the literature.³⁰

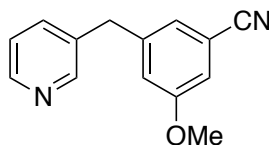


1,4-Diisopropyl-2,4,6-triphenyl-1,4-dihydropyridine (4-35): ¹H NMR (400 MHz, CDCl₃) δ 7.67 – 7.60 (m, 4H), 7.50 – 7.43 (m, 2H), 7.42 – 7.29 (m, 8H), 7.20 – 7.12 (m, 1H), 5.29 (s, 2H), 3.30 (hept, *J* = 6.9 Hz, 1H), 2.01 (hept, *J* = 6.8 Hz, 1H), 0.78 (d, *J* = 6.8 Hz, 6H), 0.58 (d, *J* = 6.9 Hz, 6H); ¹³C NMR (101 MHz, CDCl₃) δ 151.7, 145.2, 140.9, 128.2, 128.0, 127.9, 127.7, 126.8, 125.1, 115.3, 53.6, 47.0, 39.5, 22.6, 18.4; HRMS (ESI+) [*M*+*H*]⁺ calculated for C₂₉H₃₂N: 394.2529, found 394.2513.

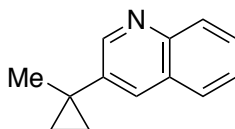


***tert*-Butyl 4-(benzofuran-5-yl)piperidine-1-carboxylate (4-51).** Prepared via General Procedure B using 1-(1-(*tert*-butoxycarbonyl)piperidin-4-yl)-2,4,6-triphenylpyridin-1-ium tetrafluoroborate. The crude mixture was purified by silica gel chromatography (2–10% ethyl acetate/hexanes) to give **4-51** (run 1: 218 mg, 72%; run 2: 210 mg, 70%) as a white solid: ¹H NMR (600 MHz, CDCl₃) δ 7.62 – 7.58 (m, 1H), 7.44 – 7.40 (m, 2H), 7.17 – 7.12 (m, 1H), 6.73 (s, 1H), 4.37 – 4.17 (br m, 2H), 2.92 – 2.77 (m, 2H), 2.74 (tt, *J* = 12.2, 3.6 Hz, 1H), 1.89 – 1.83 (m, 2H), 1.73 – 1.62 (m, 2H), 1.49 (s, 9H); ¹³C NMR (151 MHz, CDCl₃) δ 154.9, 153.7, 145.3, 140.5, 127.6, 123.4,

118.7, 111.2, 106.5, 79.4, 44.5 (br), 42.7, 33.8, 28.5. The spectral data matches that reported in the literature.⁹

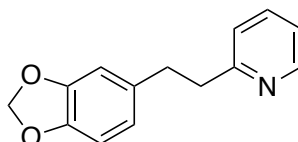


3-Methoxy-5-(pyridin-3-ylmethyl)benzonitrile (4-52). Prepared via General Procedure B using 2,4,6-triphenyl-1-(pyridin-3-ylmethyl)pyridin-1-ium tetrafluoroborate. The crude mixture was purified by silica gel chromatography (20–60% ethyl acetate/hexanes) to give **4-52** (run 1: 129 mg, 58%, run 2: 127 mg, 57%) as an off-white solid (mp 74–78 °C): ¹H NMR (400 MHz, CDCl₃) δ 8.54 – 8.46 (m, 2H), 7.49 – 7.41 (m, 1H), 7.26 – 7.23 (m, 1H), 7.08 – 7.04 (m, 1H), 7.03 – 6.98 (m, 1H), 6.95 – 6.90 (m, 1H), 3.97 (s, 2H), 3.80 (s, 3H); ¹³C NMR (101 MHz, CDCl₃) δ 159.9, 150.1, 148.3, 142.8, 136.3, 134.8, 124.8, 123.7, 120.0, 118.6, 114.8, 113.4, 55.6, 38.6; FTIR (neat) 3029, 2923, 2841, 2228, 1591, 1292, 1059, 718 cm⁻¹; HRMS (ESI+) [M+H]⁺ calculated for C₁₄H₁₃N₂O: 225.1022, found 255.1021.

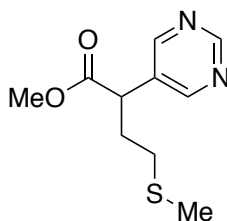


3-(1-Methylcyclopropyl)quinoline (4-53). Prepared via General Procedure B using 1-(1-methylcyclopropyl)-2,4,6-triphenylpyridin-1-ium tetrafluoroborate. The crude mixture was purified by silica gel chromatography (5–20% ethyl acetate/hexanes) to give **4-53** (run 1: 61 mg, 33%, run 2: 65 mg, 36%) as a yellow oil: ¹H NMR (400 MHz, CDCl₃) δ 8.84 (d, *J* = 2.3 Hz, 1H), 8.06 (d, *J* = 8.4 Hz, 1H), 7.99 – 7.93 (m, 1H), 7.76 (d, *J* = 8.1 Hz, 1H), 7.69 – 7.60 (m, 1H), 7.56 – 7.47 (m, 1H), 1.51 (s, 3H),

1.00 (t, $J = 5.4$ Hz, 2H), 0.87 (t, $J = 5.4$ Hz, 2H); ^{13}C NMR (151 MHz, CDCl_3) δ 151.0, 146.5, 139.6, 132.9, 129.1, 128.5, 127.9, 127.3, 126.6, 25.6, 18.4, 15.0; FTIR (neat) 3076, 3001, 2958, 2925, 2870, 1492, 1016, 750 cm^{-1} ; HRMS (ESI+) $[\text{M}+\text{H}]^+$ calculated for $\text{C}_{13}\text{H}_{14}\text{N}$: 184.1121; found 184.1116.

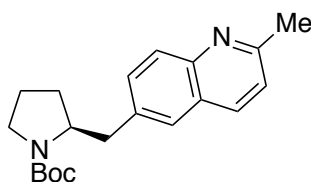


2-(2-(Benzo[d][1,3]dioxol-5-yl)ethyl)pyridine (4-54). Prepared via General Procedure A using 1-(2-(benzo[d][1,3]dioxol-5-yl)ethyl)-2,4,6-triphenylpyridin-1-ium tetrafluoroborate. The crude mixture was purified by silica gel chromatography (5–40% ether/hexanes) to give **4-54** (run 1: 83 mg, 36%; run 2: 77 mg, 34%) as a yellow oil: ^1H NMR (400 MHz, CDCl_3) δ 8.57 – 8.54 (m, 1H), 7.56 (td, $J = 7.7, 1.9$ Hz, 1H), 7.13 – 7.05 (m, 2H), 6.71 (d, $J = 7.9$ Hz, 1H), 6.69 (d, $J = 1.6$ Hz, 1H), 6.63 (dd, $J = 7.9, 1.7$ Hz, 1H), 5.91 (s, 2H), 3.07 – 3.01 (m, 2H), 3.00 – 2.94 (m, 2H); ^{13}C NMR (101 MHz, CDCl_3) δ 161.2, 149.5, 147.6, 145.8, 136.4, 135.5, 123.1, 121.34, 121.31, 109.1, 108.3, 100.9, 40.7, 35.9. The spectral data matches that reported in the literature.³¹



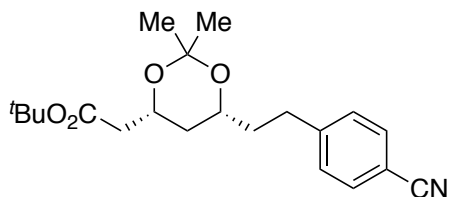
Methyl 4-(methylthio)-2-(pyrimidin-5-yl)butanoate (4-55). Prepared via General Procedure B using 1-(1-methoxy-4-(methylthio)-1-oxobutan-2-yl)-2,4,6-triphenylpyridin-1-ium tetrafluoroborate. The crude mixture was purified via silica gel

chromatography (5–30% ethyl acetate/hexanes) to give **4-55** (run 1: 113 mg, 50%; run 2: 116 mg, 51%) as a pale yellow oil: ^1H NMR (400 MHz, CDCl_3) δ 9.15 (s, 1H), 8.71 (s, 2H), 3.87 – 3.82 (m, 1H), 3.71 (s, 3H), 2.54 – 2.34 (m, 3H), 2.12 – 2.01 (m, 1H), 2.07 (s, 1H); ^{13}C NMR (101 MHz, CDCl_3) δ 172.6, 158.1, 156.7, 132.1, 52.8, 45.4, 31.9, 31.6, 15.4; FTIR (neat) 2917, 1736, 1561, 1412, 1203, 728 cm^{-1} ; HRMS (ESI+) $[\text{M}+\text{H}]^+$ calculated for $\text{C}_{10}\text{H}_{15}\text{N}_2\text{O}_2\text{S}$: 227.0849, found 227.0851.

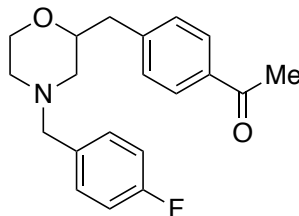


***tert*-Butyl (S)-2-((2-methylquinolin-6-yl)methyl)pyrrolidine-1-carboxylate (4-56).** Prepared via General Procedure B using (S)-1-((1-(*tert*-butoxycarbonyl)pyrrolidin-2-yl)methyl)-2,4,6-triphenylpyridin-1-ium tetrafluoroborate. The crude mixture was purified via silica gel chromatography (10–50% ethyl acetate/hexanes) to give 4-56 (run 1: 191 mg, 59%; run 2: 182 mg, 56%) as a yellow oil (mixture of rotamers): ^1H NMR (400 MHz, CDCl_3) δ 8.03 – 7.92 (m, br, 2H), 7.62 – 7.49 (m, br, 2H), 7.31 – 7.26 (m, br, 1H, *overlaps with CHCl₃*), 4.16 – 4.02 (m, br, 1H), 3.44 – 3.15 (m, br, 3H), 2.80 – 2.65 (m, br, 1H), 2.74 (s, br, 3H), 1.81 – 1.70 (m, br, 4H), 1.51 (s, br, 9H); ^{13}C NMR (101 MHz, CDCl_3) δ 158.5 (major), 158.3 (minor), 154.6 (minor), 154.6 (major), 146.6, 136.8 (minor), 135.9 (major), 132.0 (minor), 131.4 (major), 128.5 (major), 128.2 (minor), 127.4, 127.3, 126.5, 122.2 (major), 122.0 (minor), 79.4 (major), 79.2 (minor), 58.7, 46.9 (minor), 46.3 (major), 40.5 (major), 39.5 (minor), 29.8 (major), 29.0 (minor), 28.6, 25.3, 23.5 (minor), 22.7 (major); FTIR (neat) 2972, 2875, 1691, 1395, 1170, 1116, 772 cm^{-1} ; HRMS (ESI+) $[\text{M}+\text{H}]^+$ calculated for $\text{C}_{20}\text{H}_{27}\text{N}_2\text{O}_2$: 327.2067, found 327.2066. The enantiomeric excess was determined to

be >99% by chiral HPLC analysis (CHIRALPAK IA, 0.2 mL/min, 2% *i*-PrOH/hexanes, $\lambda=210$ nm); $t_R(\text{major}) = 103.75$ min, $t_R(\text{minor}) = 111.85$ min.

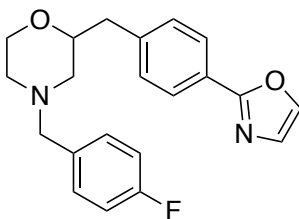


***tert*-Butyl 2-((4*R*,6*R*)-6-(4-cyanophenethyl)-2,2-dimethyl-1,3-dioxan-4-yl)acetate (4-58)**. Prepared via General Procedure B using 1-(2-((4*R*,6*R*)-6-(2-(*tert*-butoxy)-2-oxoethyl)-2,2-dimethyl-1,3-dioxan-4-yl)ethyl)-2,4,6-triphenylpyridin-1-ium tetrafluoroborate. The crude mixture was purified via silica gel chromatography (5–60% ether/hexanes) to give 4-58 (run 1: 191 mg, 53%; run 2: 219 mg, 61%) as a clear oil: ^1H NMR (400 MHz, CDCl_3) δ 7.59 (d, $J = 8.2$ Hz, 2H), 7.30 (d, $J = 8.2$ Hz, 2H), 4.23 (dtd, $J = 11.5, 6.5, 2.5$ Hz, 1H), 3.86 – 3.74 (m, 1H), 2.91 – 2.65 (m, 2H), 2.45 (dd, $J = 15.2, 6.9$ Hz, 1H), 2.31 (dd, $J = 15.2, 6.3$ Hz, 1H), 1.90 – 1.76 (m, 1H), 1.78 – 1.64 (m, 1H), 1.56 (dt, $J = 12.7, 2.4$ Hz, 1H), 1.46 (s, 9H), 1.43 (s, 3H), 1.41 (s, 3H), 1.29 – 1.19 (m, 1H); ^{13}C NMR (101 MHz, CDCl_3) δ 170.3, 147.8, 132.2, 129.3, 119.1, 109.7, 98.8, 80.7, 67.5, 66.2, 42.6, 37.3, 36.5, 31.4, 30.1, 28.1, 19.8; FTIR (neat) 2980, 2227, 1729, 1368, 1159, 845 cm^{-1} ; HRMS (ESI+) $[\text{M}+\text{H}]^+$ calculated for $\text{C}_{21}\text{H}_{30}\text{NO}_4$: 360.2169, found 360.2167.



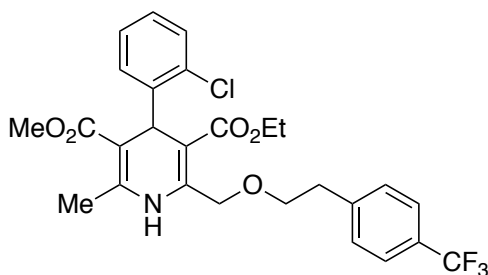
1-(4-((4-(4-Fluorobenzyl)morpholin-2-yl)methyl)phenyl)ethan-1-one (4-59).

Prepared via General Procedure A using 1-((4-(4-fluorobenzyl)morpholin-2-yl)methyl)-2,4,6-triphenylpyridin-1-ium tetrafluoroborate. The crude mixture was purified by silica gel chromatography (20–75% ethyl acetate/hexanes w/ 1% Et₃N) to give **4-59** (run 1: 244 mg, 77%; run 2: 258 mg, 82%) as a pale yellow oil: ¹H NMR (400 MHz, CDCl₃) δ 7.92 – 7.85 (m, 2H), 7.33 – 7.28 (m, 2H), 7.28 – 7.21 (m, 2H, overlaps with CHCl₃), 7.04 – 6.94 (m, 2H), 3.88 – 3.80 (m, 1H), 3.80 – 3.71 (m, 1H), 3.59 (td, *J* = 11.3, 2.5 Hz, 1H), 3.51 – 3.35 (m, 2H), 2.86 (dd, *J* = 13.9, 7.7 Hz, 1H), 2.78 – 2.66 (m, 2H), 2.65 – 2.55 (m, 1H), 2.58 (s, 3H), 2.13 (td, *J* = 11.3, 3.3 Hz, 1H), 1.99 – 1.89 (m, 1H); ¹³C NMR (101 MHz, CDCl₃) δ 198.0, 162.2 (d, *J* = 245.1 Hz), 144.2, 135.52, 133.46 (d, *J* = 3.1 Hz), 130.7 (d, *J* = 8.0 Hz), 129.6, 128.6, 115.2 (d, *J* = 21.2 Hz), 76.2, 67.0, 62.5, 58.4, 52.8, 40.3, 26.8; ¹⁹F NMR (376 MHz, CDCl₃) δ -115.59; FTIR (neat) 2935, 2805, 1682, 1268, 842 cm⁻¹; HRMS (ESI⁺) [M+H]⁺ calculated for C₂₀H₂₃FNO₂: 328.1707, found 328.1703.



4-(4-Fluorobenzyl)-2-(4-(oxazol-2-yl)benzyl)morpholine (4-60). Prepared via General Procedure A using 1-((4-(4-fluorobenzyl)morpholin-2-yl)methyl)-2,4,6-

triphenylpyridin-1-ium tetrafluoroborate on a 4 mmol scale. The crude mixture was purified by silica gel chromatography (10–15% ethyl acetate/hexanes) to give **4-60** (1041 mg, 74%) as a pale yellow oil: ^1H NMR (600 MHz, CDCl_3) δ 7.96 (d, $J = 8.3$ Hz, 2H), 7.69 (s, 1H), 7.30 (d, $J = 8.1$ Hz, 2H), 7.28 – 7.23 (m, 2H, overlaps with CHCl_3), 7.22 (s, 1H), 6.99 (t, $J = 8.7$ Hz, 2H), 3.87 – 3.81 (m, 1H), 3.81 – 3.74 (m, 1H), 3.65 – 3.57 (m, 1H), 3.48 (d, $J = 13.0$ Hz, 1H), 3.39 (d, $J = 13.0$ Hz, 1H), 2.87 (dd, $J = 14.0, 7.4$ Hz, 1H), 2.76 – 2.69 (m, 2H), 2.60 (d, $J = 11.2$ Hz, 1H), 2.17 – 2.10 (m, 1H), 1.95 (t, $J = 10.5$ Hz, 1H); ^{13}C NMR (151 MHz, CDCl_3) δ 162.05 (d, $J = 244.9$ Hz), 162.04, 140.8, 138.3, 133.4 (d, $J = 3.2$ Hz), 130.5 (d, $J = 7.9$ Hz), 129.7, 128.4, 126.4, 125.7, 115.1 (d, $J = 21.2$ Hz), 76.2, 66.9, 62.4, 58.3, 52.7, 40.1; ^{19}F NMR (565 MHz, CDCl_3) δ -115.72; FTIR (neat) 3125, 3040, 2935, 2856, 2805, 1921, 1509, 1221, 1112, 846, 715 cm^{-1} ; HRMS (ESI+) $[\text{M}+\text{H}]^+$ calculated for $\text{C}_{21}\text{H}_{22}\text{FN}_2\text{O}_2$: 353.1660, found 353.1654.



3-Ethyl **5-methyl** **4-(2-chlorophenyl)-6-methyl-2-((4-(trifluoromethyl)phenoxy)methyl)-1,4-dihydropyridine-3,5-dicarboxylate** (**4-61**). Prepared via General Procedure A using 1-(2-((4-(2-chlorophenyl)-3-(ethoxycarbonyl)-5-(methoxycarbonyl)-6-methyl-1,4-dihydropyridin-2-yl)methoxy)ethyl)-2,4,6-triphenylpyridin-1-ium tetrafluoroborate. The crude mixture was purified via silica gel chromatography (5–40% ethyl acetate/hexanes) to give **4-61**

(run 1: 326 mg, 61%; run 2: 357 mg, 67%) as a yellow oil: ^1H NMR (400 MHz, CDCl_3) δ 7.61 (d, $J = 7.7$ Hz, 2H), 7.43 – 7.35 (m, 2H), 7.31 (dd, $J = 7.7, 1.7$ Hz, 1H), 7.22 (dd, $J = 8.0, 1.4$ Hz, 1H), 7.16 – 7.07 (m, 1H), 7.08 – 6.99 (m, 1H), 6.68 (s, 1H), 5.36 (s, 1H), 4.79 – 4.62 (m, 2H), 4.10 – 3.97 (m, 2H), 3.88 – 3.73 (m, 2H), 3.60 (s, 3H), 3.02 (t, $J = 6.3$ Hz, 2H), 2.08 (s, 3H), 1.17 (t, $J = 7.1$ Hz, 3H); ^{13}C NMR (101 MHz, CDCl_3) δ 167.93, 167.14, 145.61, 145.12, 143.64, 142.96, 132.35, 131.46, 129.28, 129.27, 129.04 (q, $J = 32.5$ Hz), 127.40, 126.82, 125.56 (q, $J = 3.7$ Hz), 123.71 (q, $J = 271.7$ Hz), 103.92, 101.43, 71.44, 67.68, 59.84, 50.84, 37.18, 35.95, 19.26, 14.28; ^{19}F NMR (376 MHz, CDCl_3) δ -62.43; HRMS (ESI+) $[\text{M}+\text{H}]^+$ calculated for $\text{C}_{27}\text{H}_{28}\text{ClF}_3\text{NO}_5$: 538.1603, found 538.1590.

REFERENCES

1. Tasker, S. Z.; Standley, E. A.; Jamison, T. F., *Nature* **2014**, *509*, 299.
2. Weix, D. J., *Accounts of Chemical Research* **2015**, *48*, 1767-1775.
3. Everson, D. A.; Weix, D. J., *The Journal of Organic Chemistry* **2014**, *79*, 4793-4798.
4. Everson, D. A.; Shrestha, R.; Weix, D. J., *J. Am. Chem. Soc.* **2010**, *132*, 920-921.
5. Everson, D. A.; Jones, B. A.; Weix, D. J., *J. Am. Chem. Soc.* **2012**, *134*, 6146-6159.
6. Huihui, K. M. M.; Caputo, J. A.; Melchor, Z.; Olivares, A. M.; Spiewak, A. M.; Johnson, K. A.; DiBenedetto, T. A.; Kim, S.; Ackerman, L. K. G.; Weix, D. J., *J. Am. Chem. Soc.* **2016**, *138*, 5016-5019.
7. Biswas, S.; Weix, D. J., *J. Am. Chem. Soc.* **2013**, *135*, 16192-16197.
8. Wang, S.; Qian, Q.; Gong, H., *Org. Lett.* **2012**, *14*, 3352-3355.
9. Molander, G. A.; Traister, K. M.; O'Neill, B. T., *The Journal of Organic Chemistry* **2014**, *79*, 5771-5780.
10. Molander, G. A.; Traister, K. M.; O'Neill, B. T., *The Journal of Organic Chemistry* **2015**, *80*, 2907-2911.
11. Wang, X.; Wang, S.; Xue, W.; Gong, H., *J. Am. Chem. Soc.* **2015**, *137*, 11562-11565.
12. Wang, X.; Ma, G.; Peng, Y.; Pitsch, C. E.; Moll, B. J.; Ly, T. D.; Wang, X.; Gong, H., *J. Am. Chem. Soc.* **2018**, *140*, 14490-14497.
13. Zhang, P.; Le, C. C.; MacMillan, D. W. C., *J. Am. Chem. Soc.* **2016**, *138*, 8084-8087.

14. Bhone, V. R.; O'Neill, B. T.; Buchwald, S. L., *Angewandte Chemie International Edition* **2015**, *55*, 1849-1853.
15. Czaplik, W. M.; Mayer, M.; Jacobi von Wangelin, A., *Angewandte Chemie International Edition* **2008**, *48*, 607-610.
16. Amatore, M.; Gosmini, C., *Chemistry – A European Journal* **2010**, *16*, 5848-5852.
17. Yu, X.; Yang, T.; Wang, S.; Xu, H.; Gong, H., *Org. Lett.* **2011**, *13*, 2138-2141.
18. Xu, H.; Zhao, C.; Qian, Q.; Deng, W.; Gong, H., *Chemical Science* **2013**, *4*, 4022-4029.
19. Liu, J.-H.; Yang, C.-T.; Lu, X.-Y.; Zhang, Z.-Q.; Xu, L.; Cui, M.; Lu, X.; Xiao, B.; Fu, Y.; Liu, L., *Chemistry – A European Journal* **2014**, *20*, 15334-15338.
20. Zhao, C.; Jia, X.; Wang, X.; Gong, H., *J. Am. Chem. Soc.* **2014**, *136*, 17645-17651.
21. Feng, C.; Cunningham, D. W.; Easter, Q. T.; Blum, S. A., *J. Am. Chem. Soc.* **2016**, *138*, 11156-11159.
22. Roth, B. D., US4681893A, 1987/07/21/, 1987.
23. Kato, S.; Morie, T.; Yoshida, N., *CHEMICAL & PHARMACEUTICAL BULLETIN* **1995**, *43*, 699-702.
24. Arrowsmith, J. E.; Campbell, S. F.; Cross, P. E.; Stubbs, J. K.; Burges, R. A.; Gardiner, D. G.; Blackburn, K. J., *Journal of Medicinal Chemistry* **1986**, *29*, 1696-1702.
25. Gronborg, H.; Winther, B.; Brofeldt, S.; Borum, P.; Mygind, N., *Rhinology* **1983**, *21*, 3-12.
26. Pangborn, A. B.; Giardello, M. A.; Grubbs, R. H.; Rosen, R. K.; Timmers, F. J., *Organometallics* **1996**, *15*, 1518-1520.
27. Planellas, M.; Guo, W.; Alonso, F.; Yus, M.; Shafir, A.; Pleixats, R.; Parella, T., *Adv. Synth. Catal.* **2014**, *356*, 179-188.
28. Toriyama, F.; Cornella, J.; Wimmer, L.; Chen, T.-G.; Dixon, D. D.; Creech, G.; Baran, P. S., *J. Am. Chem. Soc.* **2016**, *138*, 11132-11135.

29. Wendling, T.; Risto, E.; Krause, T.; Goßen, L. J., *Chemistry – A European Journal* **2018**, *24*, 6019-6024.
30. Mierde, H. V.; Voort, P. V. D.; Verpoort, F., *Tetrahedron Letters* **2009**, *50*, 201-203.
31. Harrowven, D. C.; Sutton, B. J.; Coulton, S., *Organic & Biomolecular Chemistry* **2003**, *1*, 4047-4057.

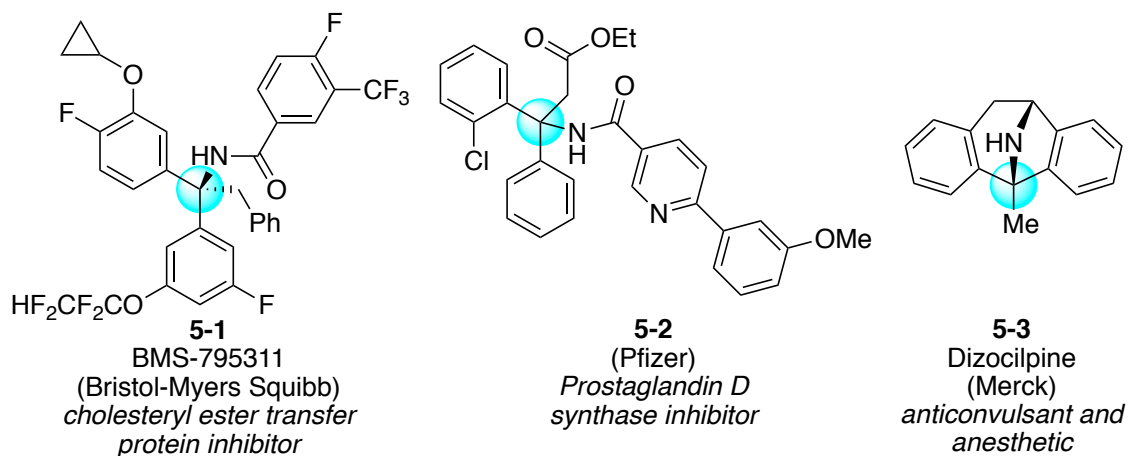
Chapter 5

COPPER-CATALYZED ENANTIOSELECTIVE ALKYNYLATION OF IMINIUM IONS TO FORM α -DIARYL TETRASUBSTITUTED STEREOCENTERS

5.1 Introduction

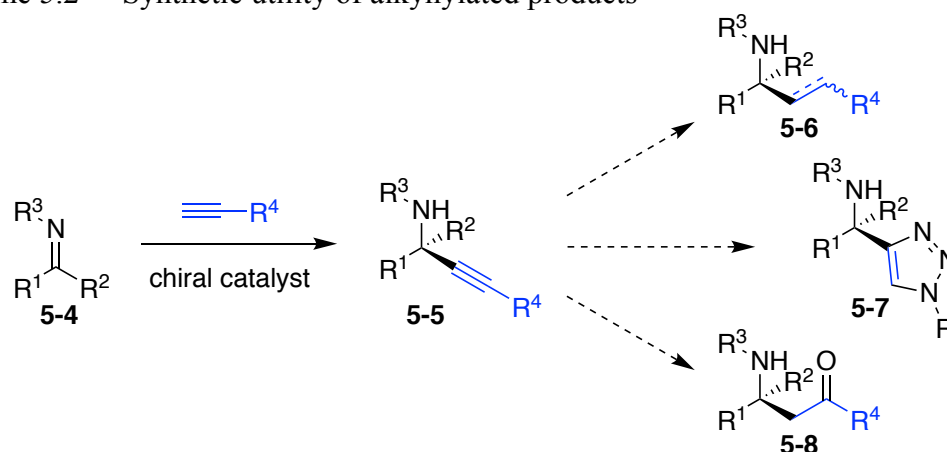
Chirality is present in a wide array of molecules ranging from simple amino acids to complex bioactive molecules. Recognizing the importance of these stereogenic centers, intense efforts have focused on the development of enantioselective methodologies to enable synthesis. In particular, amines bearing an α -diaryl tetrasubstituted stereocenter are found in a number of pharmaceutically relevant molecules (Scheme 5.1).¹⁻³ Unfortunately, construction of these stereocenters is challenging, and there are a limited number of methods that enable efficient access to these motifs.

Scheme 5.1 Examples of bioactive amines containing an α -diaryl tetrasubstituted stereocenter



An enantioselective addition of a chiral nucleophile to a prochiral ketimine (**5-4**) would allow access to amines bearing an α -tetrasubstituted stereocenter (**5-5**) (Scheme 5.2, left). Moreover, addition of an alkyne moiety would enable the incorporation of a versatile handle that can be used for further product elaboration (Scheme 5.2, right). For example, product **5-5** can be hydrogenated to form the corresponding alkene or alkane (**5-6**). The alkyne can also participate in click chemistry to form triazole **5-7**. In addition, it can be oxidized to form ketone **5-8**.

Scheme 5.2 Synthetic utility of alkynylated products

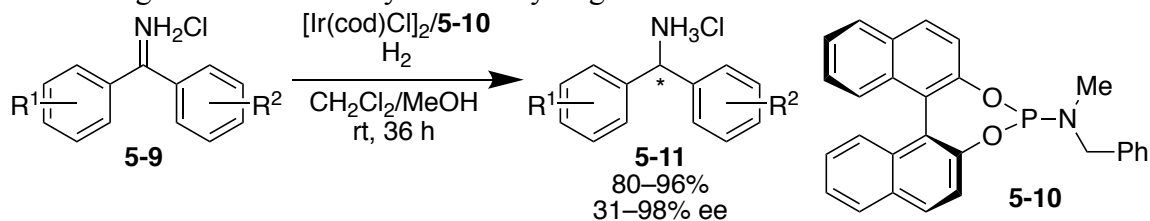


Unfortunately, enantioselective additions to diaryl ketimines remains an on-going challenge. It is very difficult for a chiral catalyst to distinguish between two similar aryl groups, thereby resulting in poor enantioselectivities. Nonetheless, there are limited examples in the literature that demonstrate the feasibility of this approach (Scheme 5.3). In 2010, the Zhang and Gosselin groups disclosed an asymmetric hydrogenation of substituted benzophenone N–H ketimines (**5-9**) using an iridium/phosphoramidite (**5-10**) catalyst system (Scheme 5.3A).⁴ Similarly, the Wang group published the enantioselective transfer hydrogenation of *ortho*-hydroxybenzophenone N–H ketimines (**5-12**) using chiral phosphoric acid (**5-13**)

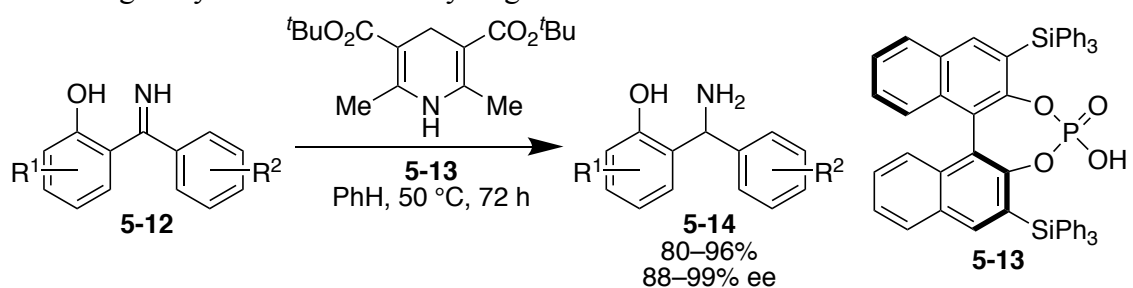
(Scheme 5.3B).⁵ In this case, a Hantzsch ester is employed as the hydrogen source. Additionally, the Feng group has demonstrated an asymmetric cyanation of ketimine **5-15** to deliver Strecker products **5-18** (Scheme 5.3C).⁶ This reaction employs a catalyst generated from titanium isopropoxide $[\text{Ti}(\text{O}^i\text{Pr})_4]$, cinchona alkaloid **5-16**, and achiral biphenol **5-17**. Notably, in every instance *ortho*-substitution on one of the aryl rings is required for good stereinduction. Chiral auxiliary based approaches have also been used, but again rely on steric differentiation of the two aryl groups to obtain good diastereomeric ratios (dr).⁷

Scheme 5.3 Enantioselective additions to diaryl ketimines

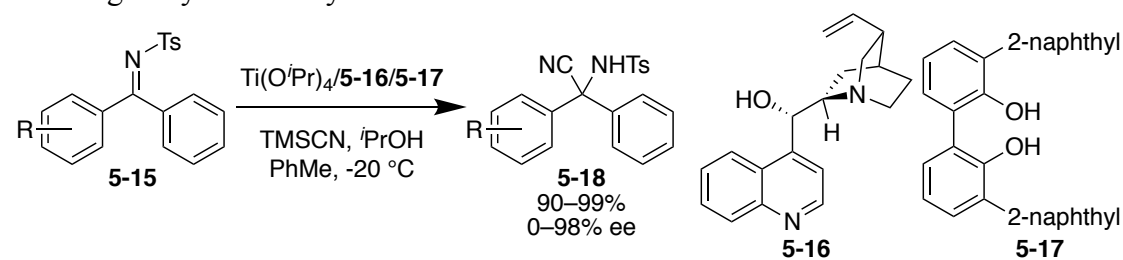
A. Zhang and Gosselin's asymmetric hydrogenation



B. Wang's asymmetric transfer hydrogenation

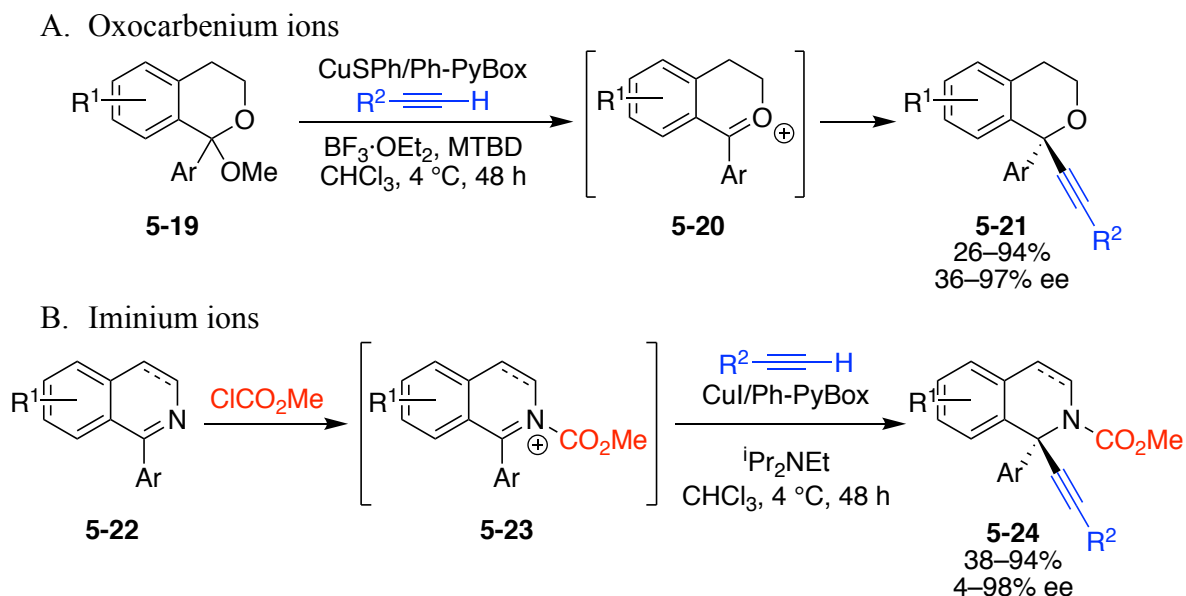


C. Feng's asymmetric cyanation



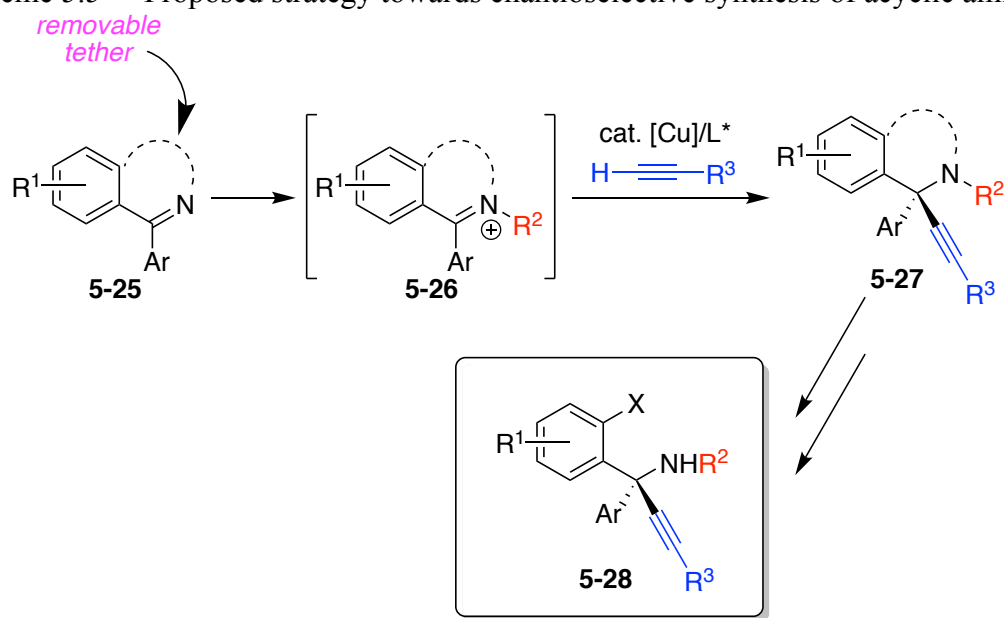
Previously, our group has developed copper-catalyzed enantioselective alkyne additions to isochroman acetals and isoquinolines to form these types of α -diaryl tetrasubstituted stereocenters (Scheme 5.4).⁸ In the former case, a Lewis acid ($\text{BF}_3 \cdot \text{OEt}_2$) is used to ionize the racemic acetal substrate (**5-19**) to form prochiral oxocarbenium ion intermediate **5-20** (Scheme 5.4A).⁹⁻¹¹ This cation is then susceptible to addition of a chiral ligand-bound copper-acetylide to form alkynylated product **5-21** bearing an α -diaryl tetrasubstituted stereocenter. An analogous reaction can be performed on *N*-acyl iminium ion **5-23**, formed from the acylation of ketimine **5-22** with methyl chloroformate (Scheme 5.4B).¹² This delivers isoquinoline products **5-24** bearing a similar tetrasubstituted stereocenter. Notably, in both cases, the substrates are designed so that an alkyl tether can be used to differentiate the faces of the diaryl oxocarbenium or iminium ion, resulting in the formation of *cyclic* products.

Scheme 5.4 Watson's copper-catalyzed enantioselective alkyne additions



Having developed methods for the enantioselective alkylation of these types of cyclic substrates, we envisioned designing substrates containing a removable tether (**5-25**), which would allow us to access *acyclic* amines bearing an α -diaryl tetrasubstituted stereocenter (**5-28**) (Scheme 5.5). Effectively, the tether would allow for differentiation of the ketimine faces to afford high levels of enantioselectivity in the alkynylated product (**5-27**). The tether can then be cleaved to reveal the desired acyclic product (**5-28**). This approach would circumvent many of the issues associated with the differentiation of two similar aryl groups in acyclic substrates.

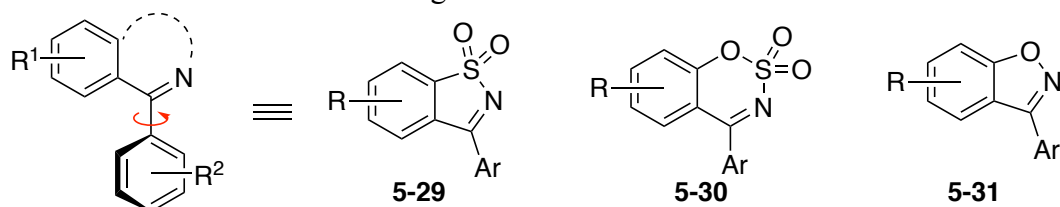
Scheme 5.5 Proposed strategy towards enantioselective synthesis of acyclic amines



With this intrinsic protecting group anchoring strategy in mind,^{13, 14} I designed several substrates that contained a suitable tether (Scheme 5.6). The two aryl groups can be differentiated based on the freedom of rotation exhibited by the pendant aryl ring versus the tethered aryl ring. It is also possible that the π -faces are more

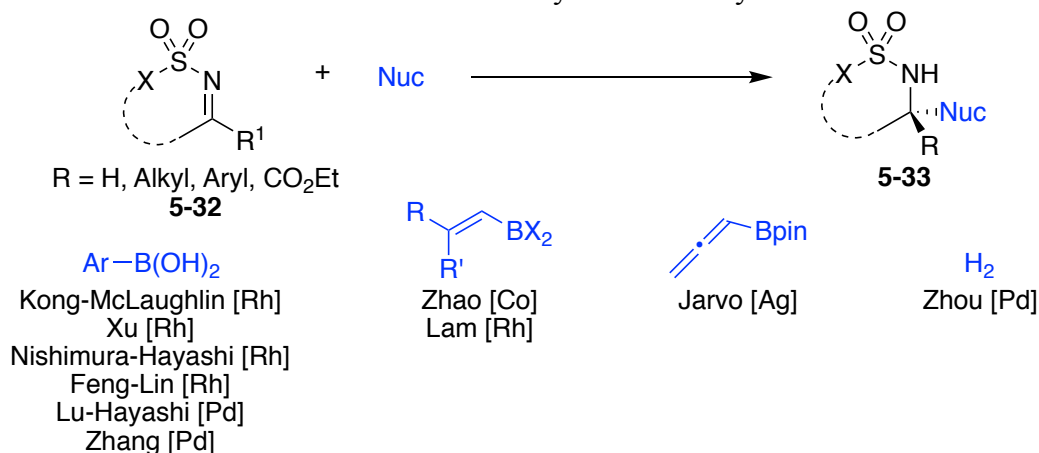
electronically differentiated because of the tether onto nitrogen (lone pair vs alkyl group). Cyclic 5- and 6-membered *N*-sulfonyl ketimines (**5-29** & **5-30**) as well as benzisoxazole (**5-31**) were chosen as model substrates.

Scheme 5.6 Substrates containing a removable tether



Enantioselective additions of a variety of nucleophiles to cyclic *N*-sulfonyl imines have been reported including arylations,¹⁵⁻²⁰ vinylations,^{21, 22} propargylations,²³ and hydrogenations²⁴ (Scheme 5.7). More importantly, the sulfonyl group can be cleaved with little or no loss of enantiopurity of the α -stereocenter. Aryl sulfamates and sulfonamides have also been shown to participate in a variety of cross-coupling reactions.²⁵⁻²⁹ Excitingly, isoxazolidines, the resultant products from isoxazole **5-31**, have proven to be a privileged scaffold for organic and medicinal chemistry.³⁰

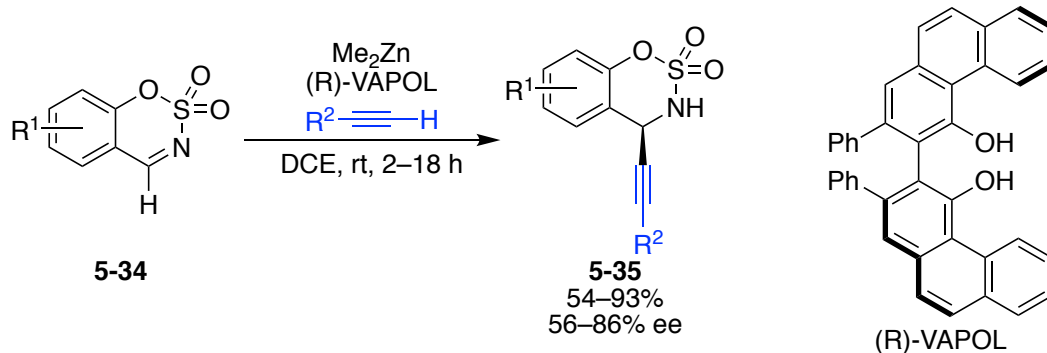
Scheme 5.7 Enantioselective additions to cyclic *N*-sulfonyl imines



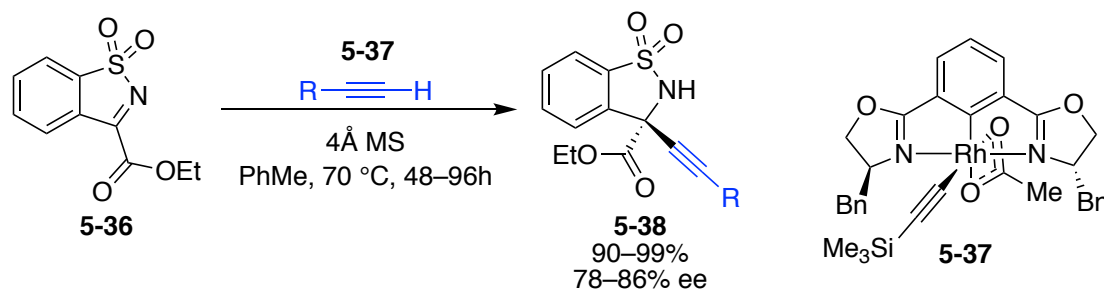
In comparison to these previously established methods, examples of enantioselective *alkynylations* of cyclic *N*-sulfonyl imines are much more limited. The Pedro group has shown that an asymmetric addition of an alkyne to aldimine **5-34** can be achieved using dimethylzinc and a chiral VAPOL ligand (Scheme 5.8A).³¹ Additionally, Morimoto and Ohshima have demonstrated that a chiral (Phebox)Rhodium(III) complex (**5-37**) can be used to catalyze the enantioselective alkynylation of α -ketiminoesters (**5-36**) (Scheme 5.8B).³² However, enantioselective alkynylations of cyclic *N*-sulfonyl ketimines to set α -diaryl tetrasubstituted stereocenters has not yet been achieved. With that in mind, I set out to develop an asymmetric copper-catalyzed alkynylation of cyclic ketimines bearing a removable tether en-route to this challenging class of products.

Scheme 5.8 Enantioselective alkynylations of cyclic *N*-sulfonyl imines

A. Pedro (aldimine)



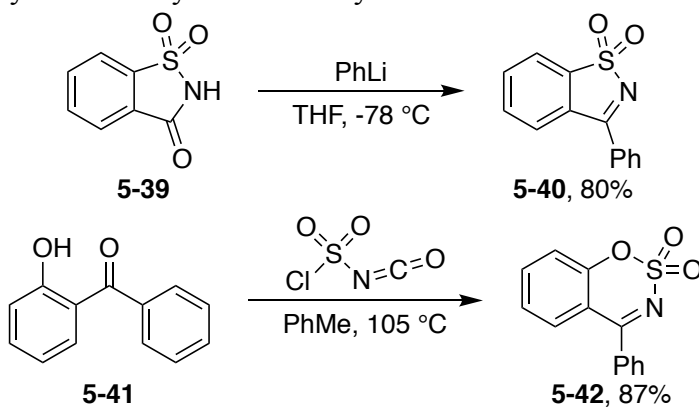
B. Morimoto and Ohshima (α -ketiminoesters)



5.2 Results and Discussion

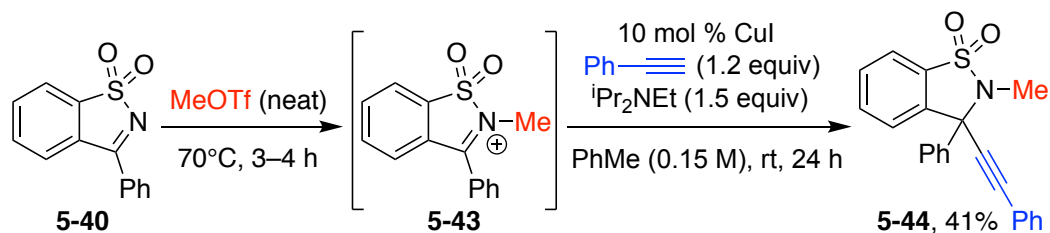
Initial screening began with 5- and 6-membered sulfonyl ketimines **5-40** and **5-42**. These substrates can be easily synthesized in a single step in excellent yields and in multi-gram quantities (Scheme 5.9). Excitingly, these products can simply be recrystallized and require no column chromatography for isolation. This route also allows for the rapid incorporation of a variety of aryl groups.

Scheme 5.9 Synthesis of cyclic *N*-sulfonyl ketimines **5-40** and **5-42**



Unfortunately, these substrates were unreactive towards alkylation under a variety of conditions tried, including activation with a Lewis acid. I hypothesized that formation of the corresponding iminium ion intermediate would increase the electrophilicity of the α -carbon and enhance reactivity. Indeed, when **5-40** was treated with methyl triflate to form methylated iminium ion **5-43**, alkynylated product **5-44** was afforded in 41% yield under standard conditions (Scheme 5.10). Notably, iminium intermediate **5-43** required elevated temperatures to form (70 °C) and was used without purification. Other methylating reagents such as methyl iodide and dimethyl sulfate were ineffective at promoting this transformation.

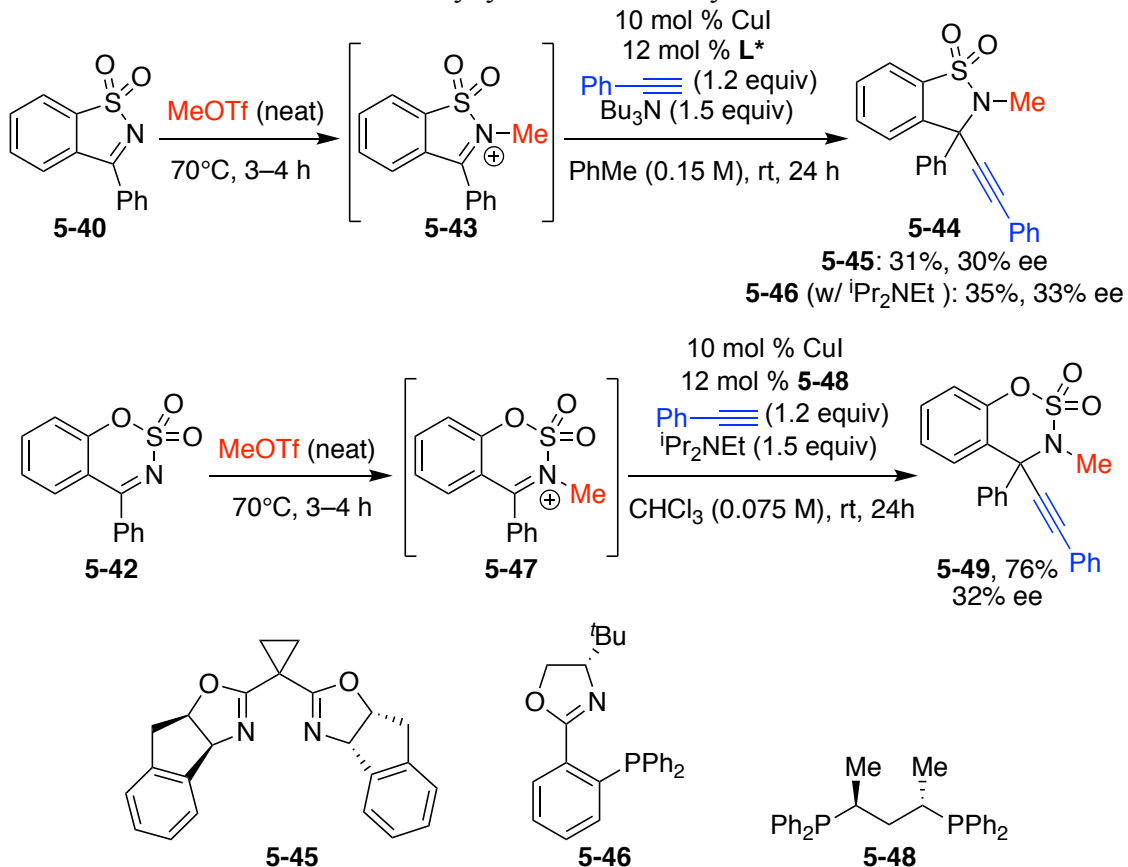
Scheme 5.10 Methylation and alkylation of sulfonyl ketimine **5-40**



Yield determined by ^1H NMR analysis using 1,3,5-trimethoxybenzene as internal standard.

I then turned my attention towards the identification of a suitable chiral ligand that would impart enantioselectivity in this reaction. Our group has shown that bis(oxazoline) (Box) and pyridine bis(oxazoline) (PyBox) ligands are privileged ligand architectures for copper-catalyzed alkylation of cyclic iminium and oxocarbenium ions. Preliminary screening efforts identified IndaBox ligand **5-45** as a promising lead. However, upon extensive screening of various parameters such as copper source, base, solvent, temperature, and concentration, alkylation product **5-44** was only observed in 31% yield and 30% *ee* (Scheme 5.11, top). PHOX ligand **5-46** also demonstrated similar reactivity and selectivity, giving 35% yield and 33% *ee*.

Scheme 5.11 Enantioselective alkynylations of sulfonyl ketimines **5-40** and **5-42**

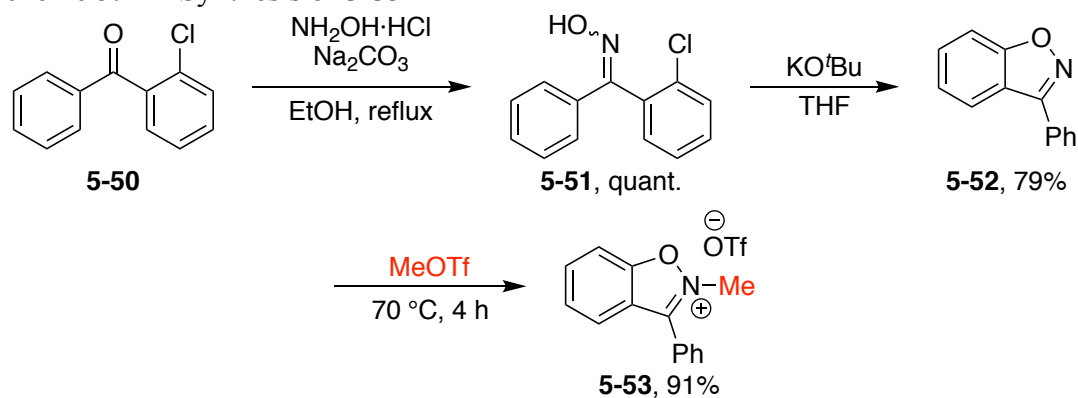


Yields determined by ^1H NMR analysis using 1,3,5-trimethoxybenzene as internal standard. Enantiomeric excesses determined by chiral HPLC analysis

Simultaneously, 6-membered sulfonyl ketimine **5-42** was tested under similar conditions. In this case, chiral bidentate phosphine ligand BDPP (**5-48**) was found to afford the highest level of stereinduction (Scheme 5.11, middle). Intense screening efforts revealed that the use of a halogenated solvent such as CHCl_3 under dilute conditions (0.075 M) afforded the desired product **5-49** in 76% yield and 32% *ee*. Further efforts to increase the yields and *ee*'s are on-going in the group.

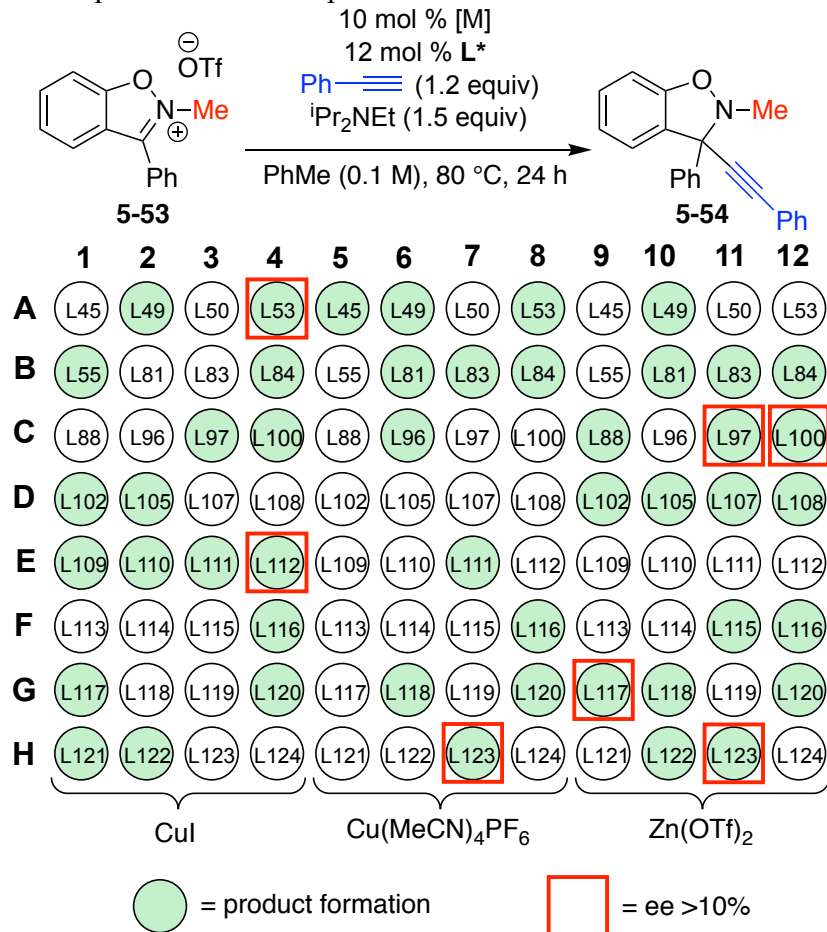
Meanwhile, I focused my efforts towards the use of benzisoxazole substrate **5-52**, which can be synthesized in two steps from commercial reagents (Scheme 5.12, top). Excitingly, the iminium intermediate is stable and can be isolated as the corresponding triflate salt. Upon treatment of benzisoxazole **5-52** with methyl triflate, iminium salt **5-53** precipitates from solution and can be obtained as a white, crystalline solid (Scheme 5.12, bottom).

Scheme 5.12 Synthesis of **5-53**



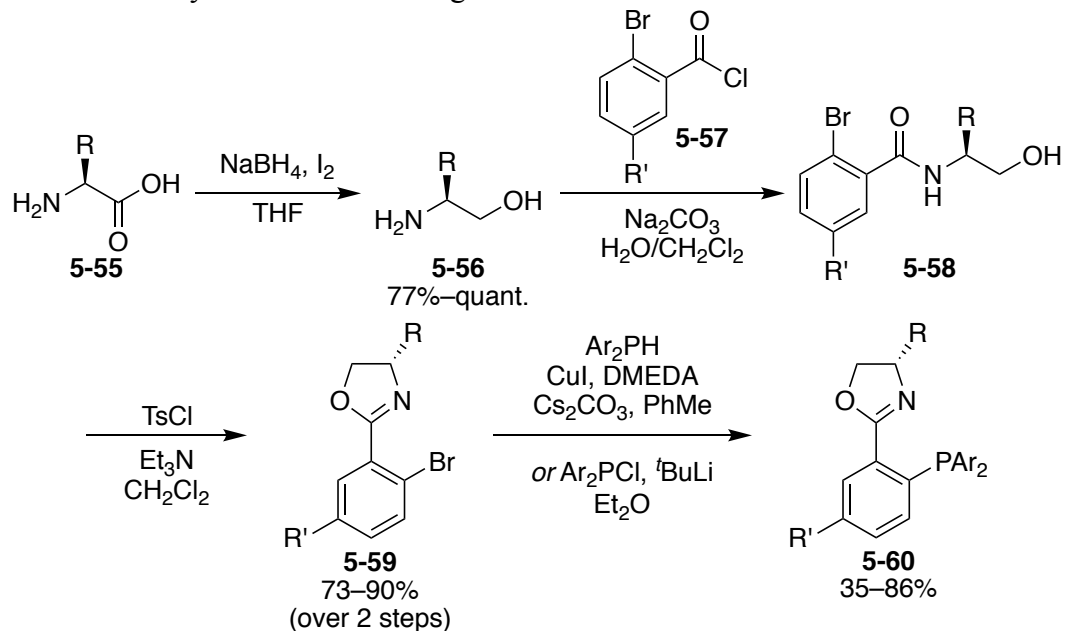
With **5-53** in hand, I decided that this substrate was perfect for high-throughput experimentation (HTE). A representative HTE plate is shown in Scheme 5.13. This set-up enables rapid screening of a variety of parameters in a 96-well format using a minimal amount of starting material (< 5 mg). I tested a number of chiral ligands including diamines, diols, phosphines, phosphoramidites, amino alcohols, and P–N ligands to identify a lead ligand class (See Appendix E for ligand structures).

Scheme 5.13 Representative HTE plate



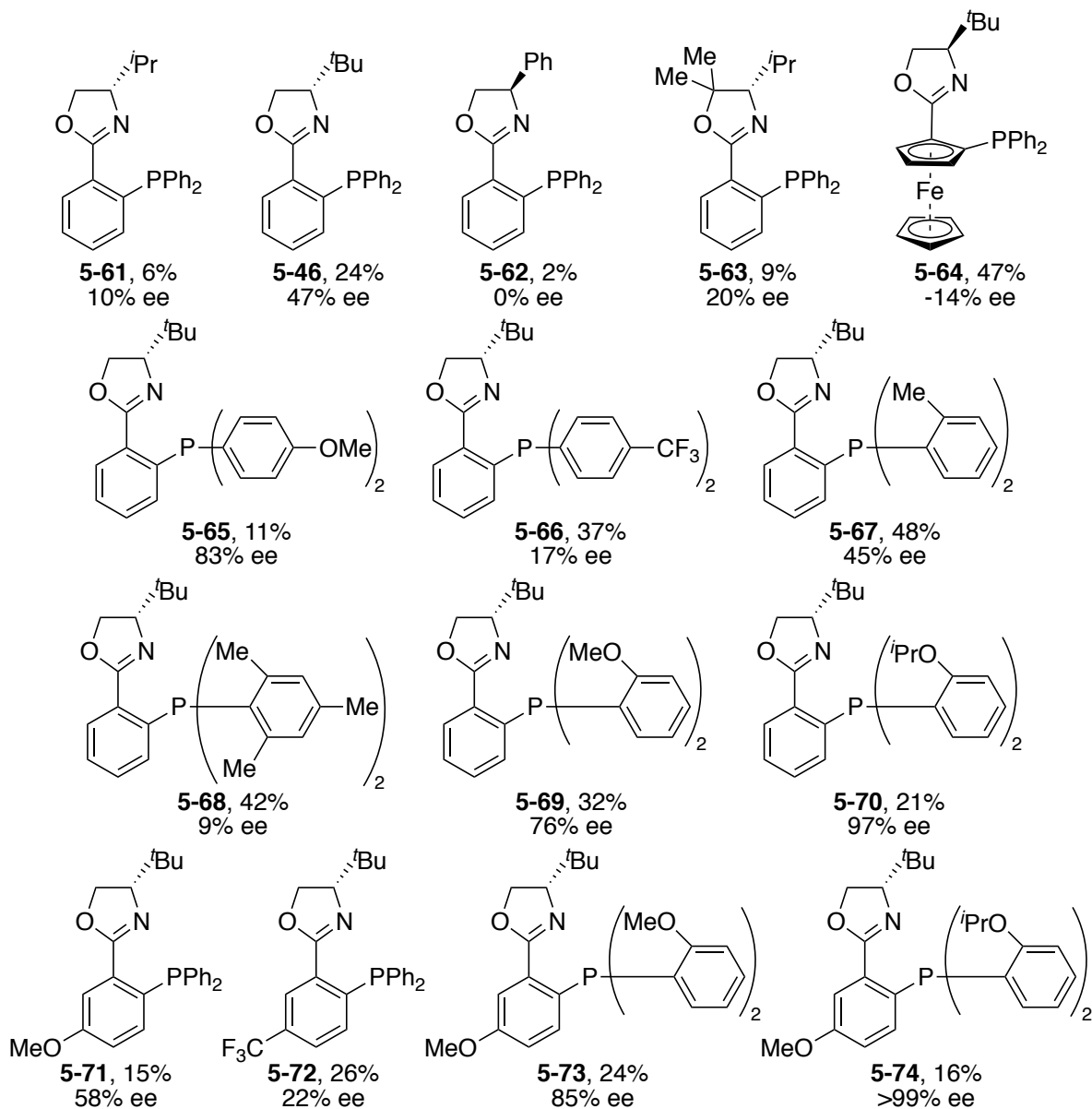
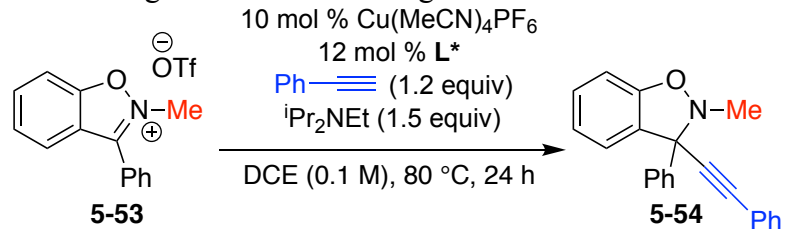
Upon screening a variety of chiral ligands, I identified phosphinooxazolines (PHOX) as a promising ligand class. These ligands are highly tunable and can be easily synthesized (Scheme 5.14).^{33, 34} The stereogenic center (R group) on the oxazoline ring can be introduced from a chiral amino alcohol (**5-56**), which is often derived from an amino acid (**5-55**). The R' group on the aryl ring can be installed from a substituted 2-bromobenzoyl chloride (**5-57**). Finally, the diarylphosphino group can be obtained from the corresponding diarylphosphine or diarylphosphine chloride.

Scheme 5.14 Synthesis of PHOX ligands



I synthesized a library of PHOX ligands to probe various steric and electronic effects on the reactivity and selectivity of the alkylation reaction (Scheme 5.15). Upon testing a variety of substituents on the oxazoline ring, I found that a bulky *tert*-butyl group (**5-46**) afforded the best reactivity and selectivity, compared to other groups such as isopropyl (**5-61**) or phenyl (**5-62**). The incorporation of a number of different diarylphosphines revealed that electron-donating groups on the aryl (OMe, **5-65**) increased the *ee* substantially compared to electron-withdrawing groups (CF₃, **5-66**). Moreover, an *ortho*-substituent afforded increased yield (*o*-tolyl, **5-67**). However, further steric bulk lead to low *ee* (mesityl, **5-68**). Finally, a bulky, electron-rich *ortho*-substituent (O^{*i*}Pr, **5-70**) afforded excellent selectivity (97% *ee*). The electronic character of the backbone aryl group was found to also influence selectivity. Again, an electron-donating group resulted in increased levels of enantioselectivity (OMe, **5-71**). In combining these observations, ligand **5-74** afforded the desired product in >99% *ee*, albeit in low yield.

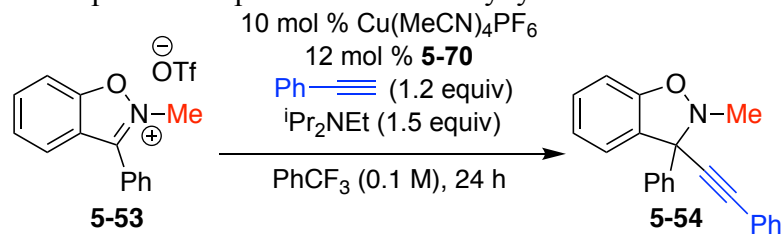
Scheme 5.15 Screening of various PHOX ligands^a



^aConditions: **5-53** (0.10 mmol), [Cu] (10 mol %), L* (12 mol %), alkyne (1.2 equiv), base (1.5 equiv), DCE (0.1 M), 80 °C, 24 h. Yield and enantiomeric excess determined by chiral SFC analysis using 1,3,5-trimethoxybenzene as internal standard.

Having identified a suitable ligand, I then turned to examine the temperature dependence of this reaction (Table 5.1). Typically for an enantioselective reaction, lower reaction temperatures can lead to increased *ee*'s. Unfortunately, the yield may be lower due to a slower rate of reaction. Surprisingly, at lower reaction temperatures (70 and 60 °C), the *ee*'s of desired product dropped substantially (entries 2 & 3). However, an improvement in yield was observed at these lower temperatures. Since these results are somewhat counterintuitive, I wanted to probe if another reaction pathway may be operational under these reaction conditions. No reaction was observed at room temperature (entry 4).

Table 5.1 Temperature dependence of the alkylation reaction^a

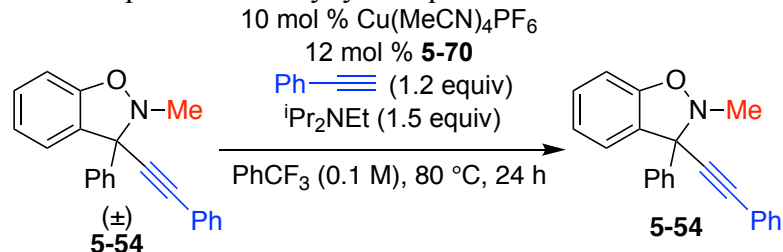


Entry	Temperature (°C)	Yield (%) ^b	ee (%) ^c
1	80	28	97
2	70	32	57
3	60	46	27

^aConditions: **5-53** (0.10 mmol), [Cu] (10 mol %), **5-70** (12 mol %), alkyne (1.2 equiv), base (1.5 equiv), PhCF₃ (0.1 M), 24 h. ^bDetermined by ¹H NMR analysis using 1,3,5-trimethoxybenzene as internal standard. ^cDetermined by chiral HPLC analysis.

With these odd results in hand, I first wanted to test if the alkynylated product **5-54** was stable under the reaction conditions. I subjected racemic product **5-54** (synthesized independently via addition of lithium phenylacetylide to **5-53**) to the standard reaction conditions (Table 5.2, entry 1). Interestingly, product decomposition was observed, and **5-54** was recovered in only 46% yield. Surprisingly, the recovered starting material was determined to be 96% *ee*, a value similar to that observed in the copper-catalyzed reaction. This result suggests a highly efficient kinetic resolution, giving high *ee*'s and yields (50% maximum theoretical yield). This result also implies that there may be a resolution event of alkynylated product **5-54** that is occurring under the alkynylation conditions. Additionally, it is plausible that the copper-catalyzed reaction proceeds to give **5-54** that is racemic or with lower *ee*, and selective decomposition of one enantiomer then leads to highly enantioenriched product.

Table 5.2 Decomposition of alkynylated product **5-54**^a



Entry	Deviation from above	Yield (%) ^b	ee (%) ^c
1	none	46	96
2	no [Cu]	98	0
3	no L*	quant.	0
4	no alkyne	<5	n.d.
5	no base	<5	n.d.

^aConditions: **5-54** (0.10 mmol), [Cu] (10 mol %), **5-70** (12 mol %), alkyne (1.2 equiv), base (1.5 equiv), PhCF₃ (0.1 M), 80 °C, 24 h. ^bDetermined by ¹H NMR analysis using 1,3,5-trimethoxybenzene as internal standard. ^cDetermined by chiral HPLC analysis.

To investigate this phenomenon further, I ran a series of control reactions to elucidate what was required for the decomposition event. In the absence of either copper or chiral ligand, no product decomposition was observed (entries 2 & 3). Interestingly, in the absence of alkyne or base, no remaining starting material **5-54** was recovered (entries 4 & 5). These results indicate that all the components of the reaction (copper, ligand, alkyne, and base) are required to promote the kinetic resolution, but also prevent complete decomposition of the alkynylated product.

Future efforts should be focused on identifying the decomposition products of this resolution reaction. Perhaps one enantiomer of alkynylated product **5-54** reacts with the chiral copper catalyst to afford some type of ring-opened or rearranged product. We are extremely interested in probing this possibility further. Unfortunately, we do not yet have a deep mechanistic understanding of this resolution event. With more evidence and mechanistic insight, I believe that this can be turned into a useful method for the kinetic resolution of related substrates.

5.3 Conclusion

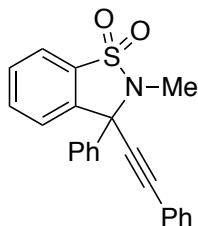
I have described my efforts towards a copper-catalyzed enantioselective alkynylation of cyclic iminium ions bearing a removable tether, en-route to acyclic amines bearing an α -diaryl tetrasubstituted stereocenter. Promising results have been obtained for both 5- and 6-membered cyclic *N*-sulfonyl ketimine substrates. Interestingly, in the case of the benzisoxazolidine product, there appears to be a kinetic resolution event occurring under the optimized reaction conditions. Further mechanistic insight may lead to the development of this method as a kinetic resolution to deliver highly enantioenriched products.

5.4 Experimental

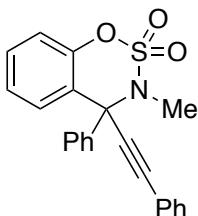
5.4.1 Enantioselective Alkynylation of Iminium Ions

5.4.1.1 General Procedure A: Reaction Optimization of *N*-sulfonyl Ketimines

In a N₂-filled glovebox: To an oven-dried 1-dram vial was added substrate (0.10 mmol, 1.0 equiv). The vial was then equipped with a micro stir bar, capped with a pierceable Teflon-coated cap, and removed from the glovebox. Methyl triflate (0.11 mmol, 1.1 equiv) was added into the vial via a N₂-purged microsyringe. The mixture was heated at 70 °C for 4 h. To a separate oven-dried 1-dram vial was added [Cu] (0.010 mmol, 10 mol %), ligand (0.012 mmol, 12 mol %), and solvent. The vial was equipped with a micro stir bar, and the resultant solution was stirred for 30 min at rt. Alkyne (0.12 mmol, 1.2 equiv) and base (0.15, 1.5 equiv) were added. The vial was removed from the glovebox, and the copper acetylide mixture was transferred to the substrate vial via a N₂-purged syringe. The resulting mixture was stirred vigorously at room temperature for 24 hours. The mixture was then diluted with Et₂O (1.5 mL) and filtered through a short plug of silica gel. The filter cake was washed with Et₂O (10 mL), and the filtrate was concentrated. 1,3,5-Trimethoxybenzene (internal standard) and CDCl₃ were added, and the yield was determined by ¹H NMR analysis. An analytical sample of the product was prepared via preparatory thin layer chromatography, and the *ee* of this sample was determined by HPLC using a chiral stationary phase.



2-Methyl-3-phenyl-3-(phenylethynyl)-2,3-dihydrobenzo[d]isothiazole 1,1-dioxide (5-44). ^1H NMR (400 MHz, CDCl_3) δ 7.93 – 7.83 (m, 1H), 7.72 – 7.64 (m, 2H), 7.60 – 7.47 (m, 4H), 7.44 – 7.30 (m, 6H), 7.24 – 7.18 (m, 1H), 2.83 (s, 3H); ^{13}C NMR (101 MHz, CDCl_3) δ 140.9, 138.1, 133.5, 132.9, 132.0, 129.7, 129.2, 129.1, 128.9, 128.4, 127.3, 125.2, 121.5, 121.2, 90.2, 84.0, 66.8, 24.7.

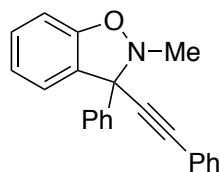


3-Methyl-4-phenyl-4-(phenylethynyl)-3,4-dihydrobenzo[e][1,2,3]oxathiazine 2,2-dioxide (5-49). ^1H NMR (400 MHz, CDCl_3) δ 7.80 – 7.73 (m, 2H), 7.62 – 7.57 (m, 2H), 7.48 – 7.35 (m, 6H), 7.34 – 7.27 (m, 1H), 7.16 – 7.08 (m, 3H), 2.90 (s, 3H); ^{13}C NMR (101 MHz, CDCl_3) δ 147.5, 140.9, 132.0, 130.3, 129.6, 129.2, 129.0, 128.8, 128.4, 127.6, 127.0, 126.1, 121.7, 118.8, 90.6, 84.4, 68.9, 31.3.

5.4.1.2 General Procedure B: Reaction Optimization of Benzisoxazole 5-53

In a N_2 -filled glovebox: To an oven-dried 1-dram vial was added [Cu] (0.010 mmol, 10 mol %), ligand (0.012 mmol, 12 mol%), and solvent. The vial was equipped with a micro stir bar, and the resultant solution was stirred for 30 min at rt. Alkyne (0.12 mmol, 1.2 equiv), base (0.15, 1.5 equiv), and **5-53** (0.10 mmol, 1.0 equiv) were

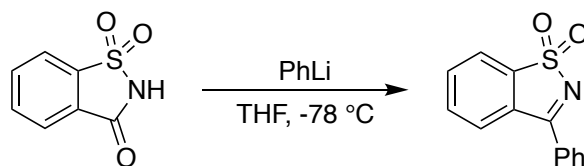
added. The vial was removed from the glovebox, and the resulting mixture was stirred vigorously at 80 °C for 24 h. The mixture was then diluted with Et₂O (1.5 mL) and filtered through a short plug of silica gel. The filter cake was washed with Et₂O (10 mL), and the filtrate was concentrated. 1,3,5-Trimethoxybenzene (internal standard) and CDCl₃ were added, and the yield was determined by ¹H NMR analysis. An analytical sample of the product was prepared via preparatory thin layer chromatography, and the *ee* of this sample was determined by SFC or HPLC using a chiral stationary phase.



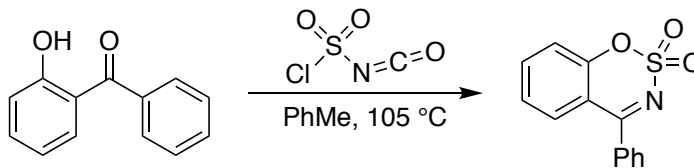
2-Methyl-3-phenyl-3-(phenylethynyl)-2,3-dihydrobenzo[d]isoxazole (5-54).

¹H NMR (600 MHz, CDCl₃) δ 7.70 (d, *J* = 7.5 Hz, 2H), 7.45 – 7.40 (m, 2H), 7.35 – 7.31 (m, 2H), 7.31 – 7.22 (m, 4H), 7.18 – 7.12 (m, 1H), 6.95 (d, *J* = 7.5 Hz, 1H), 6.86 (t, *J* = 7.5 Hz, 1H), 6.79 (d, *J* = 8.1 Hz, 1H), 2.96 (s, 3H).

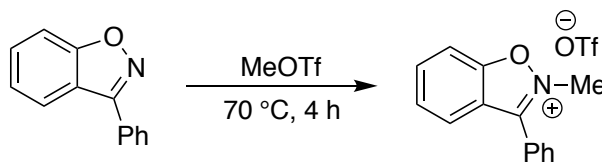
5.4.2 Preparation of Substrates



3-Phenylbenzo[d]isothiazole 1,1-dioxide (5-40). Prepared according to the literature procedure.³⁵



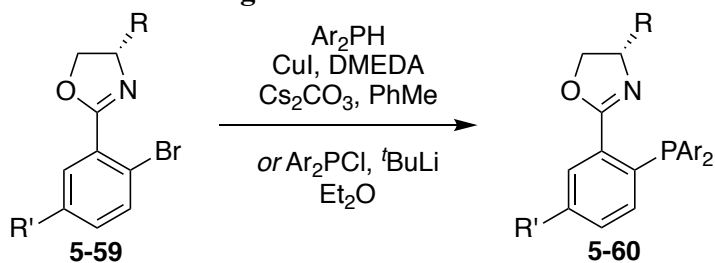
4-Phenylbenzo[*e*][1,2,3]oxathiazine 2,2-dioxide (5-42). Prepared according to the literature procedure.³⁶



3-Phenylbenzo[*d*]isoxazole (5-52). Prepared according to the literature procedure.³⁷

2-Methyl-3-phenylbenzo[*d*]isoxazol-2-ium trifluoromethanesulfonate (5-53). To an oven dried 25 mL round-bottomed flask was added benzisoxazole **5-52** (600 mg, 3.0 mmol, 1.0 equiv) and methyl triflate (0.37 mL, 3.3 mmol, 1.1 equiv). The resulting mixture was heated in an oil bath at 70 °C for 4 h. The mixture was allowed to cool to room temperature, and 2 mL of CH₂Cl₂ was added to dissolve the crude material. The solution was diluted with Et₂O and vigorously stirred to induce trituration. The resultant solid was filtered and washed with Et₂O to give **5-53** (1.0 g, 91%) as a white solid: ¹H NMR (600 MHz, CDCl₃) δ 8.07 (t, *J* = 7.9 Hz, 1H), 7.99 – 7.92 (m, 3H), 7.86 – 7.79 (m, 2H), 7.77 (t, *J* = 7.5 Hz, 2H), 7.72 (t, *J* = 7.7 Hz, 1H), 4.60 (s, 3H); ¹³C NMR (151 MHz, CDCl₃) δ 159.9, 156.4, 137.5, 134.1, 130.4, 130.1, 128.3, 124.8, 121.3, 119.7, 110.7, 40.5.

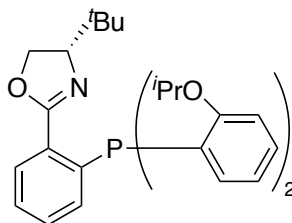
5.4.3 Preparation of PHOX Ligands



The PHOX ligands can be prepared according to a procedure adapted from the literature using the corresponding diarylphosphine.³³ In a N_2 -filled glovebox: To an oven-dried 10 mL round-bottomed flask was added CuI (8.4 mg, 0.044 mmol, 12.5 mol%), diarylphosphine (0.67 mmol, 1.88 equiv), DMEDA (33 μL , 0.31 mmol, 0.875 equiv), and toluene (1.5 mL). The resulting mixture was stirred at rt for 20 min. Aryl bromide (**5-59**) (0.35 mmol, 1.0 equiv) and Cs_2CO_3 (433 mg, 1.33 mmol, 3.75 equiv) were added along with an additional aliquot of toluene (1.5 mL). The resulting mixture was sealed, removed from the glovebox, and heated in an oil bath at 110 $^\circ\text{C}$ for 2 h. The reaction was then allowed to cool to rt. The crude mixture was filtered, washed with CH_2Cl_2 , and concentrated. The desired PHOX ligand **5-60** was then purified via silica gel chromatography.

For sterically encumbered diarylphosphino groups, the PHOX ligands can be prepared according to a procedure adapted from the literature using the corresponding diarylphosphine chloride.³⁴ To an oven-dried 10 mL round-bottomed flask was added aryl bromide (**5-59**) (0.35 mmol, 1.0 equiv) and anhydrous Et_2O (2.5 mL). The resulting solution was cooled to -78 $^\circ\text{C}$. *tert*-Butyl lithium (0.43 mmol, 1.2 equiv) was added dropwise at this temperature. The solution was stirred for an additional 1 h at -78 $^\circ\text{C}$. Diarylphosphine chloride (0.43 mmol, 1.2 equiv) was added. The reaction was warmed to rt and stirred for an additional 1 h. The crude reaction was poured into an aq. NH_4Cl solution and extracted with Et_2O (x 3). The combined organic layers were

dried with magnesium sulfate and concentrated. The desired PHOX ligand **5-60** was then purified via silica gel chromatography.



(S)-2-(2-(Bis(2-isopropoxyphenyl)phosphanyl)phenyl)-4-(tert-butyl)-4,5-

dihydrooxazole (5-70). ^1H NMR (400 MHz, CDCl_3) δ 7.92 – 7.84 (m, 1H), 7.33 (td, J = 7.6, 1.3 Hz, 1H), 7.25 – 7.19 (m, 3H), 7.09 – 7.02 (m, 1H), 6.86 – 6.73 (m, 6H), 4.53 – 4.38 (m, 2H), 4.17 – 4.01 (m, 2H), 4.00 – 3.90 (m, 1H), 1.10 (dd, J = 13.9, 6.0 Hz, 9H), 0.99 – 0.88 (m, 3H), 0.75 (s, 9H); ^{13}C NMR (101 MHz, CDCl_3) δ 159.5, 159.4, 134.8, 134.4, 129.8, 129.3, 129.3, 129.2, 129.1, 127.6, 120.2, 120.0, 111.3, 70.2, 69.6, 68.4, 33.8, 25.8, 21.9, 21.8, 21.6; ^{31}P NMR (162 MHz, CDCl_3) δ -24.44.

REFERENCES

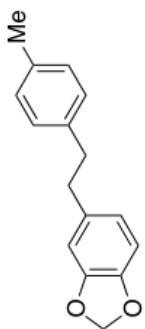
1. Qiao, J. X.; Wang, T. C.; Adam, L. P.; Chen, A. Y. A.; Taylor, D. S.; Yang, R. Z.; Zhuang, S.; Sleph, P. G.; Li, J. P.; Li, D.; Yin, X.; Chang, M.; Chen, X.-Q.; Shen, H.; Li, J.; Smith, D.; Wu, D.-R.; Leith, L.; Harikrishnan, L. S.; Kamau, M. G.; Miller, M. M.; Bilder, D.; Rampulla, R.; Li, Y.-X.; Xu, C.; Lawrence, R. M.; Poss, M. A.; Levesque, P.; Gordon, D. A.; Huang, C. S.; Finlay, H. J.; Wexler, R. R.; Salvati, M. E., *Journal of Medicinal Chemistry* **2015**, *58*, 9010-9026.
2. Crawforth, J. M.; Glossop, P. A.; Hamper, B. C.; Huang, W.; Mantell, S. J.; Neal, B. E.; Olson, K.; Thorarensen, A.; Turner, S. R., WO2009153721A1, 2009/12/23/, 2009.
3. Anderson, P.; Christy, M. E.; Evans, B. E., US4399141 (A), 1983/08/16/, 1983.
4. Hou, G.; Tao, R.; Sun, Y.; Zhang, X.; Gosselin, F., *J. Am. Chem. Soc.* **2010**, *132*, 2124-2125.
5. Nguyen, T. B.; Wang, Q.; Guéritte, F., *Chemistry – A European Journal* **2011**, *17*, 9576-9580.
6. Wang, J.; Wang, W.; Li, W.; Hu, X.; Shen, K.; Tan, C.; Liu, X.; Feng, X., *Chemistry – A European Journal* **2009**, *15*, 11642-11659.
7. Shaw, A. W.; deSolms, S. J., *Tetrahedron Letters* **2001**, *42*, 7173-7176.
8. Liu, J.; Dasgupta, S.; Watson, M. P., *Beilstein Journal of Organic Chemistry* **2015**, *11*, 2696-2706.
9. Dasgupta, S.; Rivas, T.; Watson, M. P., *Angewandte Chemie International Edition* **2015**, *54*, 14154-14158.
10. Maity, P.; Srinivas, H. D.; Watson, M. P., *J. Am. Chem. Soc.* **2011**, *133*, 17142-17145.

11. Srinivas, H. D.; Maity, P.; Yap, G. P. A.; Watson, M. P., *The Journal of Organic Chemistry* **2015**, *80*, 4003-4016.
12. Dasgupta, S.; Liu, J.; Shoffler, C. A.; Yap, G. P. A.; Watson, M. P., *Org. Lett.* **2016**, *18*, 6006-6009.
13. Zhuang, W.; Saaby, S.; Jørgensen, K. A., *Angewandte Chemie International Edition* **2004**, *43*, 4476-4478.
14. Saaby, S.; Nakama, K.; Lie, M. A.; Hazell, R. G.; Jørgensen, K. A., *Chemistry – A European Journal* **2003**, *9*, 6145-6154.
15. Kong, J.; McLaughlin, M.; Belyk, K.; Mondschein, R., *Org. Lett.* **2015**, *17*, 5520-5523.
16. Wang, H.; Jiang, T.; Xu, M.-H., *J. Am. Chem. Soc.* **2013**, *135*, 971-974.
17. Nishimura, T.; Noishiki, A.; Chit Tsui, G.; Hayashi, T., *J. Am. Chem. Soc.* **2012**, *134*, 5056-5059.
18. Chen, Y.-J.; Chen, Y.-H.; Feng, C.-G.; Lin, G.-Q., *Org. Lett.* **2014**, *16*, 3400-3403.
19. Jiang, C.; Lu, Y.; Hayashi, T., *Angewandte Chemie International Edition* **2014**, *53*, 9936-9939.
20. Yang, G.; Zhang, W., *Angewandte Chemie International Edition* **2013**, *52*, 7540-7544.
21. Huang, Y.; Huang, R.-Z.; Zhao, Y., *J. Am. Chem. Soc.* **2016**, *138*, 6571-6576.
22. Luo, Y.; Carnell, A. J.; Lam, H. W., *Angewandte Chemie International Edition* **2012**, *51*, 6762-6766.
23. Osborne, C. A.; Endean, T. B. D.; Jarvo, E. R., *Org. Lett.* **2015**, *17*, 5340-5343.
24. Wang, Y.-Q.; Yu, C.-B.; Wang, D.-W.; Wang, X.-B.; Zhou, Y.-G., *Org. Lett.* **2008**, *10*, 2071-2074.
25. Wehn, P. M.; Du Bois, J., *Org. Lett.* **2005**, *7*, 4685-4688.
26. Milburn, R. R.; Snieckus, V., *Angewandte Chemie International Edition* **2004**, *43*, 888-891.
27. Macklin, T. K.; Snieckus, V., *Org. Lett.* **2005**, *7*, 2519-2522.

28. Ramgren, S. D.; Silberstein, A. L.; Yang, Y.; Garg, N. K., *Angewandte Chemie International Edition* **2011**, *50*, 2171-2173.
29. Quasdorf, K. W.; Antoft-Finch, A.; Liu, P.; Silberstein, A. L.; Komaromi, A.; Blackburn, T.; Ramgren, S. D.; Houk, K. N.; Snieckus, V.; Garg, N. K., *J. Am. Chem. Soc.* **2011**, *133*, 6352-6363.
30. Berthet, M.; Cheviet, T.; Dujardin, G.; Parrot, I.; Martinez, J., *Chemical Reviews* **2016**, *116*, 15235-15283.
31. De Munck, L.; Monleón, A.; Vila, C.; Muñoz, M. C.; Pedro, J. R., *Organic & Biomolecular Chemistry* **2015**, *13*, 7393-7396.
32. Morisaki, K.; Sawa, M.; Yonesaki, R.; Morimoto, H.; Mashima, K.; Ohshima, T., *J. Am. Chem. Soc.* **2016**, *138*, 6194-6203.
33. Tani, K.; Behenna, D. C.; McFadden, R. M.; Stoltz, B. M., *Org. Lett.* **2007**, *9*, 2529-2531.
34. García-Fortanet, J.; Buchwald, S. L., *Angewandte Chemie International Edition* **2008**, *47*, 8108-8111.
35. Davis, F. A.; Towson, J. C.; Vashi, D. B.; ThimmaReddy, R.; McCauley, J. P.; Harakal, M. E.; Gosciniak, D. J., *The Journal of Organic Chemistry* **1990**, *55*, 1254-1261.
36. Kamal, A.; Sattur, P. B., *Synthesis* **1981**, *1981*, 272-273.
37. Shan, G.; Huang, G.-Y.; Rao, Y.; Zhang, H., *Chinese Chemical Letters* **2015**, *26*, 1236-1240.

Appendix A

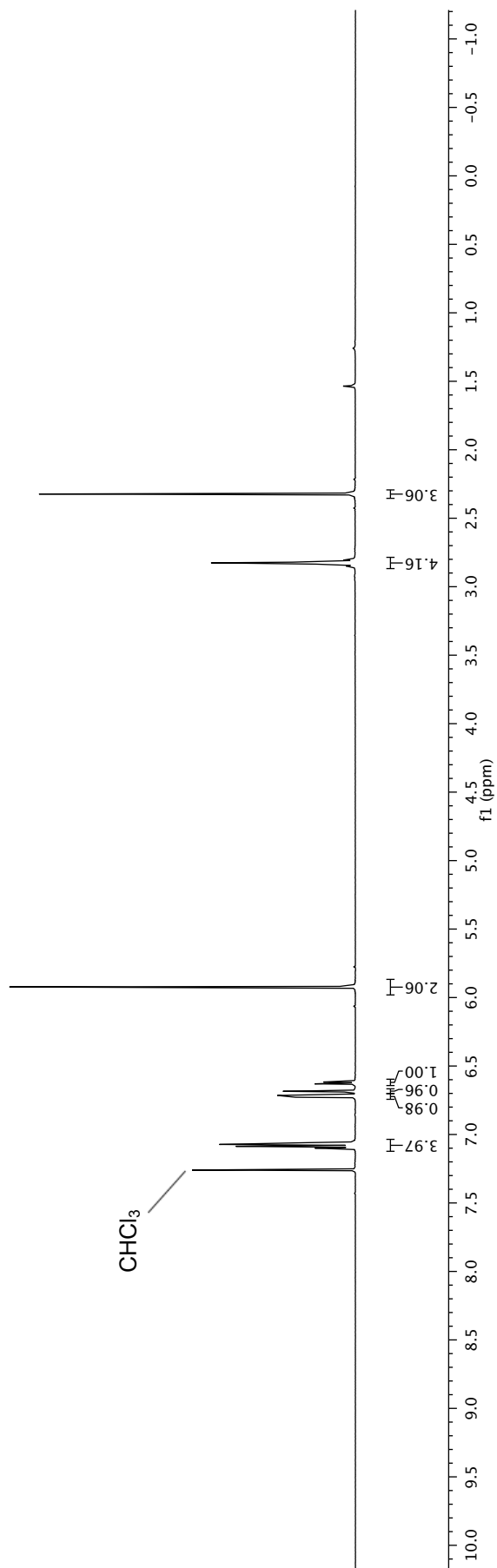
SPECTRAL AND CHROMATOGRAPHY DATA FOR CHAPTER 1

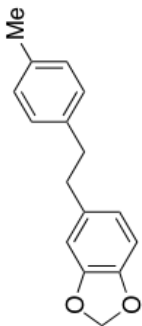


Compound 1-40
¹H NMR (600 MHz, CDCl₃)

2.857
 2.848
 2.840
 2.833
 2.828
 2.826
 2.821
 2.814
 2.806
 2.797
 2.323

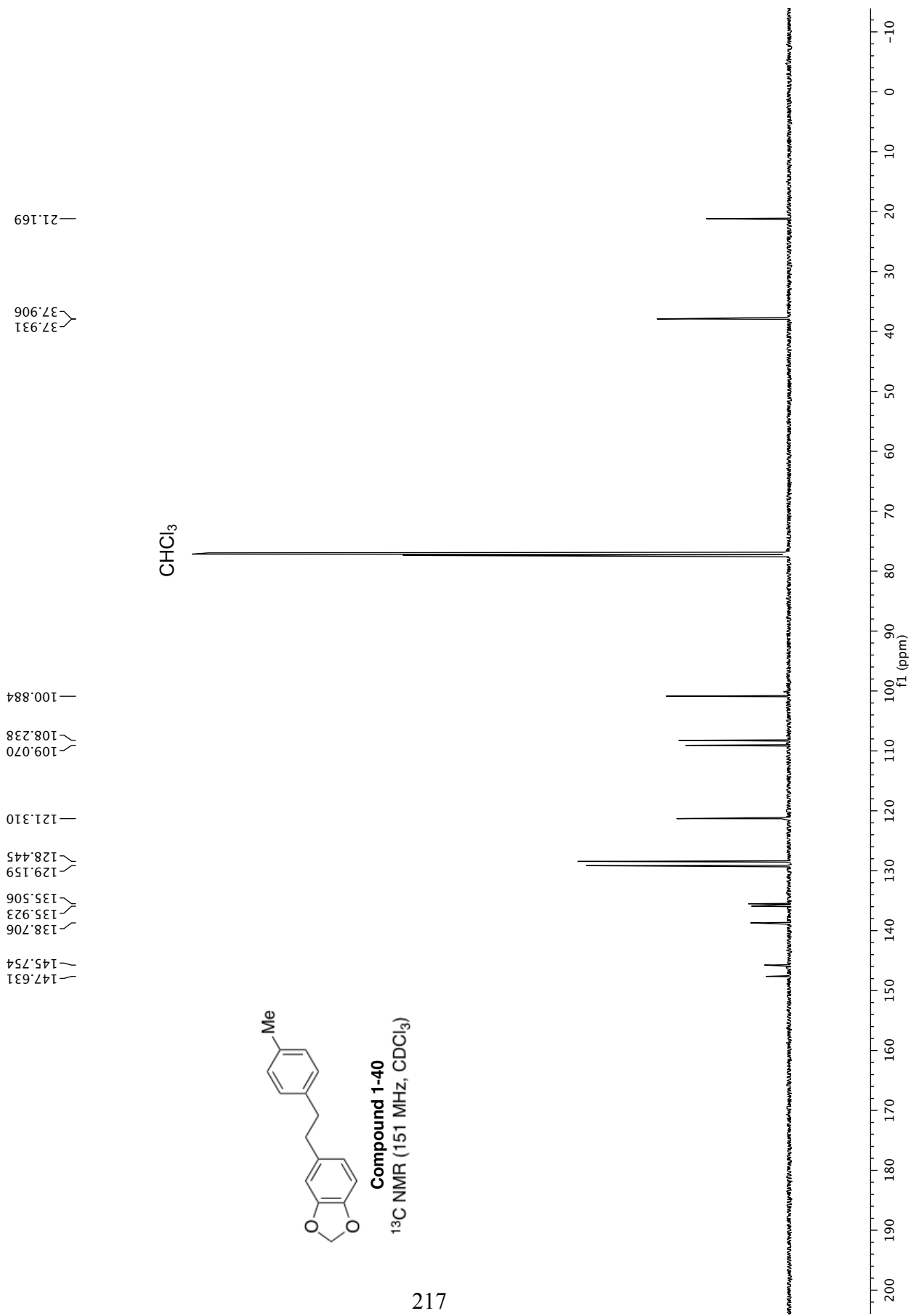
7.100
 7.086
 7.073
 7.059
 6.728
 6.715
 6.687
 6.685
 6.630
 6.627
 6.617
 6.614
 5.923

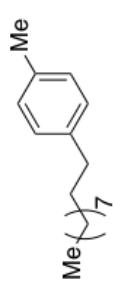




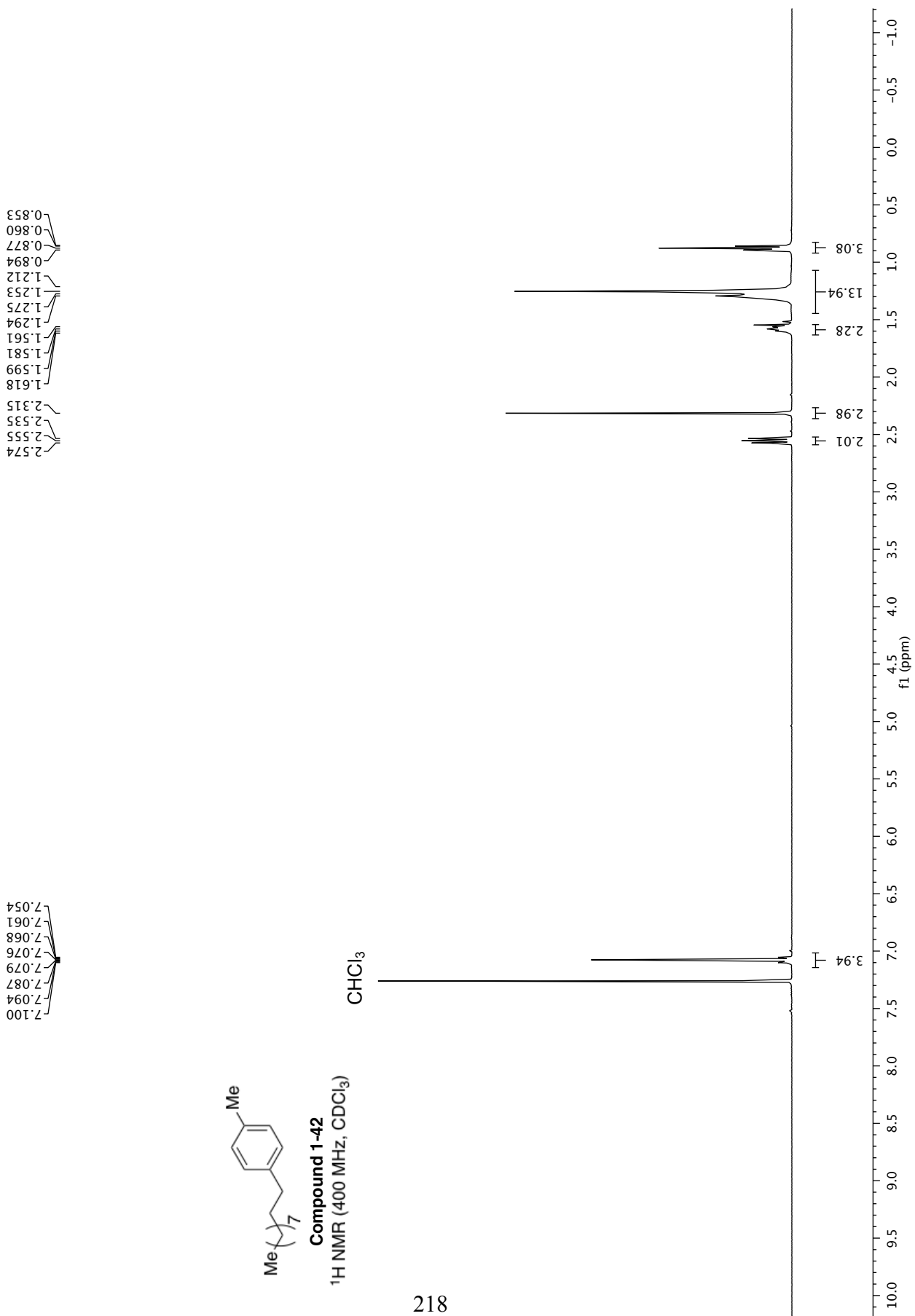
Compound 1-40

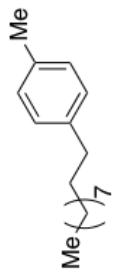
^{13}C NMR (151 MHz, CDCl_3)





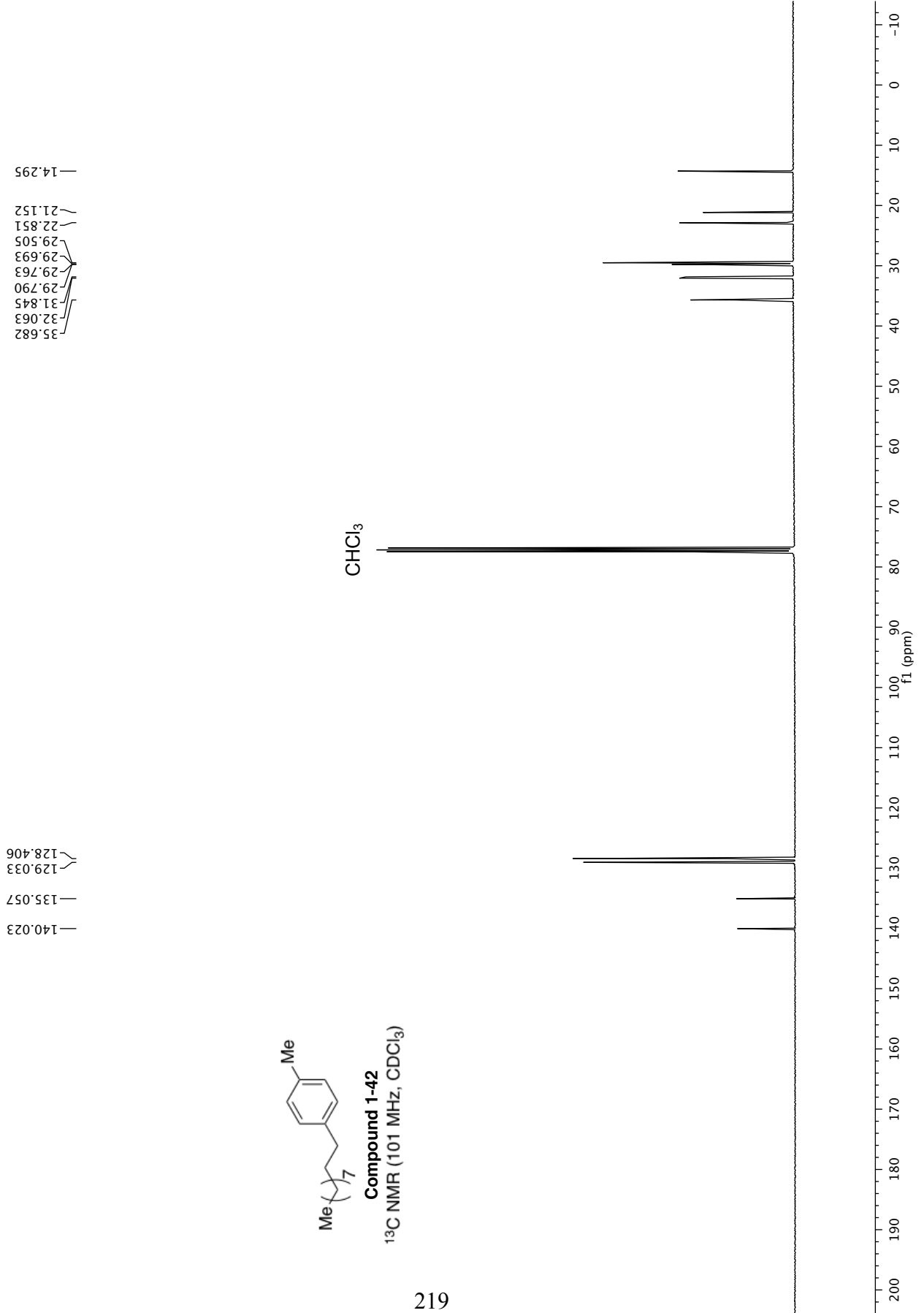
Compound 1-42
¹H NMR (400 MHz, CDCl₃)

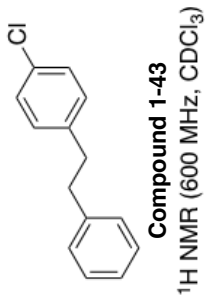




Compound 1-42

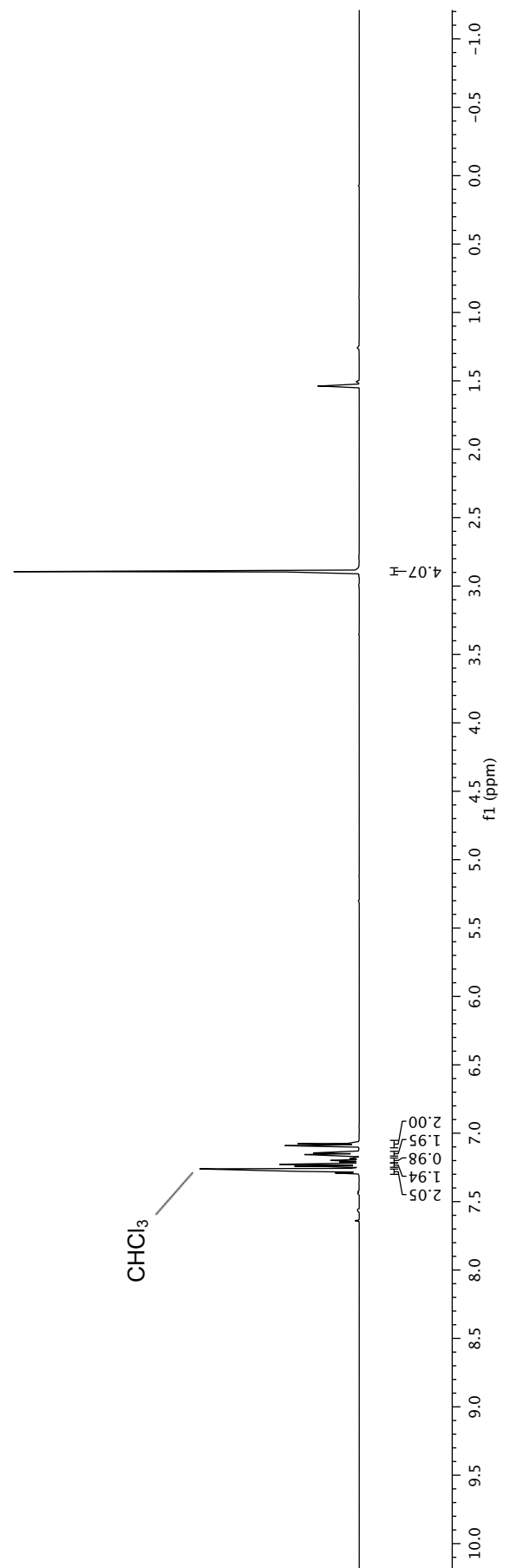
¹³C NMR (101 MHz, CDCl₃)

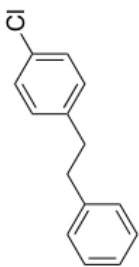




7.291
 7.279
 7.266
 7.245
 7.241
 7.238
 7.230
 7.227
 7.223
 7.211
 7.199
 7.187
 7.156
 7.144
 7.091
 7.077

2.895





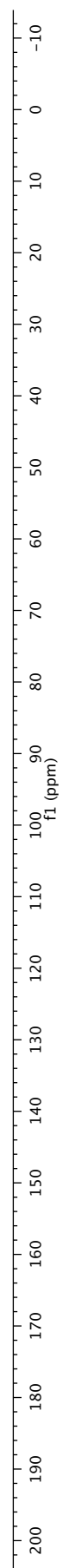
Compound 1-43

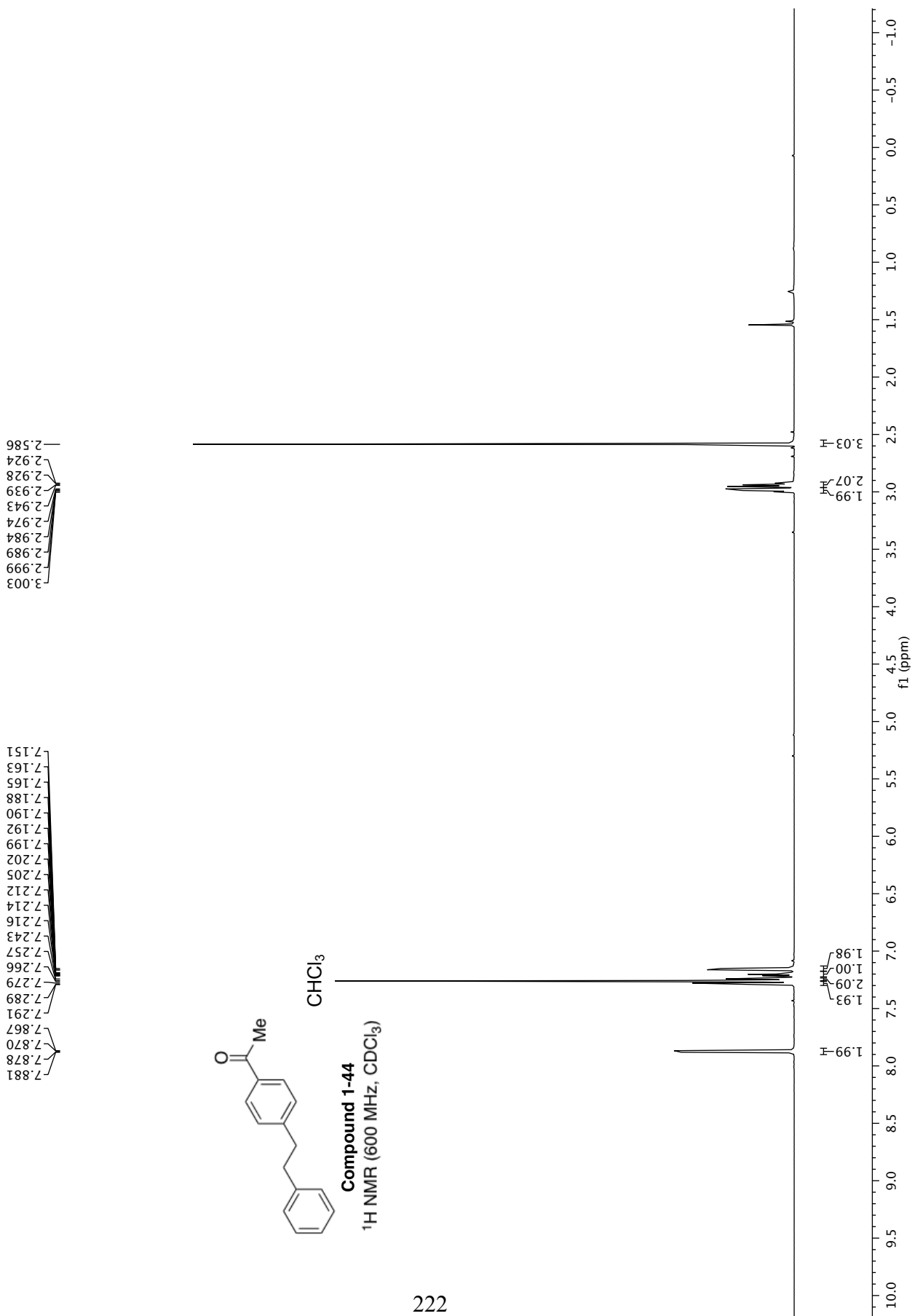
^{13}C NMR (151 MHz, CDCl_3)

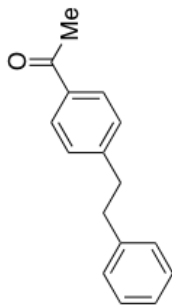
141.419
140.254
131.773
129.983
128.608
128.538
128.519
126.184

37.899
37.344

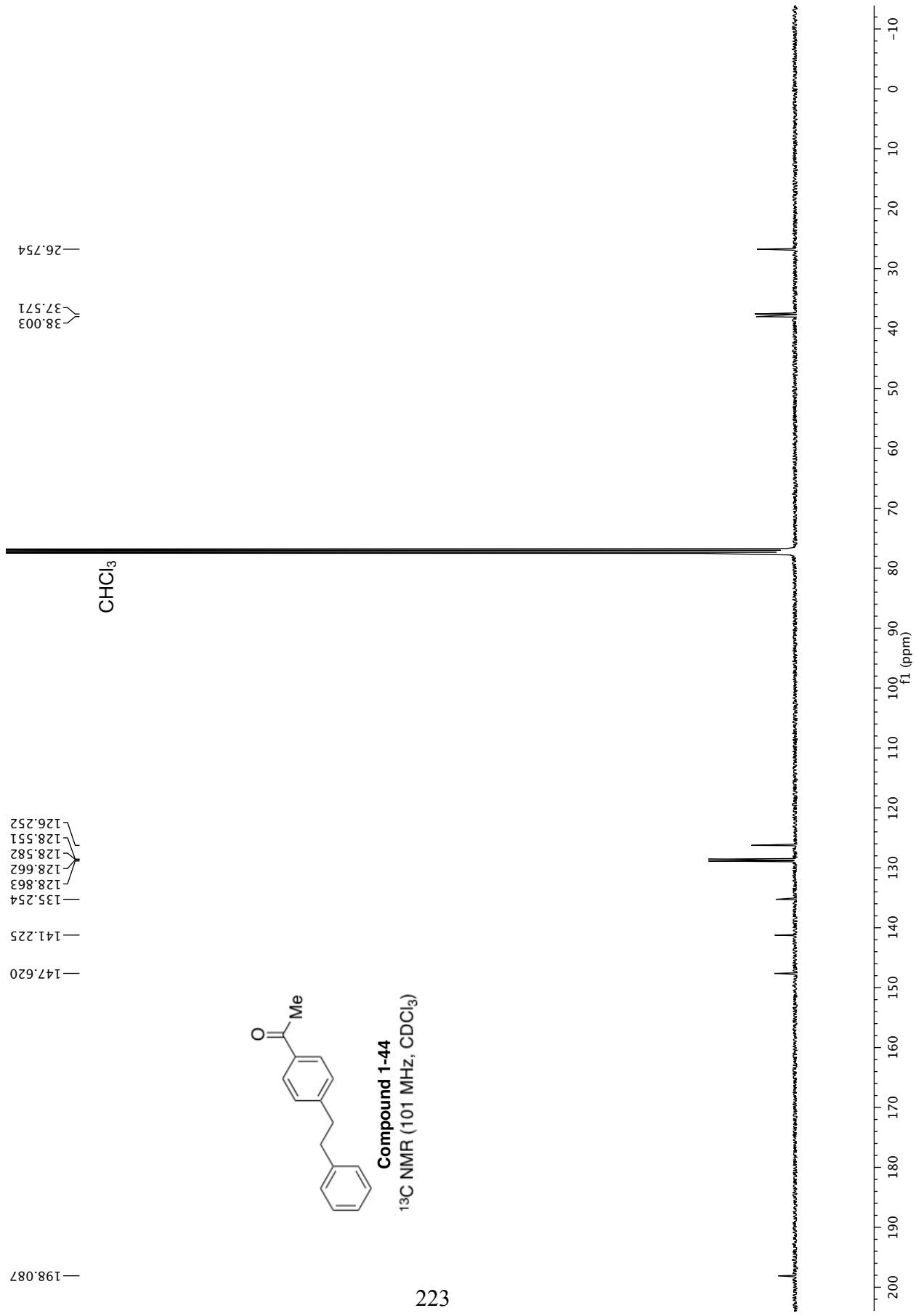
CHCl_3

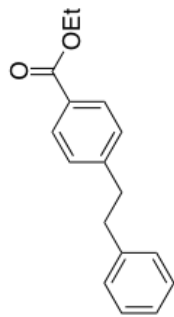




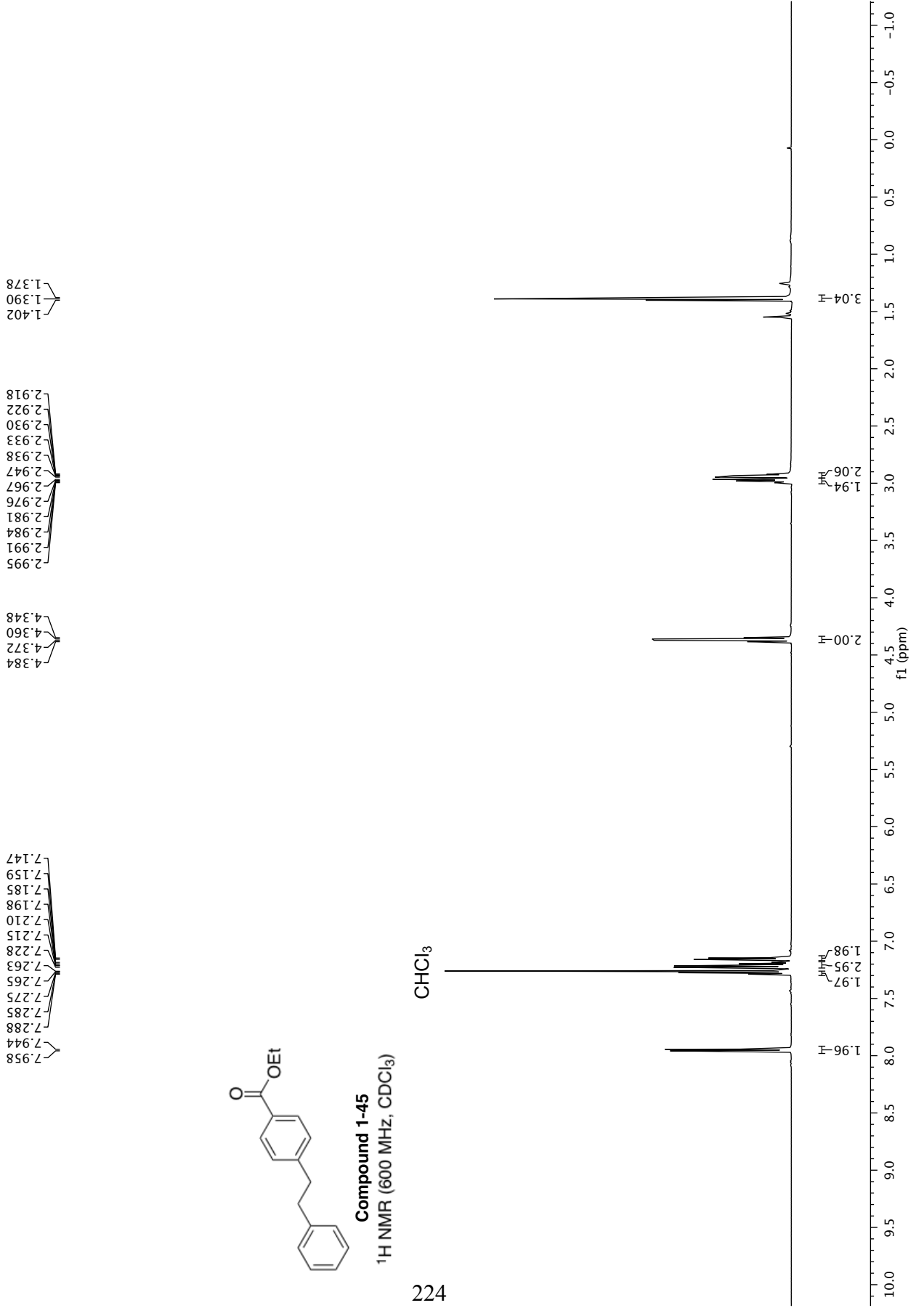


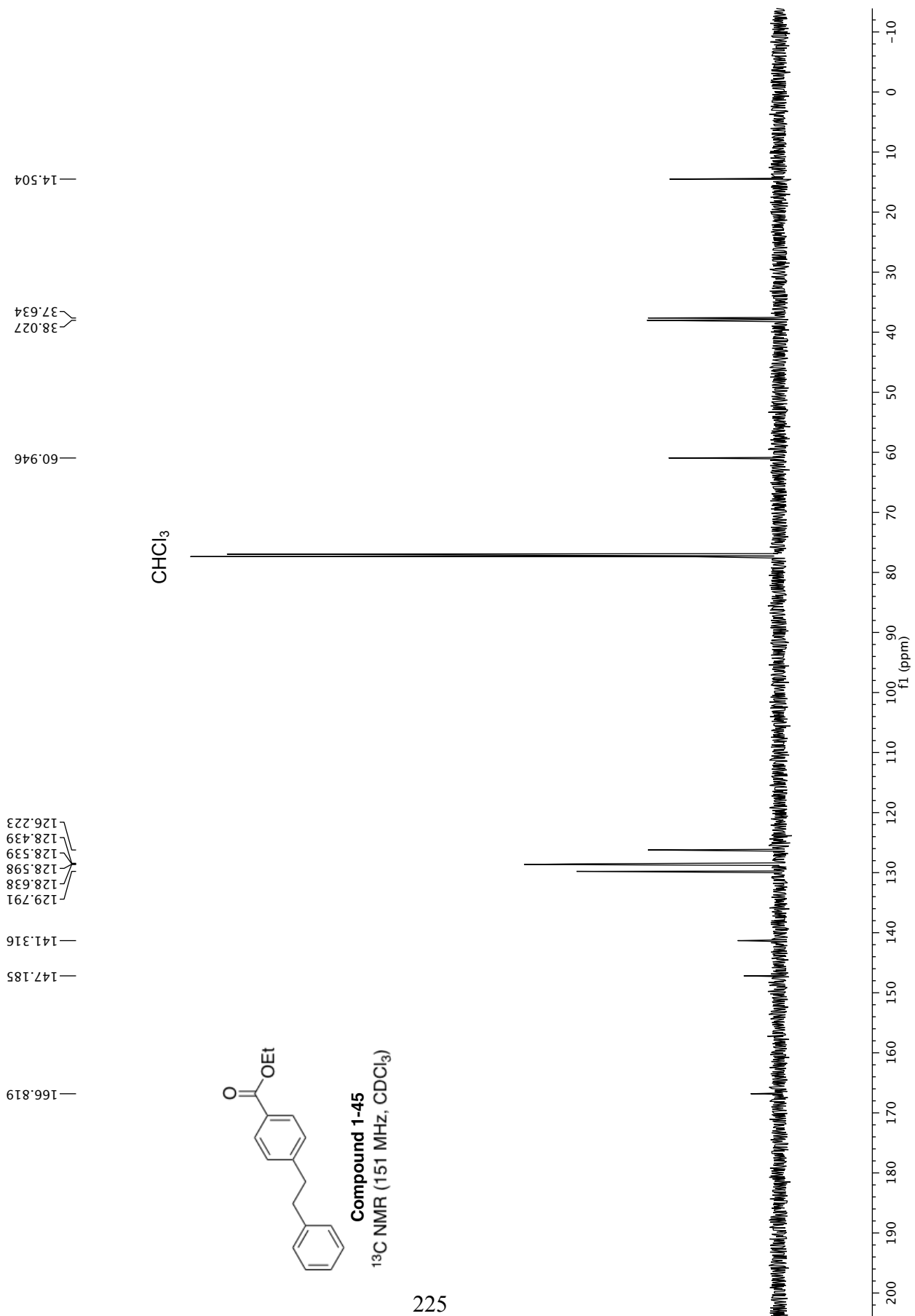
Compound 1-44
 ^{13}C NMR (101 MHz, CDCl_3)

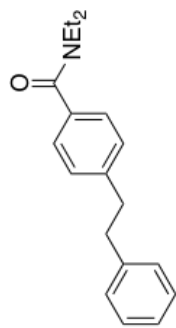




Compound 1-45
¹H NMR (600 MHz, CDCl₃)





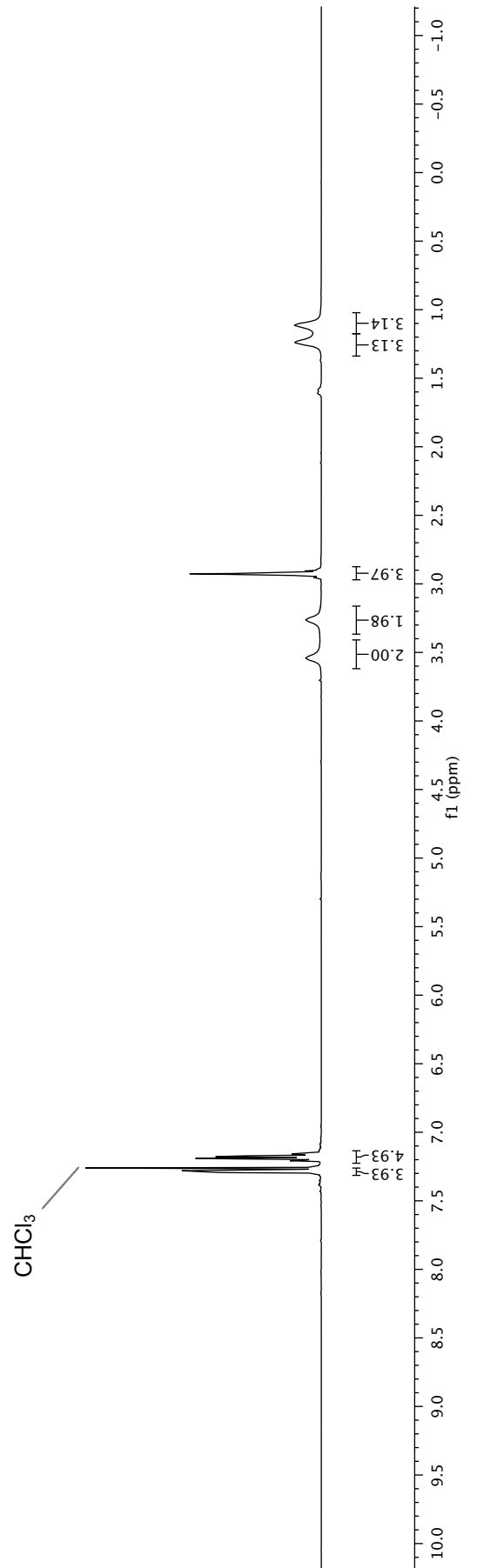


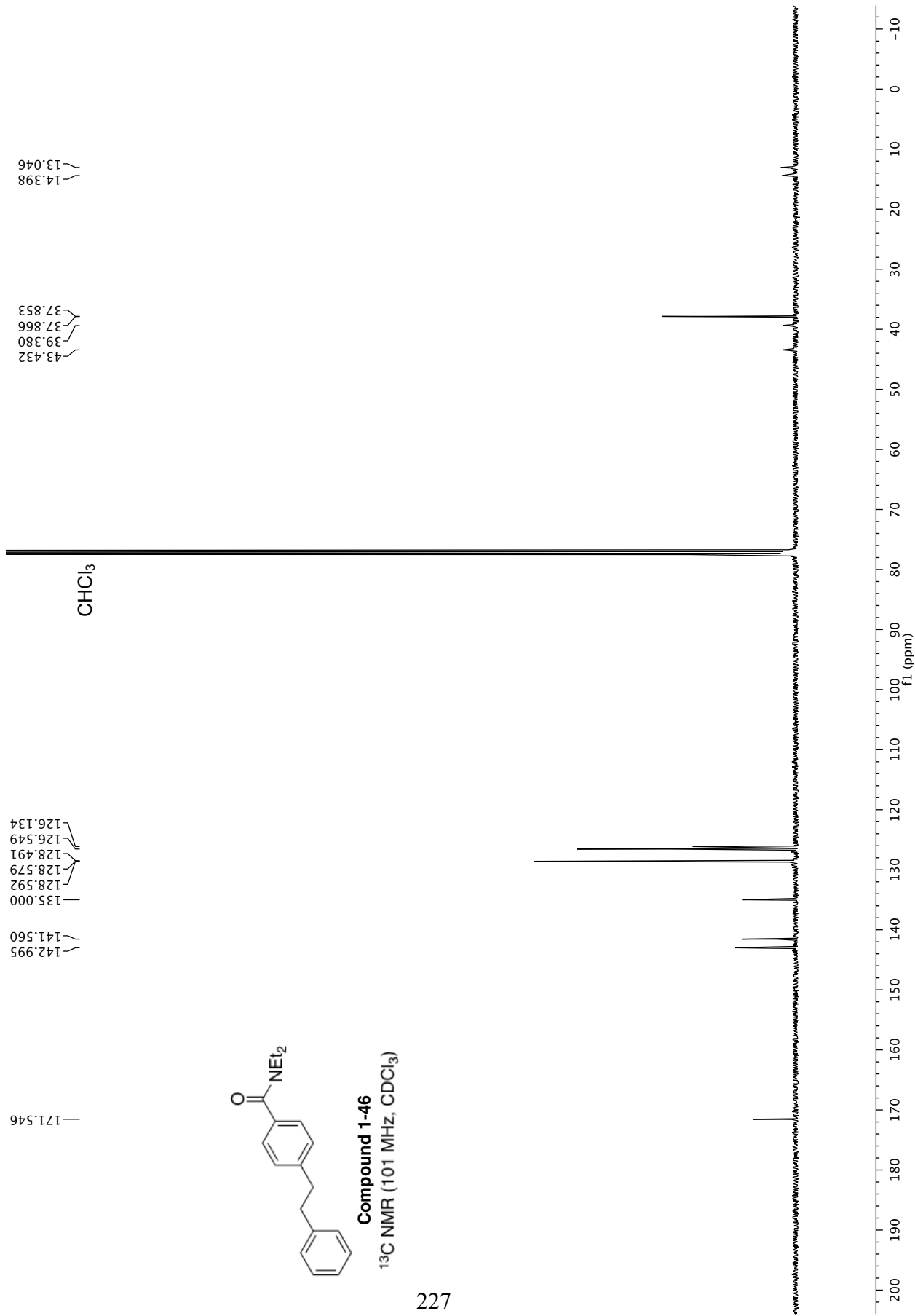
Compound 1-46

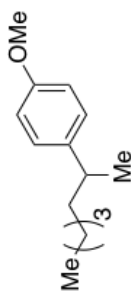
¹H NMR (600 MHz, CDCl₃)

3.541
3.263
2.958
2.951
2.942
2.936
2.930
2.926
2.920
2.915
2.905
2.898
1.238
1.112

7.294
7.291
7.288
7.284
7.281
7.276
7.263
7.208
7.206
7.196
7.178
7.175
7.172
7.161

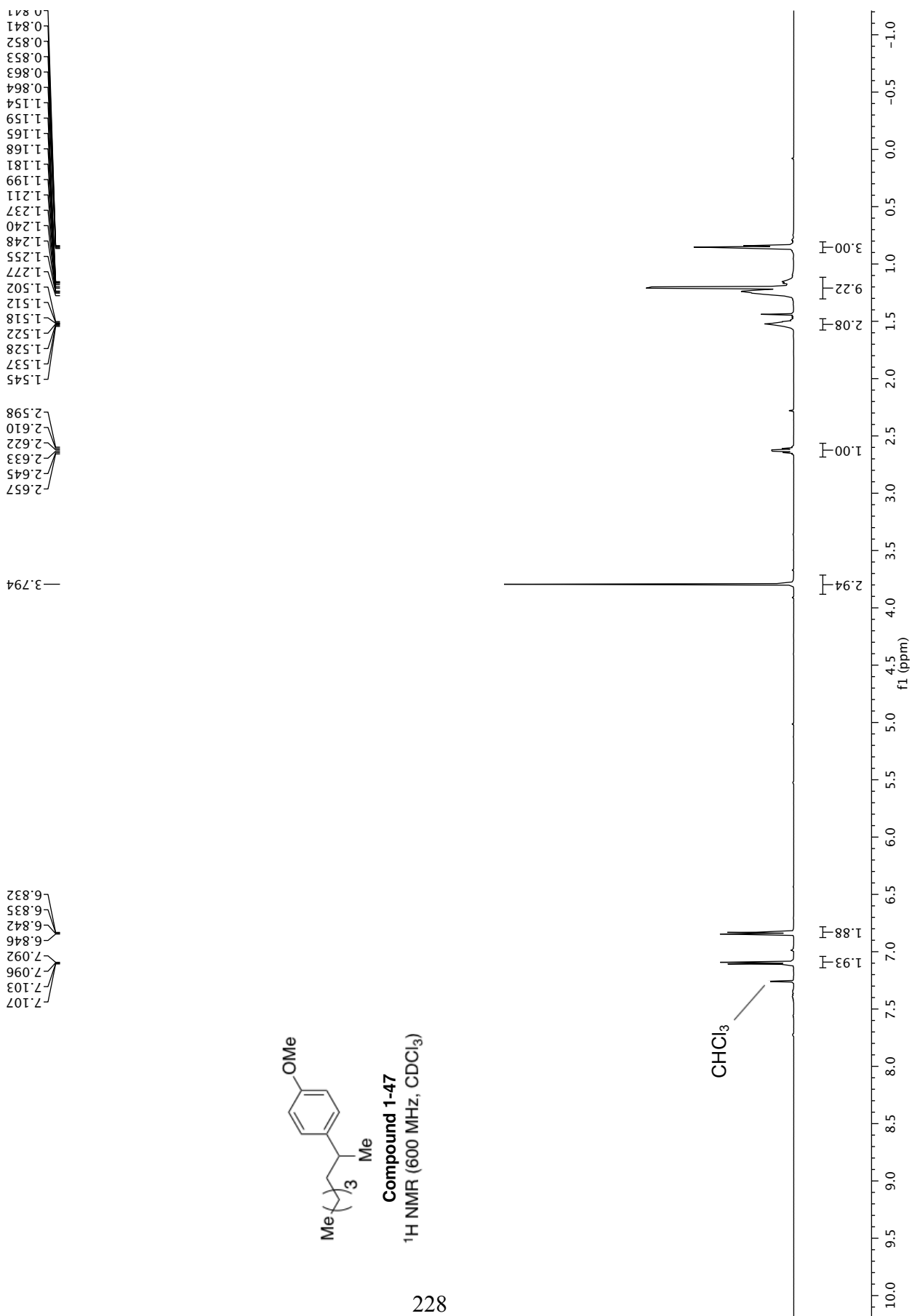


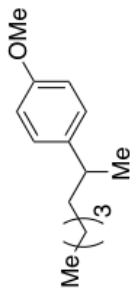




Compound 1-47
¹H NMR (600 MHz, CDCl₃)

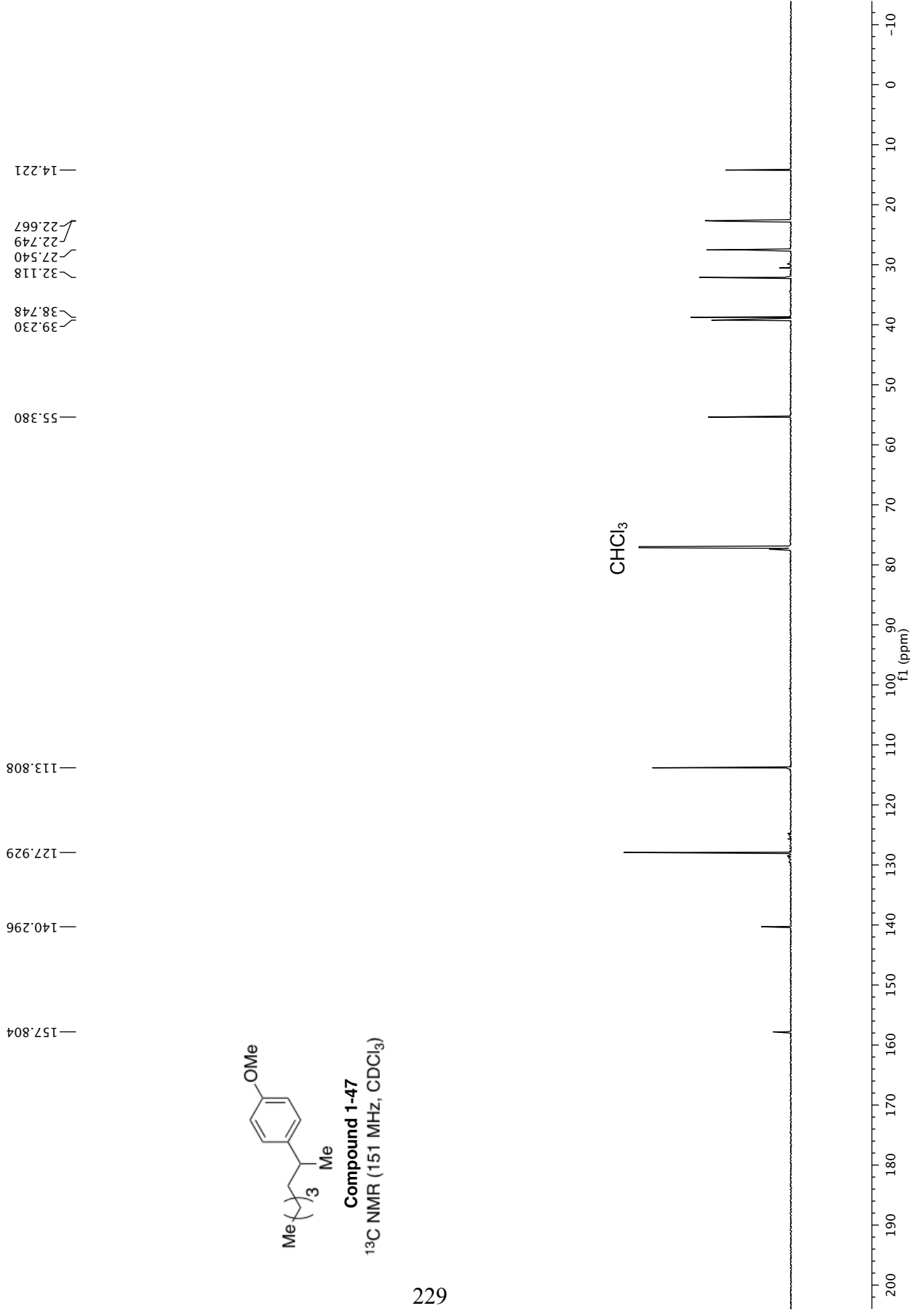
228

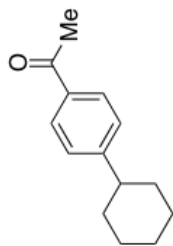




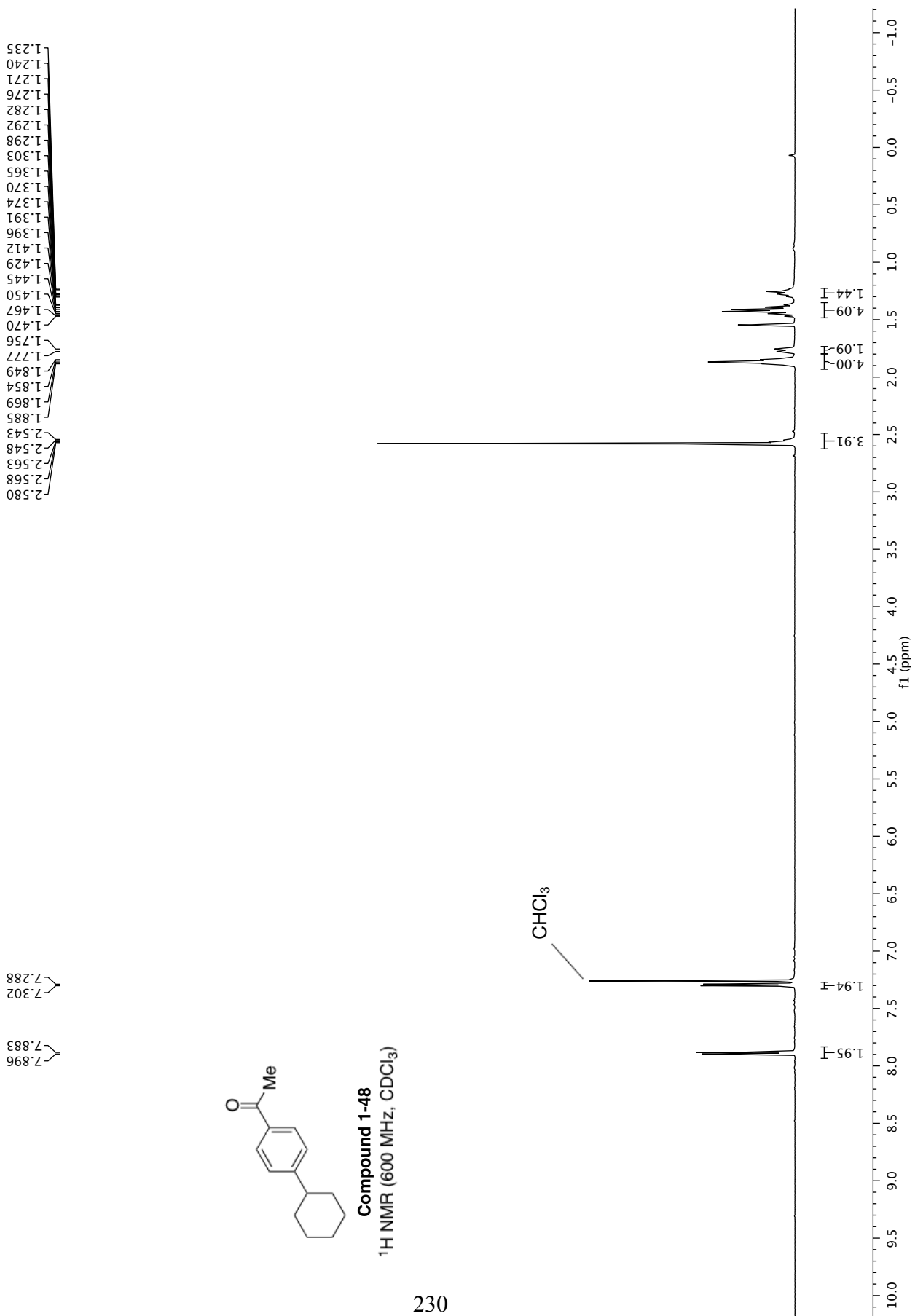
Compound 1-47

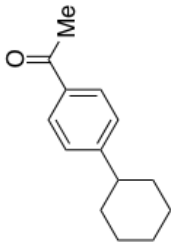
^{13}C NMR (151 MHz, CDCl_3)



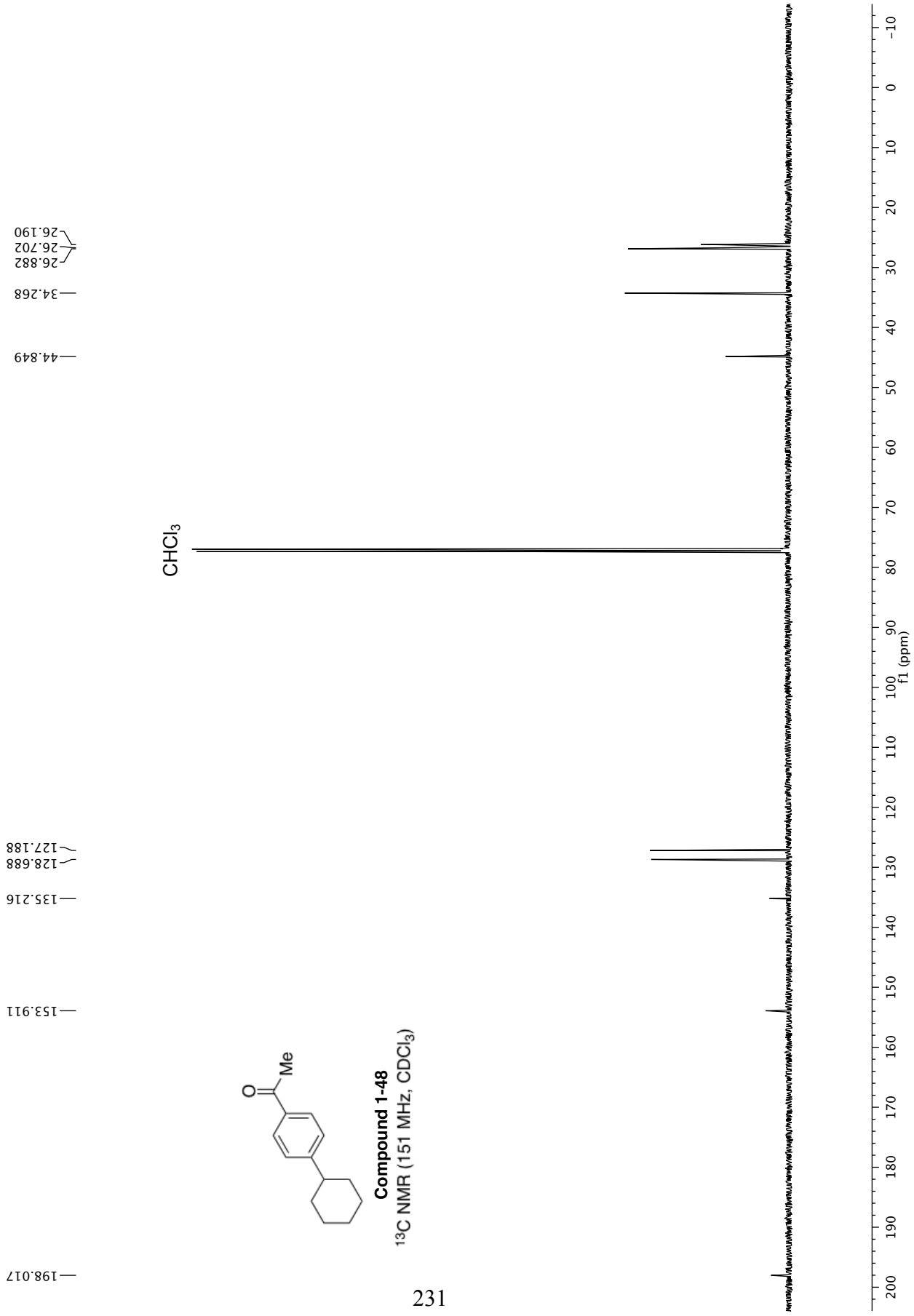


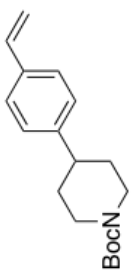
Compound 1-48
¹H NMR (600 MHz, CDCl₃)



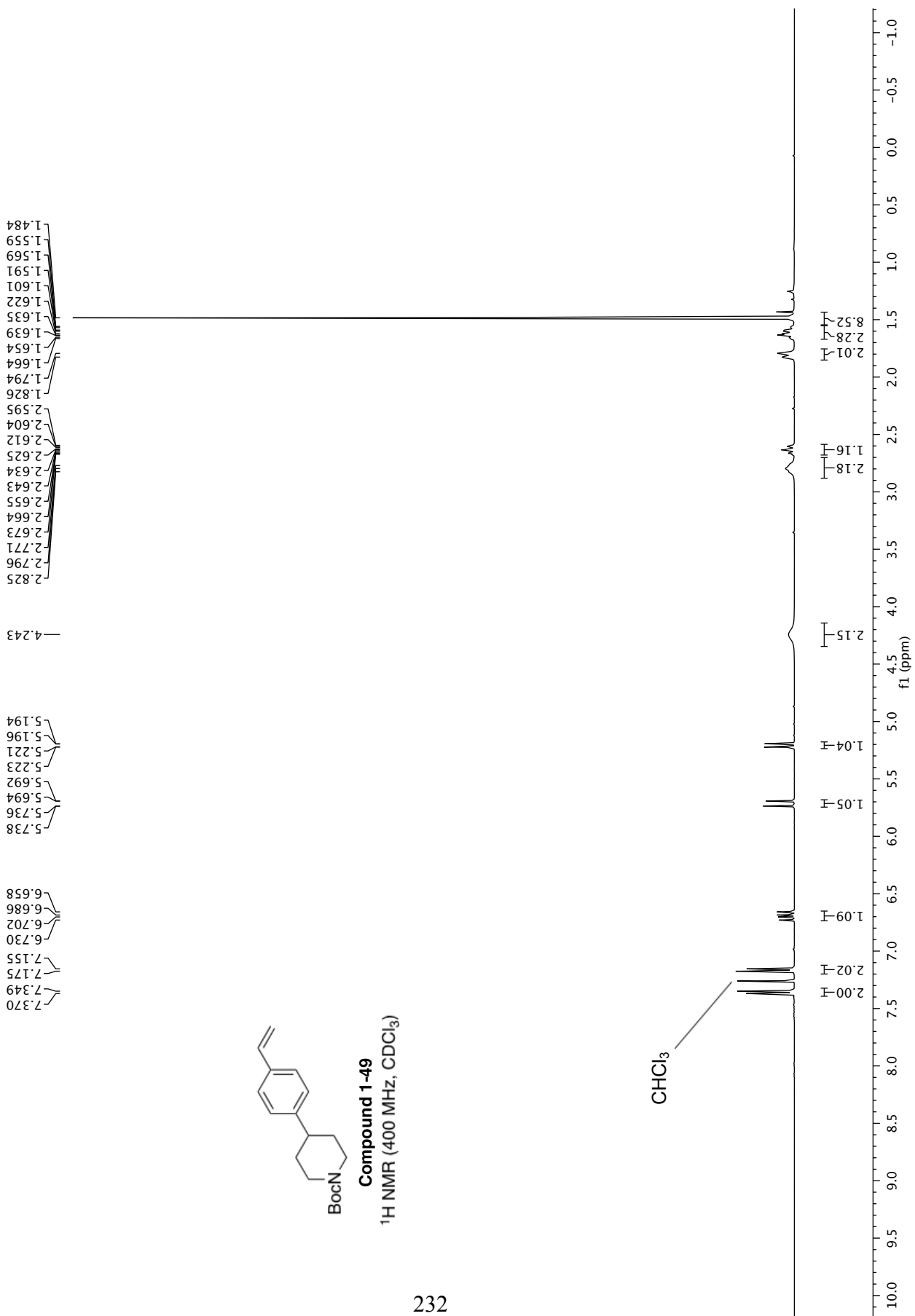


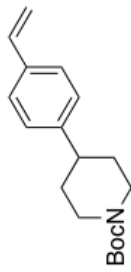
Compound 1-48
¹³C NMR (151 MHz, CDCl₃)





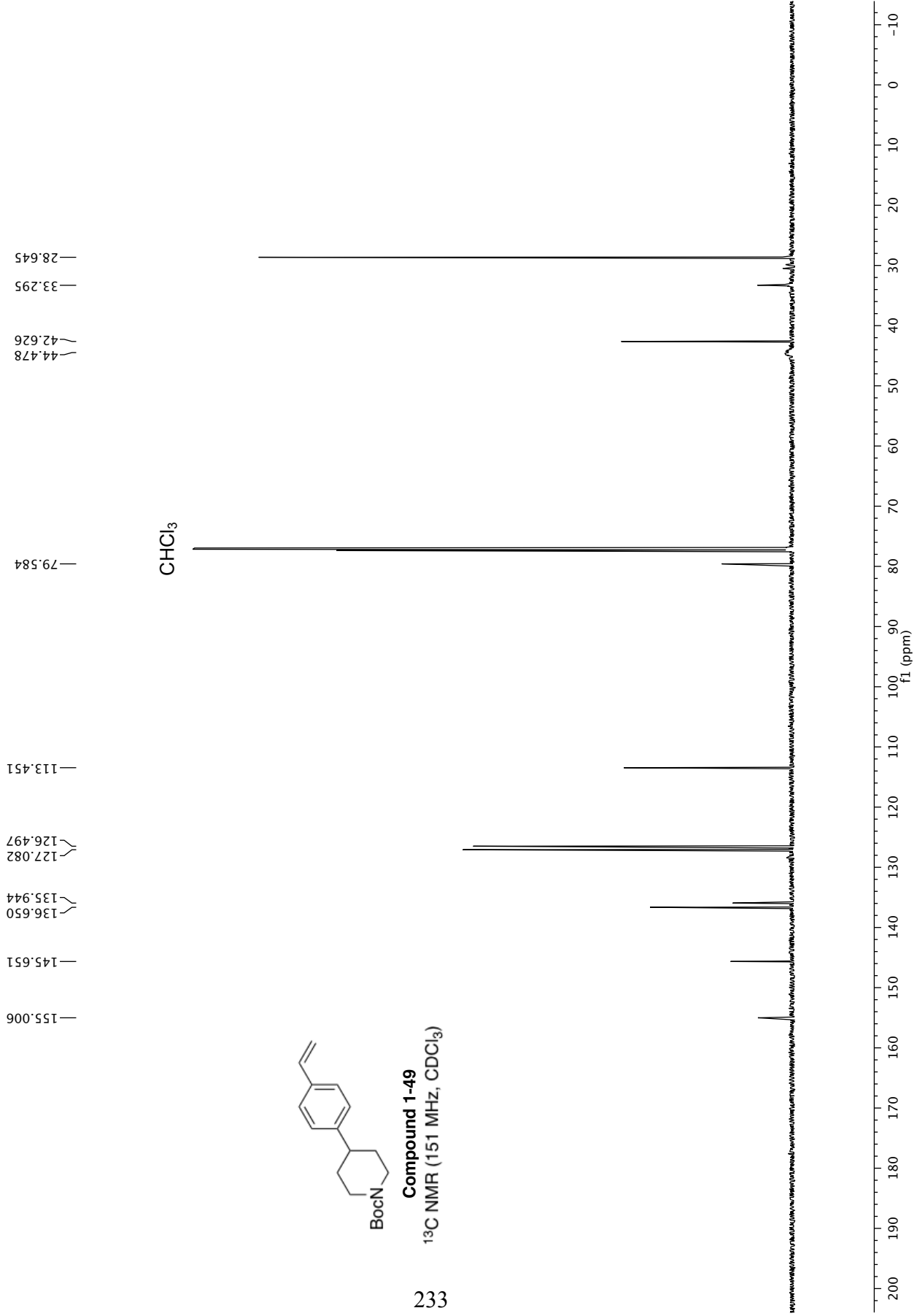
Compound 1-49
¹H NMR (400 MHz, CDCl₃)

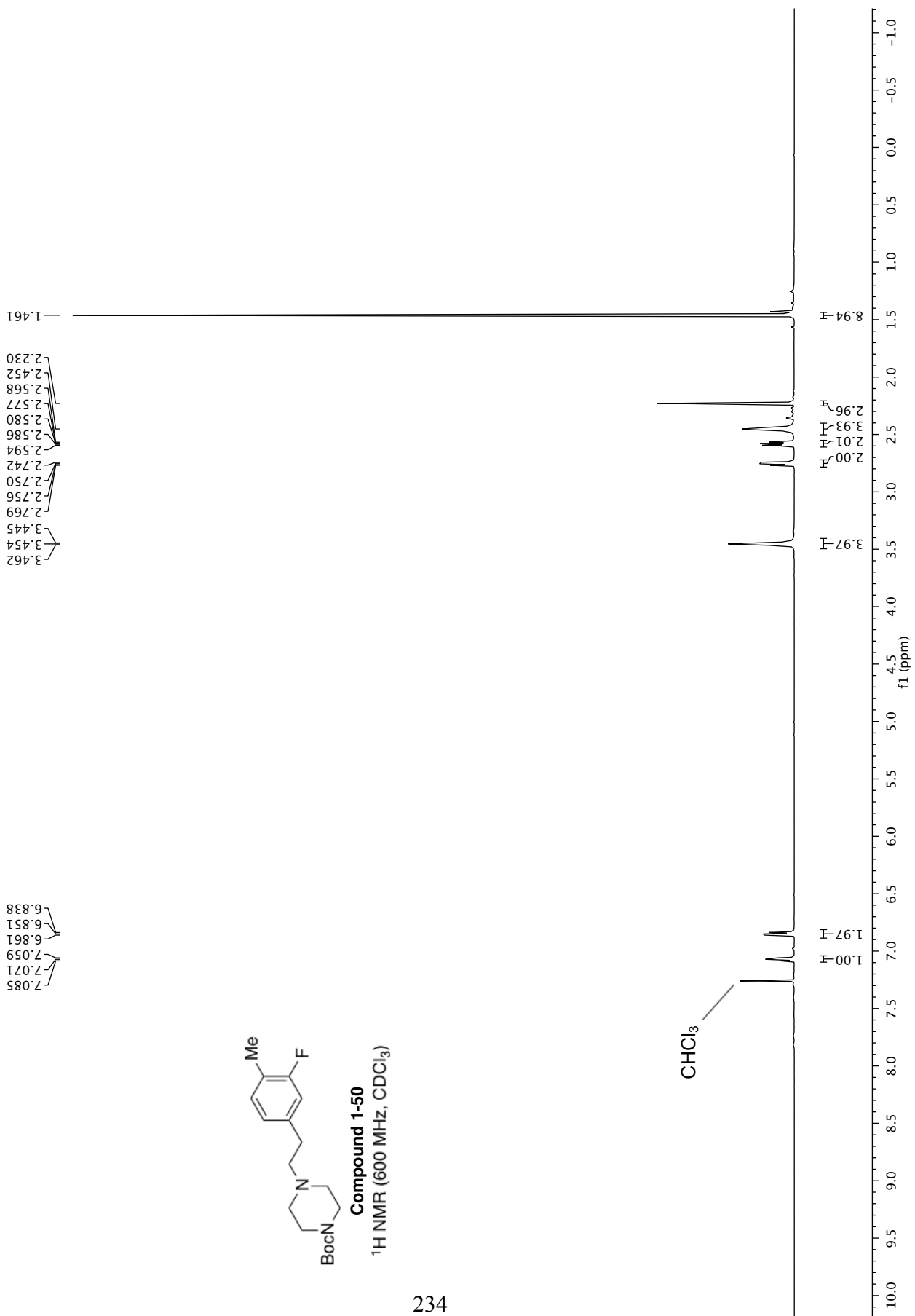
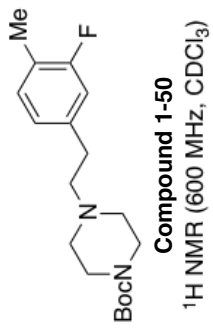


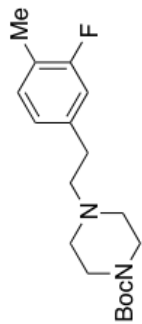


Compound 1-49

^{13}C NMR (151 MHz, CDCl_3)

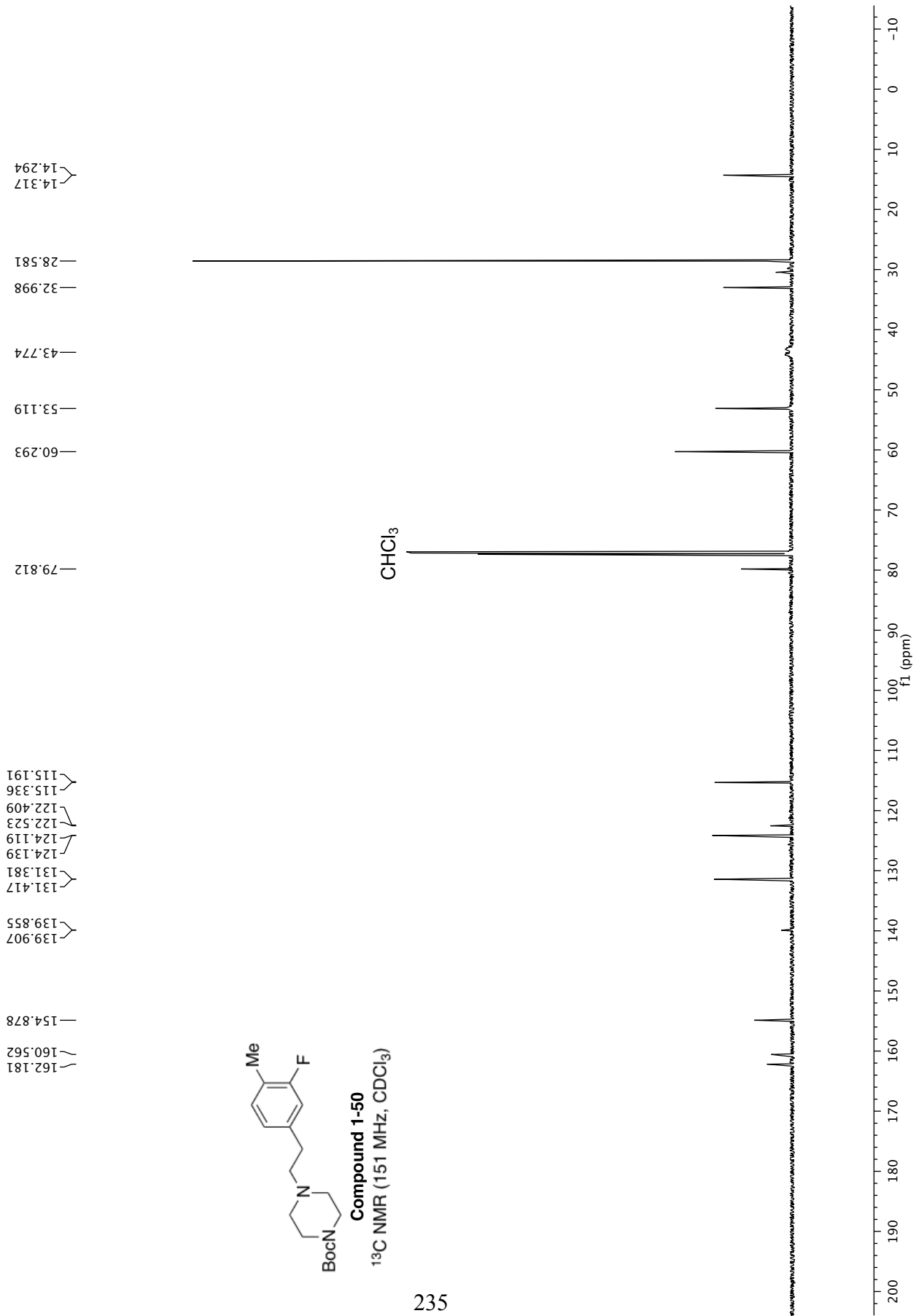


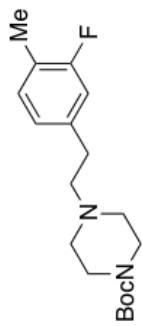




Compound 1-50

^{13}C NMR (151 MHz, CDCl_3)

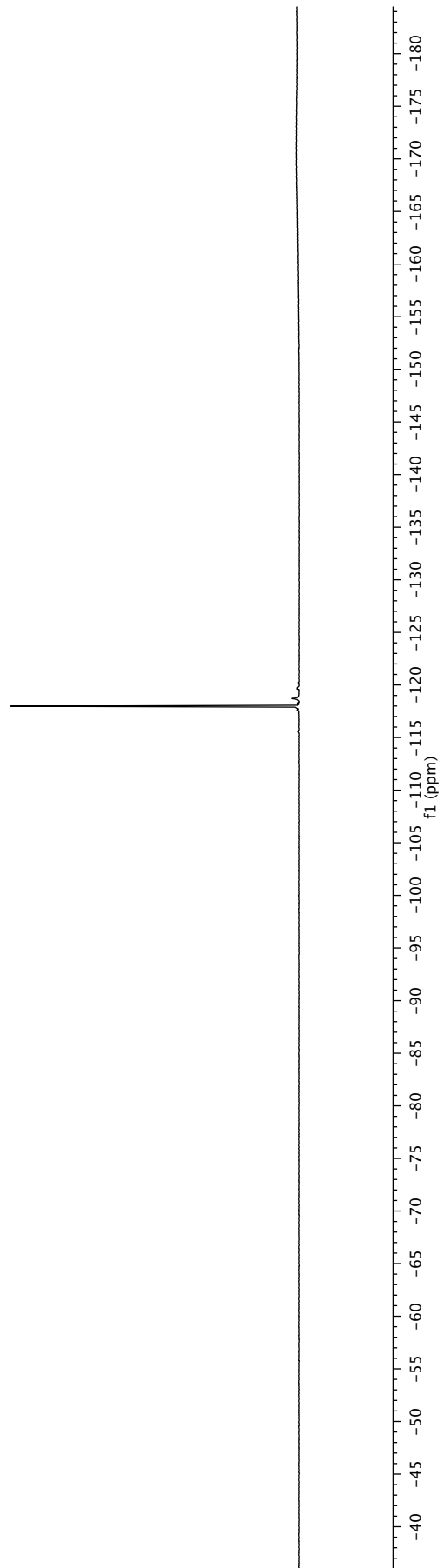


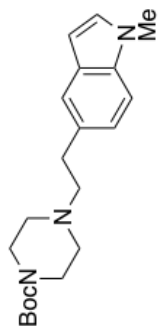


Compound 1-50

¹⁹F NMR (565 MHz, CDCl₃)

—117.975





Compound 1-51

¹H NMR (600 MHz, CDCl₃)

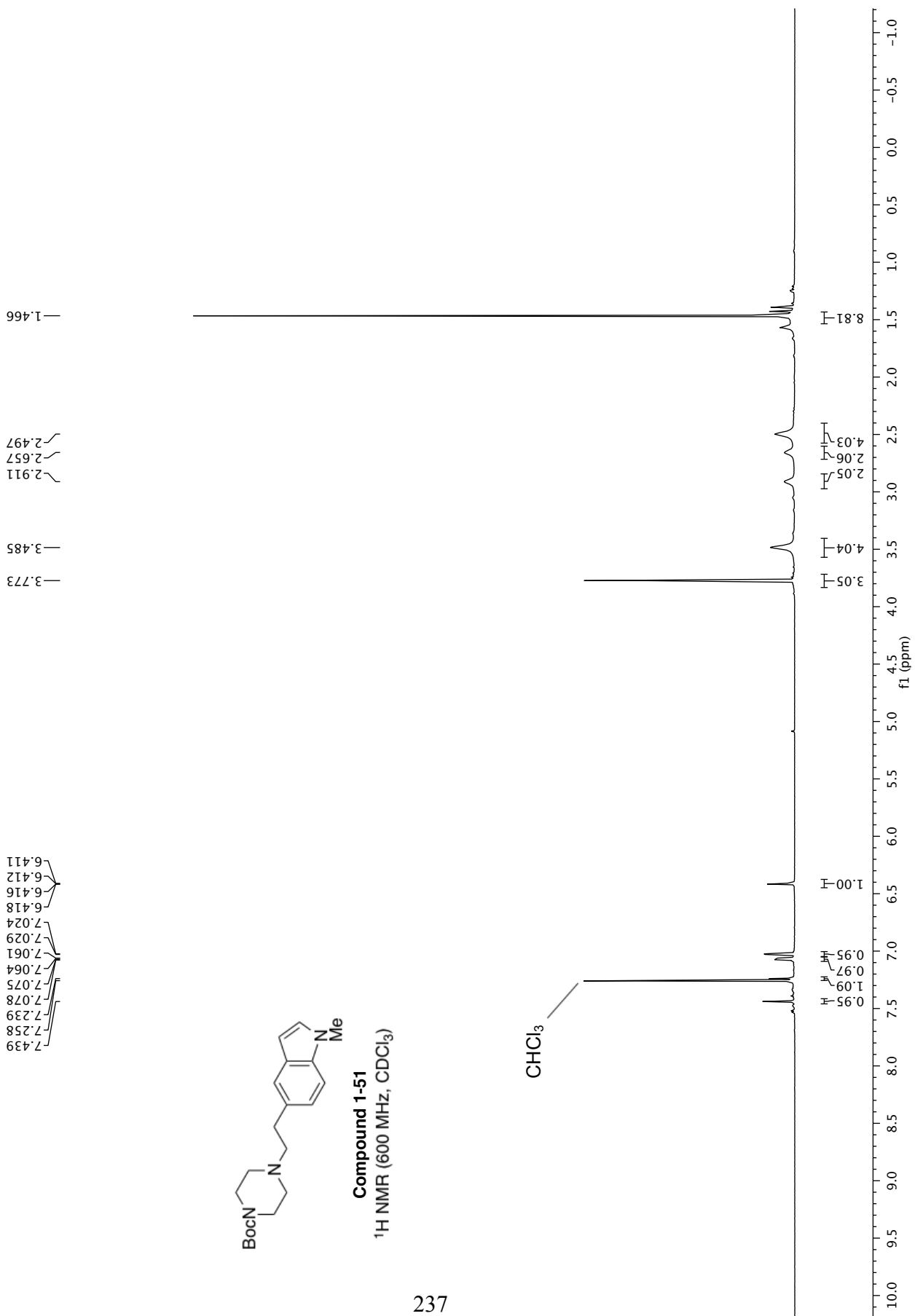
7.439
7.258
7.239
7.078
7.075
7.064
7.061
7.029
7.024
6.418
6.416
6.412
6.411

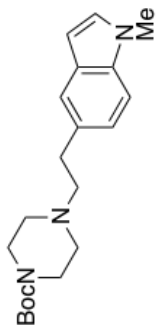
3.773
3.485

2.911
2.657
2.497

1.466

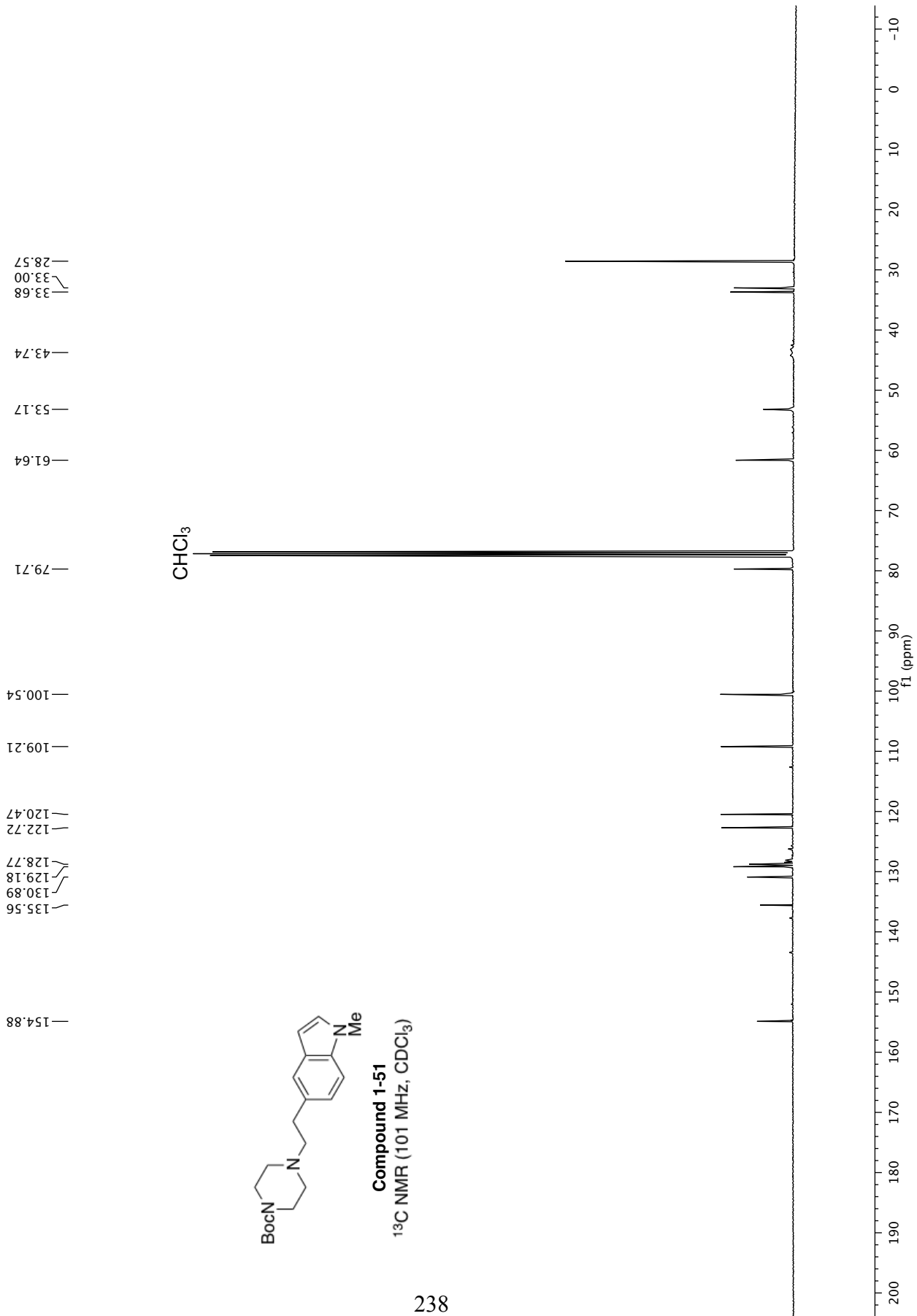
CHCl₃

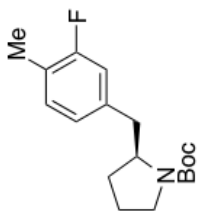




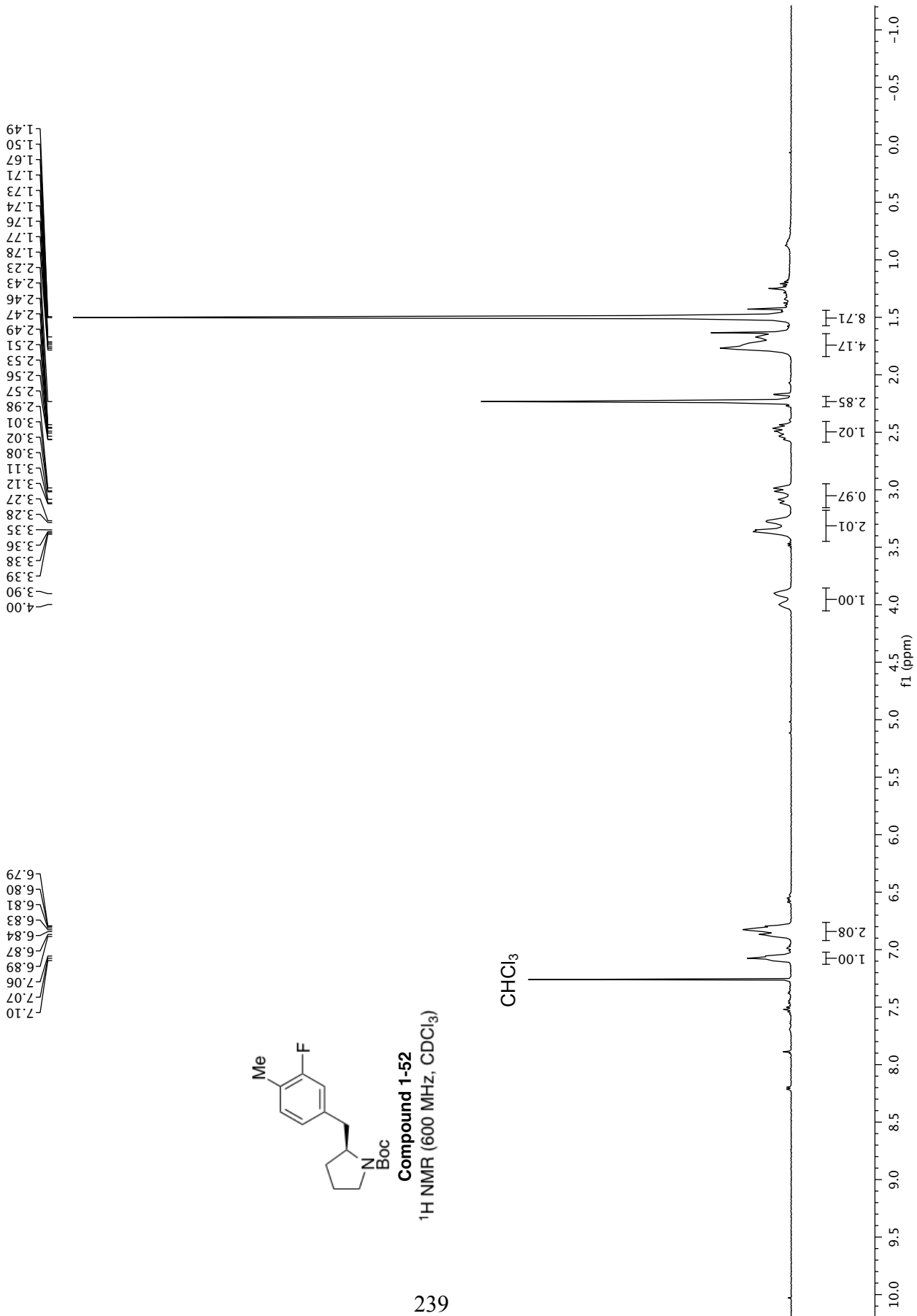
Compound 1-51

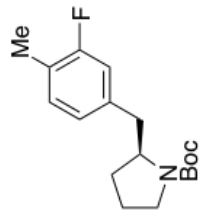
^{13}C NMR (101 MHz, CDCl_3)



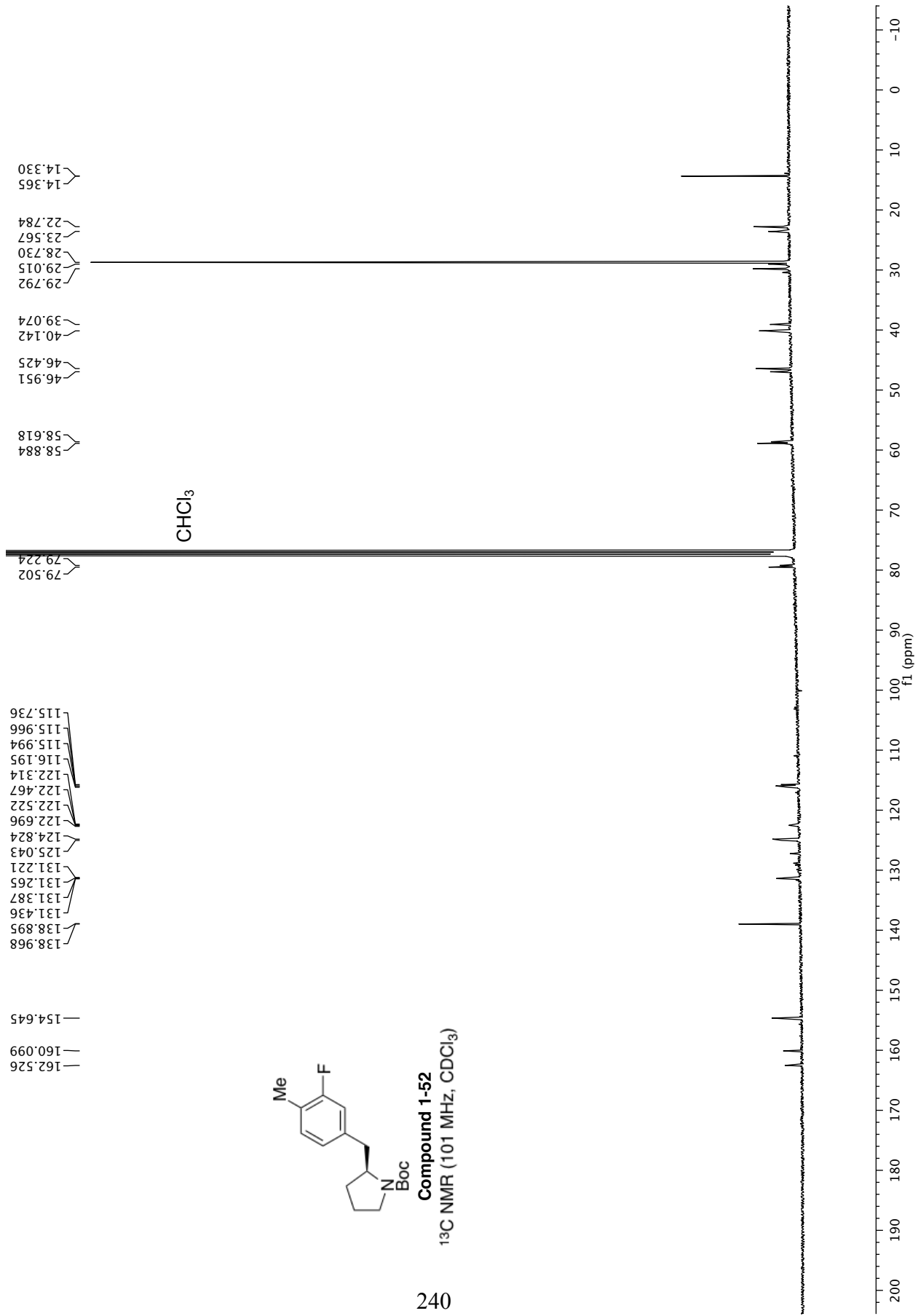


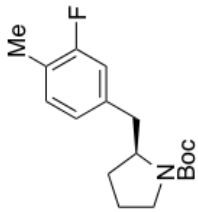
Compound 1-52
¹H NMR (600 MHz, CDCl₃)





Compound 1-52
¹³C NMR (101 MHz, CDCl₃)



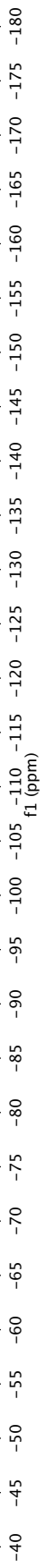


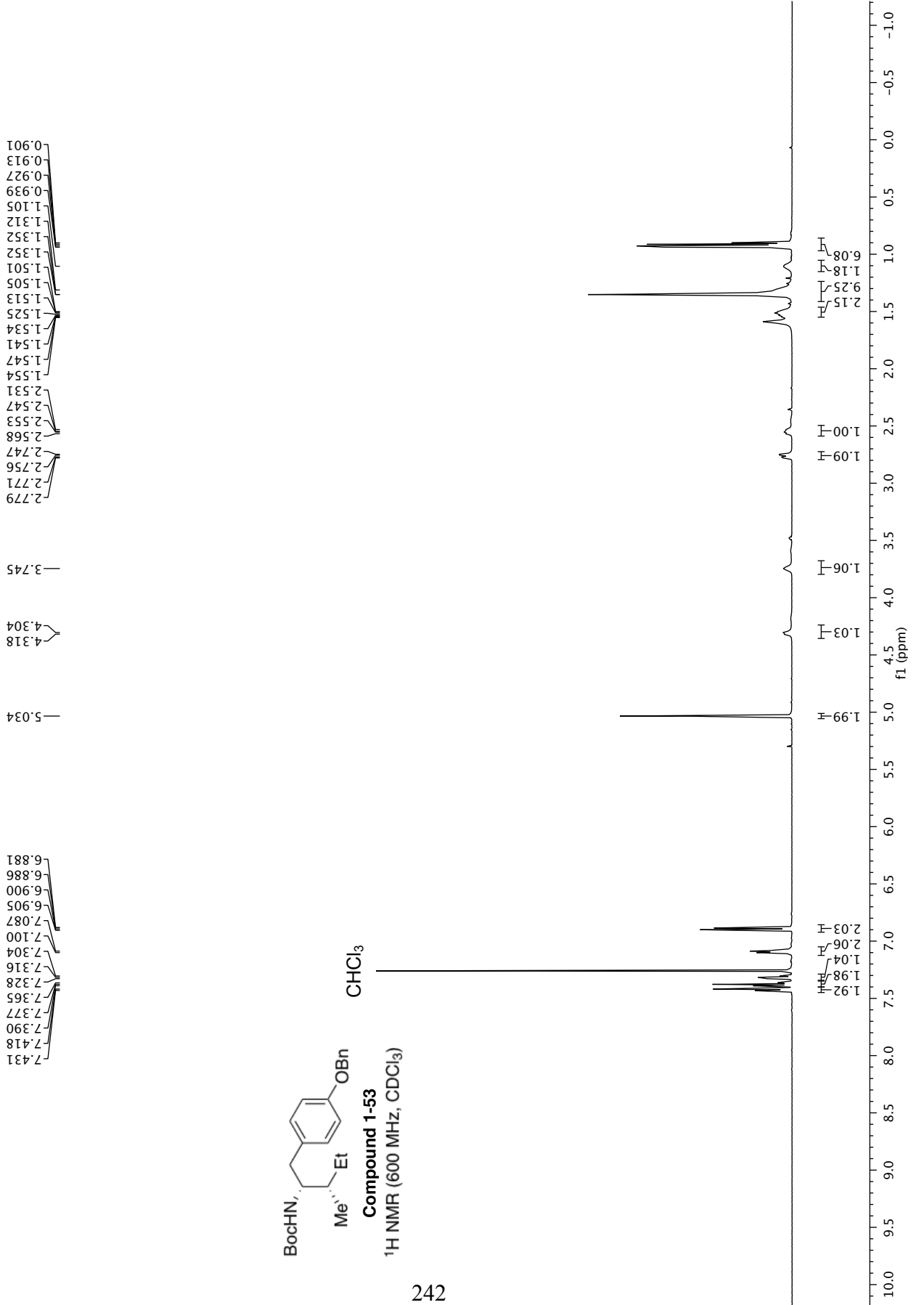
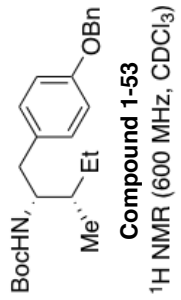
Compound 1-52

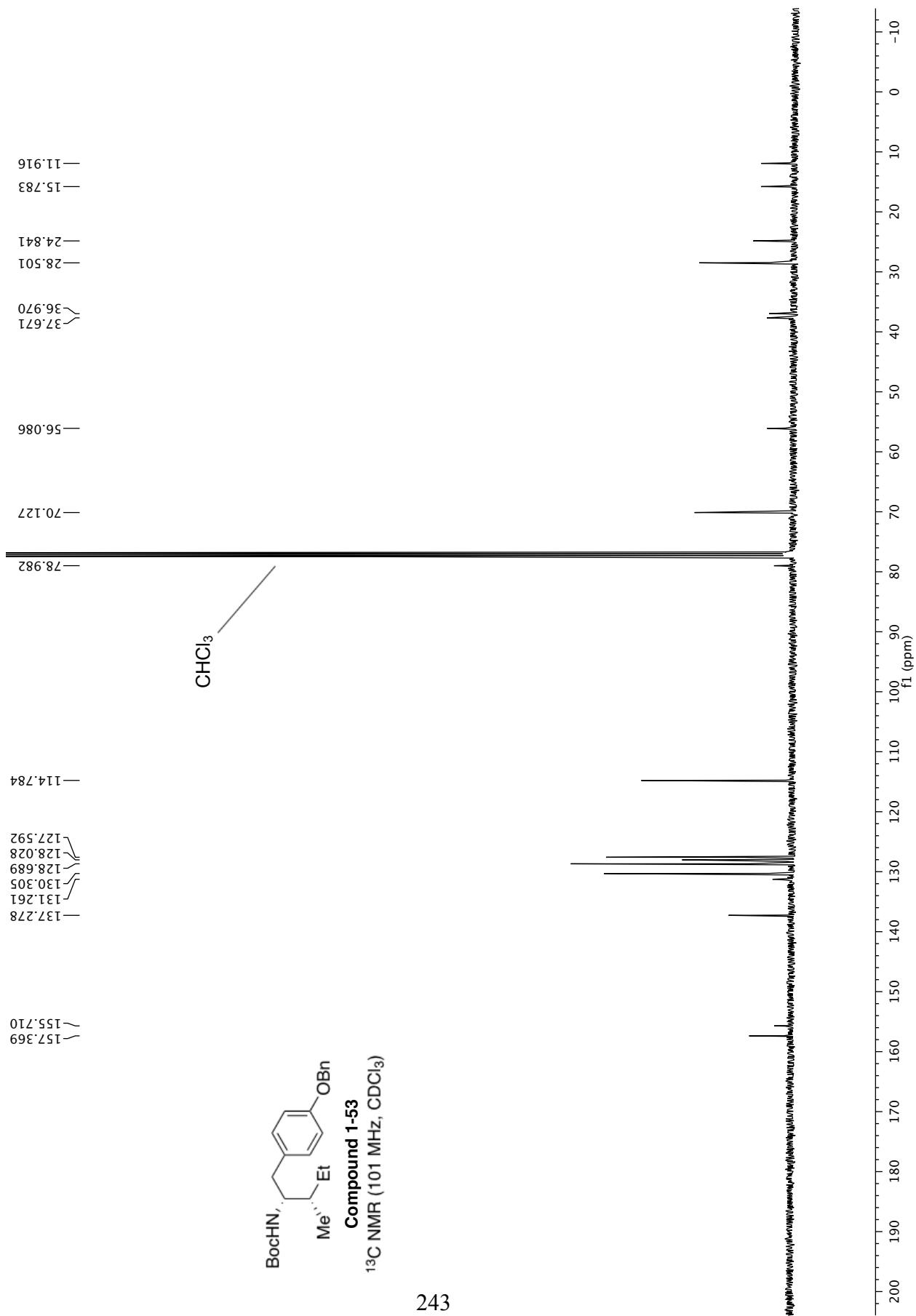
¹⁹F NMR (565 MHz, CDCl₃)

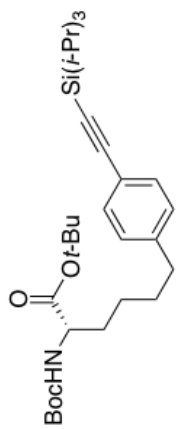
-117.98
-118.39

0.73
1.00
0.04



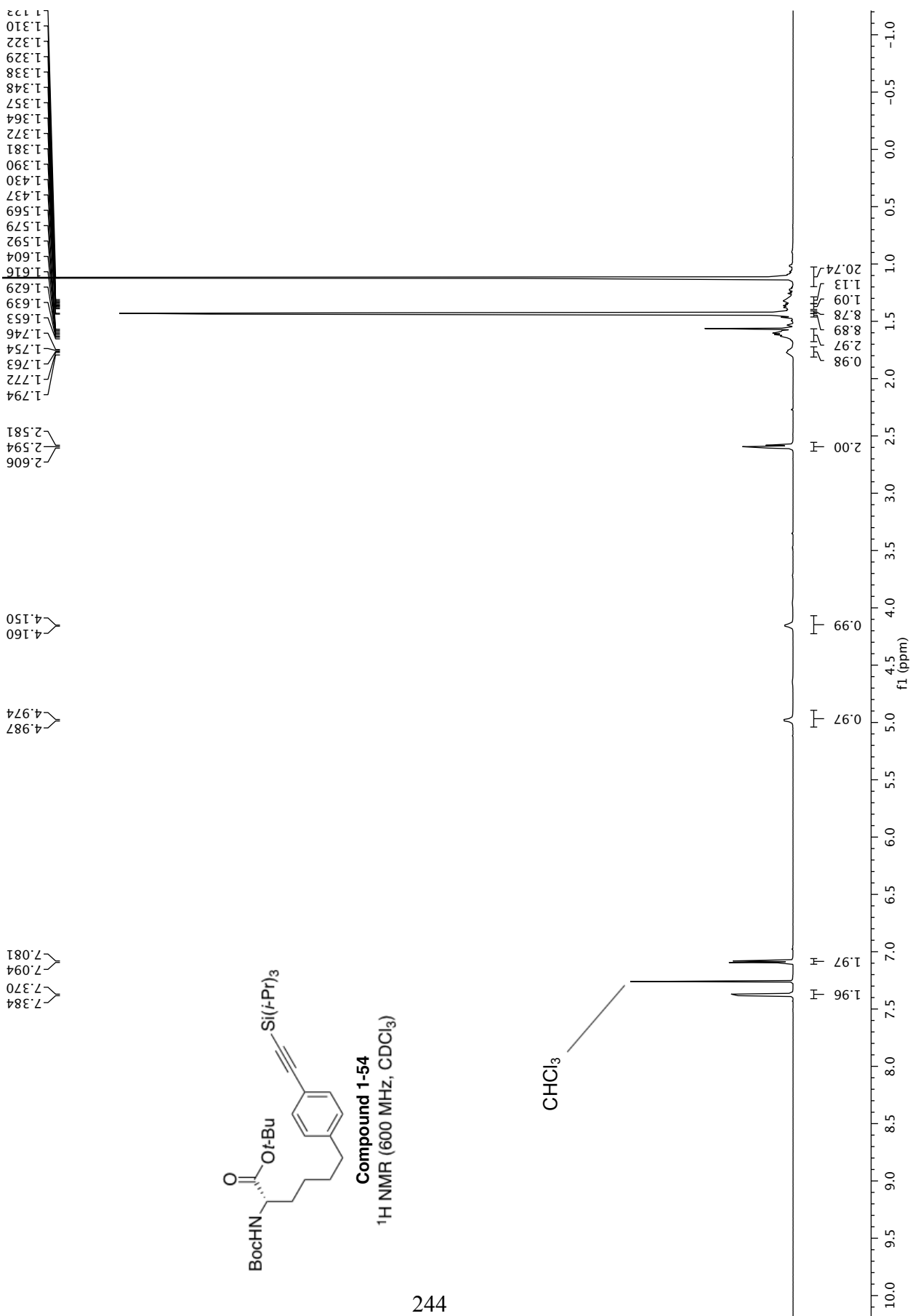


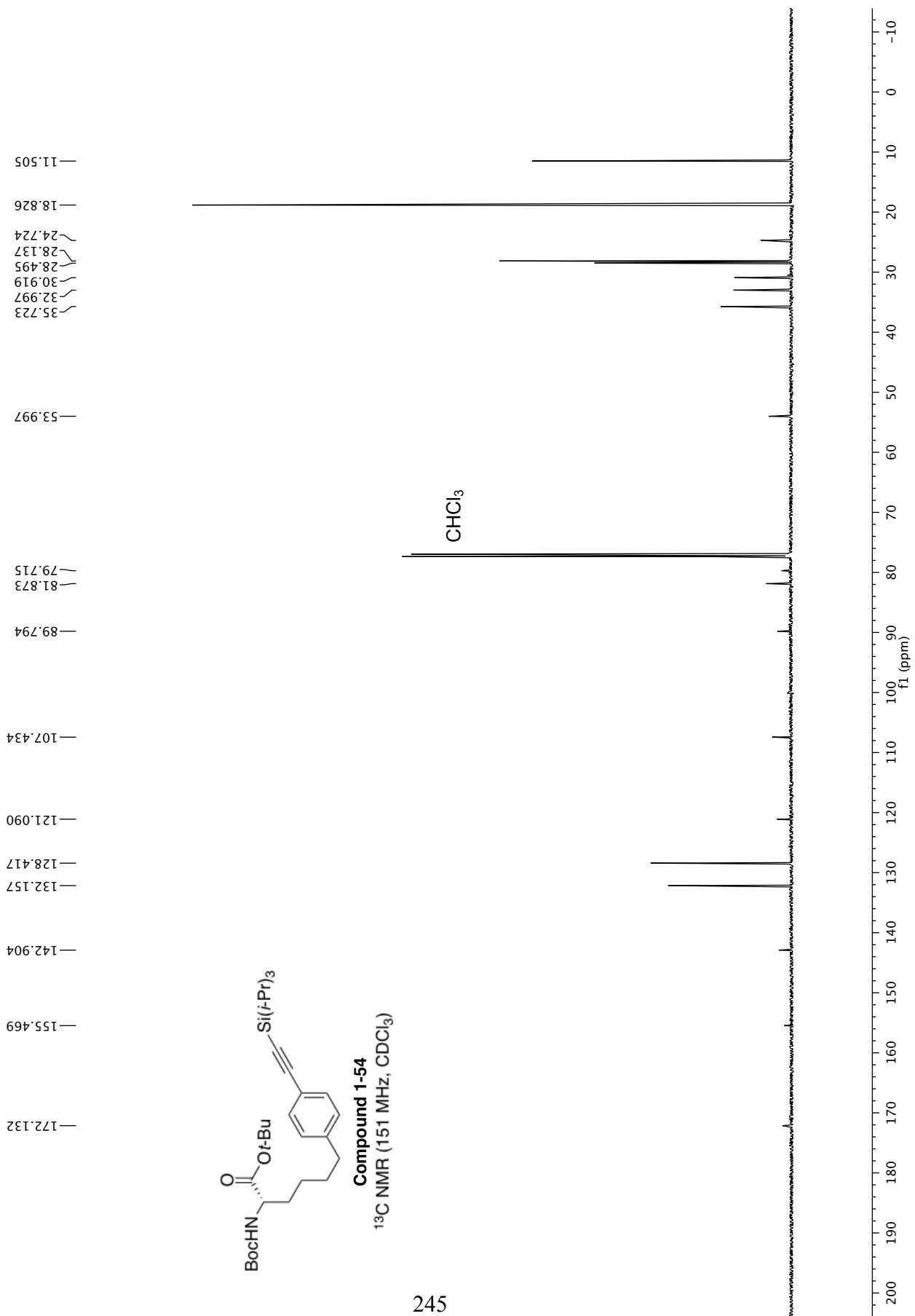




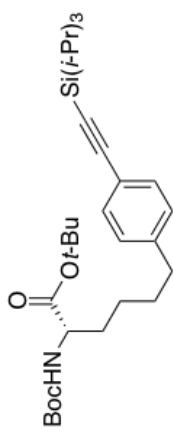
Compound 1-54

¹H NMR (600 MHz, CDCl₃)





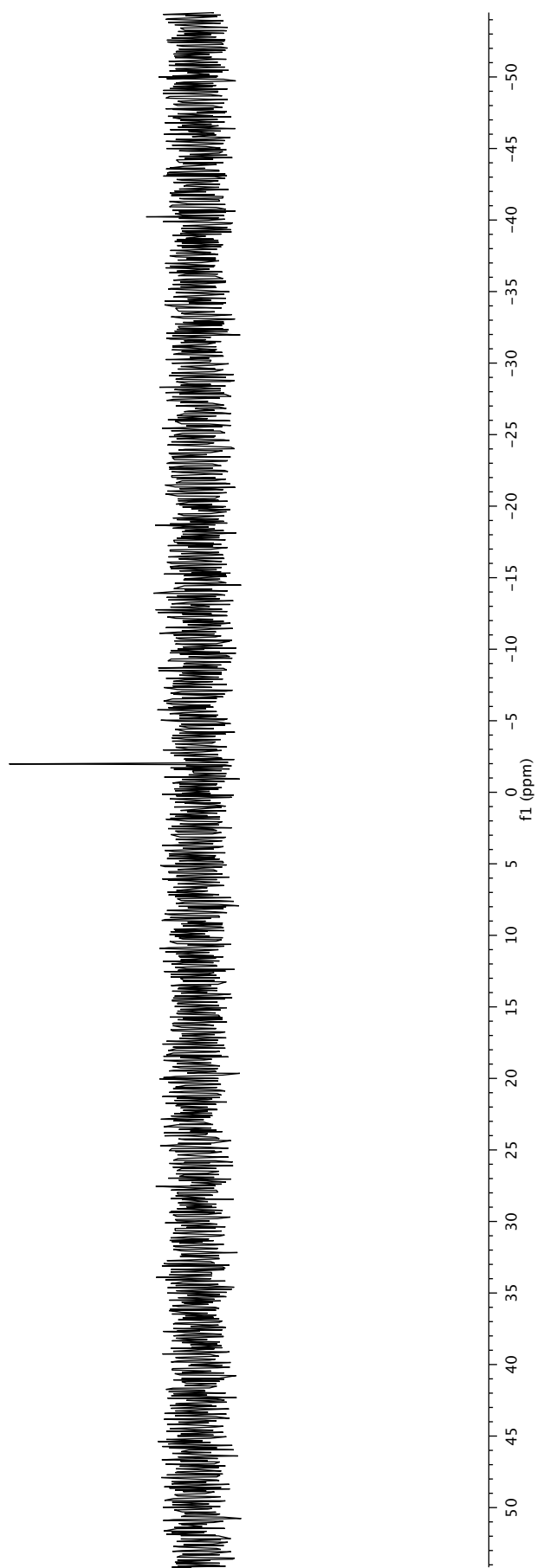
—1.983

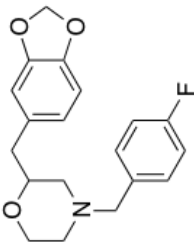


Compound 1-54

²⁹Si NMR (119 MHz, CDCl₃)

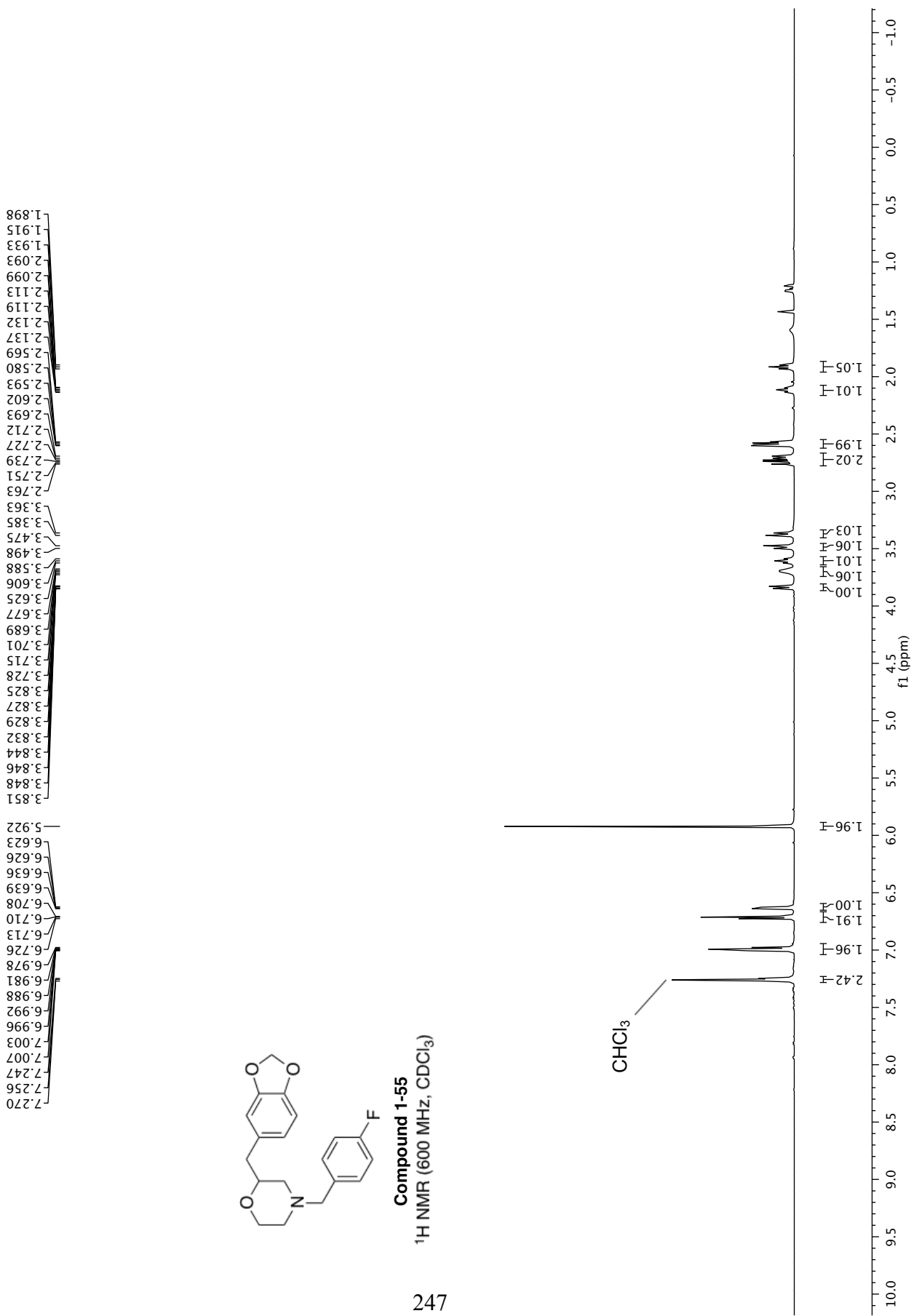
246

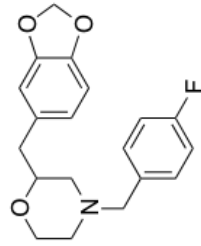




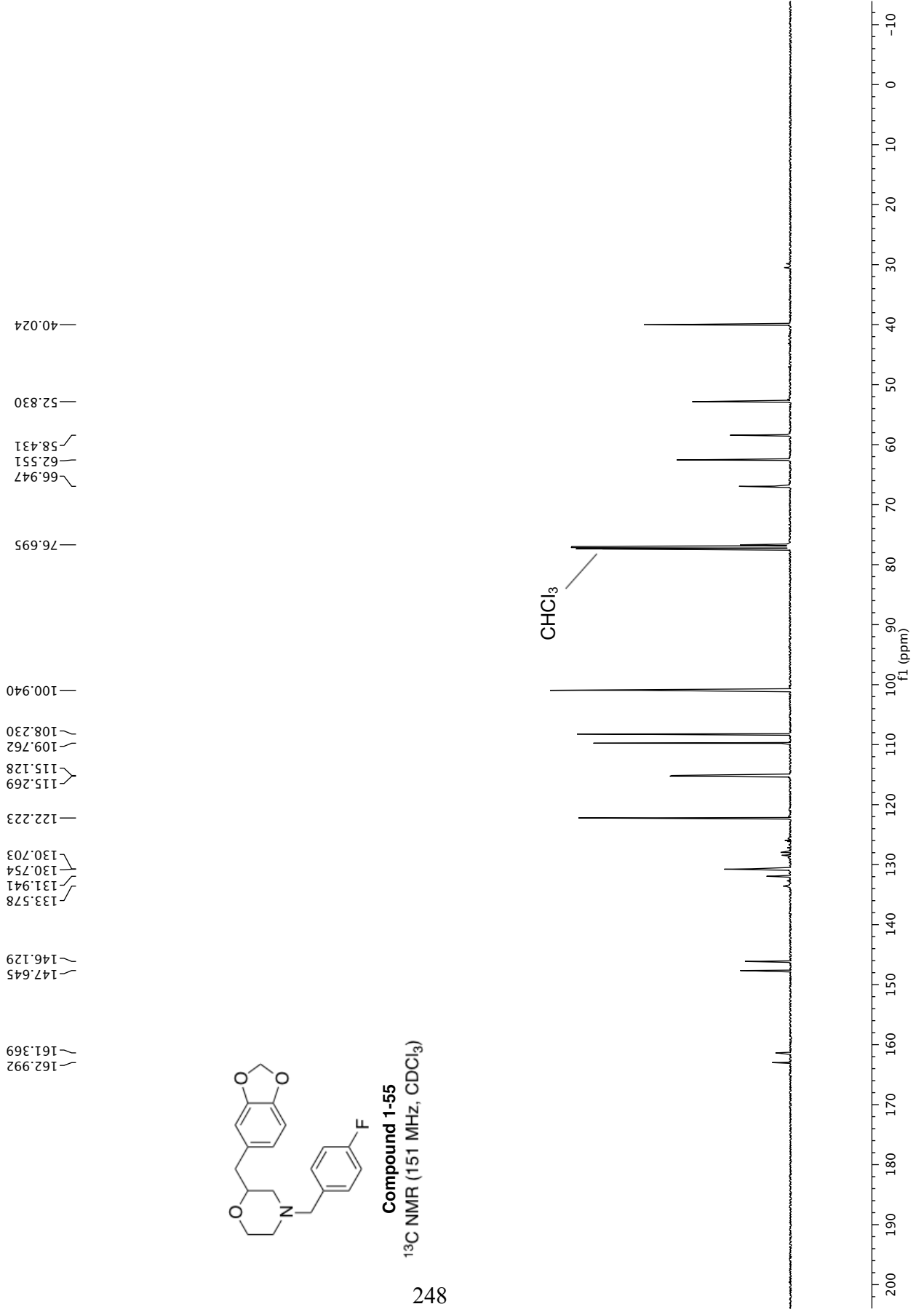
Compound 1-55
¹H NMR (600 MHz, CDCl₃)

247

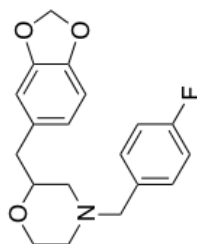




Compound 1-55
 ^{13}C NMR (151 MHz, CDCl_3)

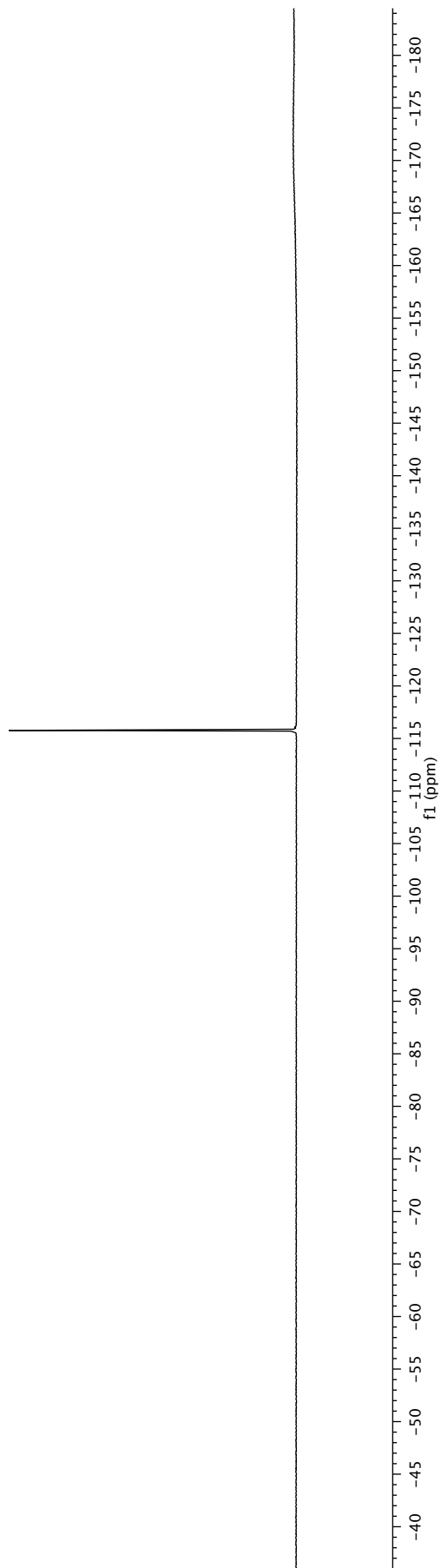


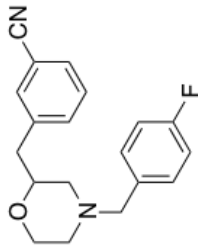
—115.769



Compound 1-55

¹⁹F NMR (565 MHz, CDCl₃)

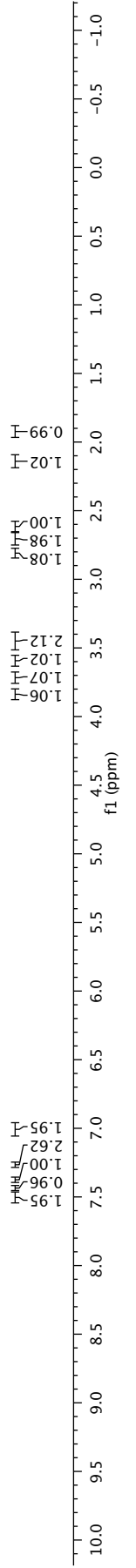


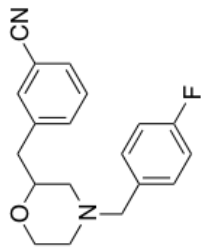


Compound 1-56
¹H NMR (600 MHz, CDCl₃)

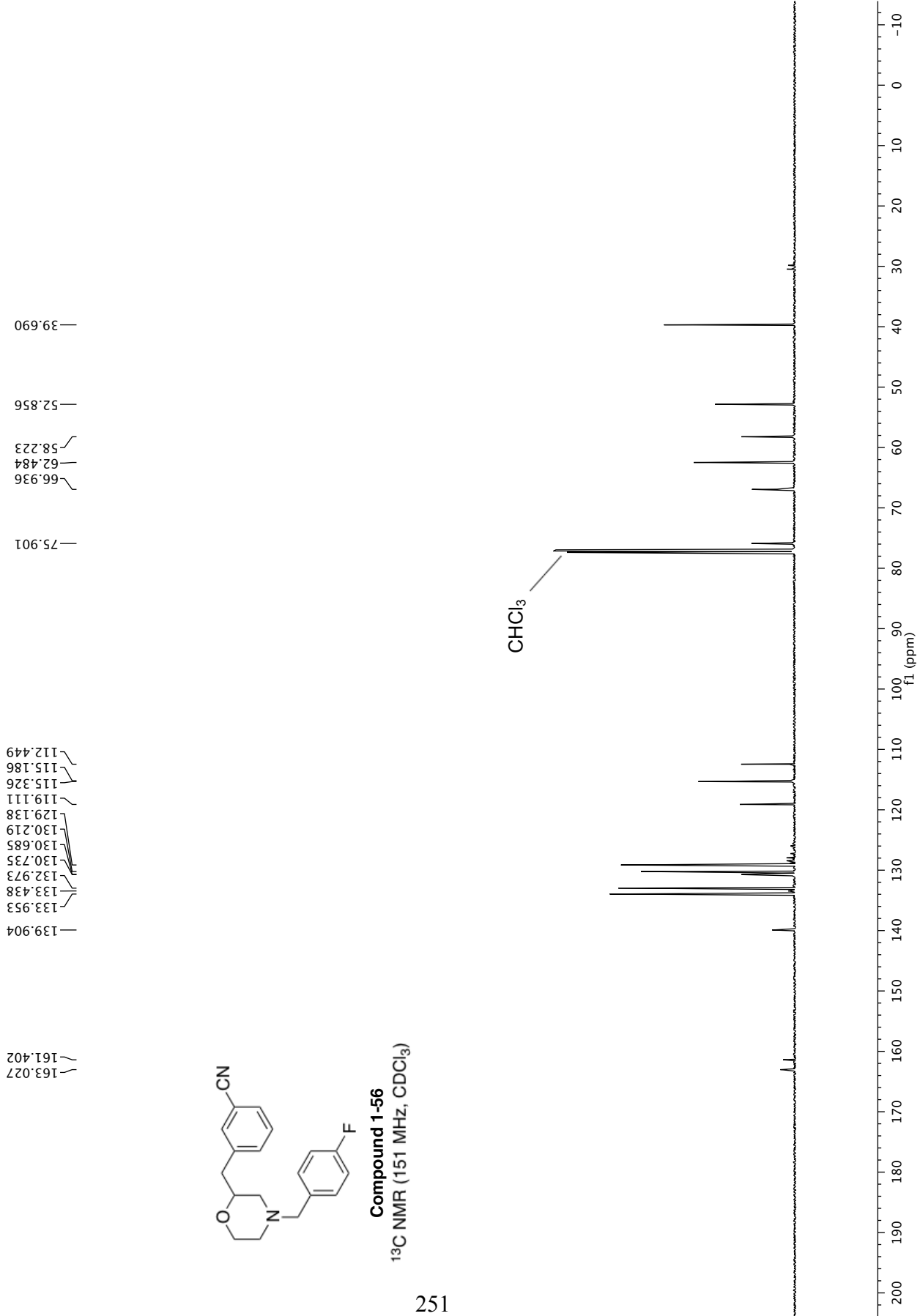
7.513
7.511
7.501
7.499
7.497
7.444
7.441
7.439
7.431
7.428
7.426
7.388
7.386
7.375
7.373
7.364
7.362
7.278
7.267
7.260
7.254
7.017
7.013
7.002
6.991
6.988
3.842
3.840
3.823
3.821
3.718
3.605
3.587
3.568
3.476
3.453
3.434
3.412
2.822
2.809
2.799
2.785
2.717
2.709
2.703
2.693
2.685
2.626
2.608
2.157
2.138
2.120
1.938
1.920
1.903

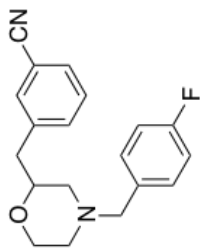
CHCl₃





Compound 1-56
 ^{13}C NMR (151 MHz, CDCl_3)

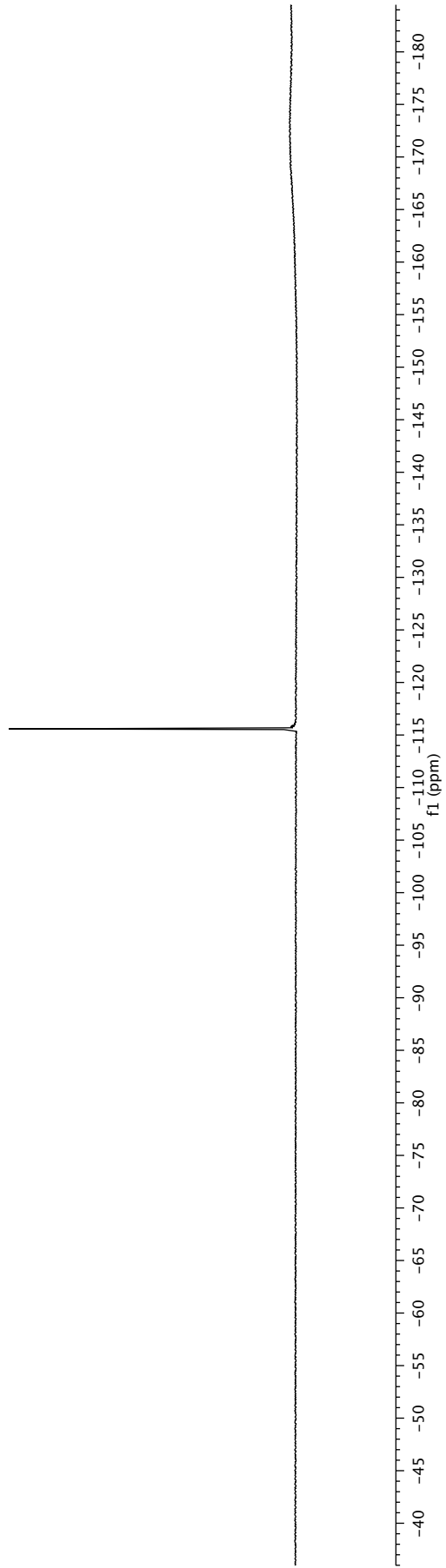


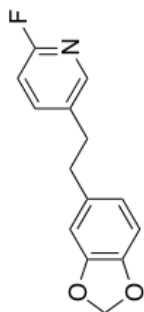


Compound 1-56
¹⁹F NMR (565 MHz, CDCl₃)

252

—115.578

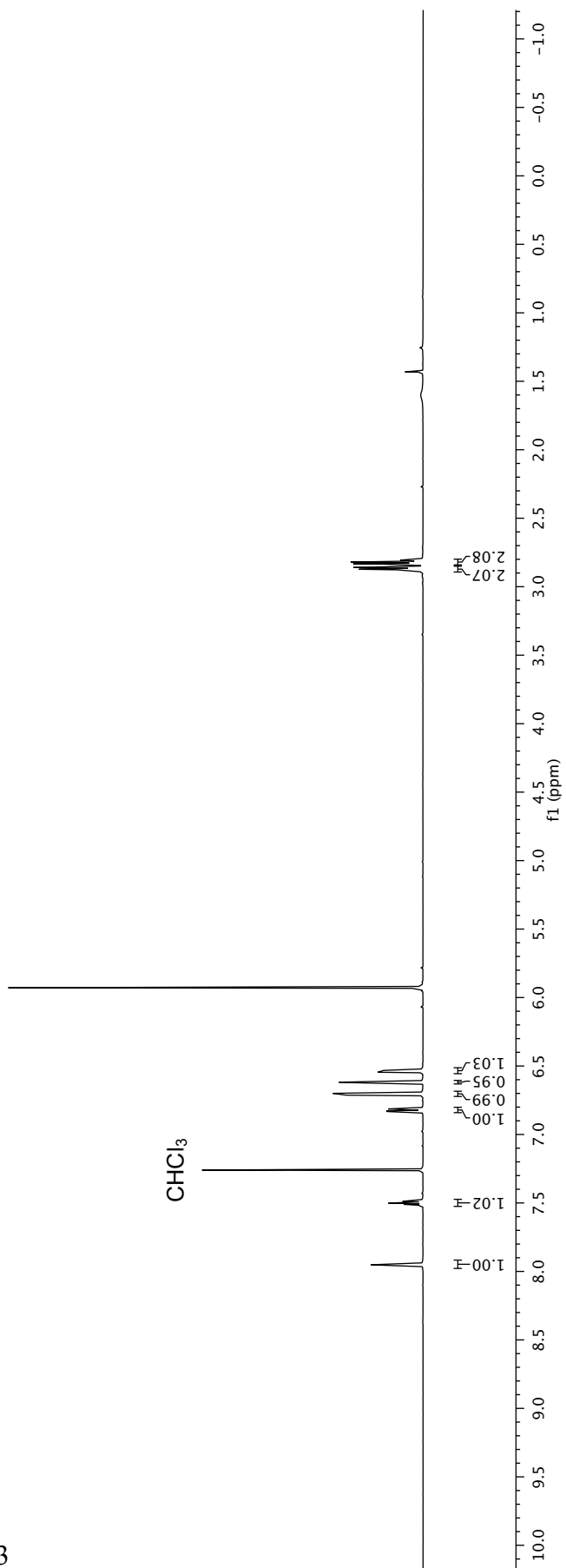


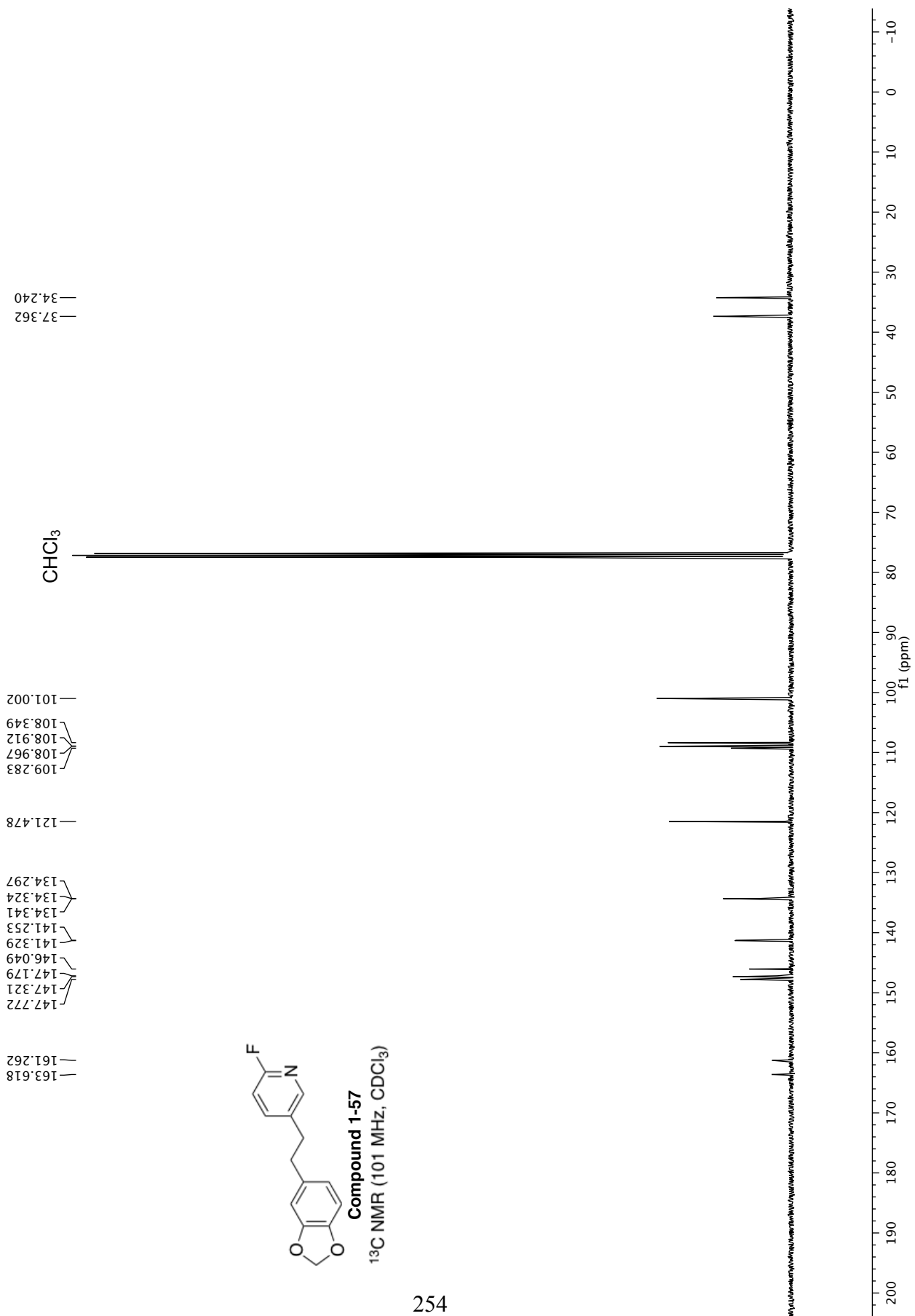


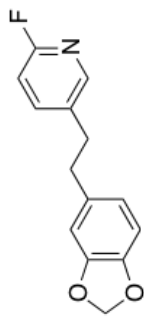
Compound 1-57
¹H NMR (600 MHz, CDCl₃)

7.955
7.952
7.515
7.511
7.501
7.497
7.488
7.484
6.832
6.828
6.819
6.814
6.713
6.700
6.621
6.618
6.545
6.543
6.532
6.530
5.929

2.887
2.884
2.873
2.860
2.833
2.823
2.820
2.809
2.806

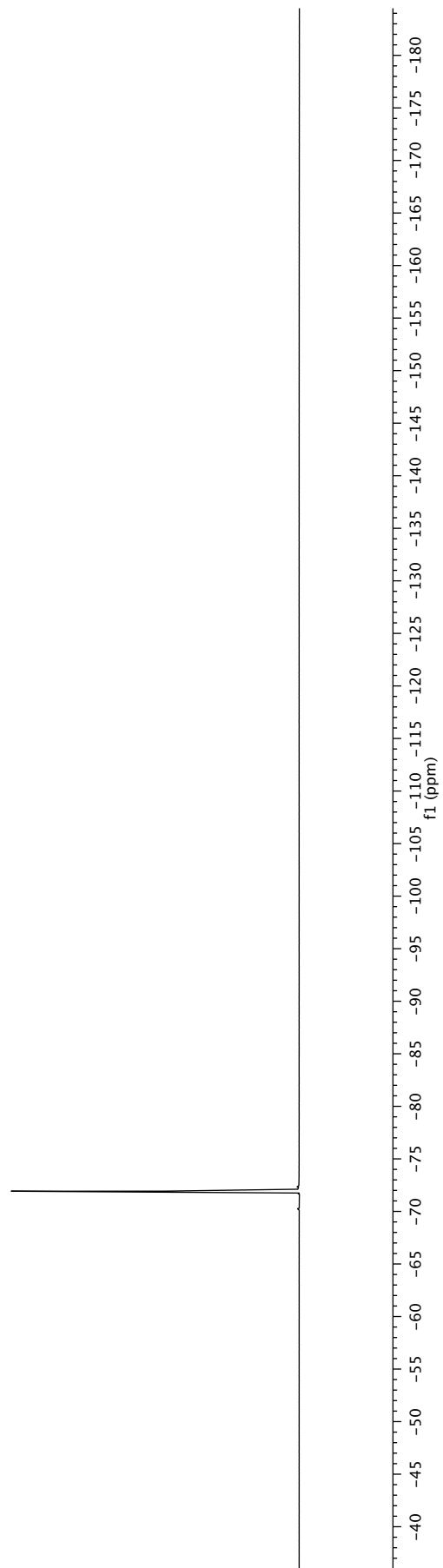


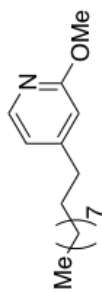




Compound 1-57
 ^{19}F NMR (376 MHz, CDCl_3)

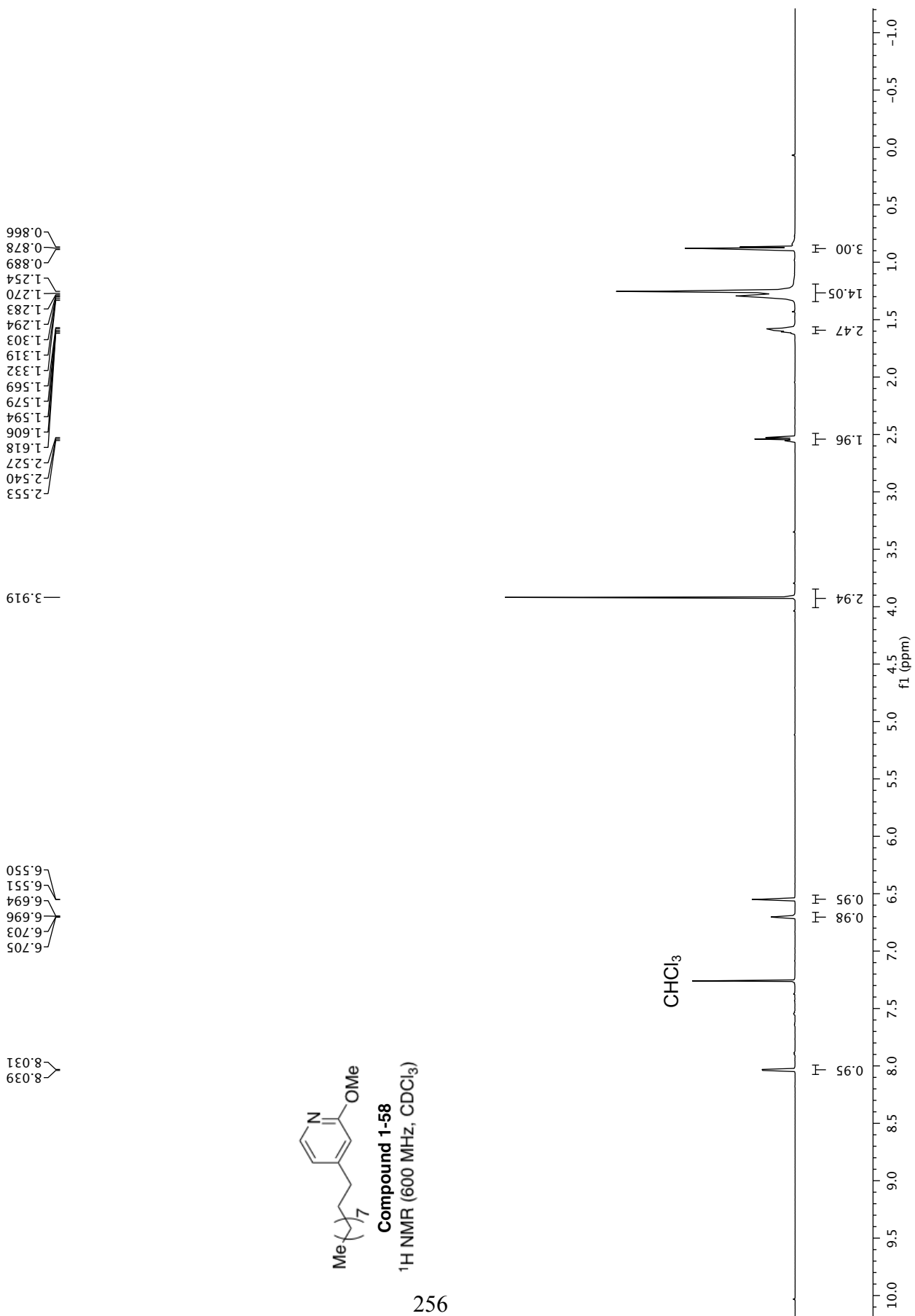
— -71.922

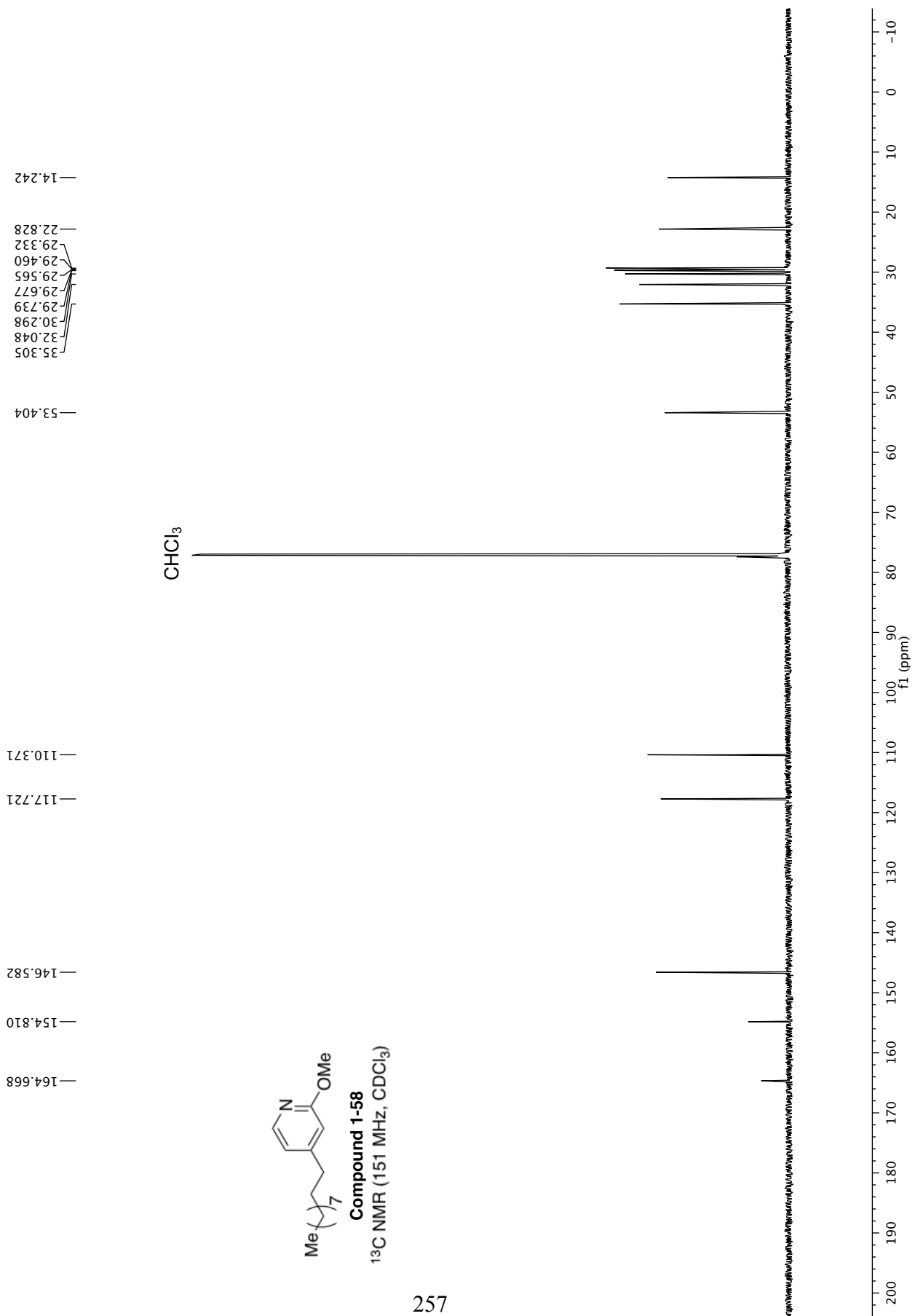


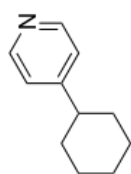


Compound 1-58

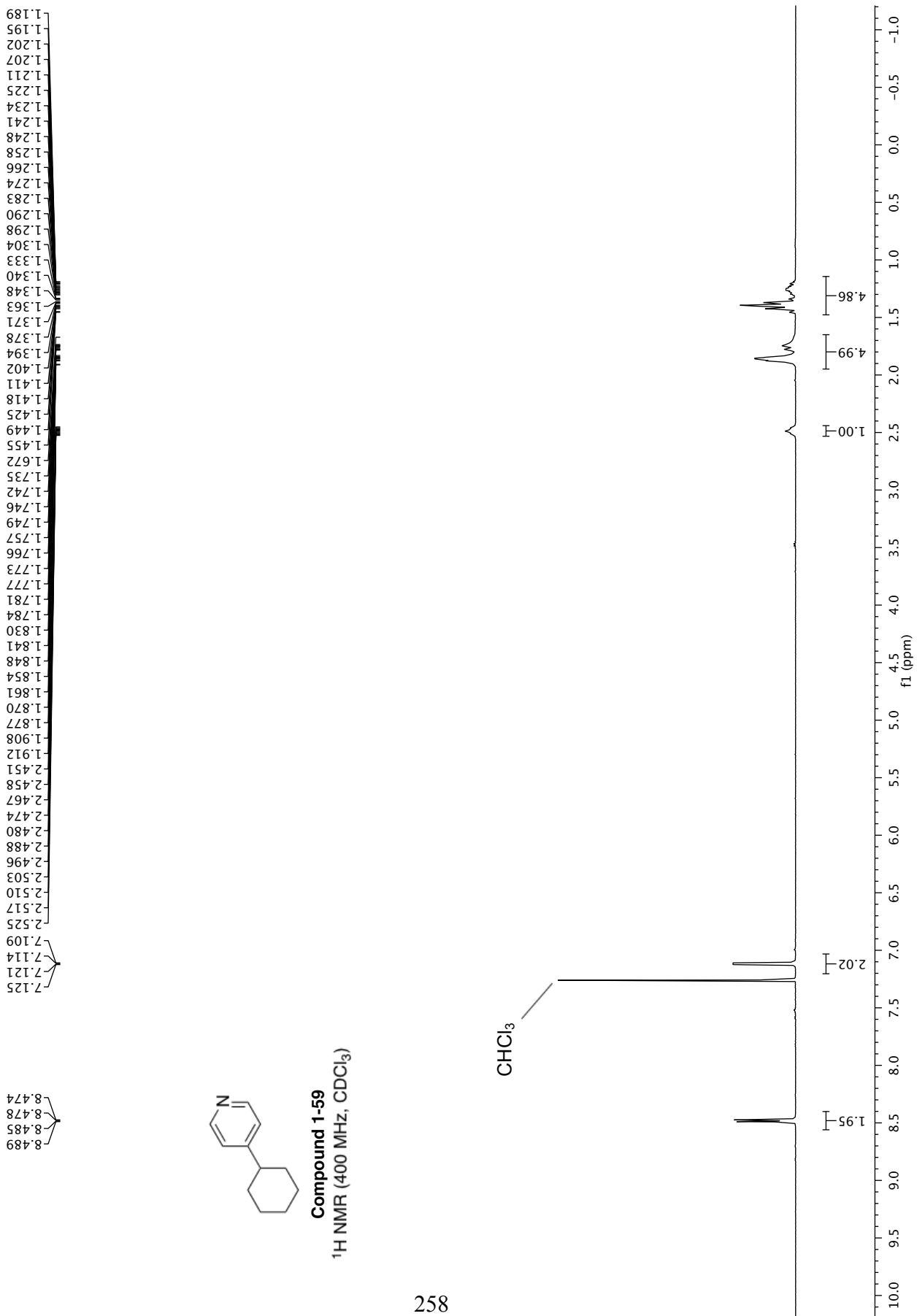
¹H NMR (600 MHz, CDCl₃)

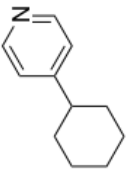




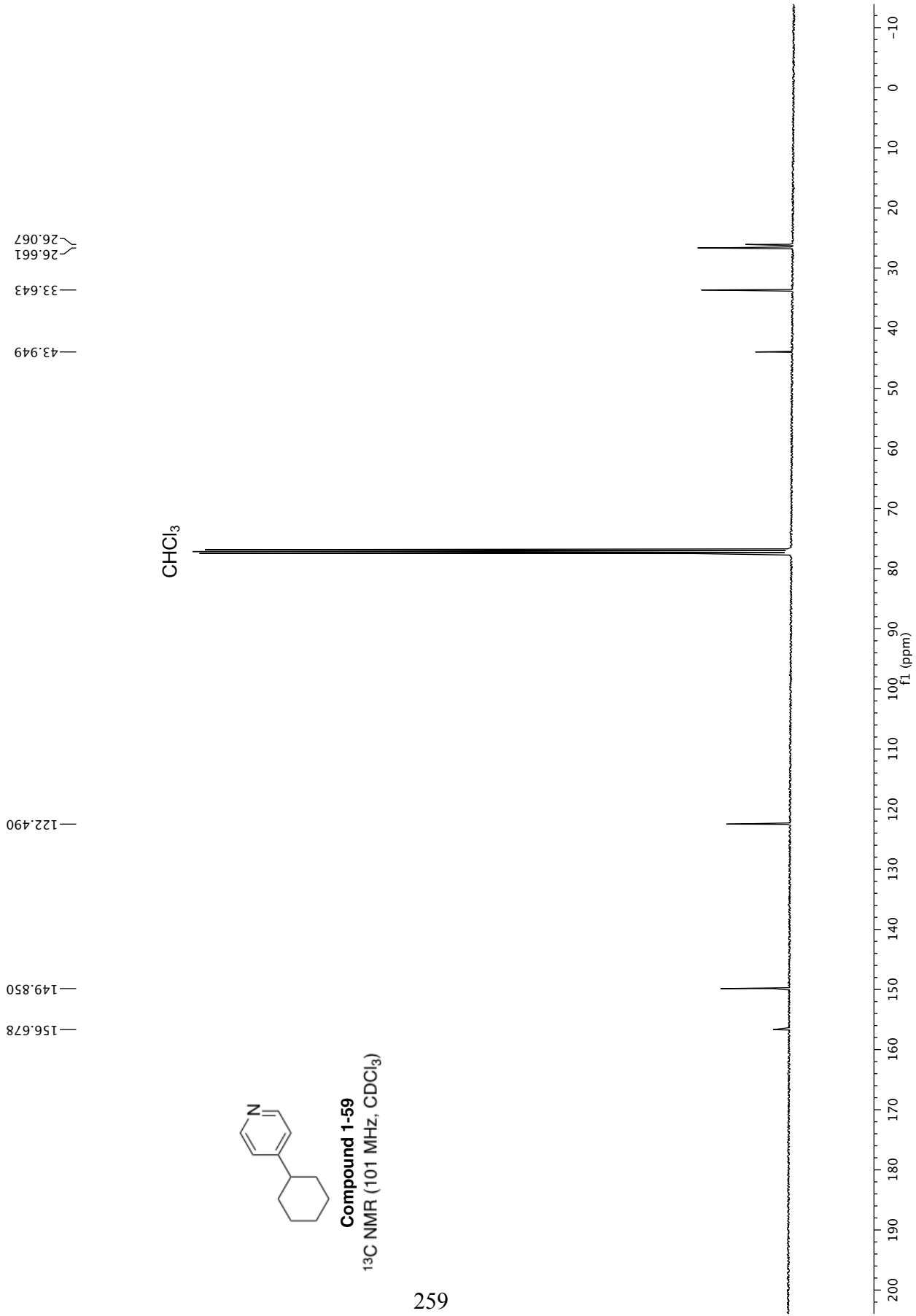


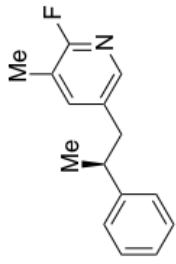
Compound 1-59
 $^1\text{H NMR}$ (400 MHz, CDCl_3)





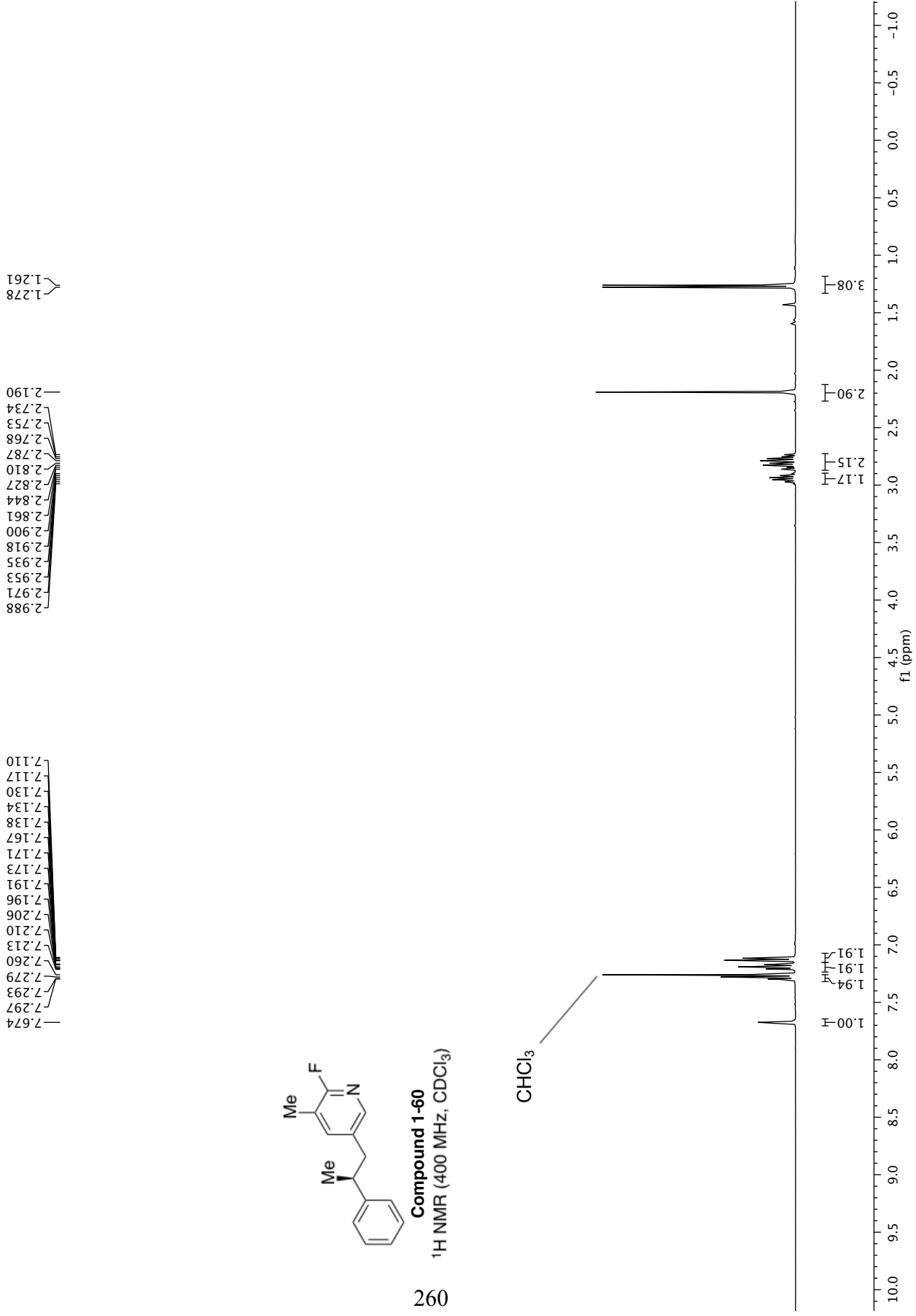
Compound 1-59
¹³C NMR (101 MHz, CDCl₃)

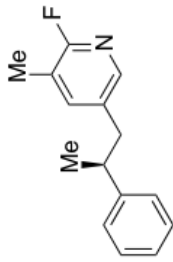




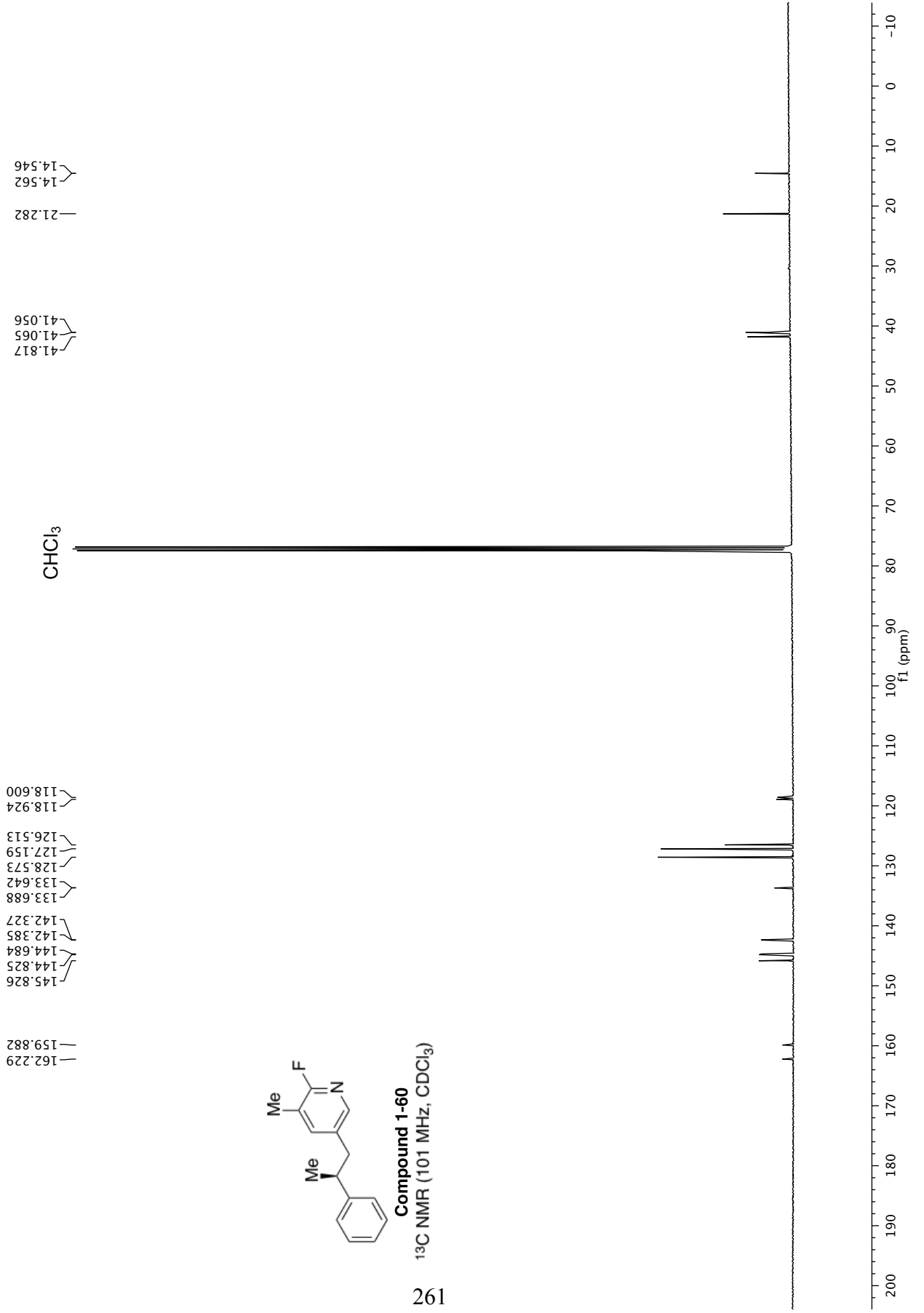
Compound 1-60
¹H NMR (400 MHz, CDCl₃)

260

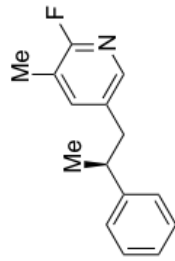




Compound 1-60
¹³C NMR (101 MHz, CDCl₃)

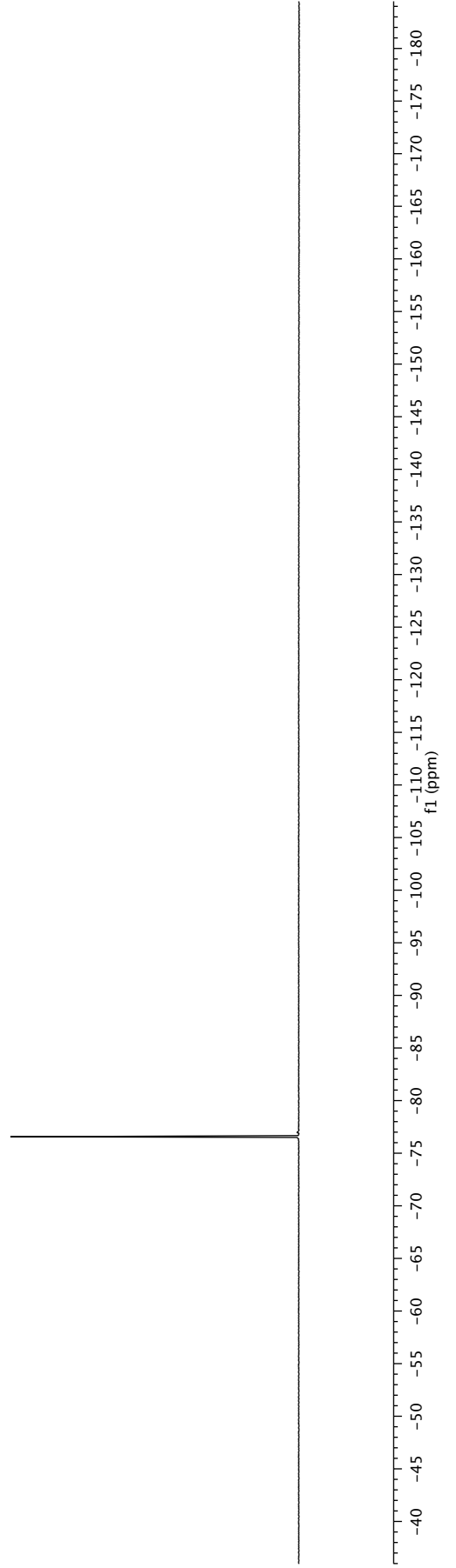


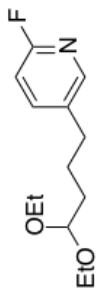
—76.561



Compound 1-60
¹⁹F NMR (376 MHz, CDCl₃)

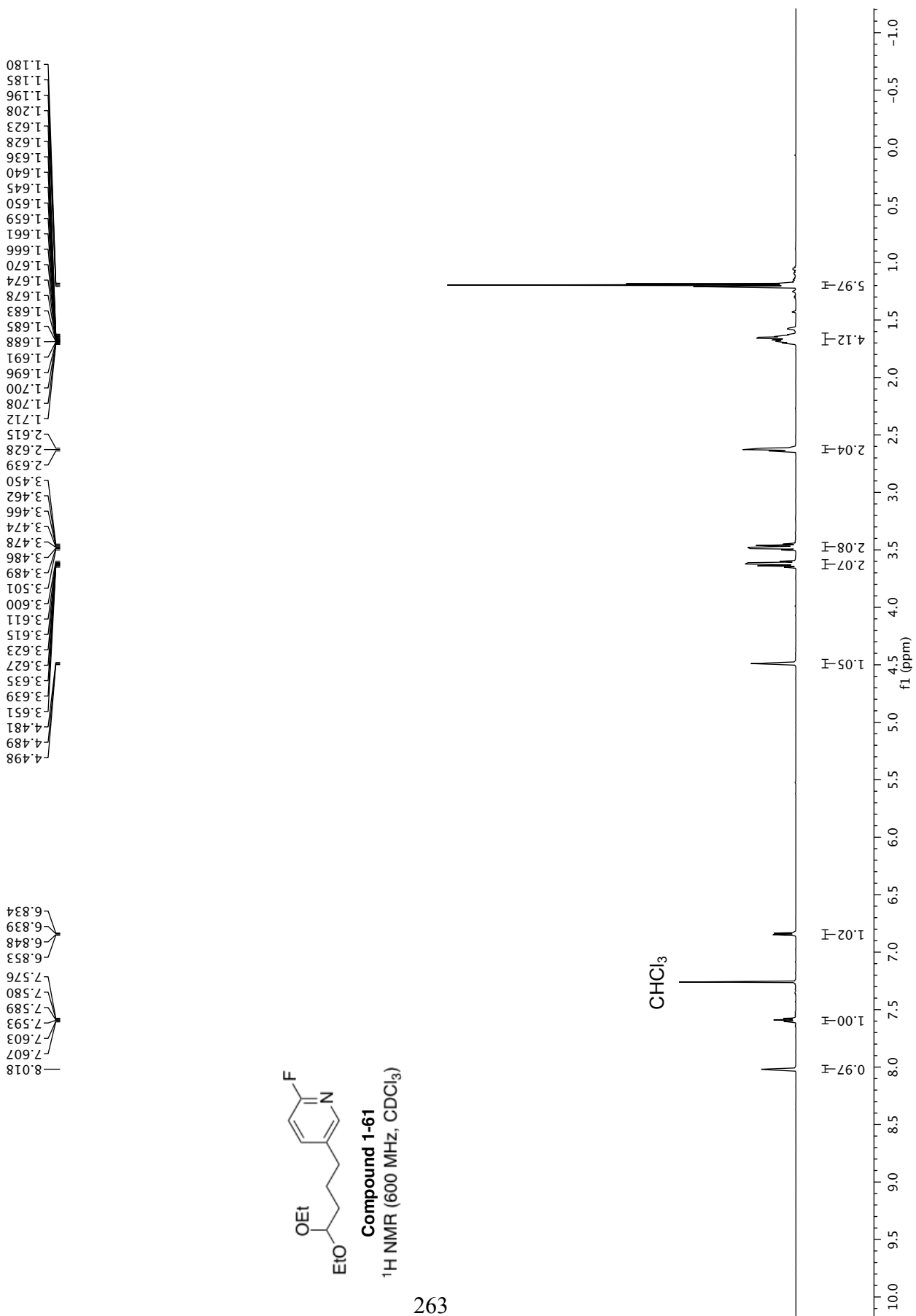
262

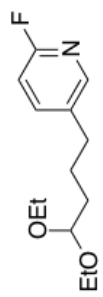




Compound 1-61

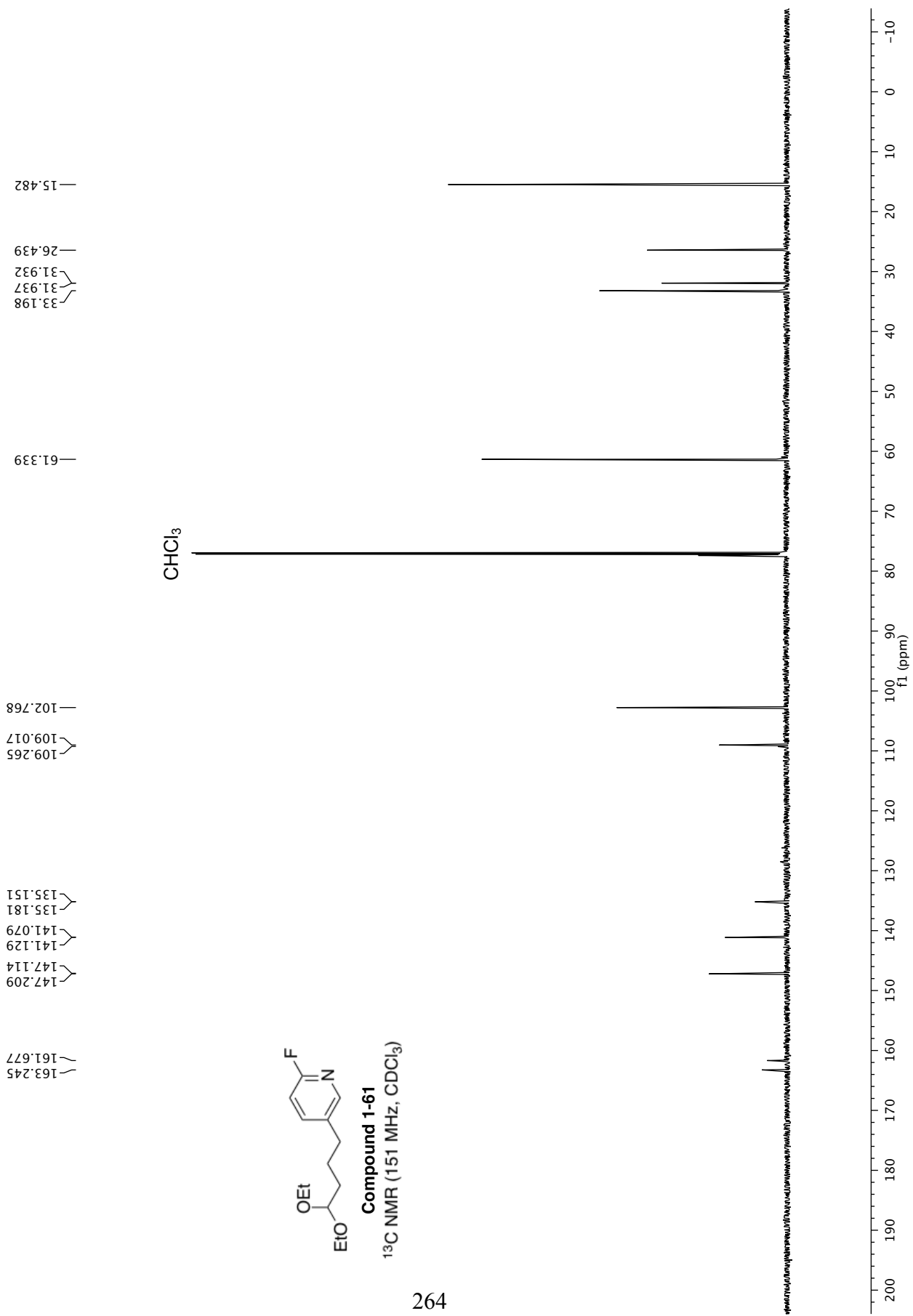
¹H NMR (600 MHz, CDCl₃)

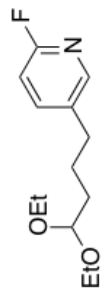




Compound 1-61

^{13}C NMR (151 MHz, CDCl_3)





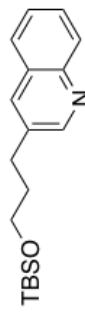
Compound 1-61
¹⁹F NMR (565 MHz, CDCl₃)

265

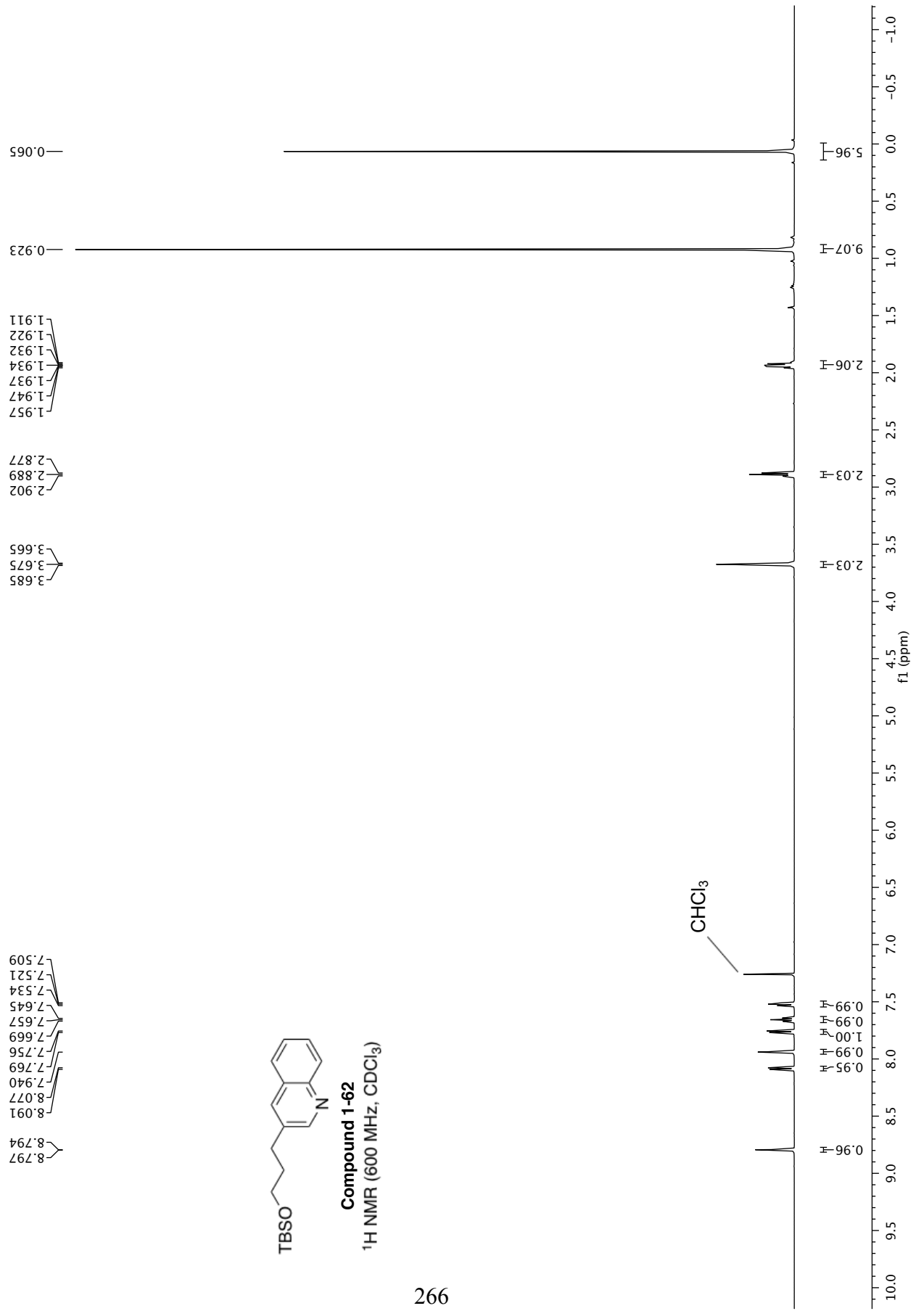
—72.271

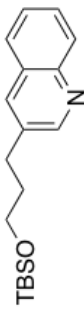


-40 -45 -50 -55 -60 -65 -70 -75 -80 -85 -90 -95 -100 -105 -110 -115 -120 -125 -130 -135 -140 -145 -150 -155 -160 -165 -170 -175 -180
f1 (ppm)



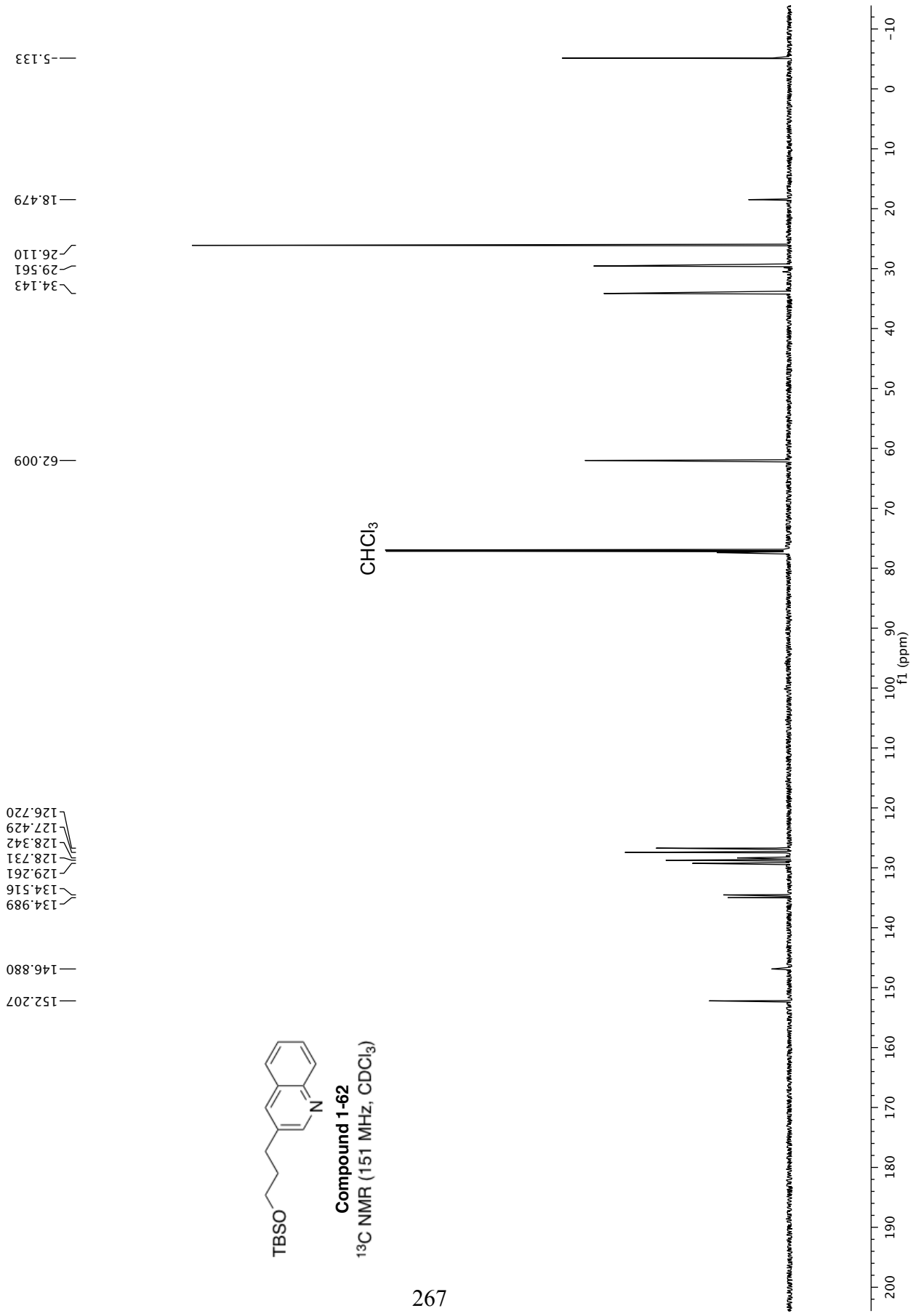
Compound 1-62
¹H NMR (600 MHz, CDCl₃)

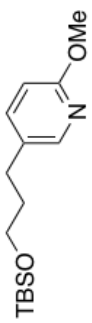




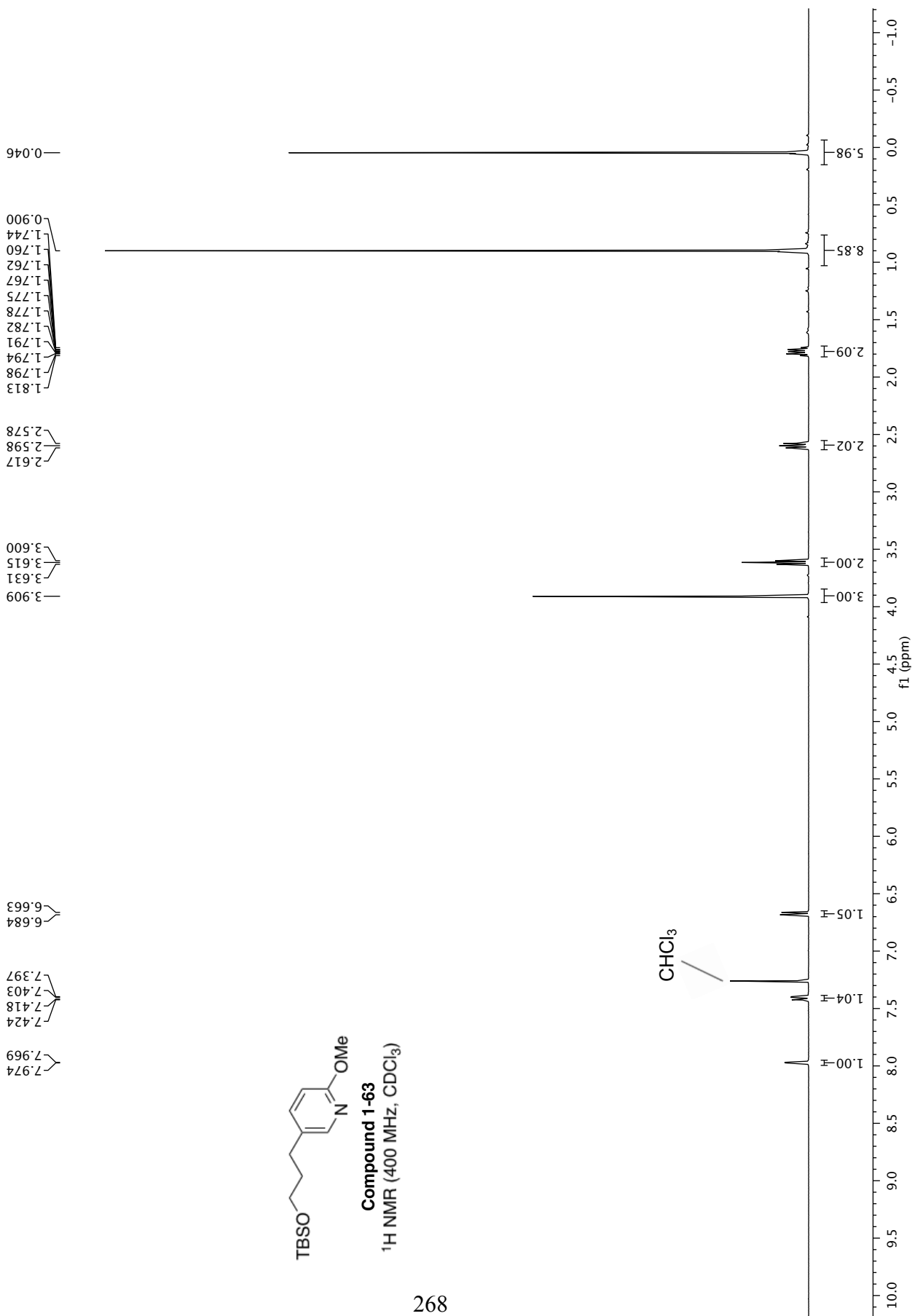
Compound 1-62

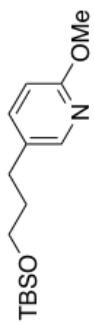
^{13}C NMR (151 MHz, CDCl_3)





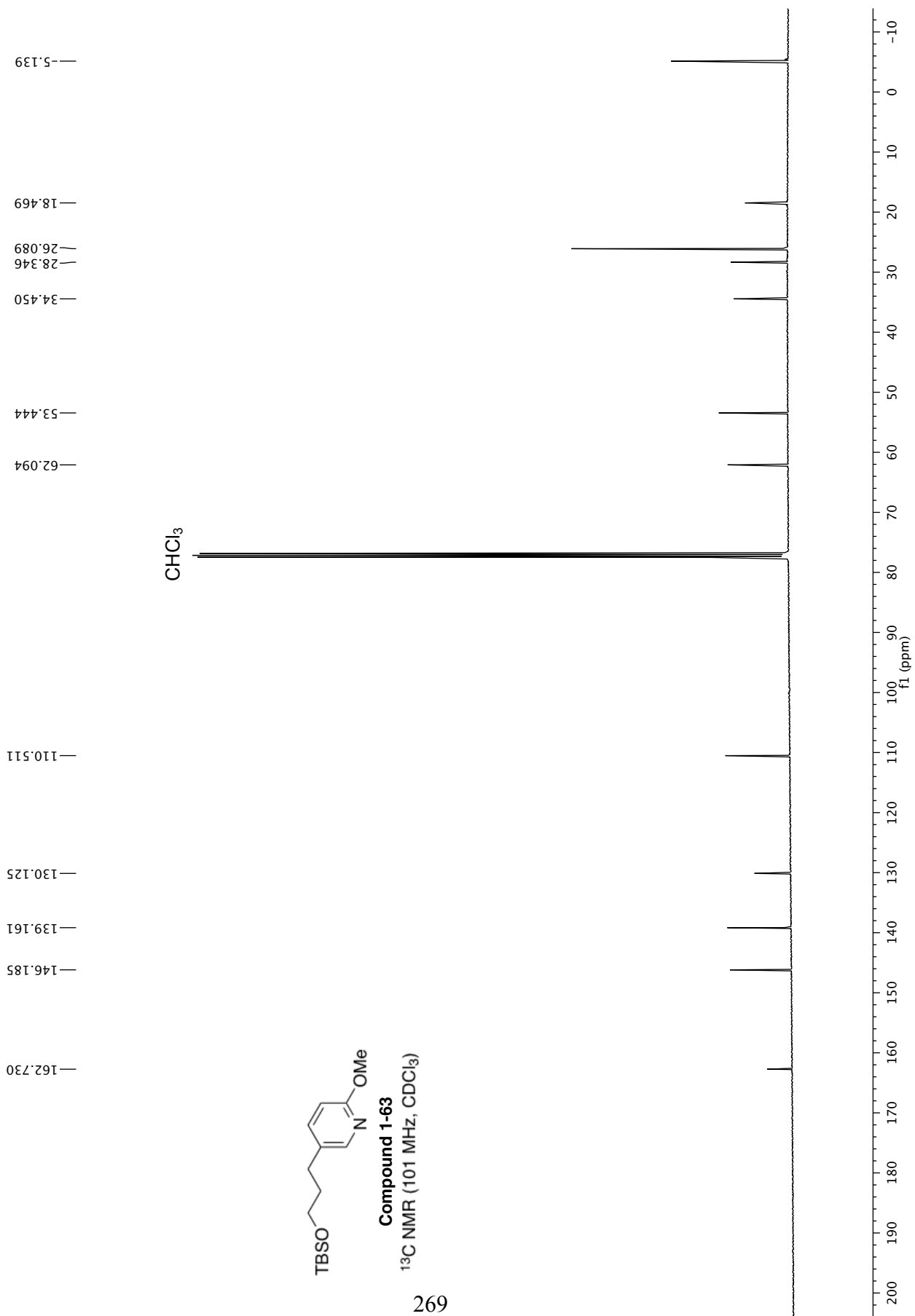
Compound 1-63
¹H NMR (400 MHz, CDCl₃)

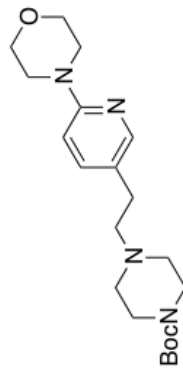




Compound 1-63

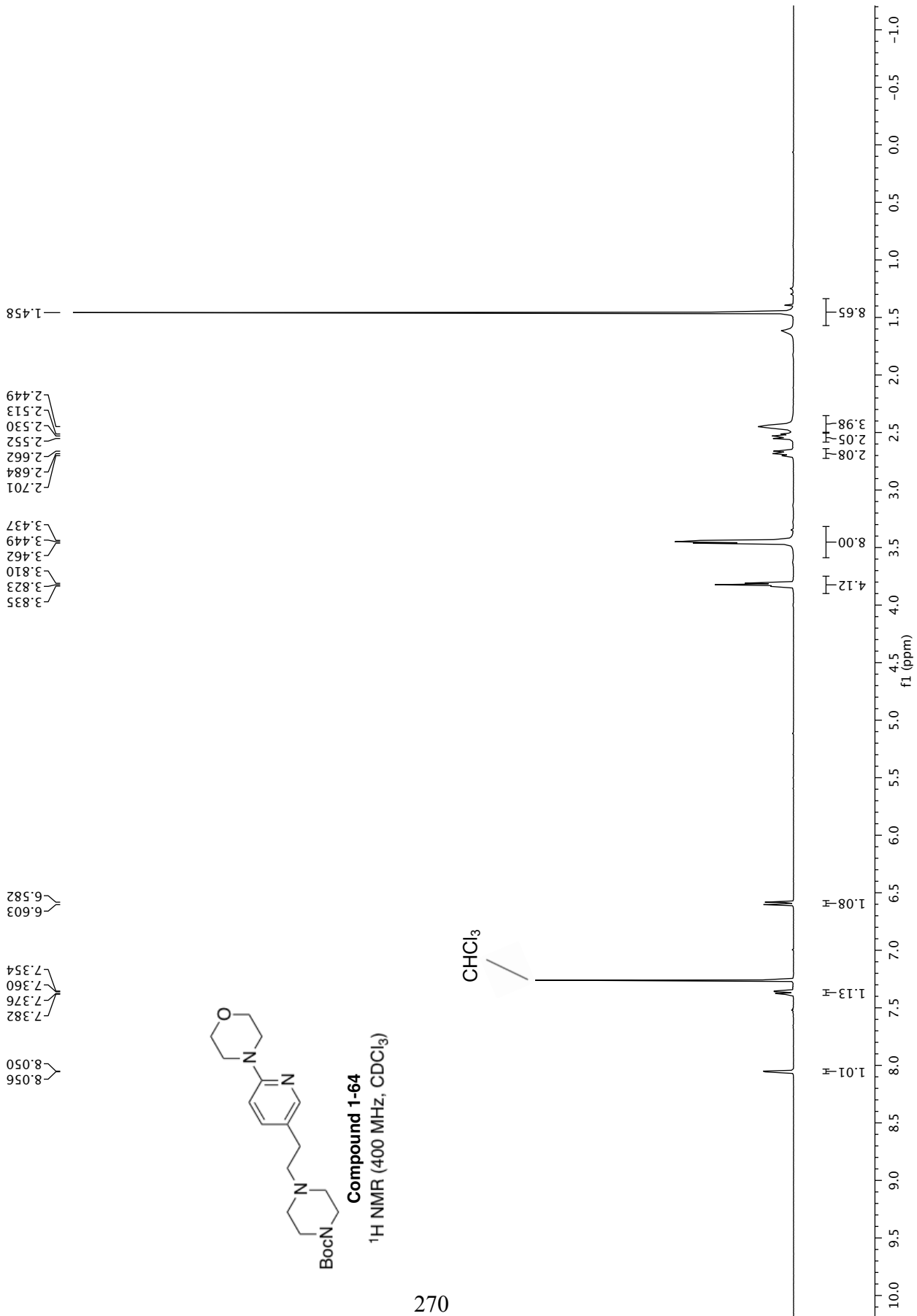
¹³C NMR (101 MHz, CDCl₃)

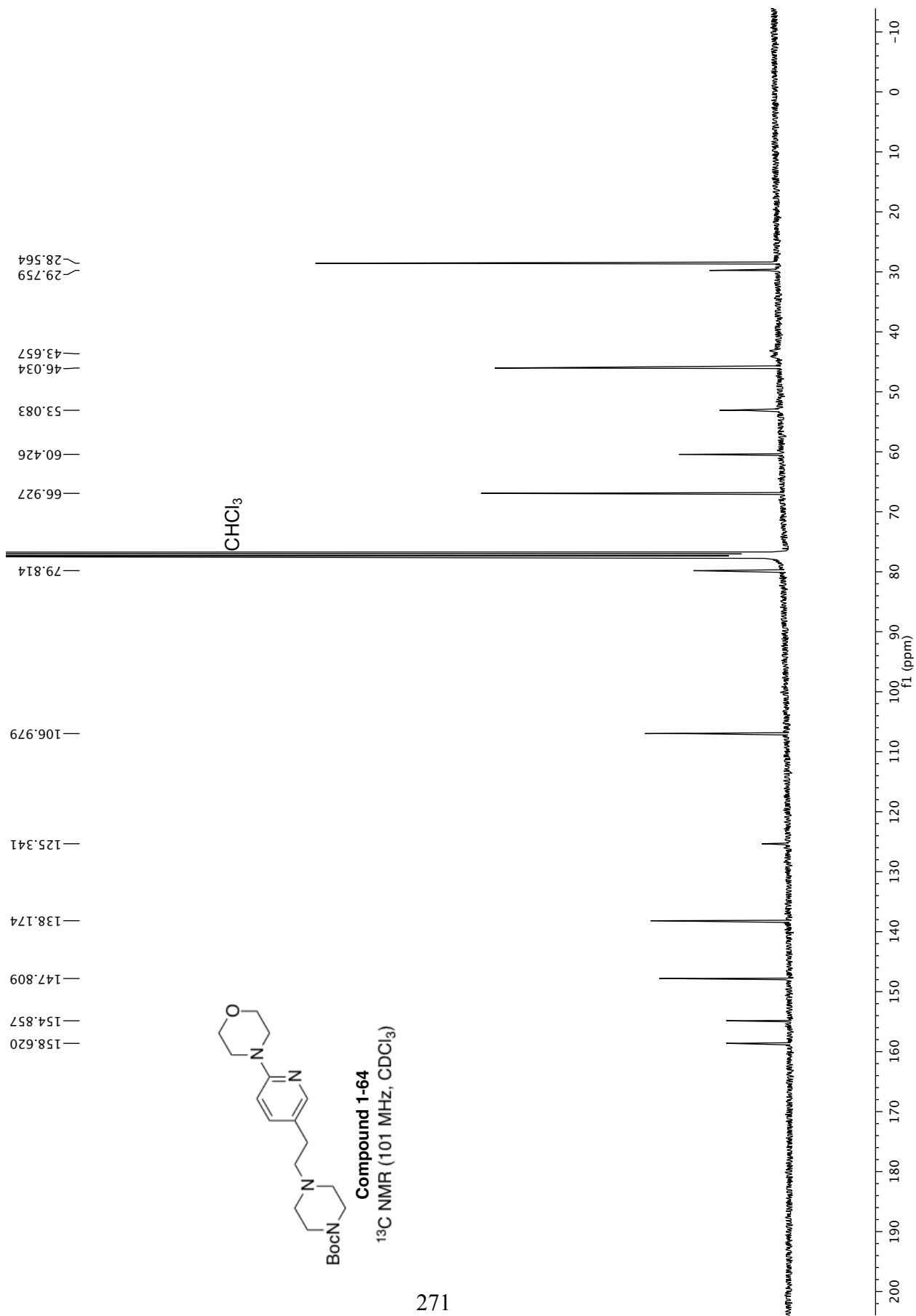


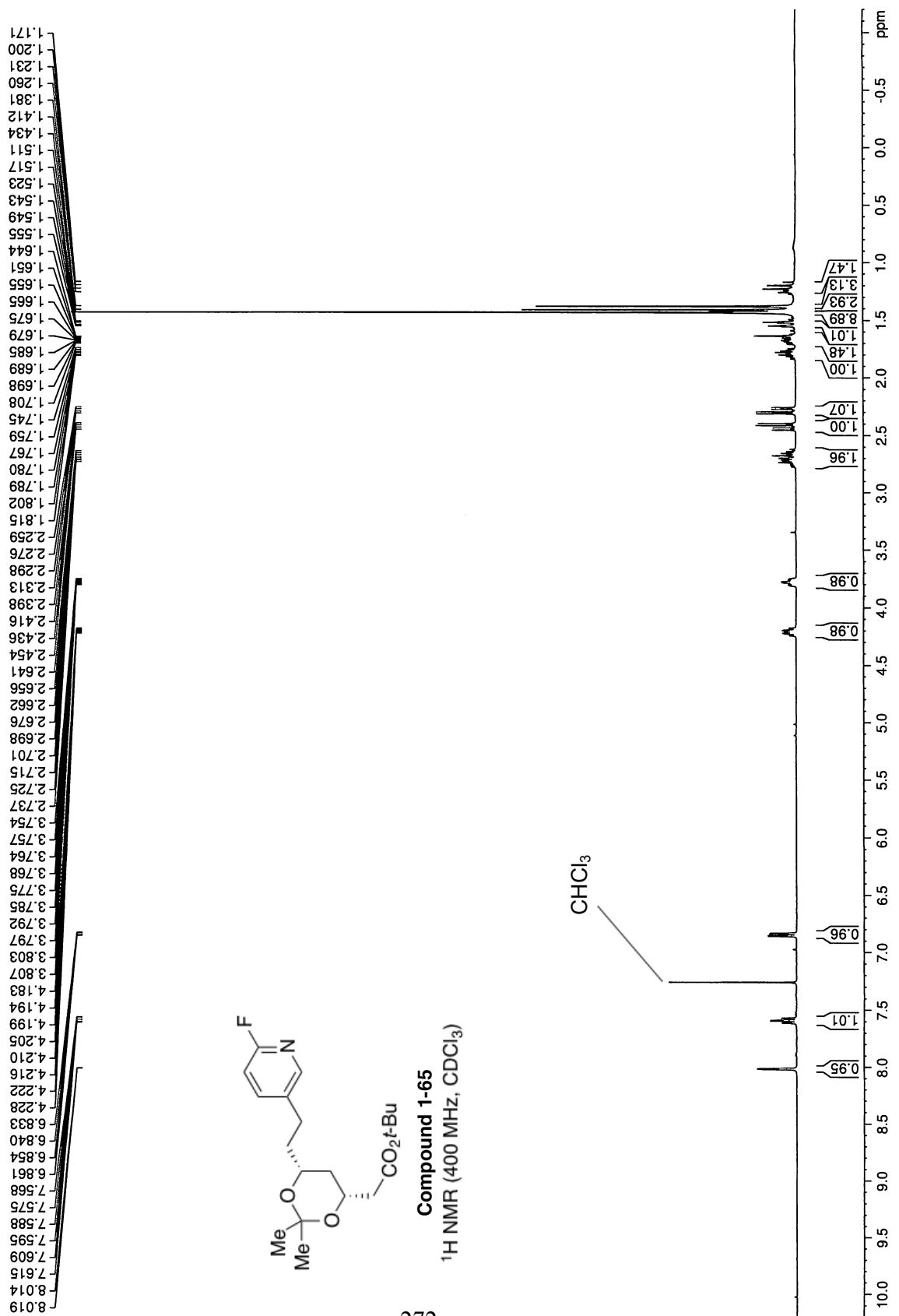


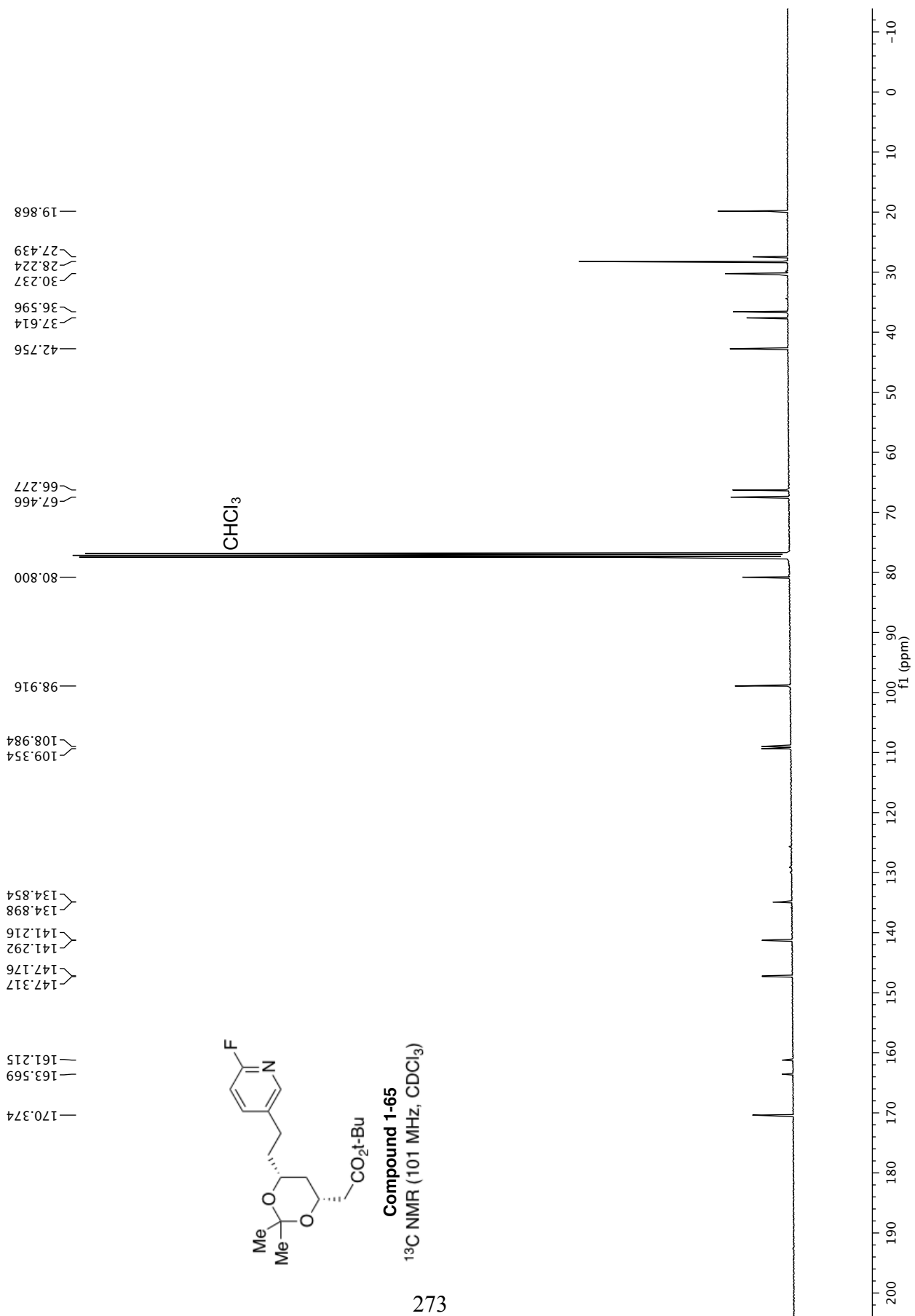
Compound 1-64

¹H NMR (400 MHz, CDCl₃)

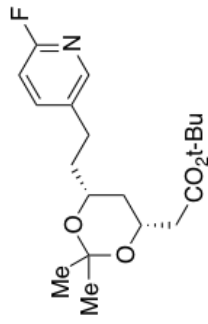






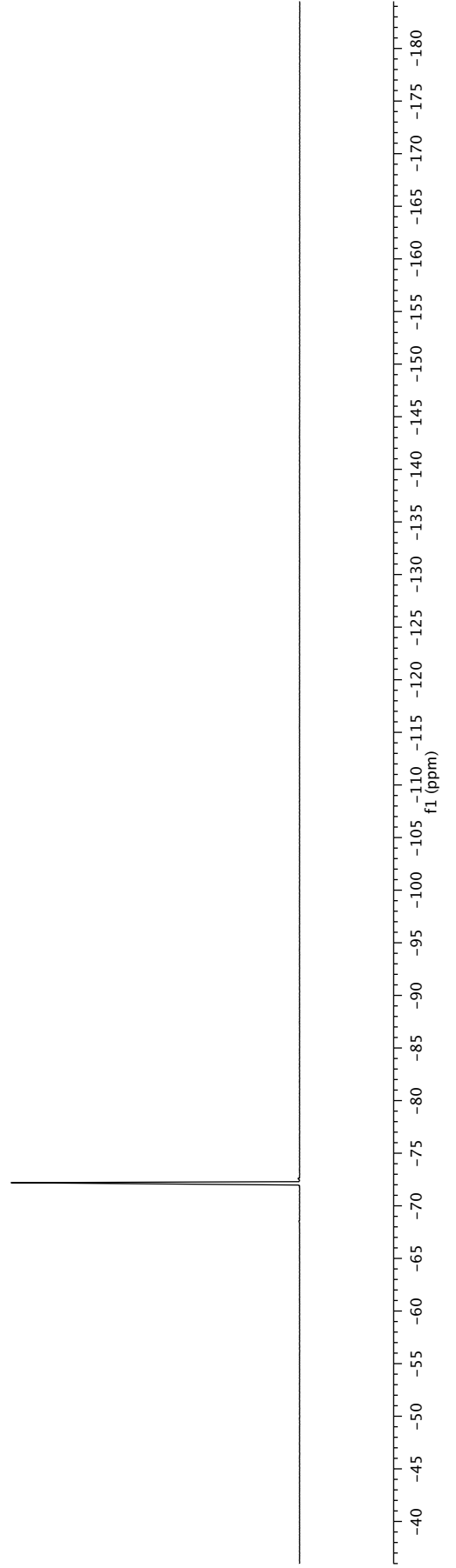


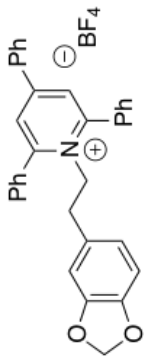
—72.197



Compound 1-65
¹⁹F NMR (376 MHz, CDCl₃)

274

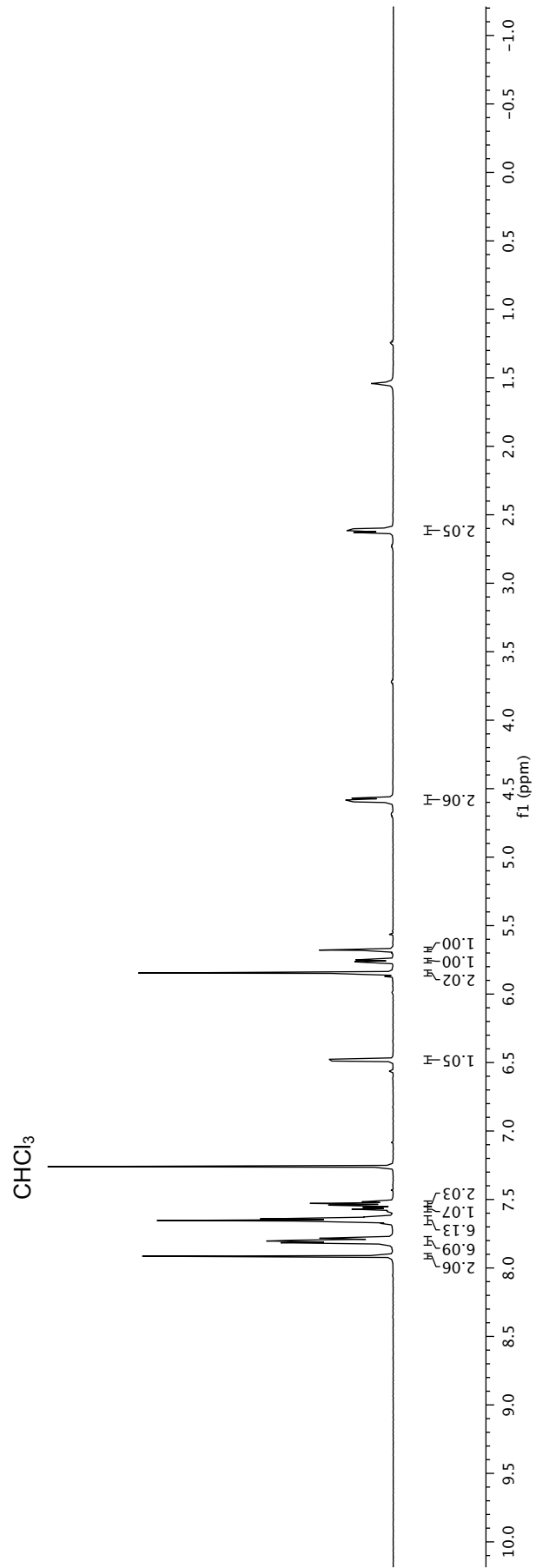


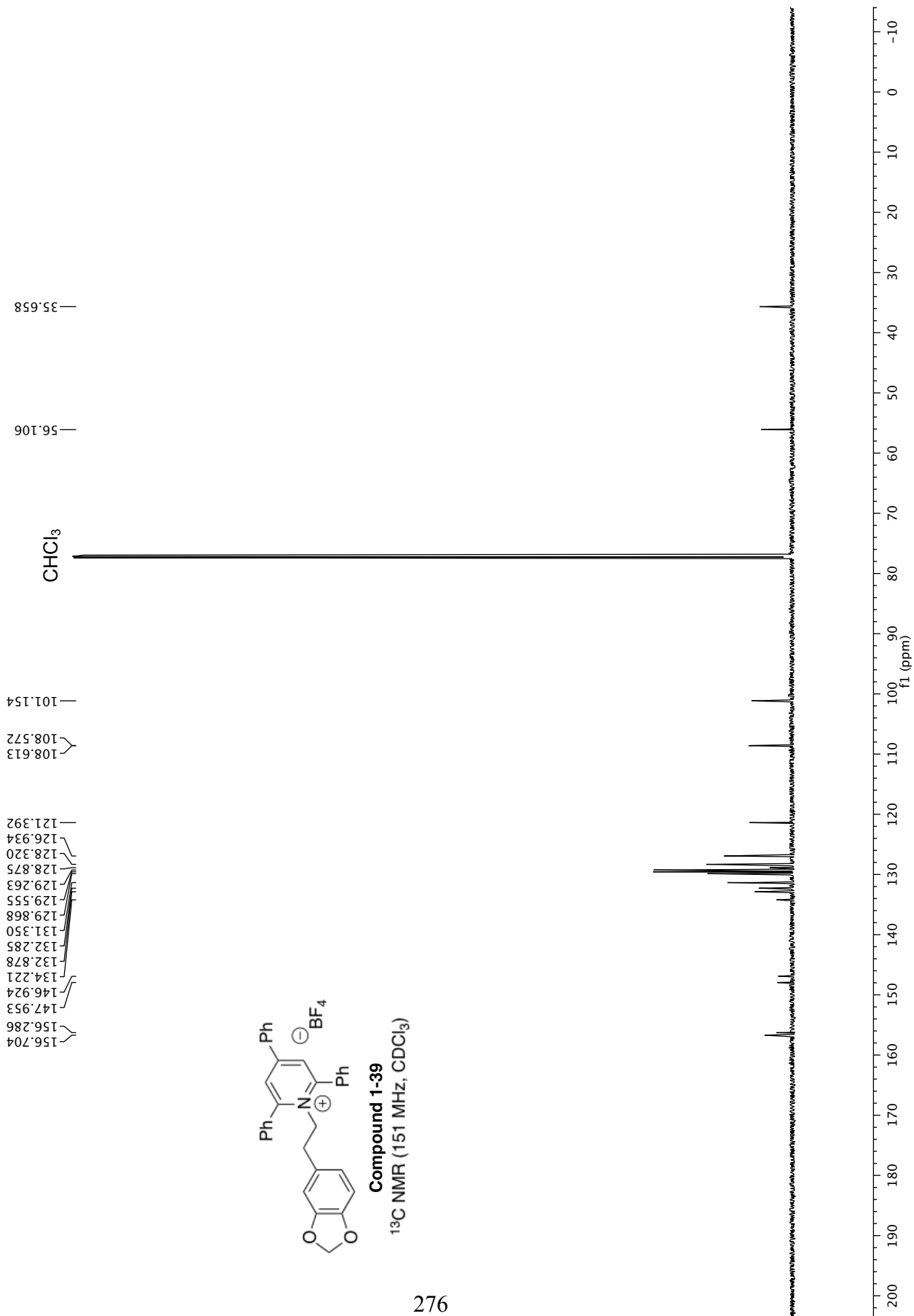


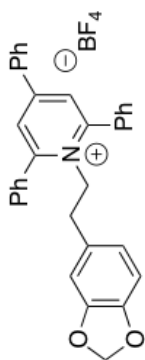
Compound 1-39

¹H NMR (600 MHz, CDCl₃)

7.914, 7.816, 7.805, 7.803, 7.798, 7.785, 7.677, 7.664, 7.654, 7.642, 7.632, 7.627, 7.584, 7.572, 7.560, 7.542, 7.529, 7.517, 6.476, 5.847, 5.765, 5.763, 5.752, 5.750, 5.679, 5.677, 4.596, 4.583, 4.569, 2.629, 2.616, 2.602



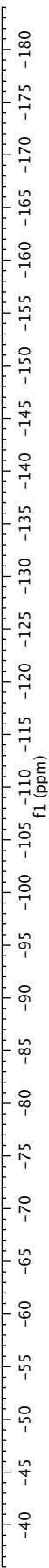


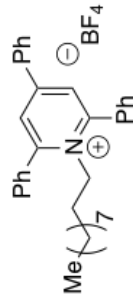


Compound 1-39

^{19}F NMR (376 MHz, CDCl_3)

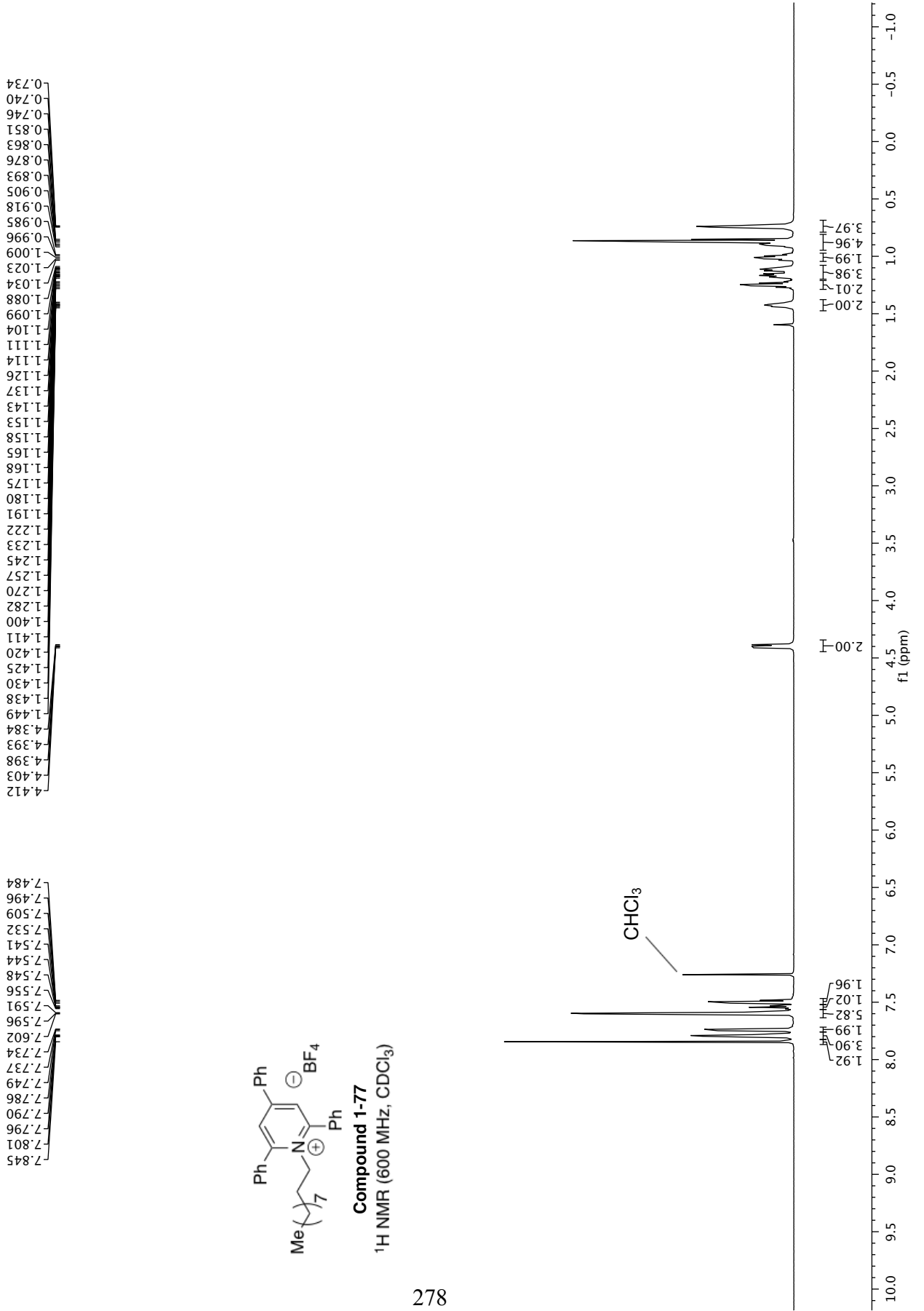
153.329
153.276

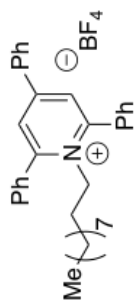




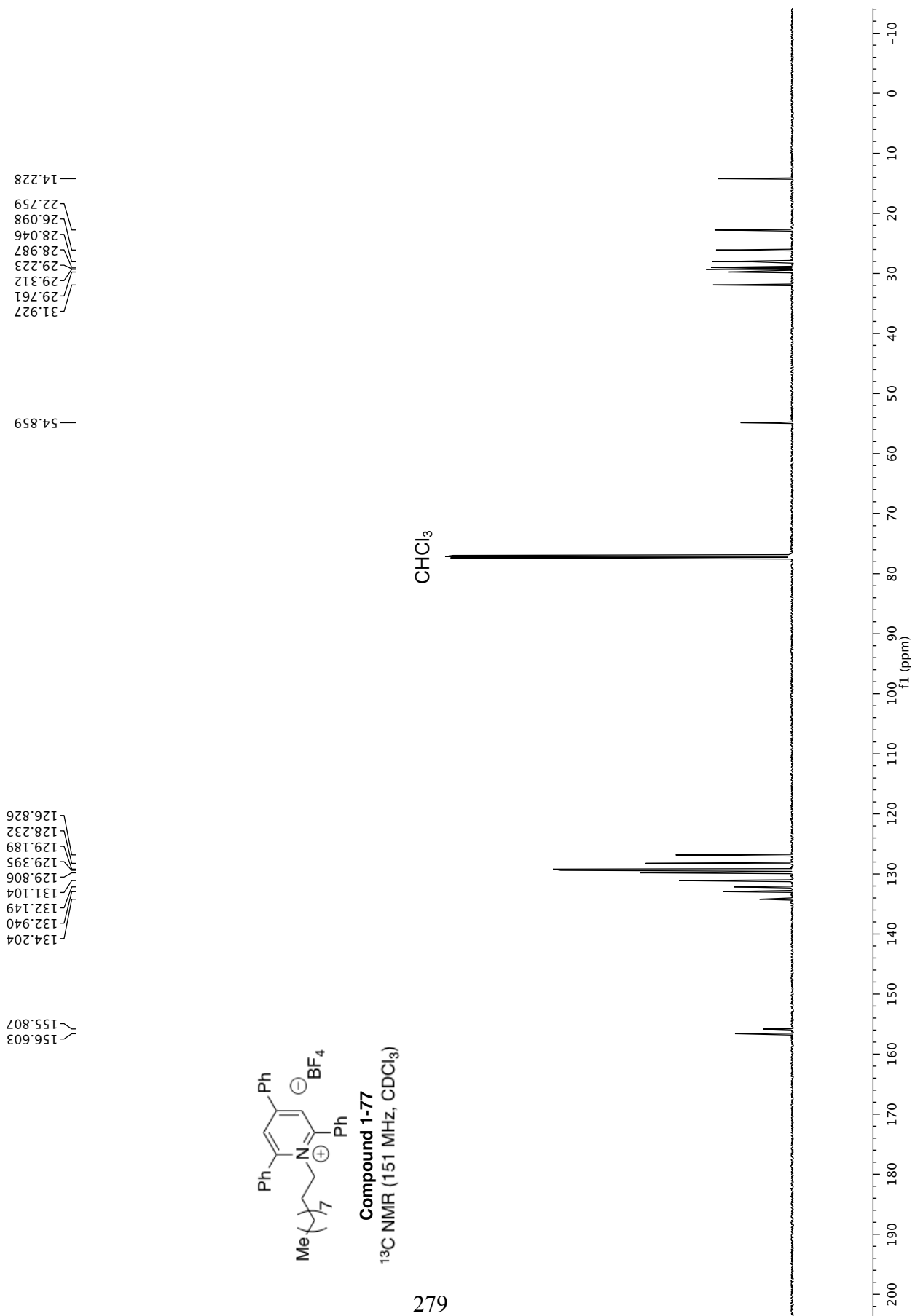
Compound 1-77

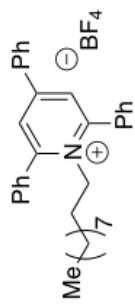
^1H NMR (600 MHz, CDCl_3)





Compound 1-77
 ^{13}C NMR (151 MHz, CDCl_3)

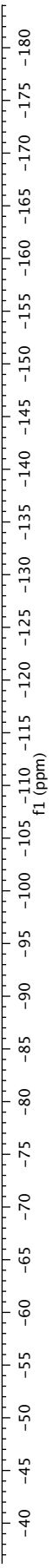




Compound 1-77
¹⁹F NMR (376 MHz, CDCl₃)

280

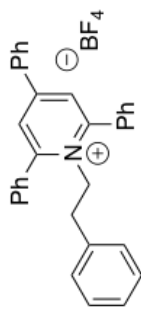
153.401
153.454



7.916
7.807
7.804
7.801
7.798
7.793
7.788
7.784
7.778
7.658
7.648
7.646
7.640
7.630
7.578
7.561
7.557
7.550
7.547
7.537
7.532
7.520
7.128
7.122
7.116
7.104
7.072
7.053
7.039
7.035
6.296
6.278
6.275

4.676
4.660
4.655
4.650
4.635

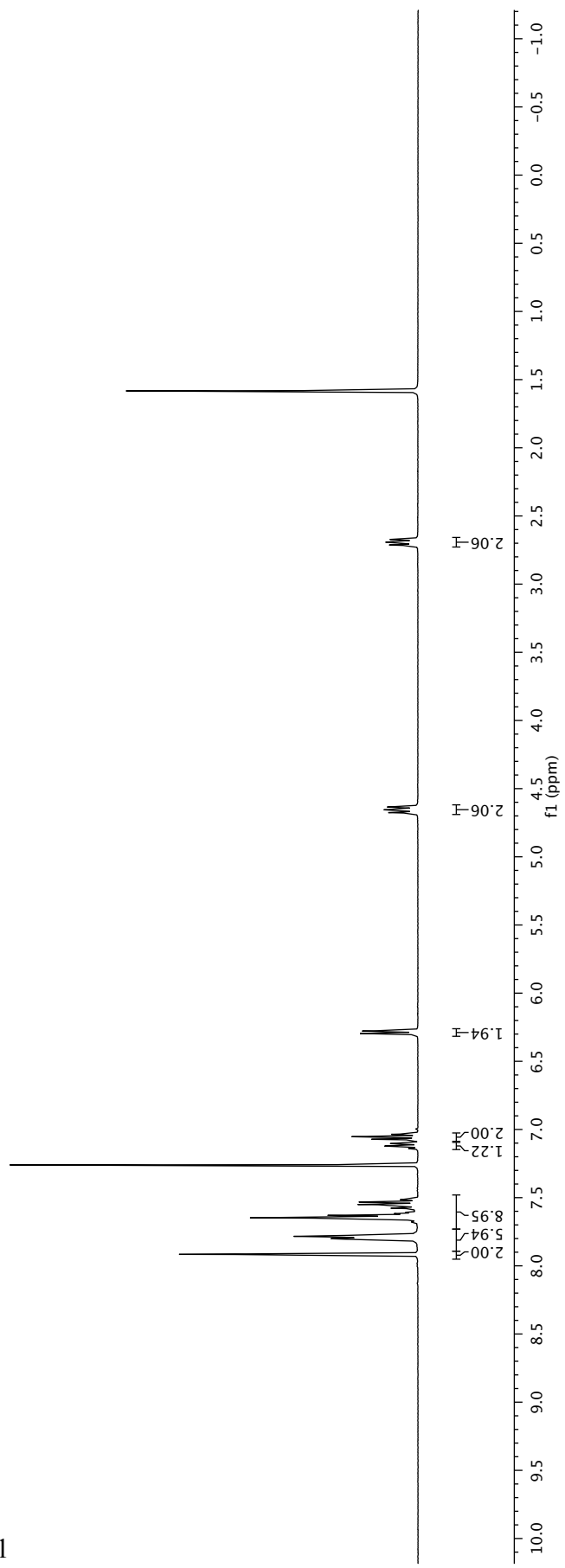
2.713
2.698
2.693
2.688
2.672

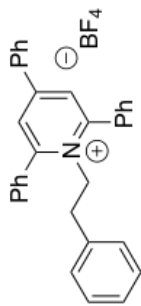


Compound 1-33
¹H NMR (400 MHz, CDCl₃)

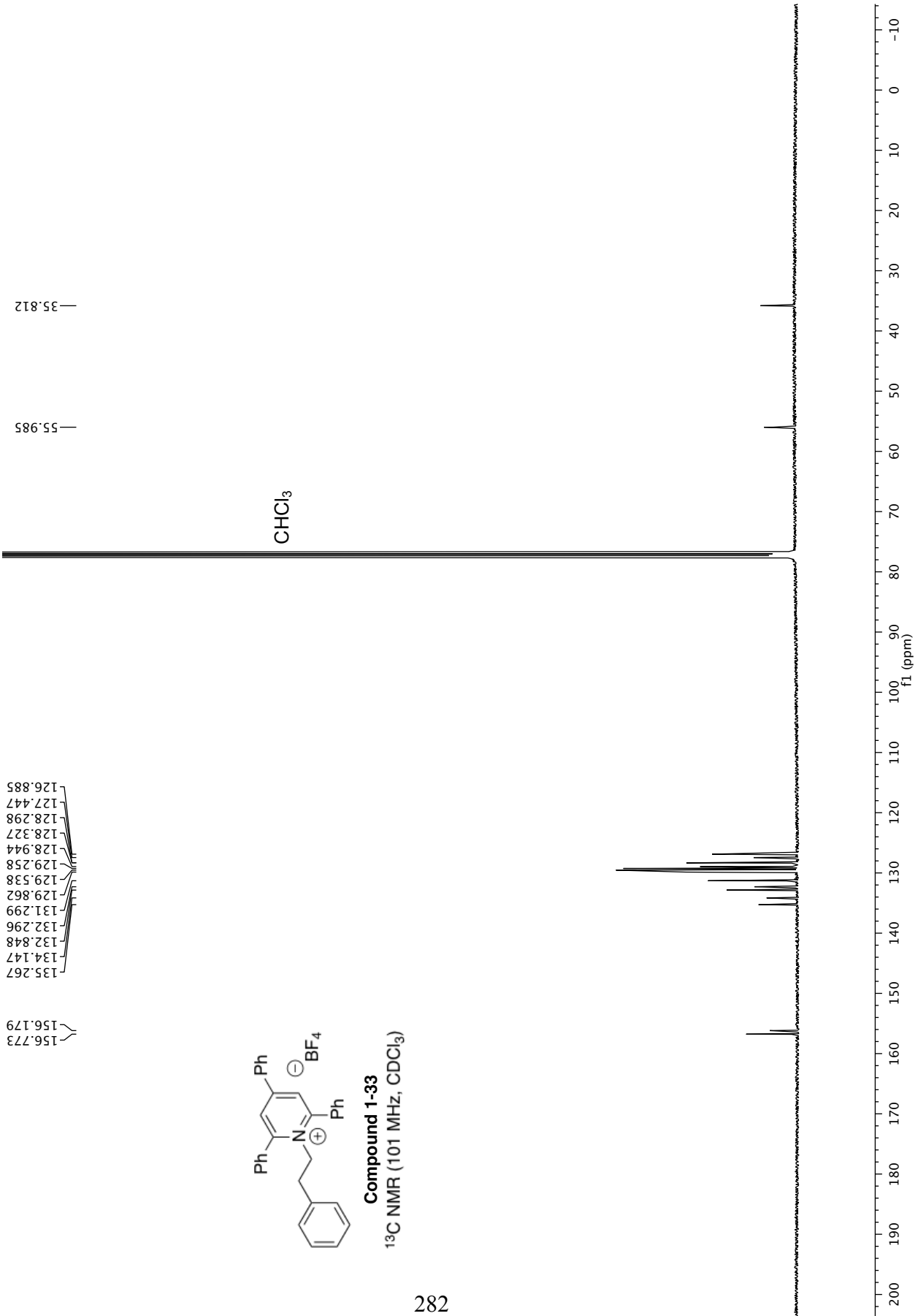
181

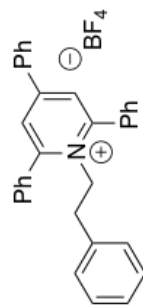
CHCl₃





Compound 1-33
 ^{13}C NMR (101 MHz, CDCl_3)

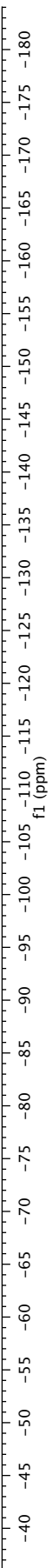


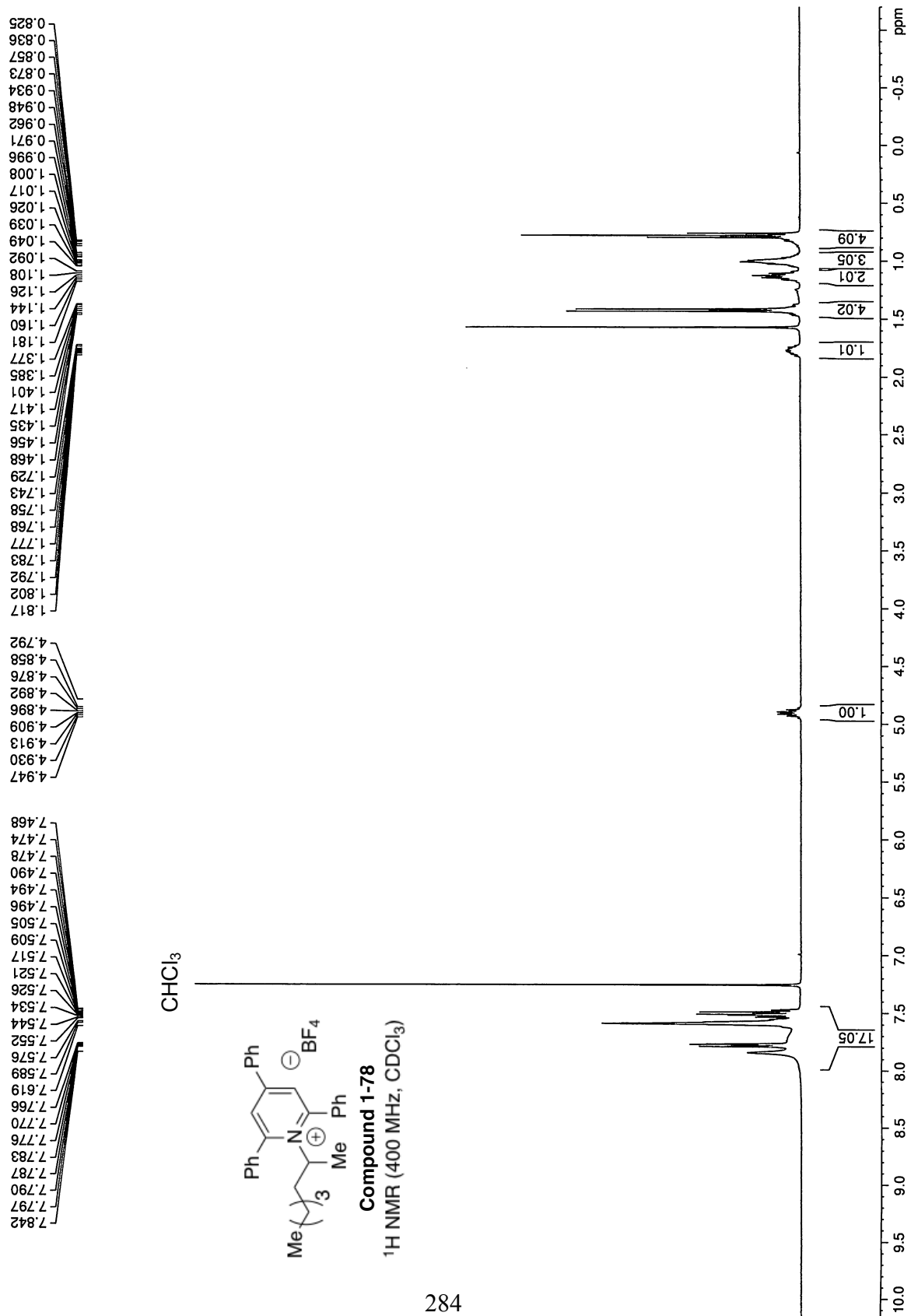


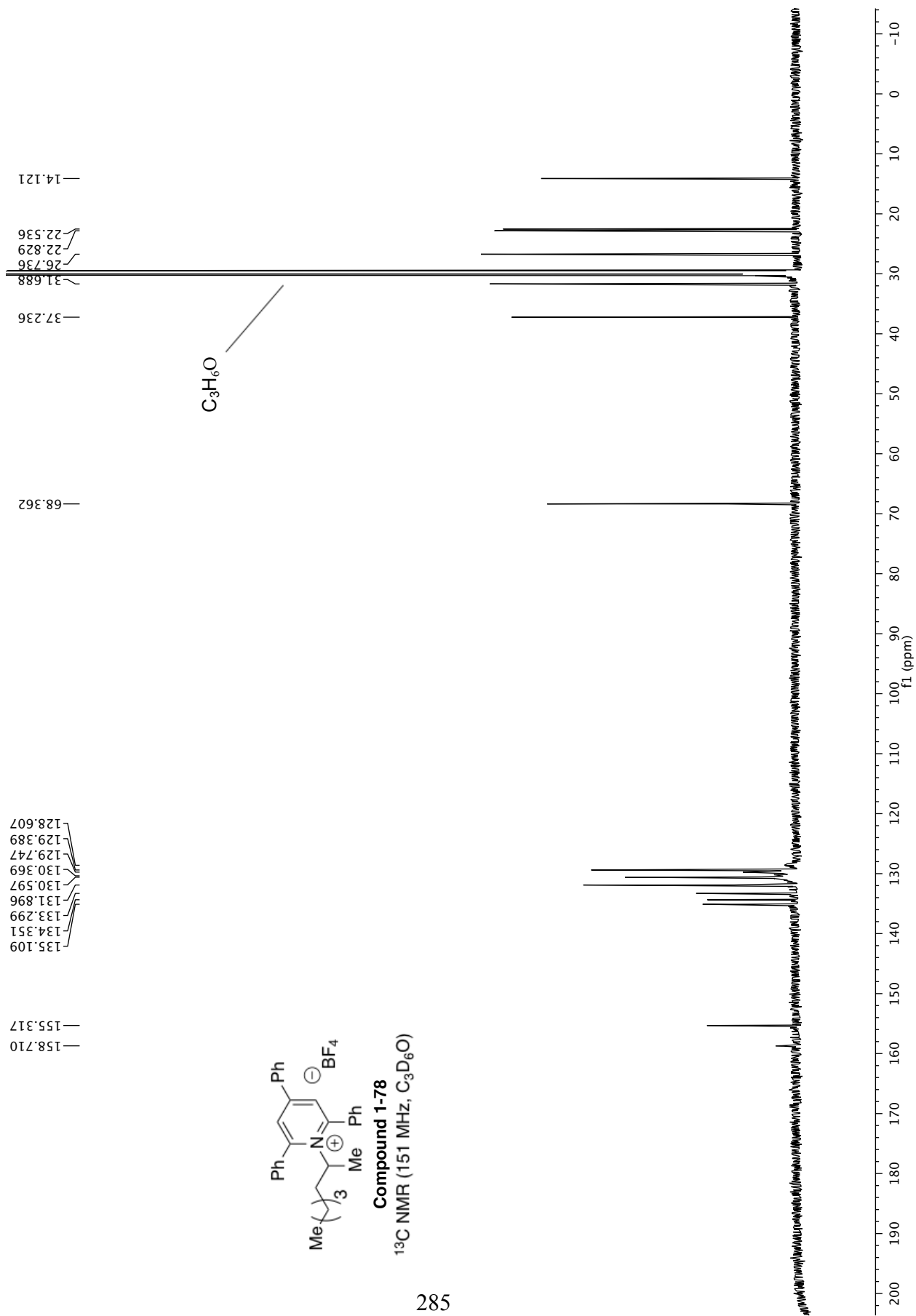
283

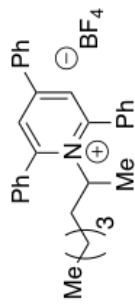
Compound 1-33
¹⁹F NMR (376 MHz, CDCl₃)

153.264
153.317





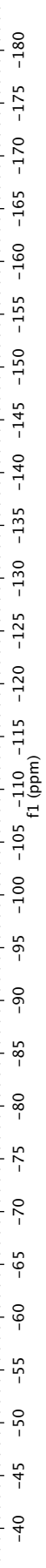




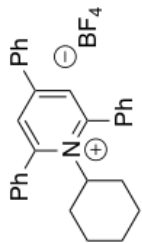
Compound 1-78
¹⁹F NMR (565 MHz, CDCl₃)

286

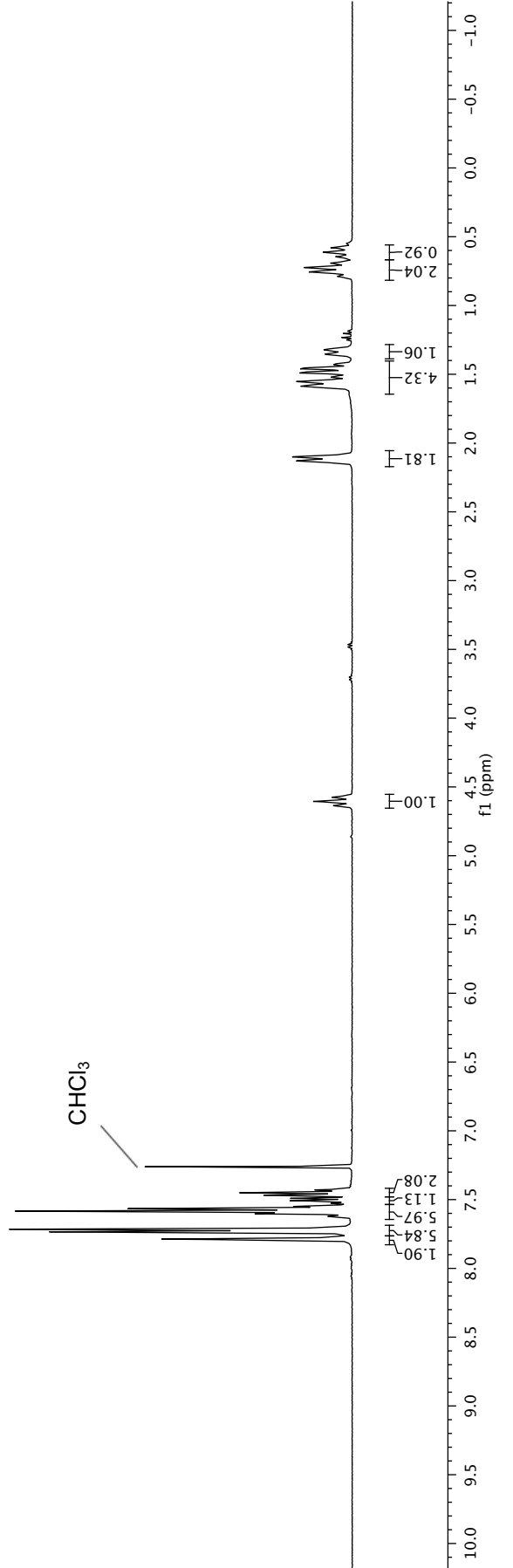
153.348
153.400

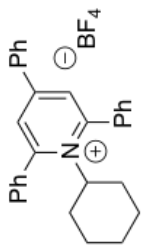


7.889
7.886
7.883
7.746
7.738
7.734
7.729
7.719
7.714
7.626
7.623
7.618
7.616
7.604
7.597
7.592
7.587
7.583
7.566
7.550
7.528
7.524
7.517
7.508
7.502
7.495
7.492
7.488
7.470
7.468
7.465
7.456
7.451
7.446
7.433
7.429
7.425
4.643
4.636
4.629
4.613
4.605
4.598
4.582
4.575
4.567
2.131
2.101
1.595
1.588
1.580
1.561
1.553
1.545
1.522
1.513
1.492
1.483
1.461
1.453
1.430
1.422
1.354
1.329
1.320
0.788
0.780
0.764
0.756
0.748
0.732
0.724
0.715
0.700
0.692
0.684
0.645
0.637
0.622
0.613
0.590
0.581
0.571



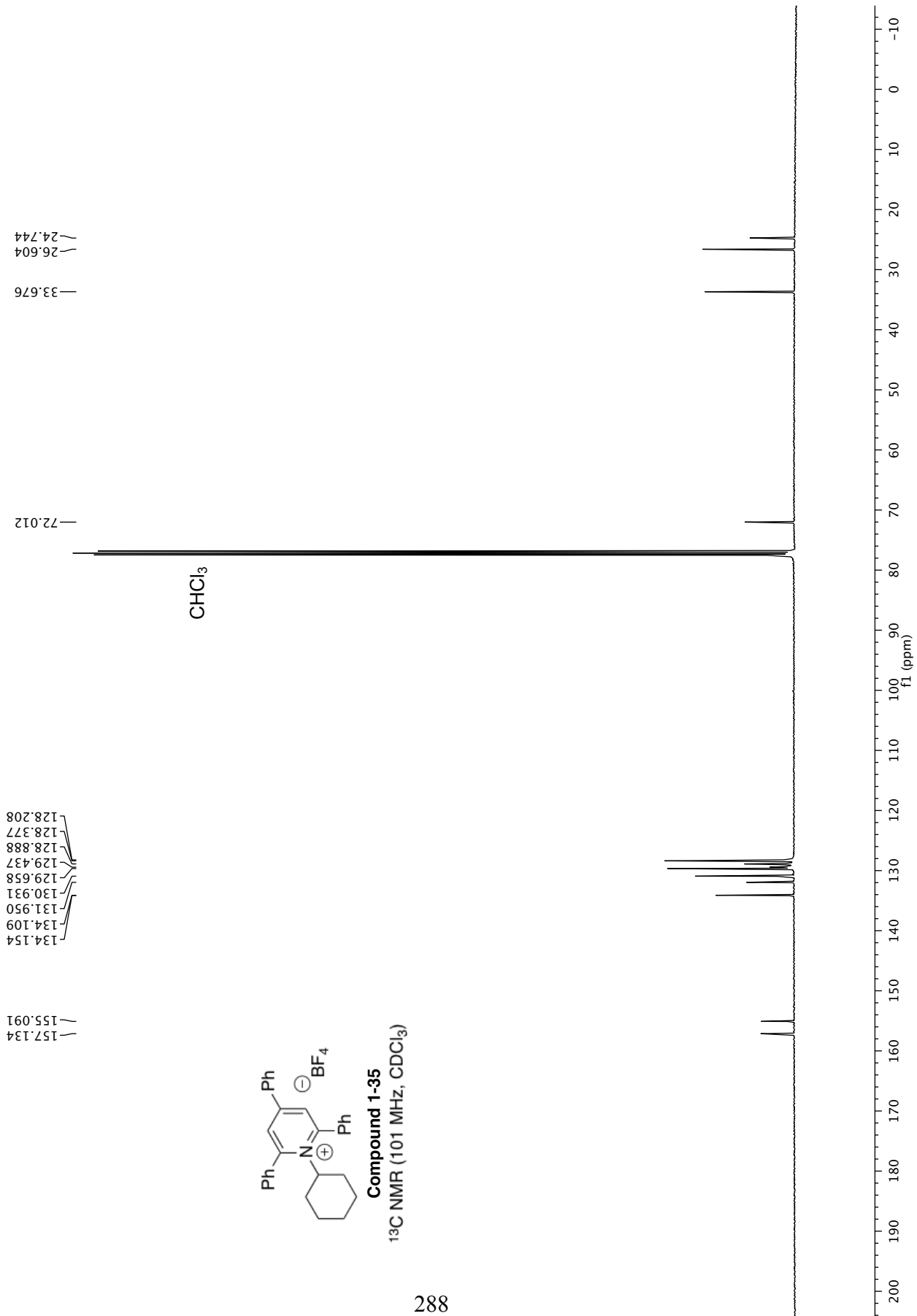
Compound 1-35
¹H NMR (400 MHz, CDCl₃)

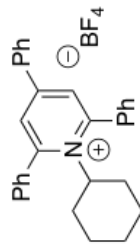




Compound 1-35

^{13}C NMR (101 MHz, CDCl_3)

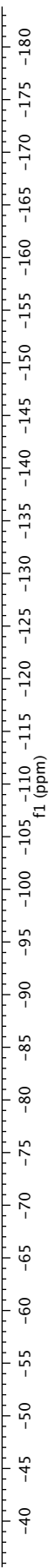


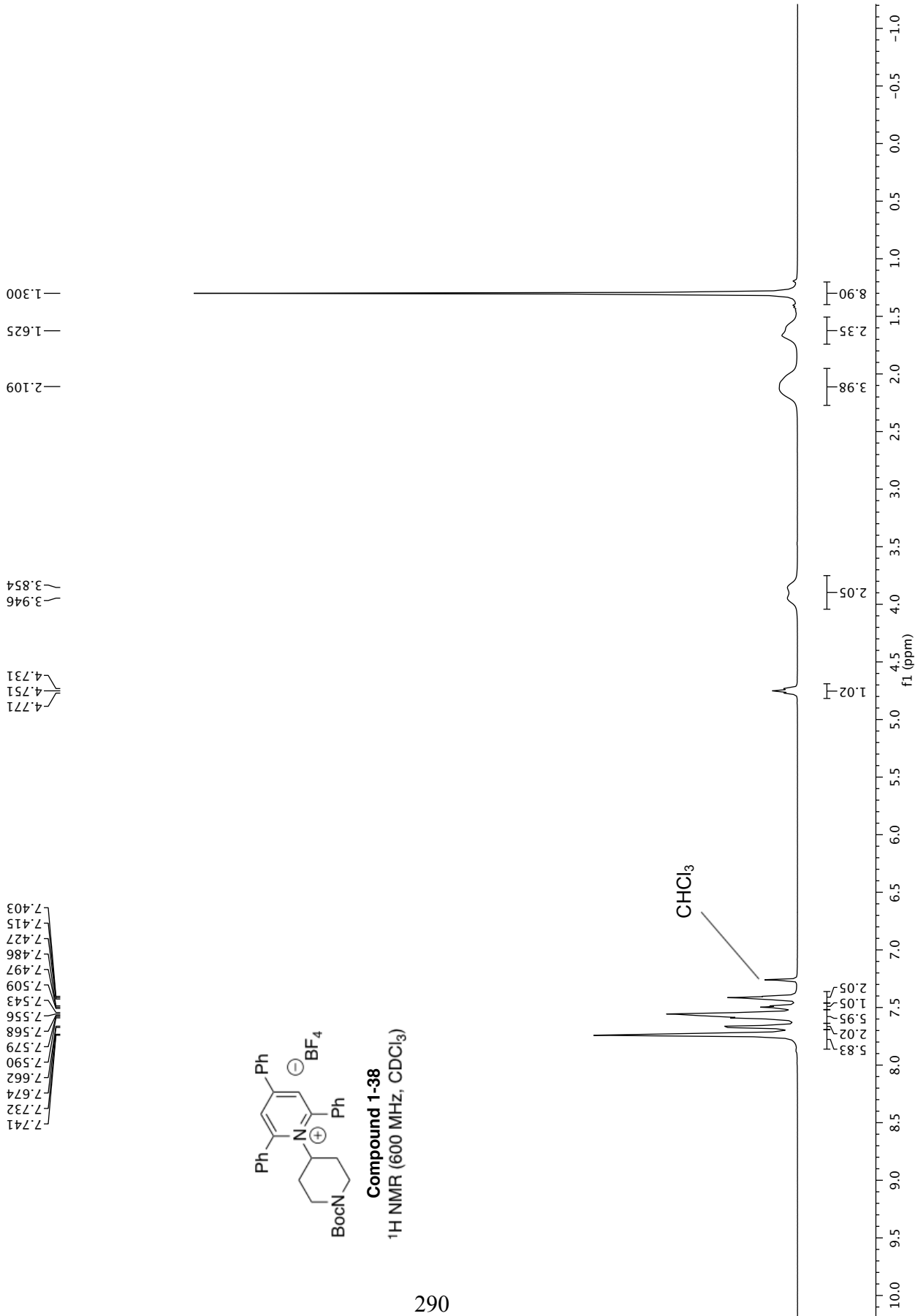


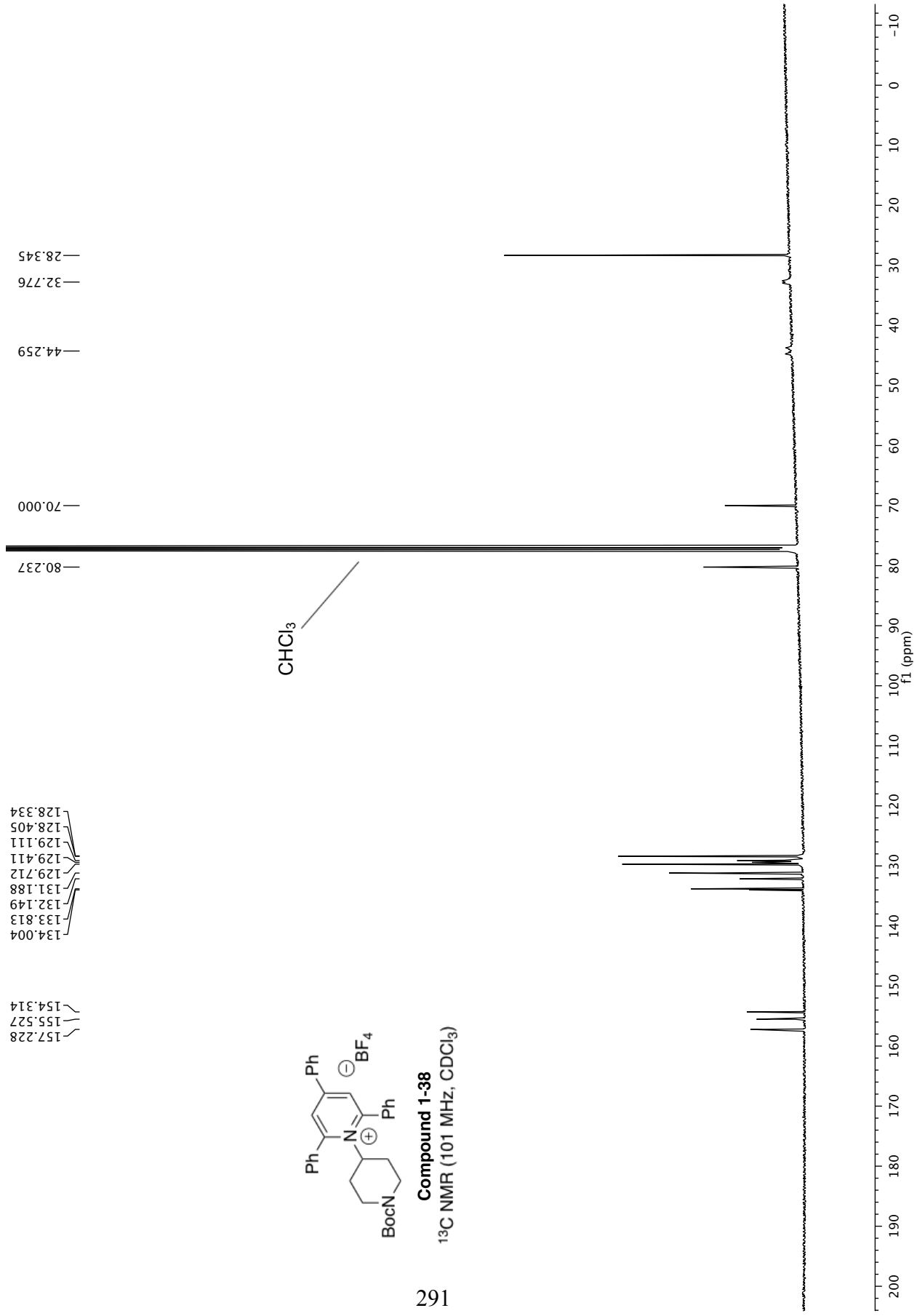
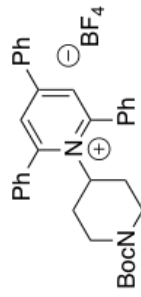
Compound 1-35
¹⁹F NMR (376 MHz, CDCl₃)

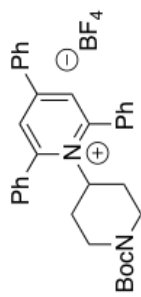
153.411
153.358

289





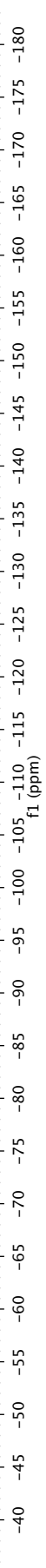
Compound 1-38
¹³C NMR (101 MHz, CDCl₃)

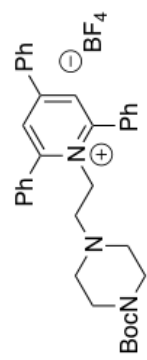
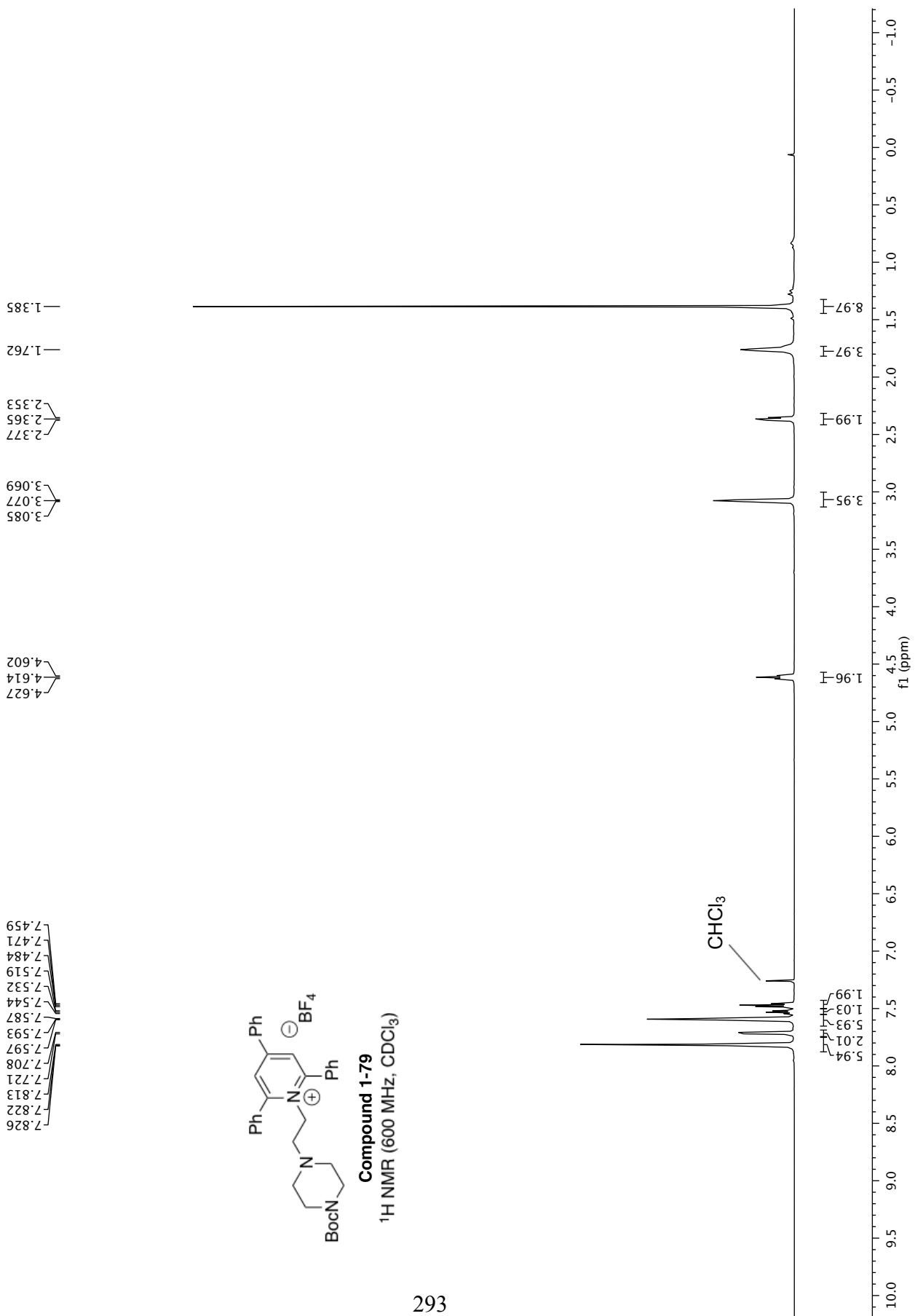


Compound 1-38
¹⁹F NMR (376 MHz, CDCl₃)

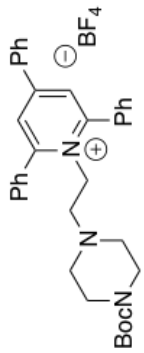
292

153.128
153.074



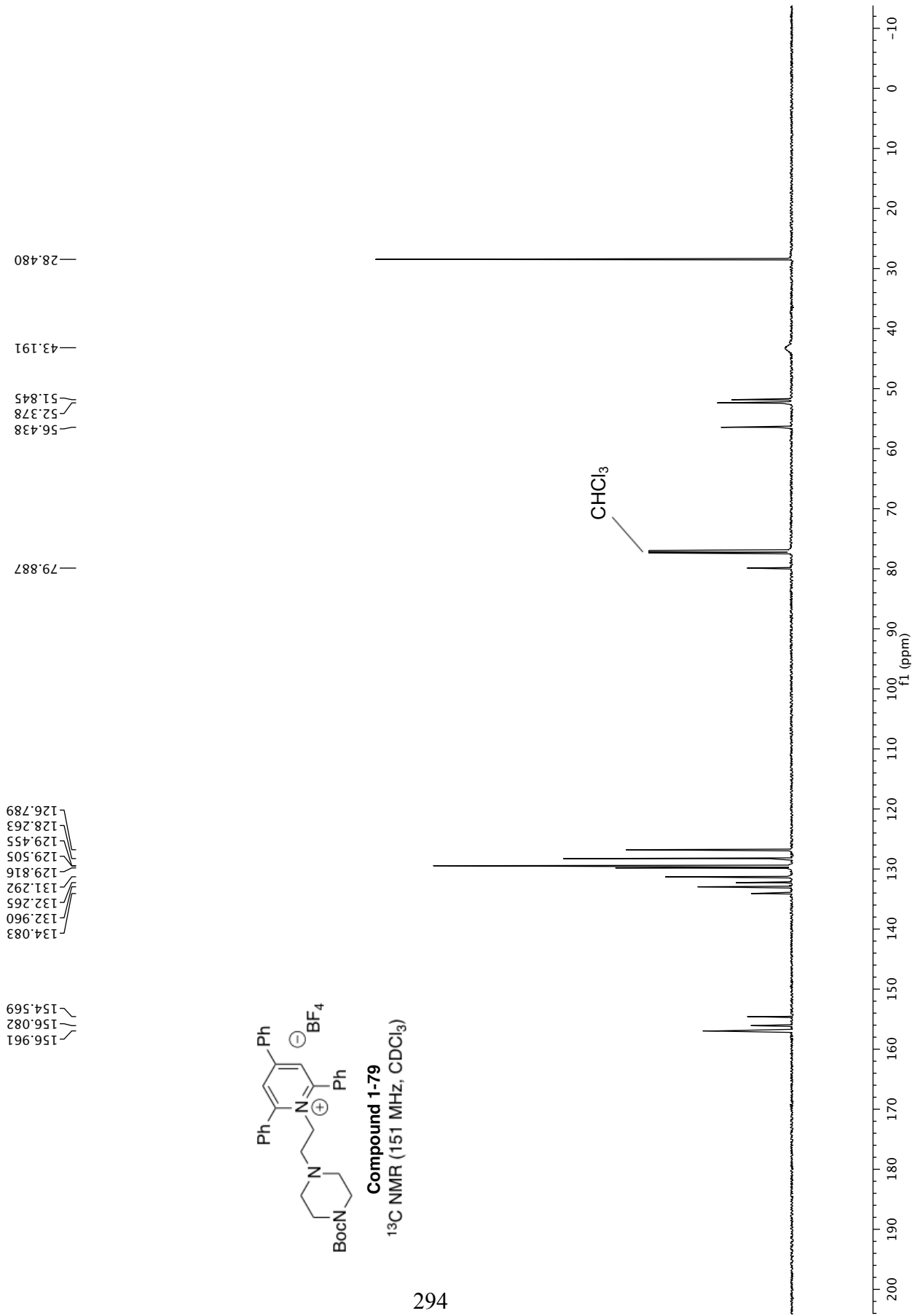


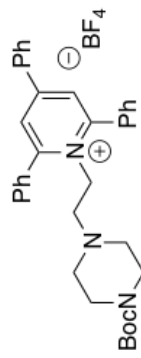
Compound 1-79
 ^1H NMR (600 MHz, CDCl_3)



Compound 1-79

^{13}C NMR (151 MHz, CDCl_3)



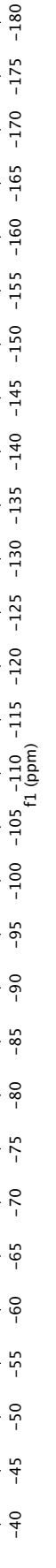


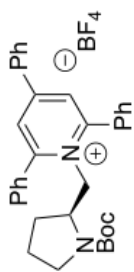
Compound 1-79

¹⁹F NMR (565 MHz, CDCl₃)

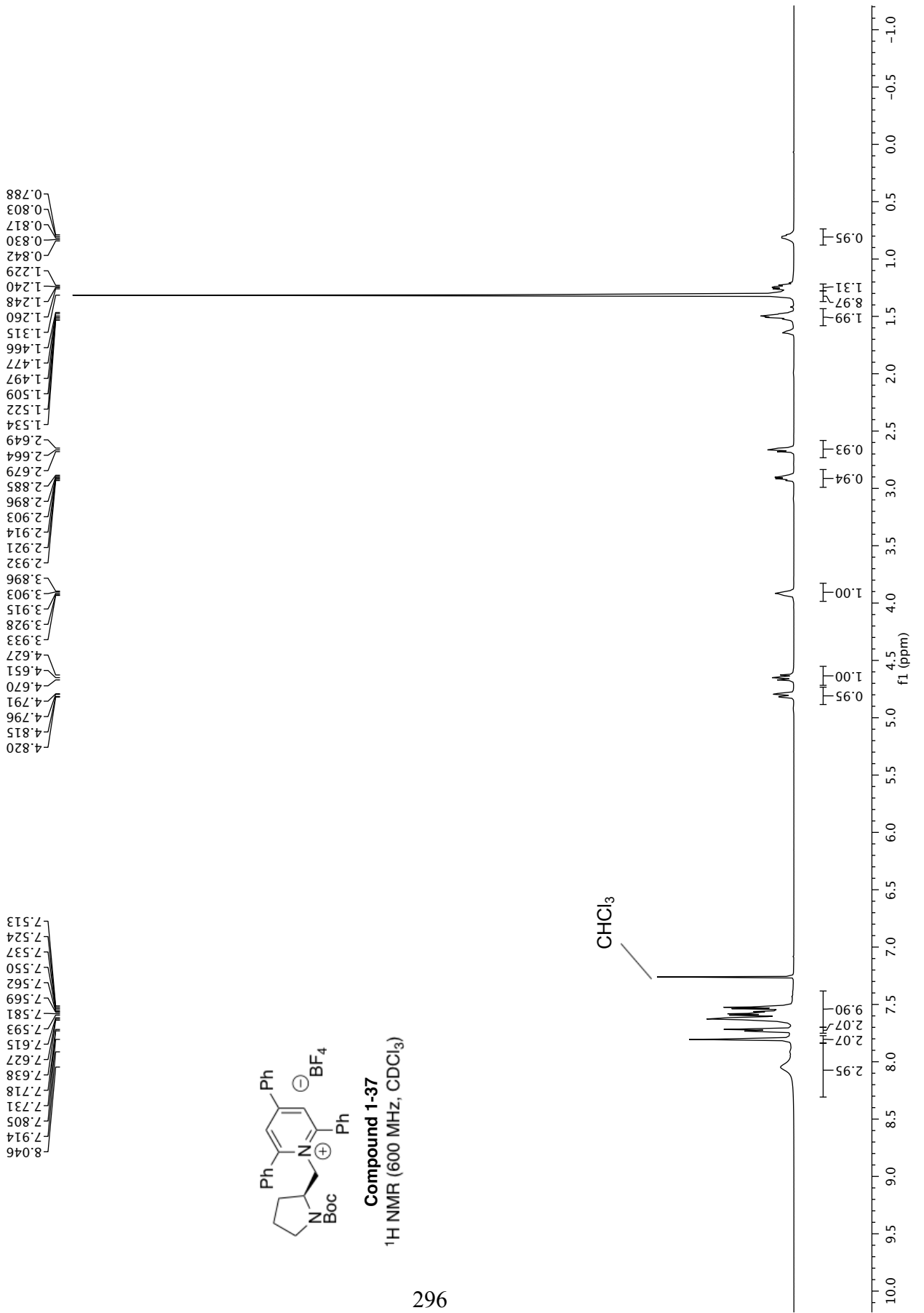
152.956
153.009

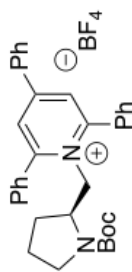
295





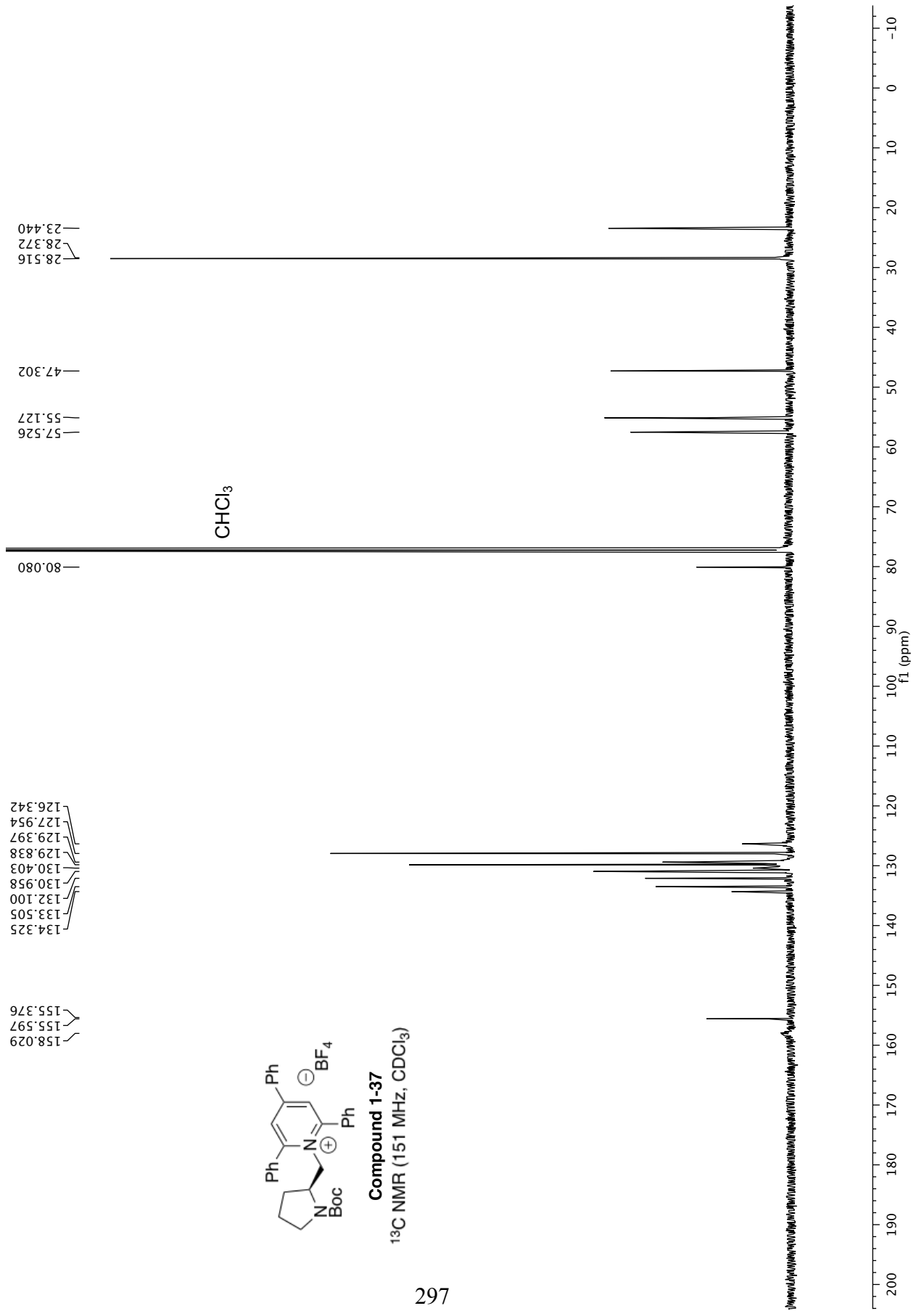
Compound 1-37
¹H NMR (600 MHz, CDCl₃)

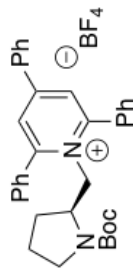




Compound 1-37

^{13}C NMR (151 MHz, CDCl_3)

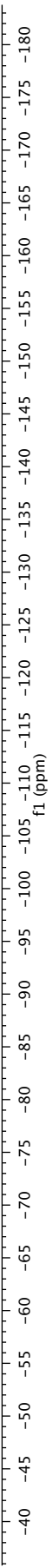


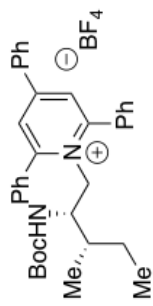


Compound 1-37
¹⁹F NMR (565 MHz, CDCl₃)

298

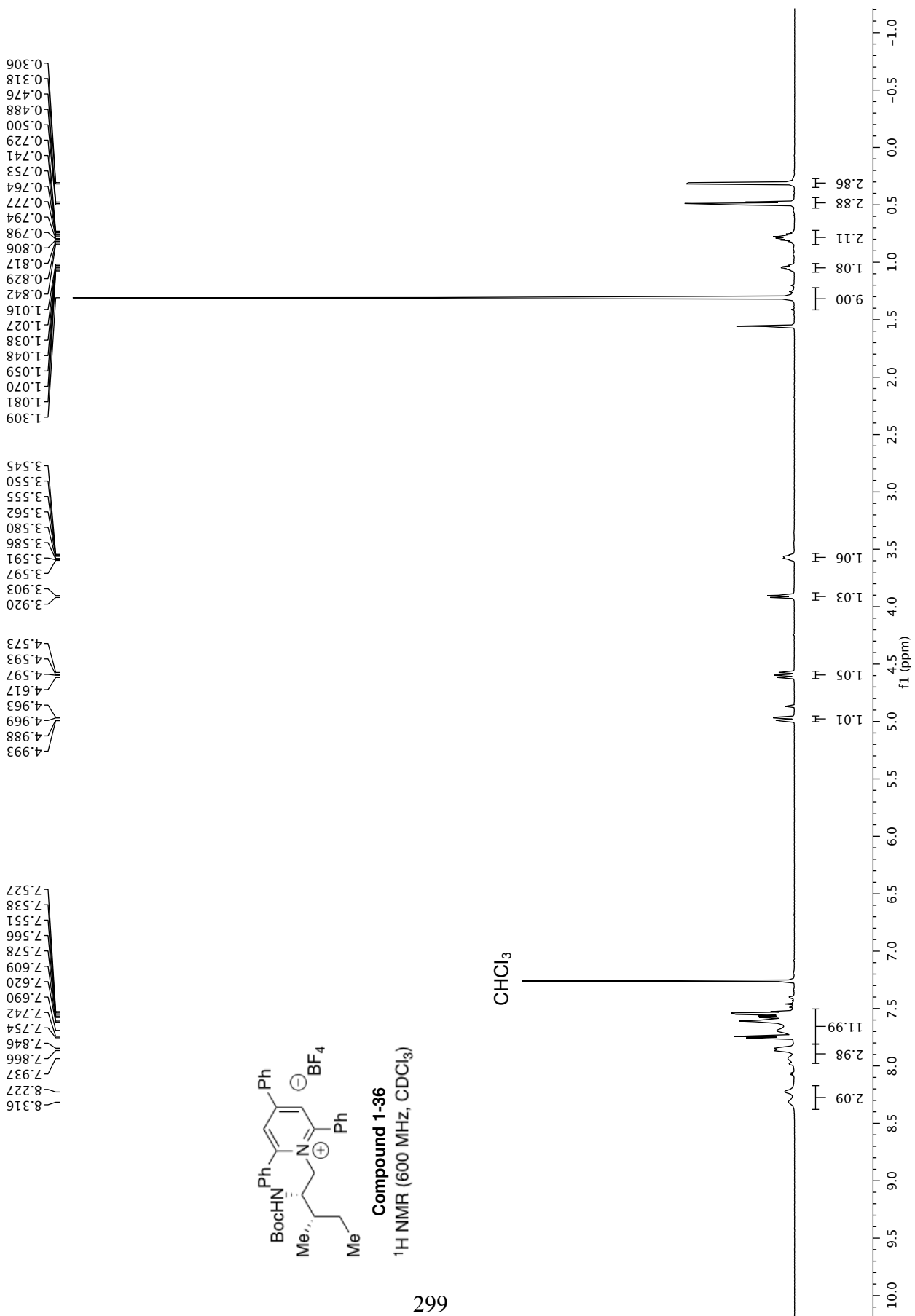
153.131
153.078

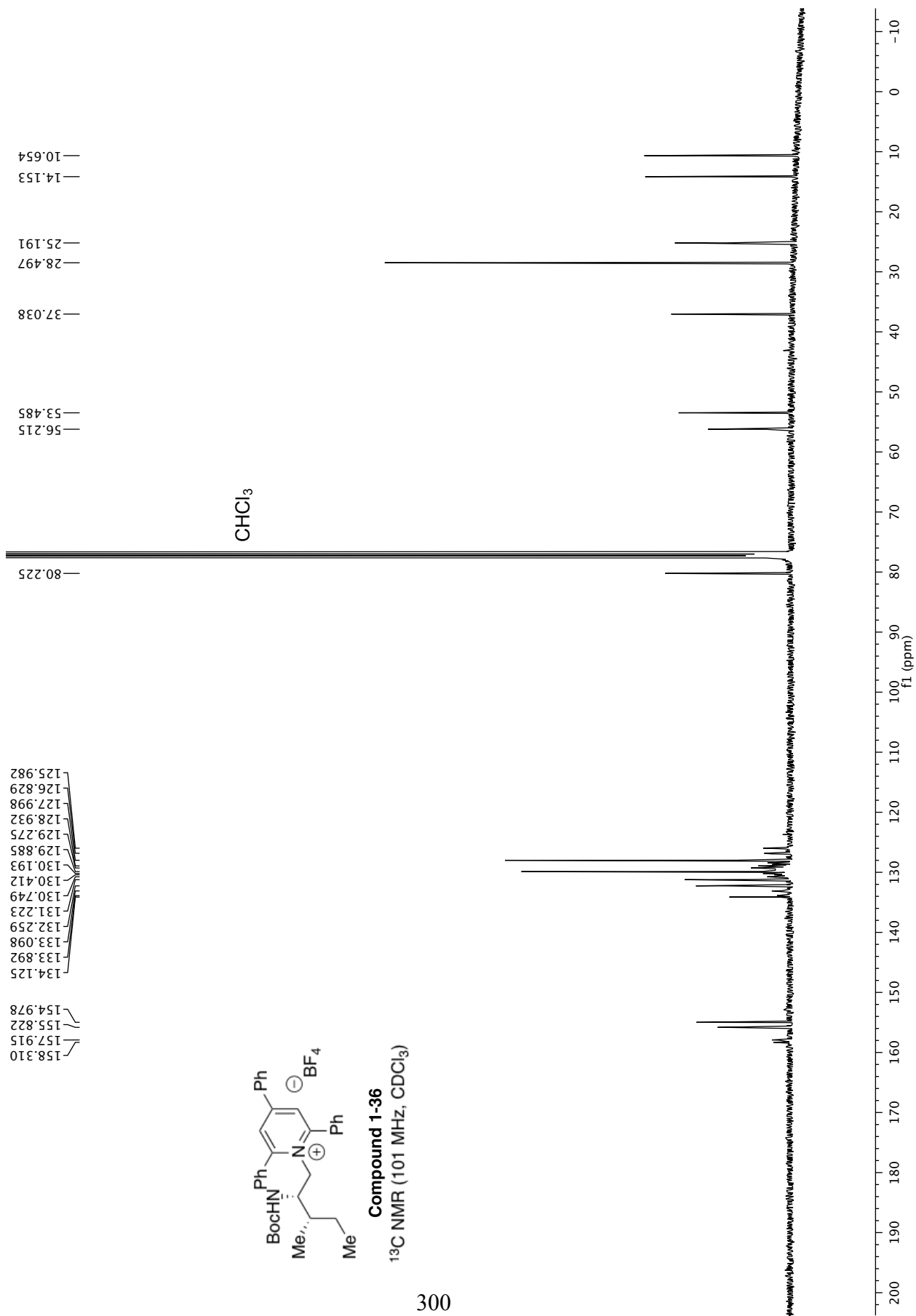


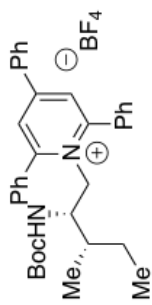


Compound 1-36

¹H NMR (600 MHz, CDCl₃)



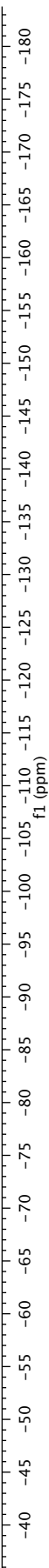


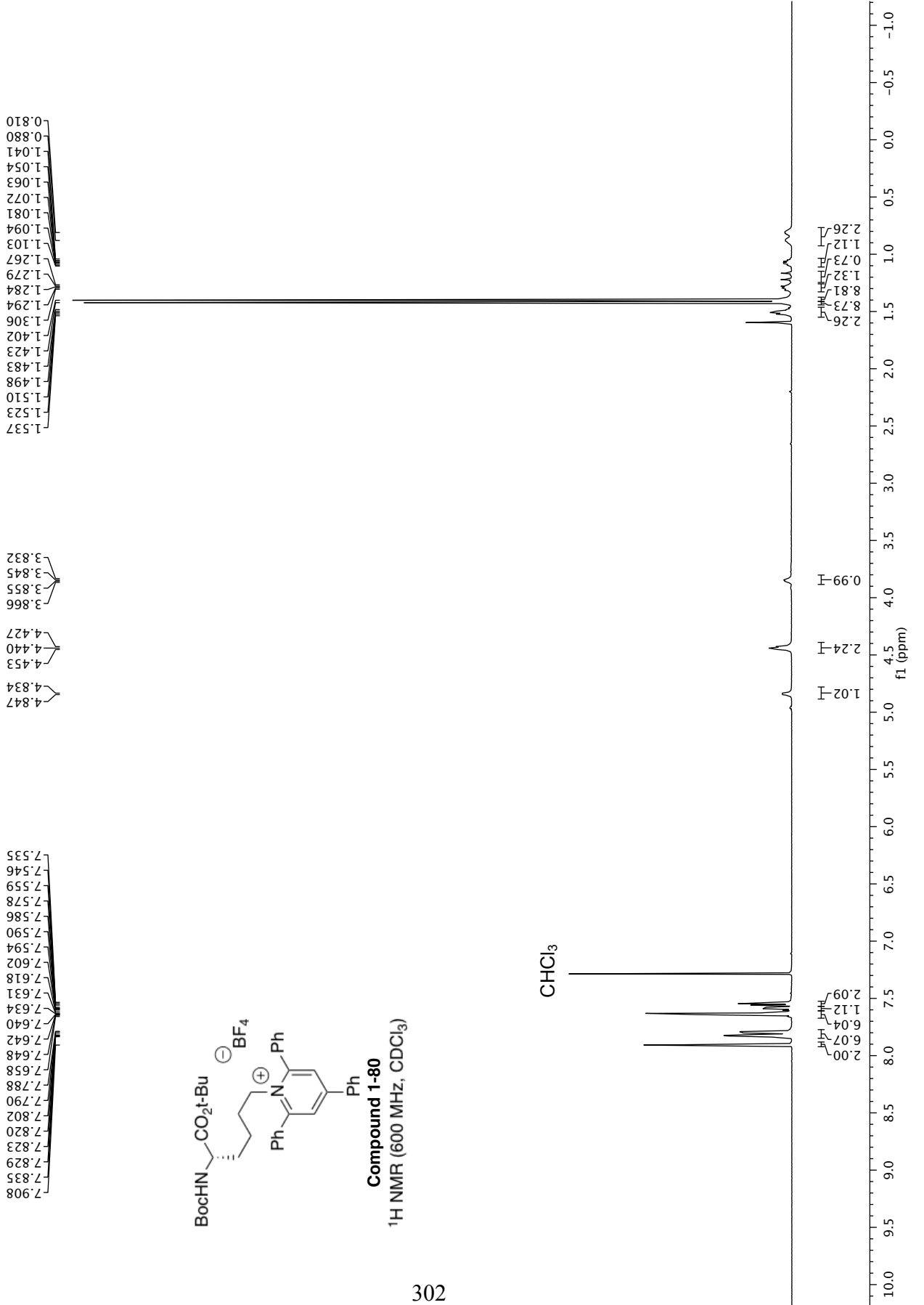


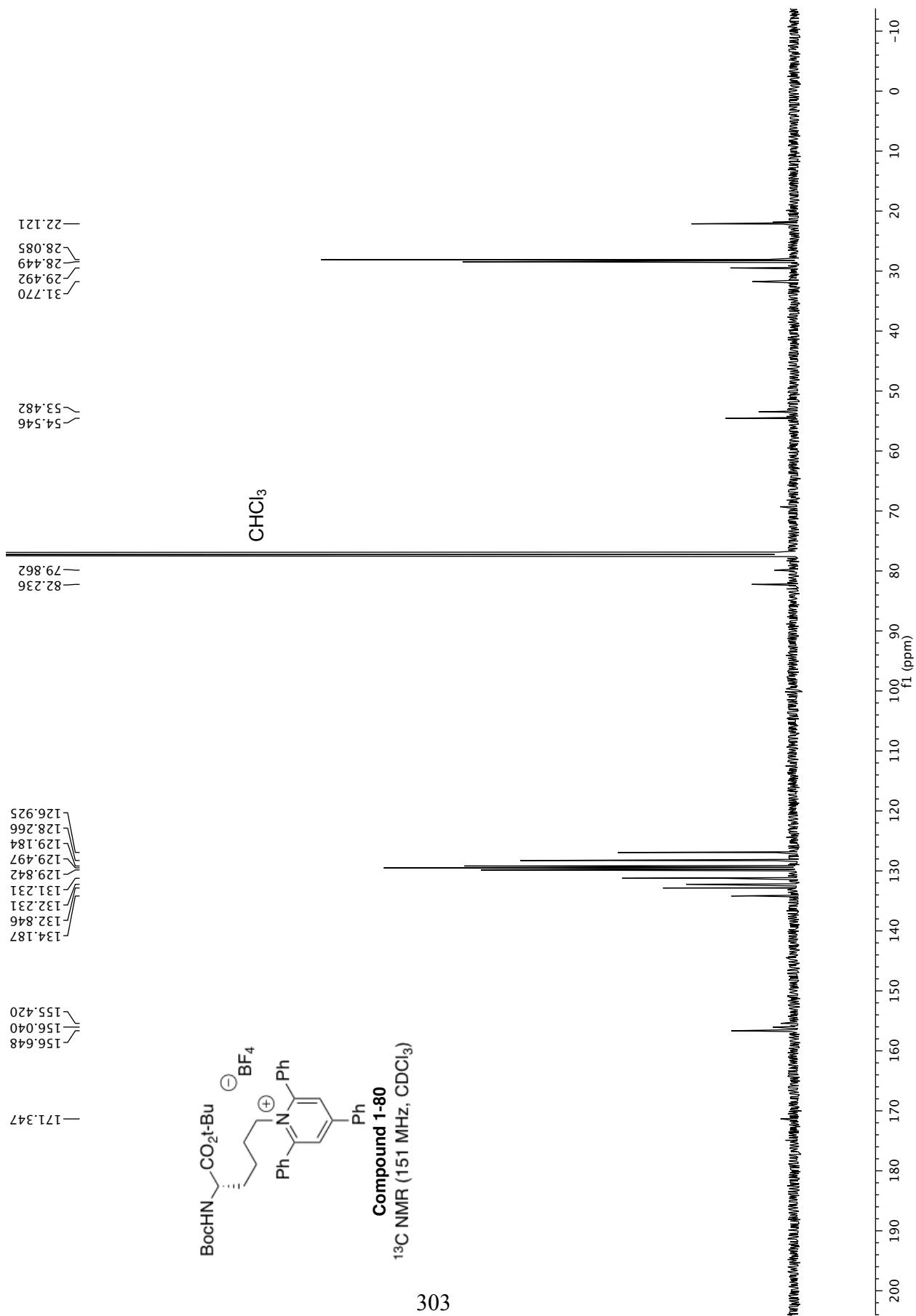
Compound 1-36

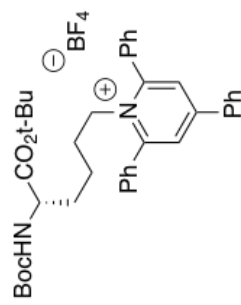
¹⁹F NMR (565 MHz, CDCl₃)

153.021
153.073





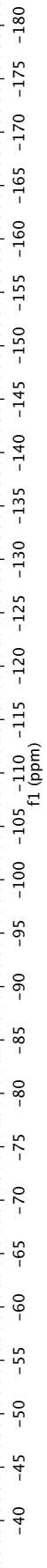




Compound 1-80

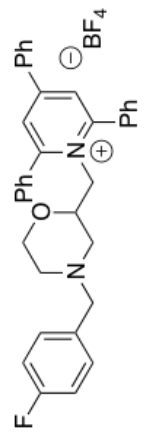
^{19}F NMR (376 MHz, CDCl_3)

153.302
153.355

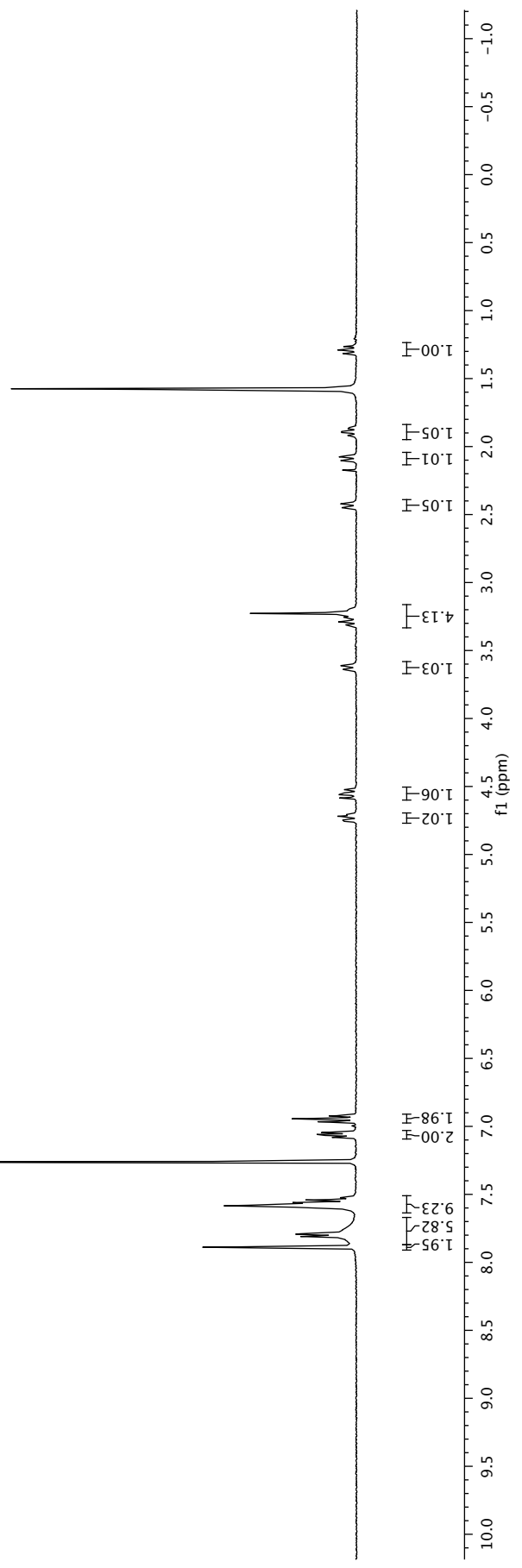


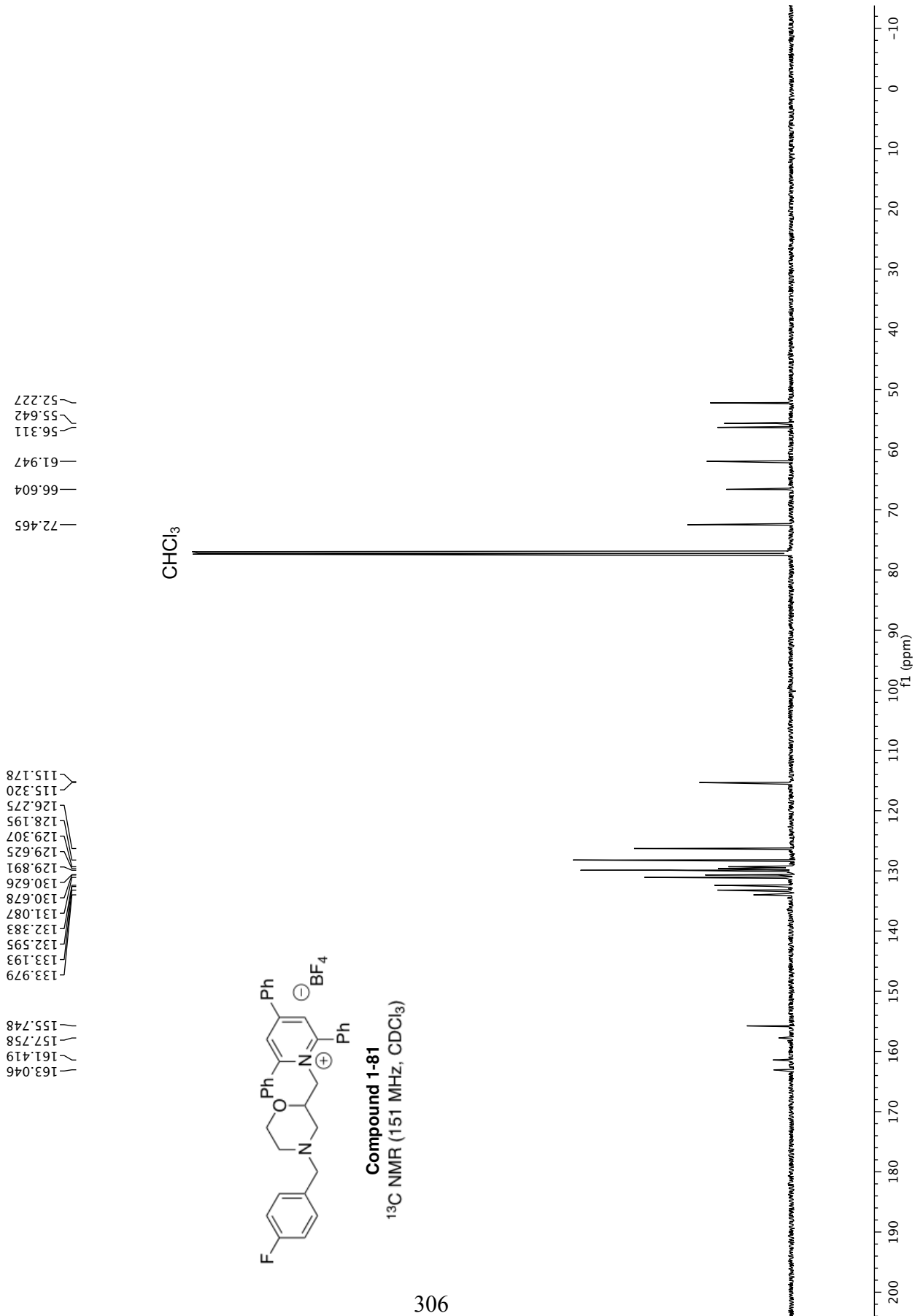
7.889
7.822
7.813
7.810
7.805
7.799
7.793
7.789
7.601
7.590
7.584
7.578
7.572
7.568
7.560
7.556
7.547
7.541
7.535
7.525
7.081
7.076
7.066
7.059
7.051
7.046
7.038
6.973
6.966
6.961
6.950
6.944
6.938
6.928
6.923
4.757
4.746
4.719
4.709
4.585
4.561
4.548
4.523
3.640
3.633
3.617
3.611
3.604
3.317
3.311
3.289
3.283
3.278
3.261
3.255
3.245
3.228
3.220
3.213
3.206
3.197
3.189
2.451
2.446
2.422
2.416
2.103
2.076
1.925
1.917
1.897
1.889
1.869
1.860
1.316
1.293
1.288
1.264

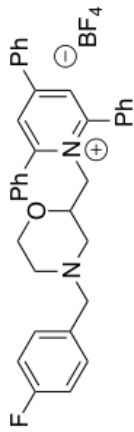
CHCl₃



Compound 1-81
¹H NMR (400 MHz, CDCl₃)







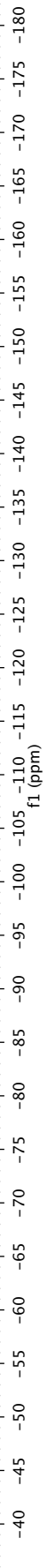
Compound 1-81

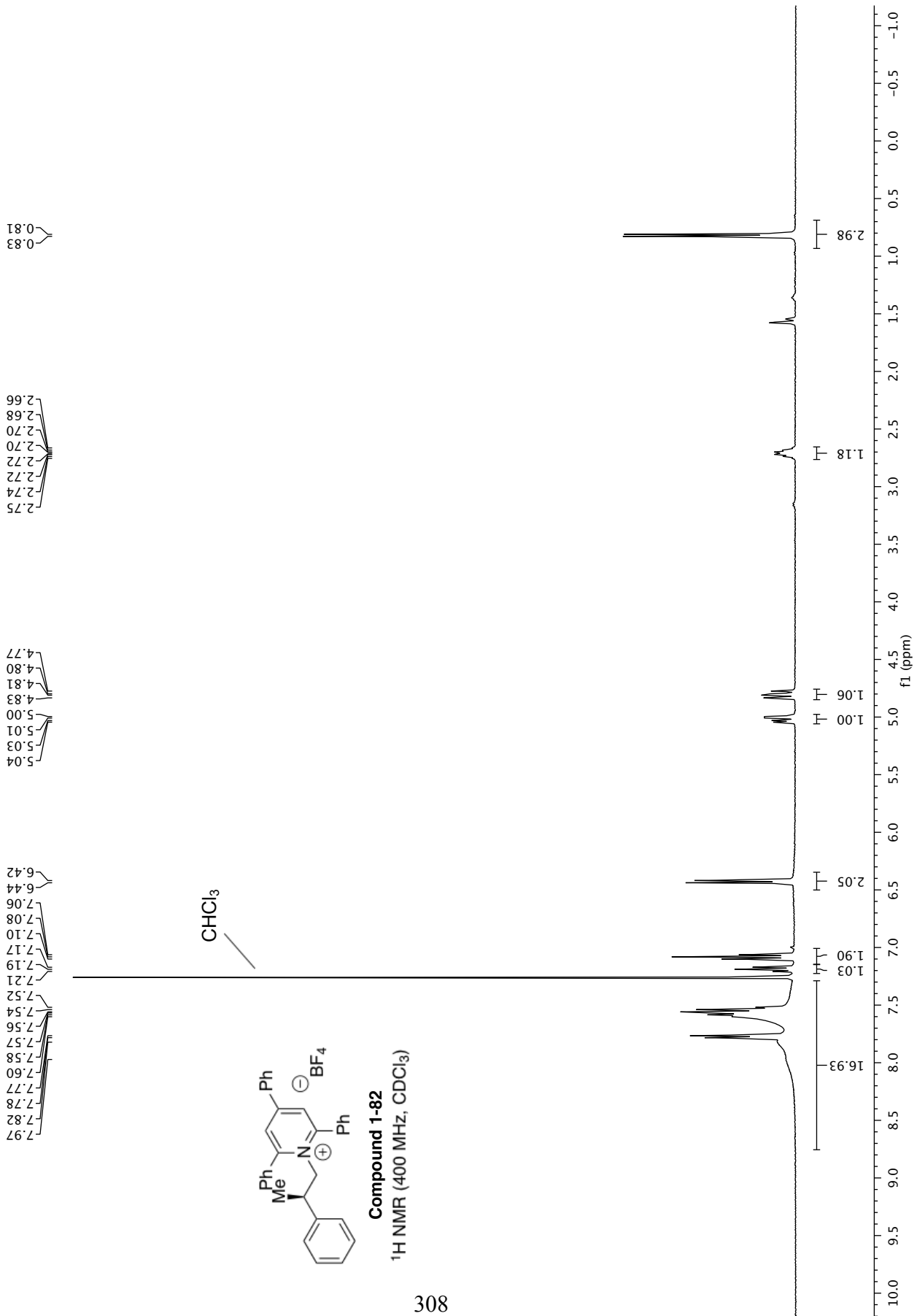
¹⁹F NMR (376 MHz, CDCl₃)

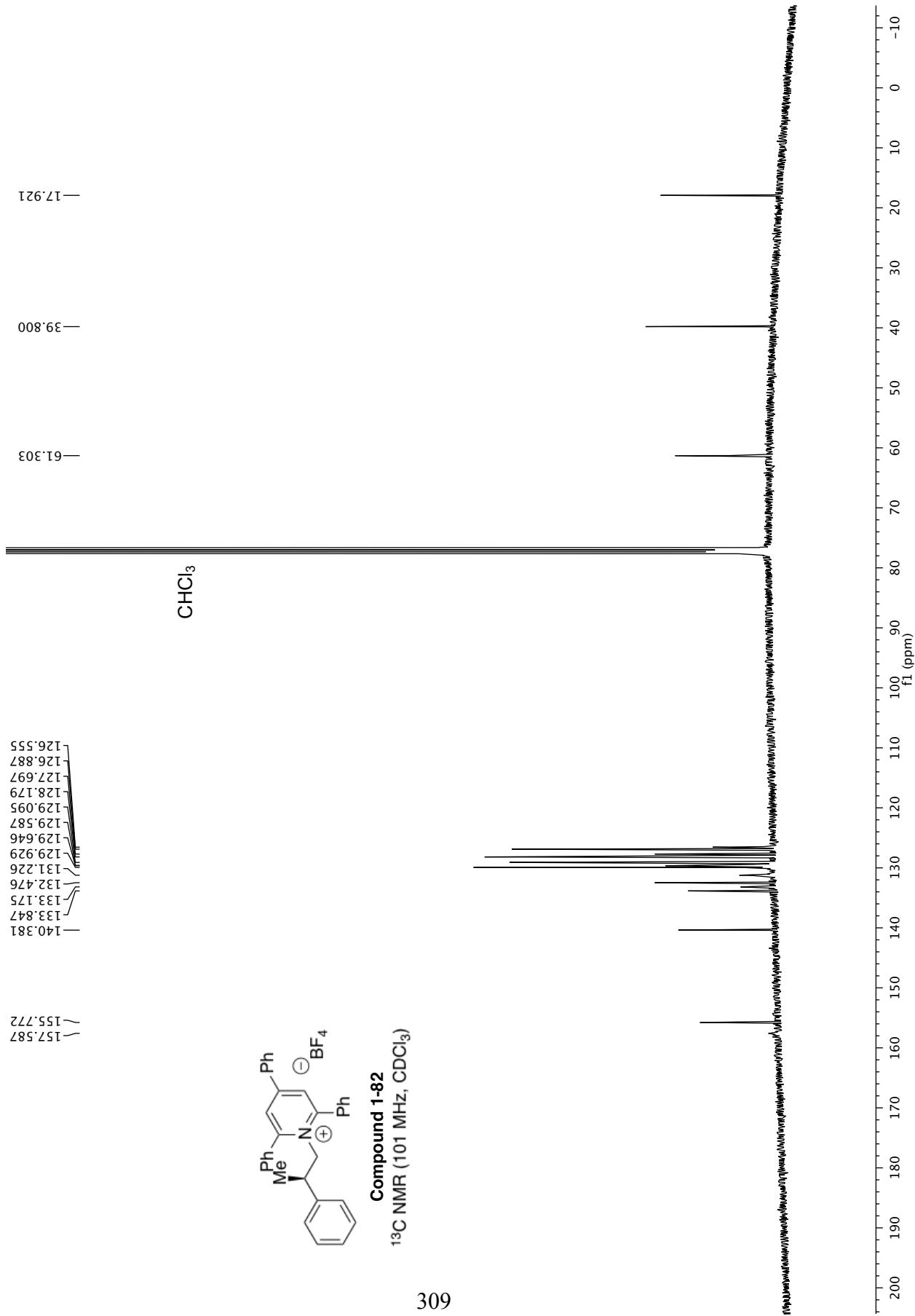
153.222
153.275

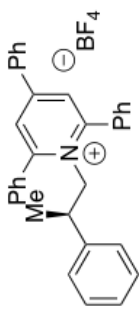
115.296

307





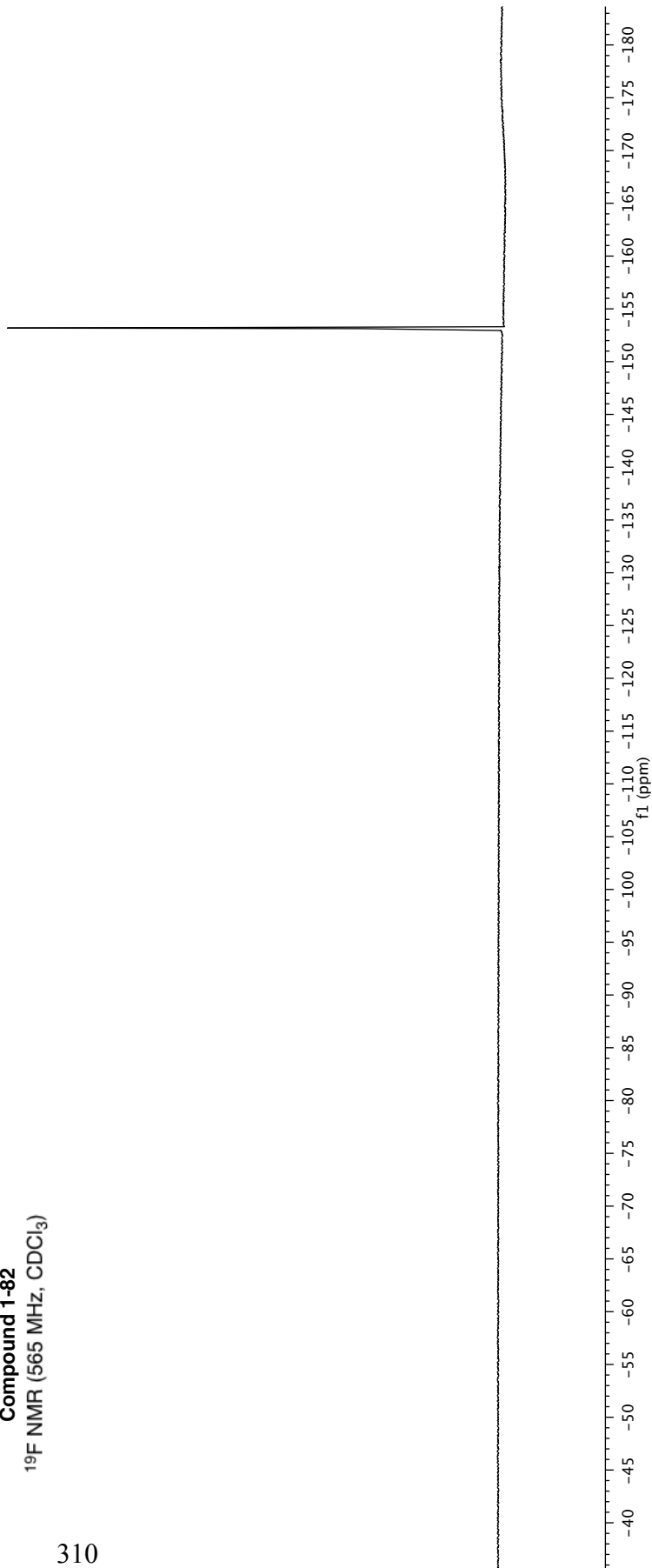




Compound 1-82

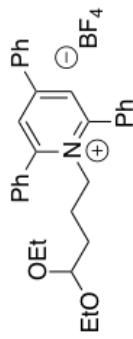
¹⁹F NMR (565 MHz, CDCl₃)

153.127
153.178



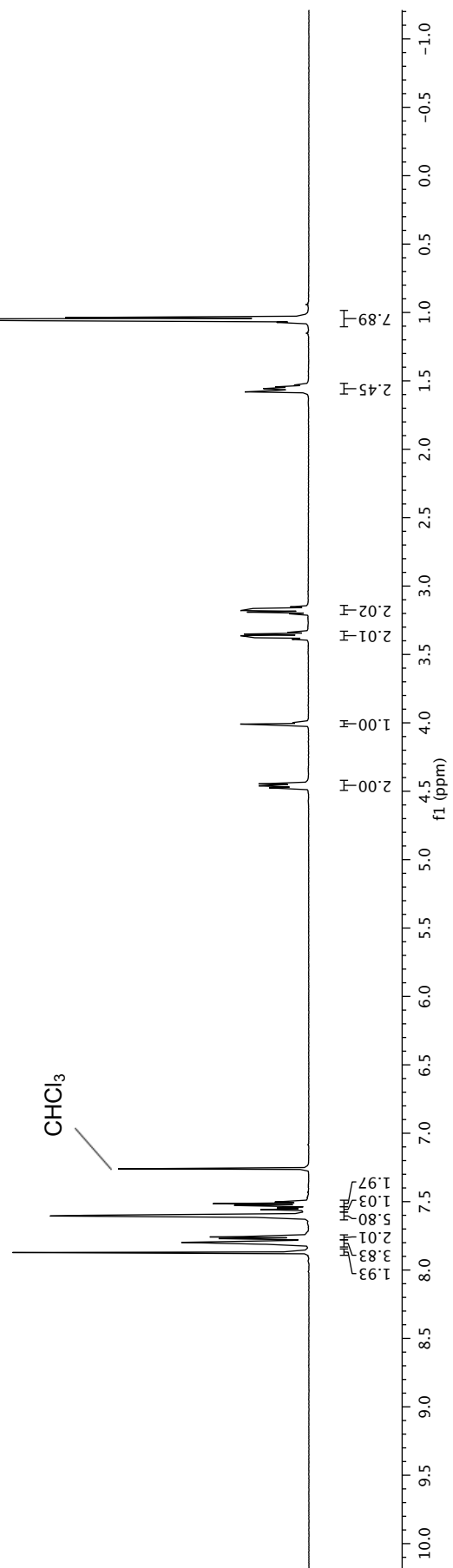
1.037
 1.049
 1.061
 1.072
 1.530
 1.539
 1.544
 1.551
 1.557
 1.562
 1.570
 3.152
 3.164
 3.167
 3.175
 3.179
 3.187
 3.191
 3.203
 3.339
 3.351
 3.354
 3.363
 3.366
 3.374
 3.378
 3.390
 4.000
 4.009
 4.018
 4.446
 4.460
 4.474

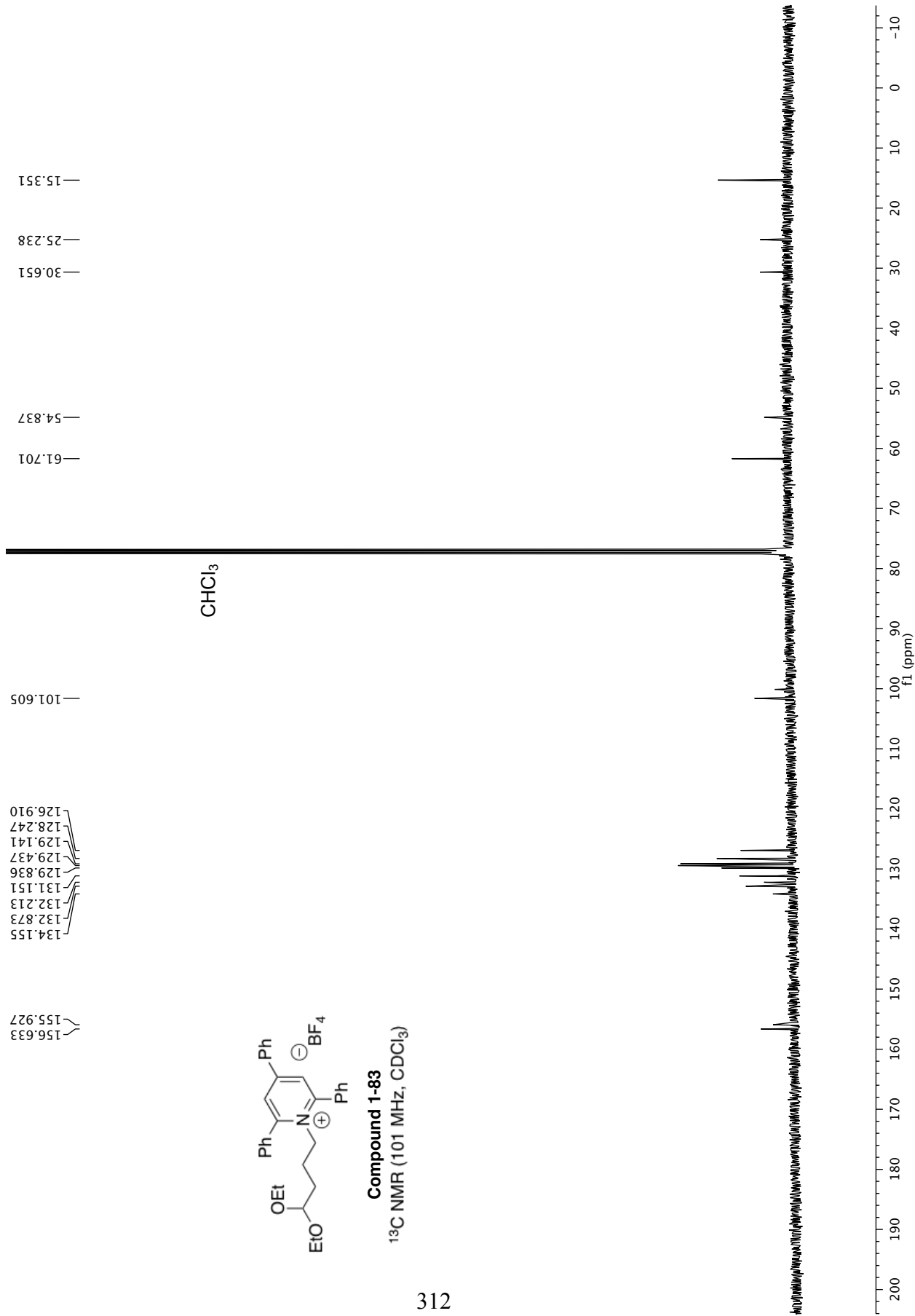
7.260
 7.503
 7.506
 7.515
 7.528
 7.546
 7.555
 7.558
 7.563
 7.571
 7.600
 7.605
 7.610
 7.756
 7.758
 7.770
 7.794
 7.798
 7.804
 7.809
 7.872

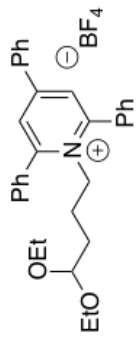


Compound 1-83

¹H NMR (600 MHz, CDCl₃)





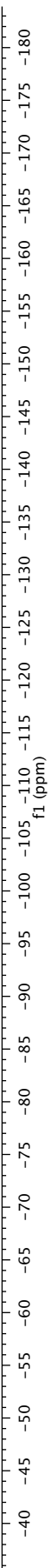


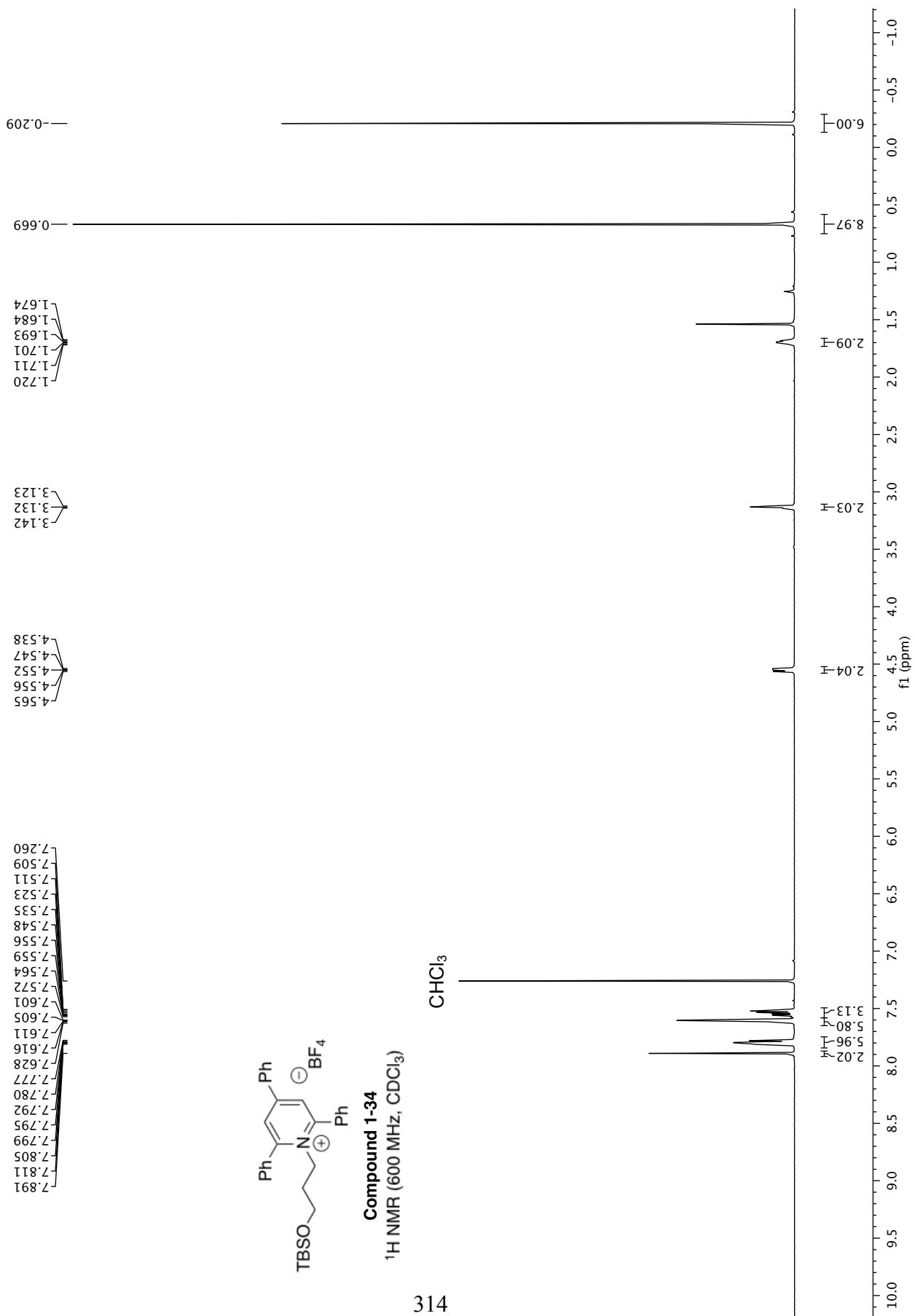
Compound 1-83

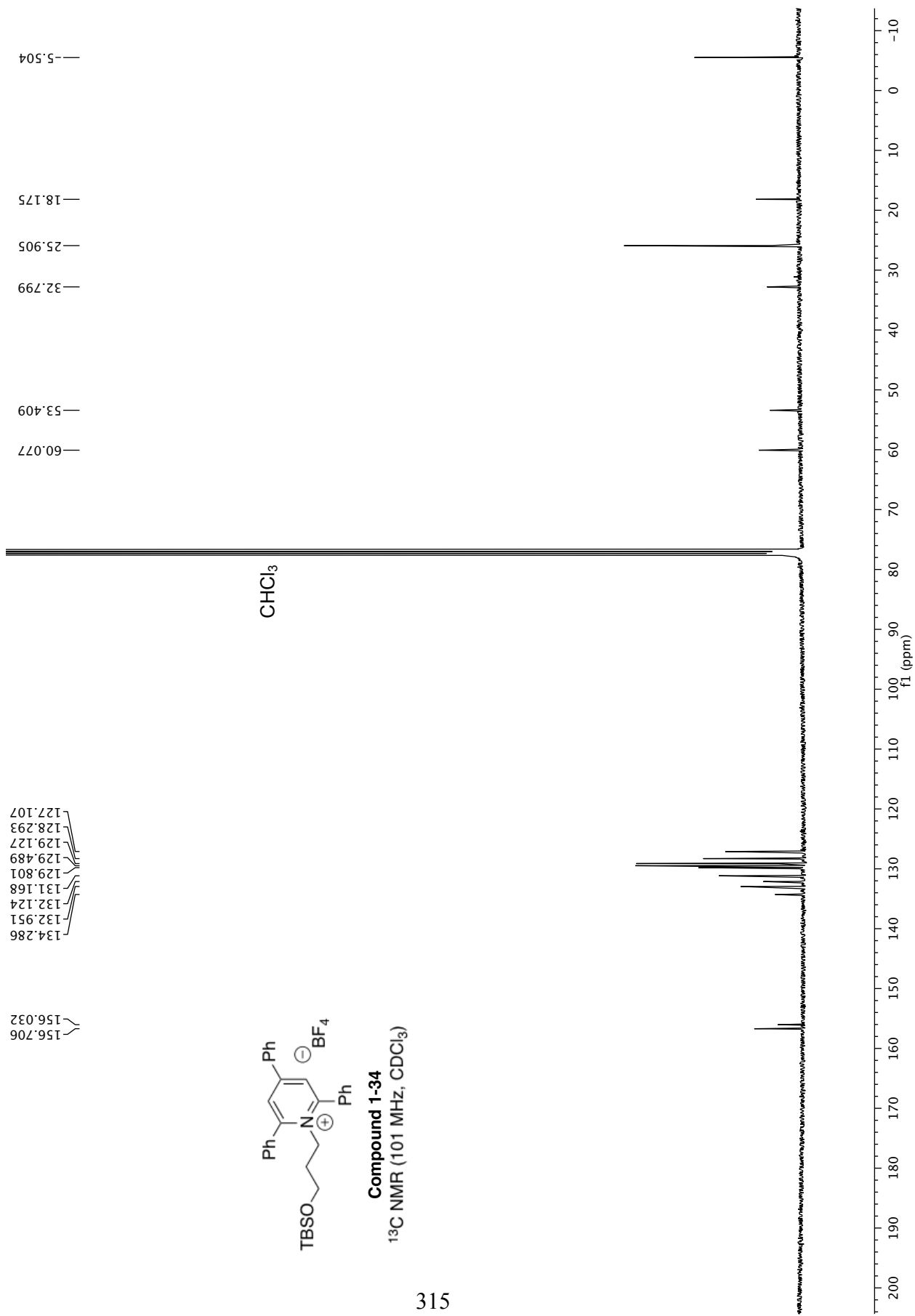
¹⁹F NMR (376 MHz, CDCl₃)

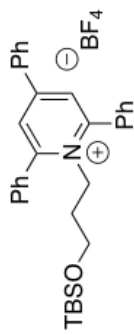
-153.464
-153.411

313







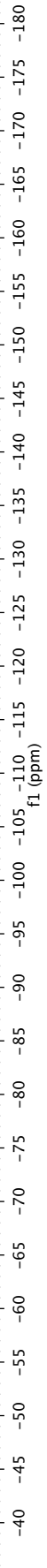


Compound 1-34

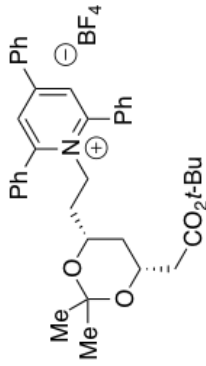
¹⁹F NMR (376 MHz, CDCl₃)

153.425
153.477

316

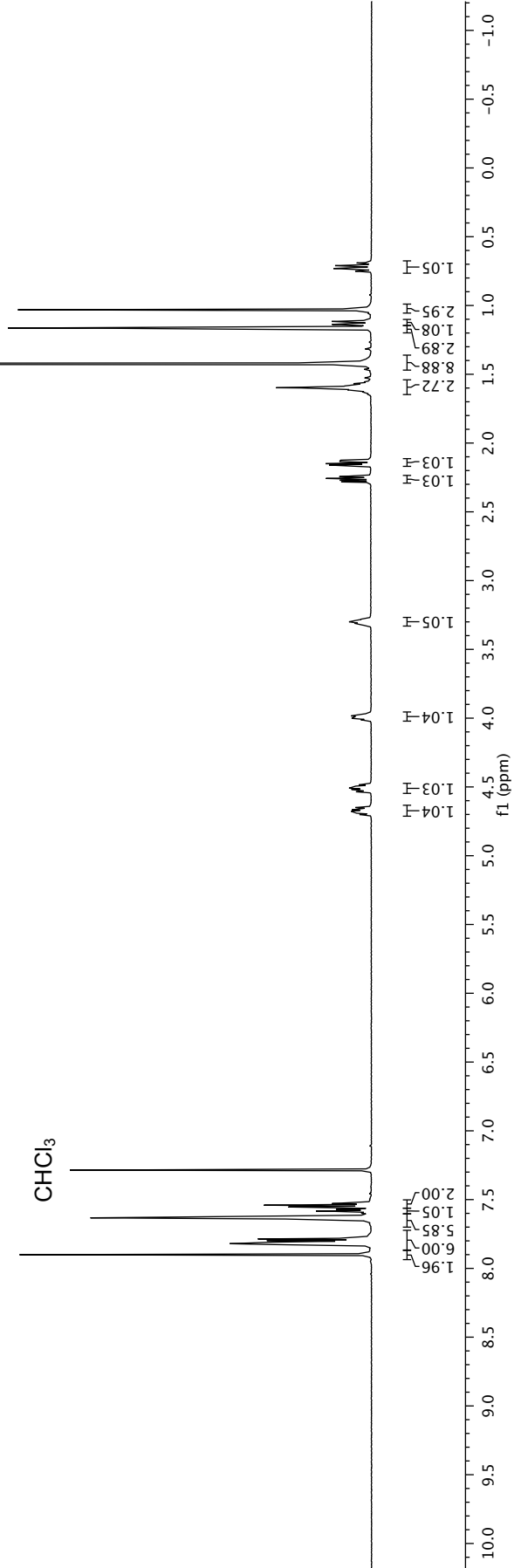


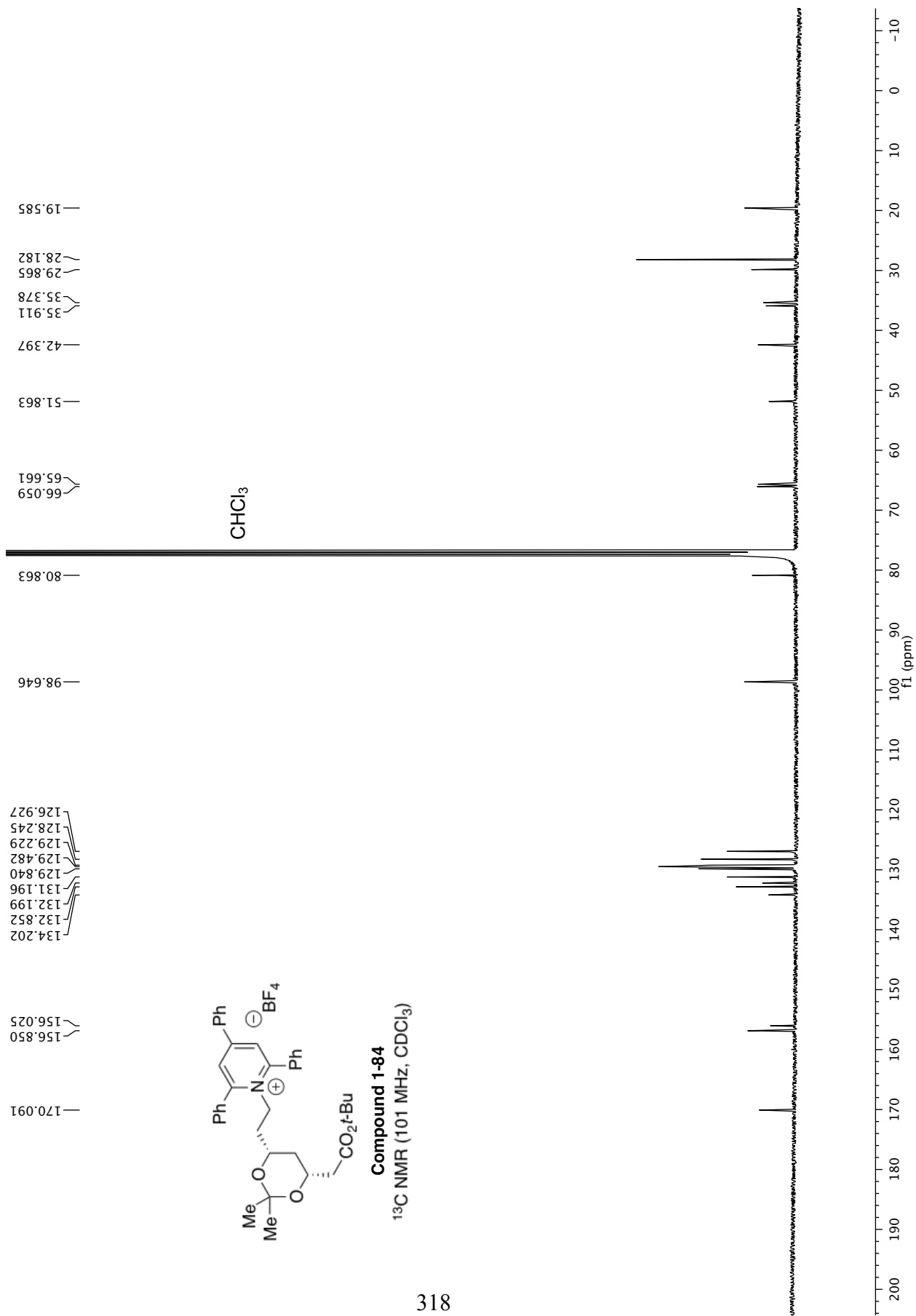
7.901
7.826
7.821
7.815
7.811
7.798
7.786
7.784
7.638
7.633
7.628
7.597
7.589
7.584
7.581
7.572
7.554
7.541
7.529
4.701
4.691
4.683
4.677
4.673
4.667
4.660
4.650
4.535
4.526
4.518
4.509
4.503
4.494
4.485
4.015
4.011
4.002
3.996
3.993
3.990
3.984
3.974
3.971
3.923
3.317
3.311
3.304
3.299
3.292
3.287
3.281
2.283
2.271
2.257
2.245
2.160
2.150
2.134
2.124
1.636
1.629
1.622
1.613
1.606
1.591
1.586
1.581
1.578
1.568
1.558
1.555
1.545
1.424
1.164
1.141
1.137
1.134
1.120
1.116
1.113
1.031
0.750
0.731
0.710
0.691

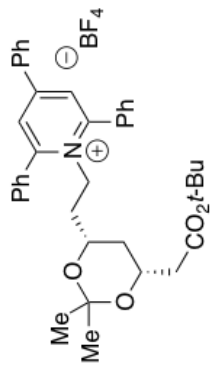


Compound 1-84
¹H NMR (600 MHz, CDCl₃)

317





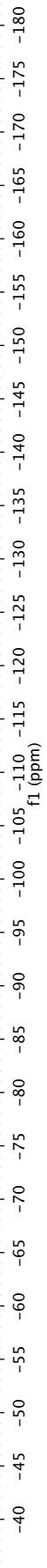


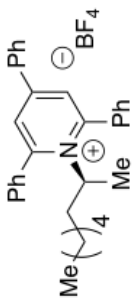
Compound 1-84

¹⁹F NMR (376 MHz, CDCl₃)

-153.319
-153.372

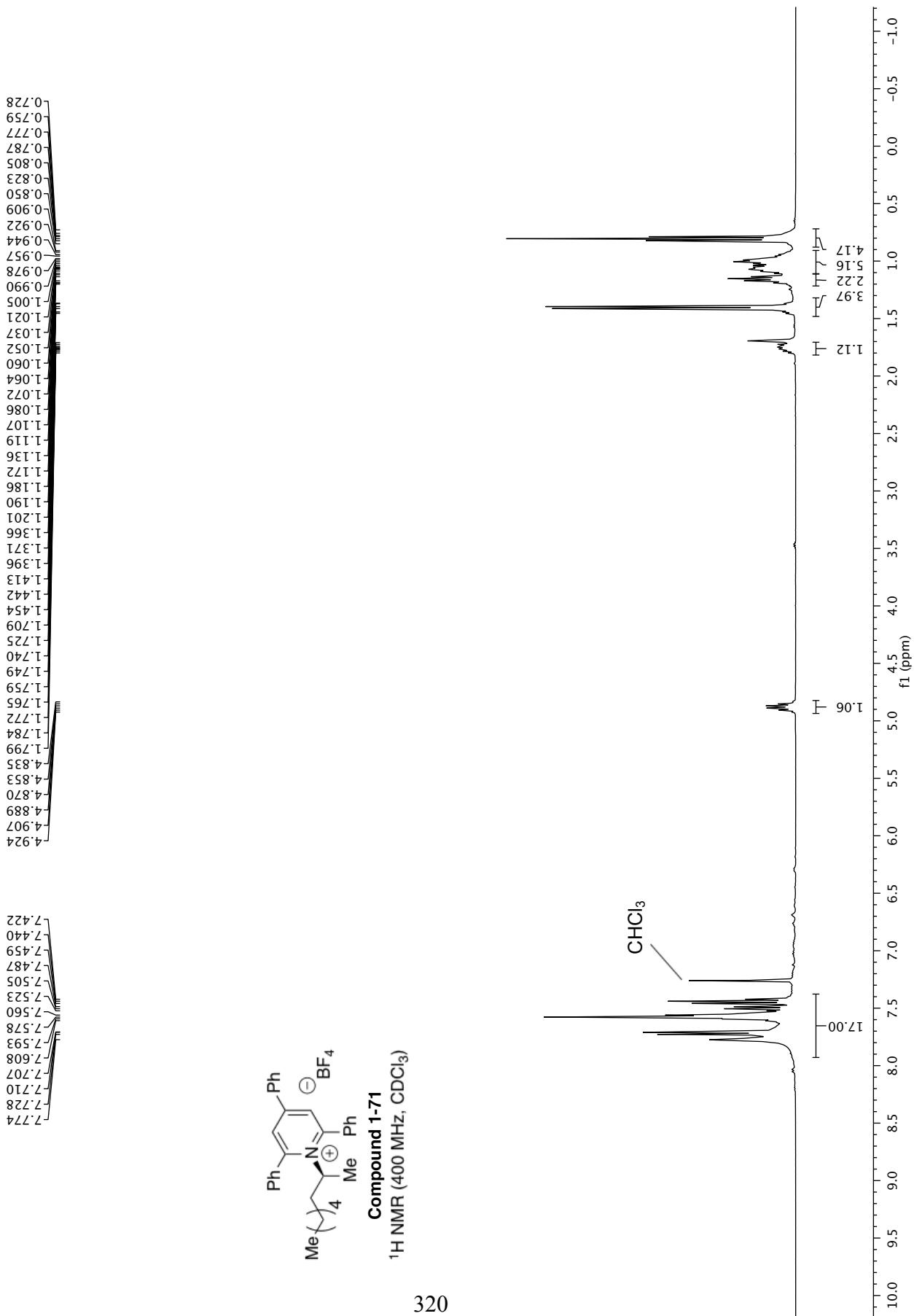
319

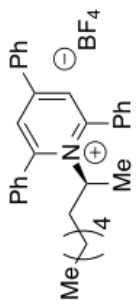




Compound 1-71

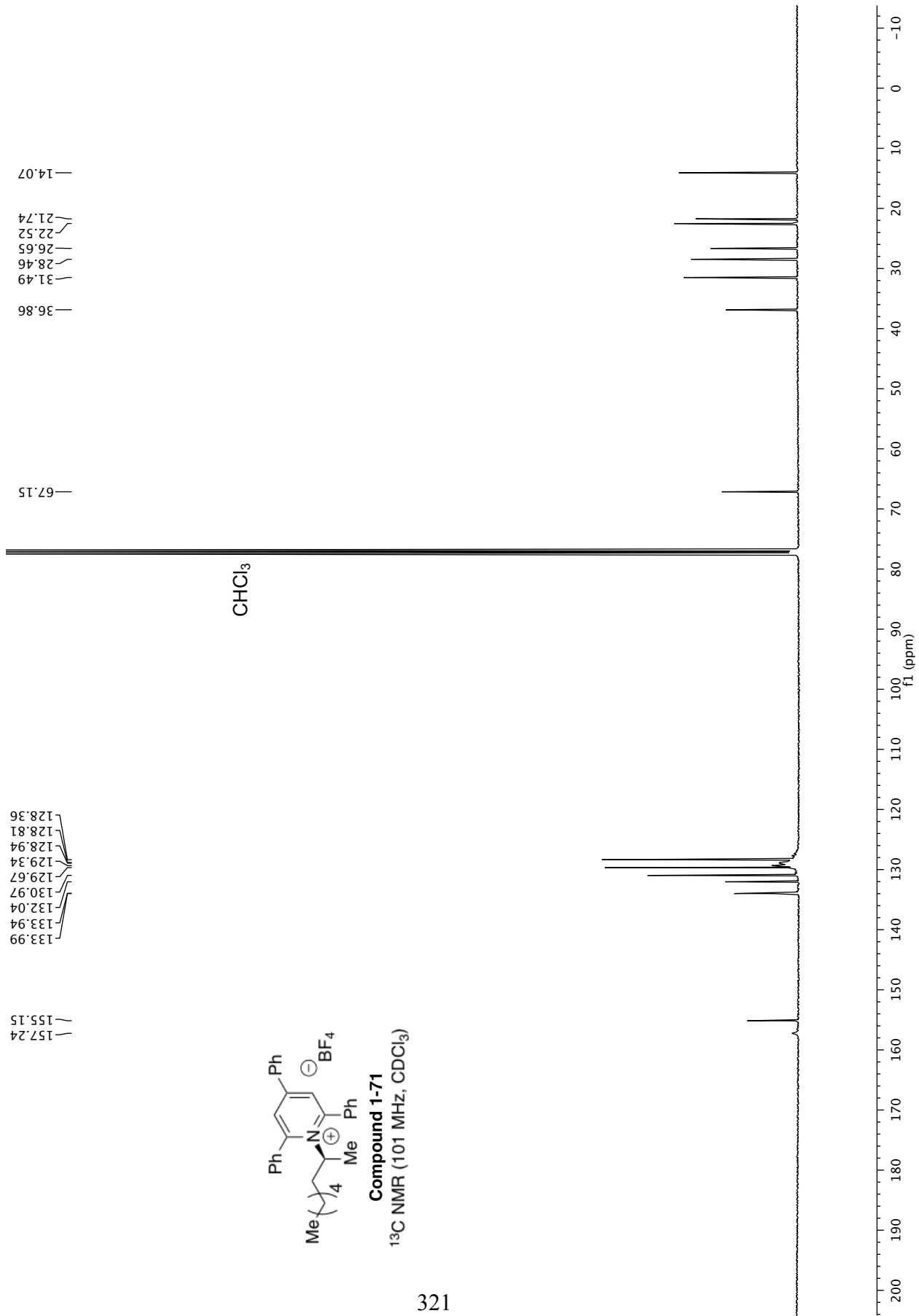
¹H NMR (400 MHz, CDCl₃)

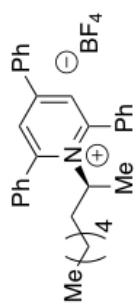




Compound 1-71

^{13}C NMR (101 MHz, CDCl_3)



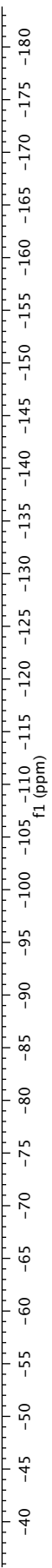


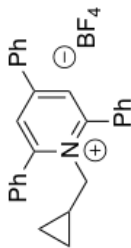
Compound 1-71

¹⁹F NMR (376 MHz, CDCl₃)

-153.25
-153.31

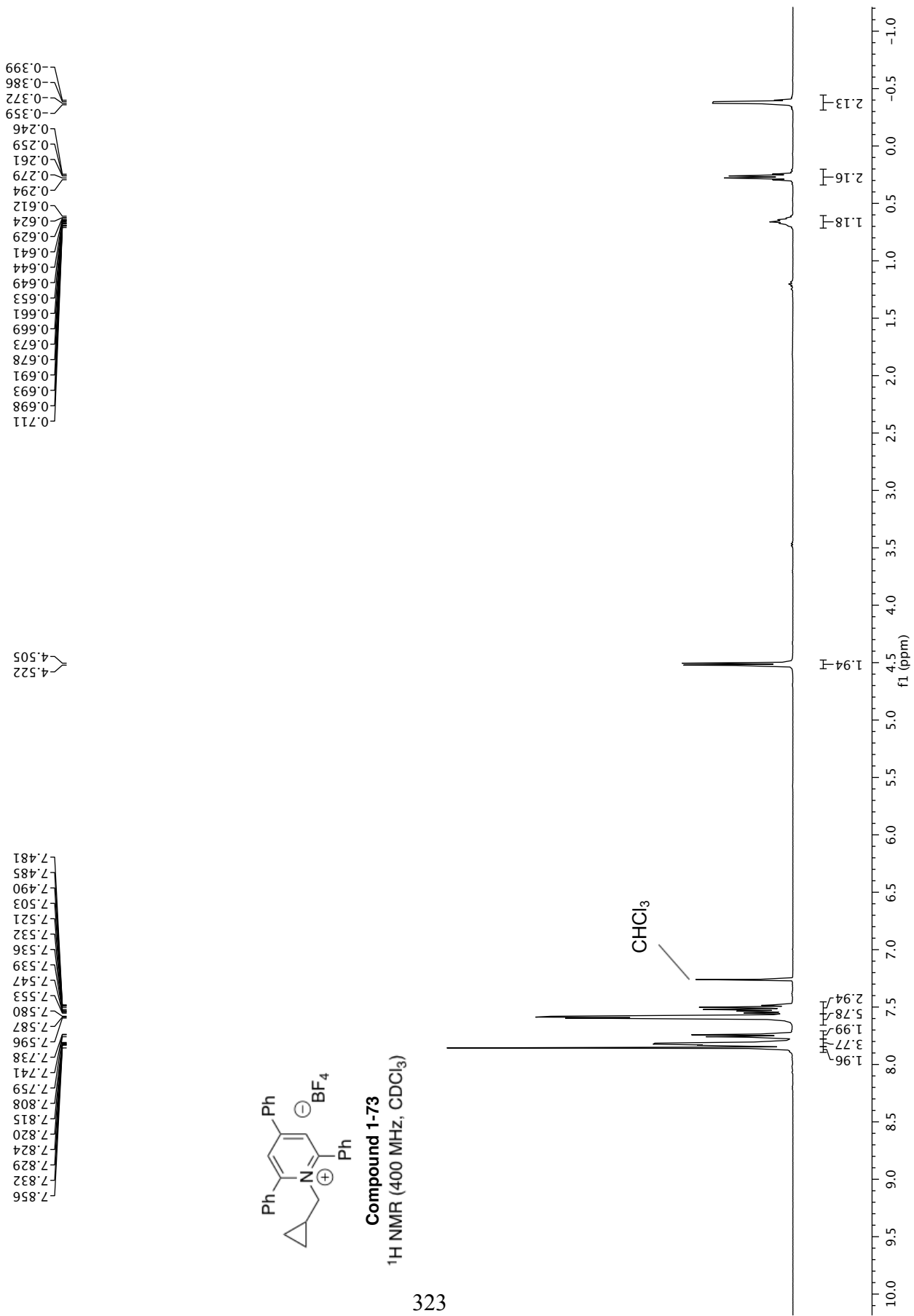
322

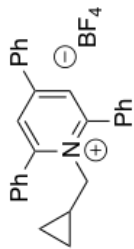




Compound 1-73
 ^1H NMR (400 MHz, CDCl_3)

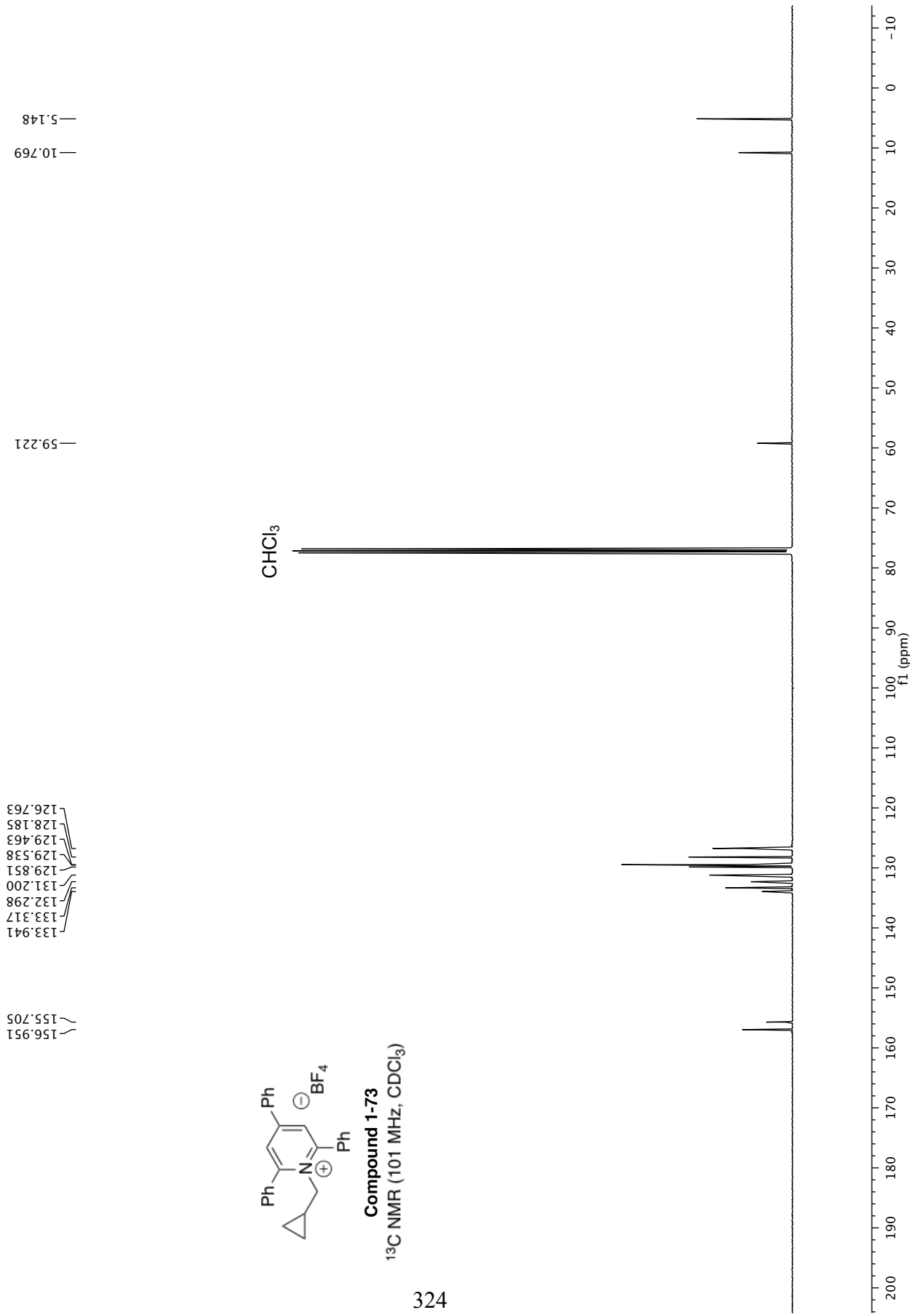
323

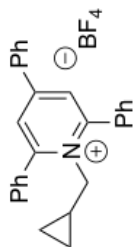




Compound 1-73

^{13}C NMR (101 MHz, CDCl_3)





Compound 1-73

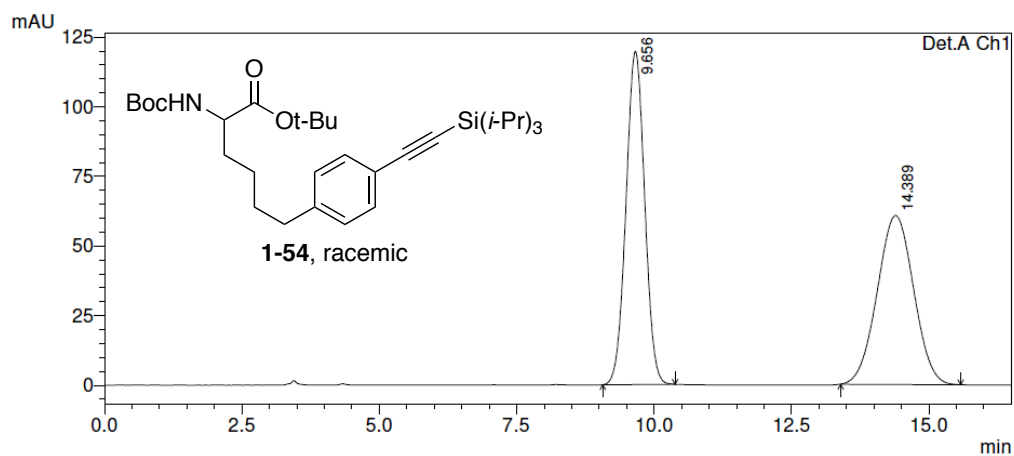
¹⁹F NMR (376 MHz, CDCl₃)

153.232
153.286

325

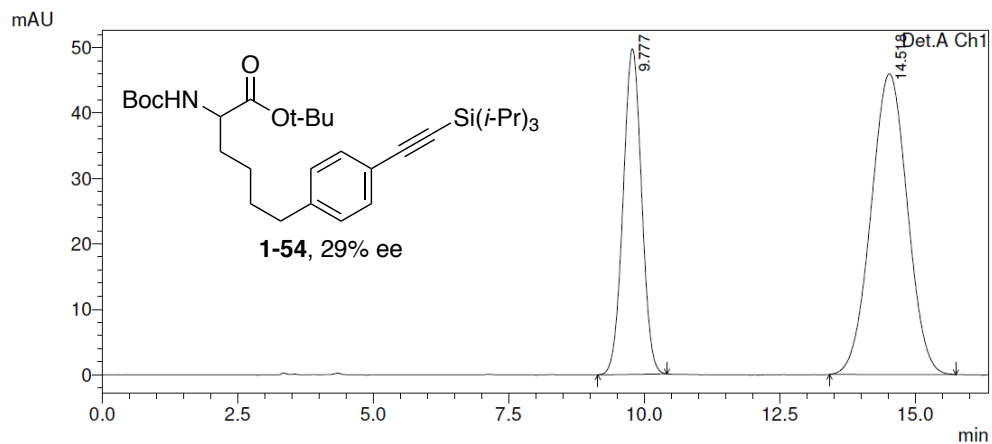
-40 -45 -50 -55 -60 -65 -70 -75 -80 -85 -90 -95 -100 -105 -110 -115 -120 -125 -130 -135 -140 -145 -150 -155 -160 -165 -170 -175 -180
f1 (ppm)

Compound 1-54, racemic (254 nm)



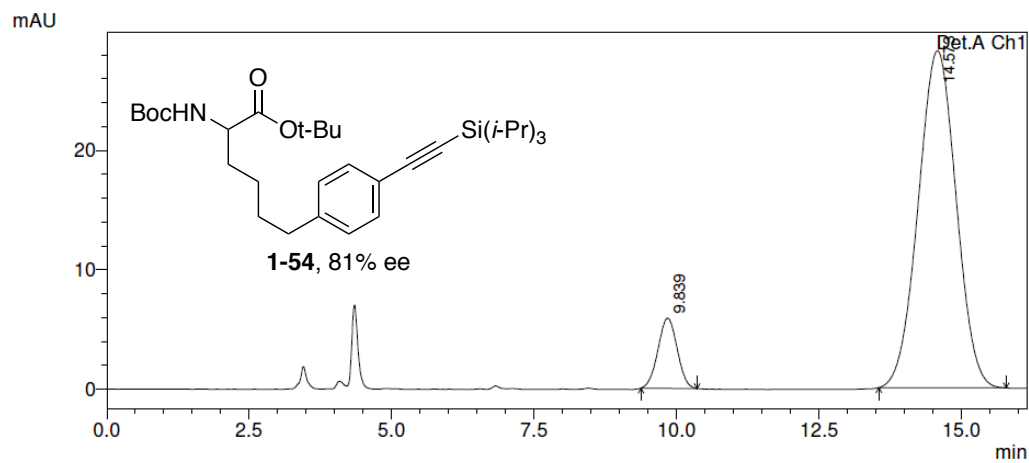
Peak#	Ret. Time	Area	Height	Area %	Height %
1	9.656	2833525	119647	50.307	66.357
2	14.389	2798895	60660	49.693	33.643
Total		5632419	180307	100.000	100.000

Compound 1-54, 29% ee (254 nm)



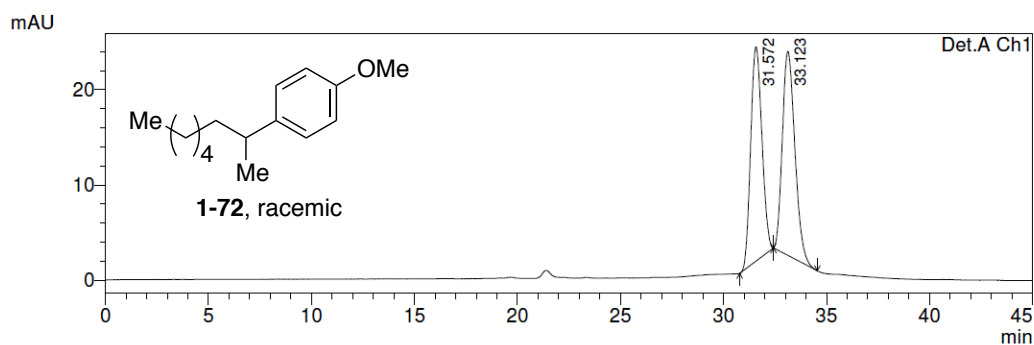
Peak#	Ret. Time	Area	Height	Area %	Height %
1	9.777	1180374	49751	35.522	51.983
2	14.518	2142537	45955	64.478	48.017
Total		3322911	95706	100.000	100.000

Compound 1-54, 81% ee (254 nm), reaction with 4-(trifluoromethyl)phenol additive



Peak#	Ret. Time	Area	Height	Area %	Height %
1	9.839	137403	5876	9.510	17.224
2	14.573	1307395	28238	90.490	82.776
Total		1444798	34114	100.000	100.000

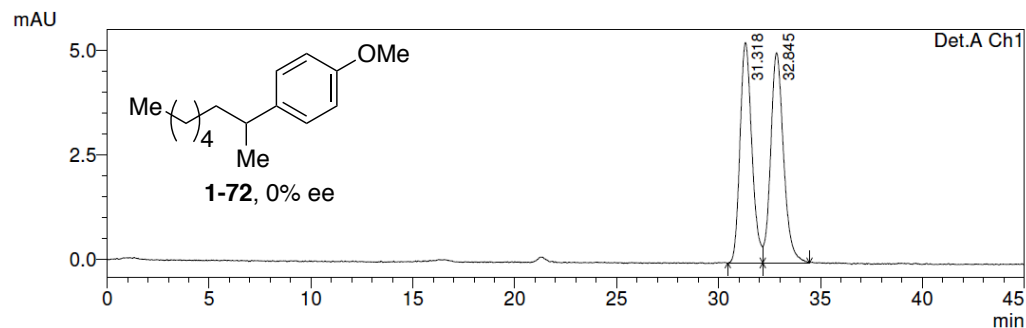
Compound 1-72, racemic (254 nm)



Detector A Ch1 254nm

Peak#	Ret. Time	Area	Height	Area %	Height %
1	31.572	850548	22514	48.386	51.255
2	33.123	907290	21411	51.614	48.745
Total		1757837	43925	100.000	100.000

Compound 1-72, 0% ee (254 nm), from cross-coupling reaction

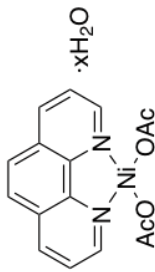


Detector A Ch1 254nm

Peak#	Ret. Time	Area	Height	Area %	Height %
1	31.318	212990	5277	49.079	51.202
2	32.845	220984	5029	50.921	48.798
Total		433974	10306	100.000	100.000

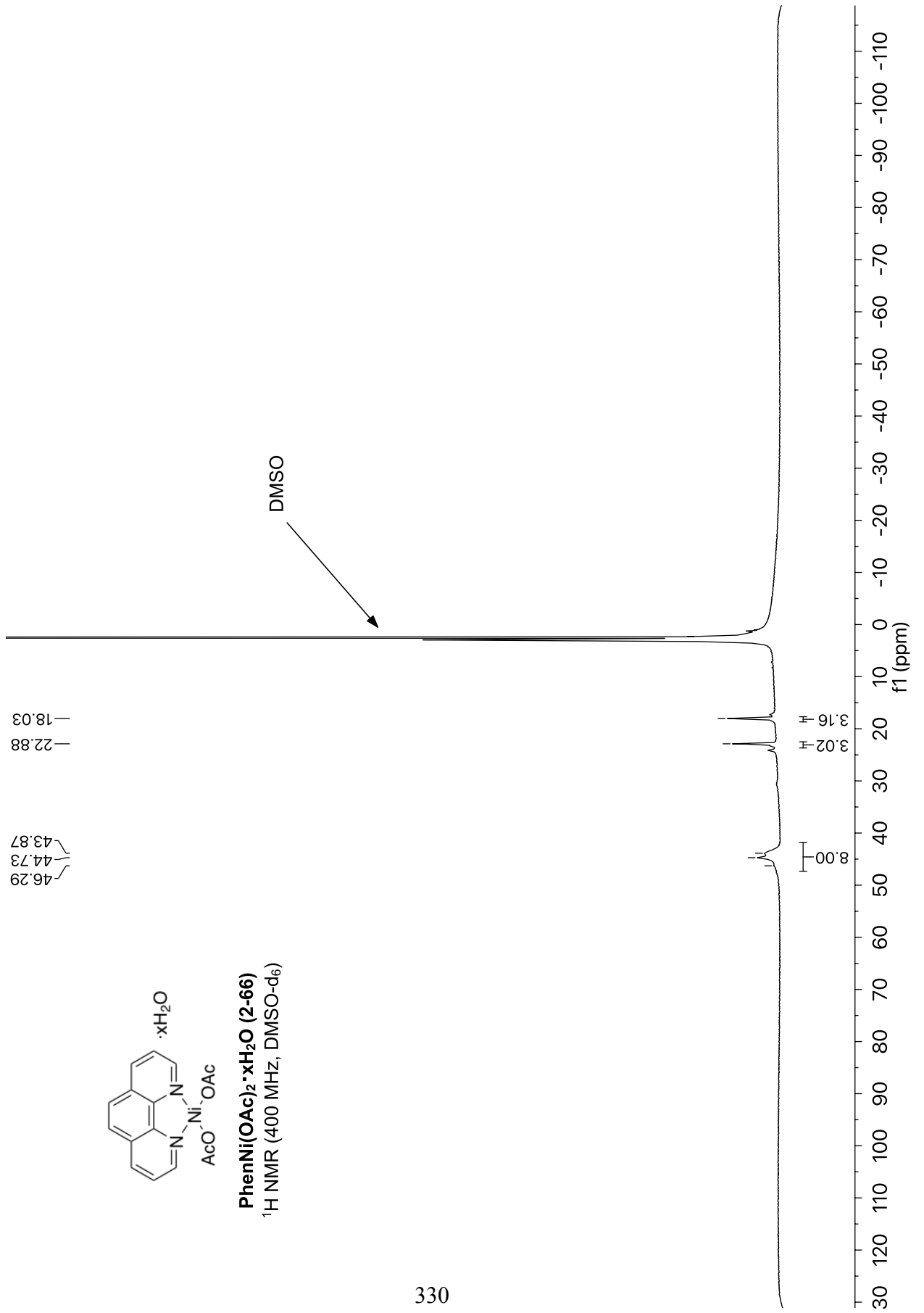
Appendix B

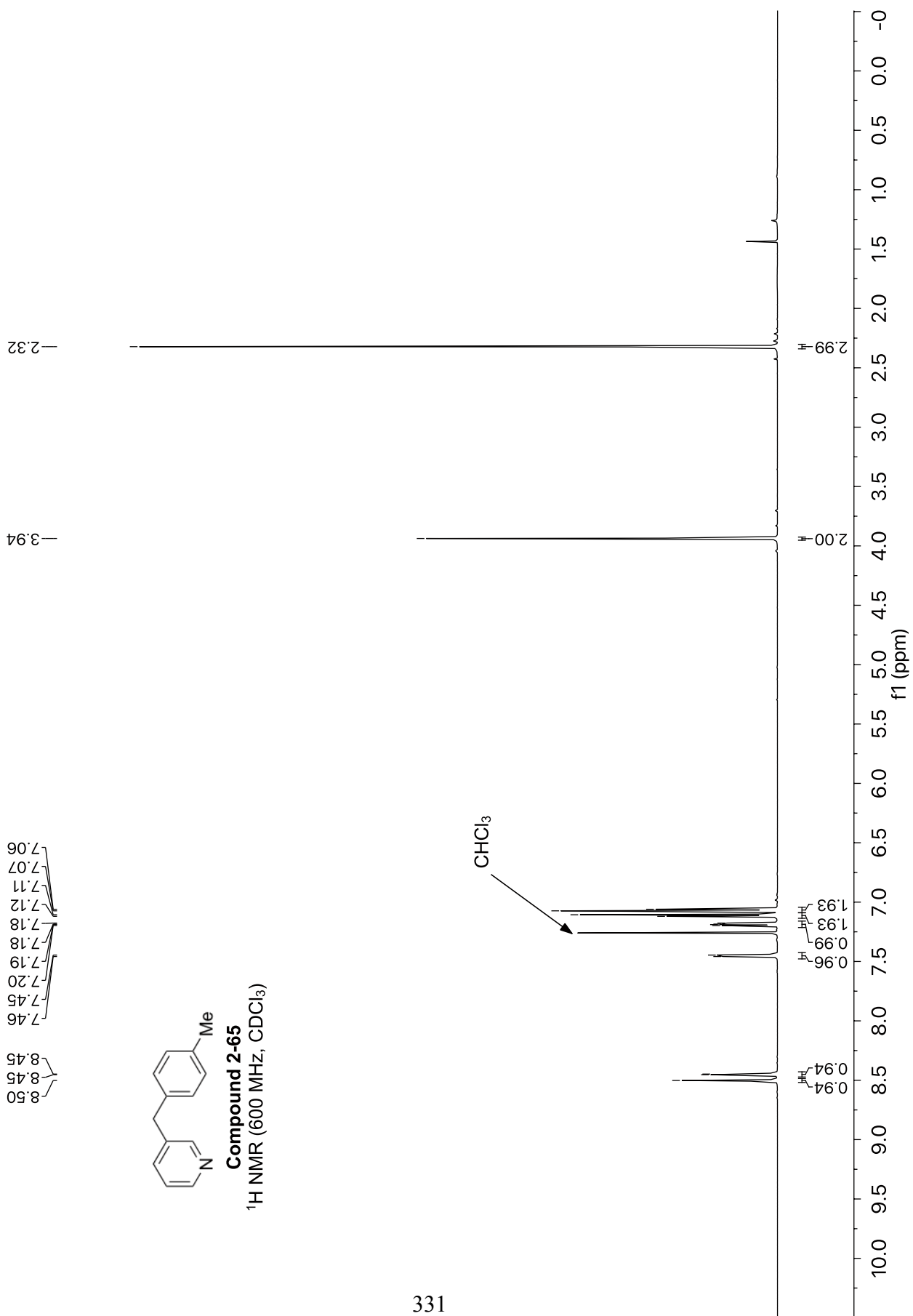
SPECTRAL AND CHROMATOGRAPHY DATA FOR CHAPTER 2

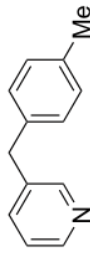


PhenNi(OAc)₂·xH₂O (2-66)

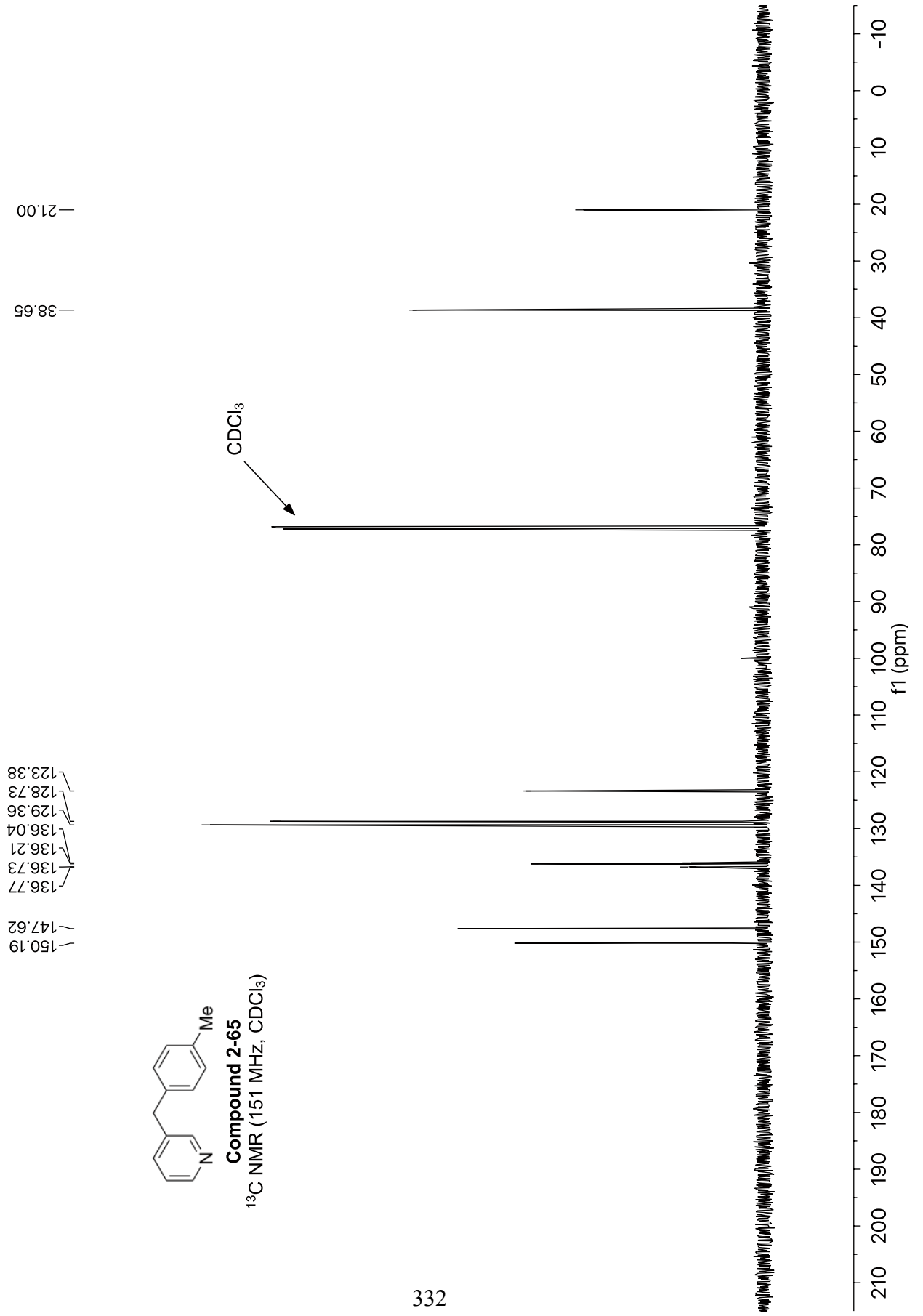
¹H NMR (400 MHz, DMSO-d₆)

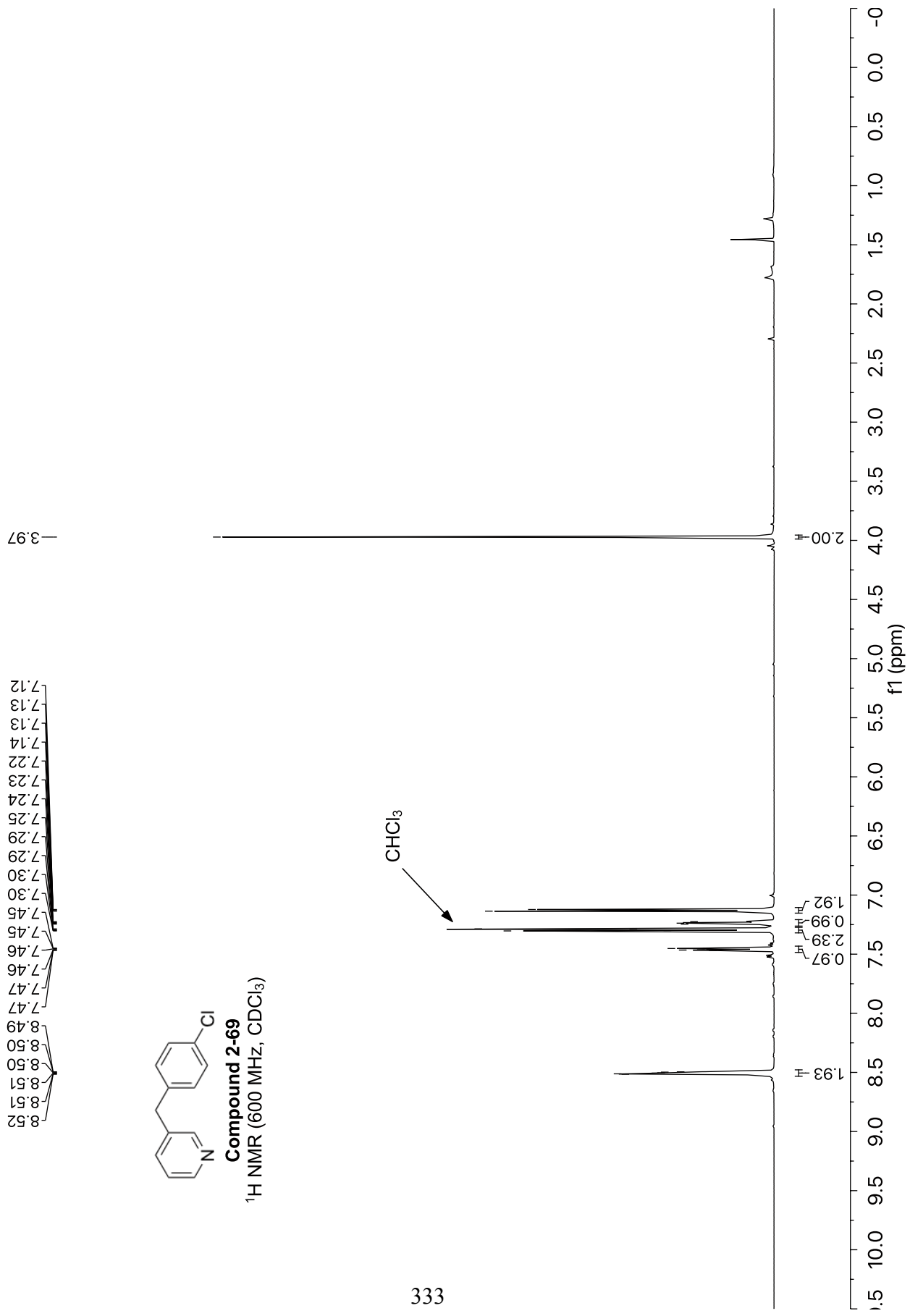


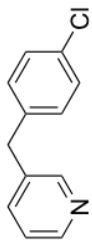




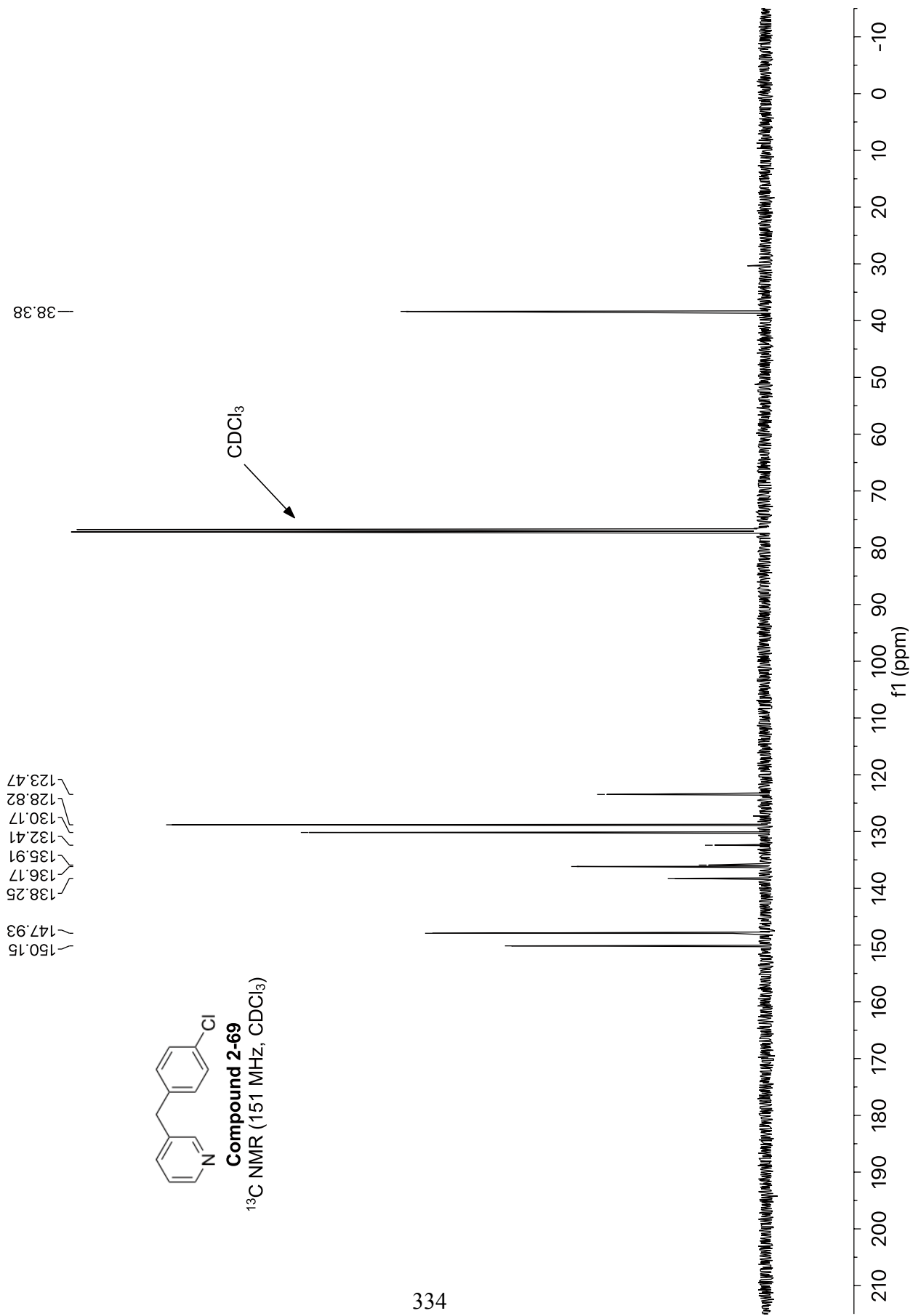
Compound 2-65
 ^{13}C NMR (151 MHz, CDCl_3)

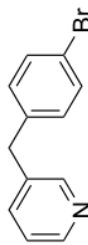






Compound 2-69
 ^{13}C NMR (151 MHz, CDCl_3)





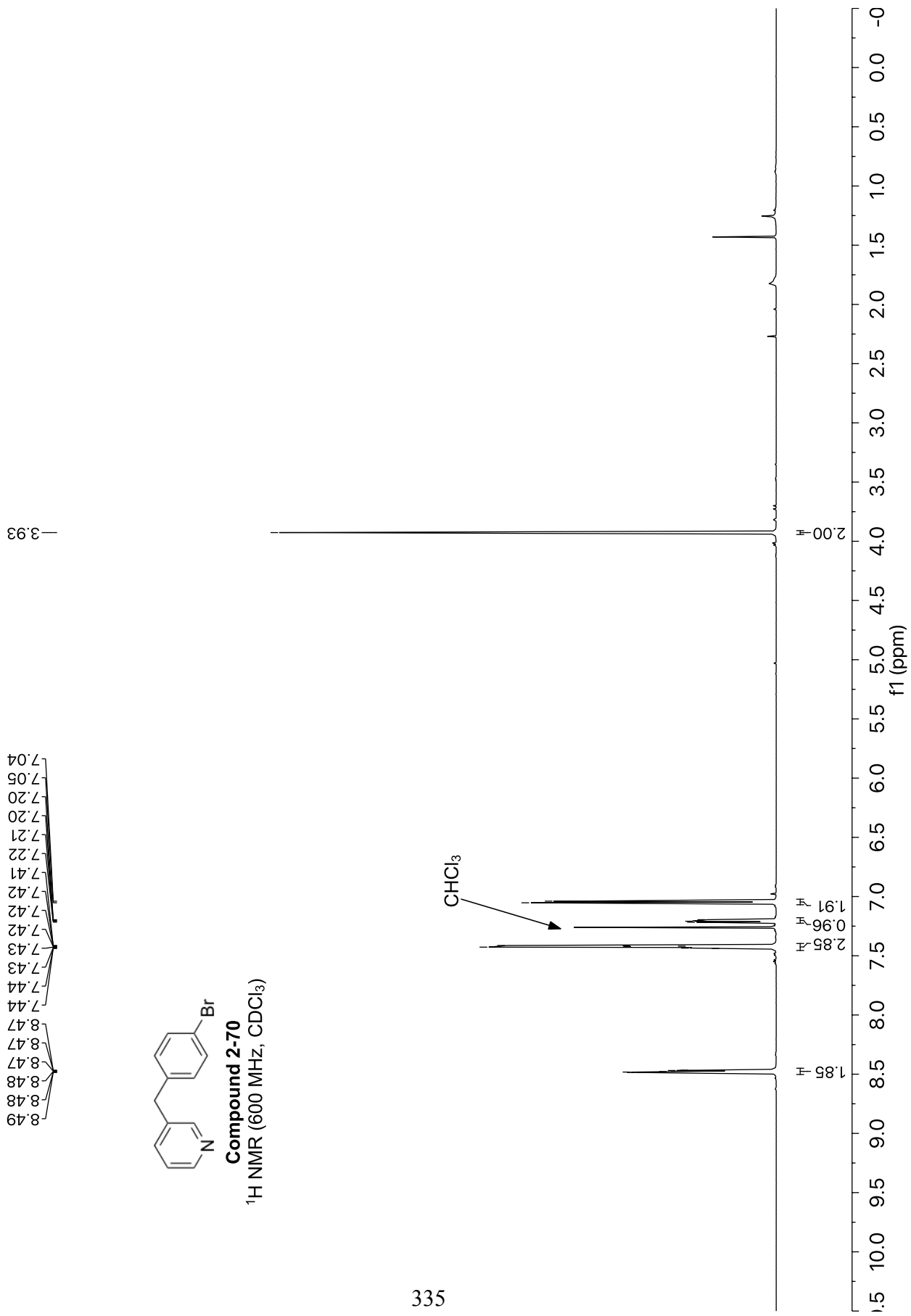
Compound 2-70

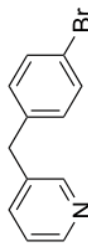
¹H NMR (600 MHz, CDCl₃)

8.49, 8.48, 8.48, 8.47, 8.47, 8.47, 8.44, 7.44, 7.43, 7.43, 7.42, 7.42, 7.41, 7.22, 7.21, 7.20, 7.20, 7.05, 7.04

3.93

335



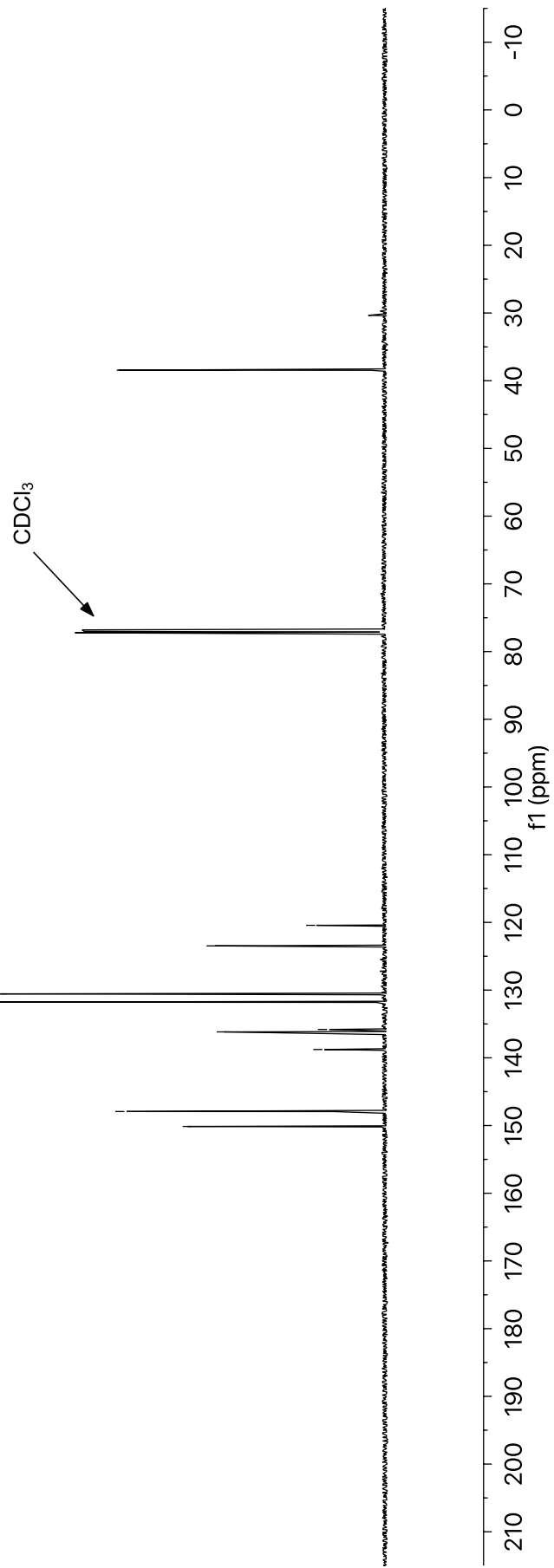


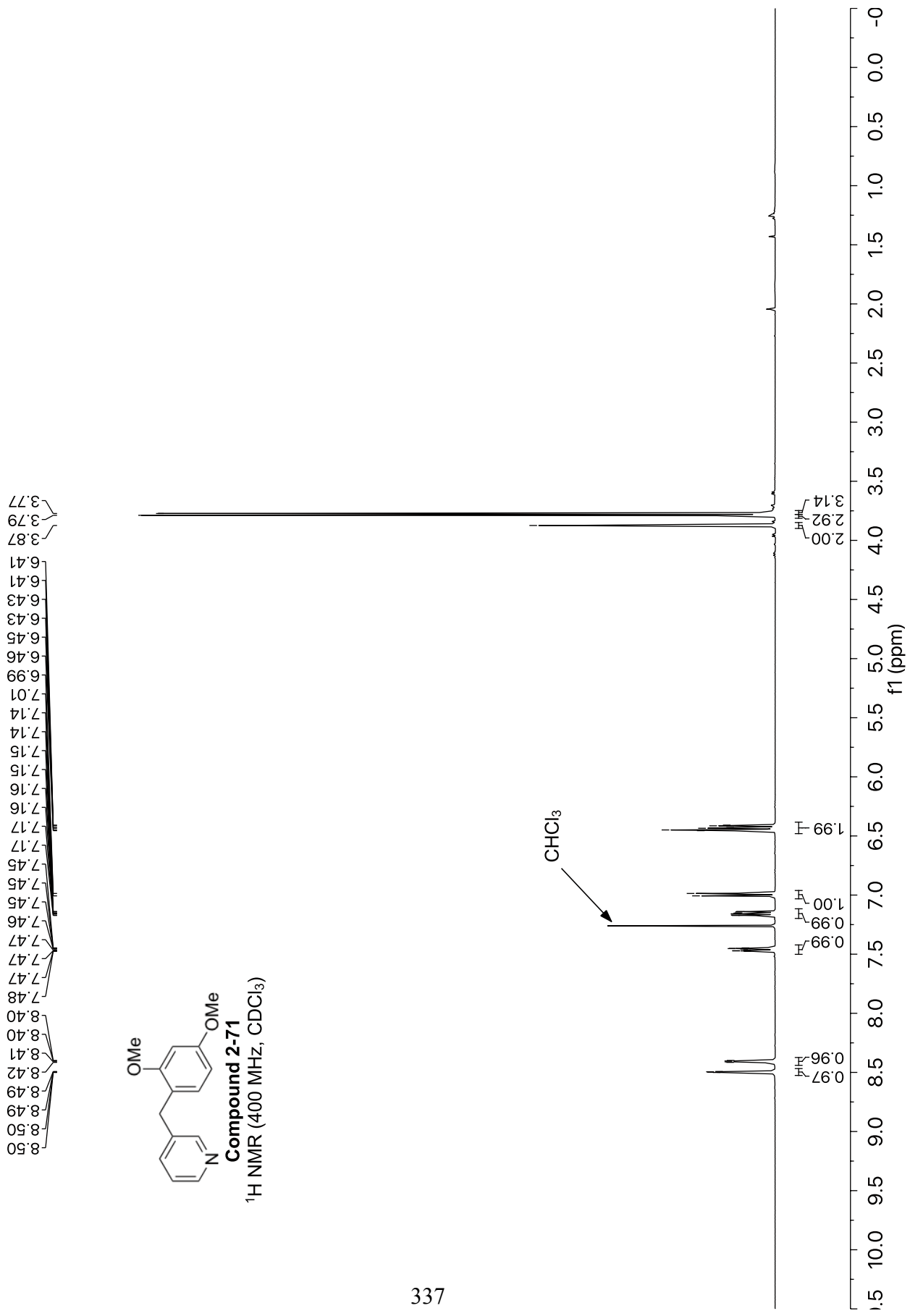
Compound 2-70
 ^{13}C NMR (151 MHz, CDCl_3)

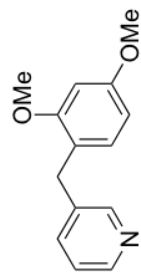
150.14
147.93
138.77
136.17
135.81
131.78
130.55
123.47
120.43

38.45

336

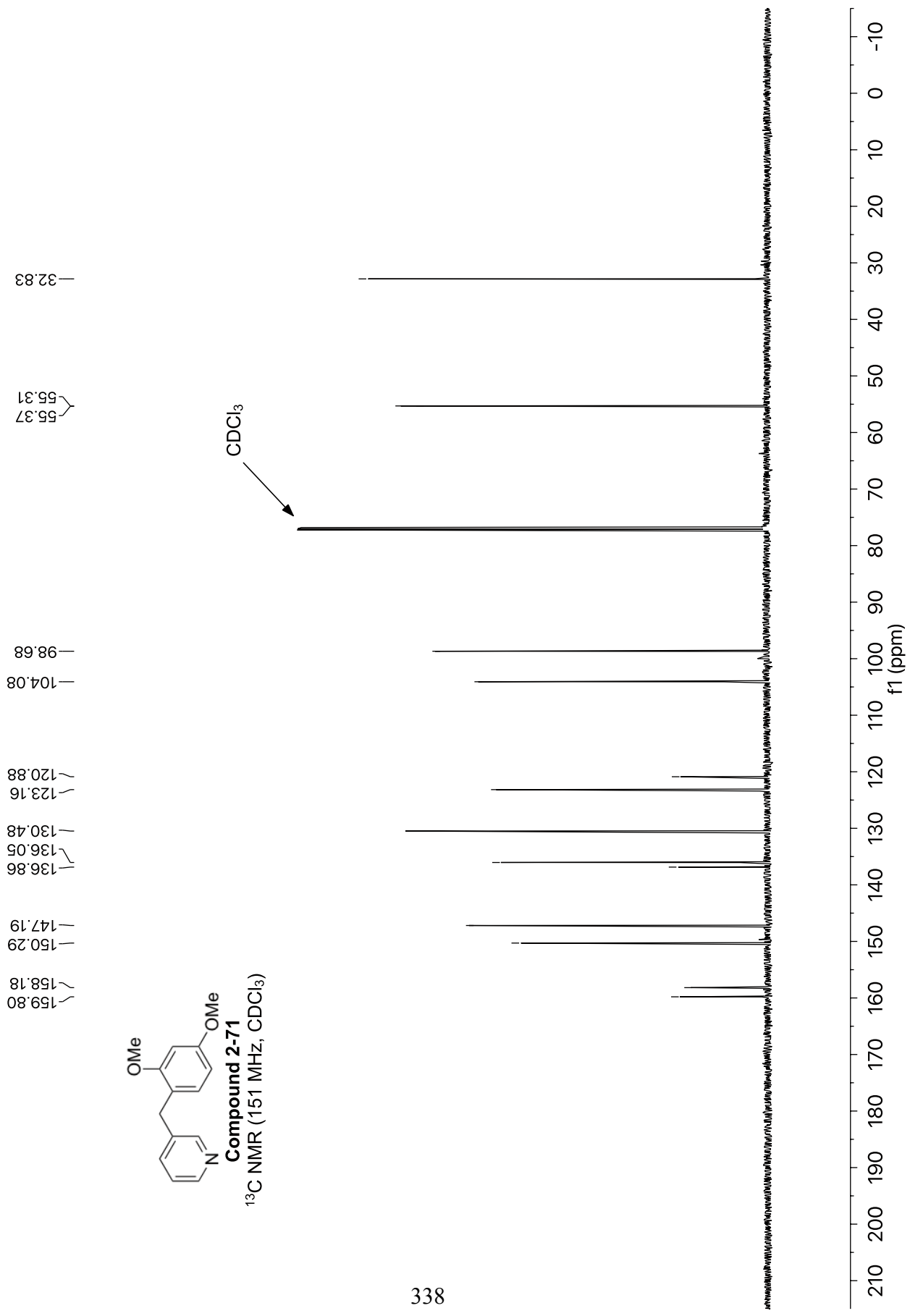


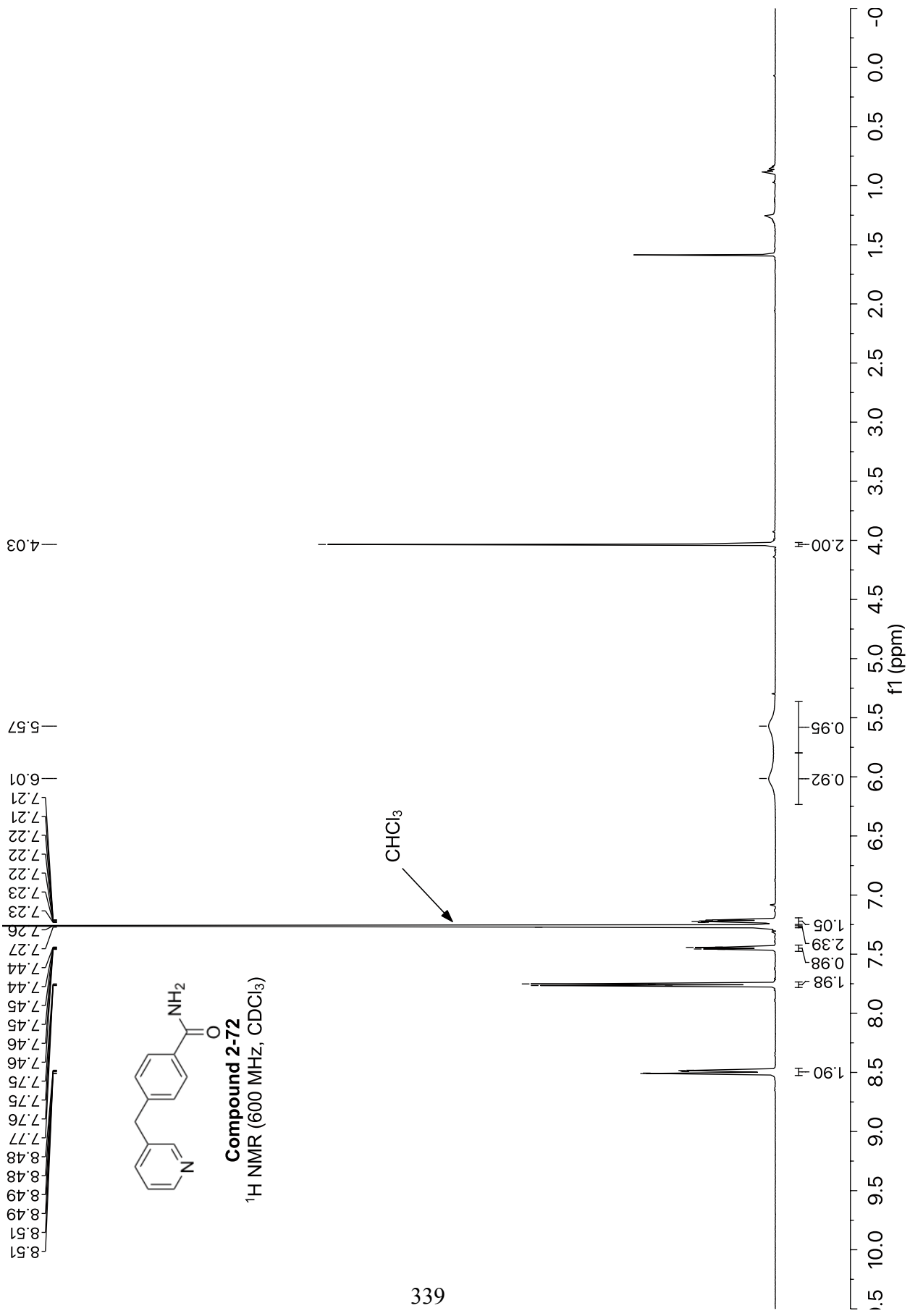


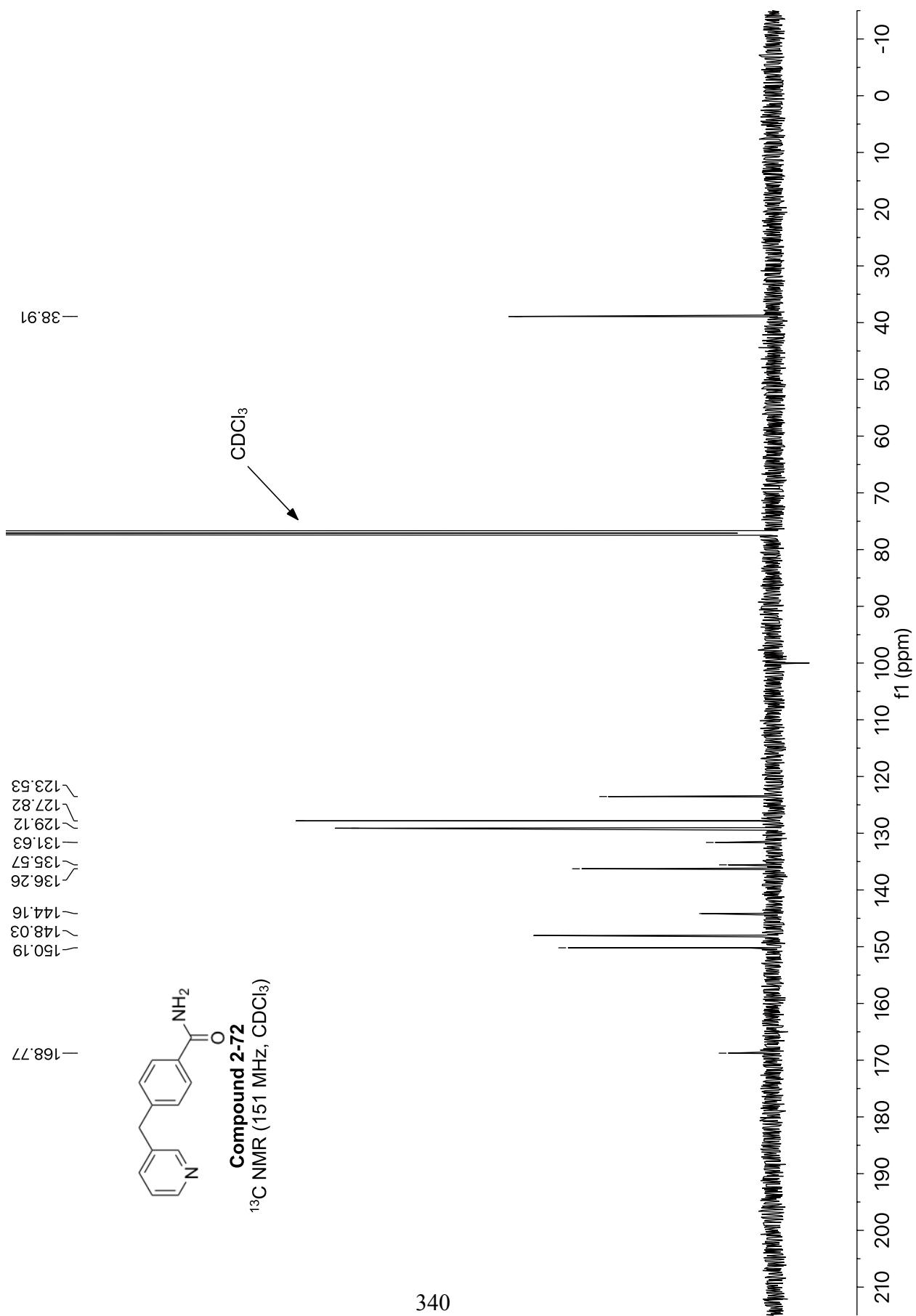


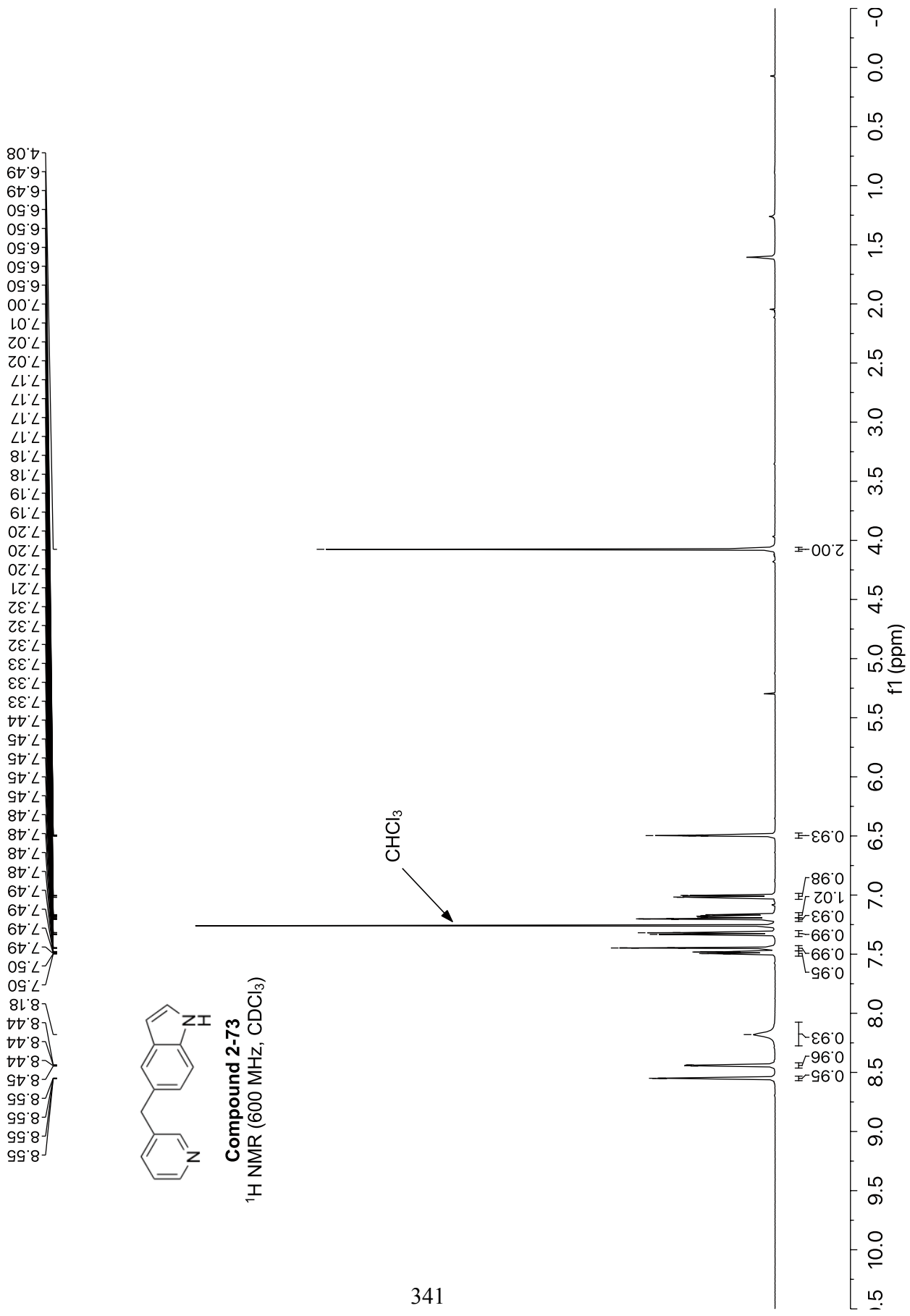
Compound 2-71

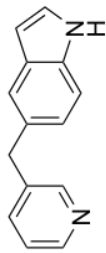
^{13}C NMR (151 MHz, CDCl_3)



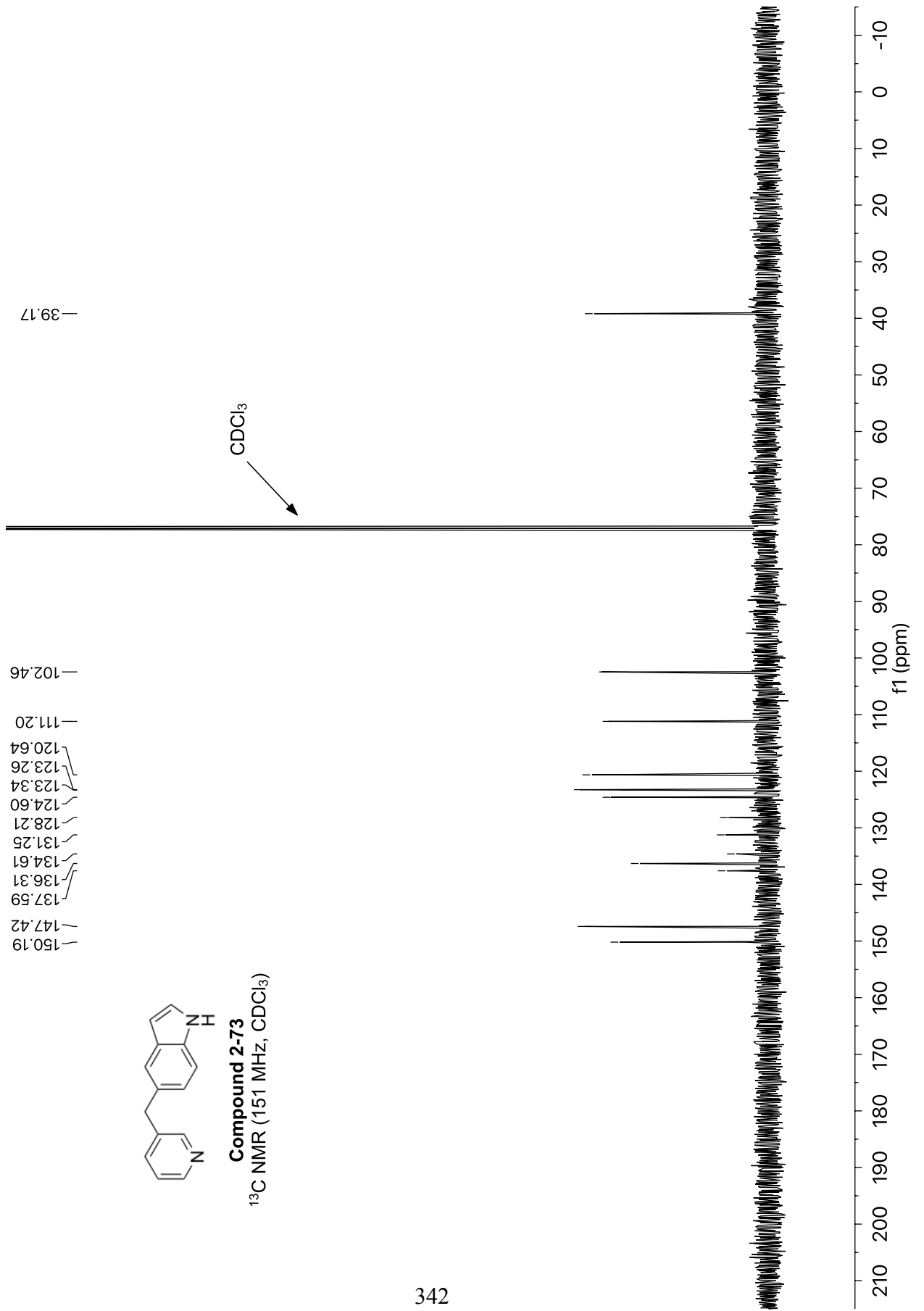


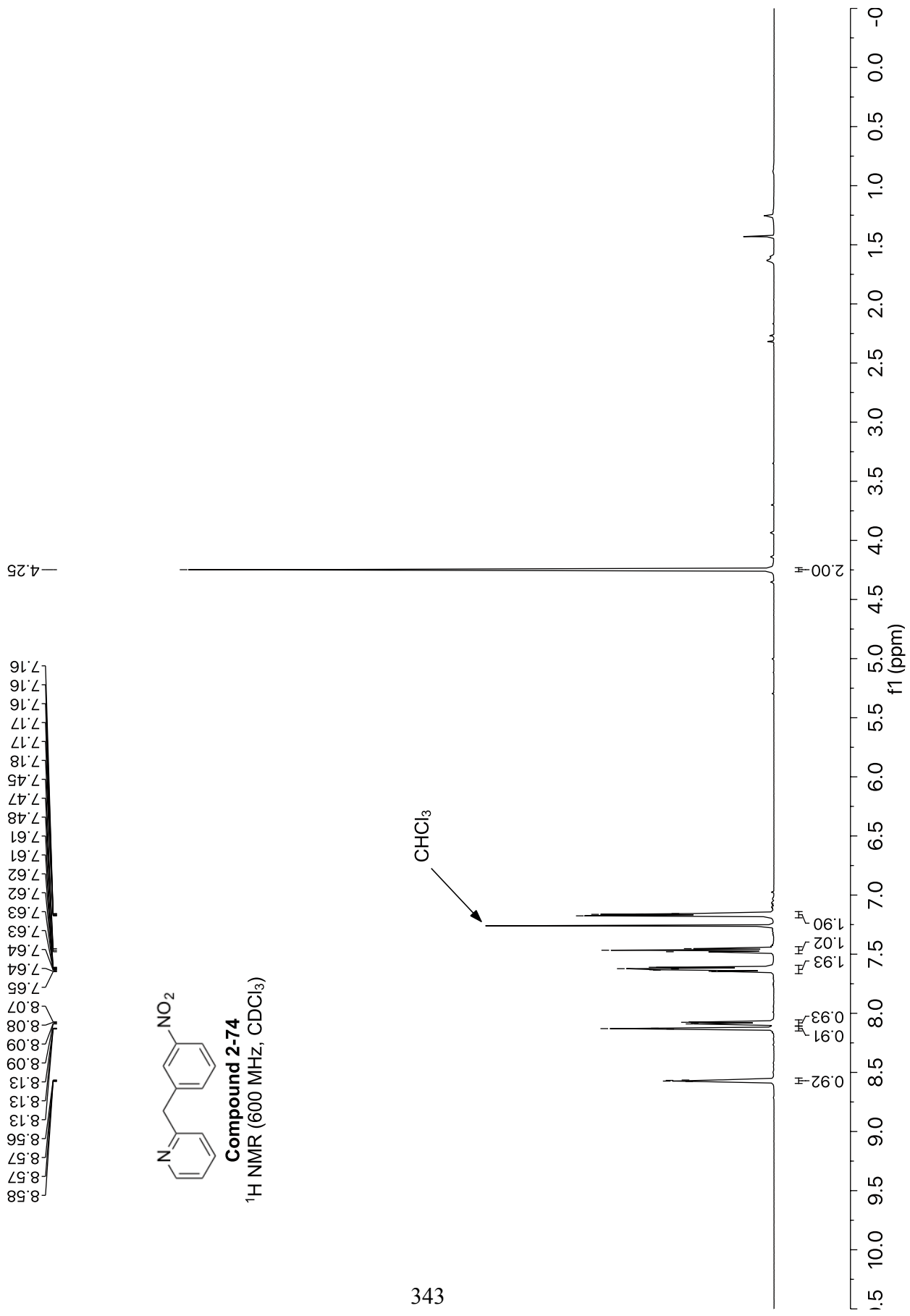


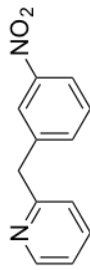




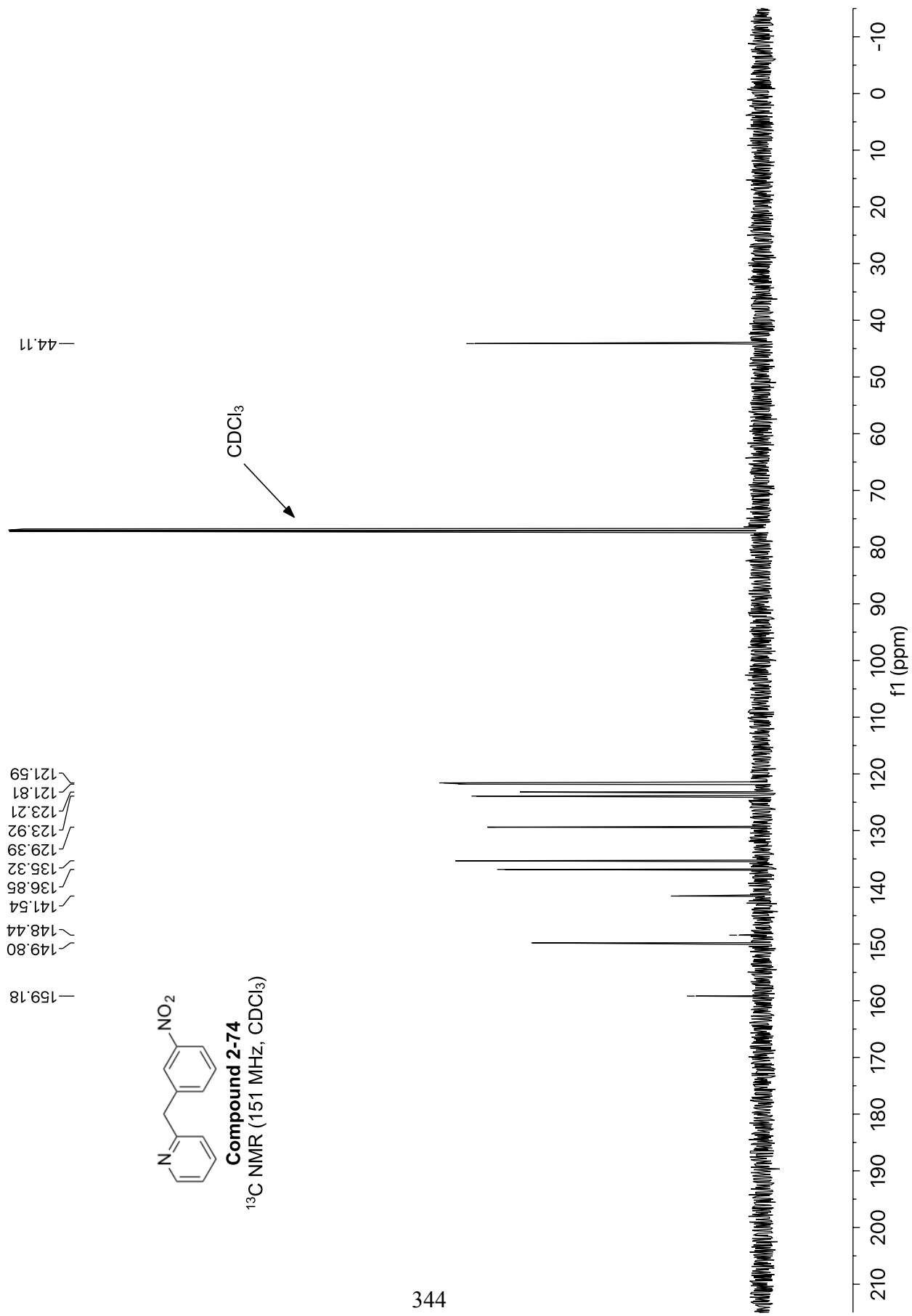
Compound 2-73
¹³C NMR (151 MHz, CDCl₃)

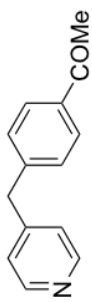




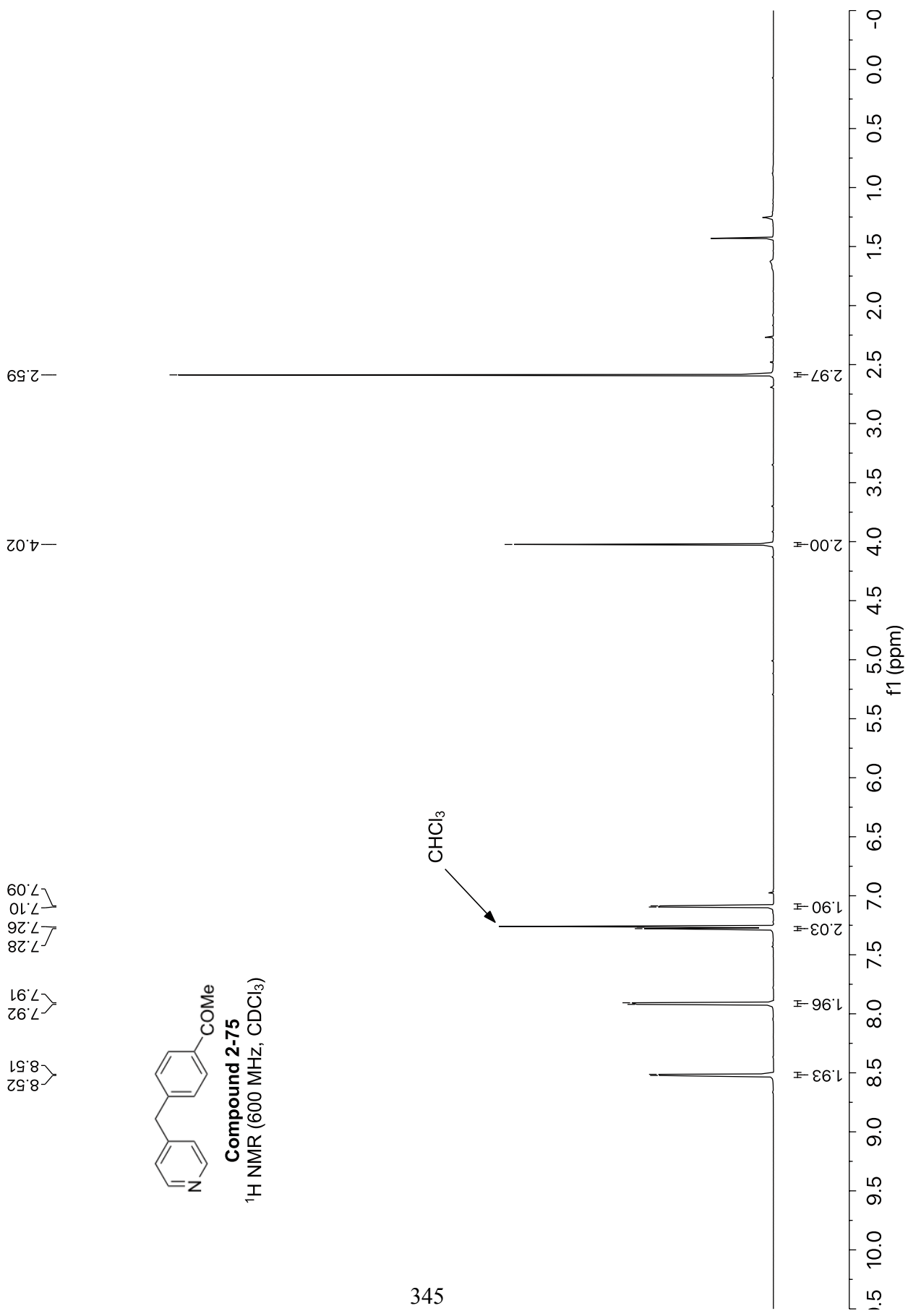


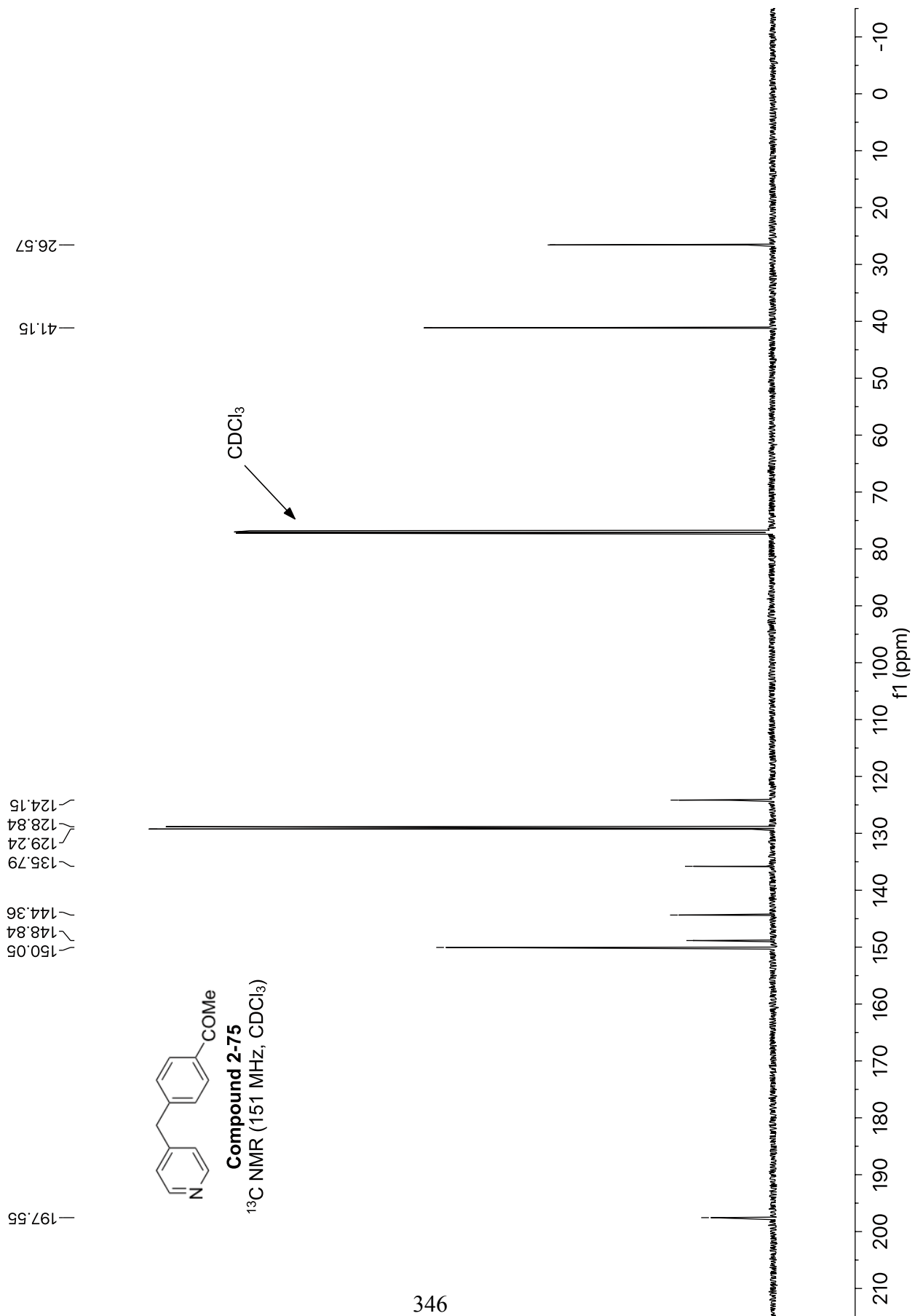
Compound 2-74
¹³C NMR (151 MHz, CDCl₃)

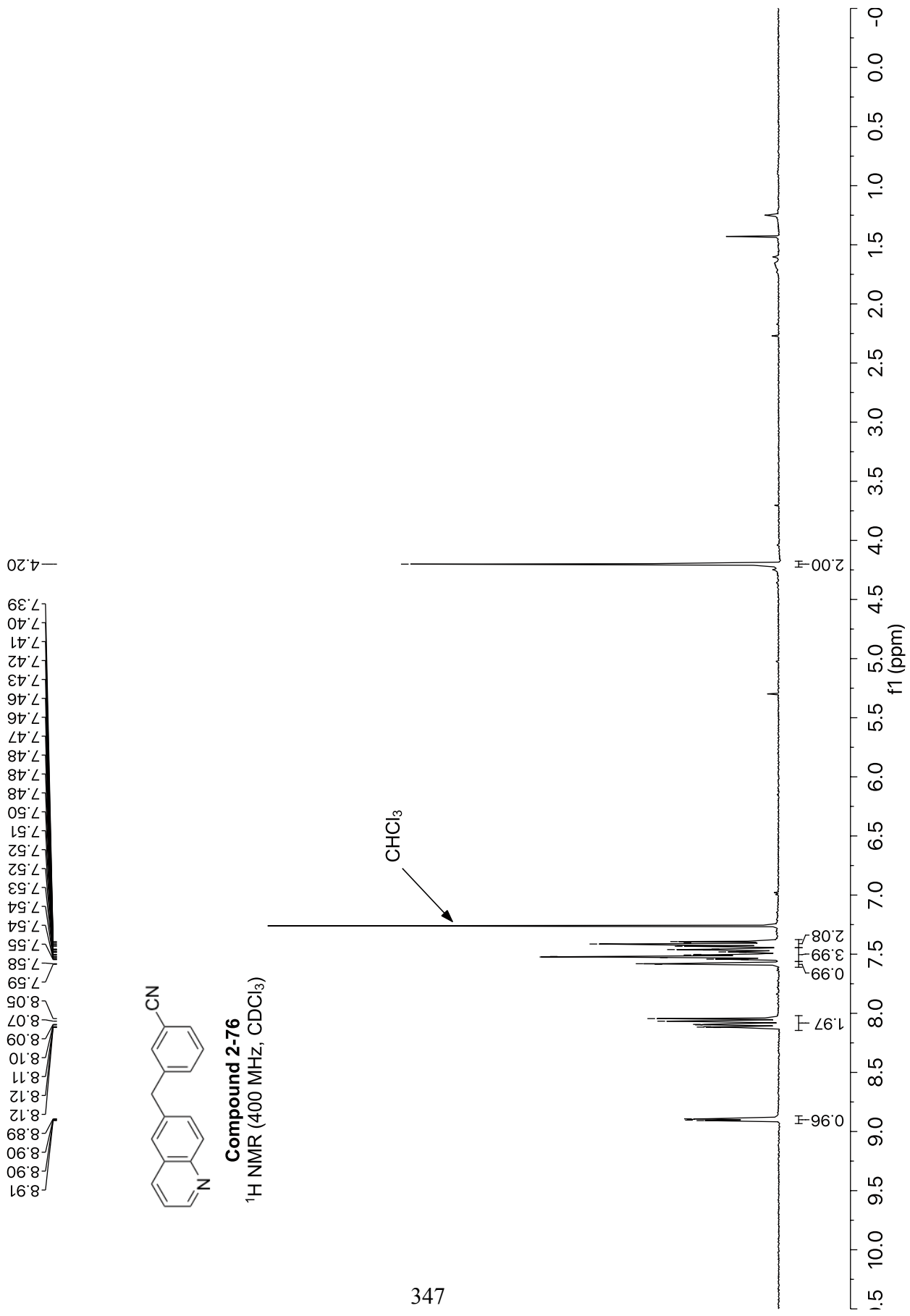


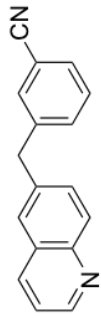


Compound 2-75
¹H NMR (600 MHz, CDCl₃)



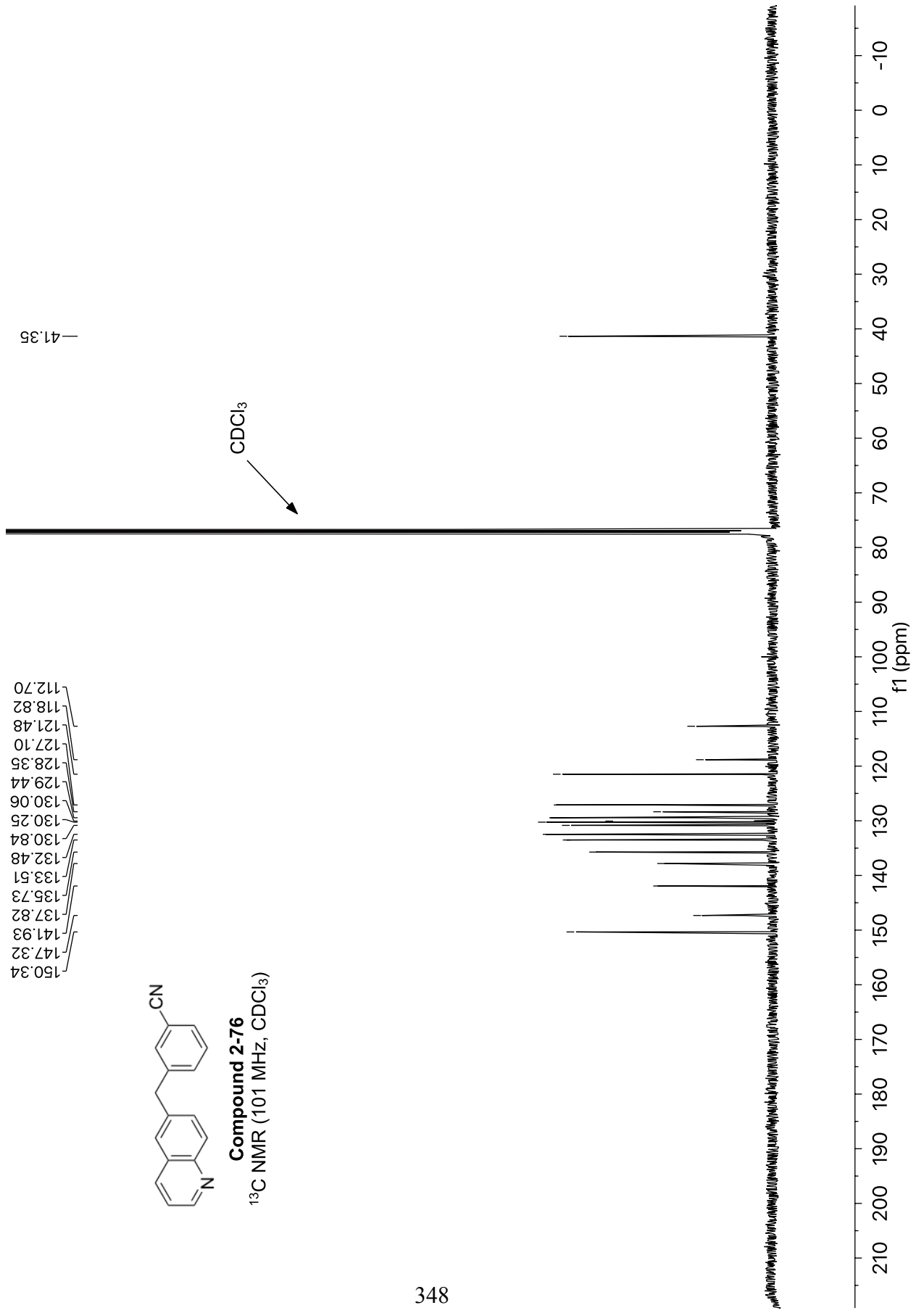


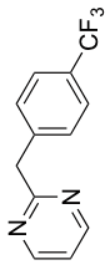




Compound 2-76

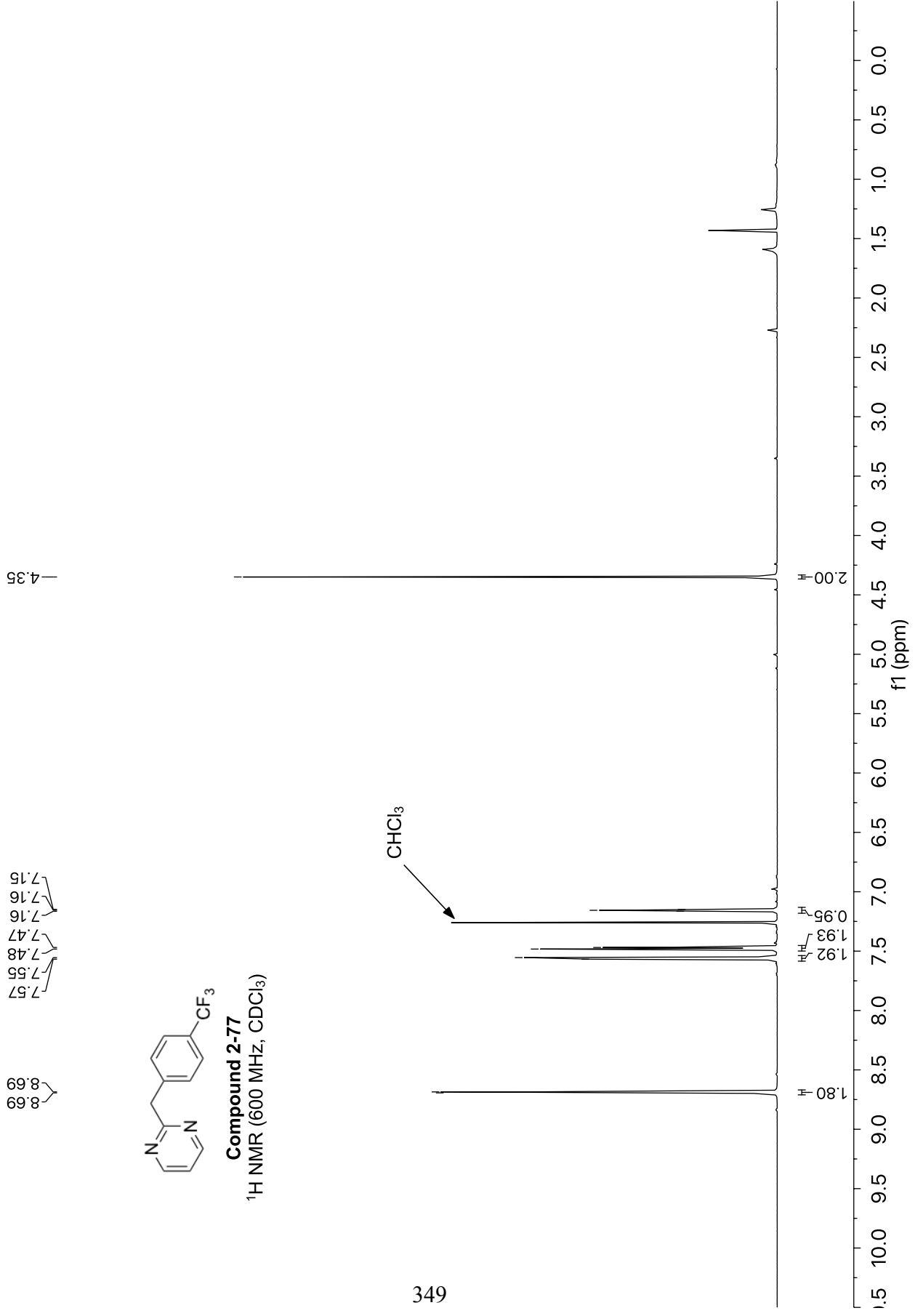
^{13}C NMR (101 MHz, CDCl_3)

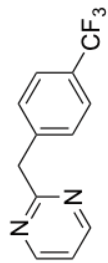




Compound 2-77

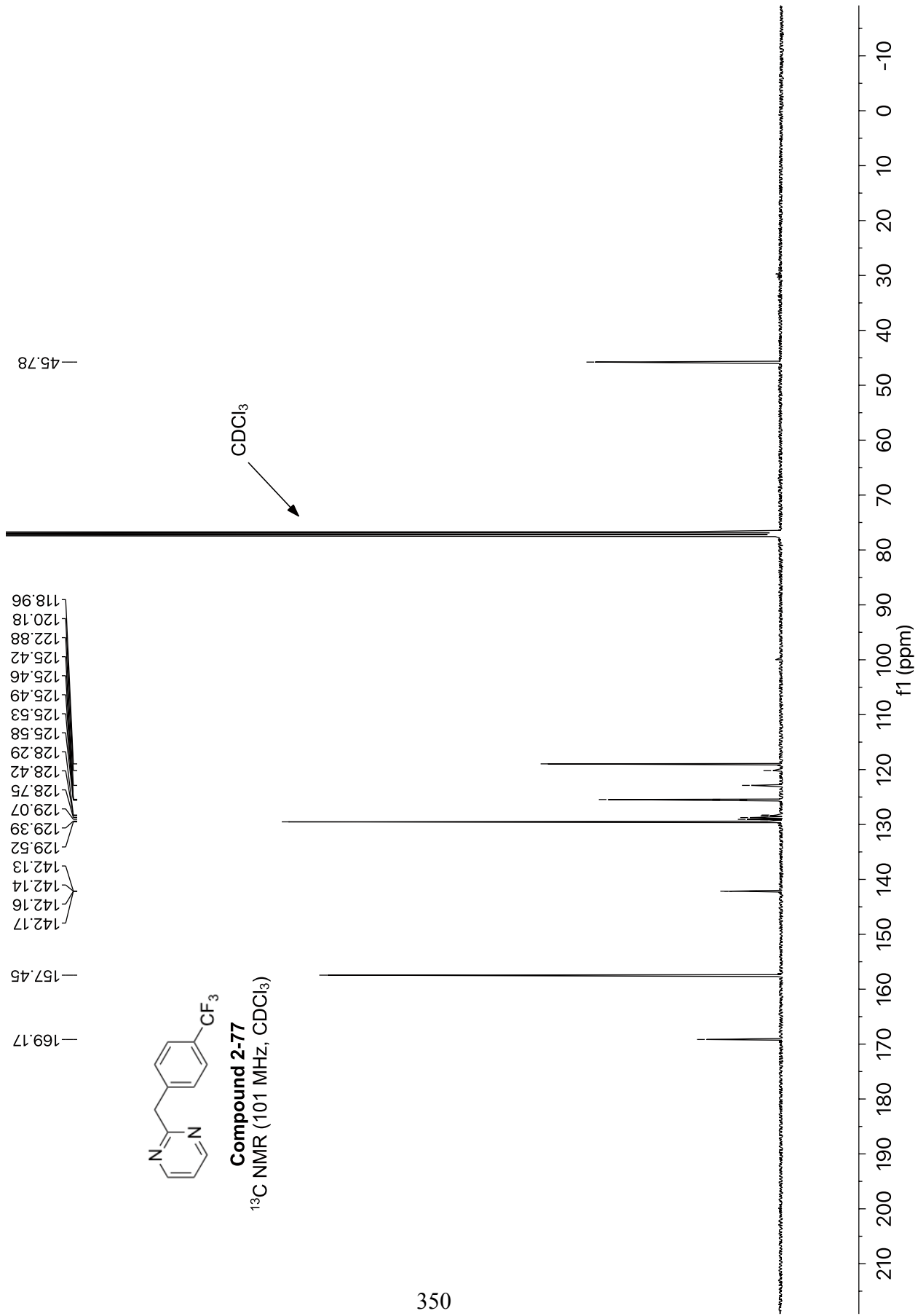
¹H NMR (600 MHz, CDCl₃)

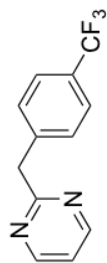




Compound 2-77

^{13}C NMR (101 MHz, CDCl_3)



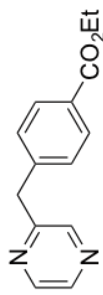


Compound 2-77
¹⁹F NMR (565 MHz, CDCl₃)

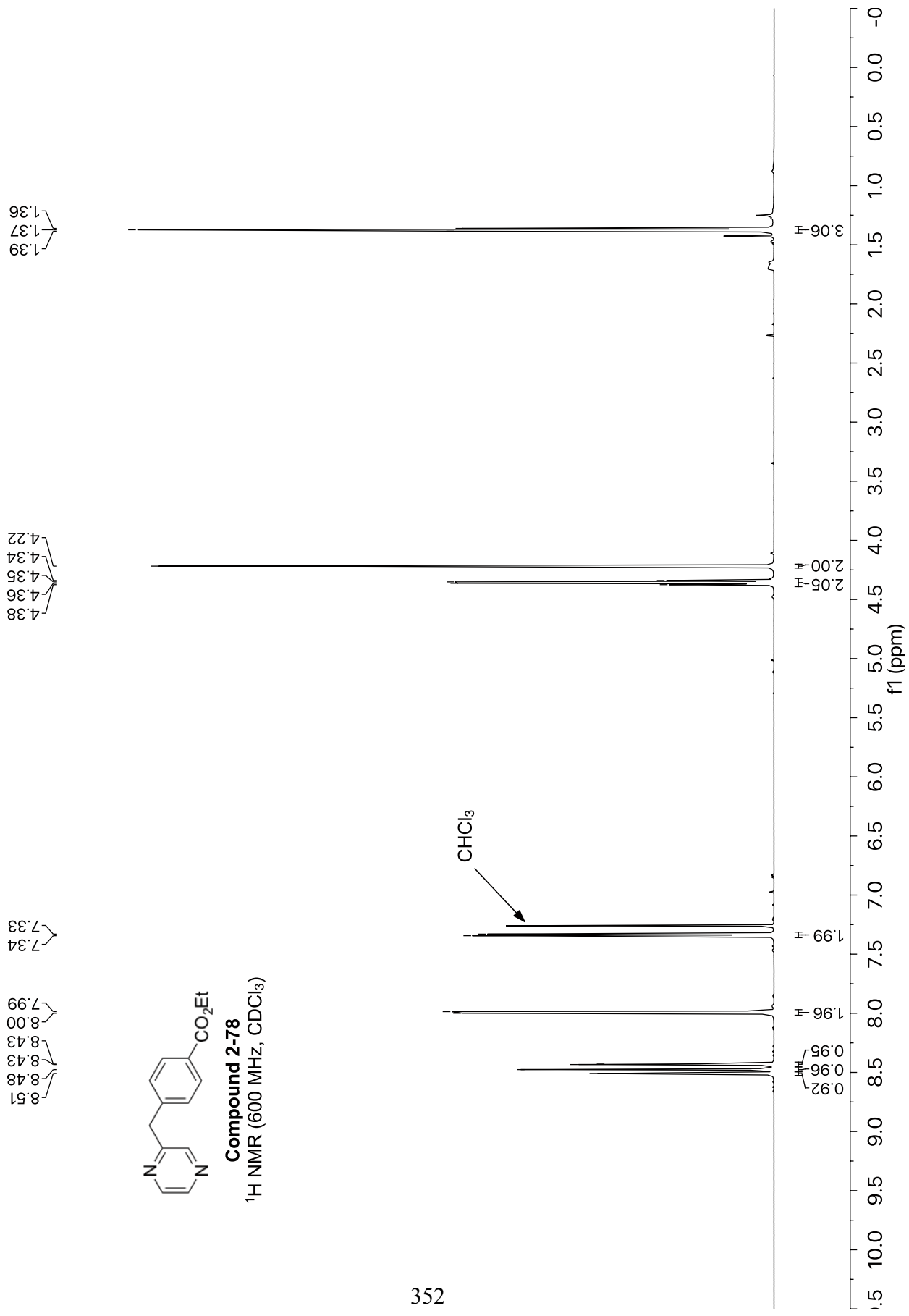
— -62.49

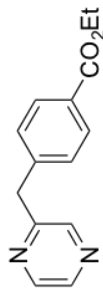


10 0 -10 -20 -30 -40 -50 -60 -70 -80 -90 -100 -110 -120 -130 -140 -150 -160 -170 -180 -190 -200 -210
f1 (ppm)

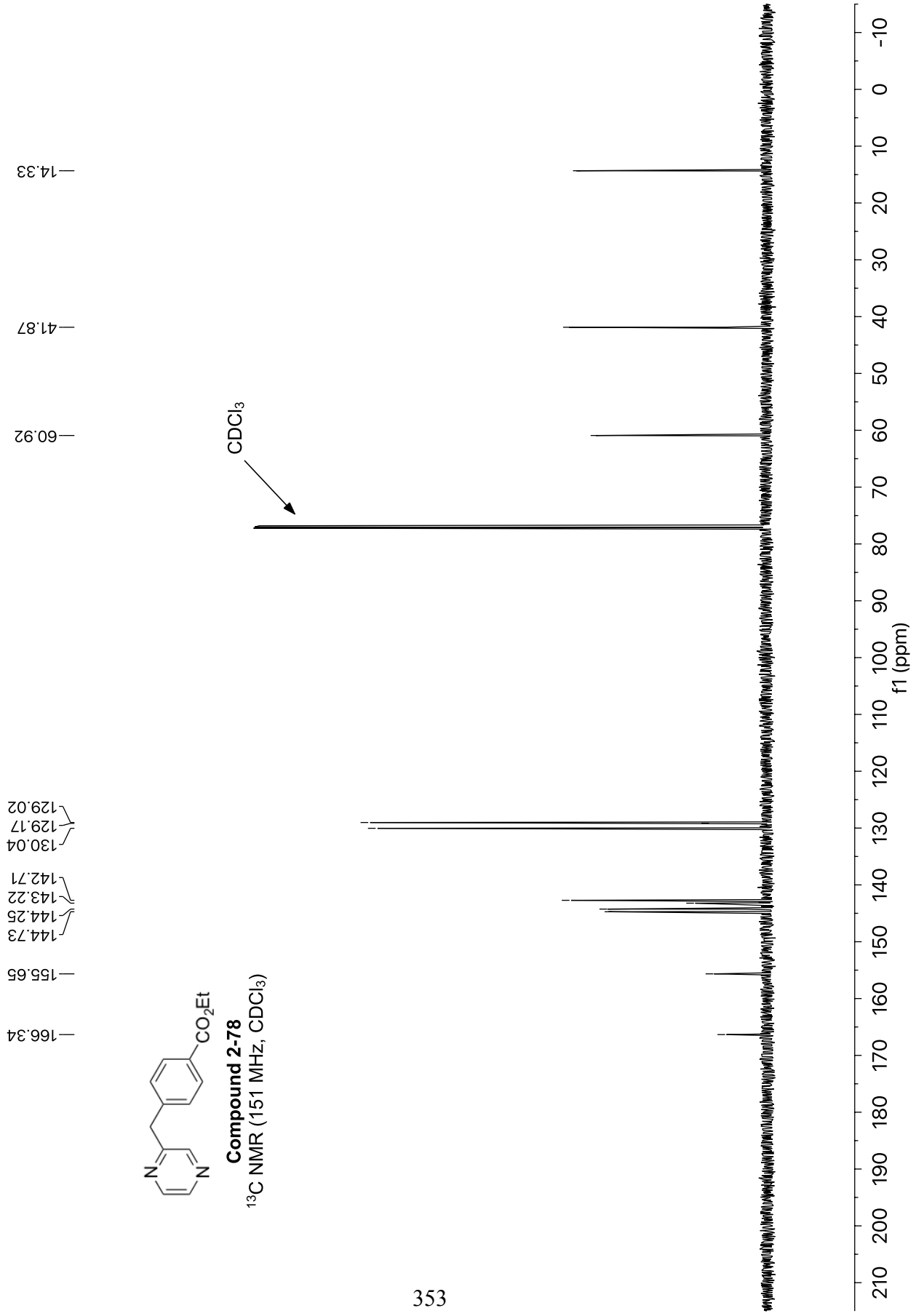


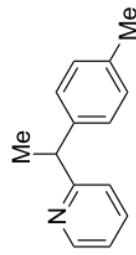
Compound 2-78
¹H NMR (600 MHz, CDCl₃)





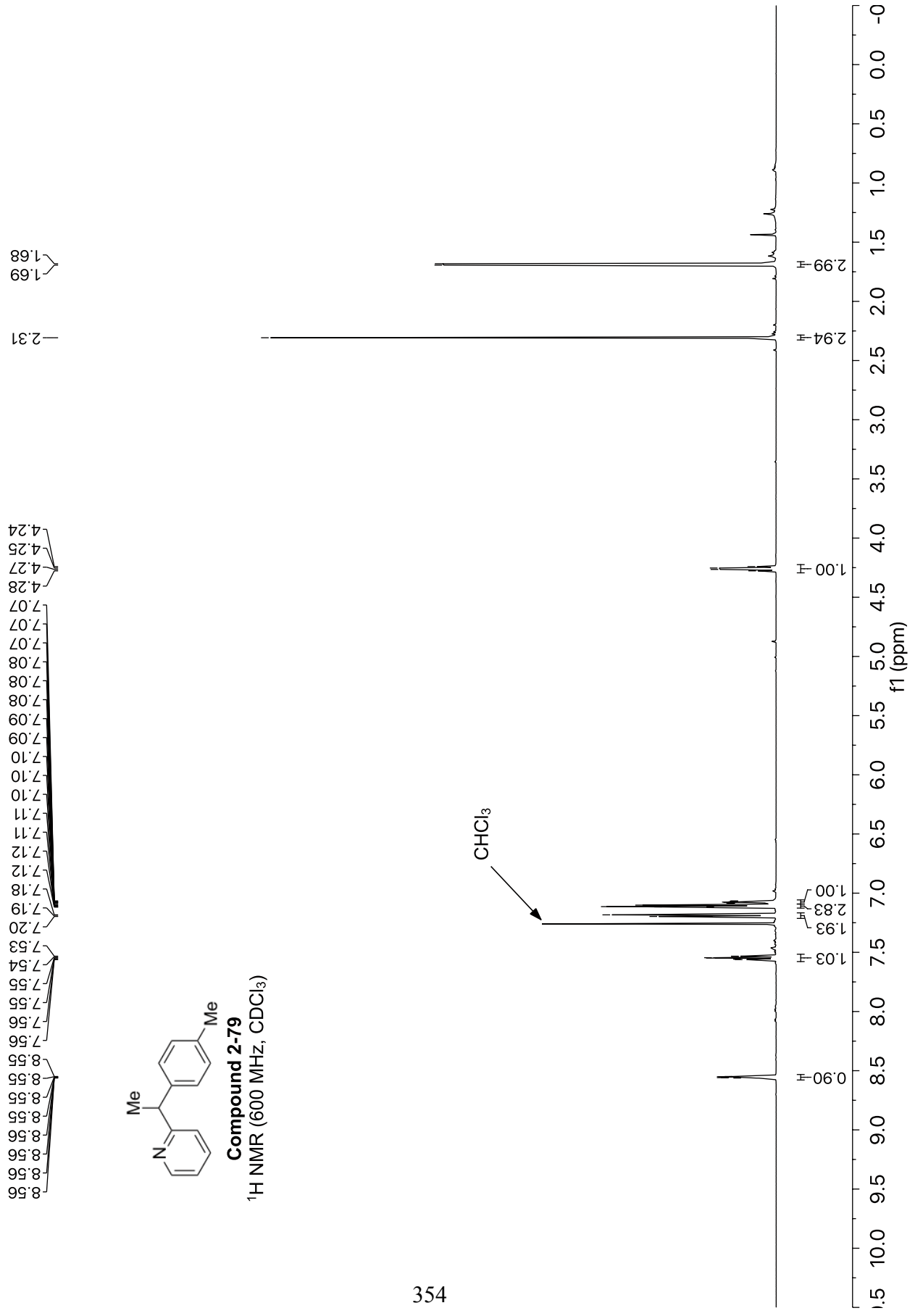
Compound 2-78
 ^{13}C NMR (151 MHz, CDCl_3)

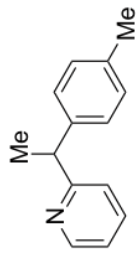




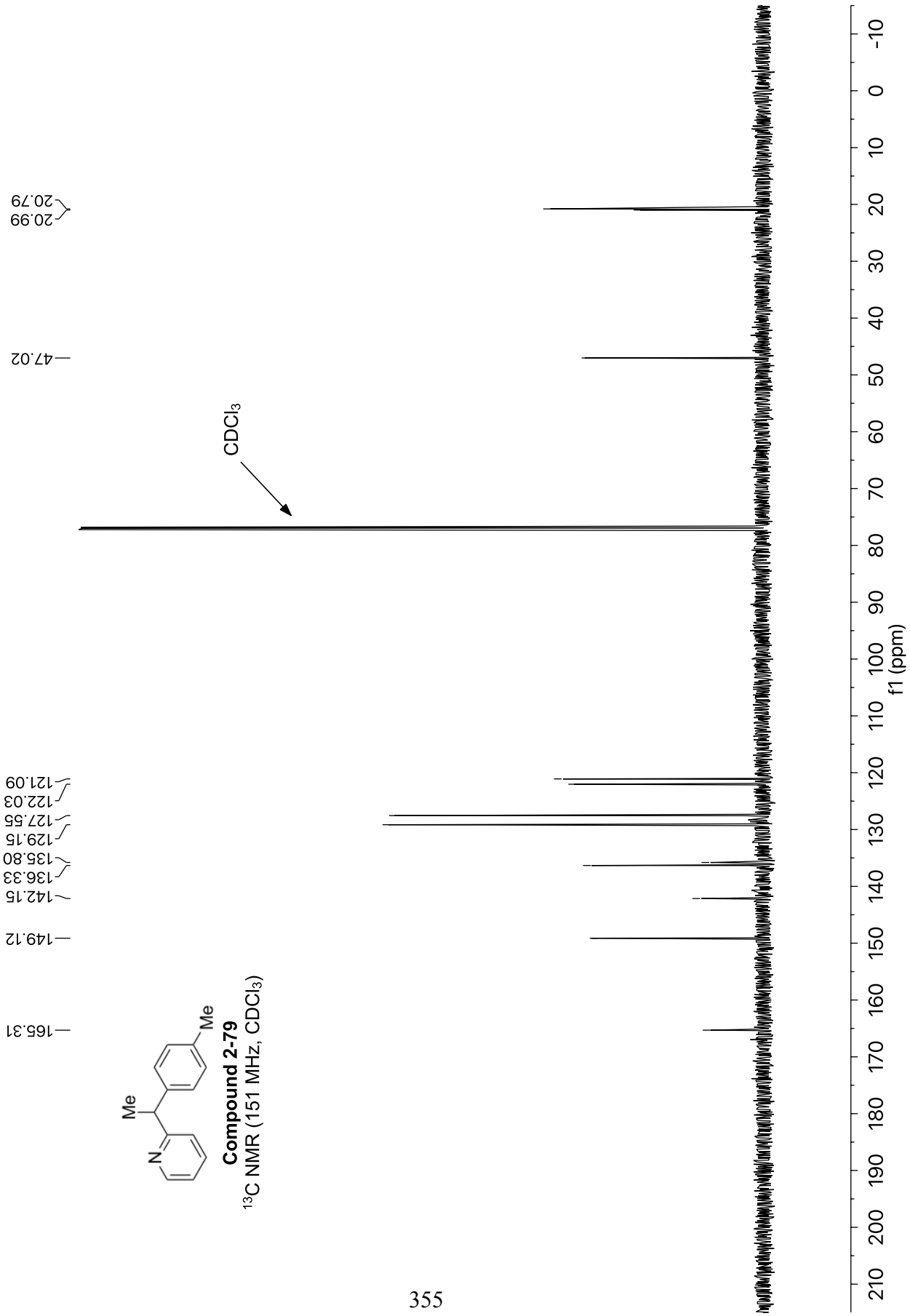
Compound 2-79

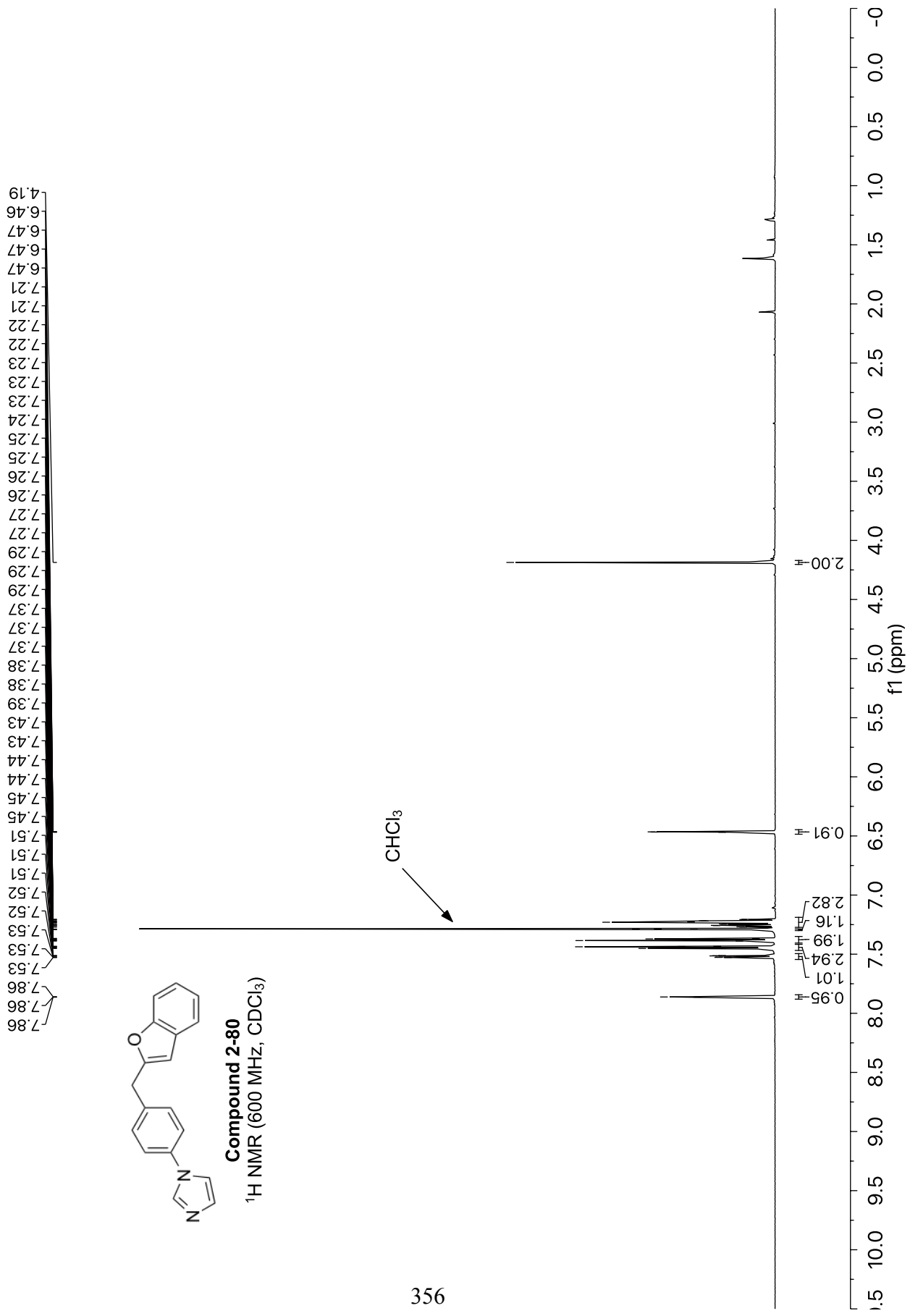
¹H NMR (600 MHz, CDCl₃)

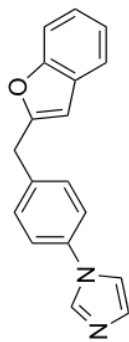




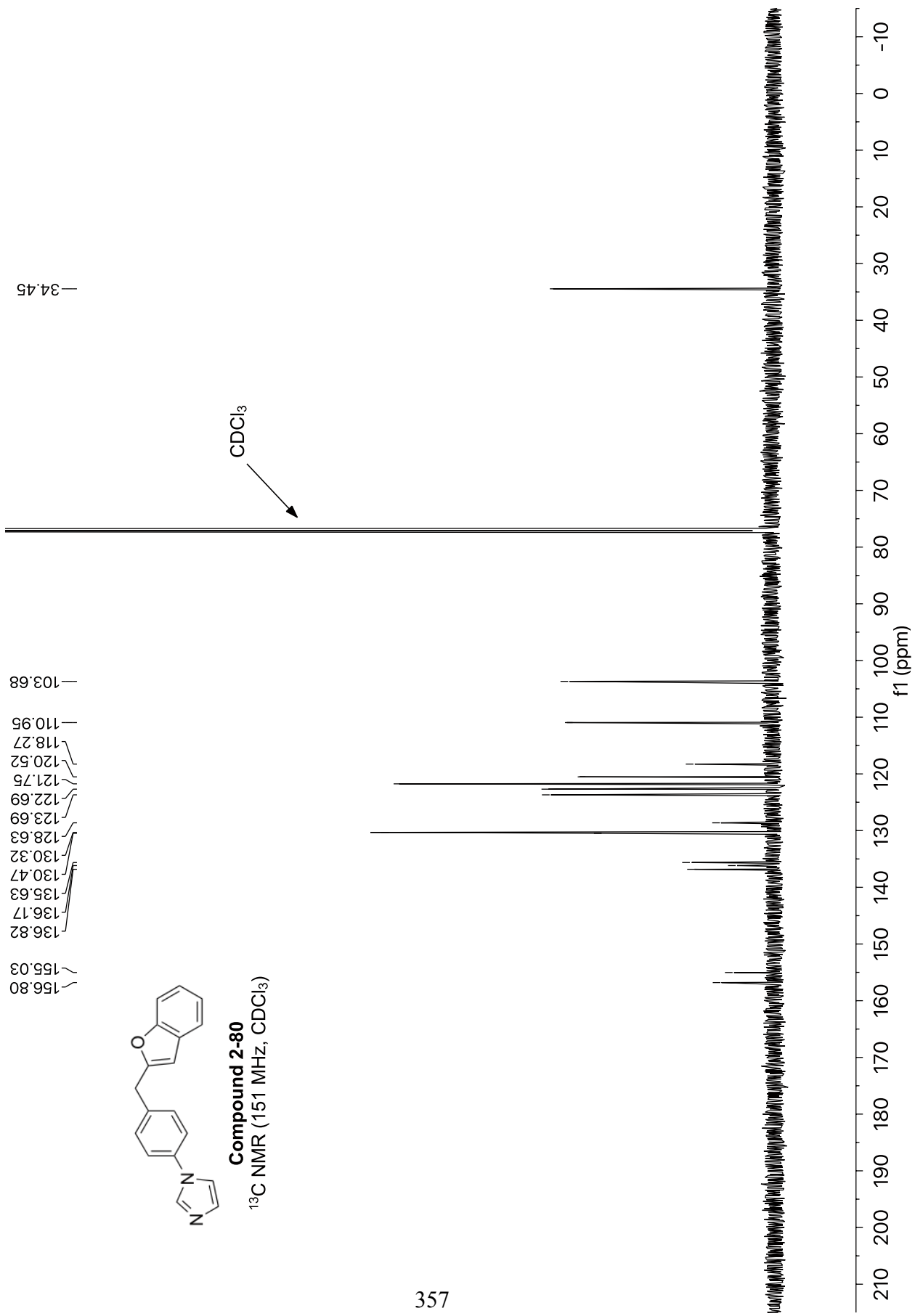
Compound 2-79
¹³C NMR (151 MHz, CDCl₃)

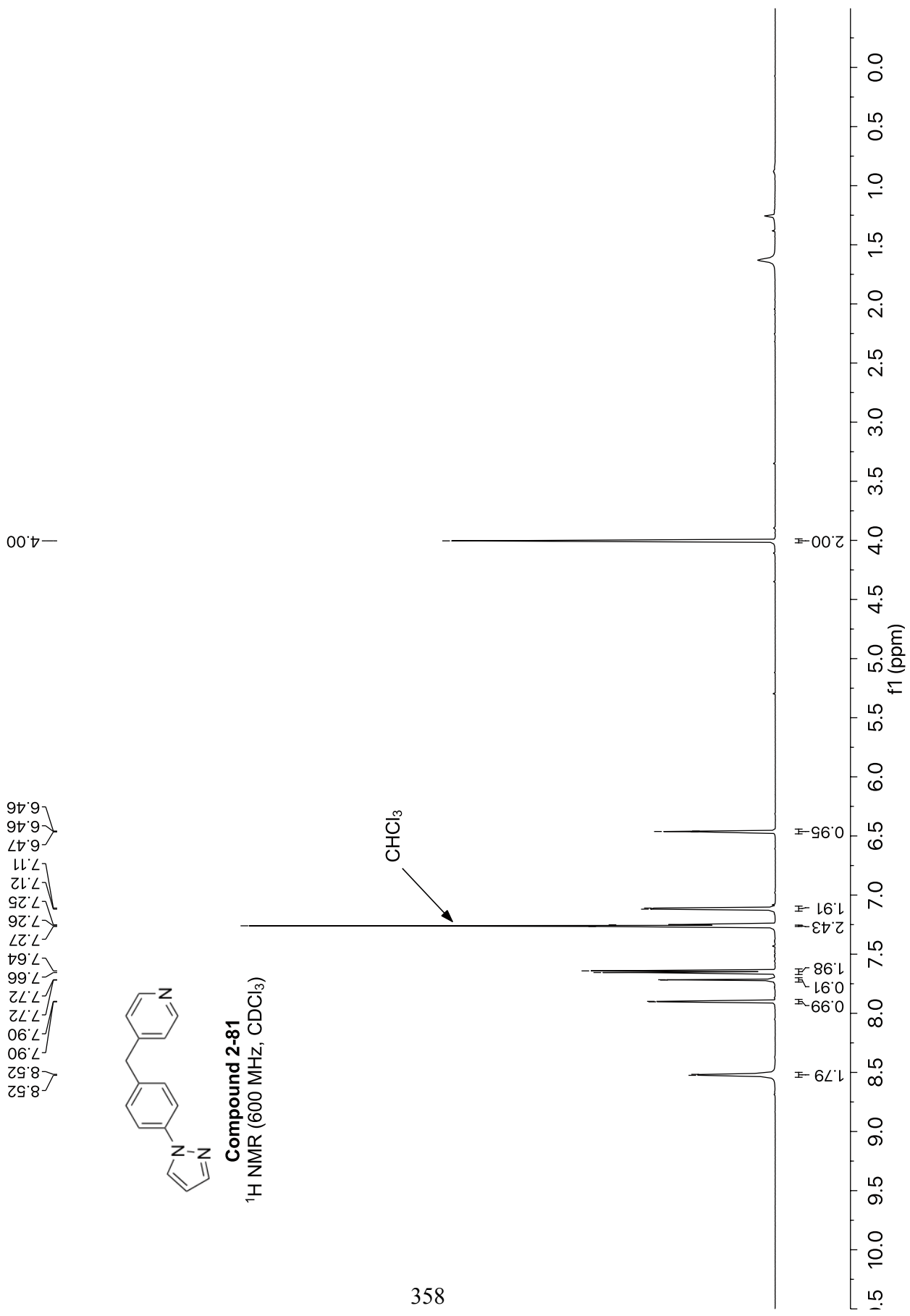


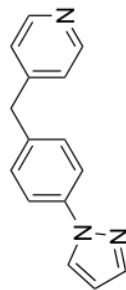




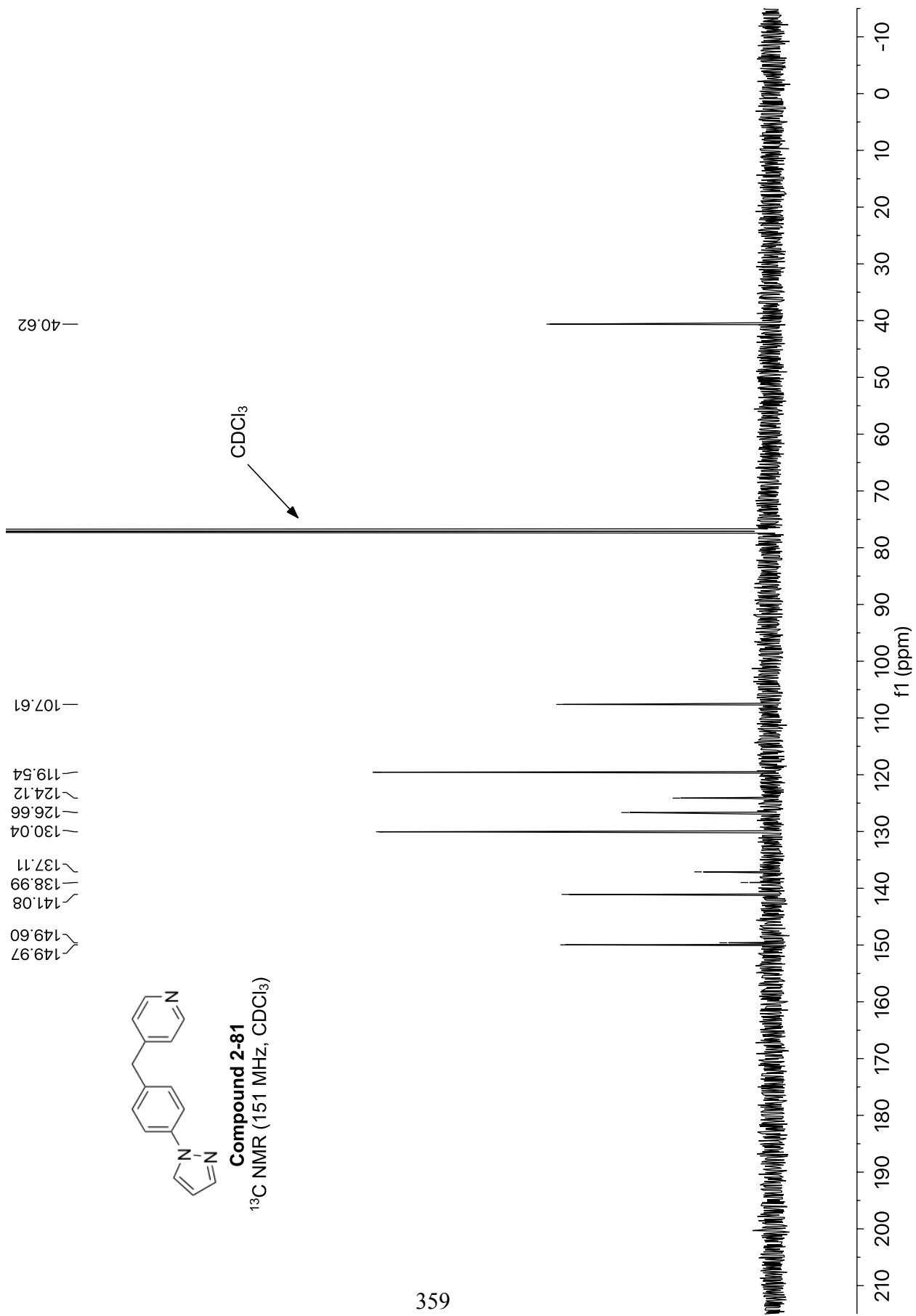
Compound 2-80
¹³C NMR (151 MHz, CDCl₃)

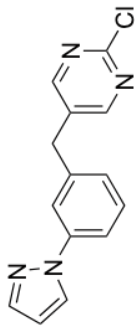




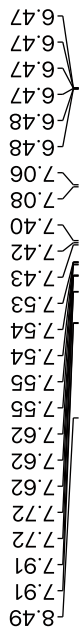


Compound 2-81
¹³C NMR (151 MHz, CDCl₃)

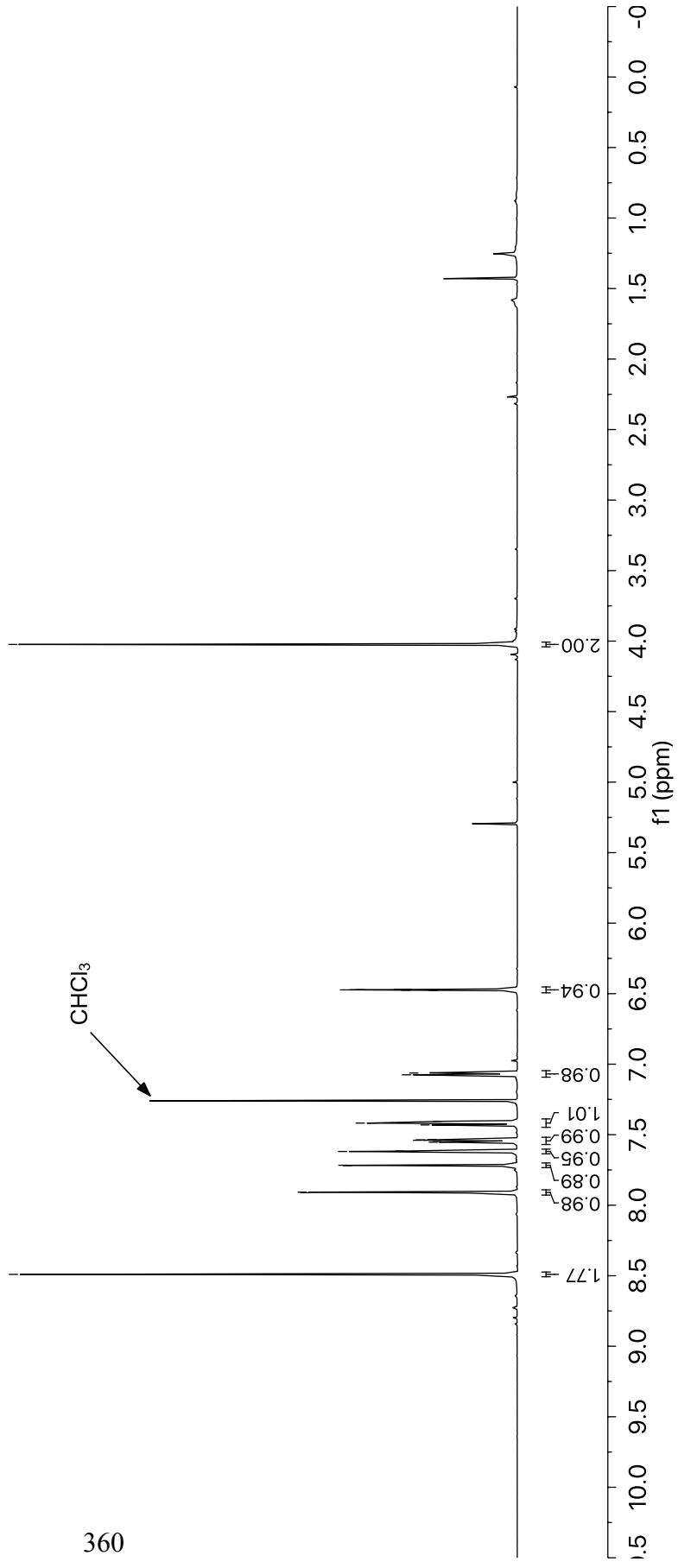


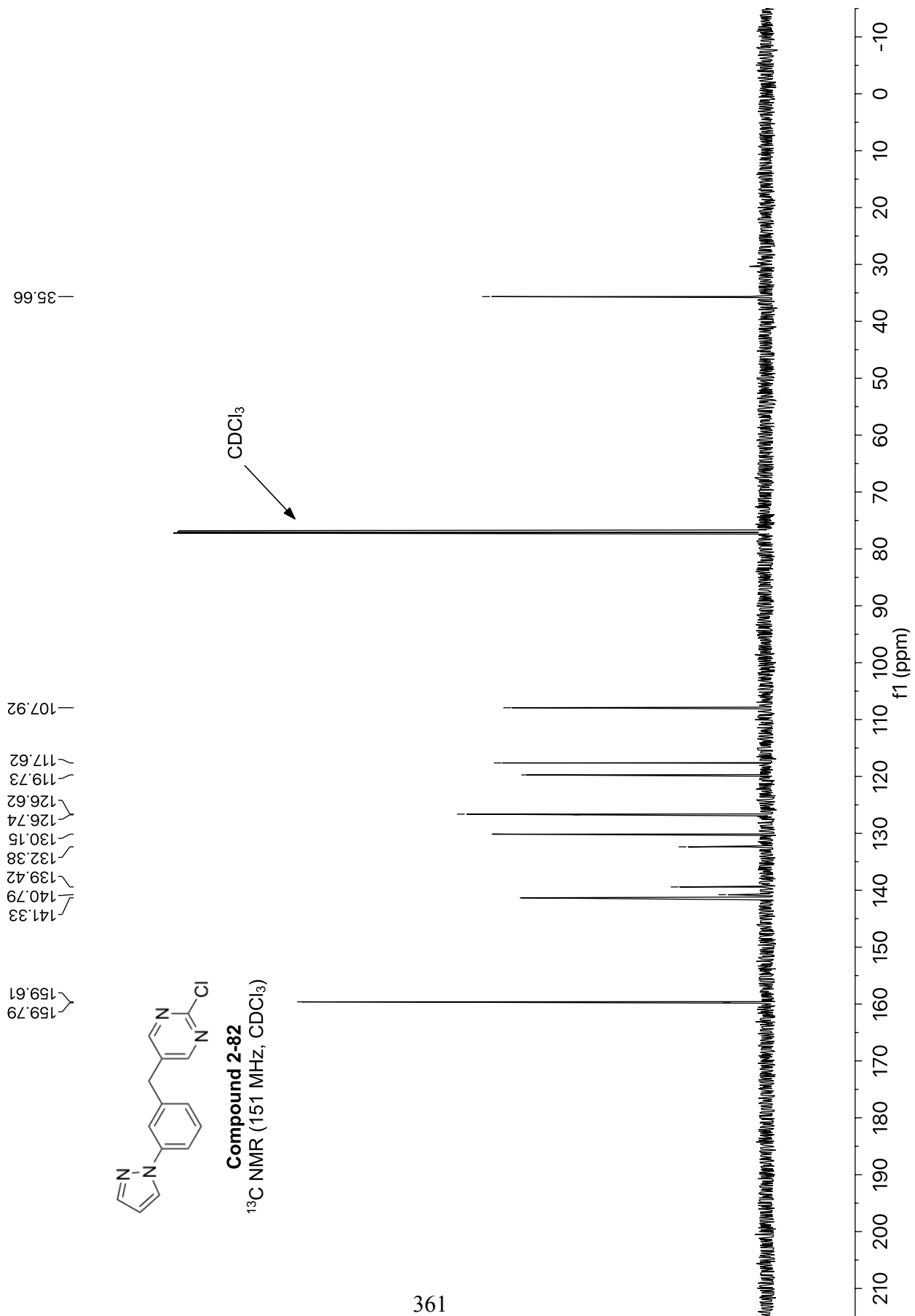


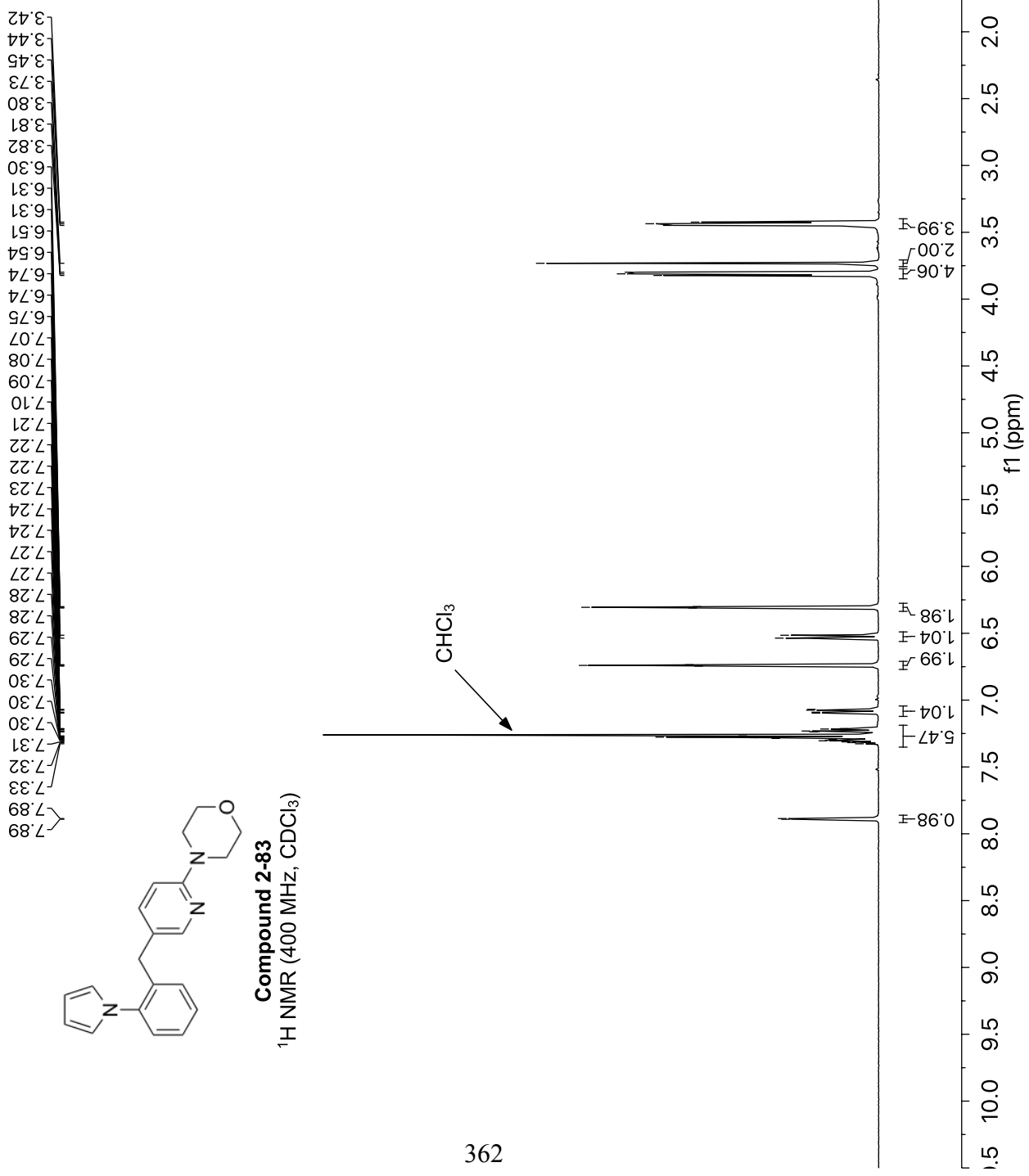
Compound 2-82
¹H NMR (600 MHz, CDCl₃)

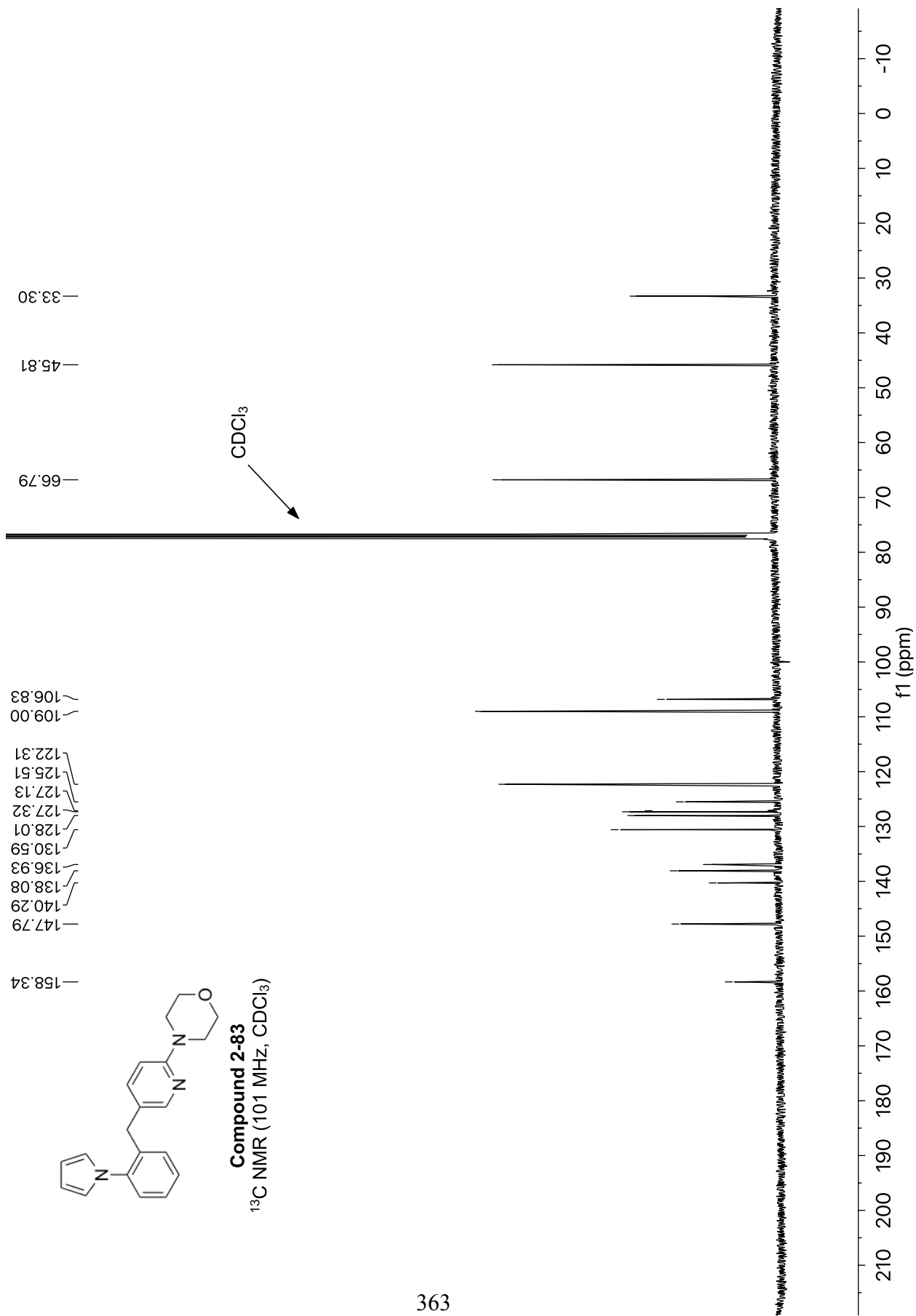


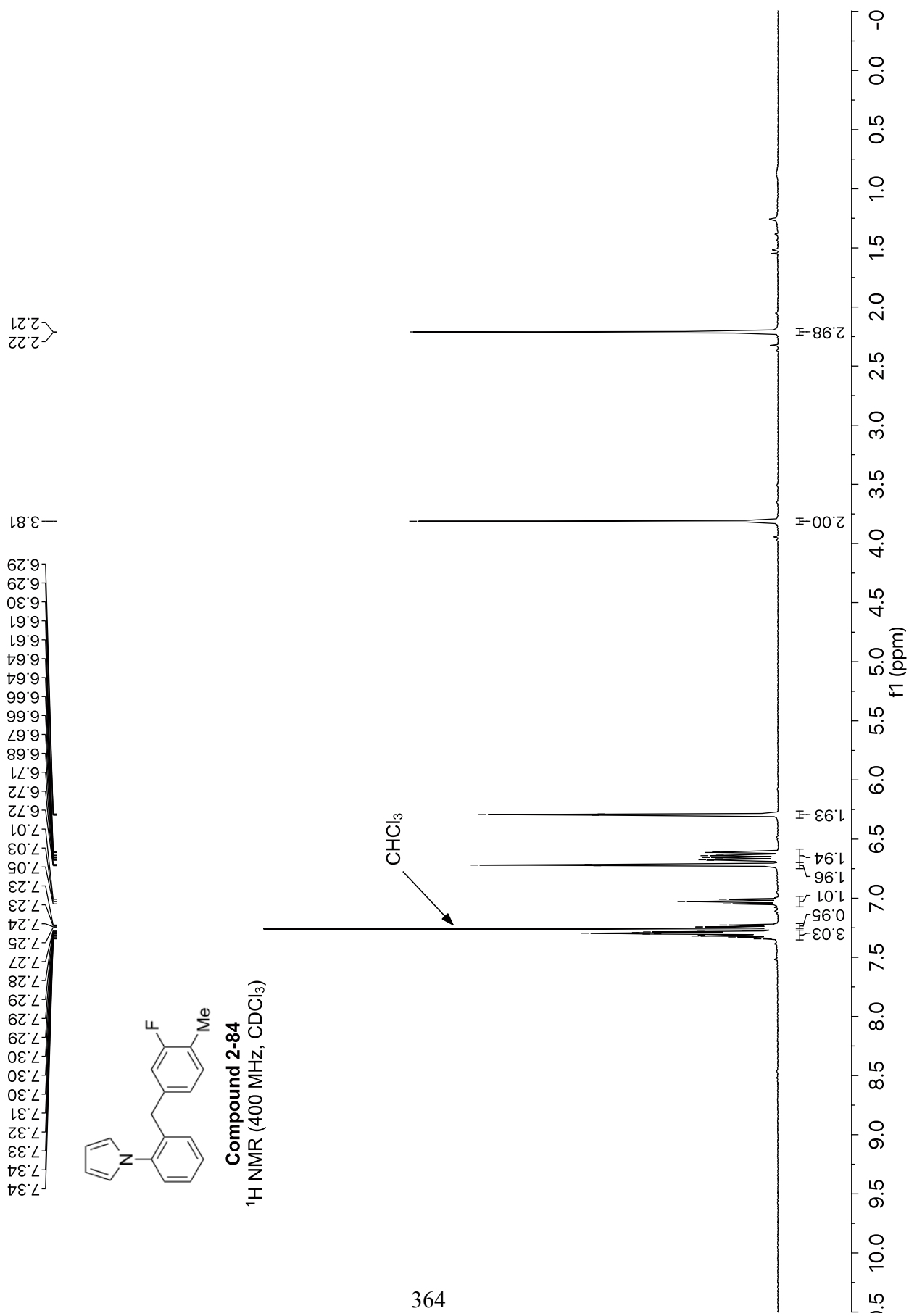
—4.02

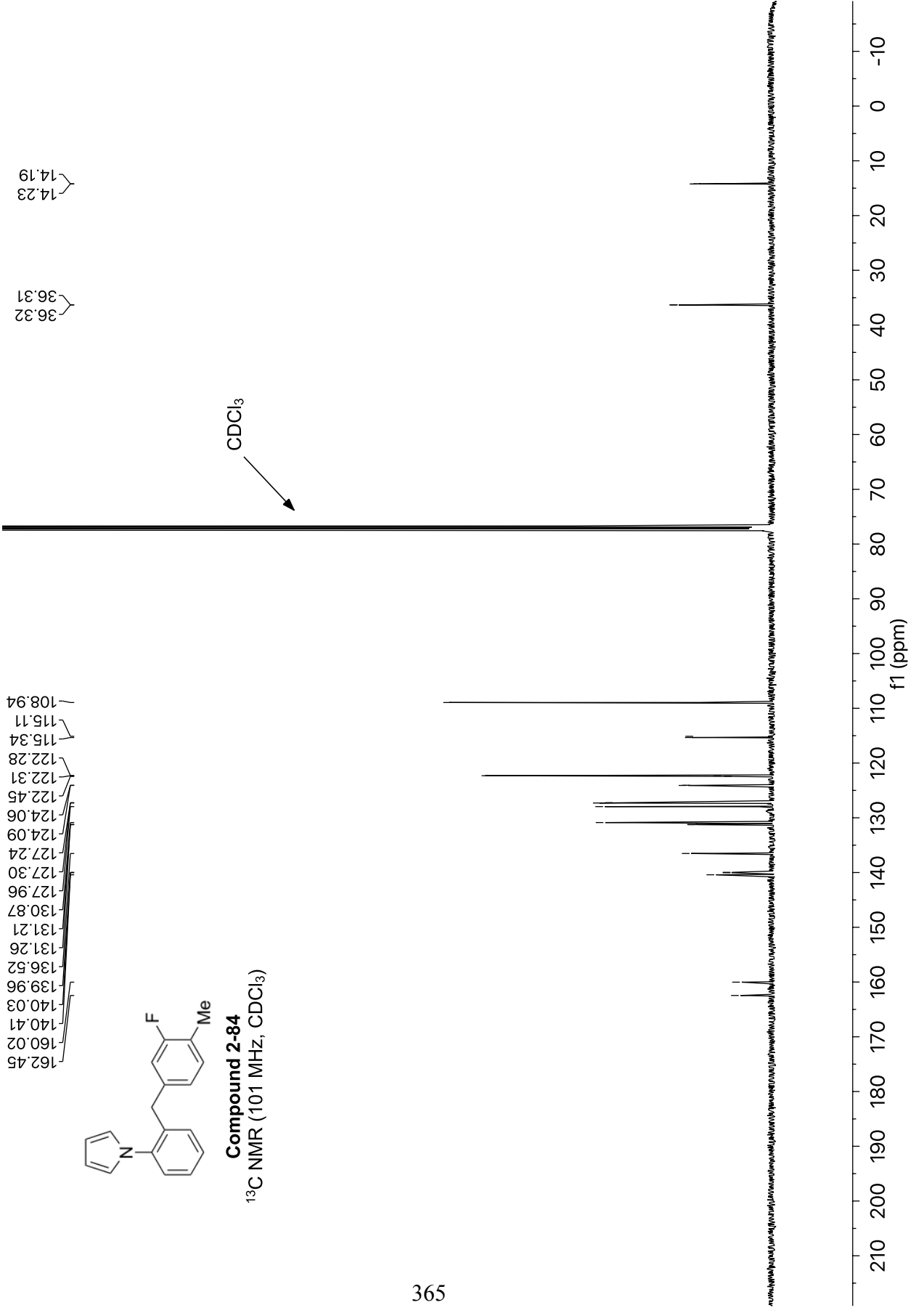


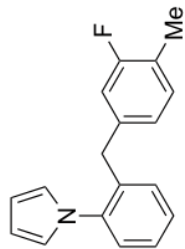










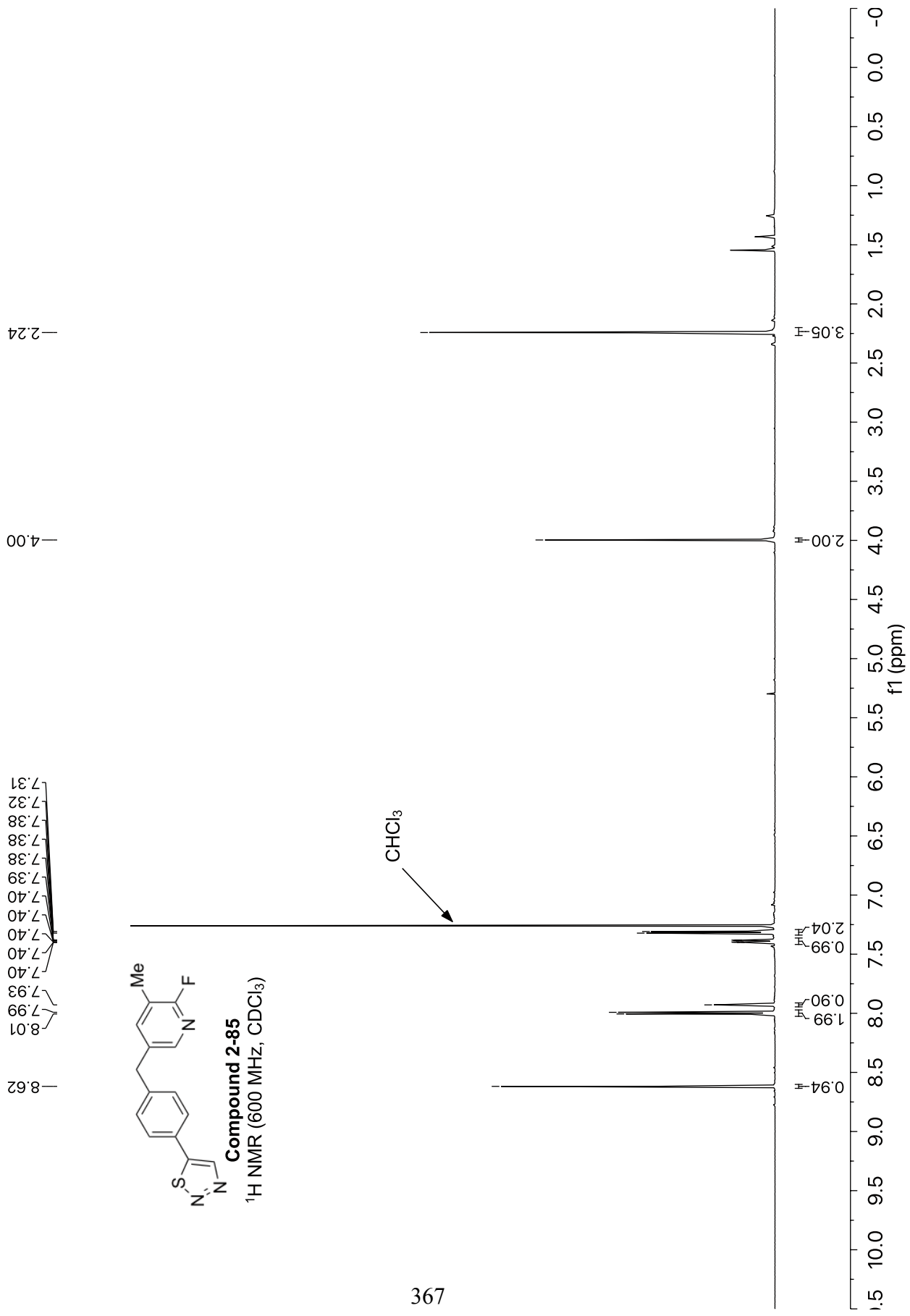


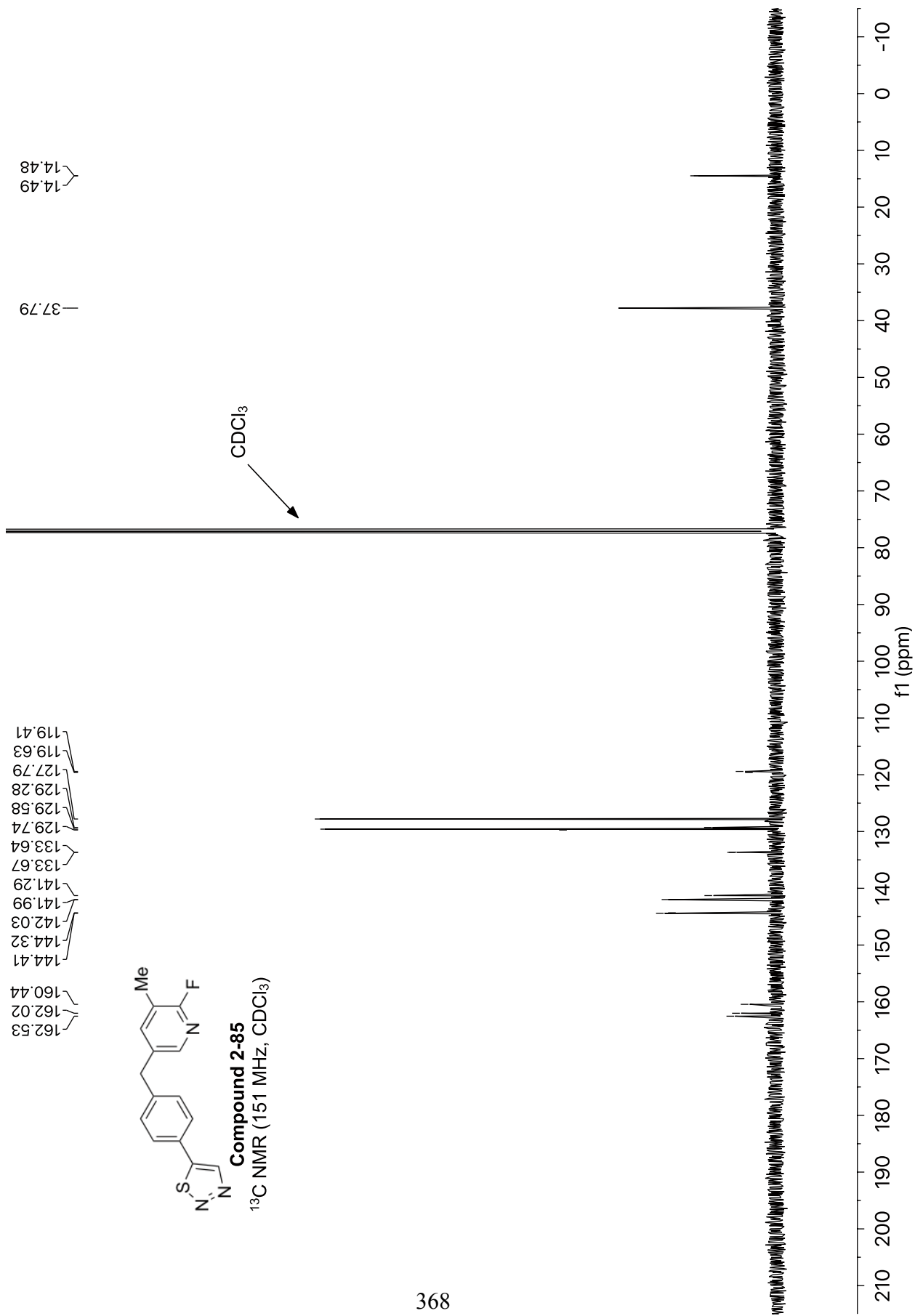
Compound 2-84
 ^{19}F NMR (565 MHz, CDCl_3)

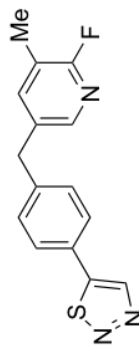
— -117.88



10 0 -10 -20 -30 -40 -50 -60 -70 -80 -90 -100 -110 -120 -130 -140 -150 -160 -170 -180 -190 -200 -210
f1 (ppm)







Compound 2-85

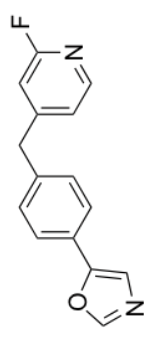
^{19}F NMR (565 MHz, CDCl_3)

— -75.62

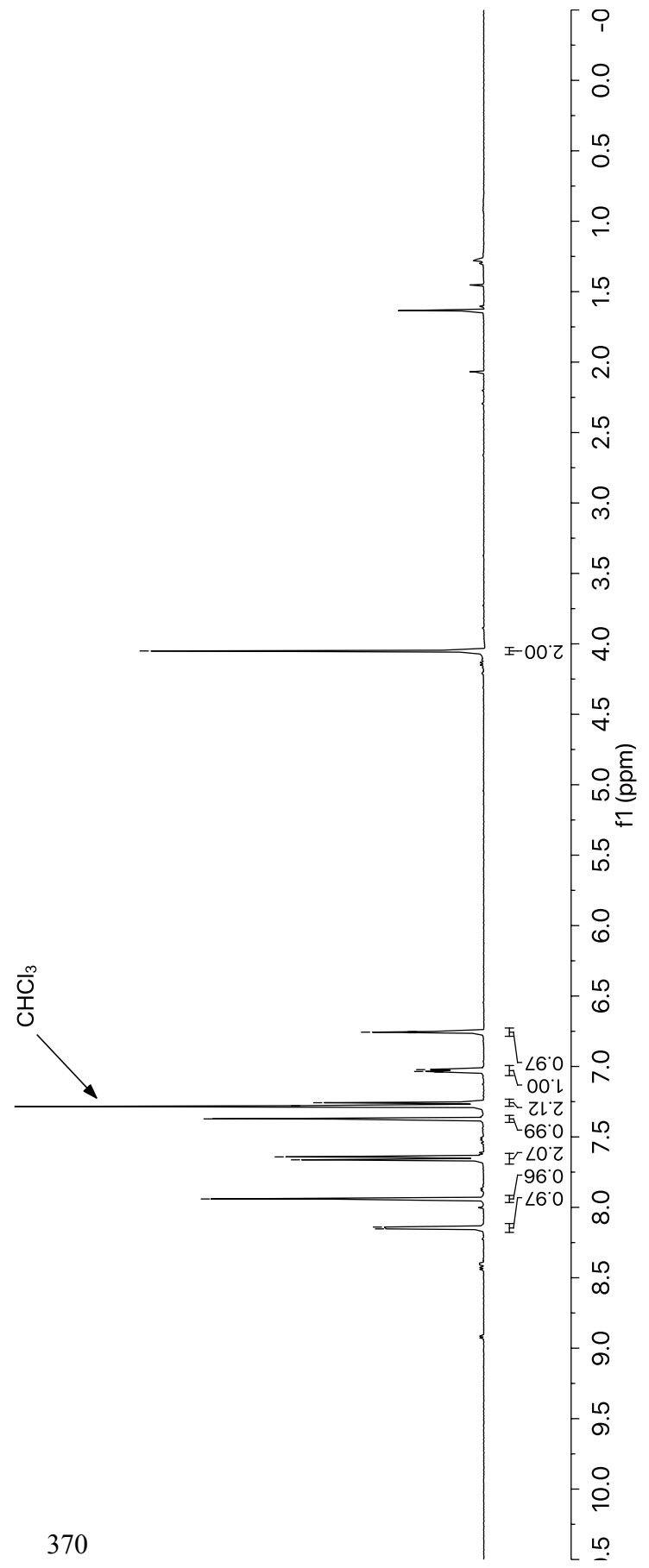


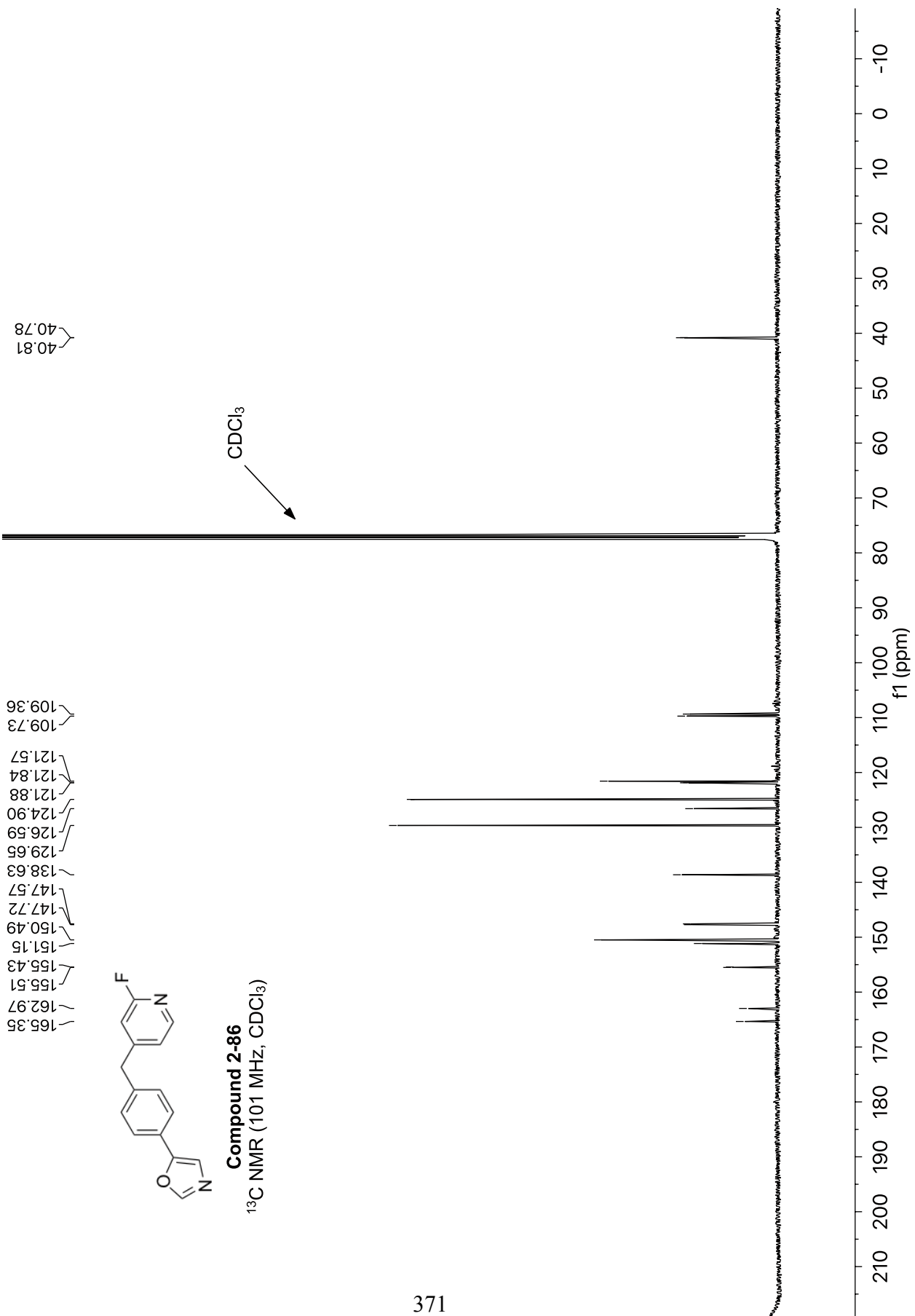
8.15
8.14
7.94
7.66
7.64
7.37
7.28
7.26
7.04
7.04
7.03
7.03
7.02
7.02
6.76
6.76
6.75

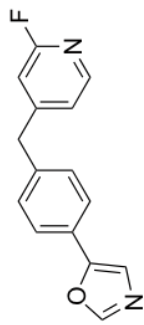
4.05



Compound 2-86
¹H NMR (400 MHz, CDCl₃)



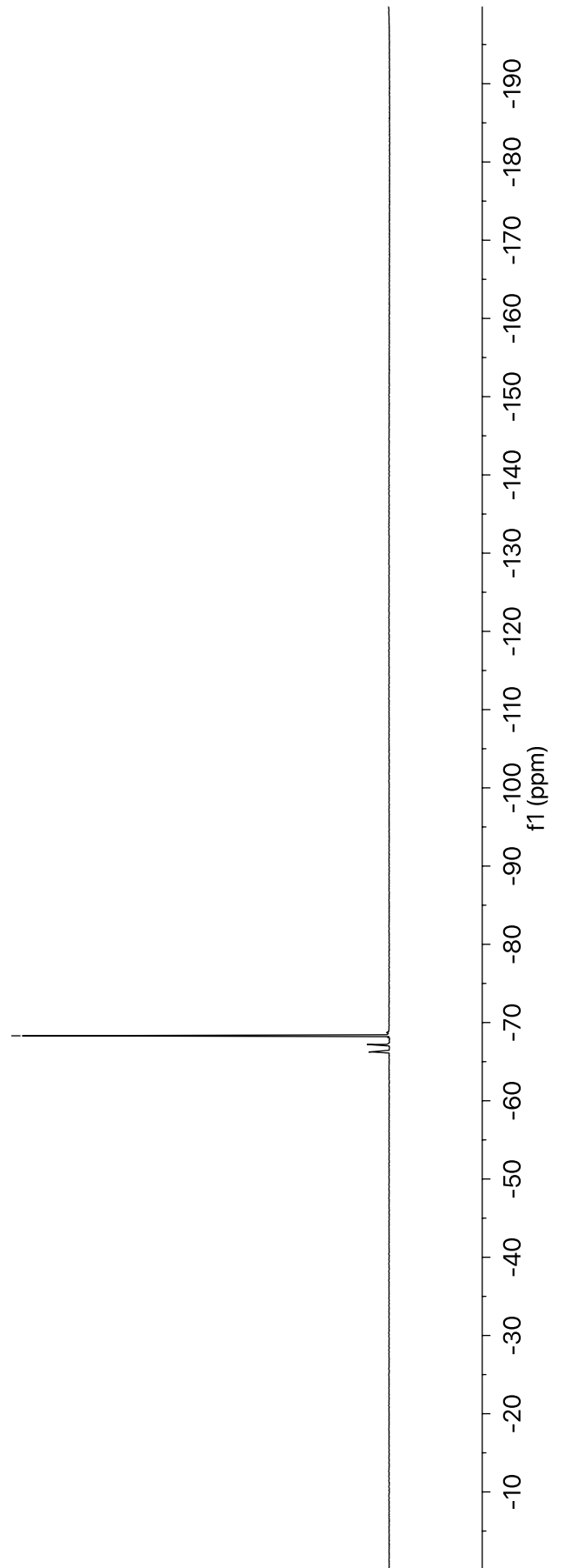


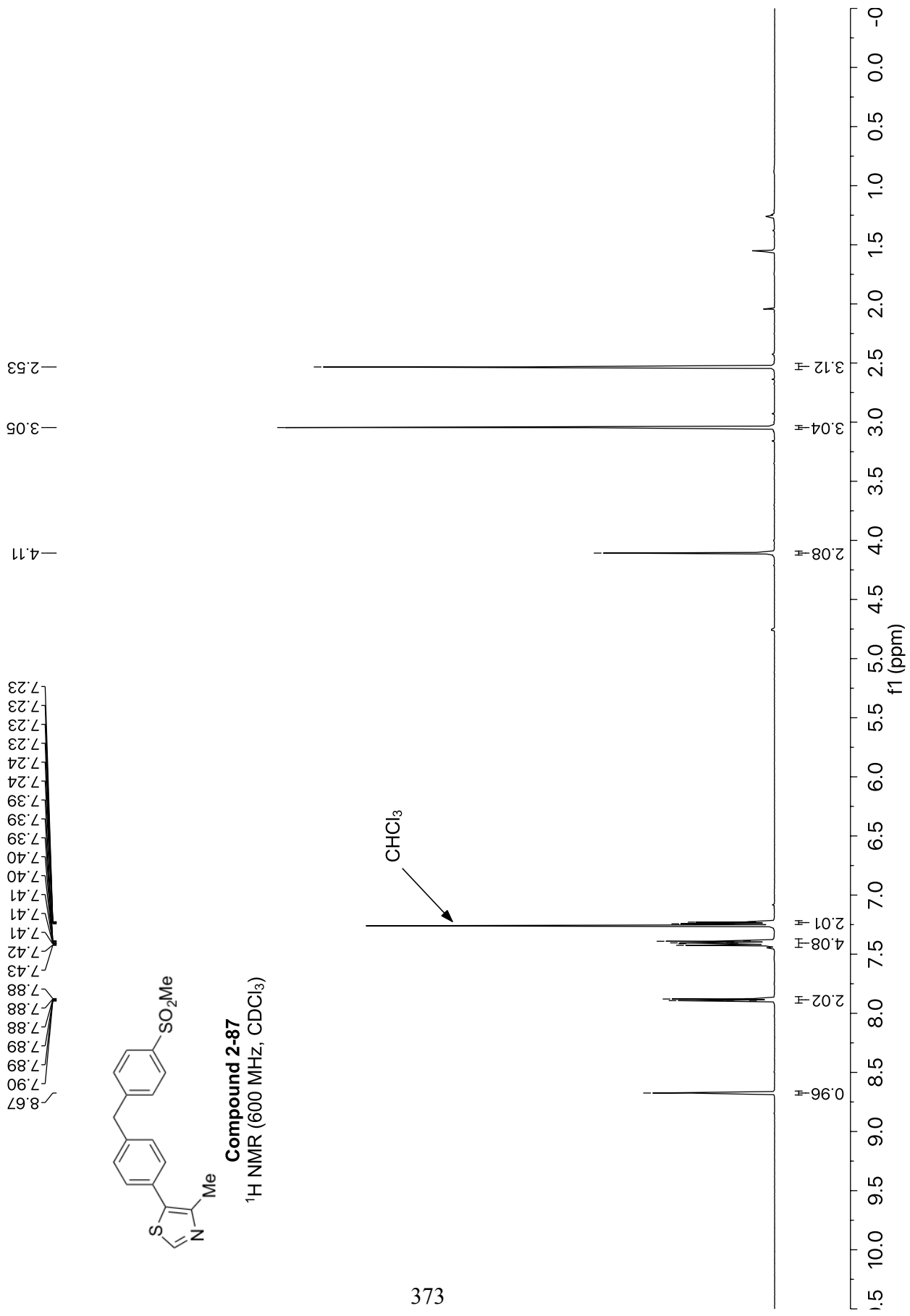


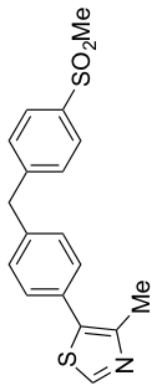
Compound 2-86
¹⁹F NMR (565 MHz, CDCl₃)

-68.31

372

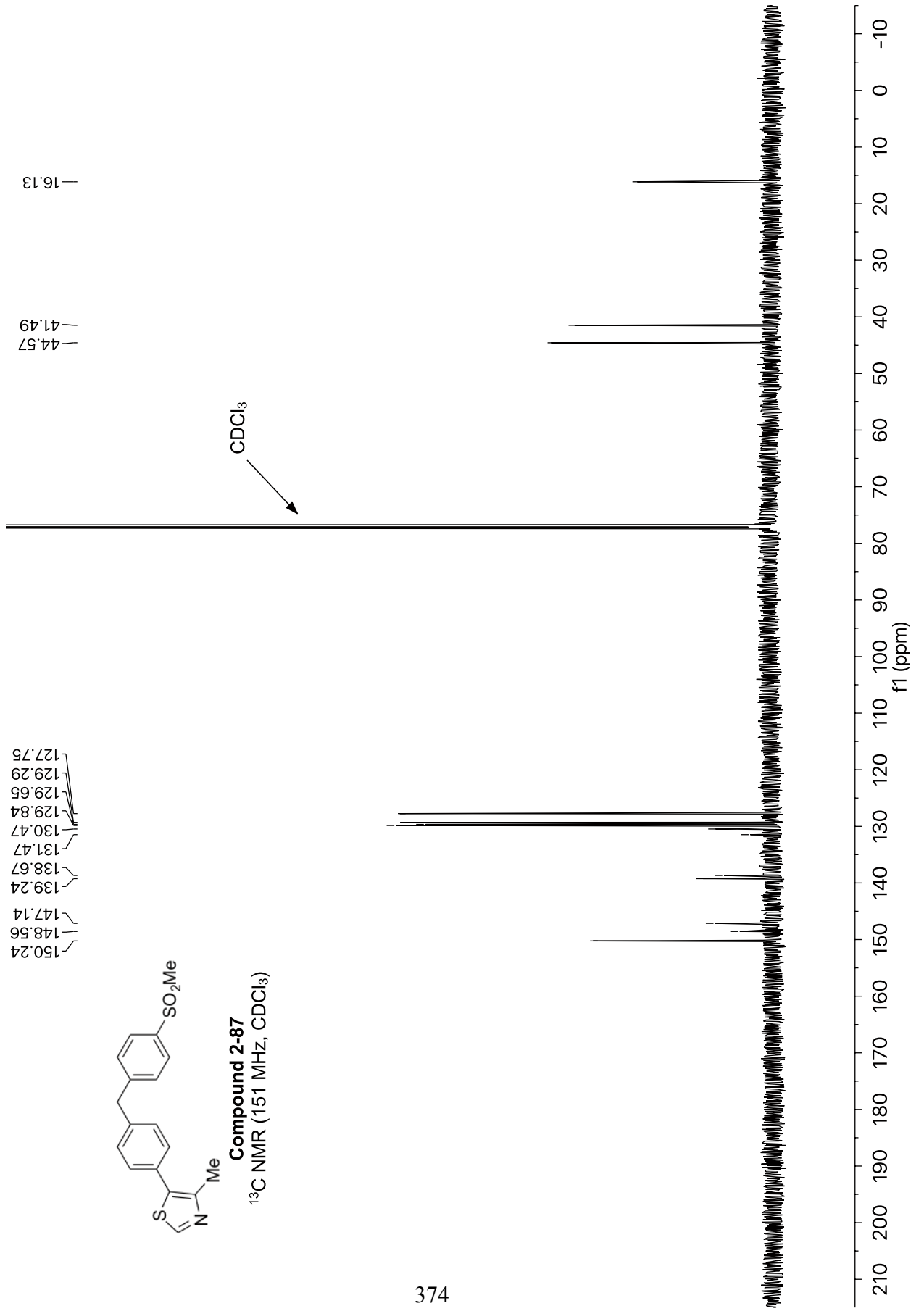


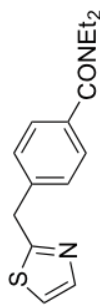




Compound 2-87

^{13}C NMR (151 MHz, CDCl_3)



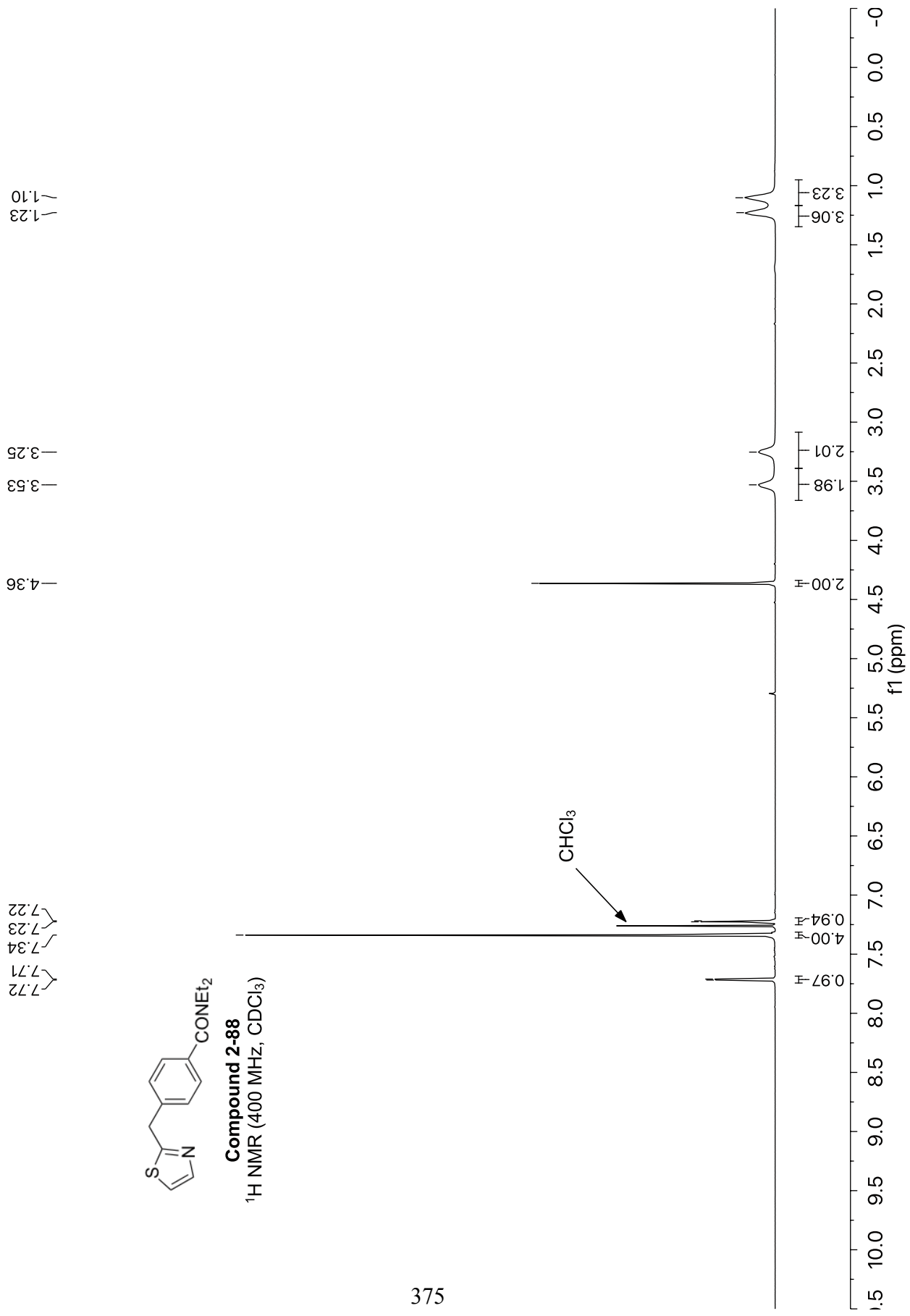


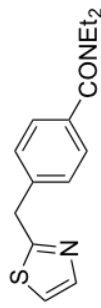
Compound 2-88

¹H NMR (400 MHz, CDCl₃)

7.72, 7.71, 7.34, 7.23, 7.22, 4.36, 3.53, 3.25, 1.23, 1.10

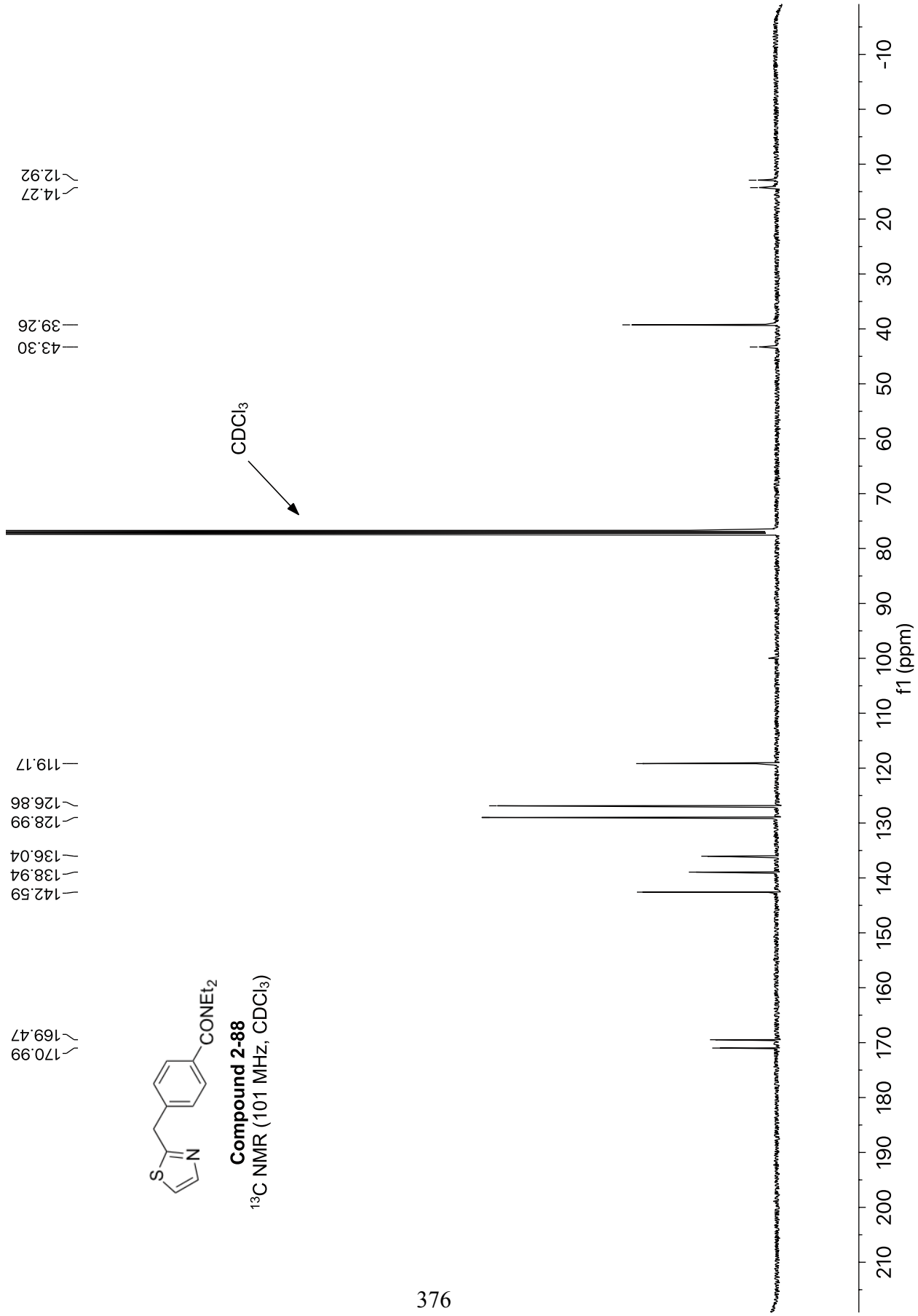
CHCl₃

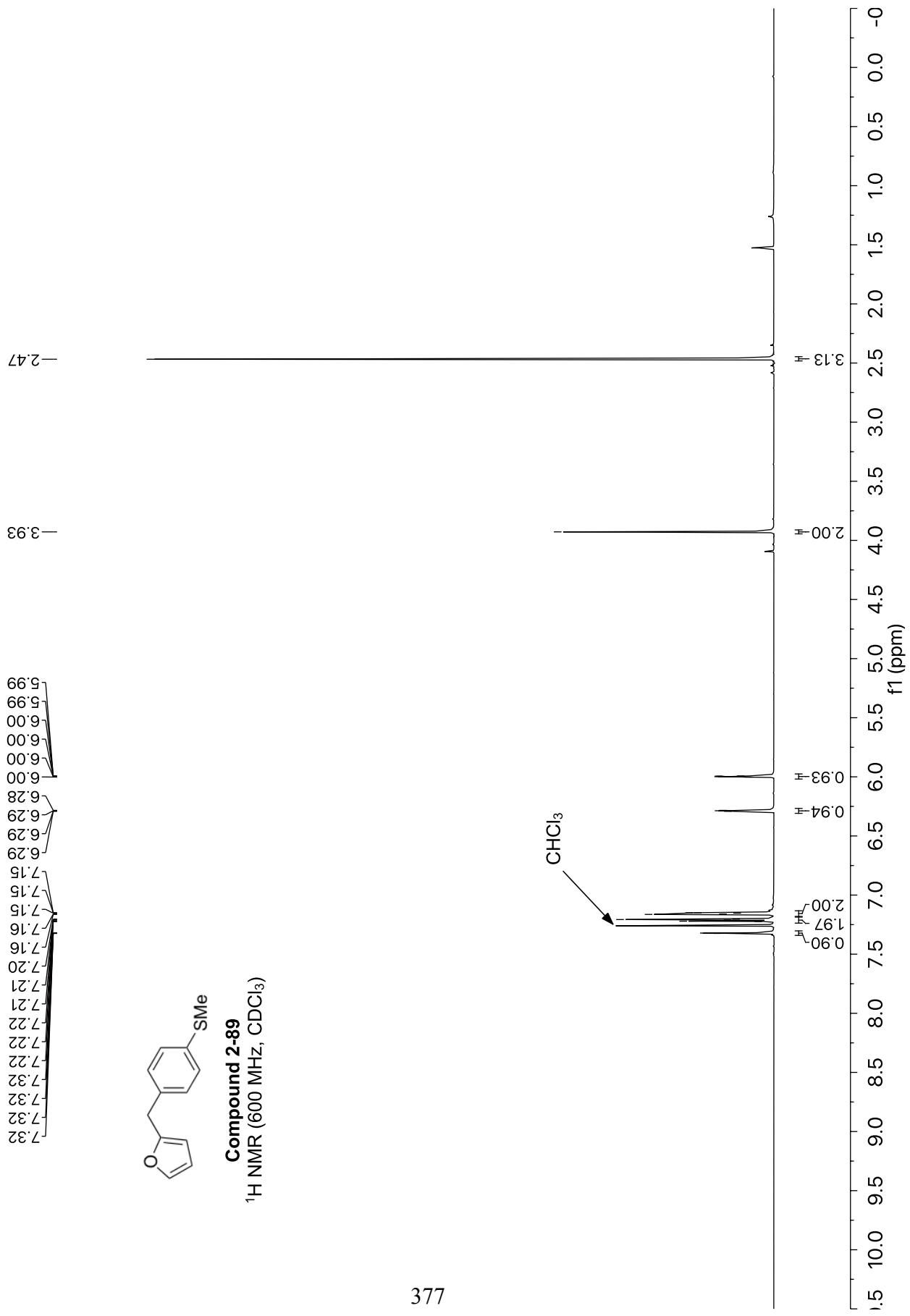


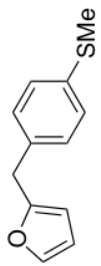


Compound 2-88

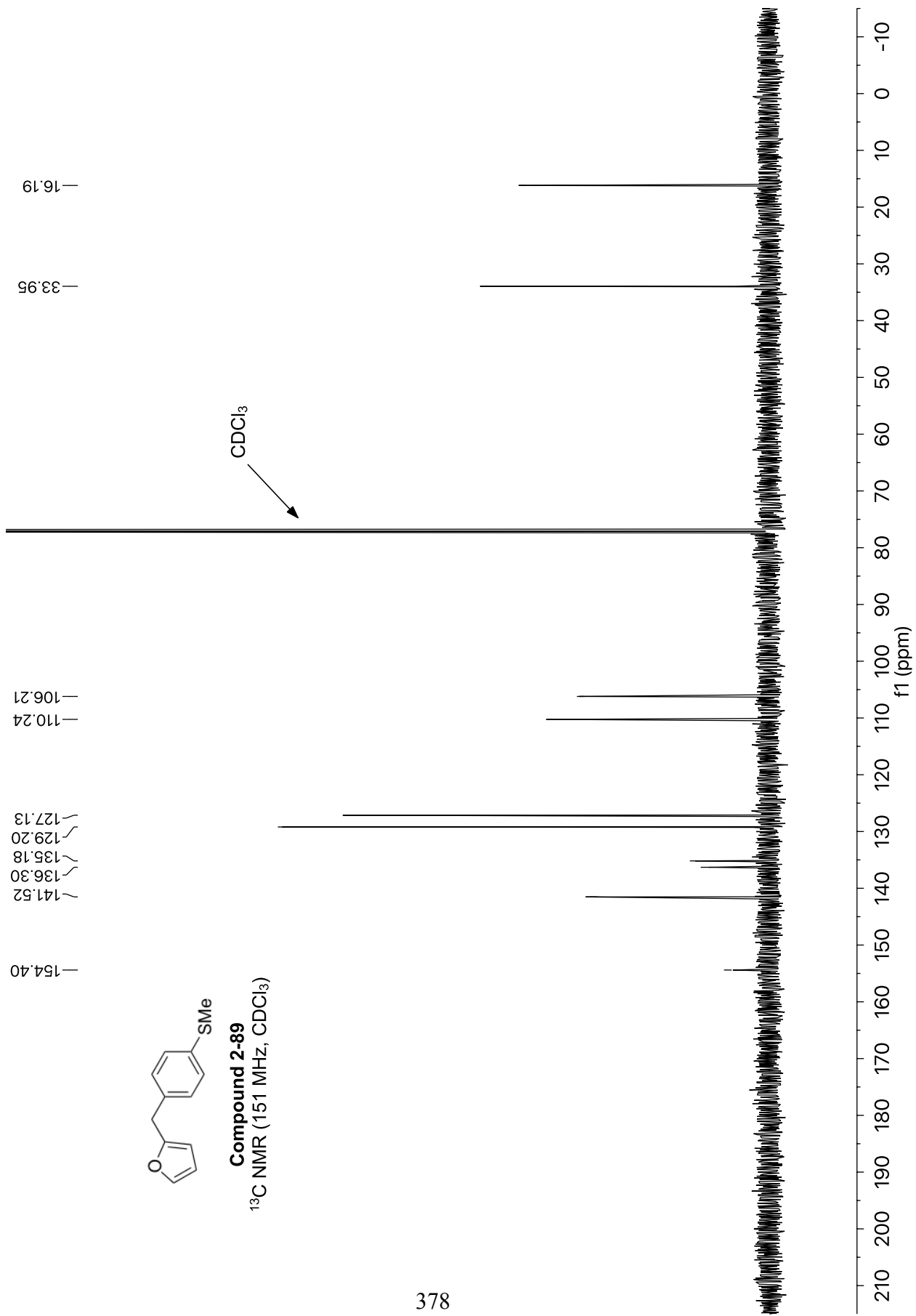
^{13}C NMR (101 MHz, CDCl_3)



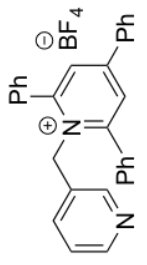




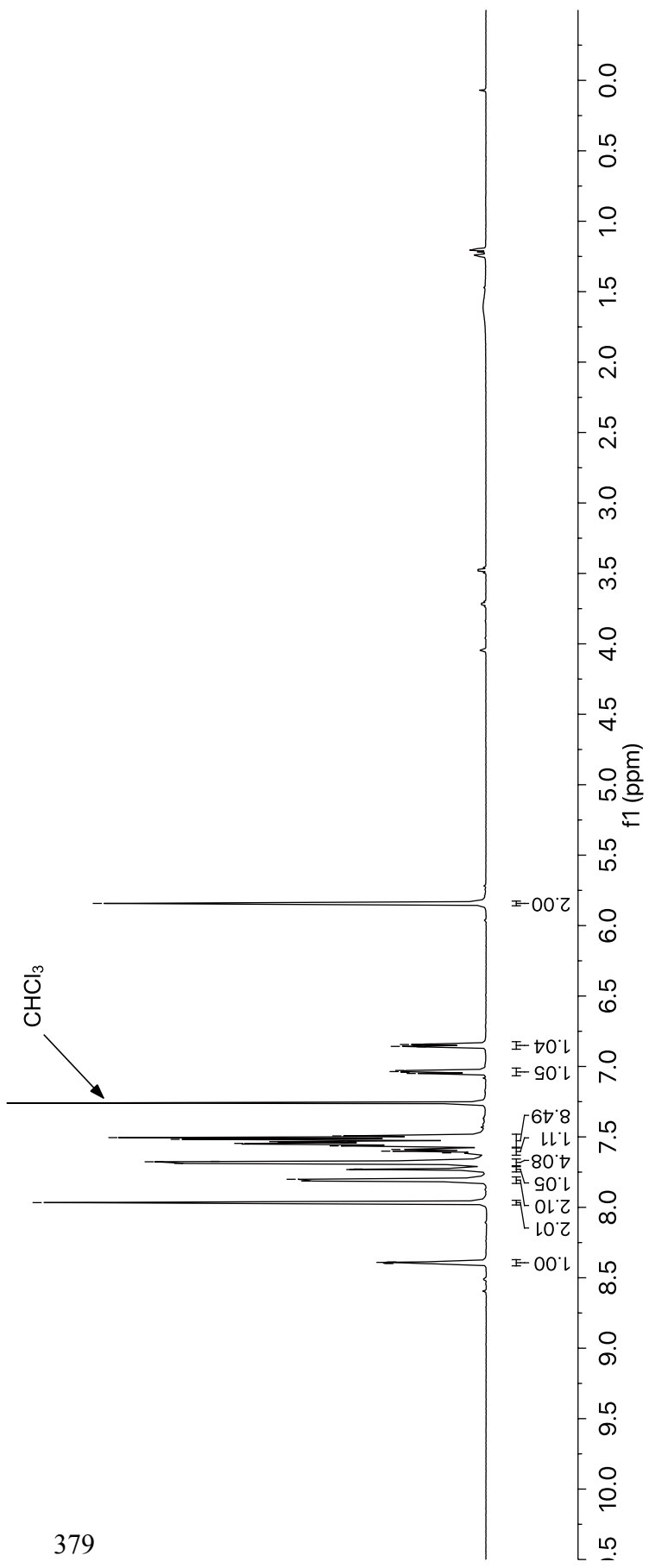
Compound 2-89
¹³C NMR (151 MHz, CDCl₃)

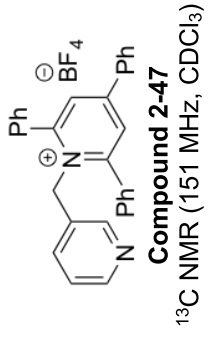
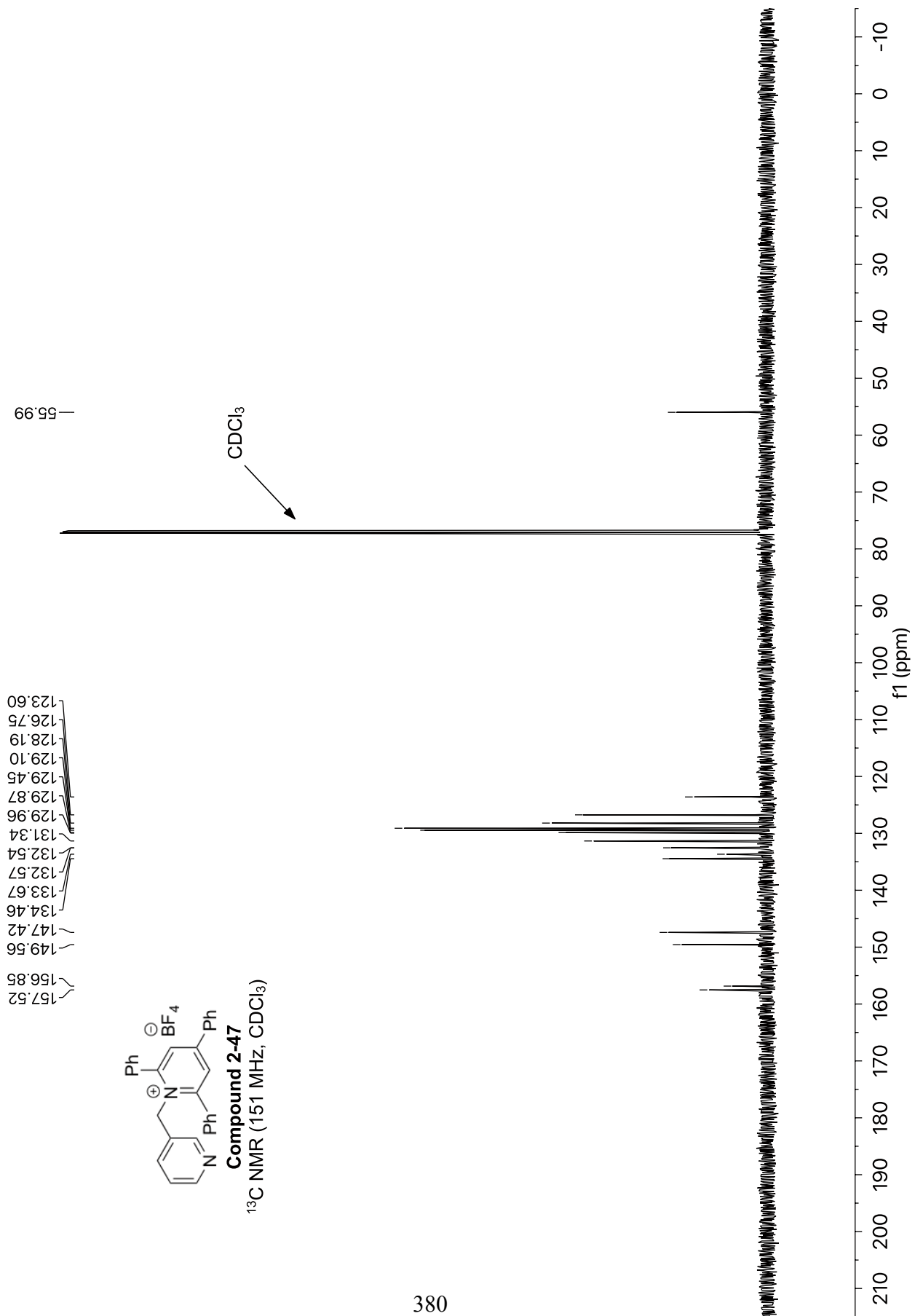


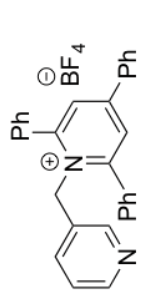
8.40
8.40
8.39
8.39
7.97
7.81
7.80
7.73
7.73
7.69
7.68
7.67
7.61
7.60
7.59
7.56
7.56
7.55
7.55
7.54
7.54
7.53
7.53
7.49
7.49
7.05
7.04
7.04
7.03
6.86
6.86
6.85
6.85
6.84
6.84
5.84



Compound 2-47
¹H NMR (600 MHz, CDCl₃)





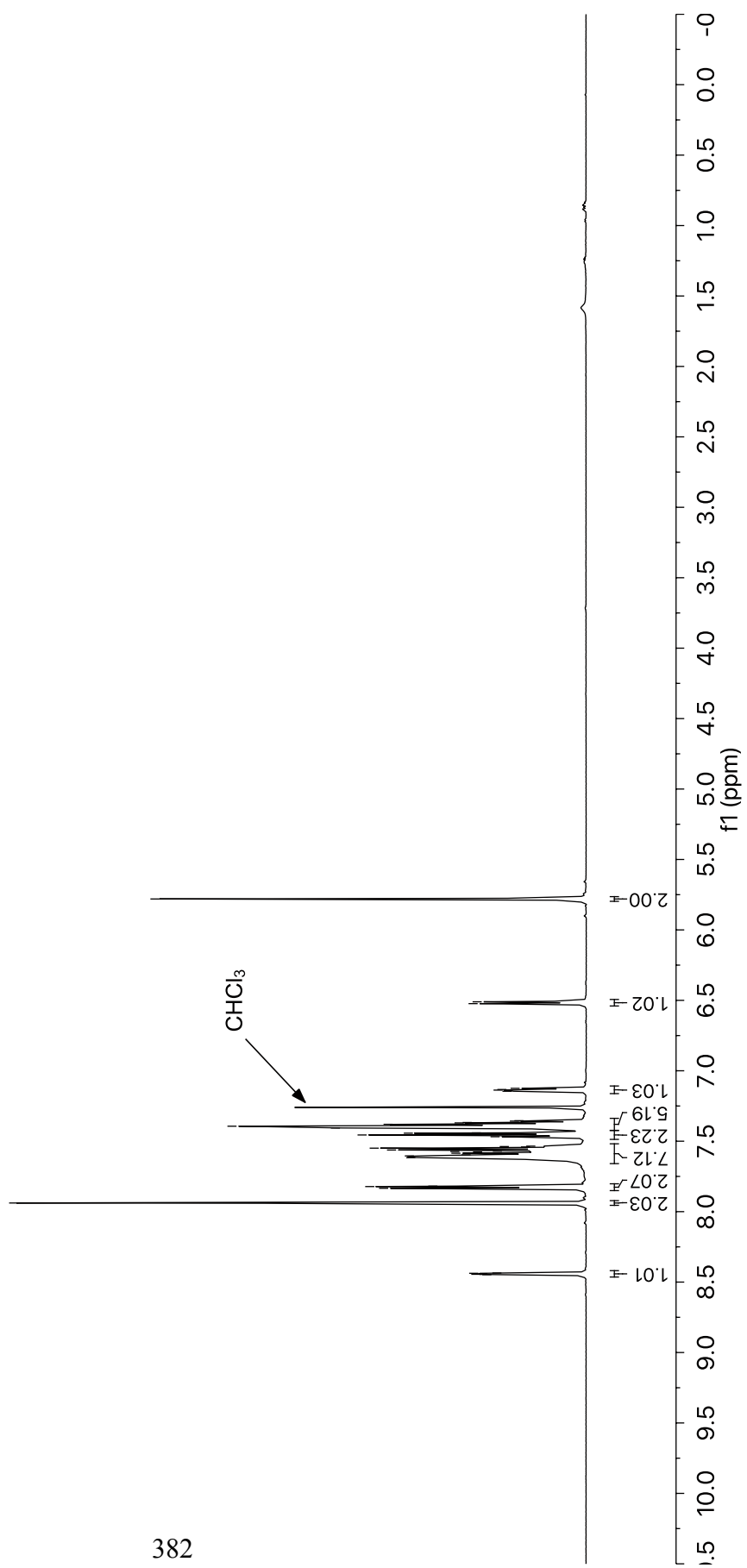
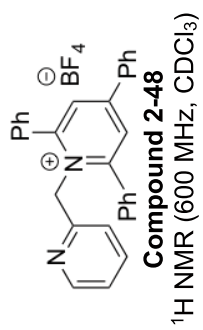


Compound 2-47
¹⁹F NMR (376 MHz, CDCl₃)

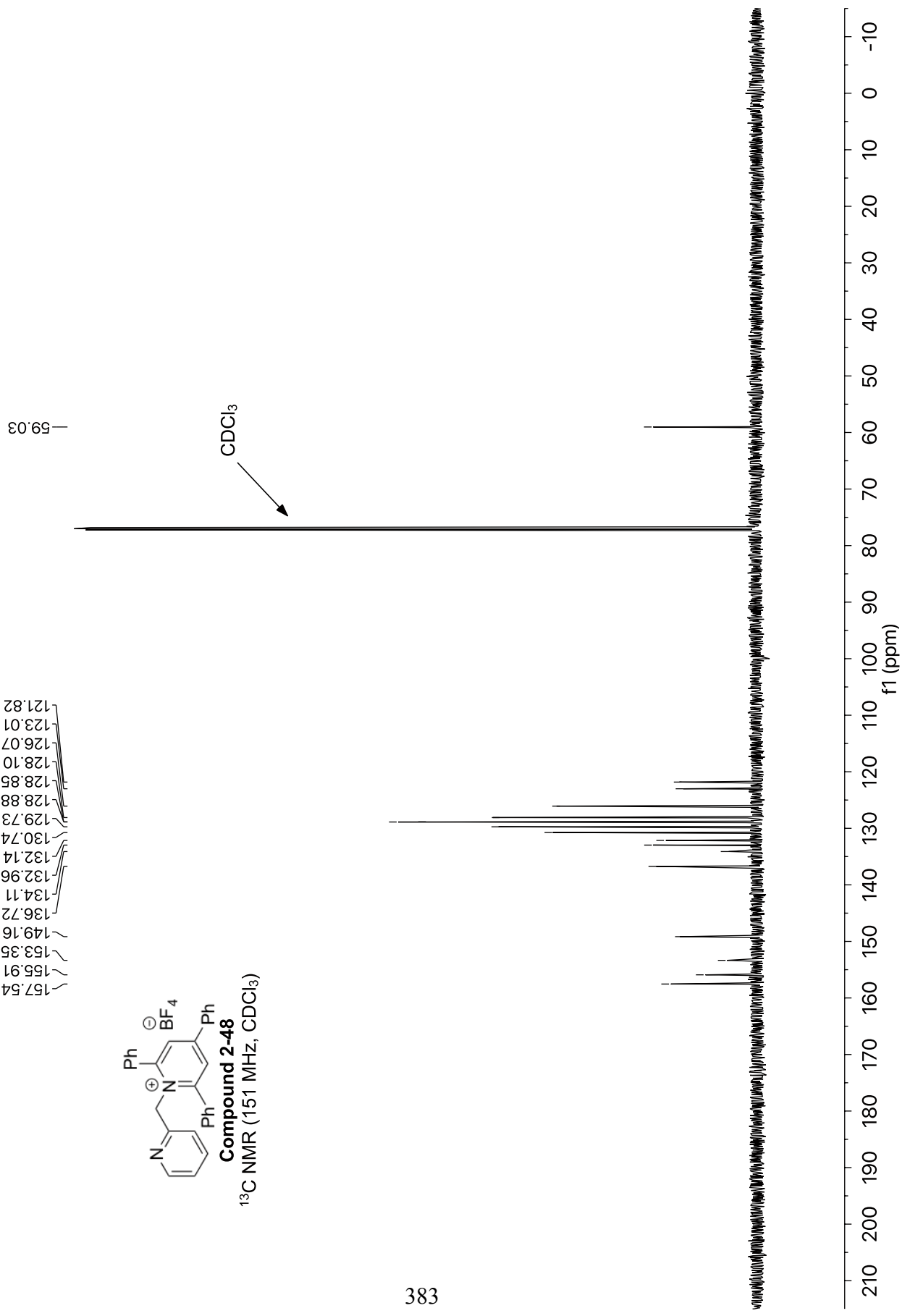
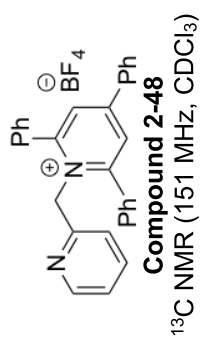
-152.68
-152.63

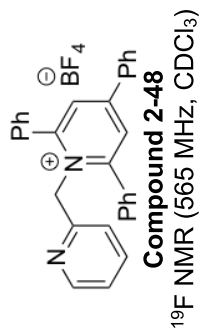
-10 -20 -30 -40 -50 -60 -70 -80 -90 -100 -110 -120 -130 -140 -150 -160 -170 -180 -190
f1 (ppm)

8.45
8.44
8.44
8.44
8.44
8.44
7.94
7.83
7.82
7.82
7.62
7.60
7.60
7.59
7.58
7.57
7.57
7.56
7.55
7.55
7.55
7.54
7.54
7.53
7.47
7.47
7.46
7.45
7.44
7.44
7.41
7.39
7.38
7.38
7.37
7.37
7.36
7.35
7.15
7.14
7.13
7.12
6.52
6.51
5.78

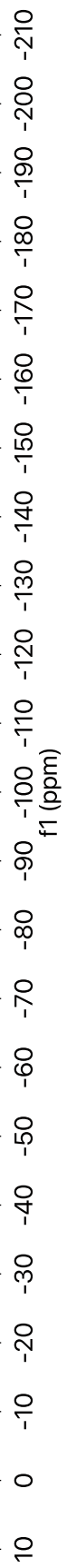


157.54
155.91
153.35
149.16
136.72
134.11
132.96
132.14
130.74
129.73
128.88
128.85
128.10
126.07
123.01
121.82

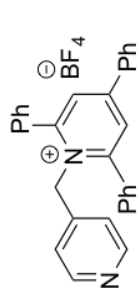




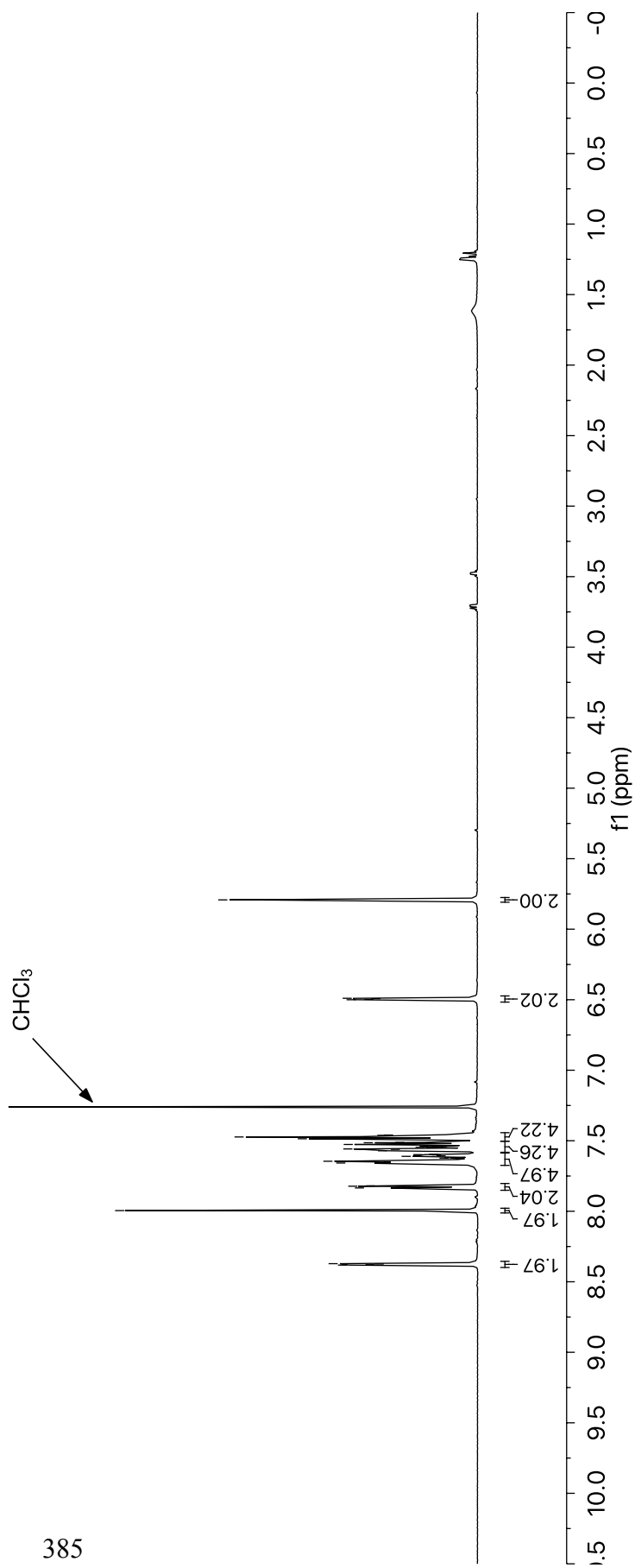
153.35
153.30

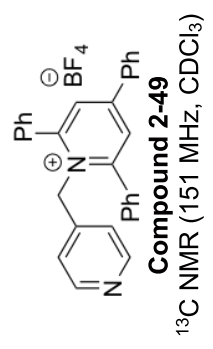
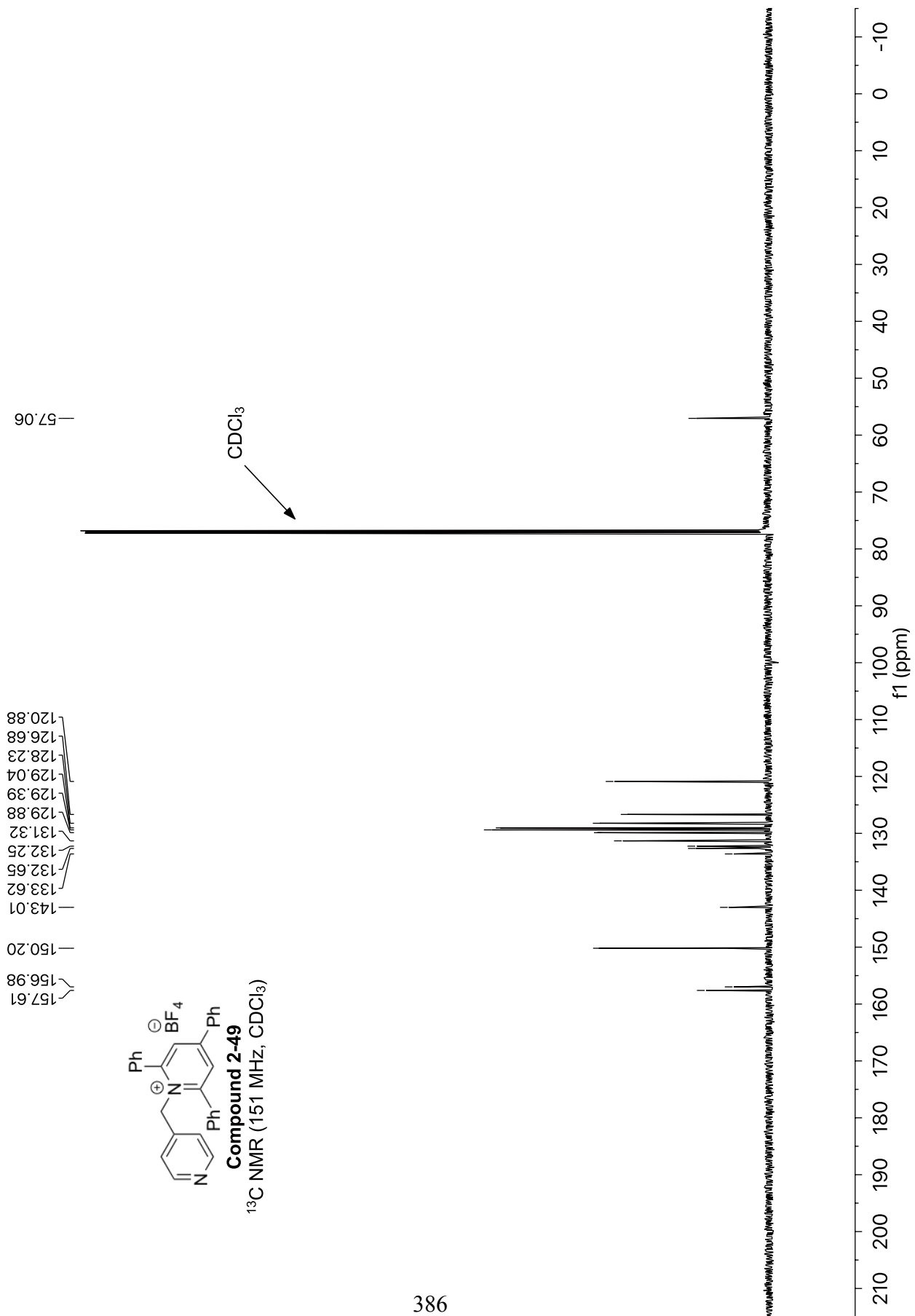


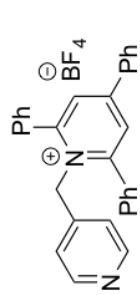
8.38
8.37
8.37
8.00
7.83
7.83
7.82
7.82
7.66
7.65
7.62
7.62
7.61
7.61
7.60
7.60
7.60
7.57
7.56
7.56
7.56
7.55
7.55
7.54
7.54
7.54
7.54
7.54
7.53
7.52
7.51
7.51
7.49
7.48
7.47
7.46
7.46
6.50
6.50
6.49
6.49
5.79



Compound 2-49
¹H NMR (600 MHz, CDCl₃)

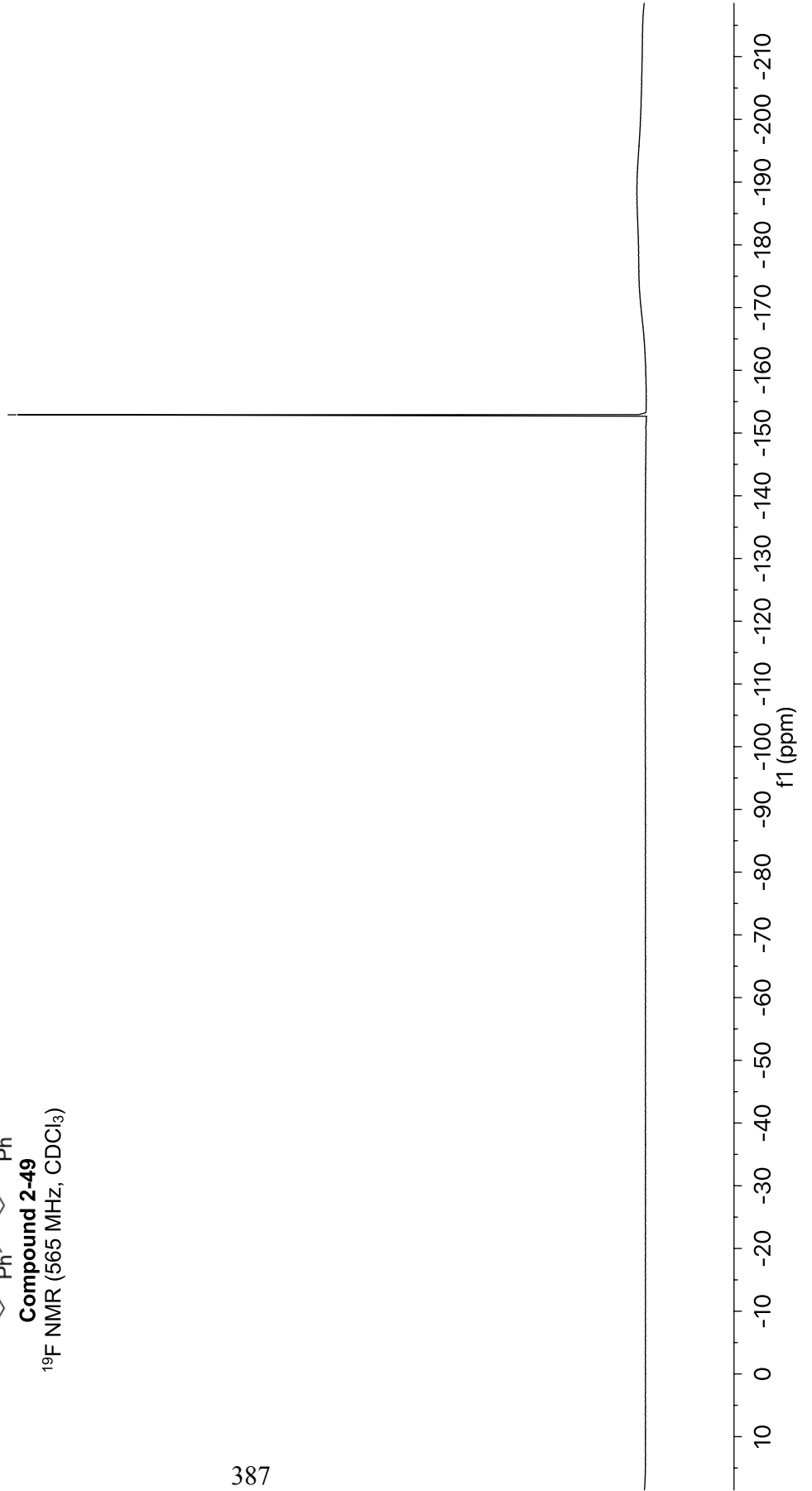




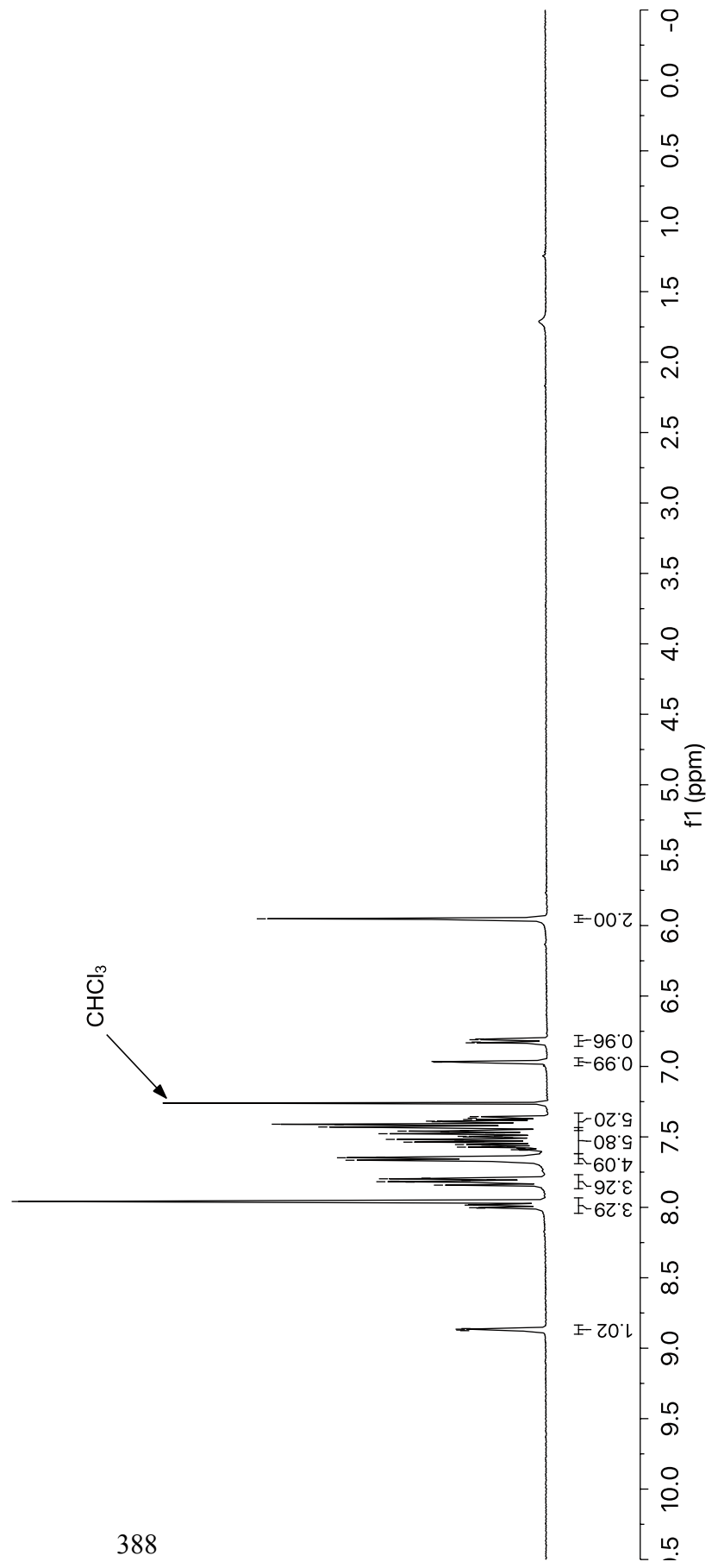
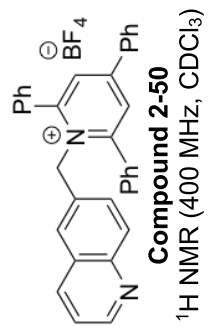


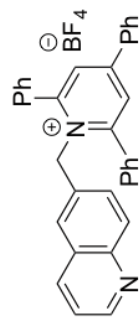
Compound 2-49
¹⁹F NMR (565 MHz, CDCl₃)

152.85
152.90



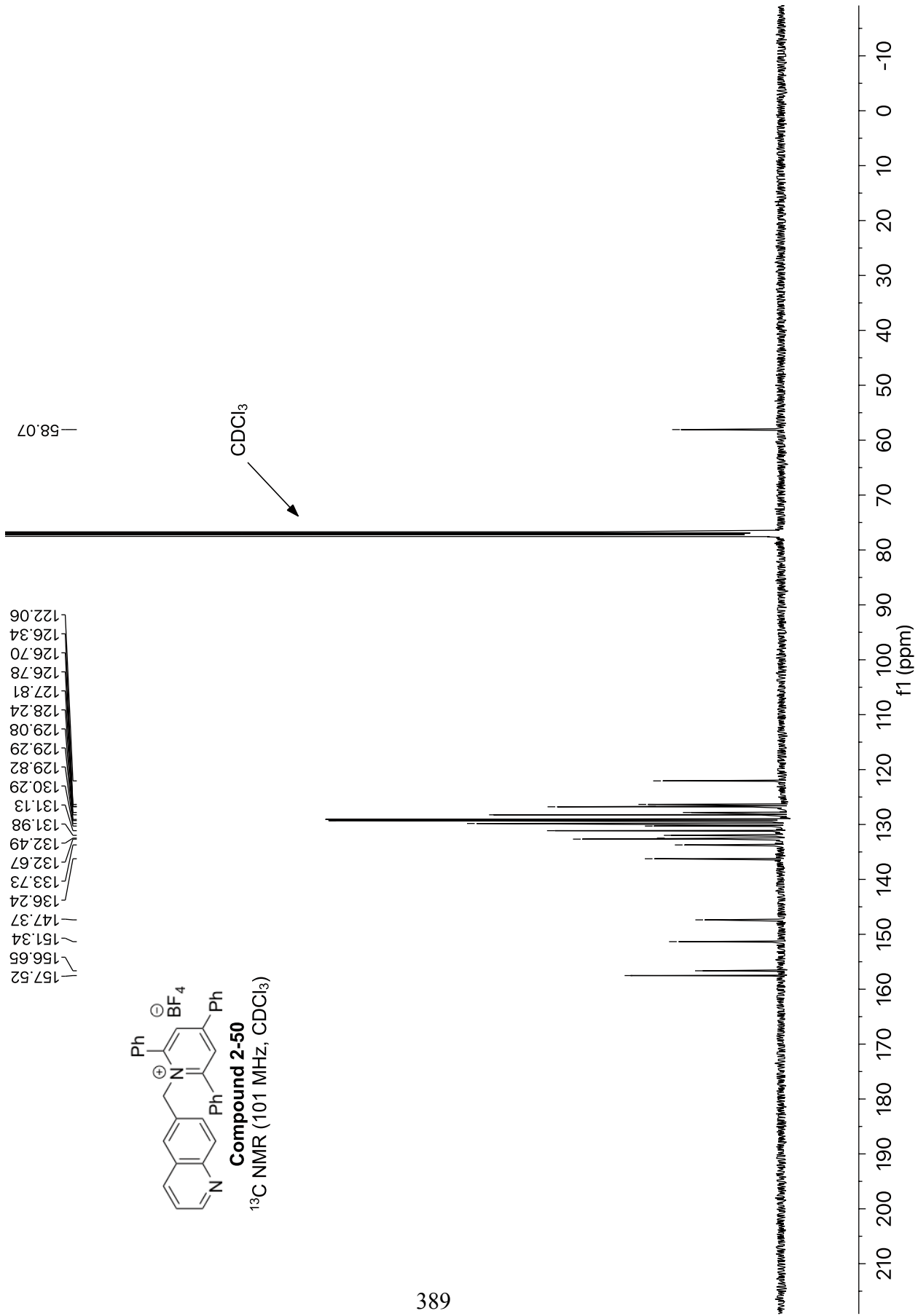
8.88
8.87
8.86
8.86
8.01
8.00
8.00
7.98
7.98
7.96
7.84
7.82
7.82
7.81
7.81
7.80
7.79
7.67
7.65
7.64
7.59
7.59
7.59
7.58
7.57
7.57
7.56
7.55
7.55
7.54
7.53
7.52
7.52
7.51
7.50
7.50
7.49
7.48
7.48
7.47
7.46
7.46
7.43
7.41
7.41
7.39
7.39
7.38
7.37
7.36
6.97
6.96
6.83
6.83
6.81
6.80
5.95

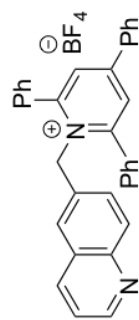




Compound 2-50

¹³C NMR (101 MHz, CDCl₃)

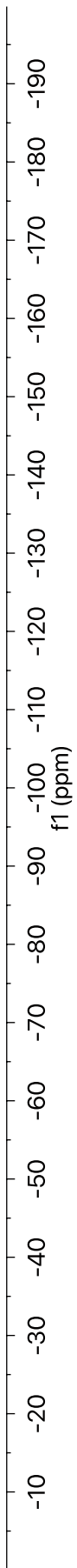




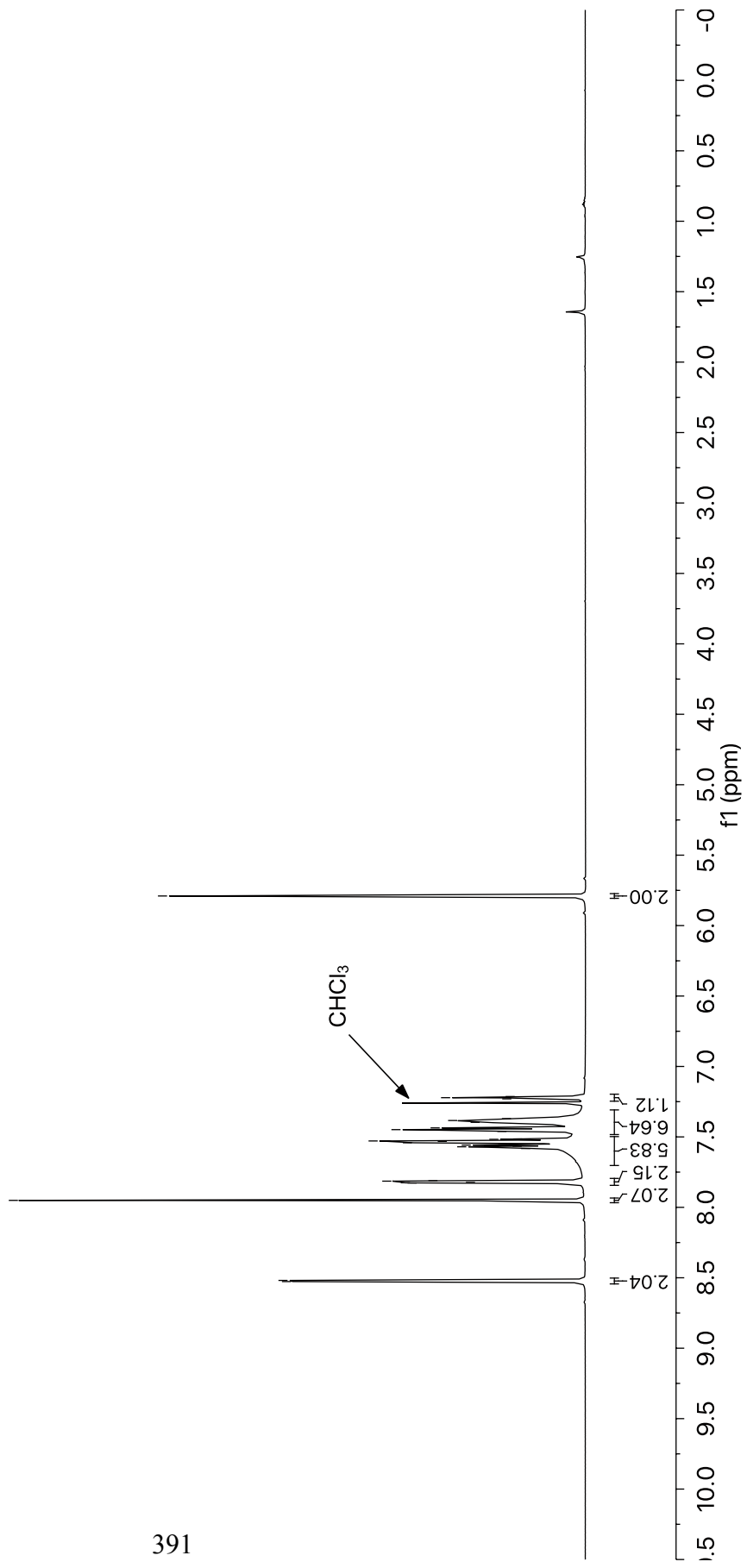
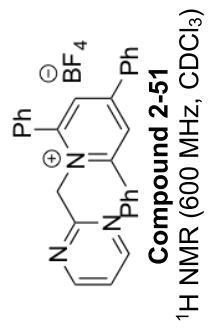
Compound 2-50

¹⁹F NMR (376 MHz, CDCl₃)

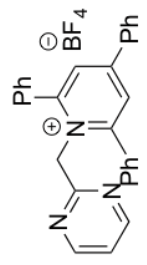
-152.55
-152.55



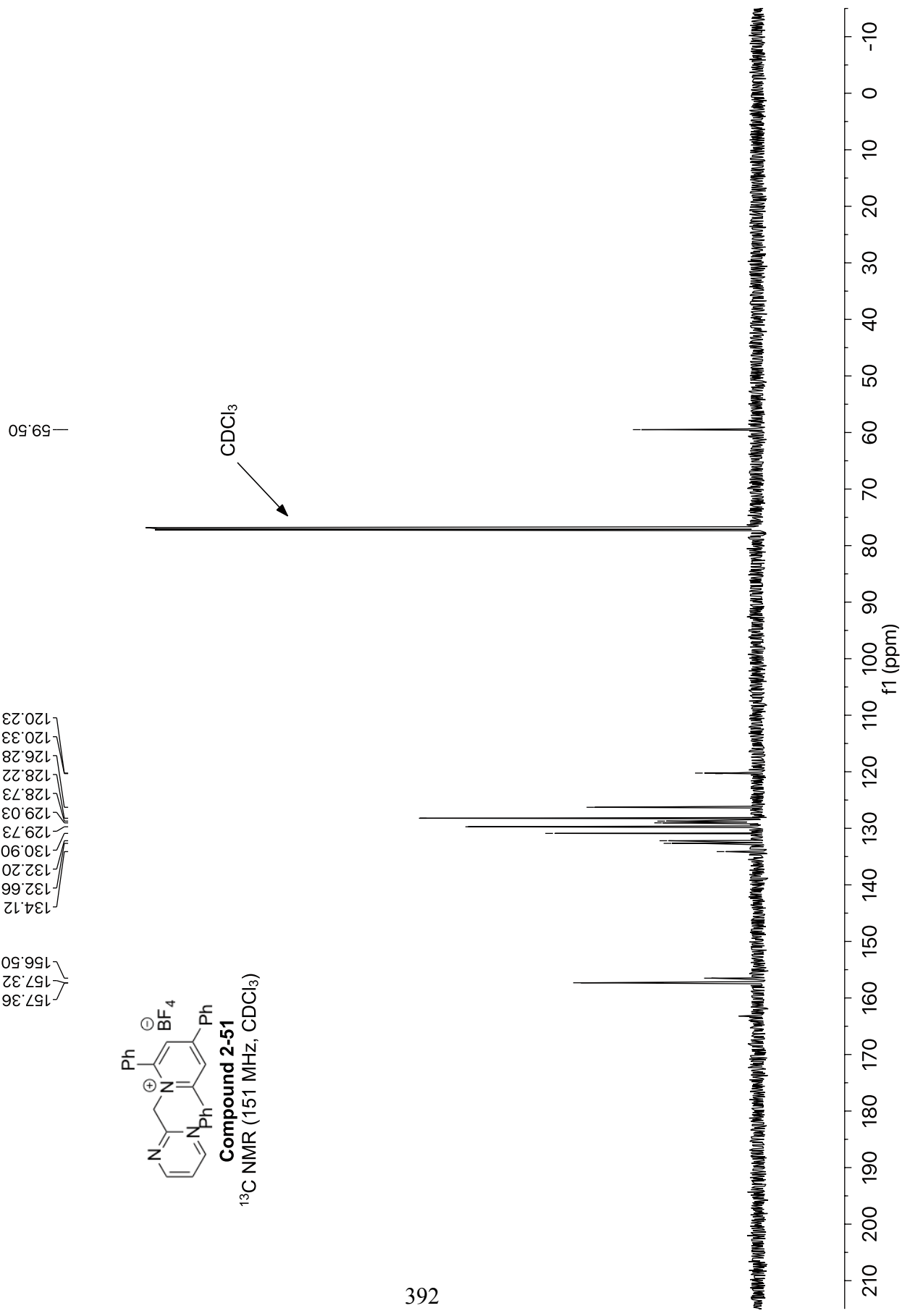
8.53
8.52
7.95
7.83
7.83
7.82
7.81
7.81
7.58
7.57
7.57
7.56
7.56
7.56
7.54
7.53
7.53
7.53
7.52
7.51
7.46
7.45
7.44
7.40
7.38
7.37
7.23
7.22
7.21
5.79

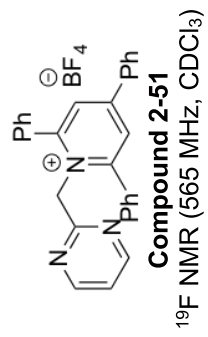


157.36
156.50
157.32
134.12
132.66
132.20
130.90
129.73
129.03
128.73
128.22
126.28
120.33
120.23

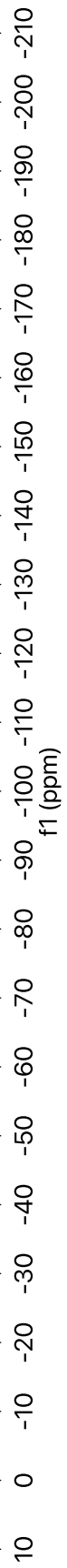


Compound 2-51
¹³C NMR (151 MHz, CDCl₃)

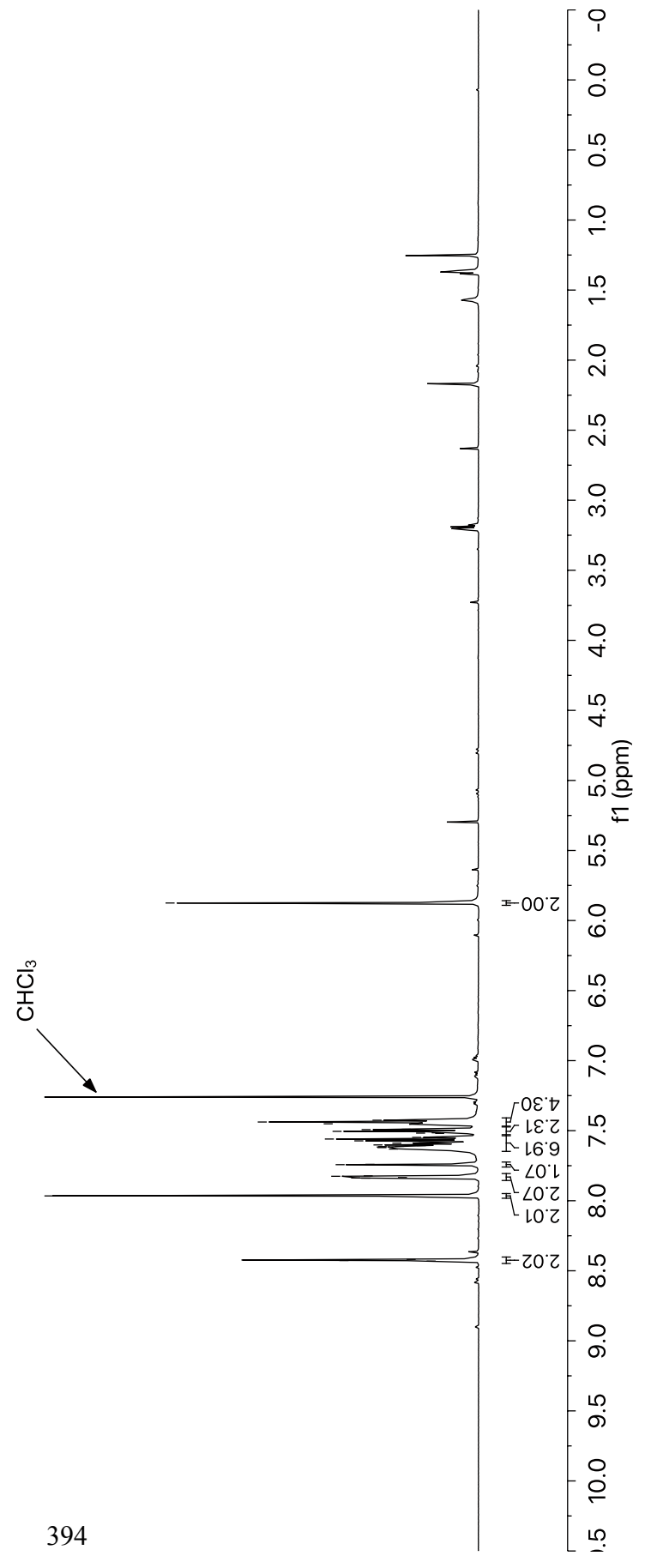
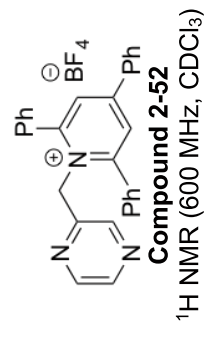


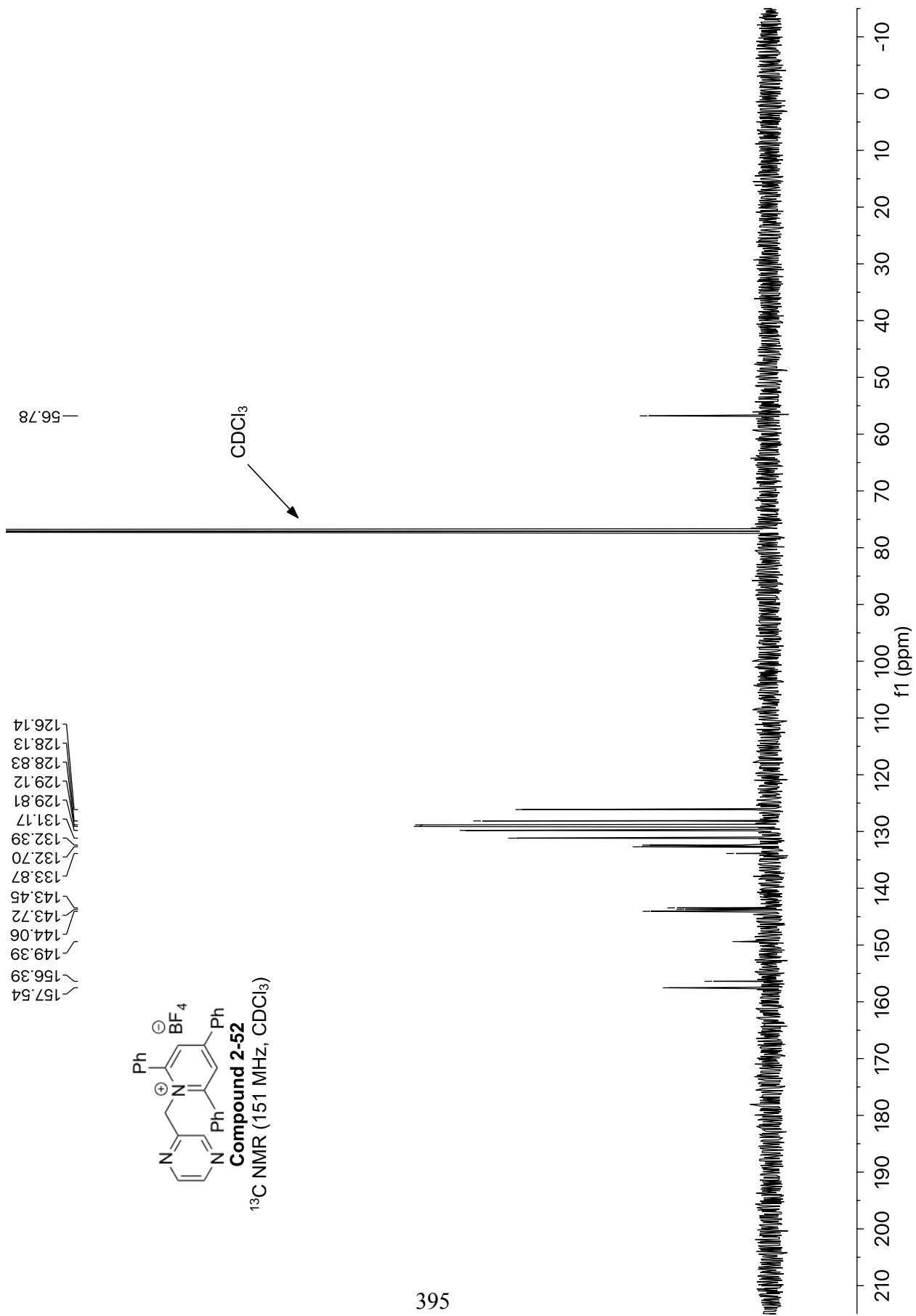
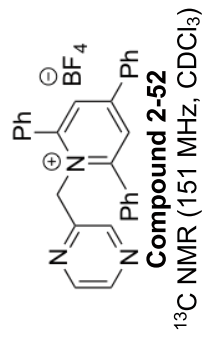


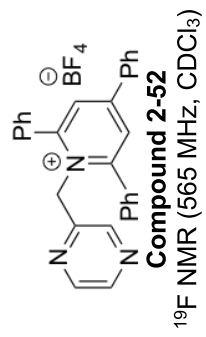
-153.48
-153.43



8.43
8.42
8.42
8.42
7.97
7.84
7.84
7.83
7.83
7.82
7.74
7.74
7.63
7.62
7.62
7.61
7.61
7.60
7.59
7.59
7.59
7.57
7.57
7.56
7.56
7.55
7.55
7.52
7.52
7.51
7.50
7.50
7.49
7.49
7.45
7.44
7.43
5.87

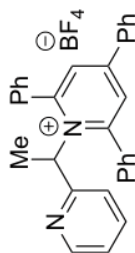
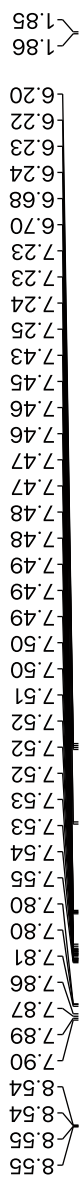




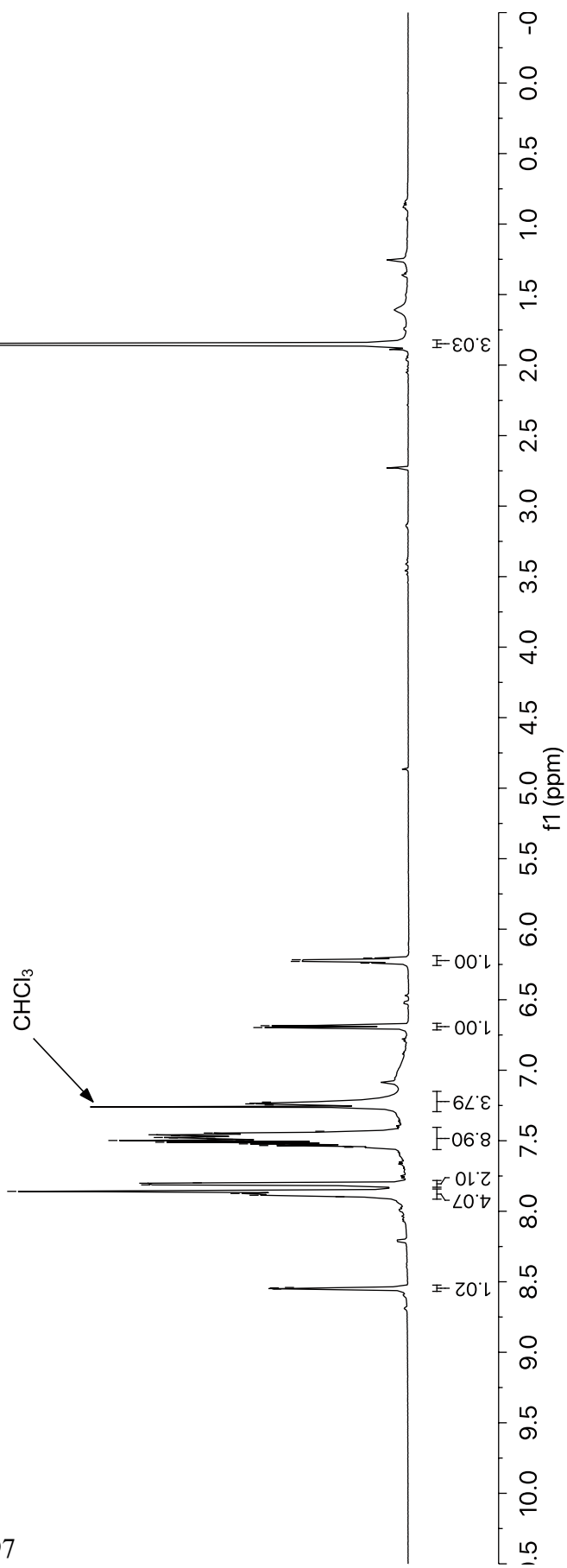


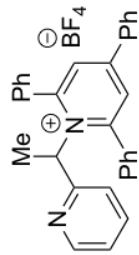
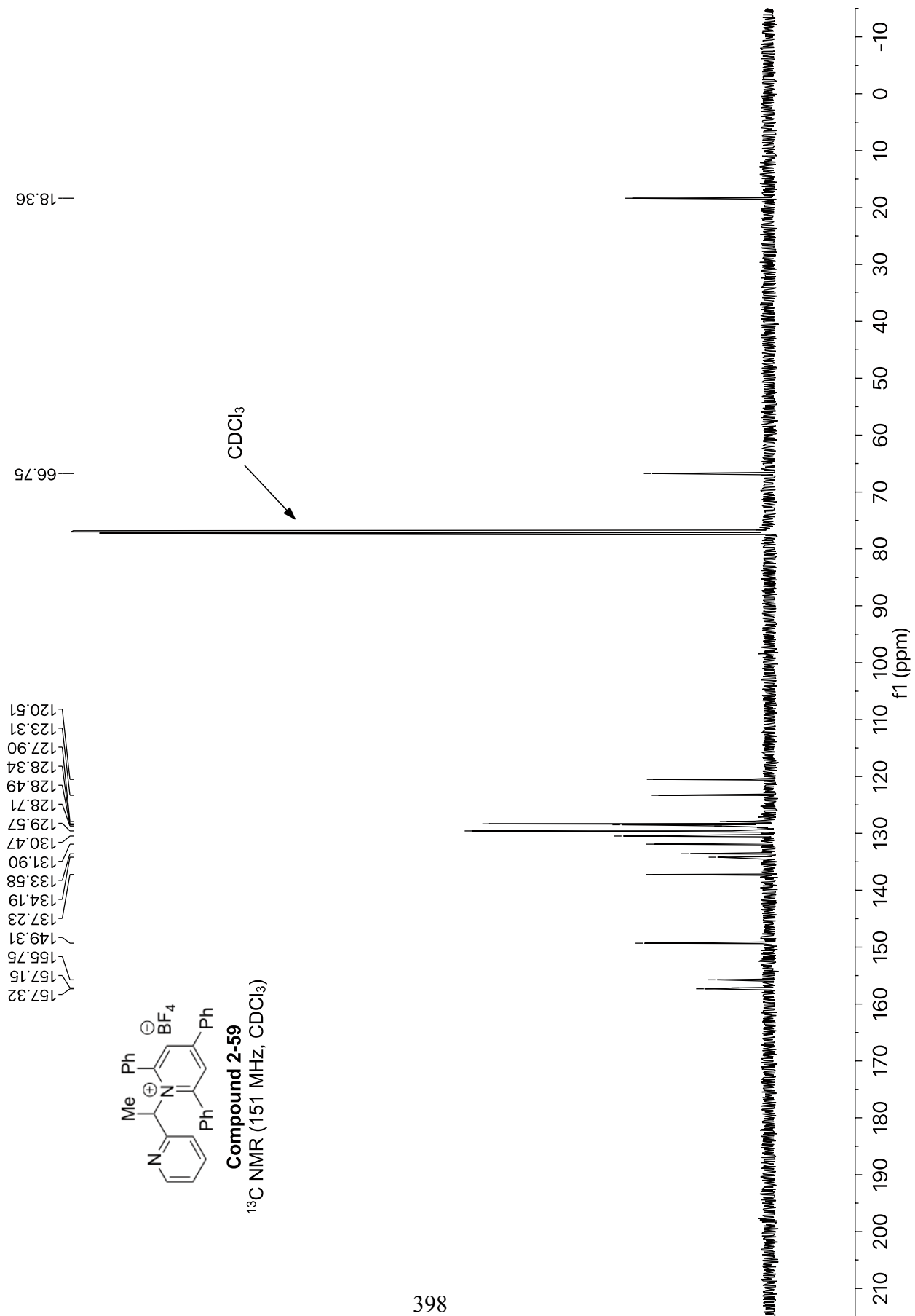
152.94
152.99

10 0 -10 -20 -30 -40 -50 -60 -70 -80 -90 -100 -110 -120 -130 -140 -150 -160 -170 -180 -190 -200 -210
f1 (ppm)

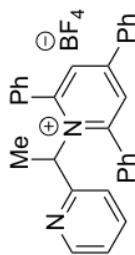


Compound 2-59
¹H NMR (600 MHz, CDCl₃)





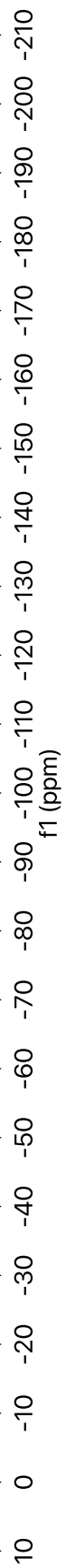
Compound 2-59
¹³C NMR (151 MHz, CDCl₃)



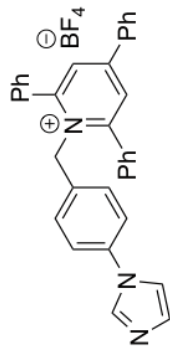
Compound 2-59

¹⁹F NMR (565 MHz, CDCl₃)

-153.31
-153.26

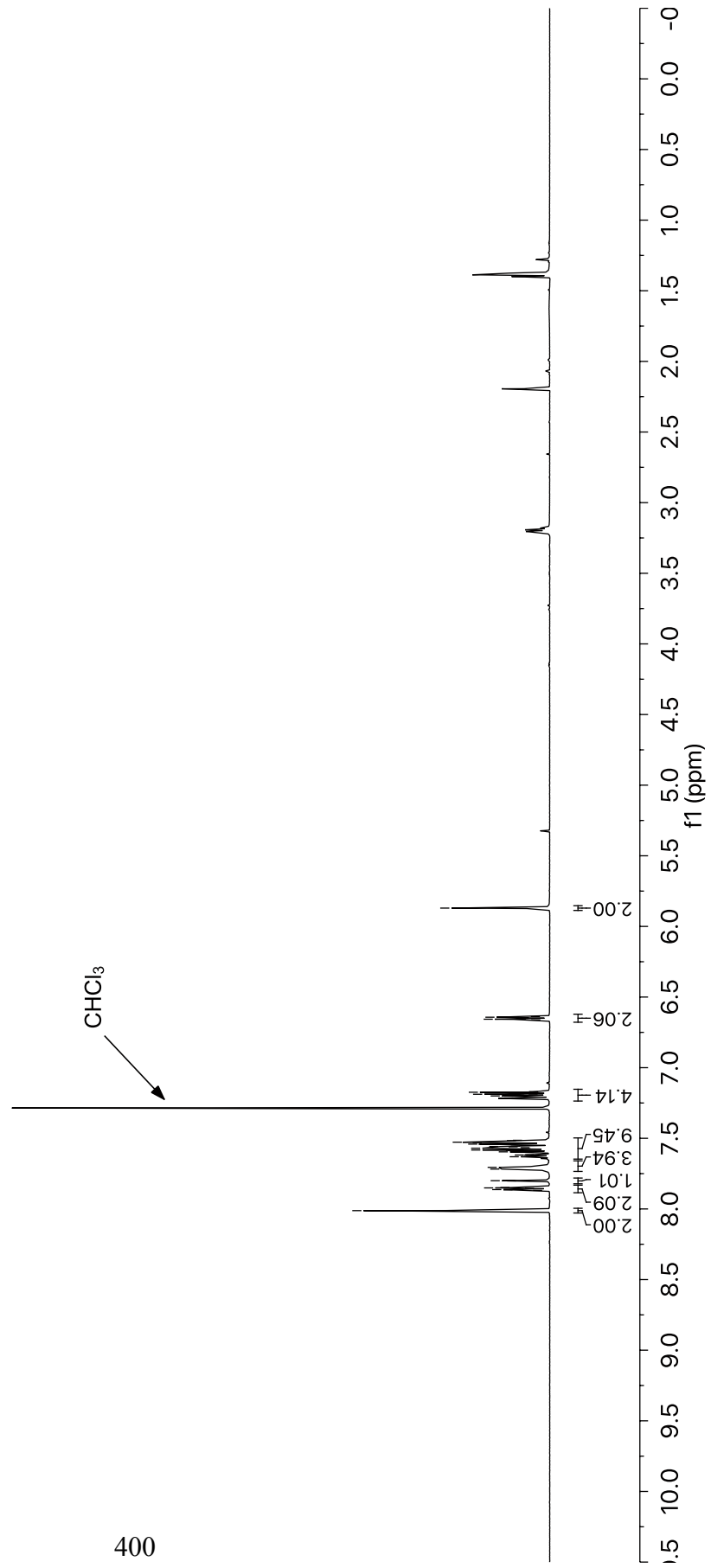


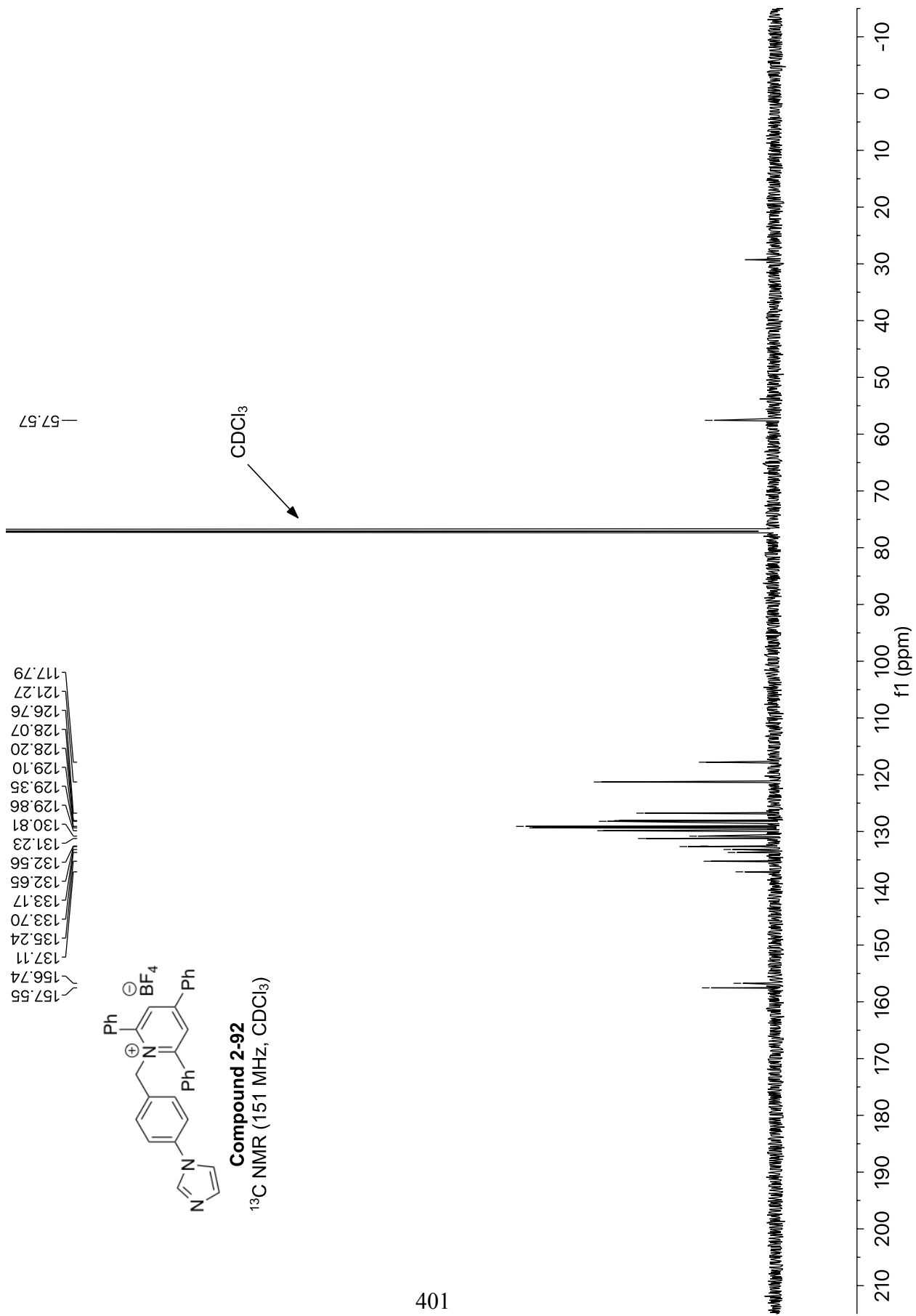
8.01
7.87
7.86
7.86
7.85
7.85
7.85
7.80
7.80
7.72
7.71
7.63
7.62
7.62
7.62
7.60
7.59
7.58
7.58
7.57
7.57
7.56
7.56
7.56
7.54
7.54
7.54
7.53
7.53
7.52
7.51
7.20
7.20
7.19
7.18
7.18
7.17
7.17
6.66
6.66
6.65
6.65
6.64
6.64
5.87

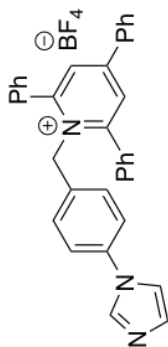


Compound 2-92

¹H NMR (600 MHz, CDCl₃)





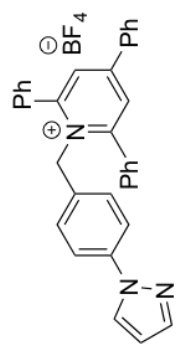


Compound 2-92

¹⁹F NMR (565 MHz, CDCl₃)

152.45
152.40

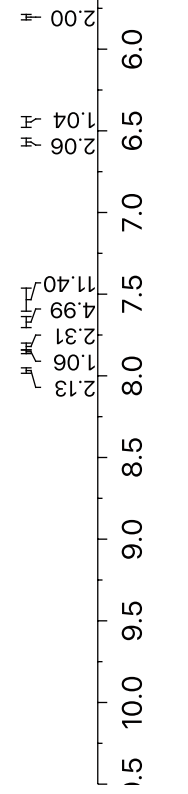
10 0 -10 -20 -30 -40 -50 -60 -70 -80 -90 -100 -110 -120 -130 -140 -150 -160 -170 -180 -190 -200 -210
f1 (ppm)

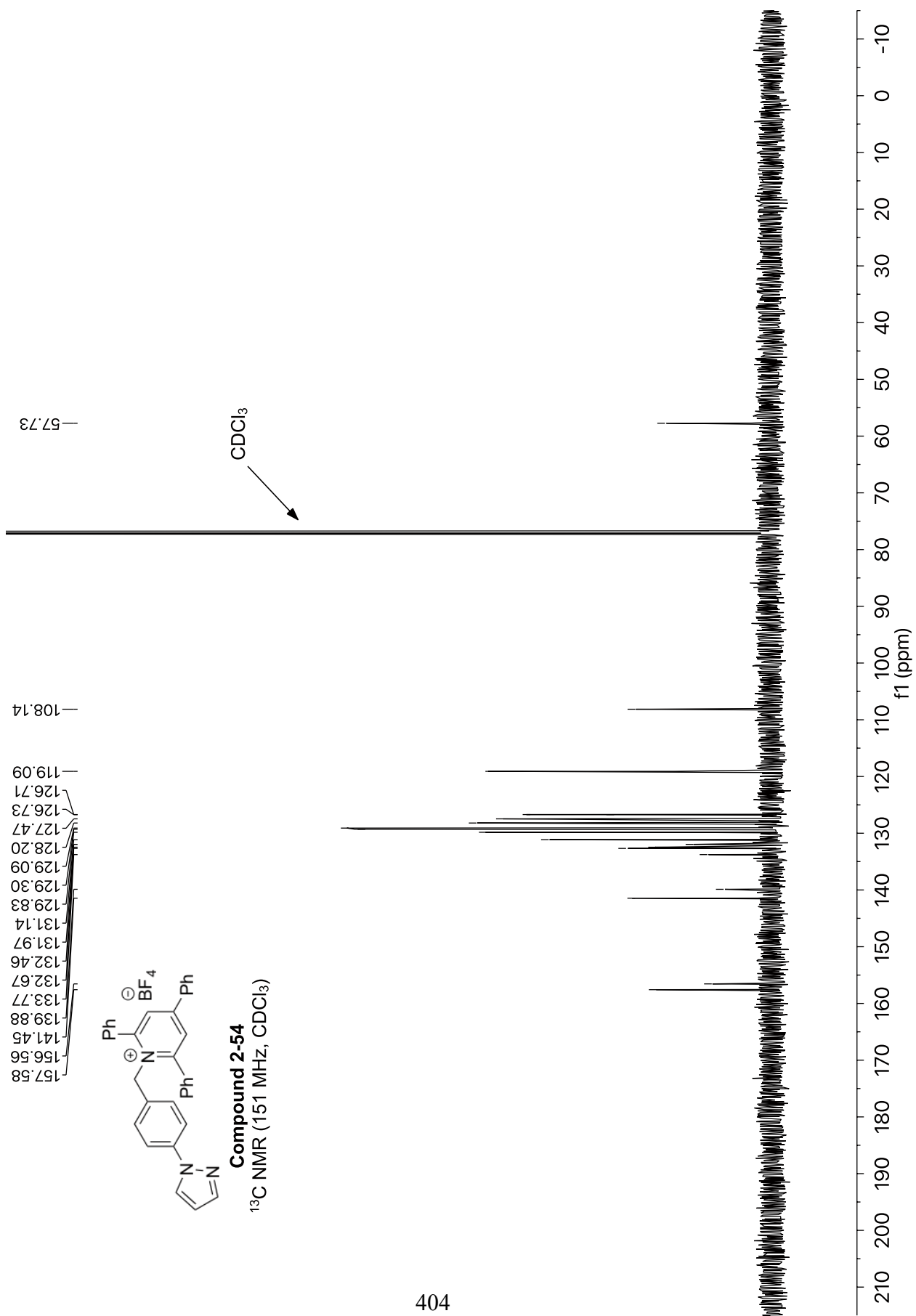


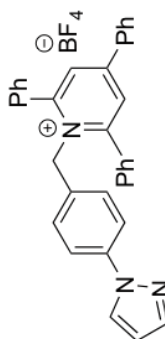
Compound 2-54

¹H NMR (600 MHz, CDCl₃)

CHCl₃







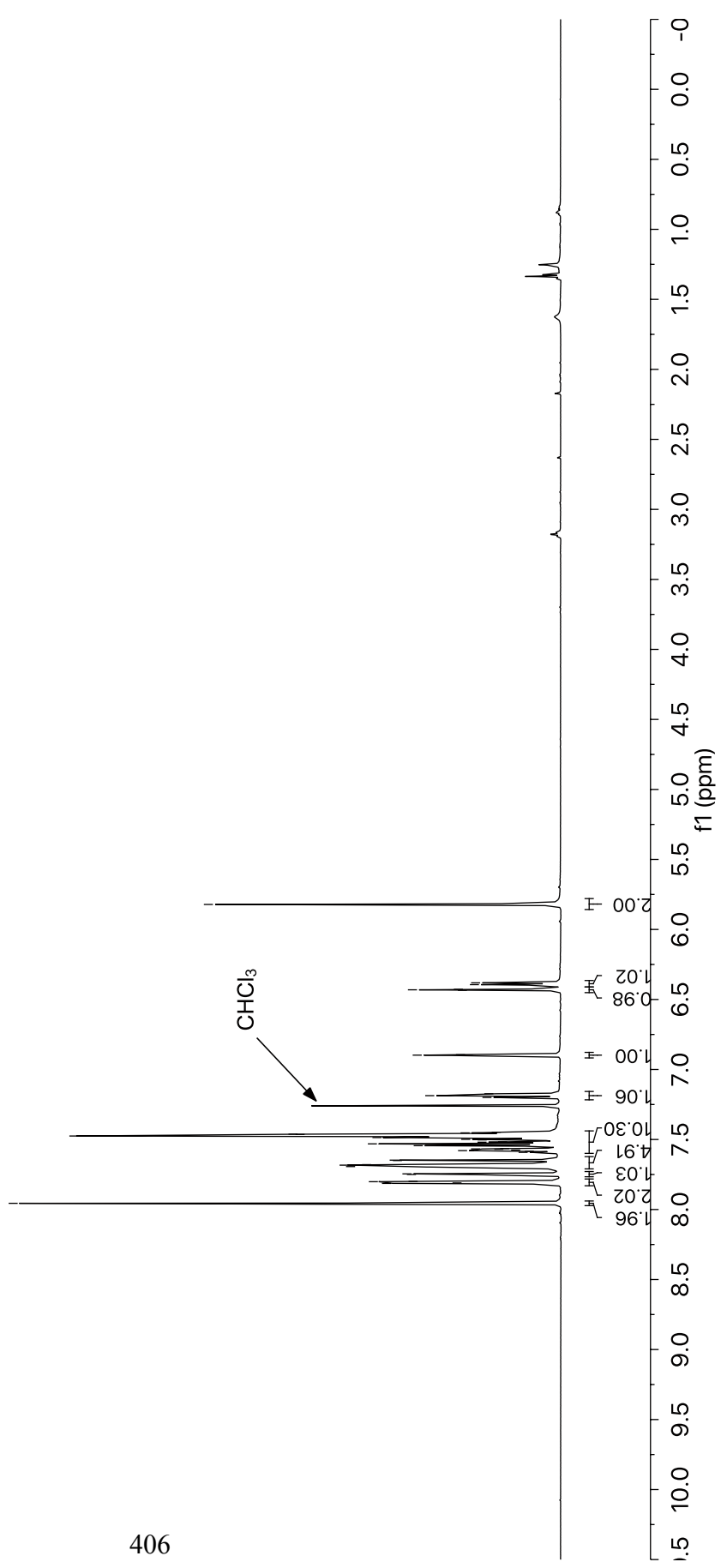
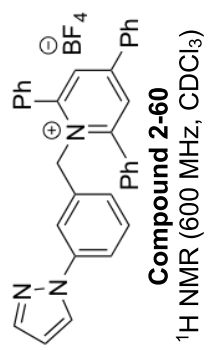
Compound 2-54

¹⁹F NMR (565 MHz, CDCl₃)

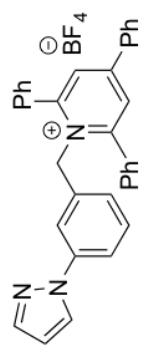
152.89
152.83

10 0 -10 -20 -30 -40 -50 -60 -70 -80 -90 -100 -110 -120 -130 -140 -150 -160 -170 -180 -190 -200 -210
f1 (ppm)

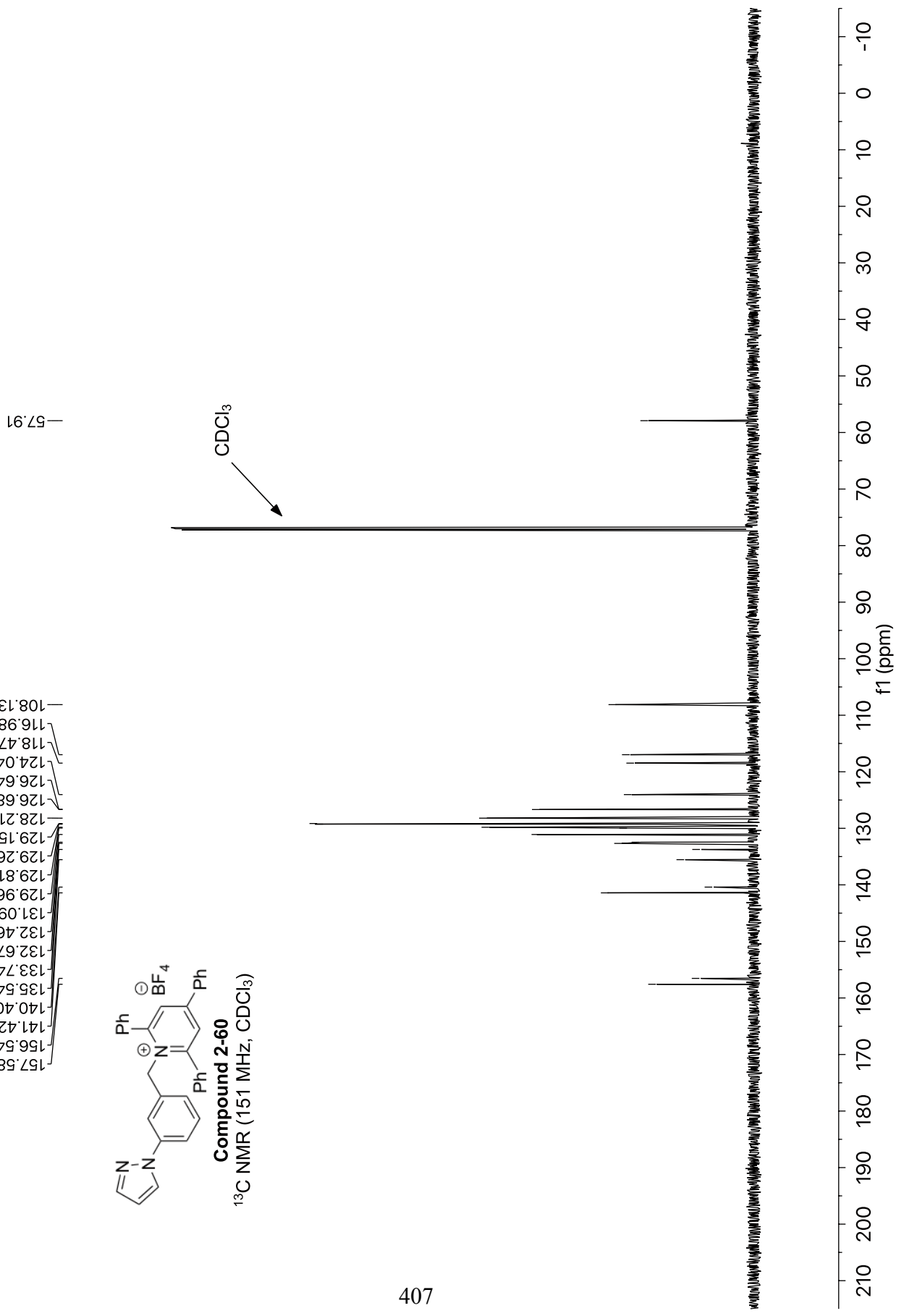
7.96
7.81
7.81
7.80
7.80
7.75
7.75
7.69
7.68
7.68
7.65
7.65
7.59
7.58
7.58
7.58
7.58
7.57
7.57
7.57
7.56
7.54
7.53
7.53
7.52
7.52
7.52
7.50
7.50
7.49
7.48
7.46
7.46
7.45
7.45
7.20
7.19
7.17
6.90
6.90
6.89
6.43
6.43
6.43
6.39
6.38
5.82

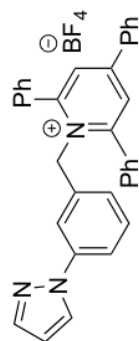


157.58
156.54
141.42
140.40
135.54
133.74
132.67
132.46
131.09
129.96
129.81
129.26
129.15
128.21
126.68
126.64
124.04
118.47
116.98
108.13



Compound 2-60
¹³C NMR (151 MHz, CDCl₃)



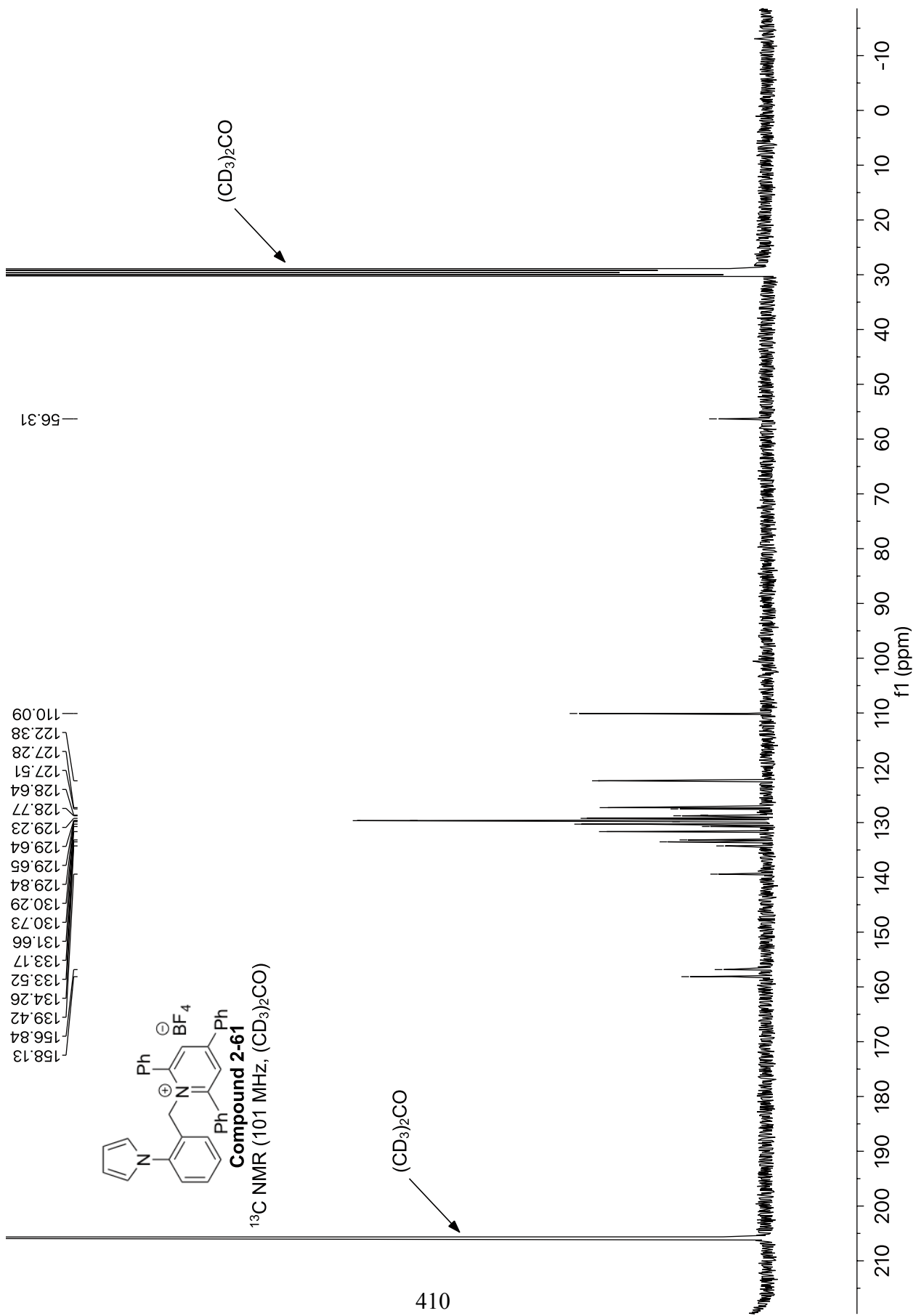


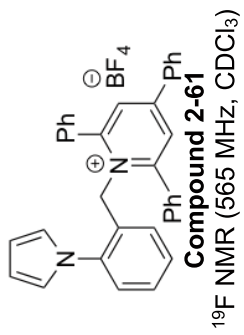
Compound 2-60

¹⁹F NMR (565 MHz, CDCl₃)

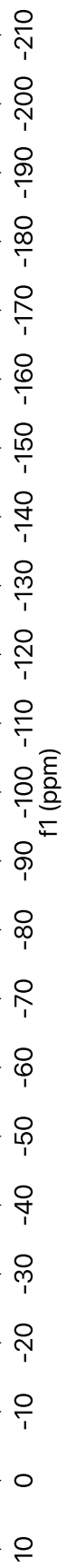
-152.75
-152.80

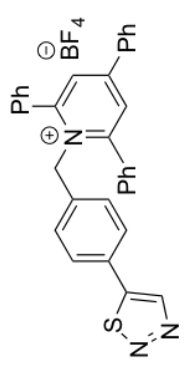
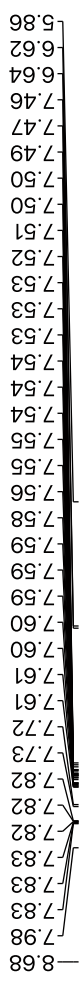
10 0 -10 -20 -30 -40 -50 -60 -70 -80 -90 -100 -110 -120 -130 -140 -150 -160 -170 -180 -190 -200 -210
f1 (ppm)



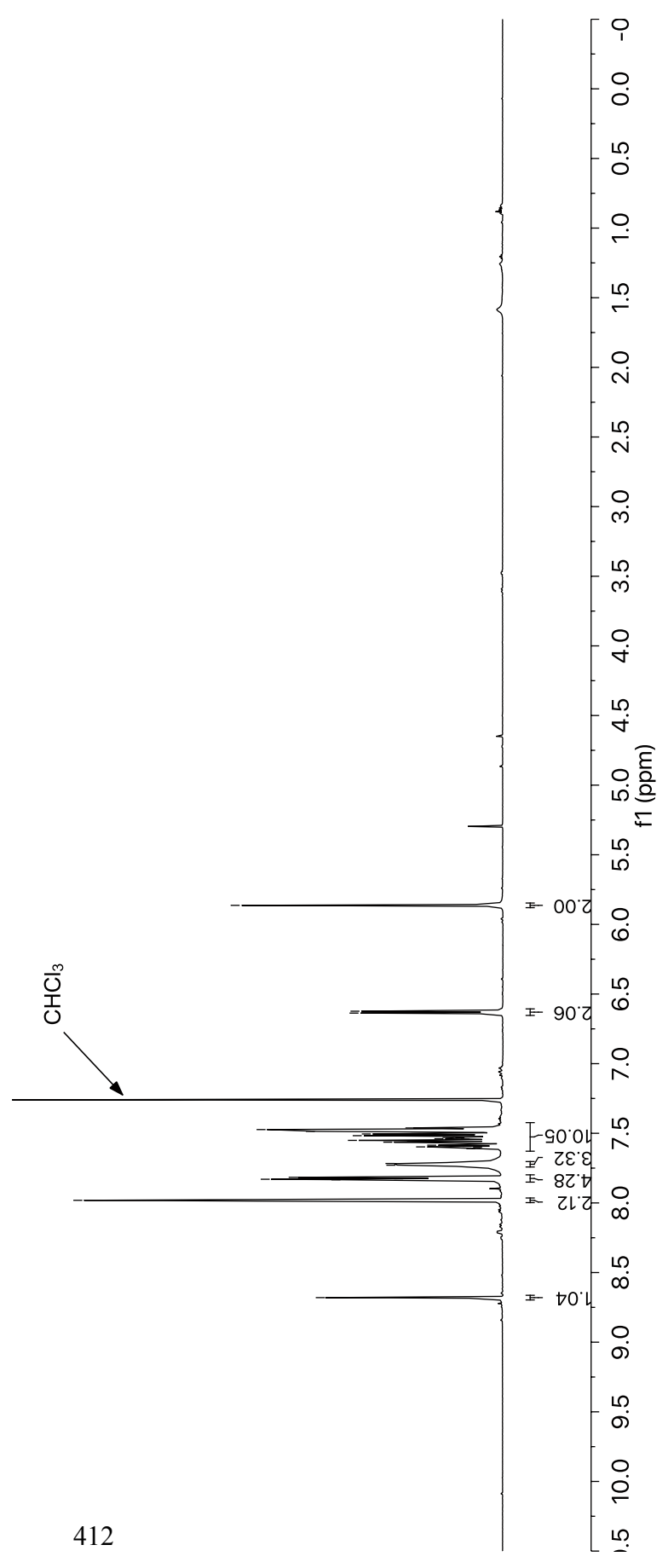


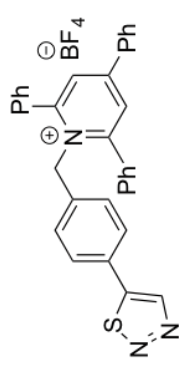
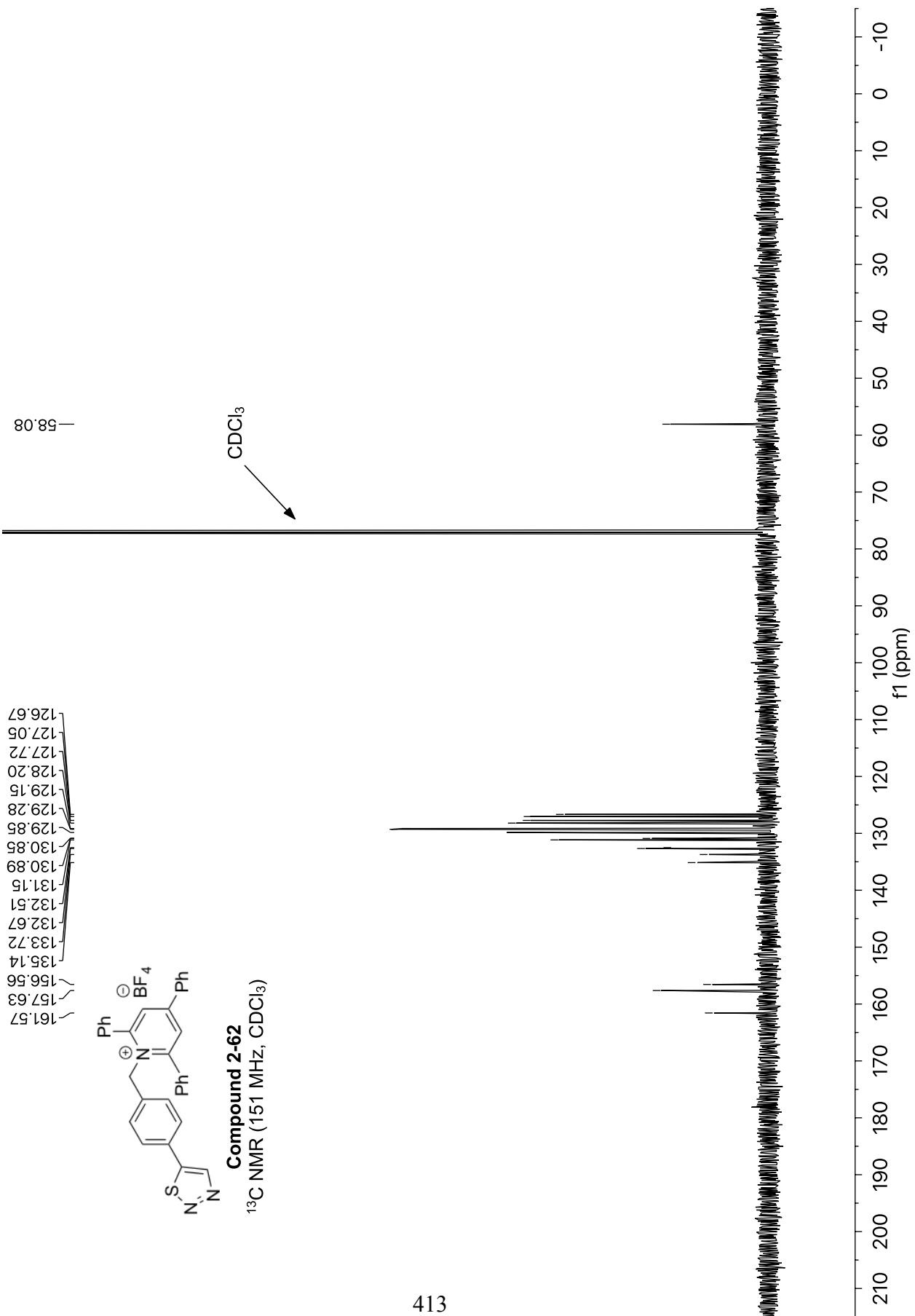
153.09
153.04



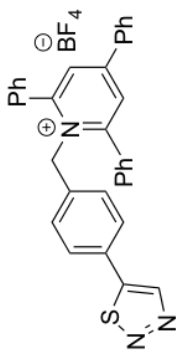


Compound 2-62
¹H NMR (600 MHz, CDCl₃)





Compound 2-62
¹³C NMR (151 MHz, CDCl₃)

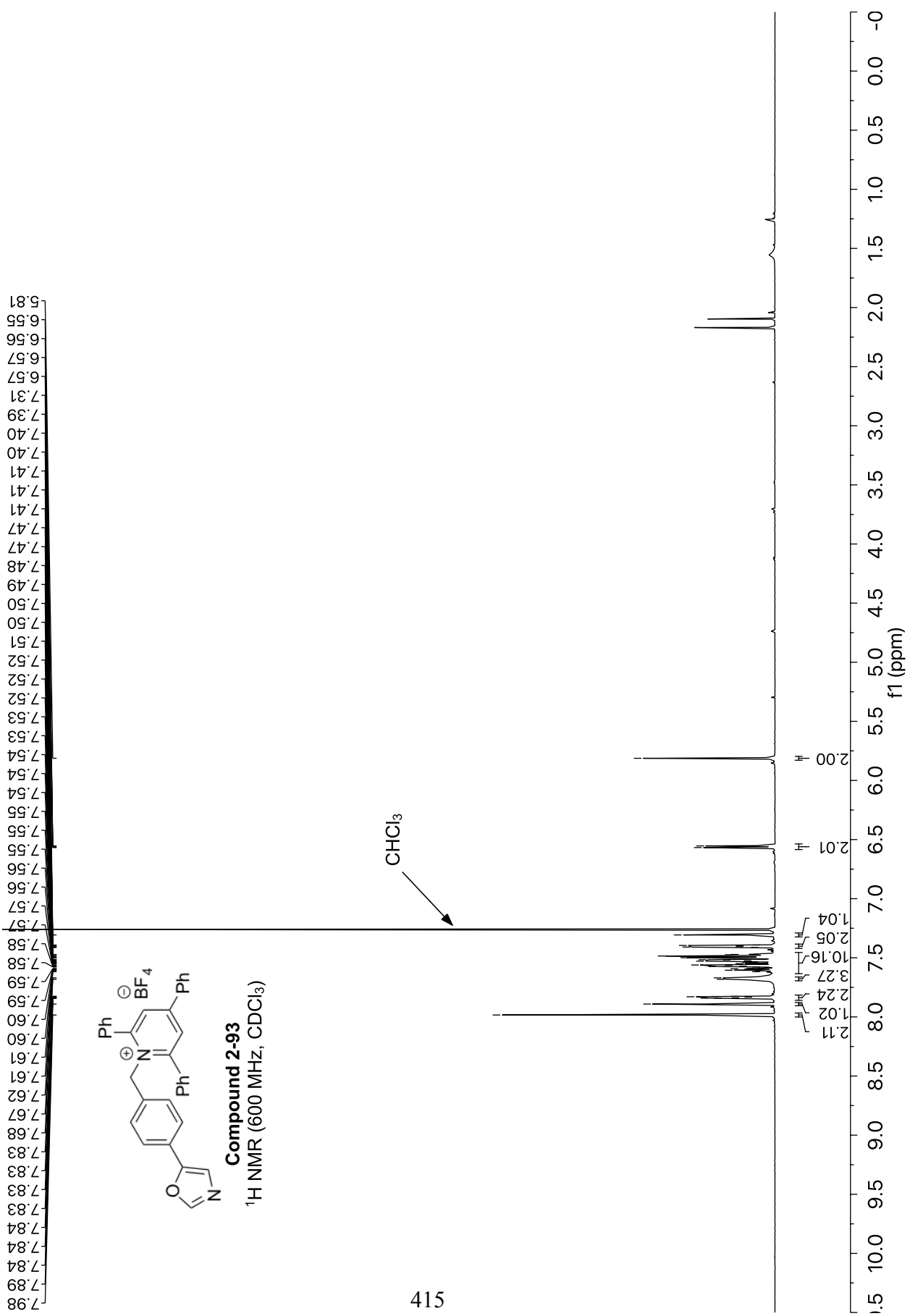


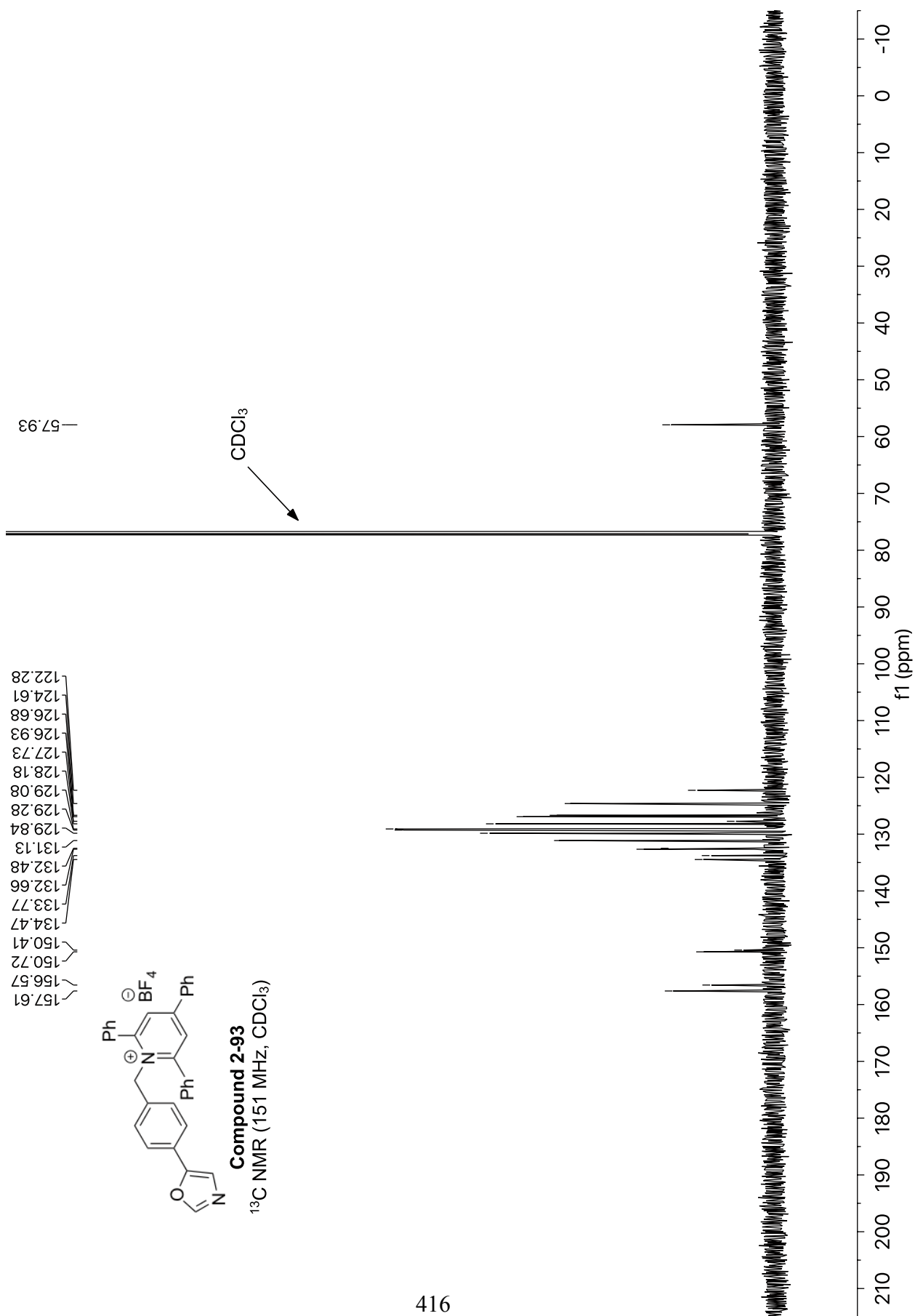
Compound 2-62

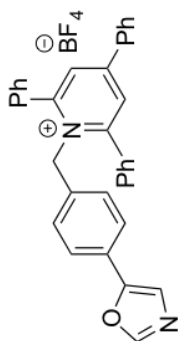
¹⁹F NMR (565 MHz, CDCl₃)

152.81
152.86

10 0 -10 -20 -30 -40 -50 -60 -70 -80 -90 -100 -110 -120 -130 -140 -150 -160 -170 -180 -190 -200 -210
f1 (ppm)



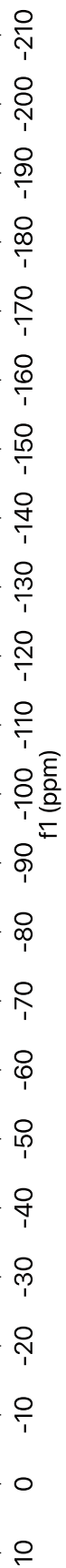


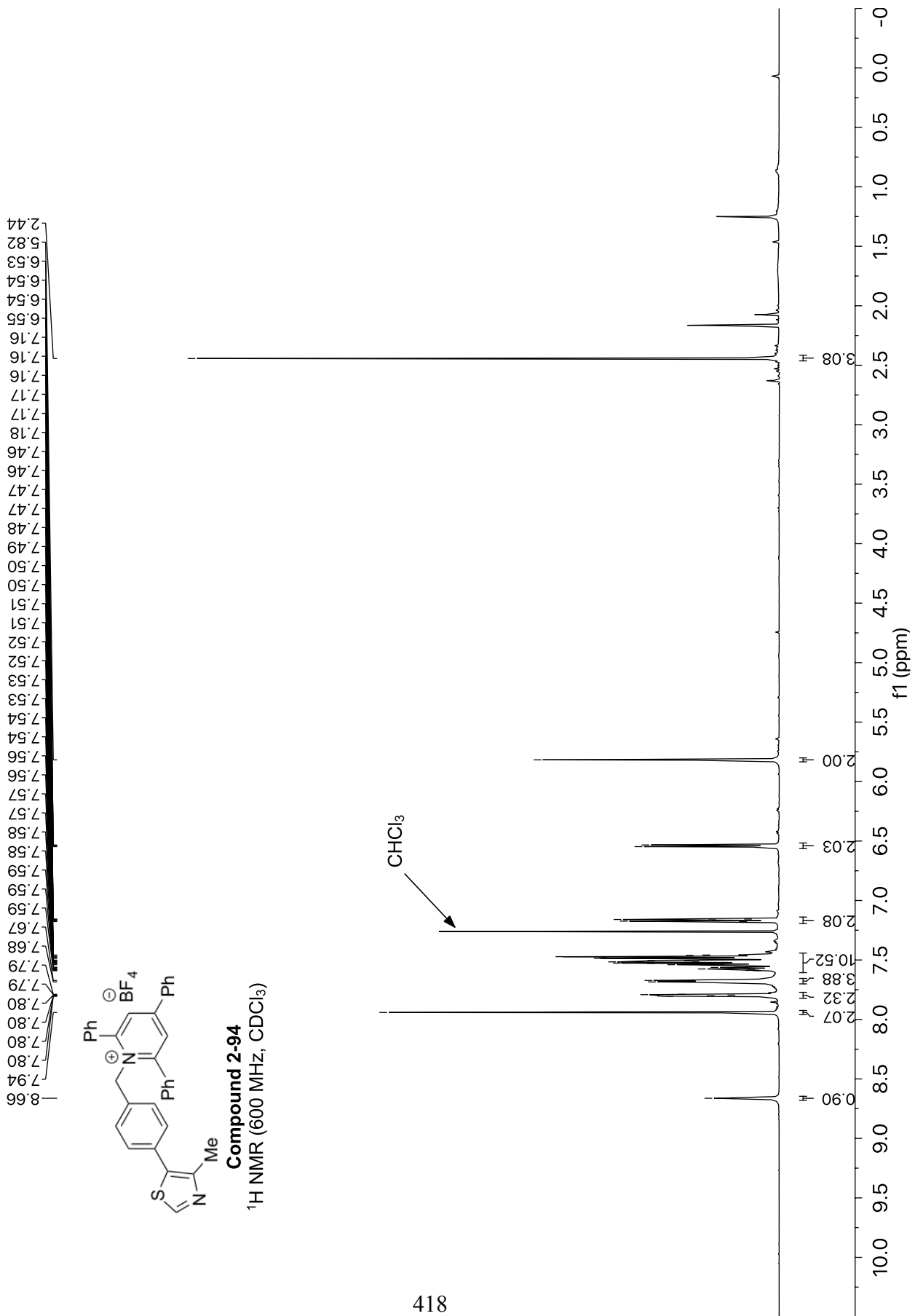


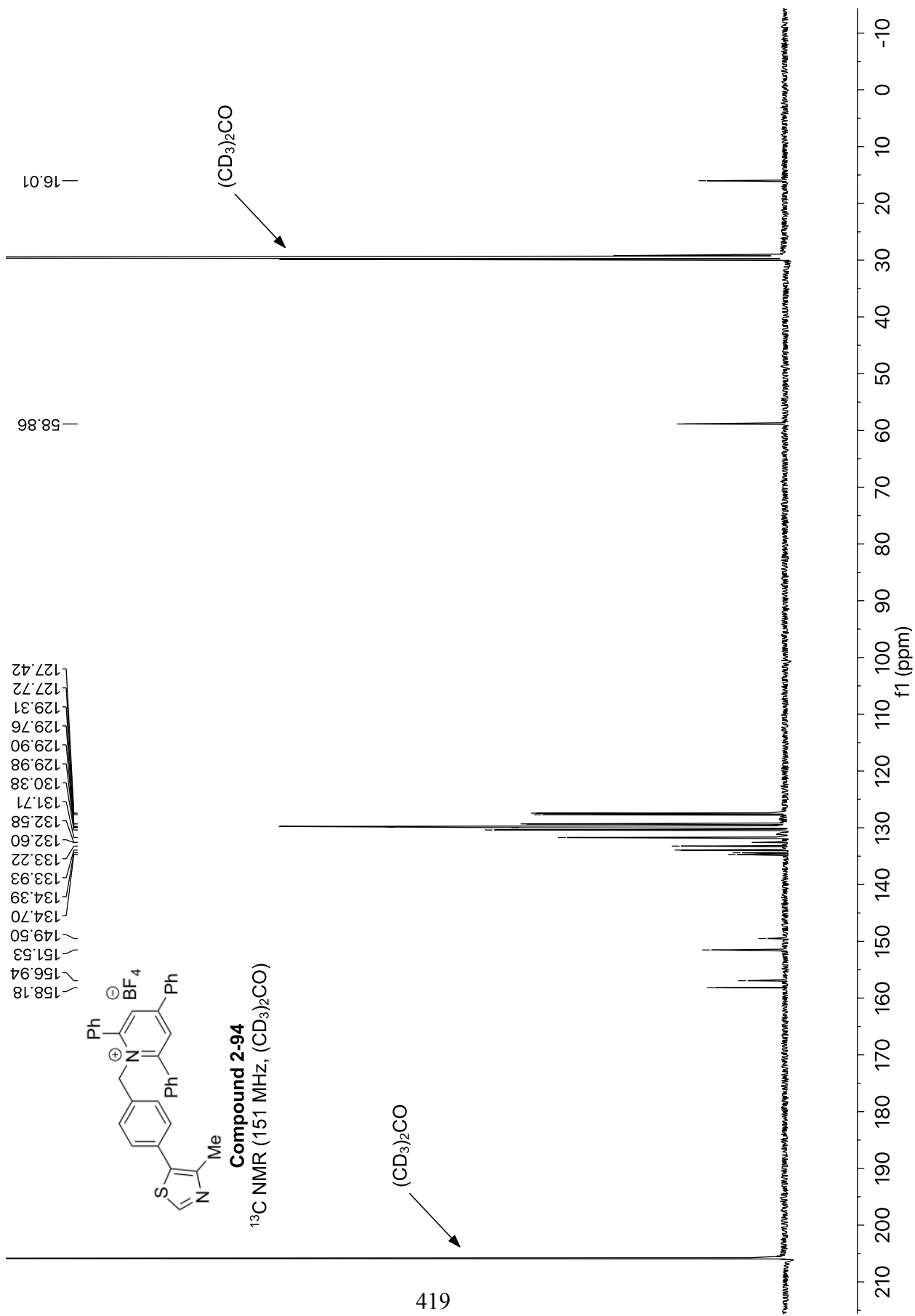
Compound 2-93

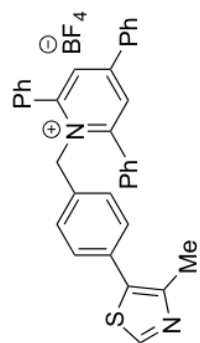
¹⁹F NMR (565 MHz, CDCl₃)

153.07
153.01









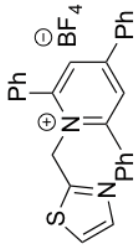
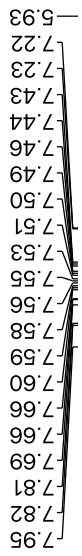
Compound 2-94

¹⁹F NMR (565 MHz, CDCl₃)

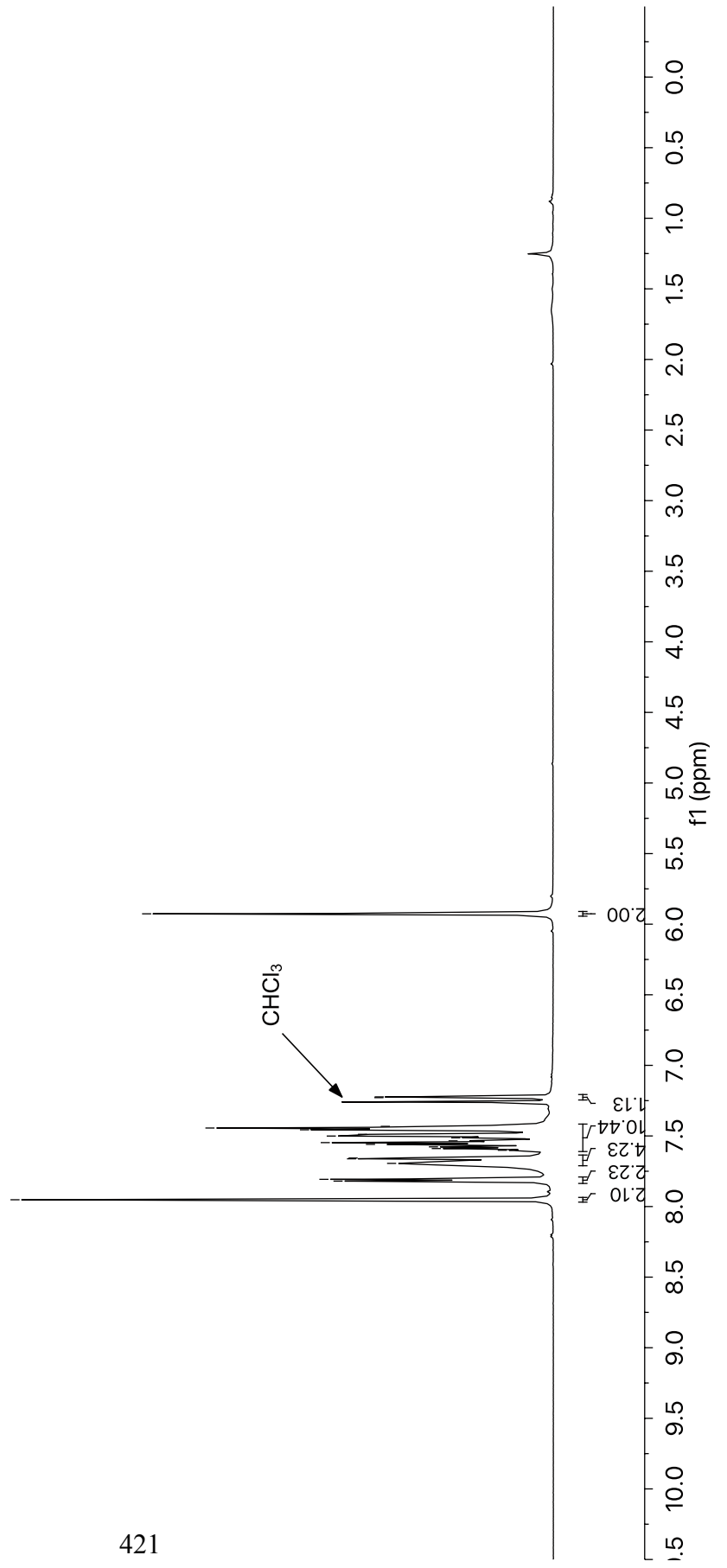
152.84
152.89

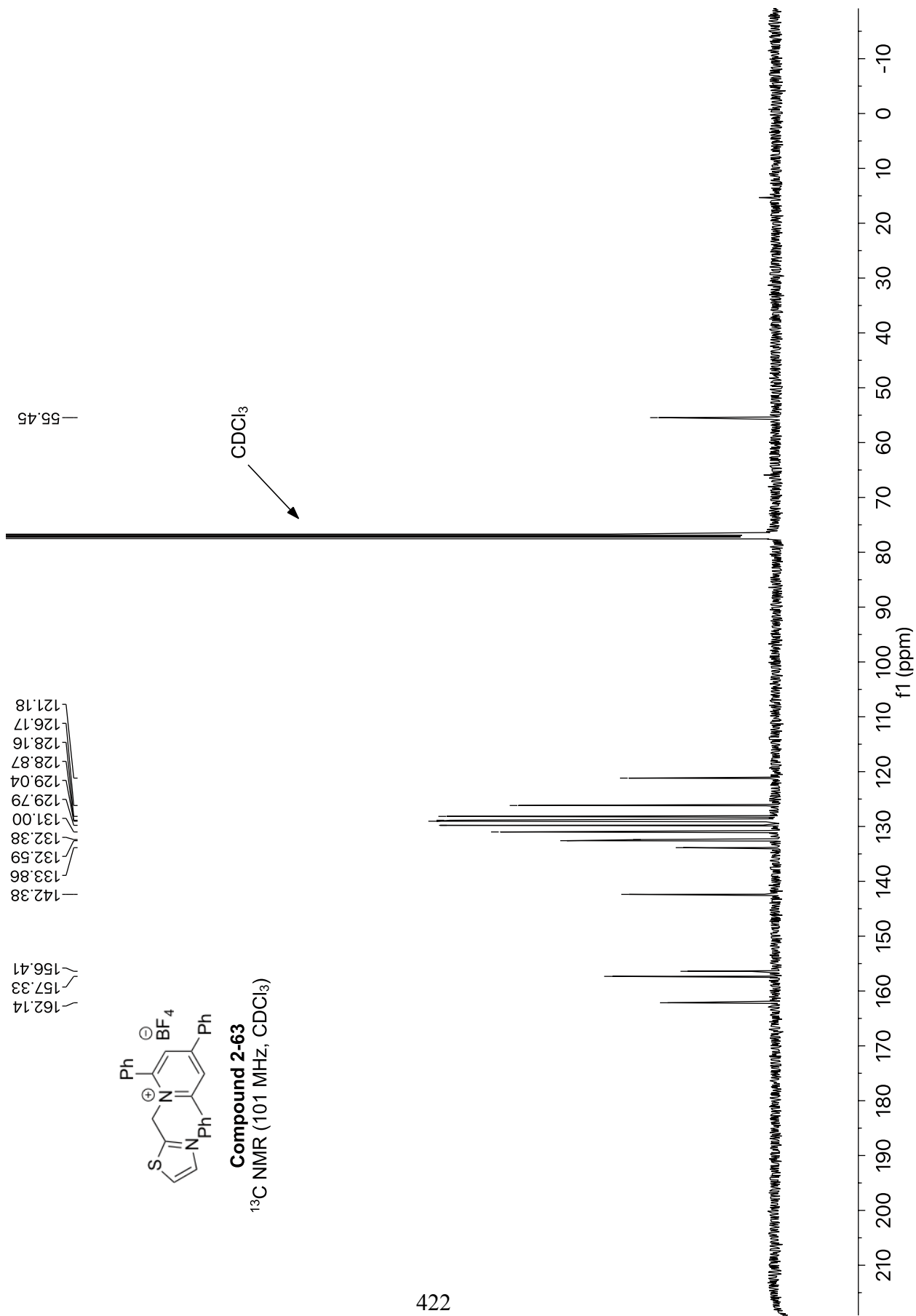
420

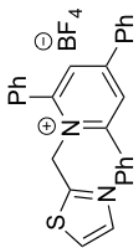
10 0 -10 -20 -30 -40 -50 -60 -70 -80 -90 -100 -110 -120 -130 -140 -150 -160 -170 -180 -190 -200 -210
f1 (ppm)



Compound 2-63
¹H NMR (600 MHz, CDCl₃)



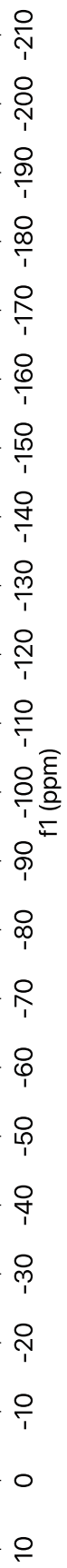




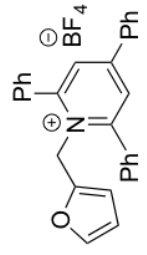
Compound 2-63

¹⁹F NMR (565 MHz, CDCl₃)

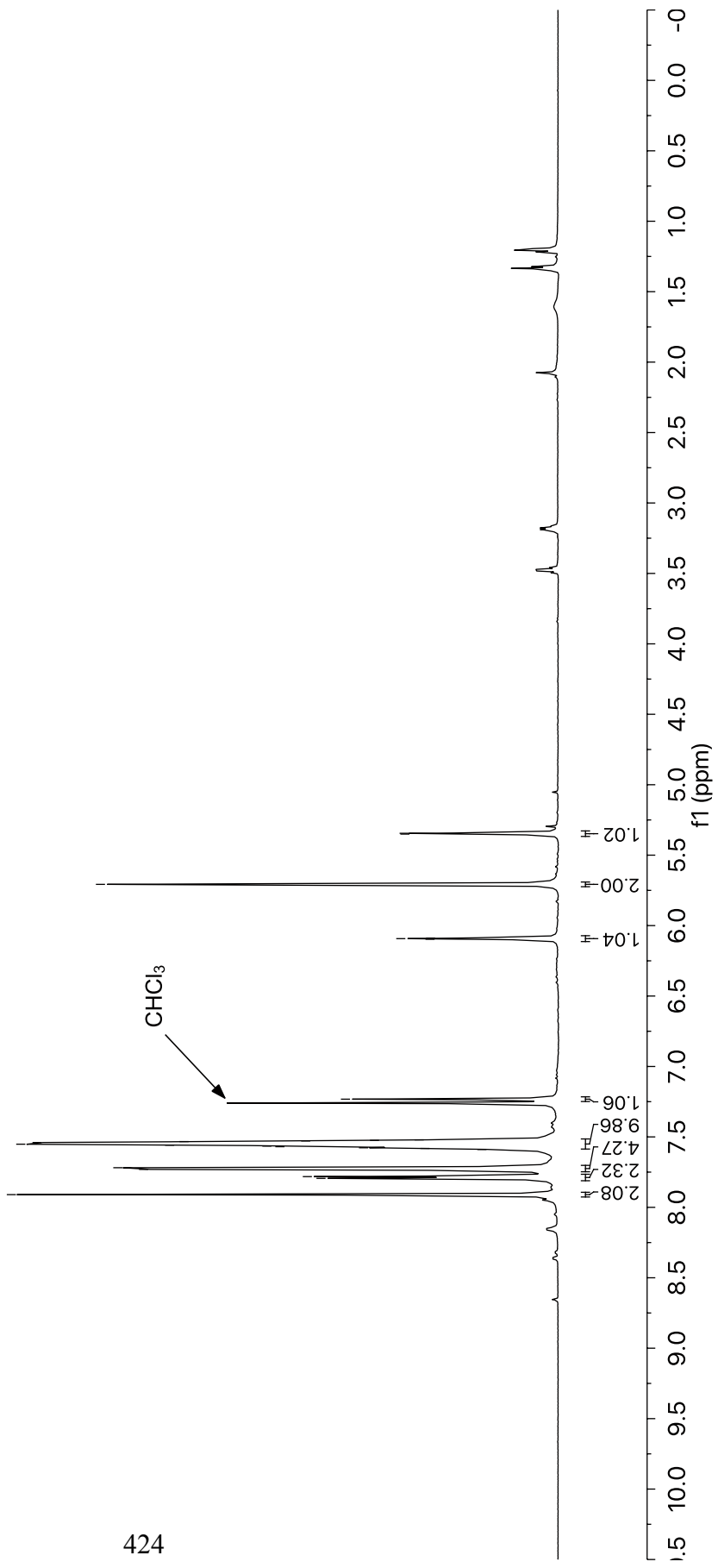
-153.29
-153.23

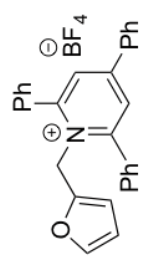
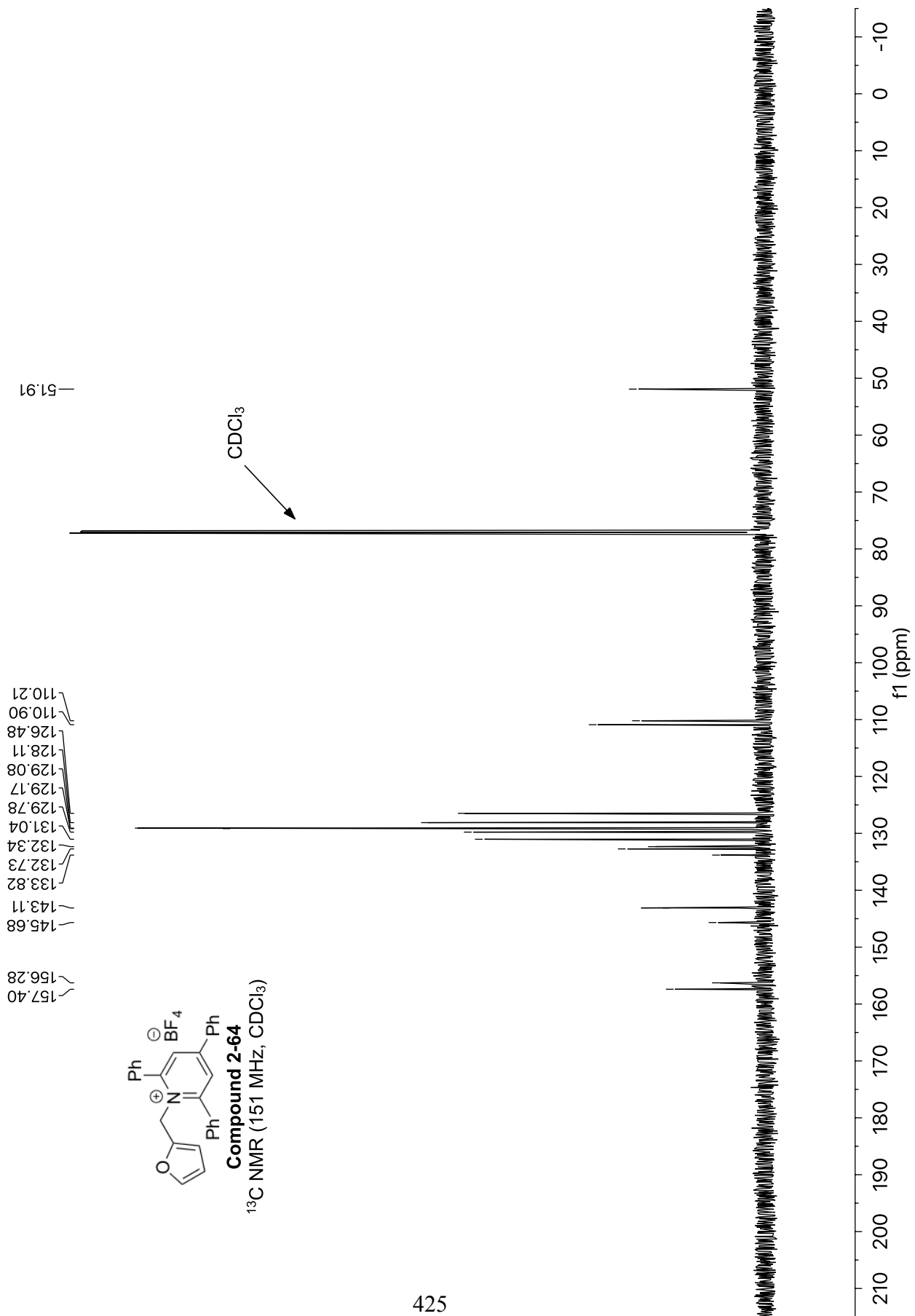


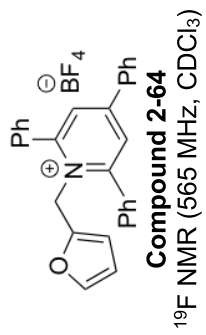
7.91
7.79
7.78
7.73
7.72
7.59
7.58
7.58
7.57
7.57
7.56
7.55
7.54
7.53
7.53
7.52
7.52
7.23
6.10
6.09
6.09
5.71
5.35
5.34



Compound 2-64
¹H NMR (600 MHz, CDCl₃)







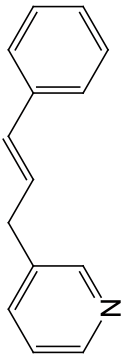
153.03
152.98

10 0 -10 -20 -30 -40 -50 -60 -70 -80 -90 -100 -110 -120 -130 -140 -150 -160 -170 -180 -190 -200 -210
f1 (ppm)

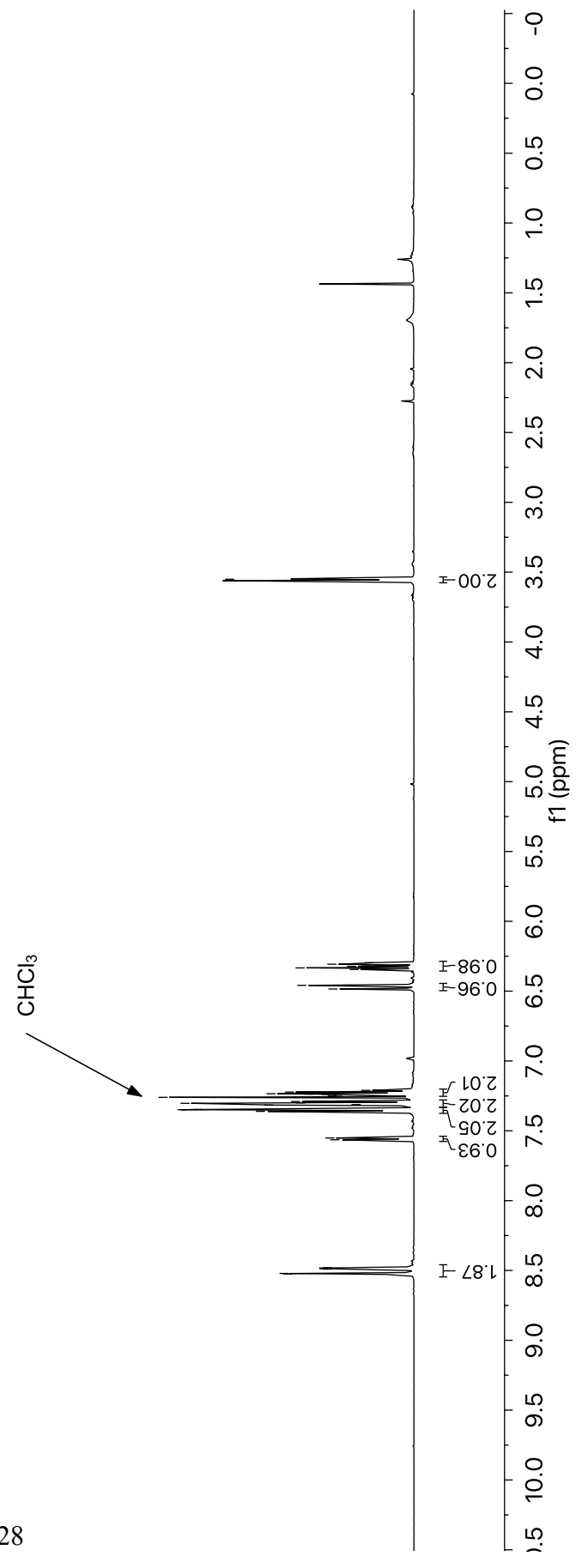
Appendix C

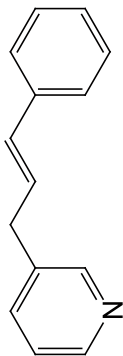
SPECTRAL AND CHROMATOGRAPHY DATA FOR CHAPTER 3

8.52
8.49
8.48
8.48
8.49
8.49
8.52
7.56
7.55
7.36
7.36
7.35
7.35
7.36
7.36
7.35
7.35
7.32
7.31
7.30
7.30
7.29
7.29
7.26
7.26
7.25
7.25
7.24
7.24
7.23
7.23
7.23
7.22
7.21
6.48
6.46
6.34
6.33
6.32
6.32
6.31
6.30
3.56
3.55



Compound 3-22
¹H NMR (600 MHz, CDCl₃)

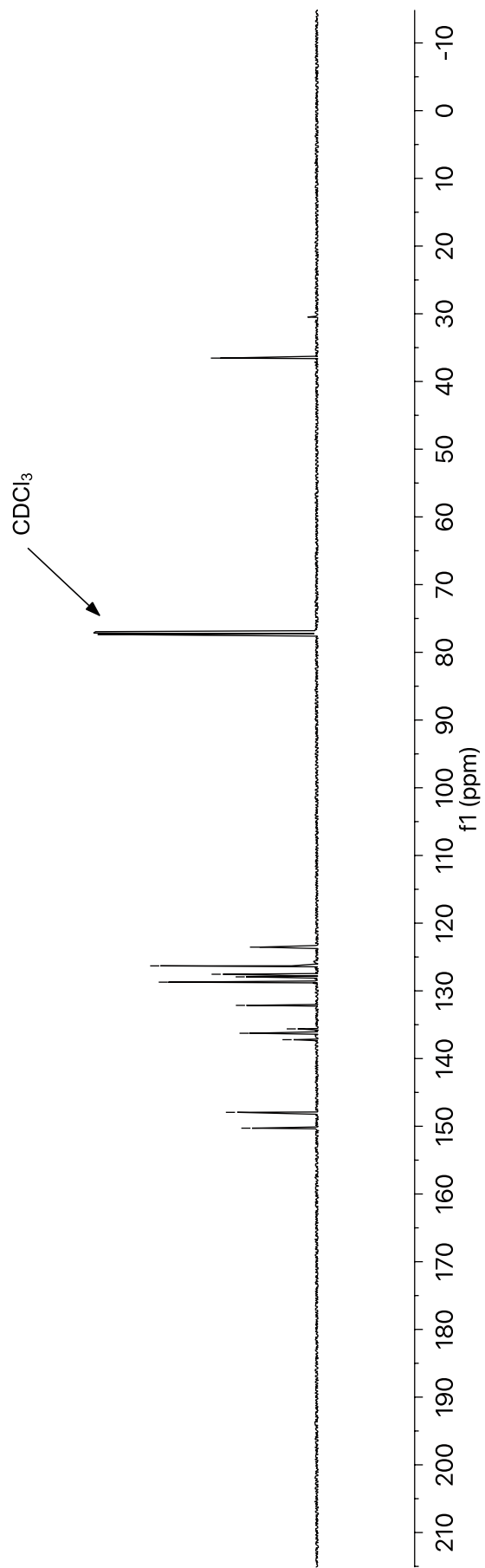


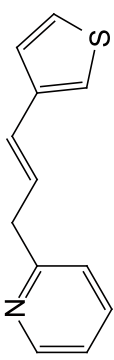
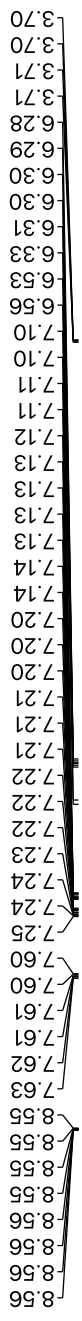


Compound 3-22
 ^{13}C NMR (151 MHz, CDCl_3)

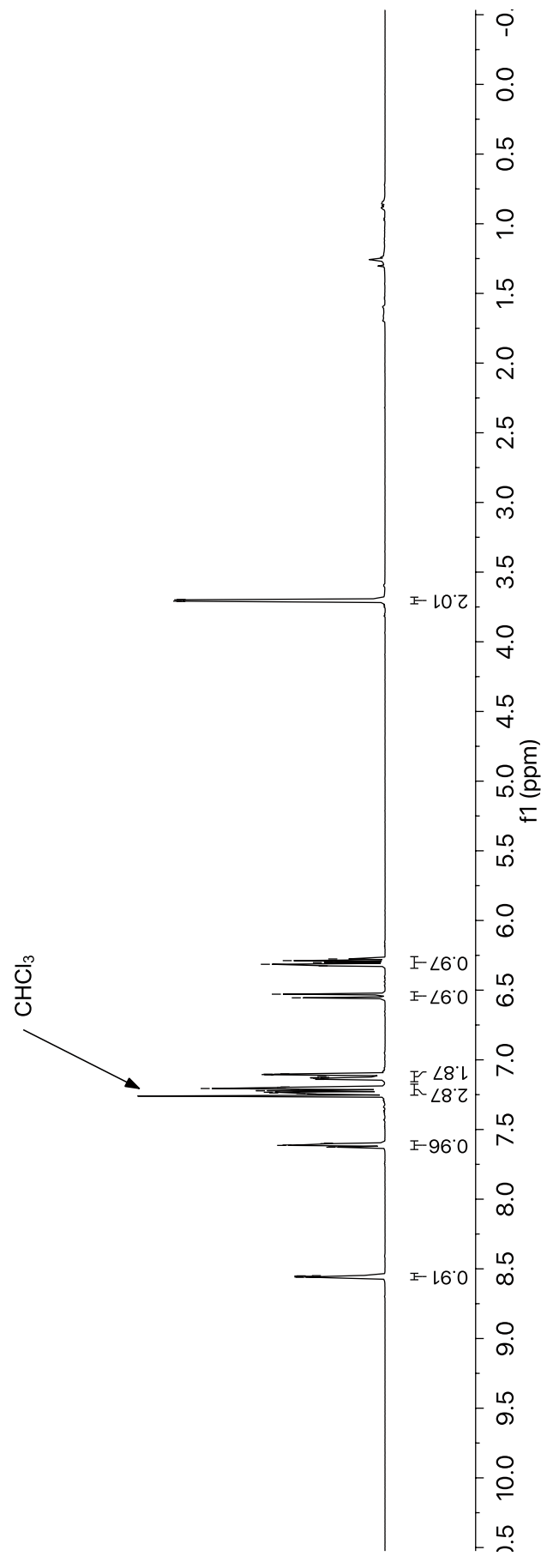
150.28
147.94
137.21
136.26
135.61
132.14
128.71
127.93
127.55
126.31
123.54

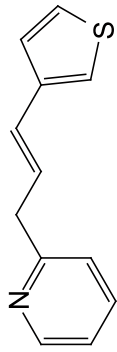
36.55





Compound 3-26
¹H NMR (600 MHz, CDCl₃)





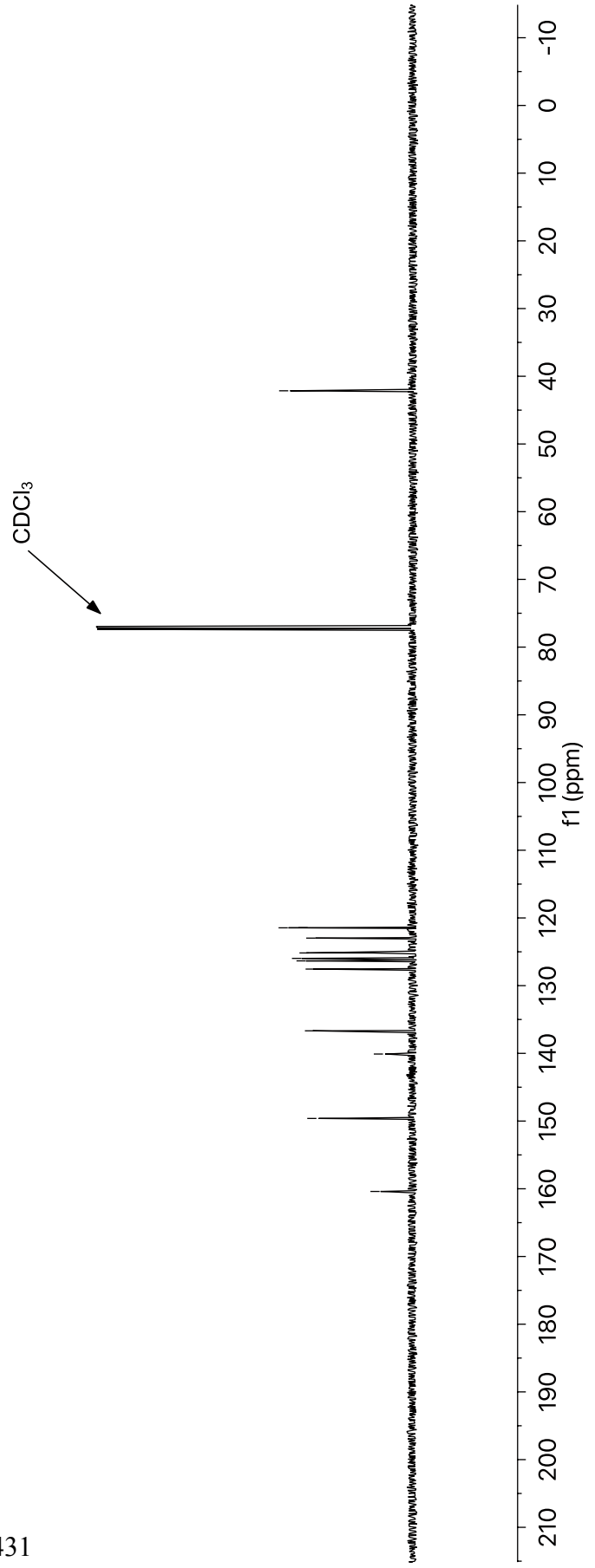
Compound 3-26

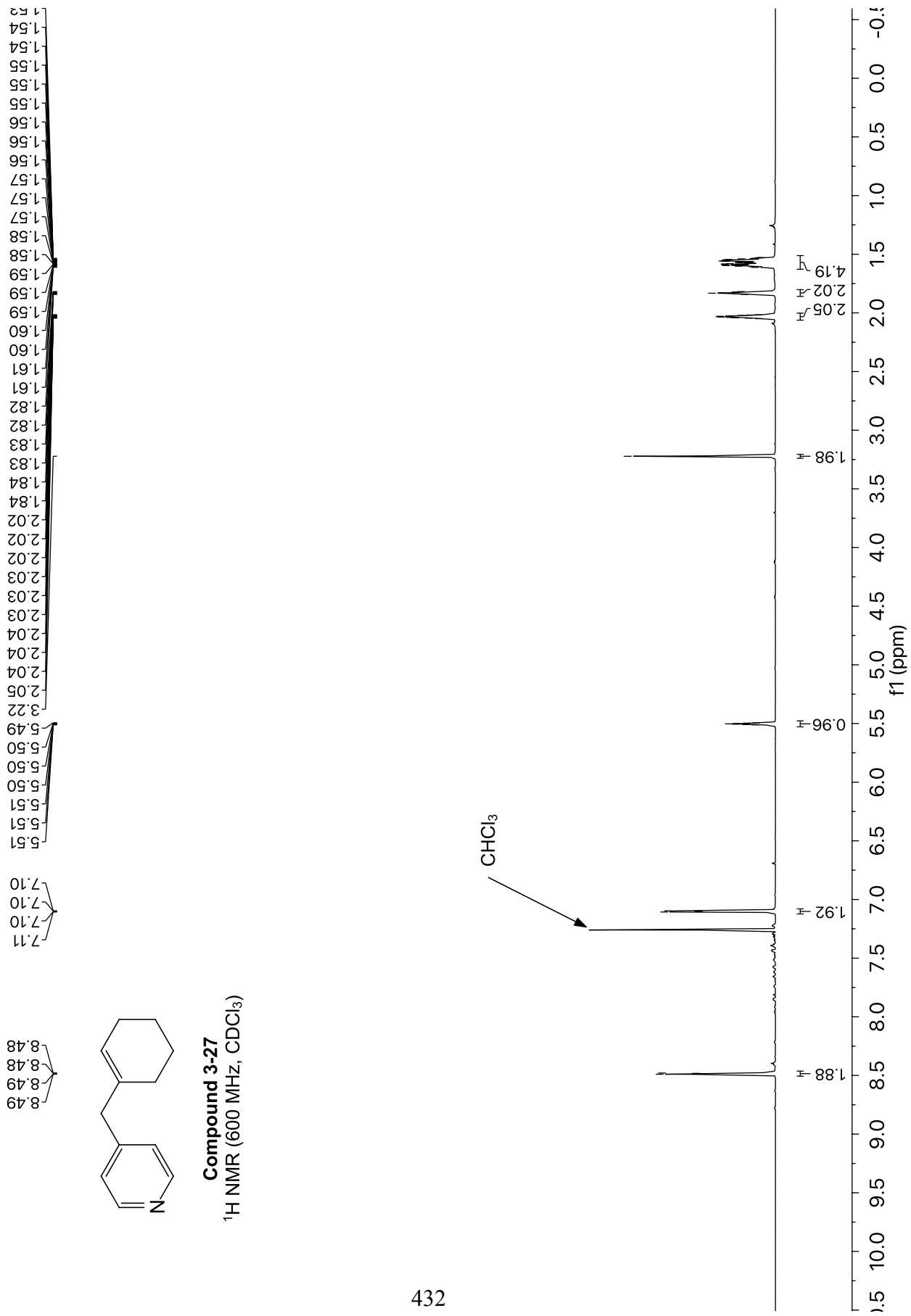
^{13}C NMR (151 MHz, CDCl_3)

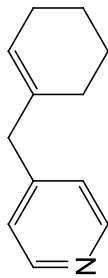
—160.39
—149.61
—140.10
—136.67
—127.55
—126.34
—125.97
—125.17
—122.98
—121.46
—121.44

—42.14

431







Compound 3-27
 ^{13}C NMR (151 MHz, CDCl_3)

28.21
25.47
22.96
22.39

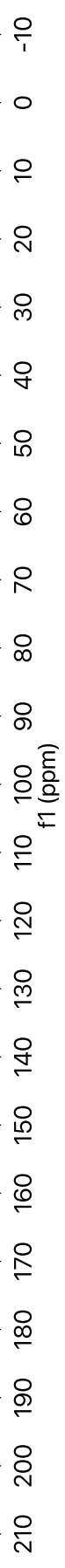
44.13

124.60
124.44

135.55

149.75
149.67

CDCl_3

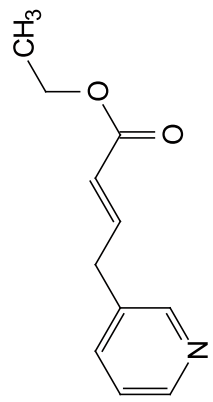


1.30
1.29
1.27

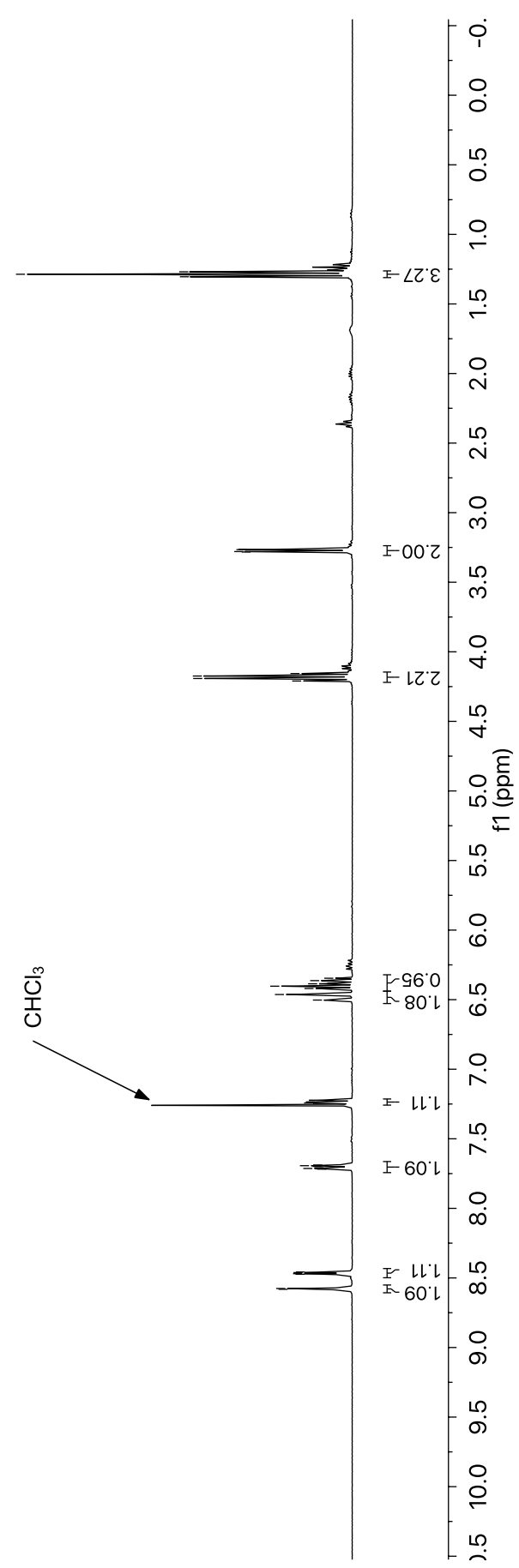
3.28
3.28
3.27
3.26

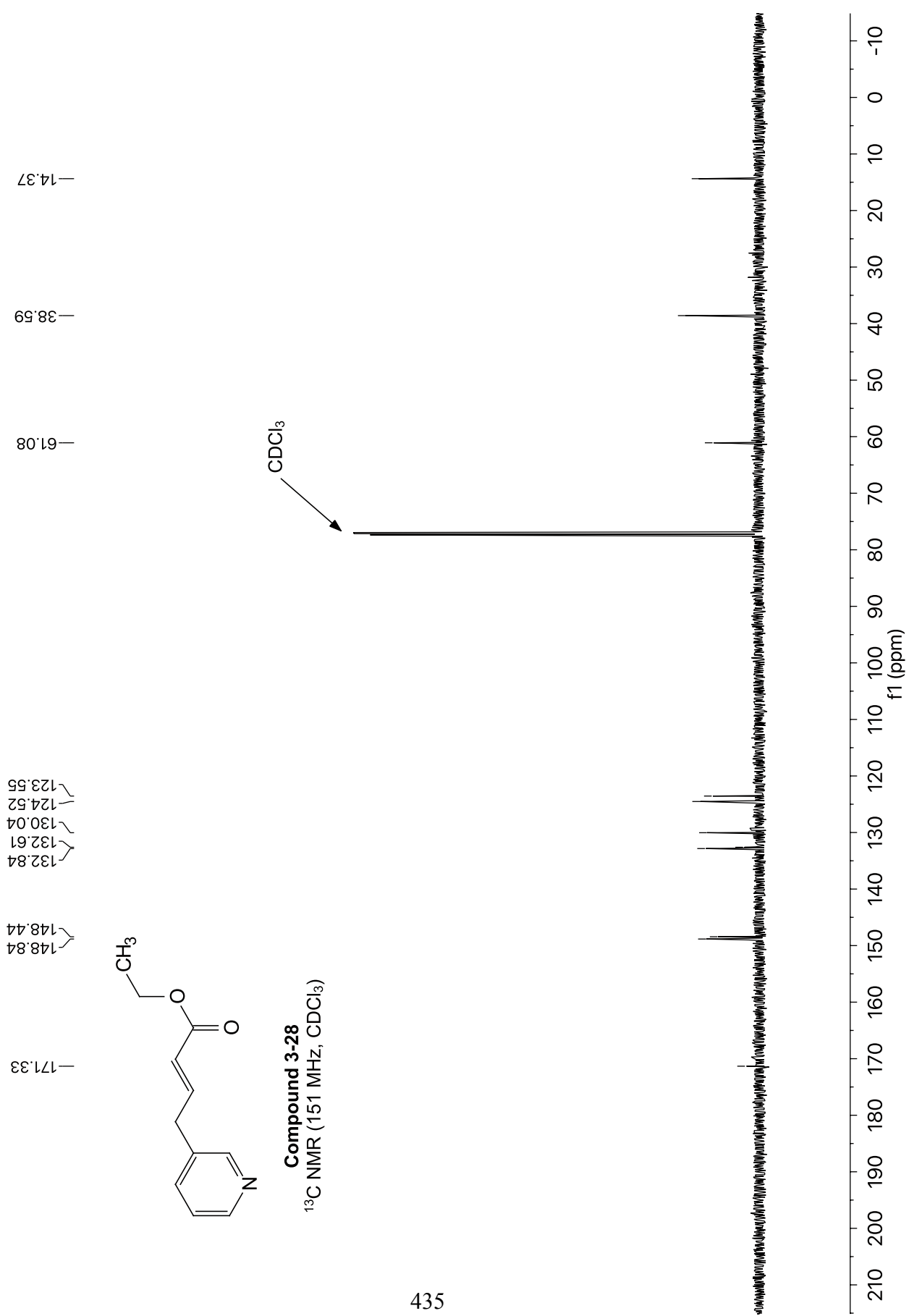
4.21
4.19
4.17
4.16

6.35
6.36
6.38
6.39
6.40
6.42
6.46
6.50
7.22
7.22
7.23
7.24
7.69
7.69
7.70
7.71
7.71
7.72
8.46
8.46
8.47
8.47
8.58
8.58

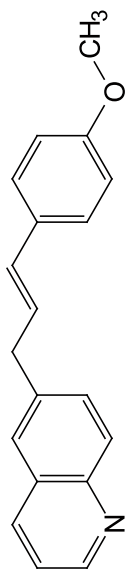


Compound 3-28
¹H NMR (600 MHz, CDCl₃)





8.88
8.88
8.87
8.87
8.11
8.11
8.10
8.10
8.09
8.06
8.04
7.65
7.65
7.64
7.63
7.62
7.62
7.39
7.38
7.37
7.37
7.37
7.32
7.31
6.86
6.84
6.48
6.45
6.31
6.30
6.29
6.28
6.27
6.26
3.80
3.72
3.71



Compound 3-29
¹H NMR (600 MHz, CDCl₃)

CHCl₃

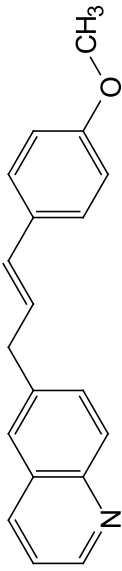
3.12
1.98

0.98
0.97
2.04
2.00
1.10
1.96
0.96
0.98
0.92

10.5 10.0 9.5 9.0 8.5 8.0 7.5 7.0 6.5 6.0 5.5 5.0 4.5 4.0 3.5 3.0 2.5 2.0 1.5 1.0 0.5 0.0

f1 (ppm)

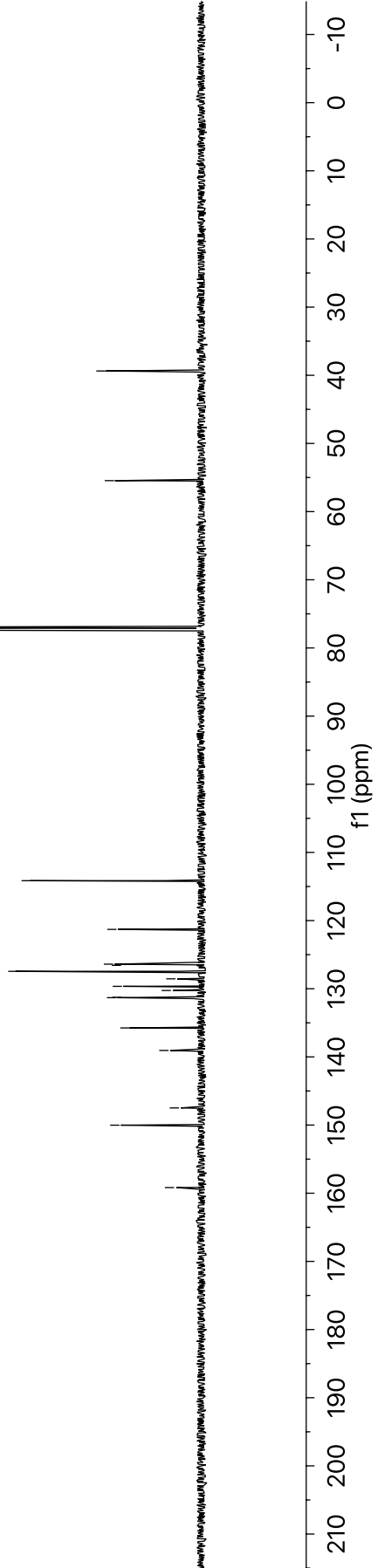
159.17
150.02
147.49
139.05
135.75
131.31
131.26
130.26
129.65
128.55
127.45
126.57
126.39
121.29
114.15



Compound 3-29
 ^{13}C NMR (151 MHz, CDCl_3)

55.46
39.37

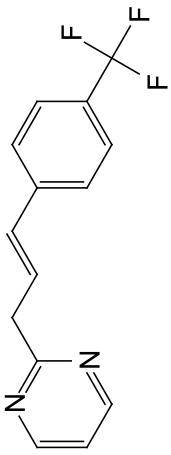
CDCl_3



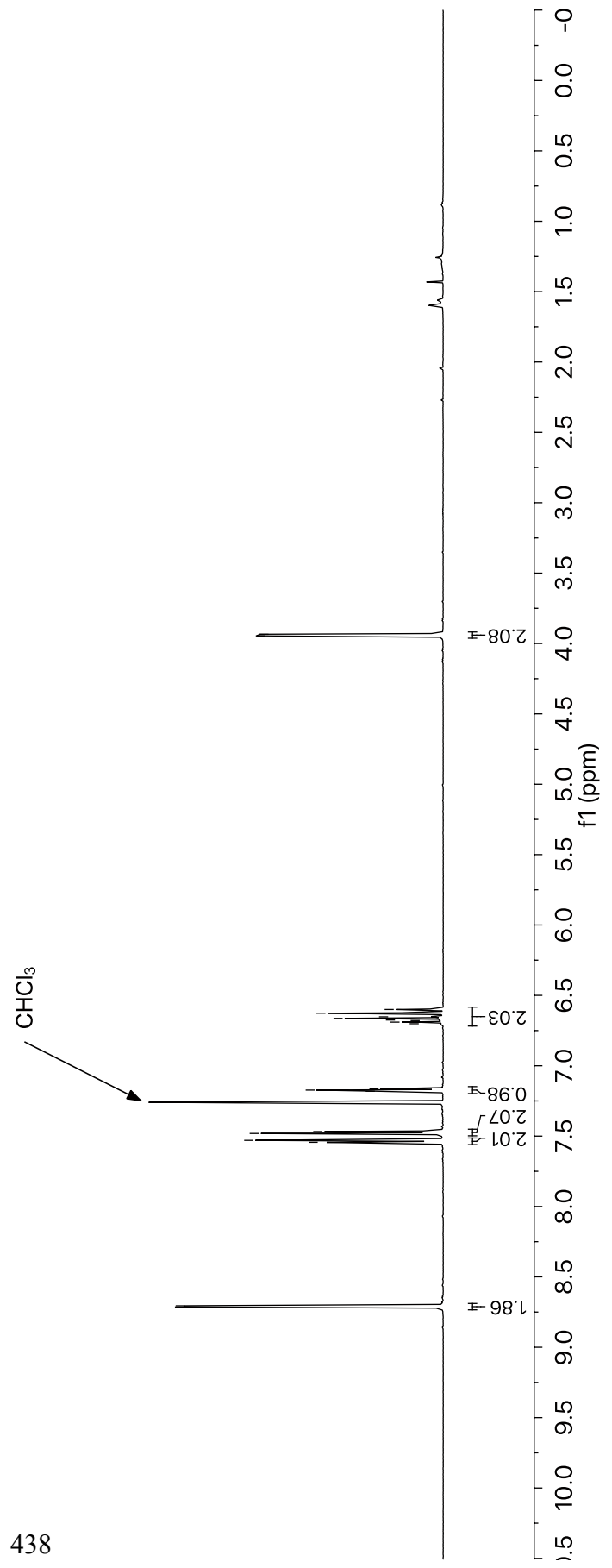
3.95
3.93

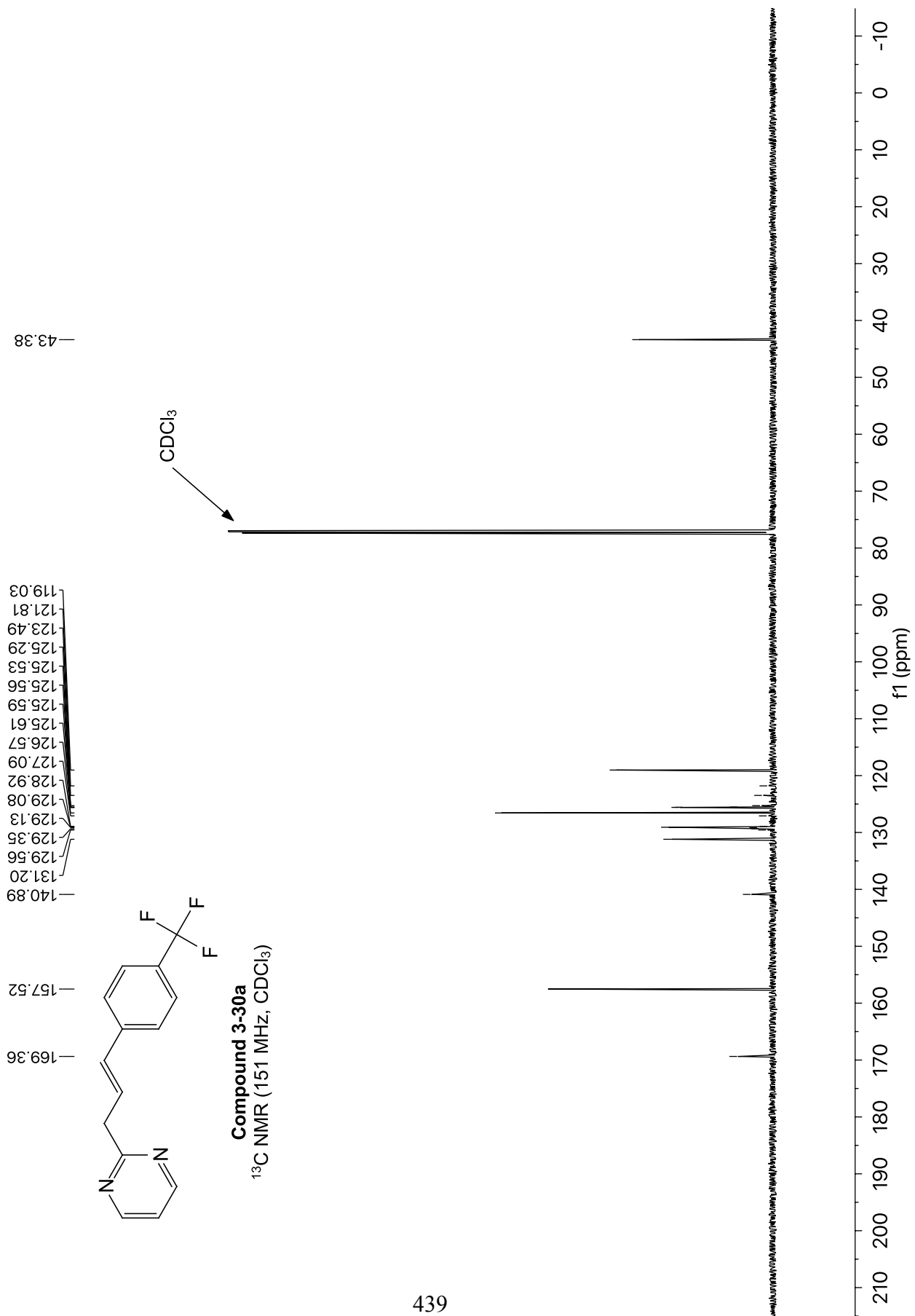
7.54
7.53
7.48
7.47
7.18
7.17
7.16
6.69
6.68
6.66
6.65
6.63
6.60

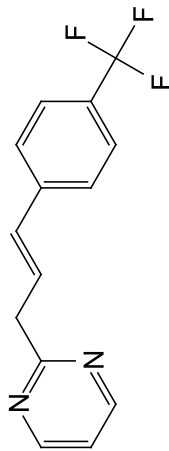
8.71
8.71



Compound 3-30a
¹H NMR (600 MHz, CDCl₃)





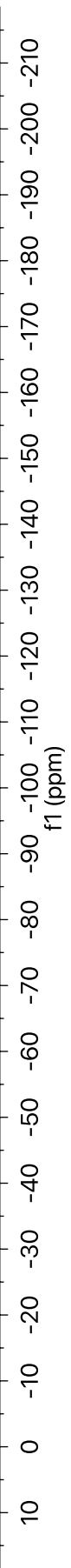


Compound 3-30a
 ^{19}F NMR (565 MHz, CDCl_3)

—62.48

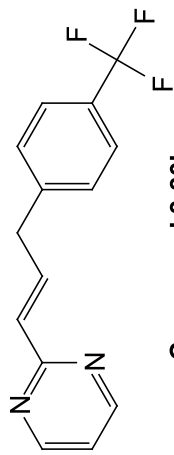


440



3.70
3.69

8.66
8.65
7.58
7.56
7.38
7.37
7.31
7.30
7.29
7.29
7.28
7.09
7.09
7.08
6.59
6.59
6.59
6.57
6.57
6.56



Compound 3-30b

¹H NMR (600 MHz, CDCl₃)

CHCl₃

2.00 H

0.90 H

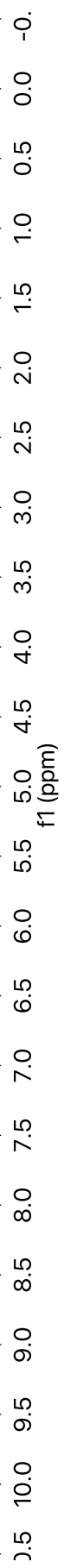
0.93 H

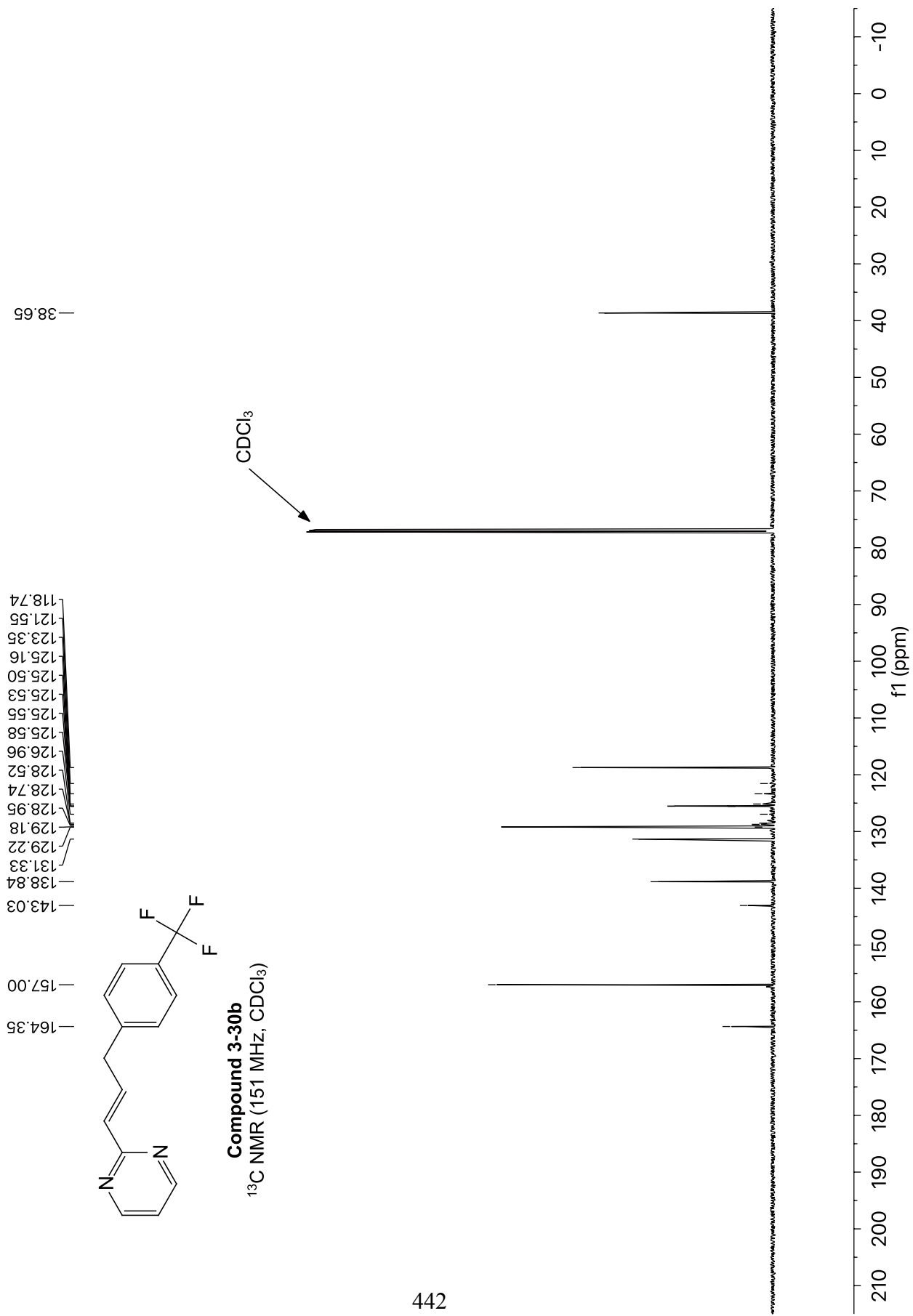
0.97 H

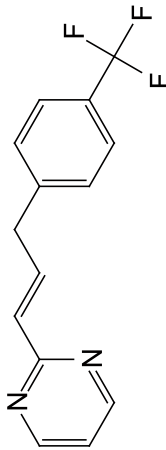
1.88 H

1.88 H

1.81 H







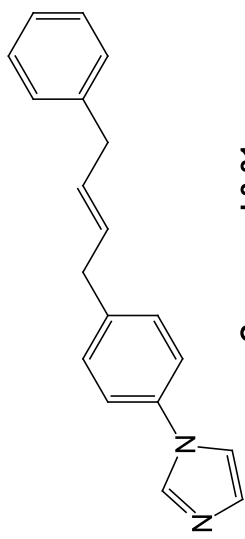
Compound 3-30b

¹⁹F NMR (565 MHz, CDCl₃)

—62.43

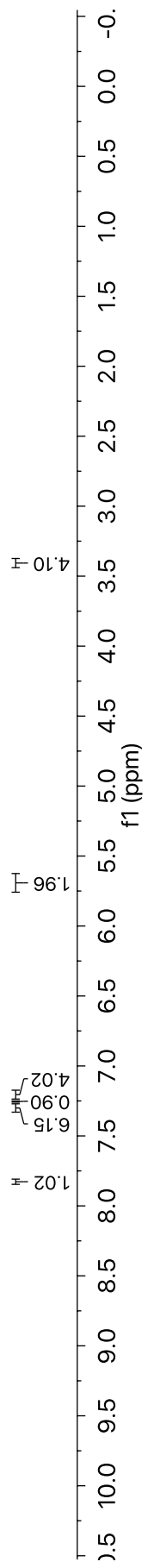
10 0 -10 -20 -30 -40 -50 -60 -70 -80 -90 -100 -110 -120 -130 -140 -150 -160 -170 -180 -190 -200 -210
f1 (ppm)

7.83
7.83
7.83
7.32
7.31
7.31
7.30
7.30
7.30
7.29
7.29
7.28
7.28
7.28
7.25
7.22
7.21
7.20
7.20
7.20
7.20
7.20
7.20
7.19
5.74
5.74
5.74
5.73
5.73
5.72
5.72
5.71
5.71
5.71
5.70
5.69
5.69
5.68
5.68
5.67
5.67
5.66
5.65
5.65
5.64
5.64
3.42
3.41
3.40
3.39



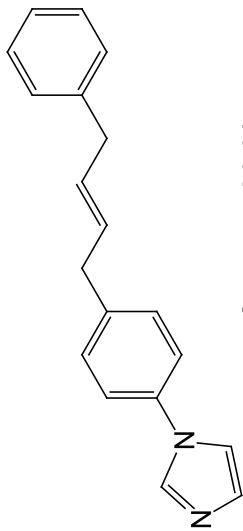
Compound 3-31
¹H NMR (600 MHz, CDCl₃)

CHCl₃



140.61
140.44
135.81
135.66
131.36
130.46
130.03
129.79
128.65
128.59
126.21
121.75
118.48

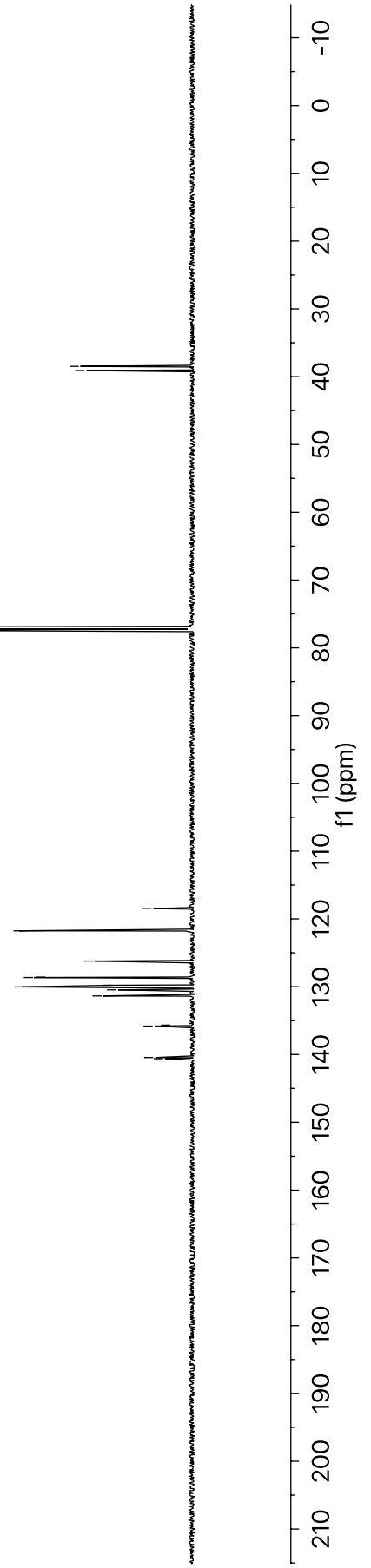
39.09
38.48

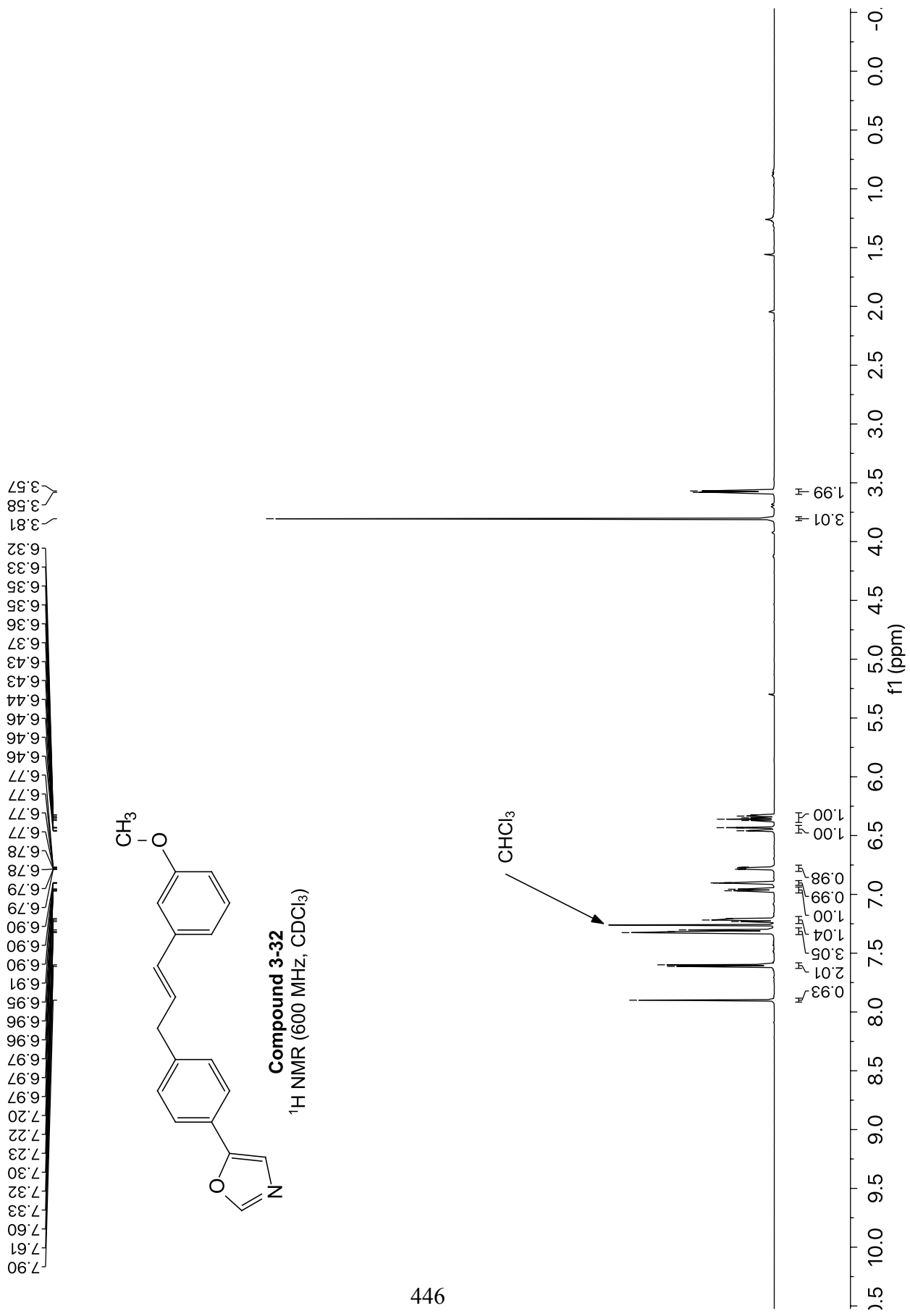


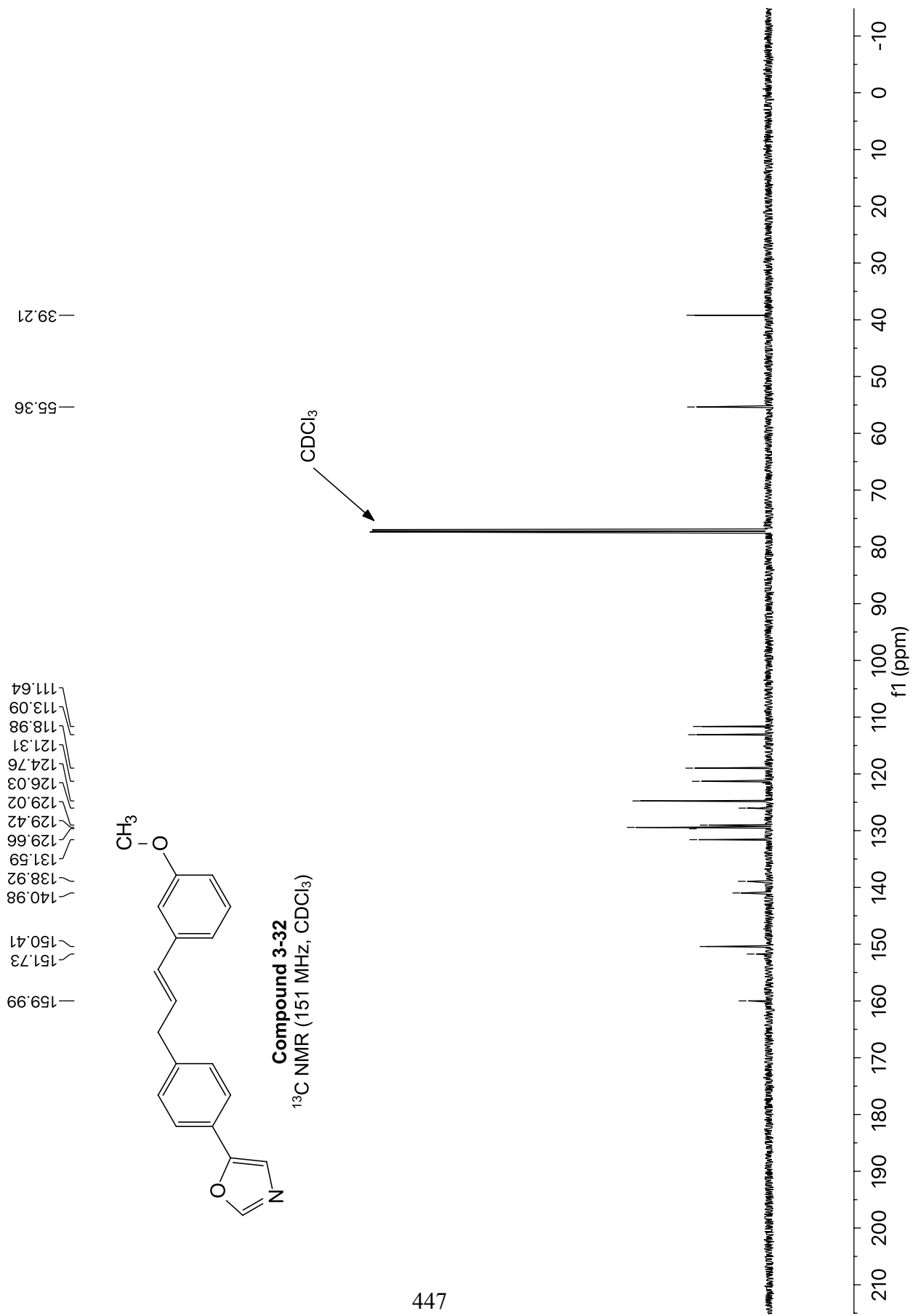
Compound 3-31
¹³C NMR (151 MHz, CDCl₃)

445

CDCl₃

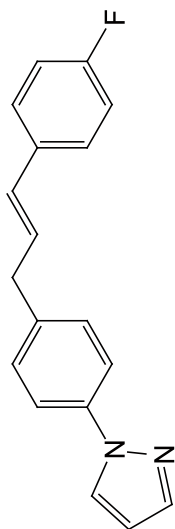






3.58
3.57
3.56
3.56

7.91
7.90
7.72
7.72
7.64
7.64
7.63
7.63
7.33
7.33
7.32
7.32
7.32
7.31
7.31
7.00
6.99
6.97
6.46
6.46
6.46
6.46
6.44
6.44
6.43
6.41
6.41
6.30
6.29
6.28
6.28
6.26
6.25



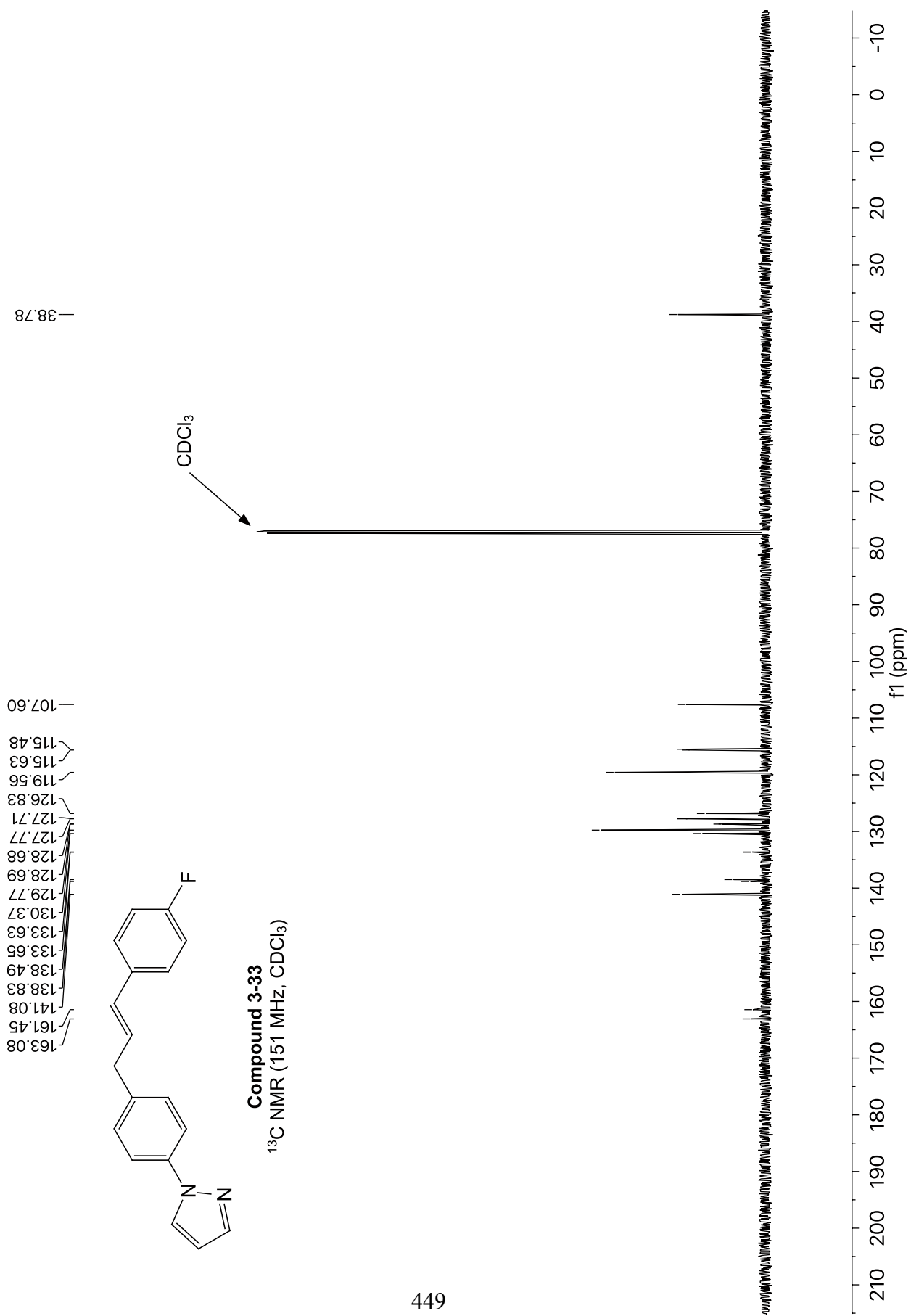
Compound 3-33
¹H NMR (600 MHz, CDCl₃)

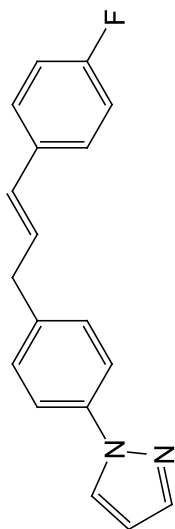
CHCl₃

1.01
0.93
1.98
4.04
2.03
1.99
1.01
2.00

10.5 10.0 9.5 9.0 8.5 8.0 7.5 7.0 6.5 6.0 5.5 5.0 4.5 4.0 3.5 3.0 2.5 2.0 1.5 1.0 0.5 0.0 -0.0

f1 (ppm)



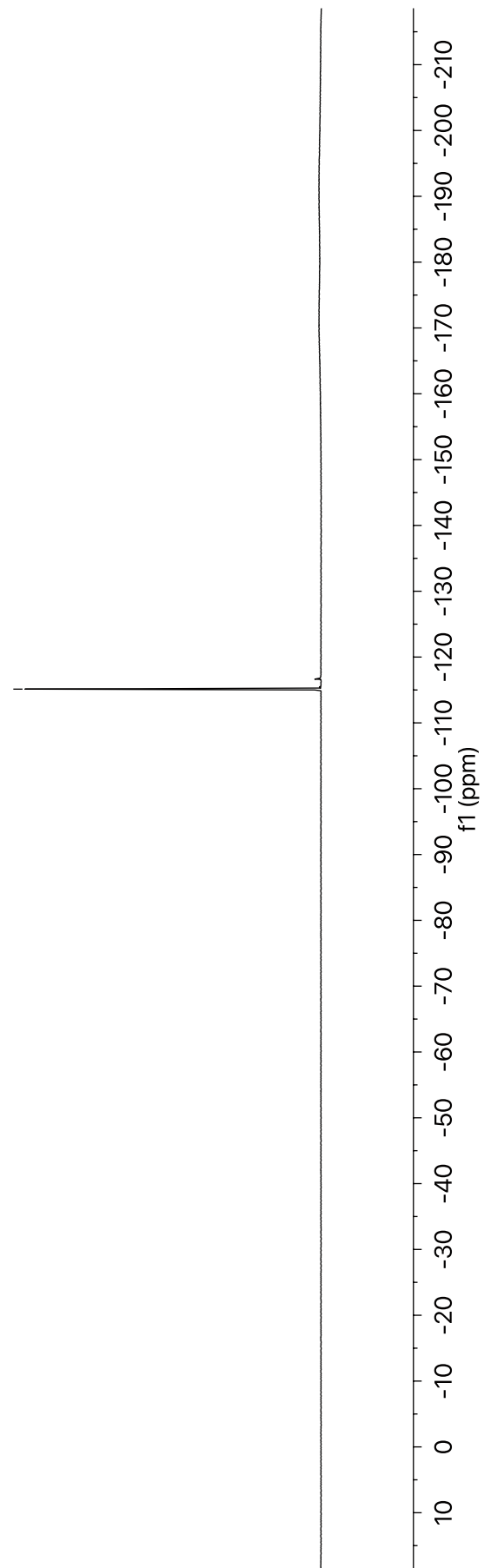


Compound 3-33

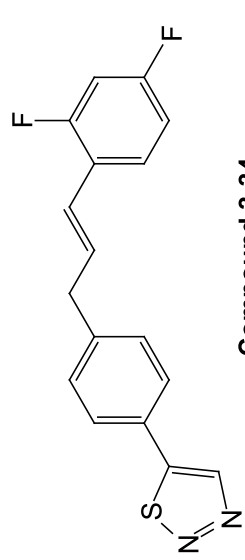
¹⁹F NMR (565 MHz, CDCl₃)

— -115.13

450

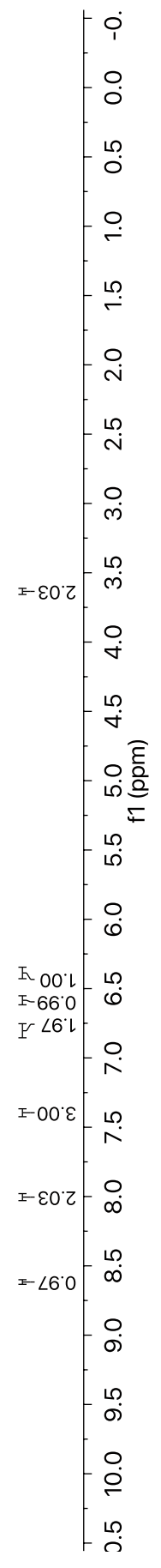


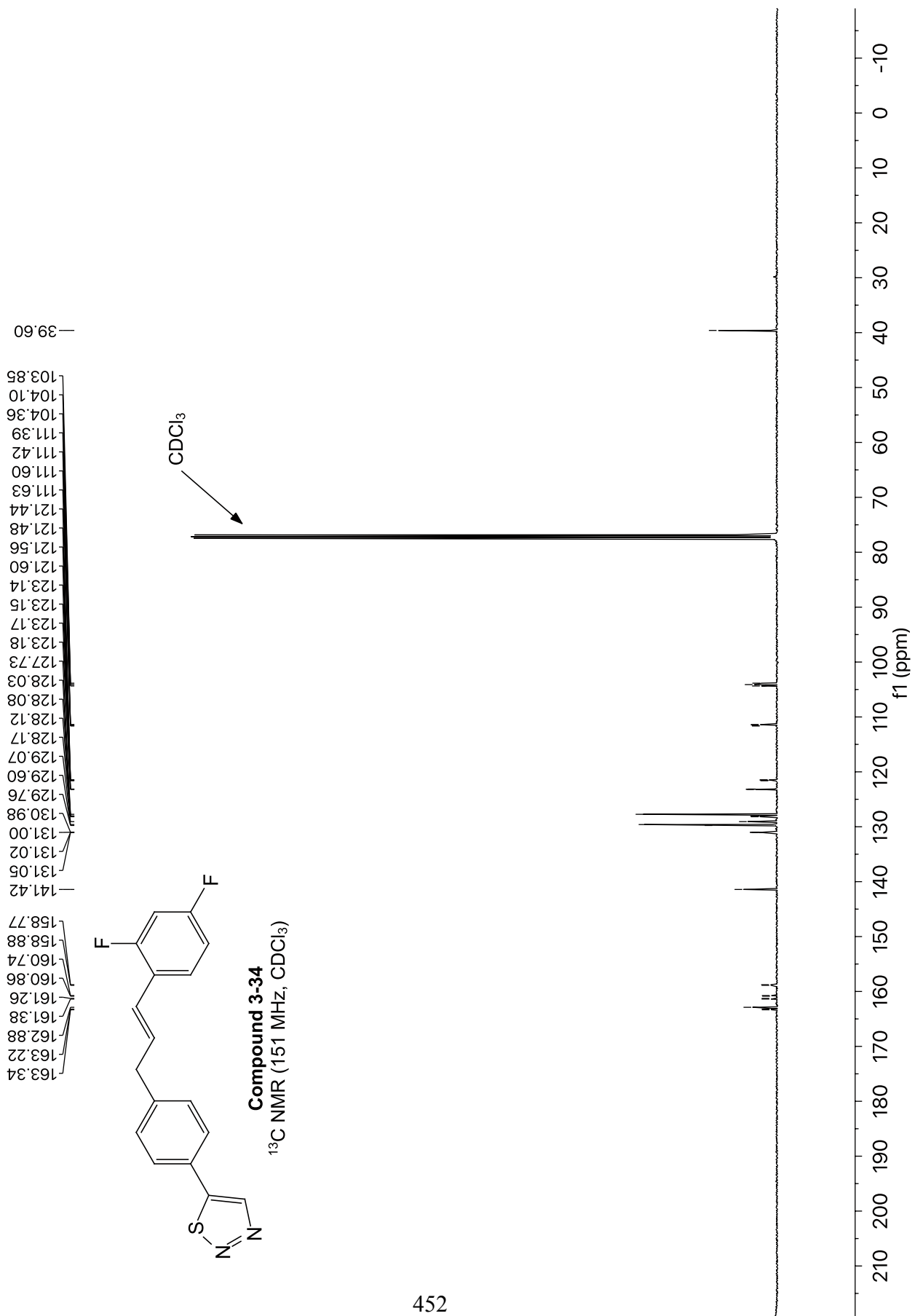
8.62
8.01
8.01
8.00
8.00
8.00
7.41
7.40
7.39
7.39
7.38
6.84
6.84
6.83
6.82
6.82
6.81
6.81
6.80
6.79
6.79
6.78
6.77
6.77
6.77
6.60
6.60
6.59
6.57
6.57
6.57
6.41
6.40
6.39
6.39
6.37
6.36
3.64
3.63

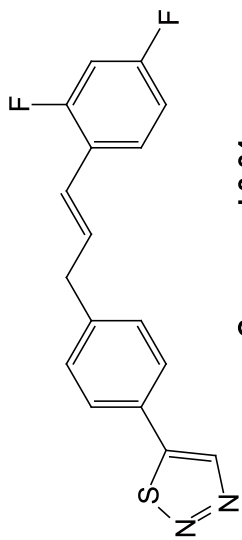


Compound 3-34
¹H NMR (600 MHz, CDCl₃)

CHCl₃

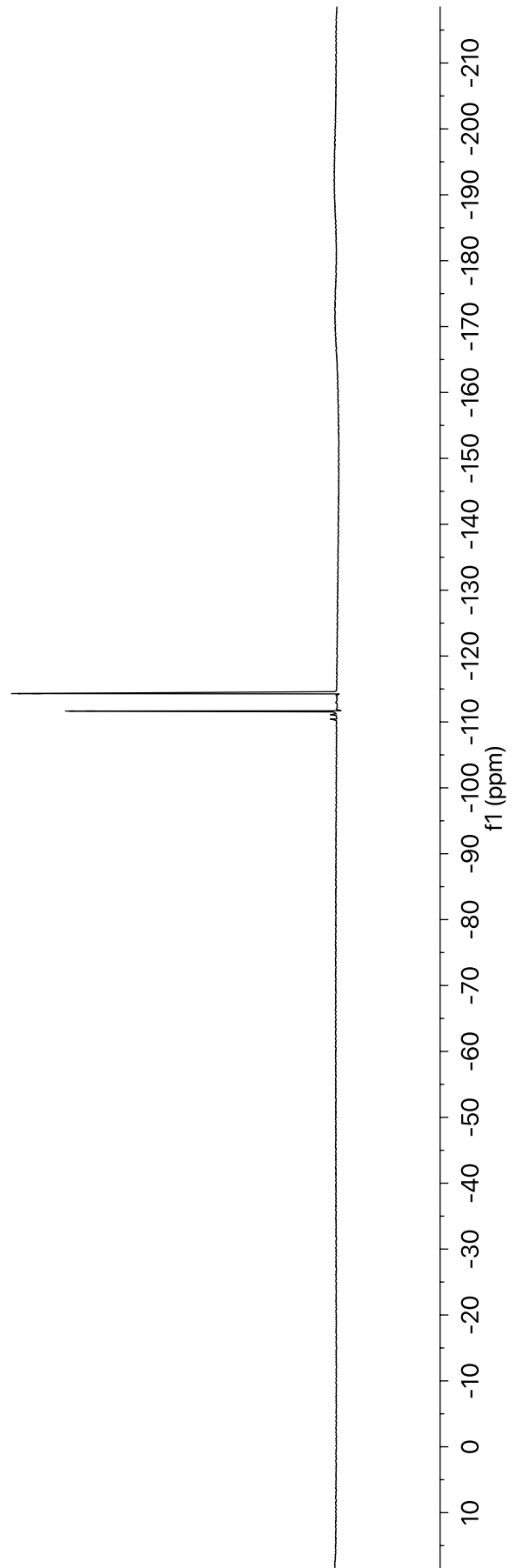


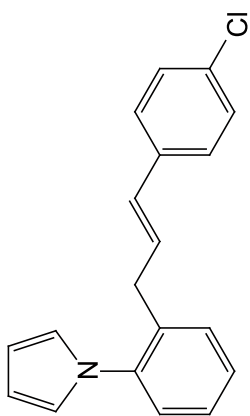
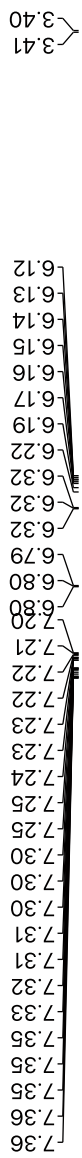




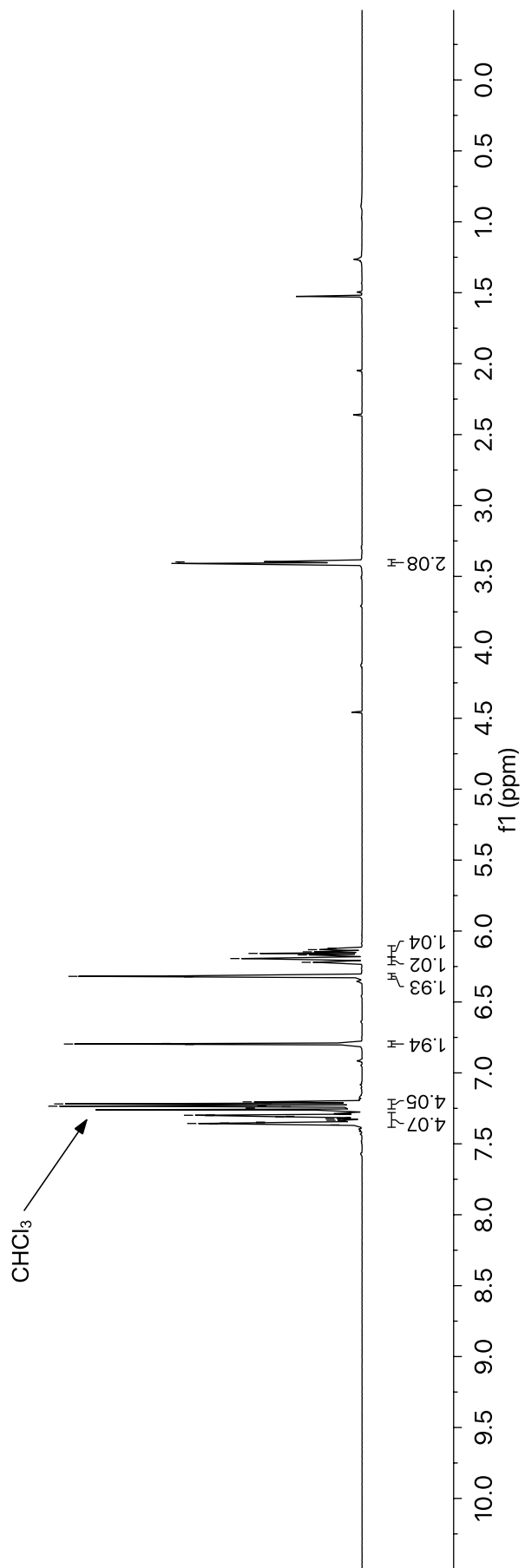
Compound 3-34
¹⁹F NMR (565 MHz, CDCl₃)

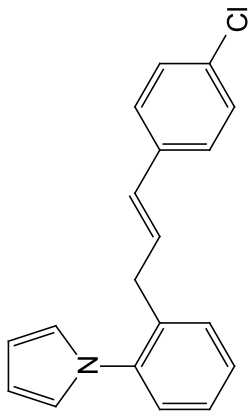
-111.65
-111.67
-114.29
-114.30





Compound 3-35
¹H NMR (600 MHz, CDCl₃)

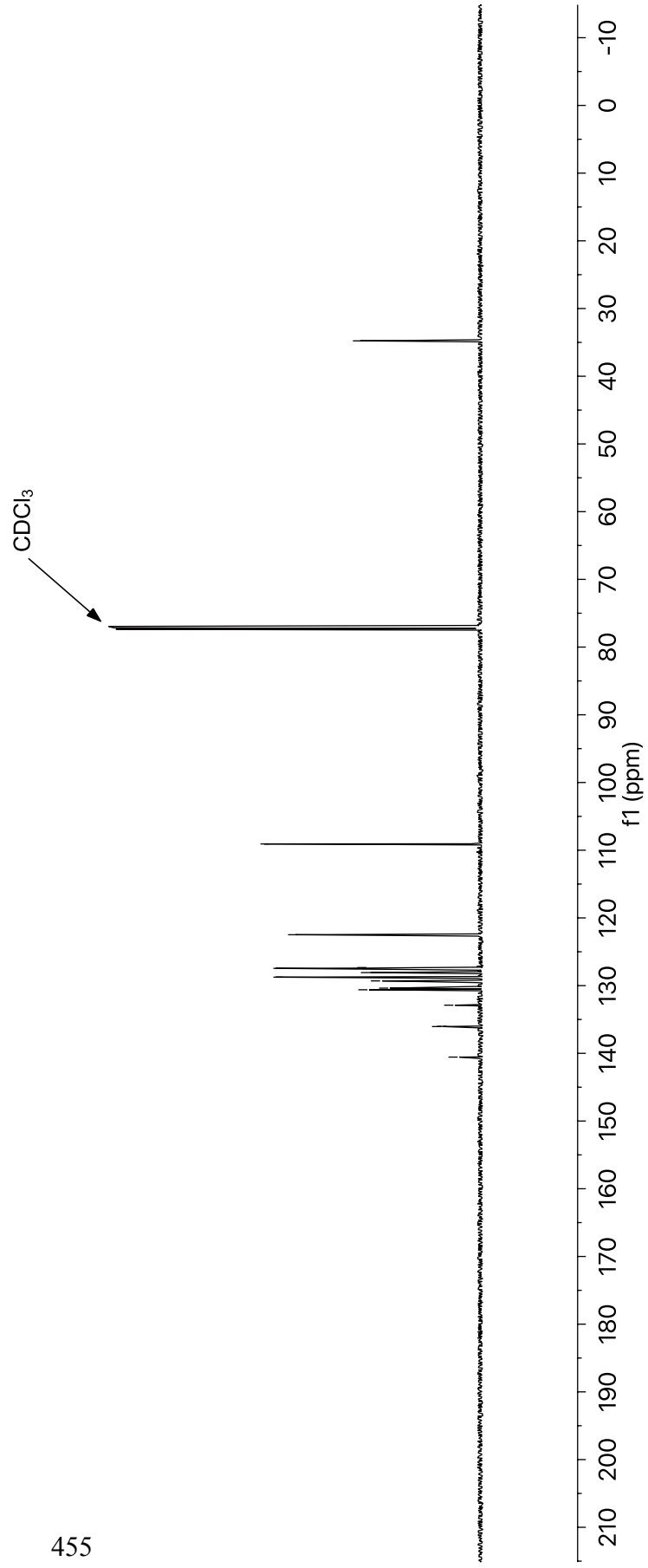


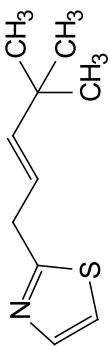


Compound 3-35
¹³C NMR (151 MHz, CDCl₃)

140.56
136.05
136.01
132.89
130.61
130.37
129.30
128.75
128.08
127.45
127.41
127.33
122.48
109.07

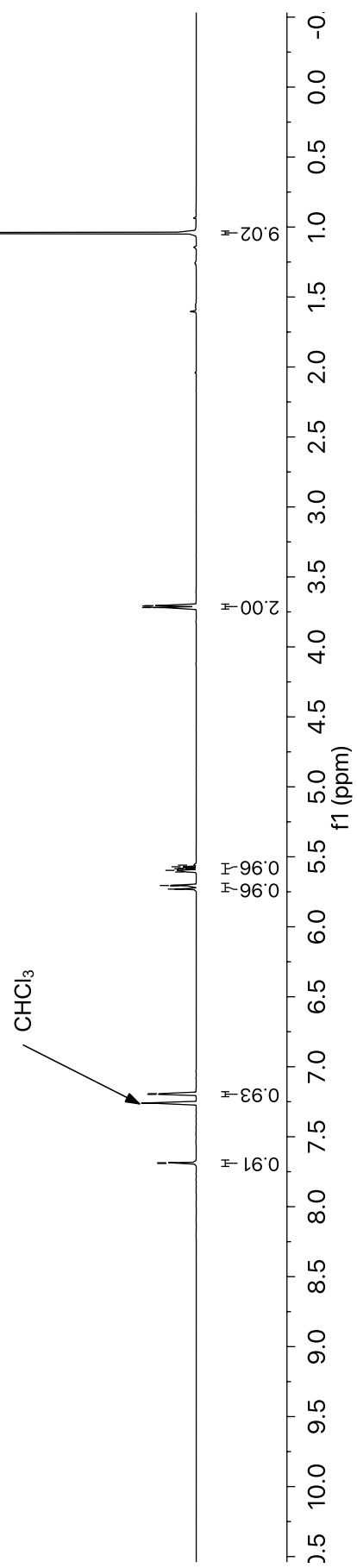
—34.77





Compound 3-36
¹H NMR (600 MHz, CDCl₃)

7.69, 7.69, 7.20, 7.19, 5.73, 5.73, 5.71, 5.71, 5.70, 5.61, 5.60, 5.59, 5.58, 5.57, 5.56, 3.72, 3.71, 3.71, 3.71, 1.04

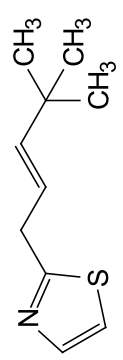


36.86
33.27
29.63

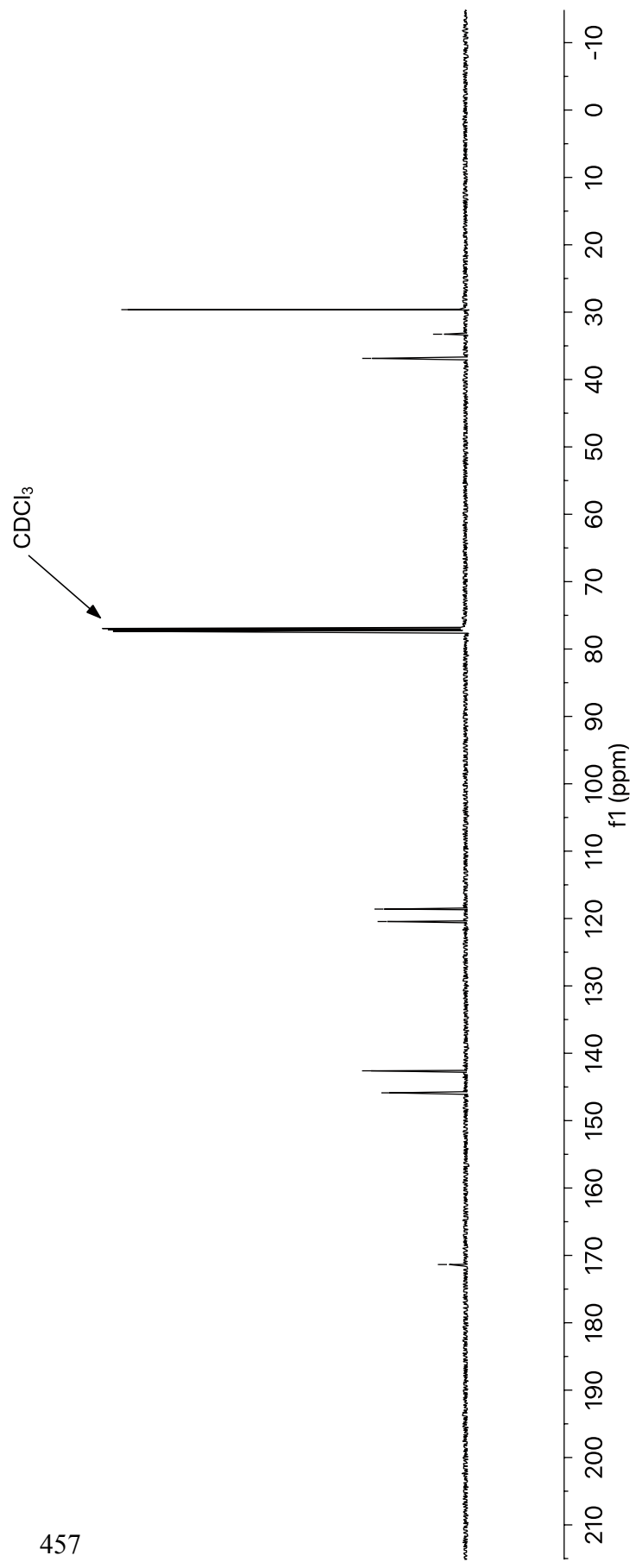
120.45
118.60

145.87
142.61

171.36

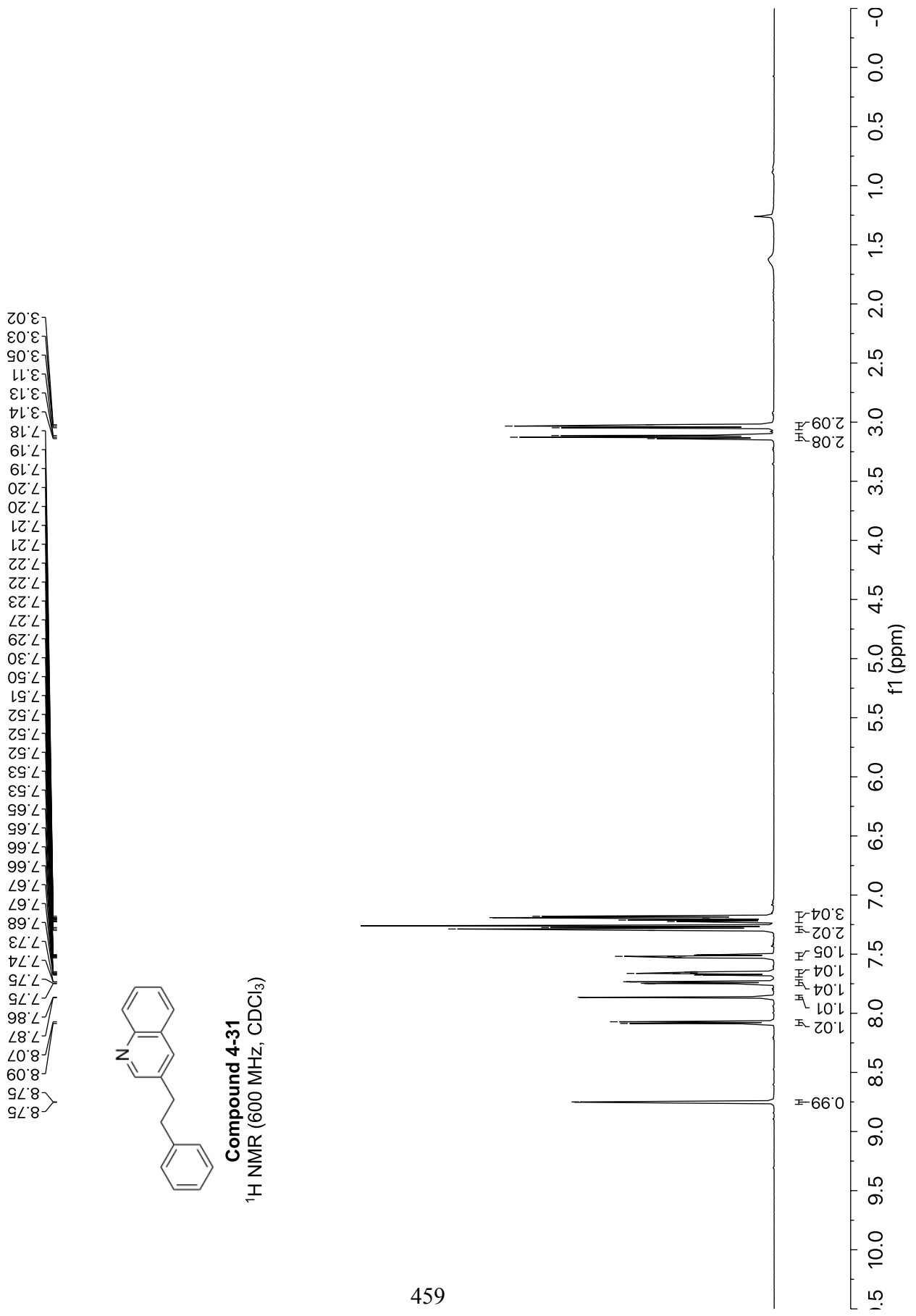


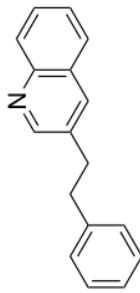
Compound 3-36
¹³C NMR (151 MHz, CDCl₃)



Appendix D

SPECTRAL AND CHROMATOGRAPHY DATA FOR CHAPTER 4

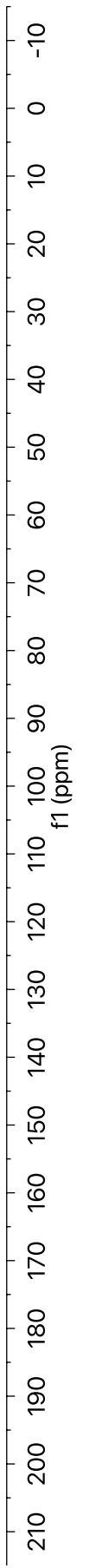


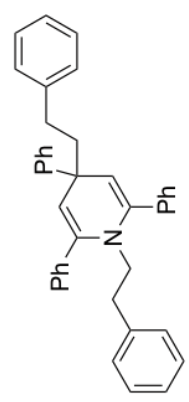
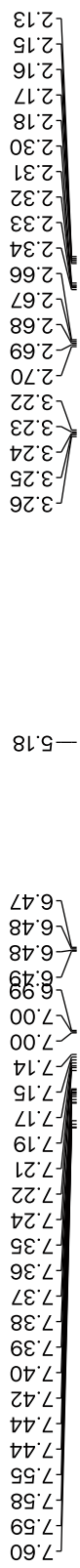


Compound 4-31
¹³C NMR (151 MHz, CDCl₃)

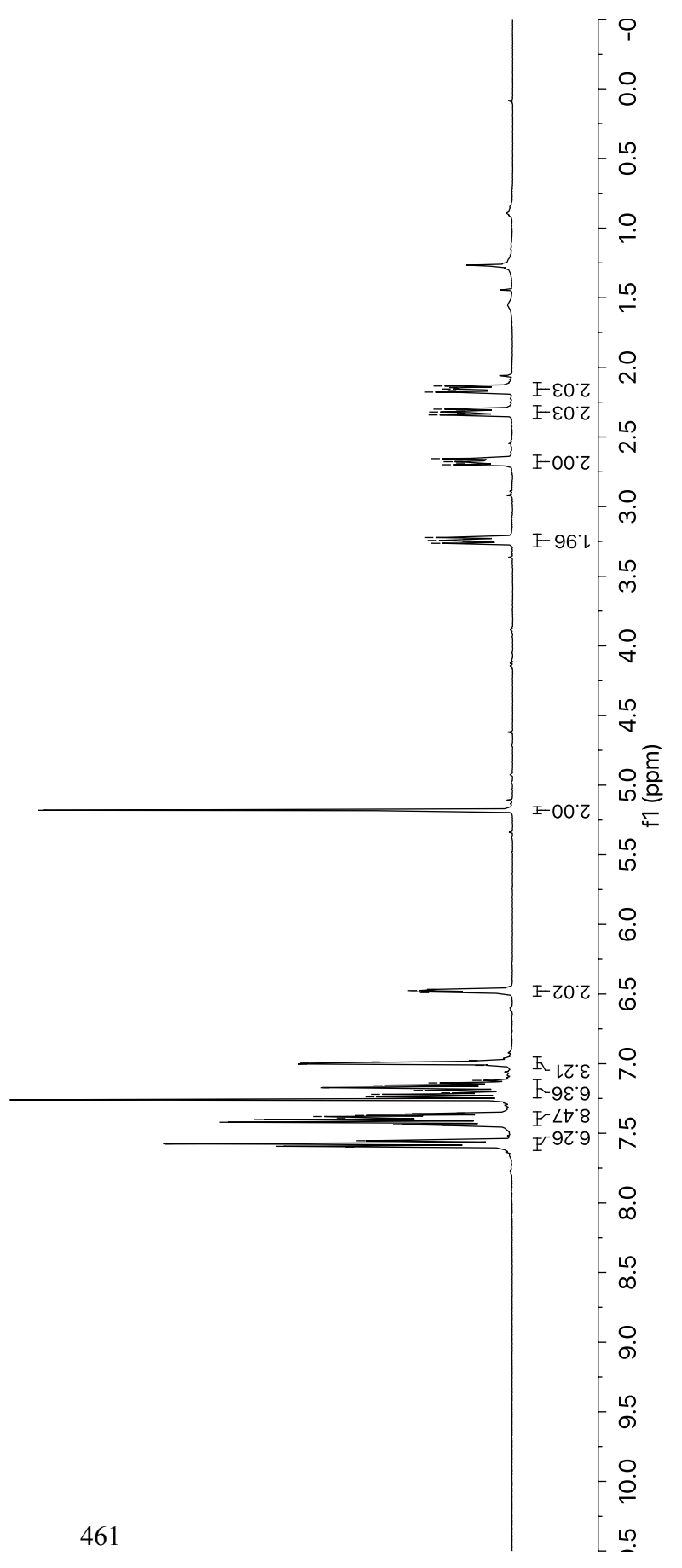
151.99
146.93
140.79
134.39
134.18
129.22
128.65
128.50
128.10
127.35
126.56
126.24

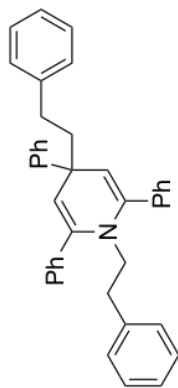
37.46
35.12



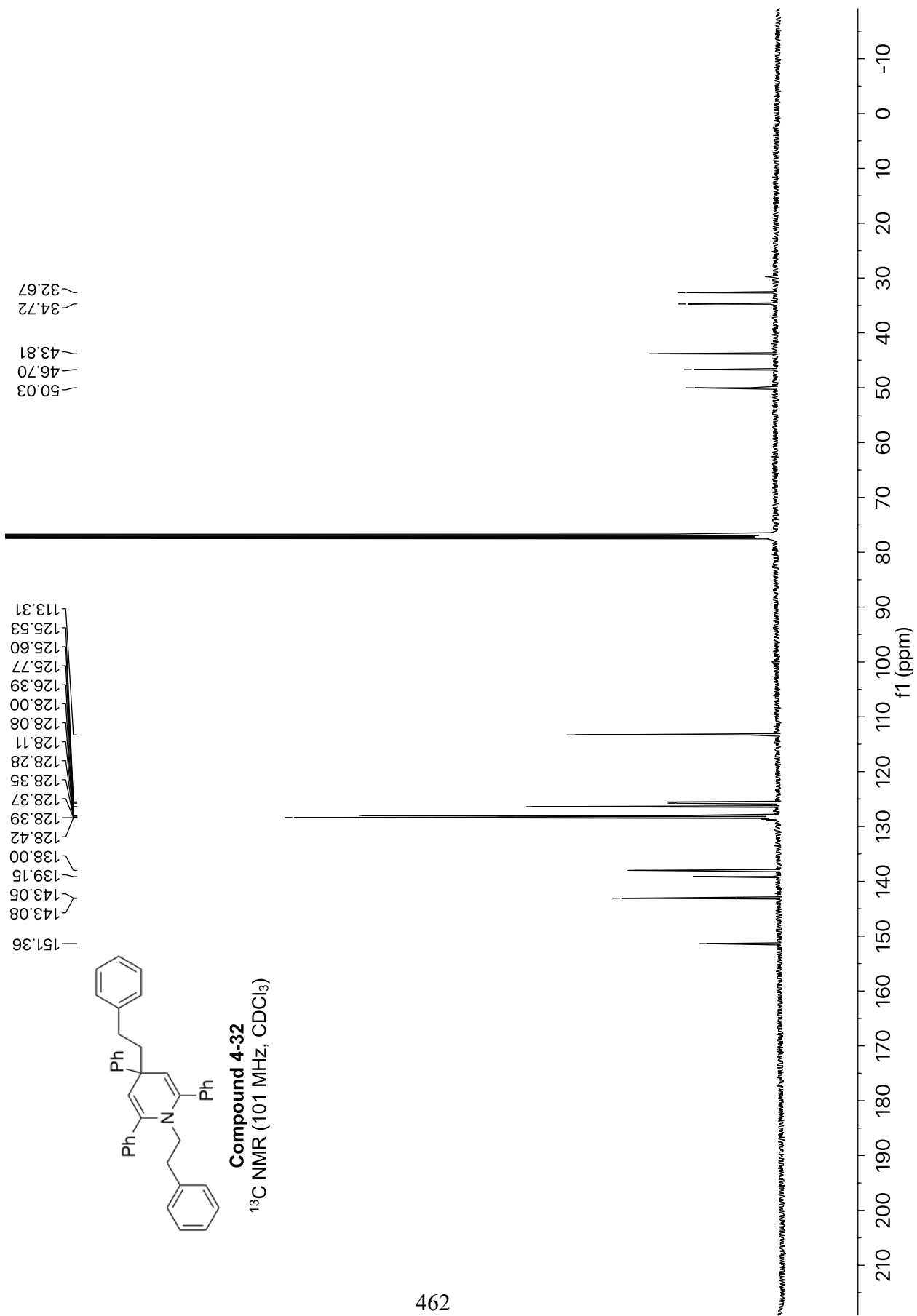


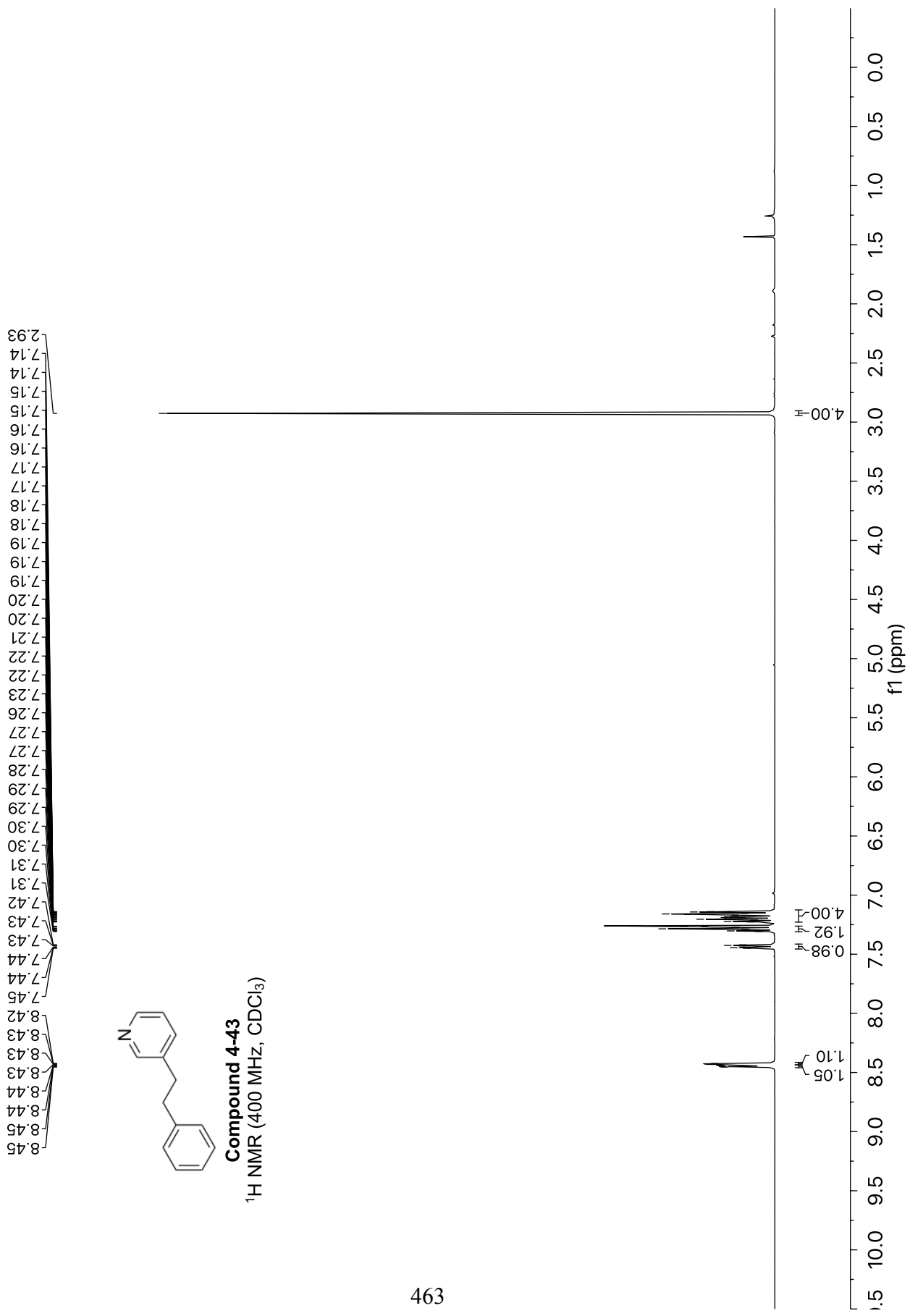
Compound 4-32
¹H NMR (400 MHz, CDCl₃)

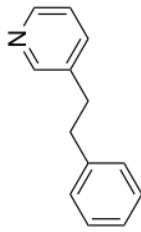




Compound 4-32
¹³C NMR (101 MHz, CDCl₃)





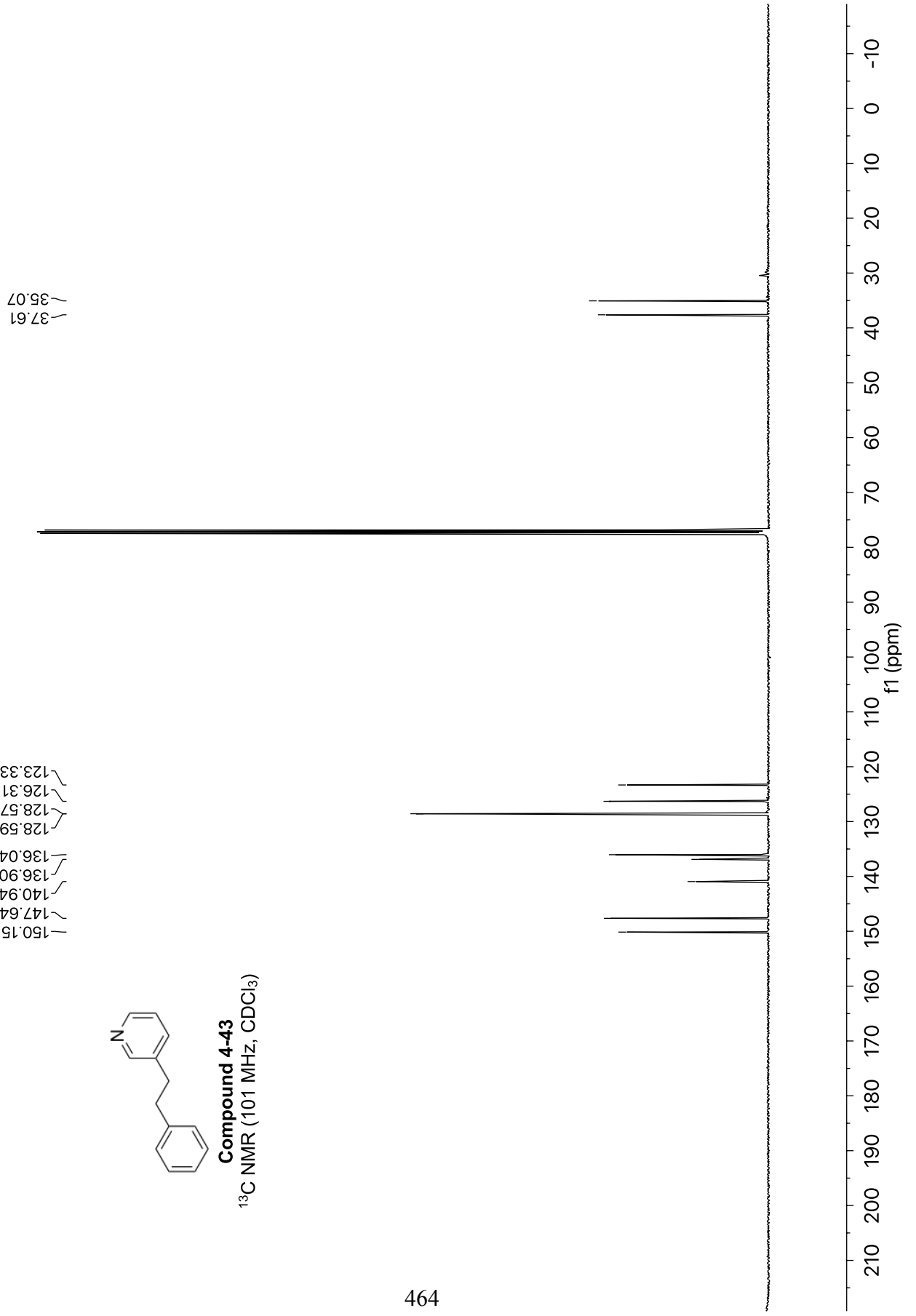


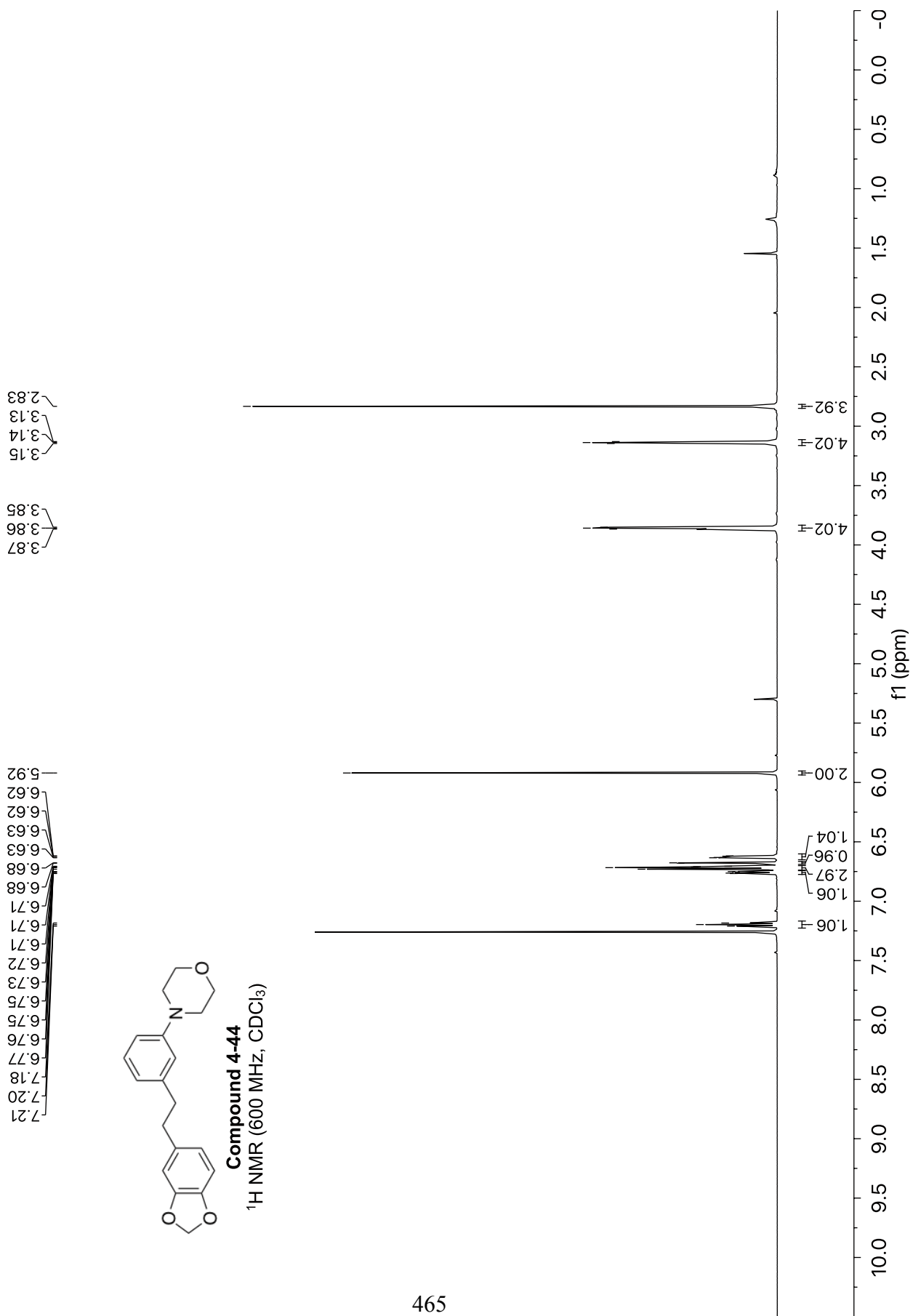
Compound 4-43

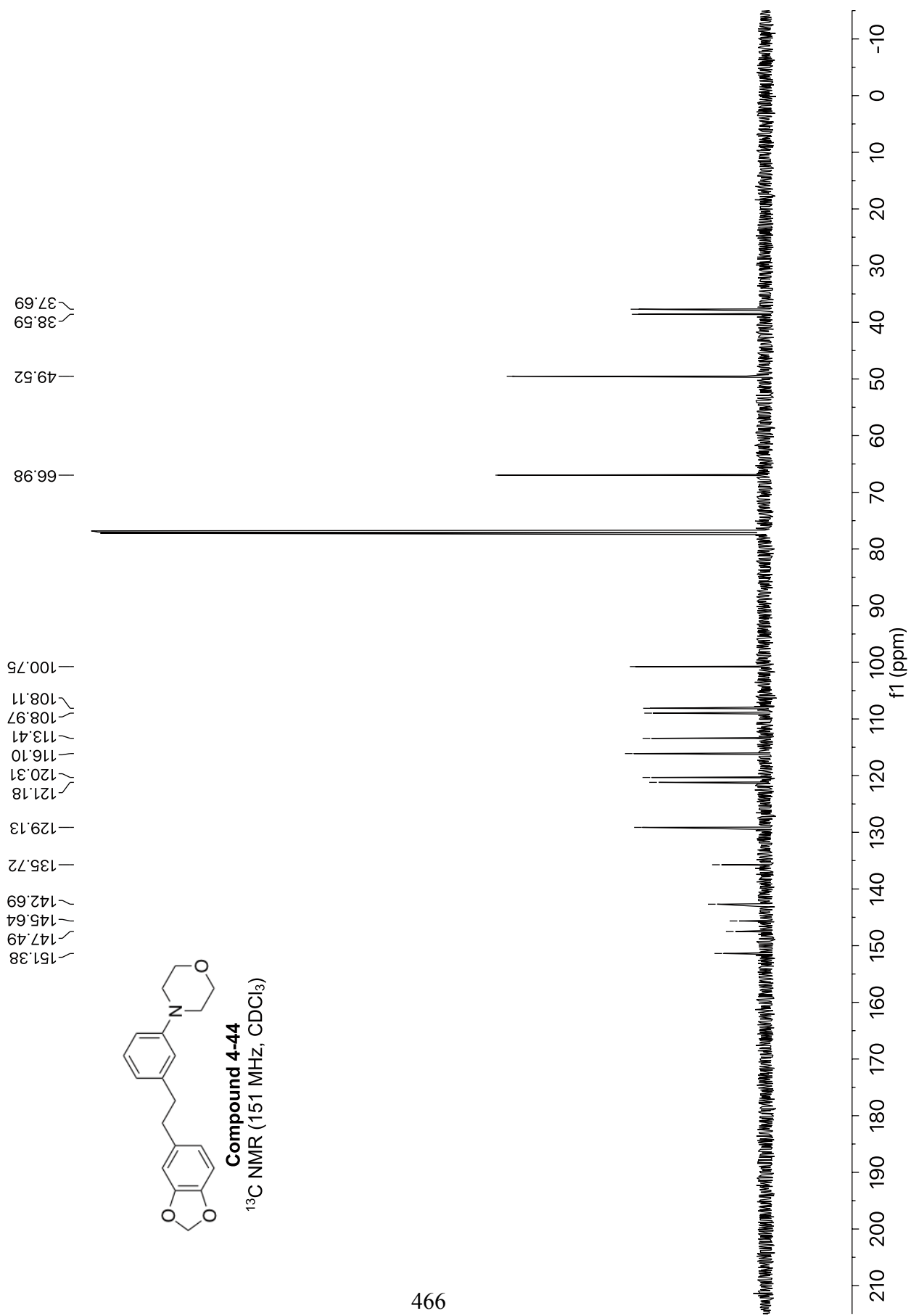
¹³C NMR (101 MHz, CDCl₃)

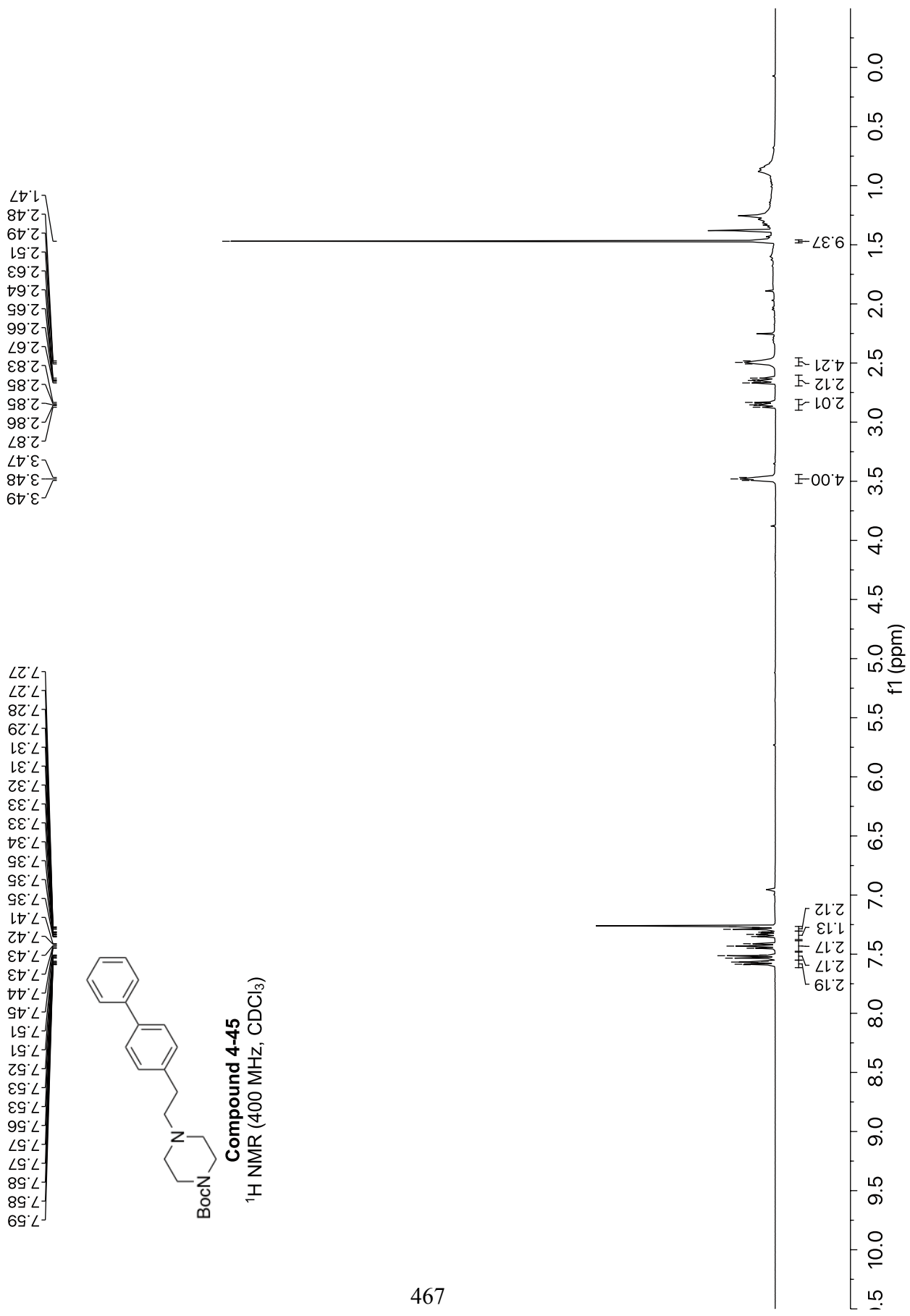
150.15
147.64
140.94
136.90
136.04
128.59
128.57
126.31
123.33

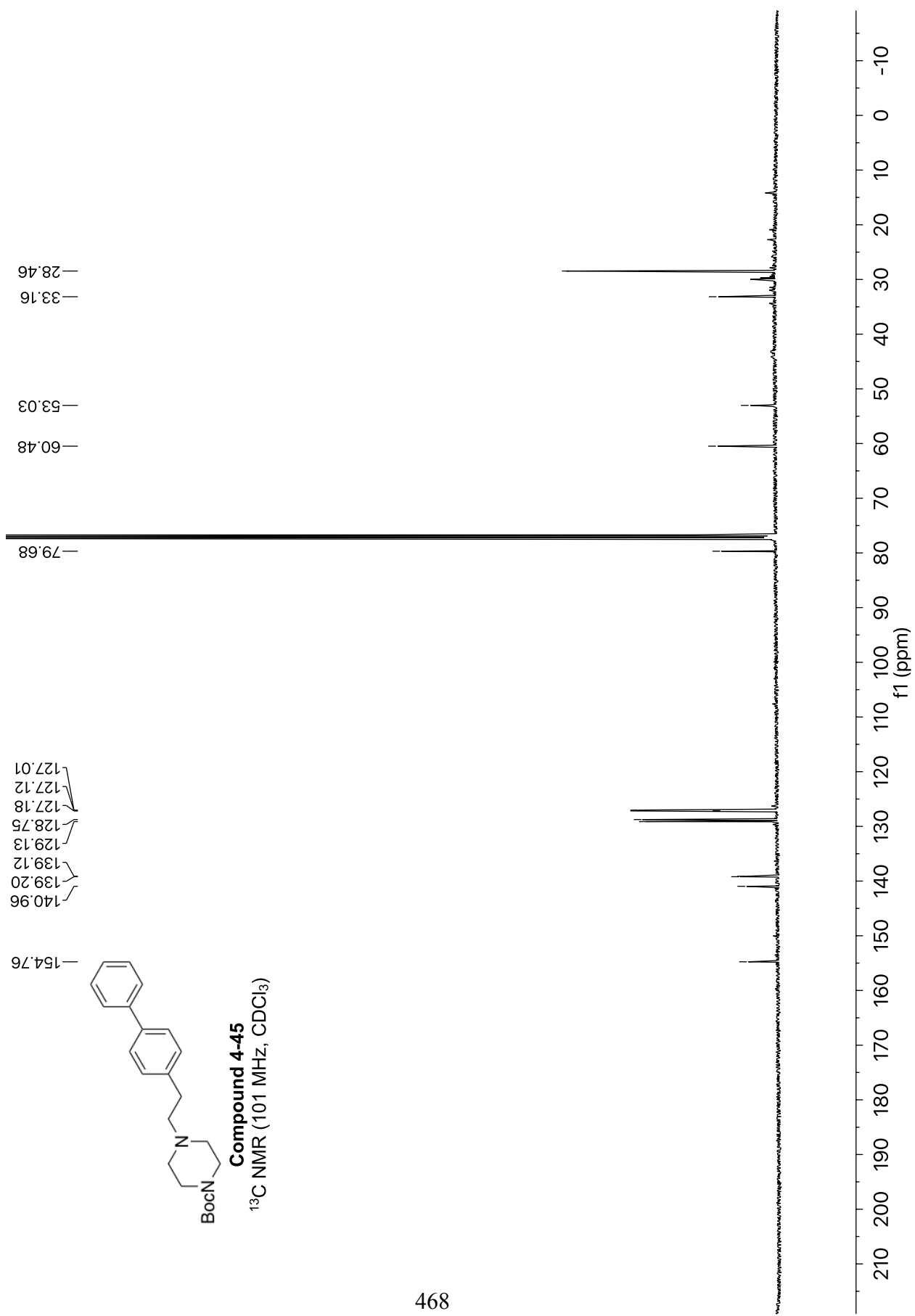
37.61
35.07

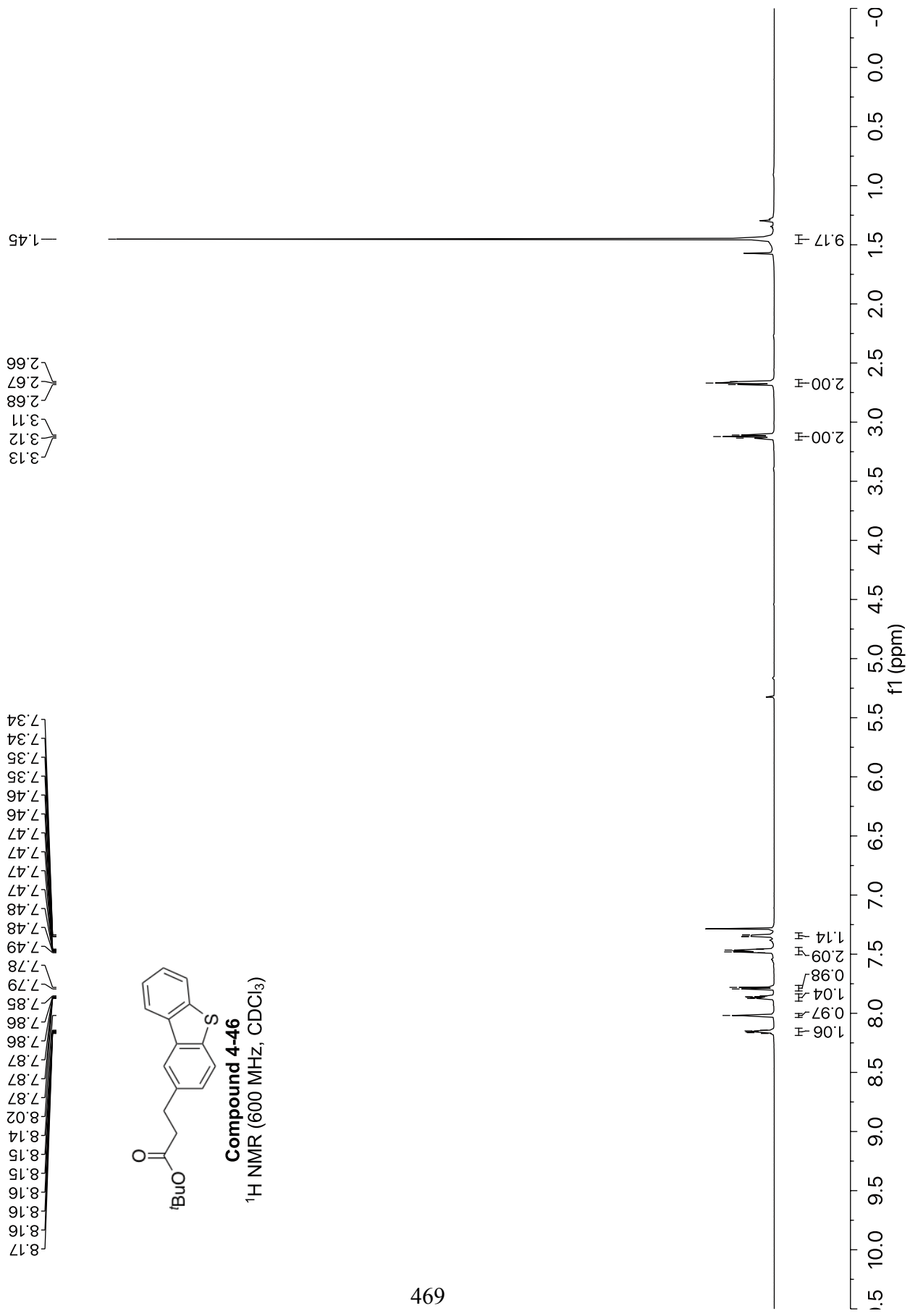


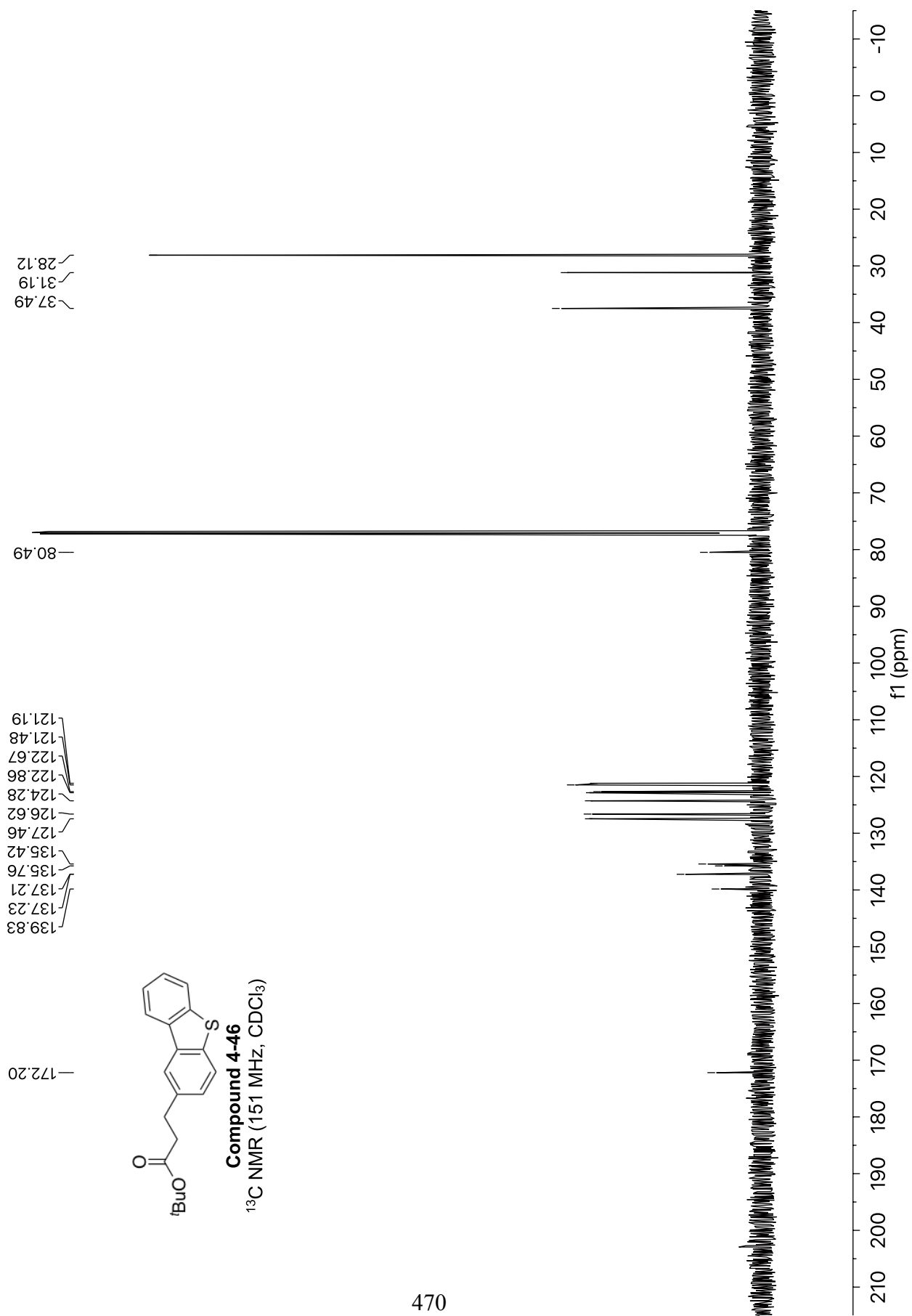


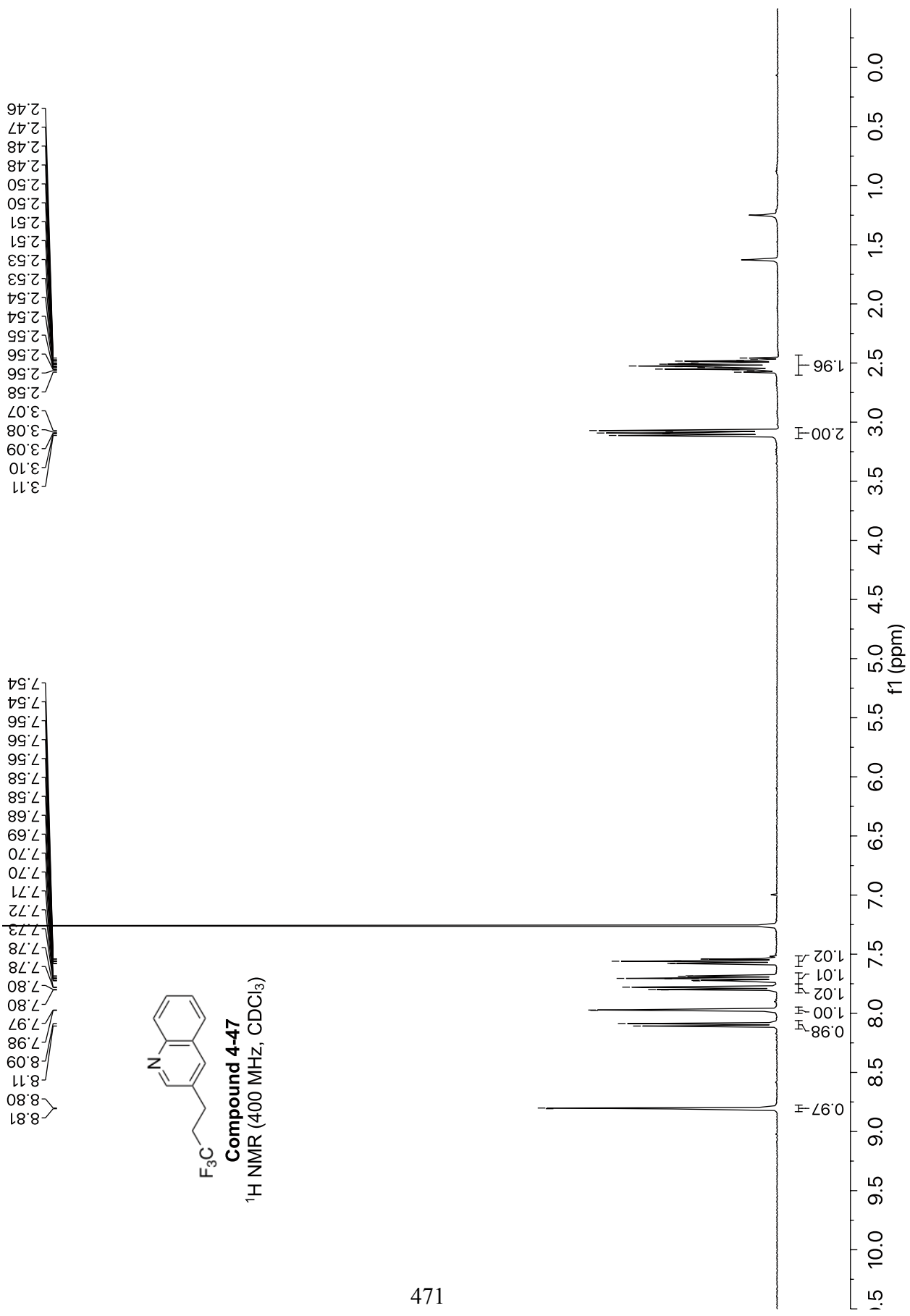


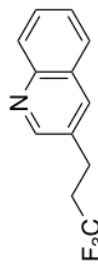






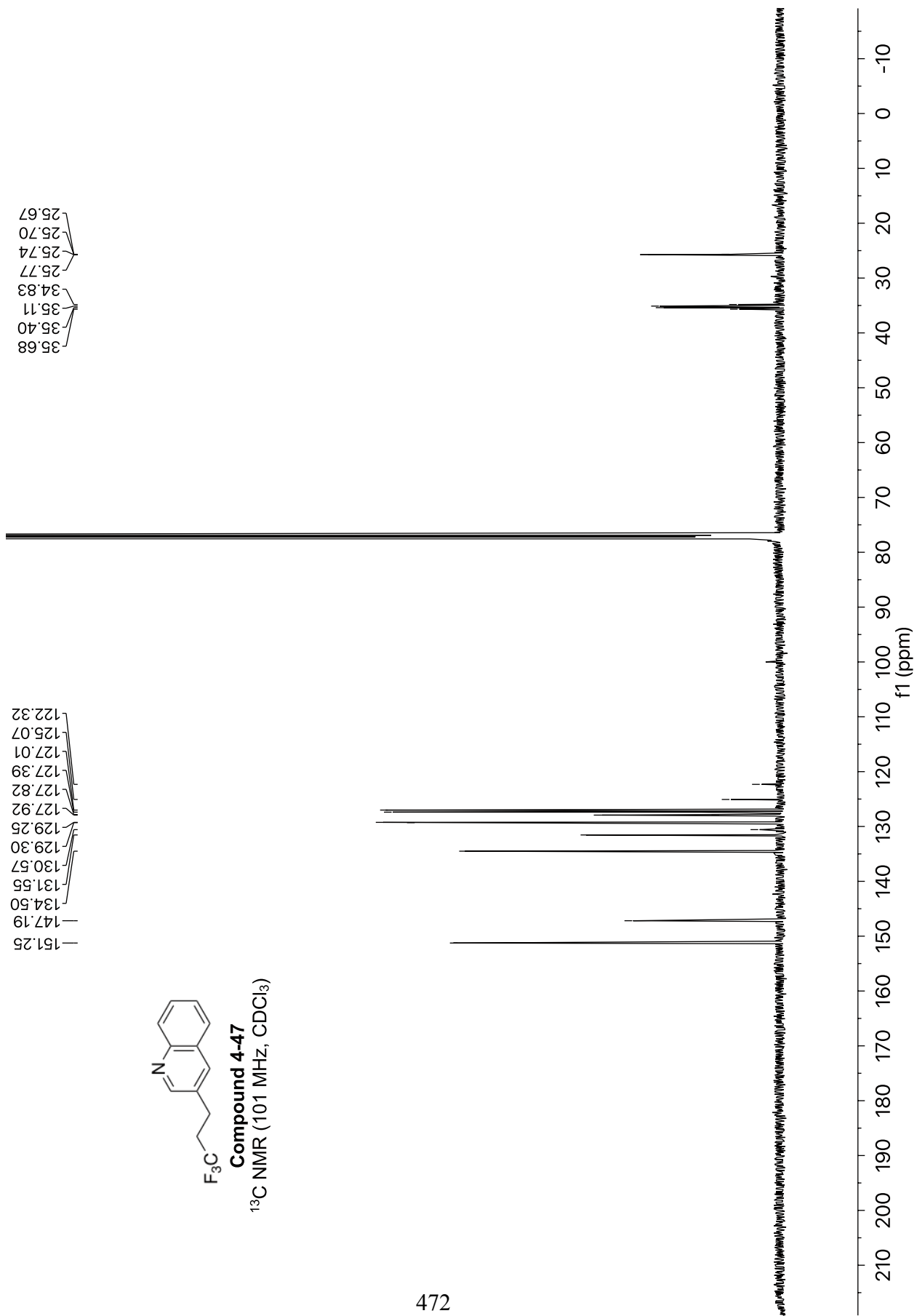


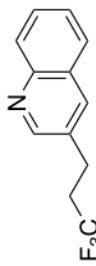




Compound 4-47

^{13}C NMR (101 MHz, CDCl_3)



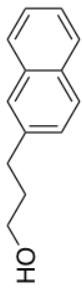


Compound 4-47
¹⁹F NMR (376 MHz, CDCl₃)

— -66.43



-10 -20 -30 -40 -50 -60 -70 -80 -90 -100 -110 -120 -130 -140 -150 -160 -170 -180 -190
f1 (ppm)

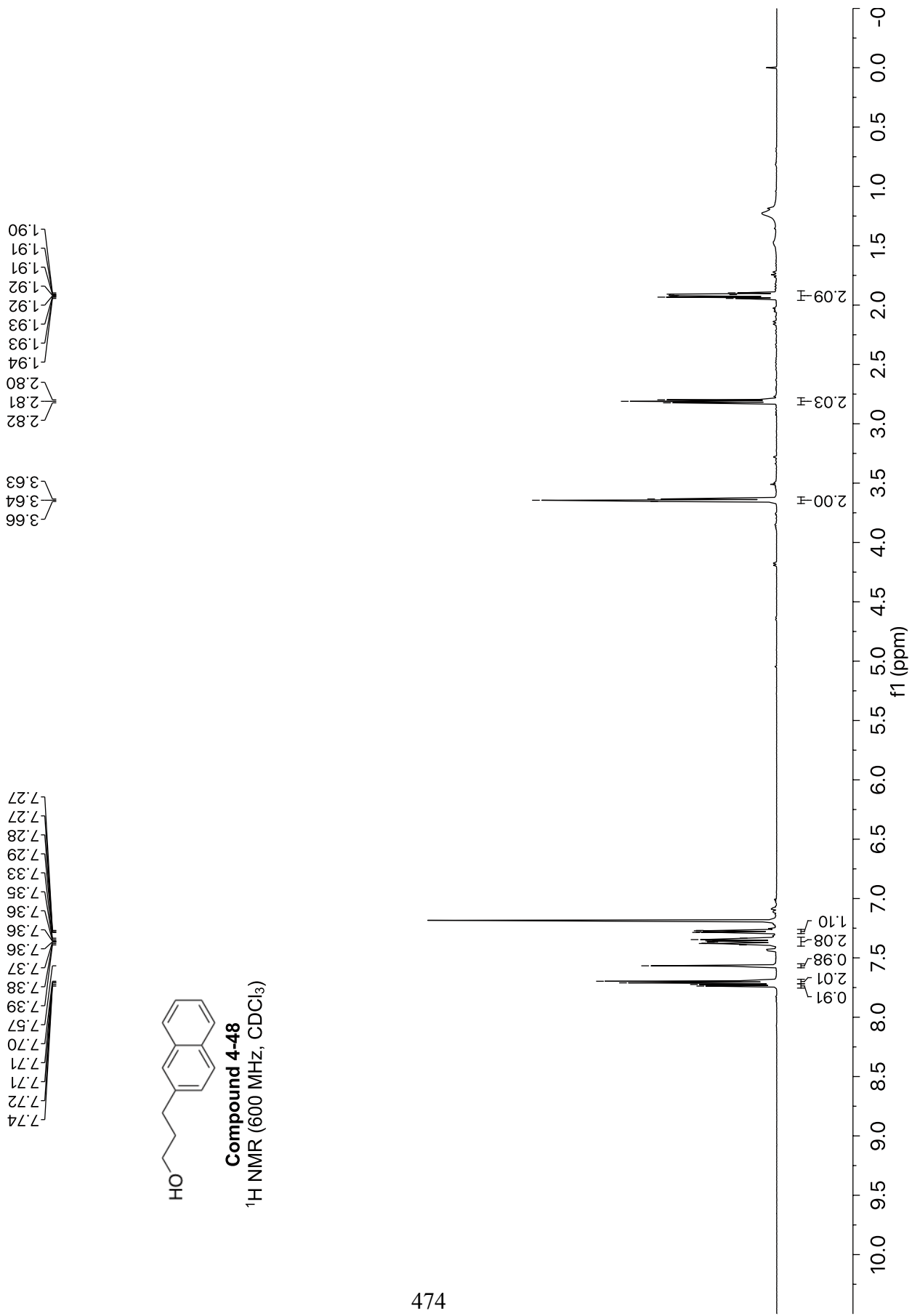


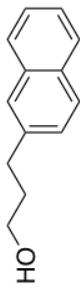
Compound 4-48
¹H NMR (600 MHz, CDCl₃)

1.90
1.91
1.91
1.92
1.92
1.93
1.93
1.94
2.80
2.81
2.82
3.63
3.64
3.66

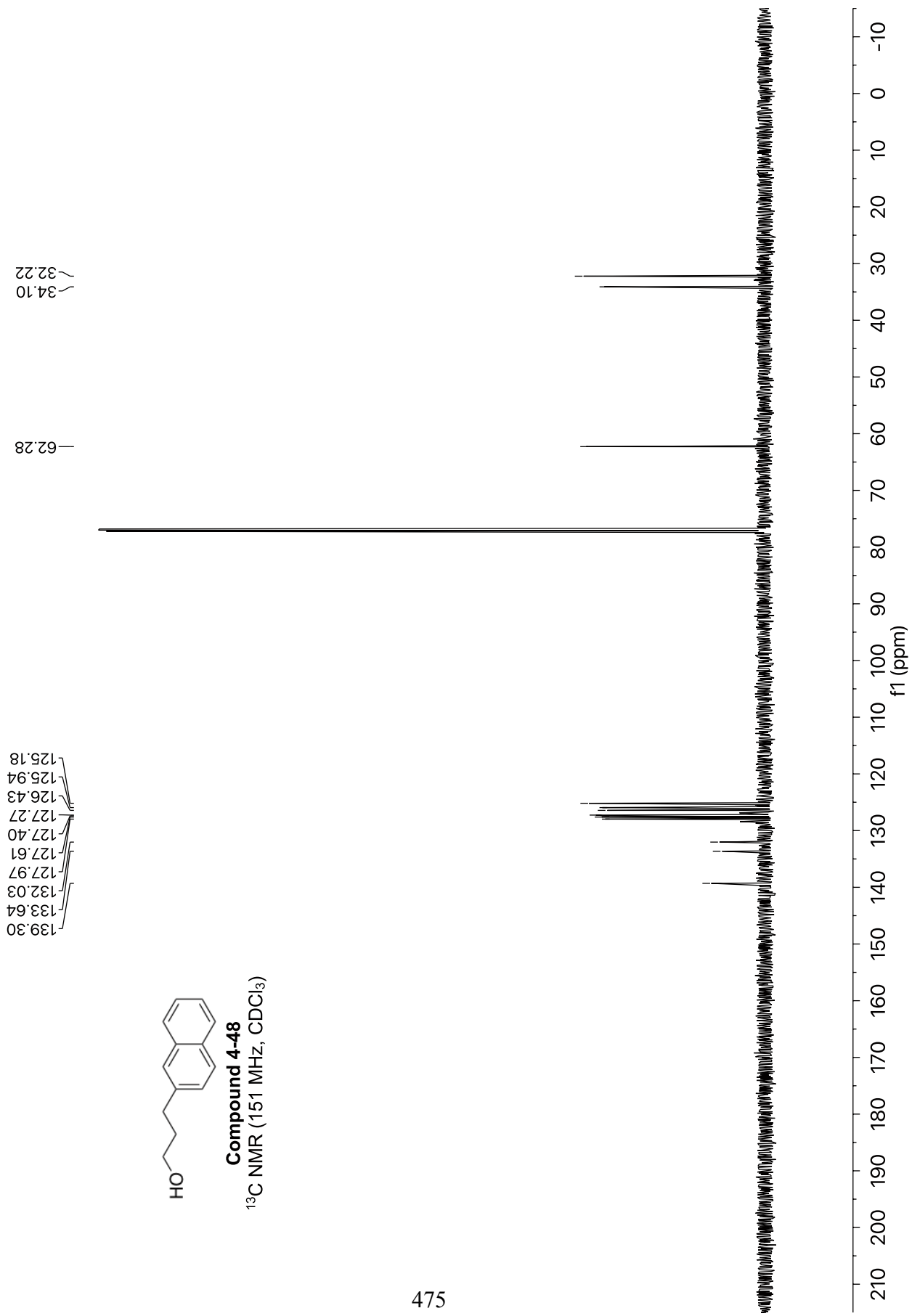
7.27
7.27
7.28
7.29
7.33
7.35
7.36
7.36
7.36
7.36
7.37
7.38
7.39
7.57
7.70
7.71
7.71
7.72
7.74

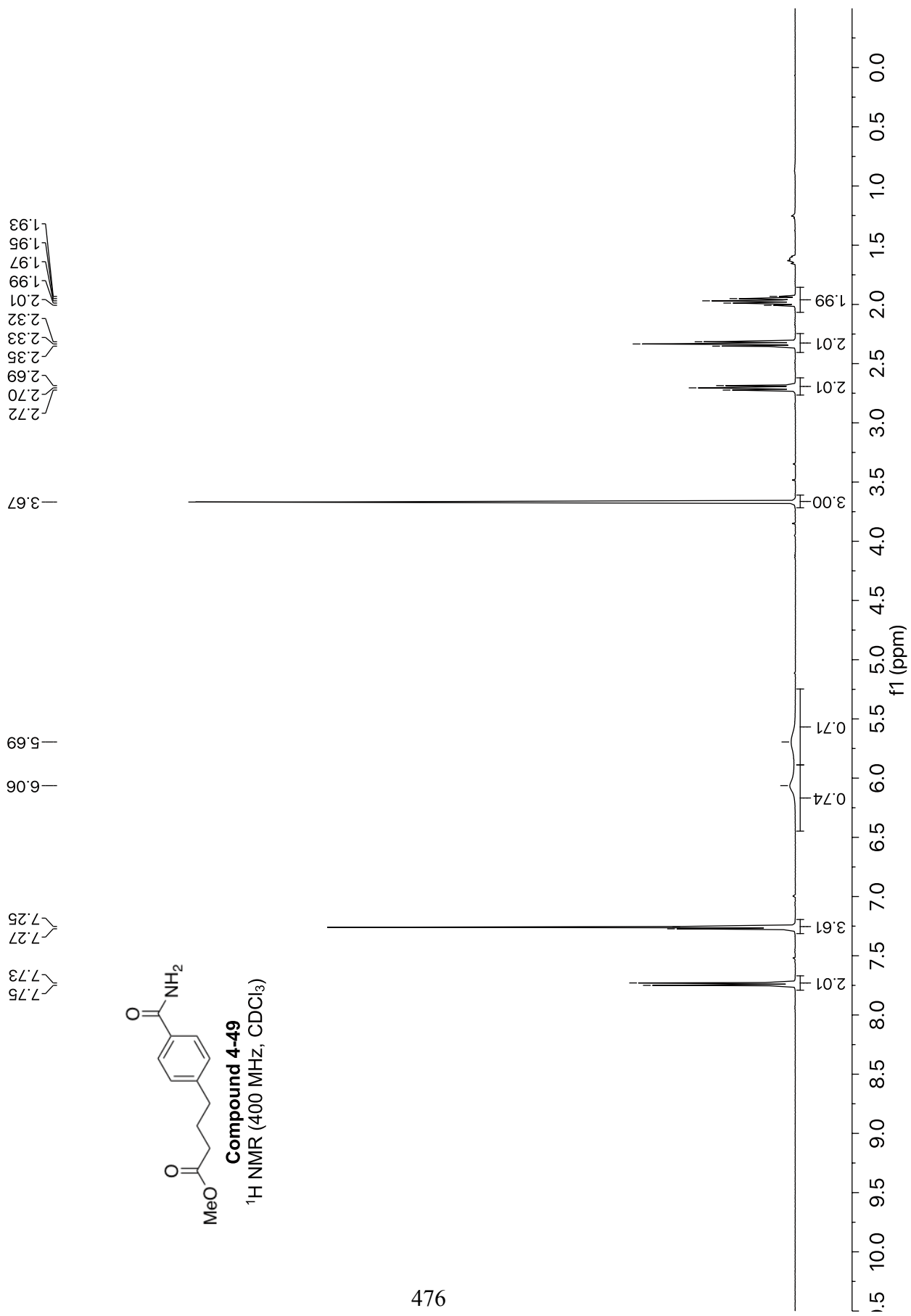
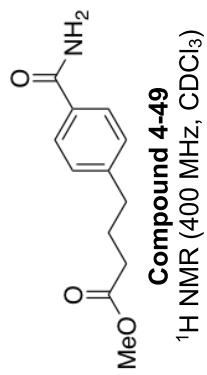
474

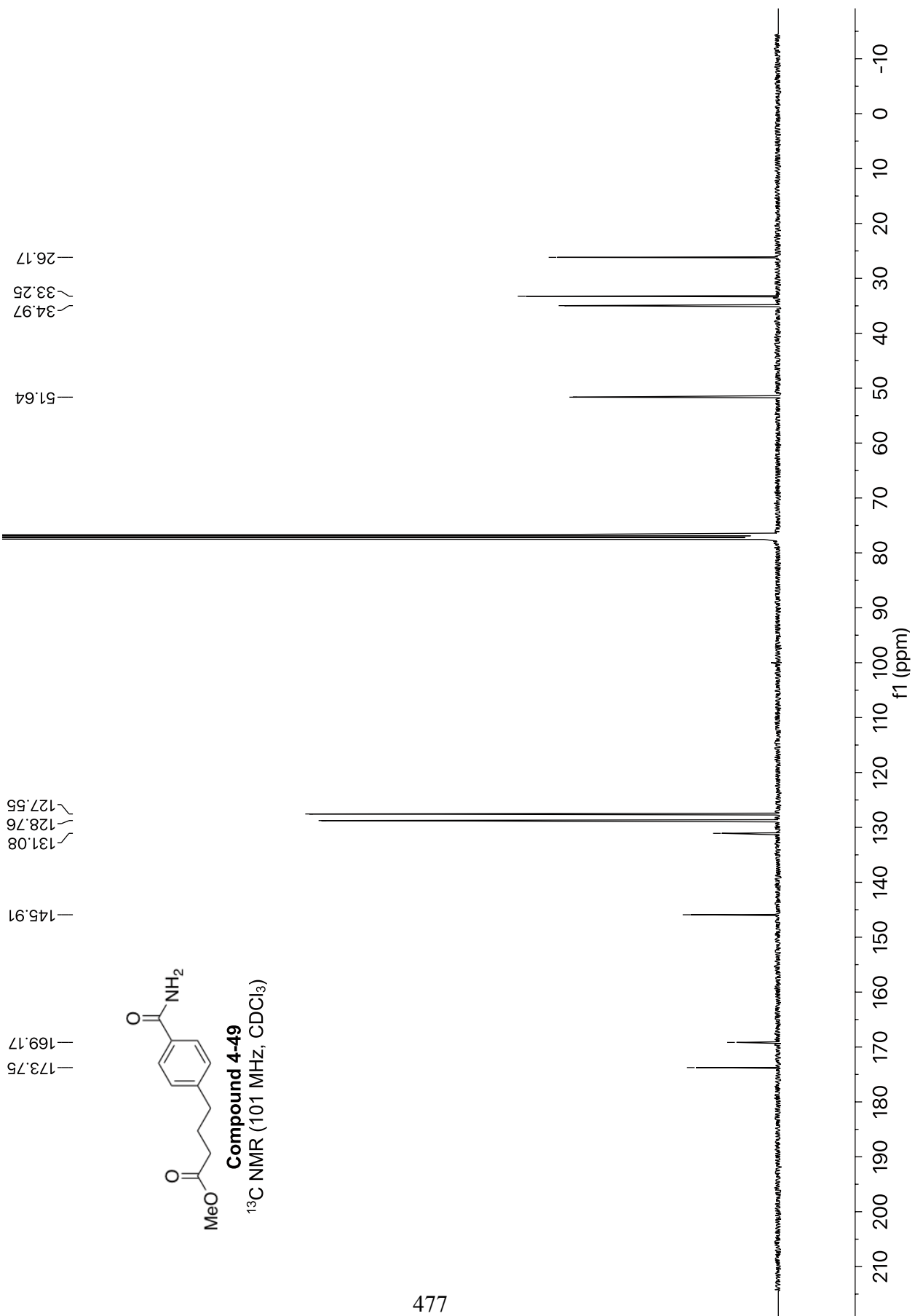


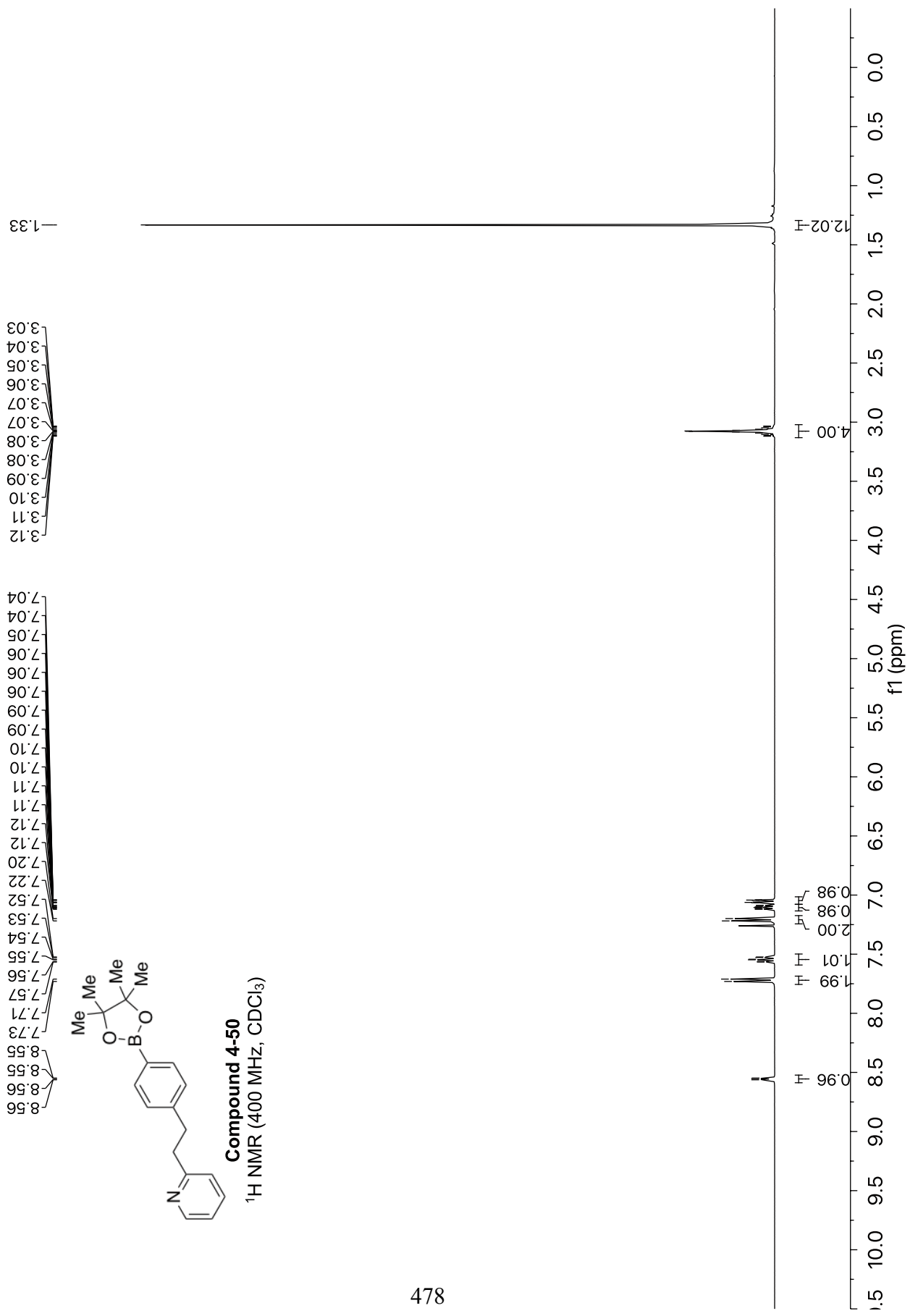


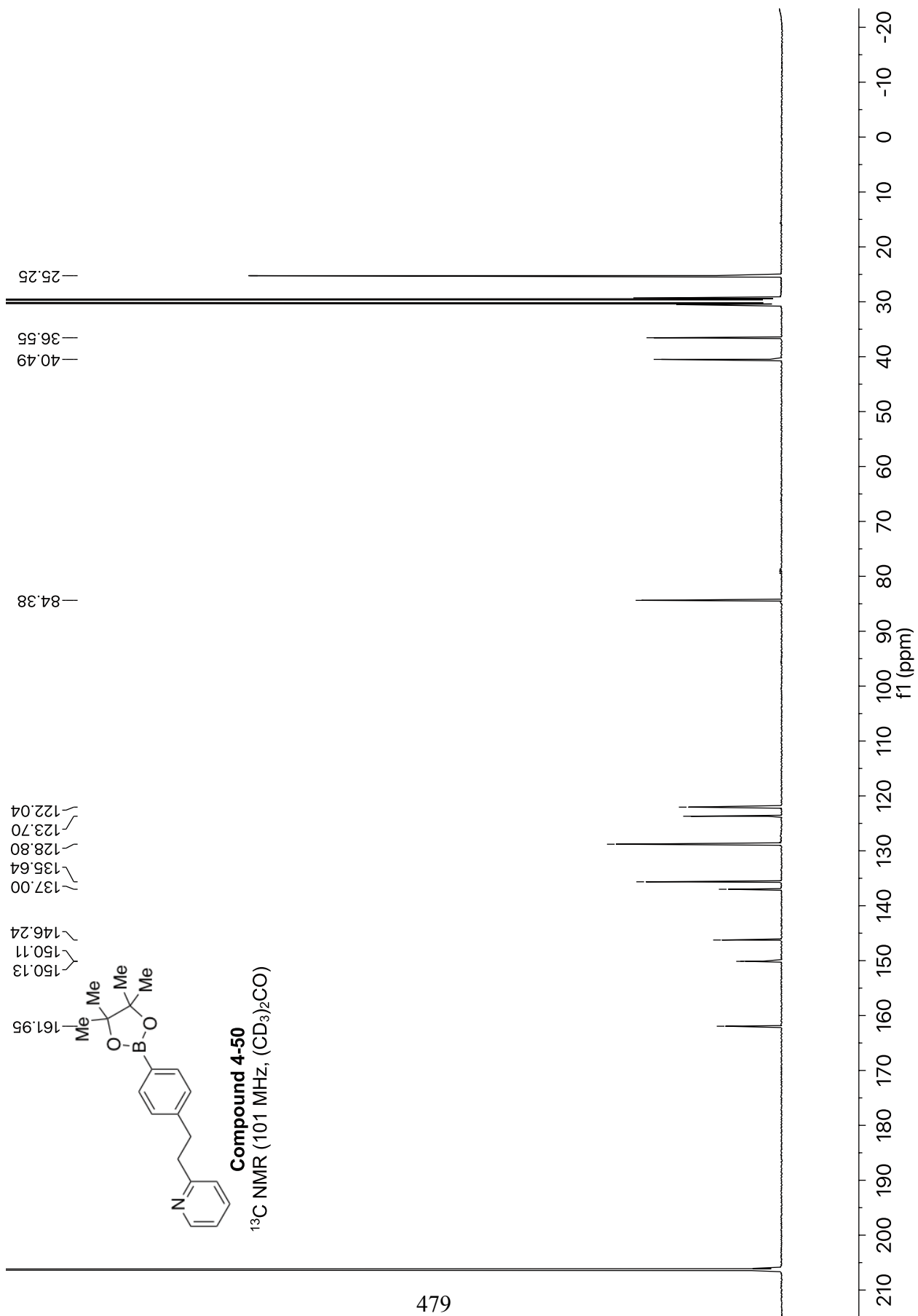
Compound 4-48
¹³C NMR (151 MHz, CDCl₃)

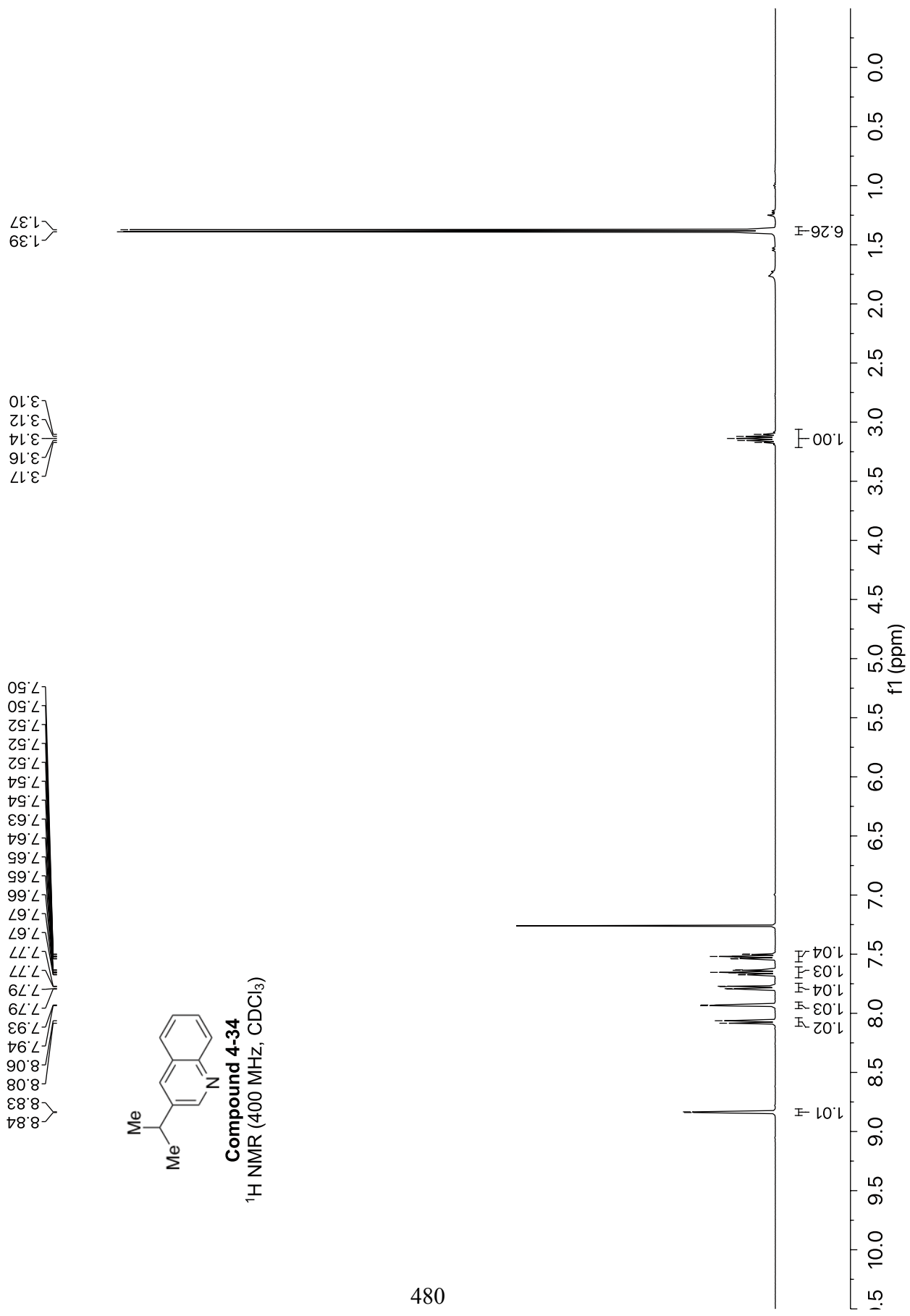


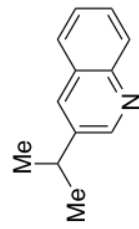






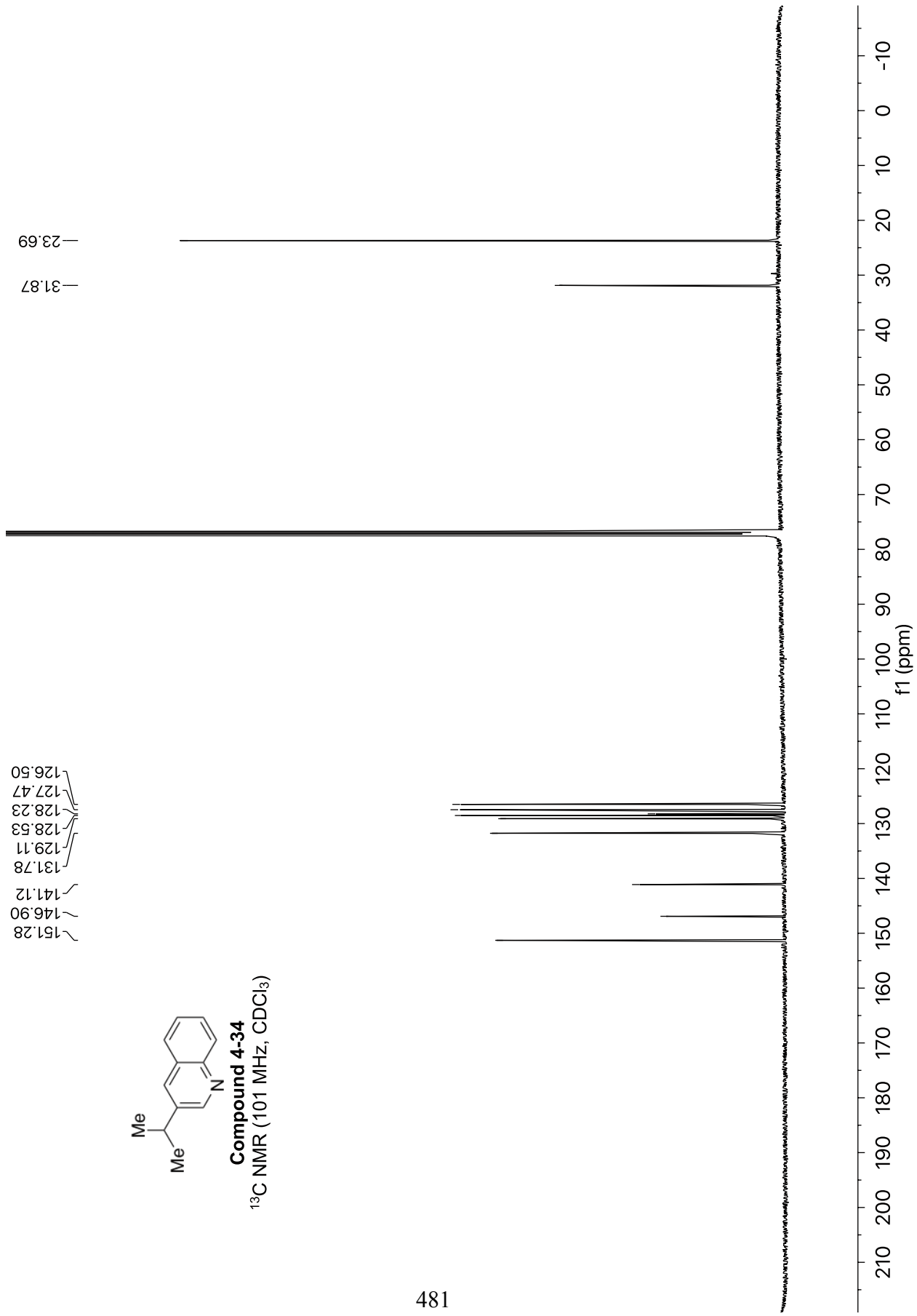


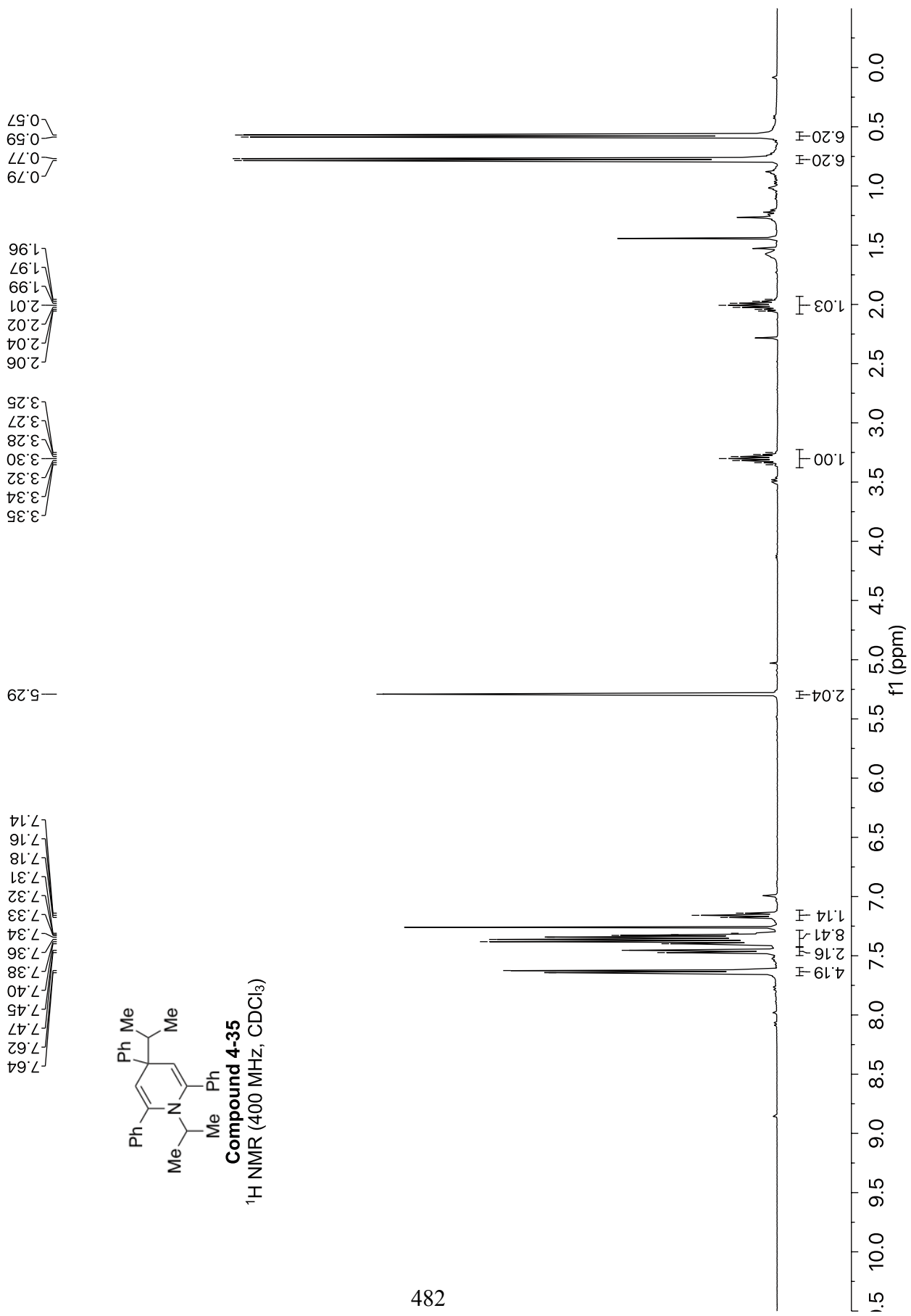
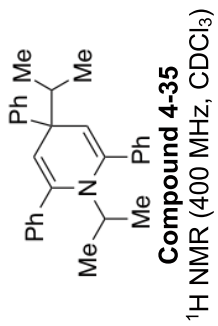


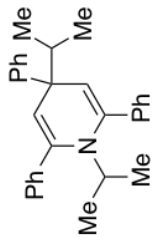


Compound 4-34

^{13}C NMR (101 MHz, CDCl_3)

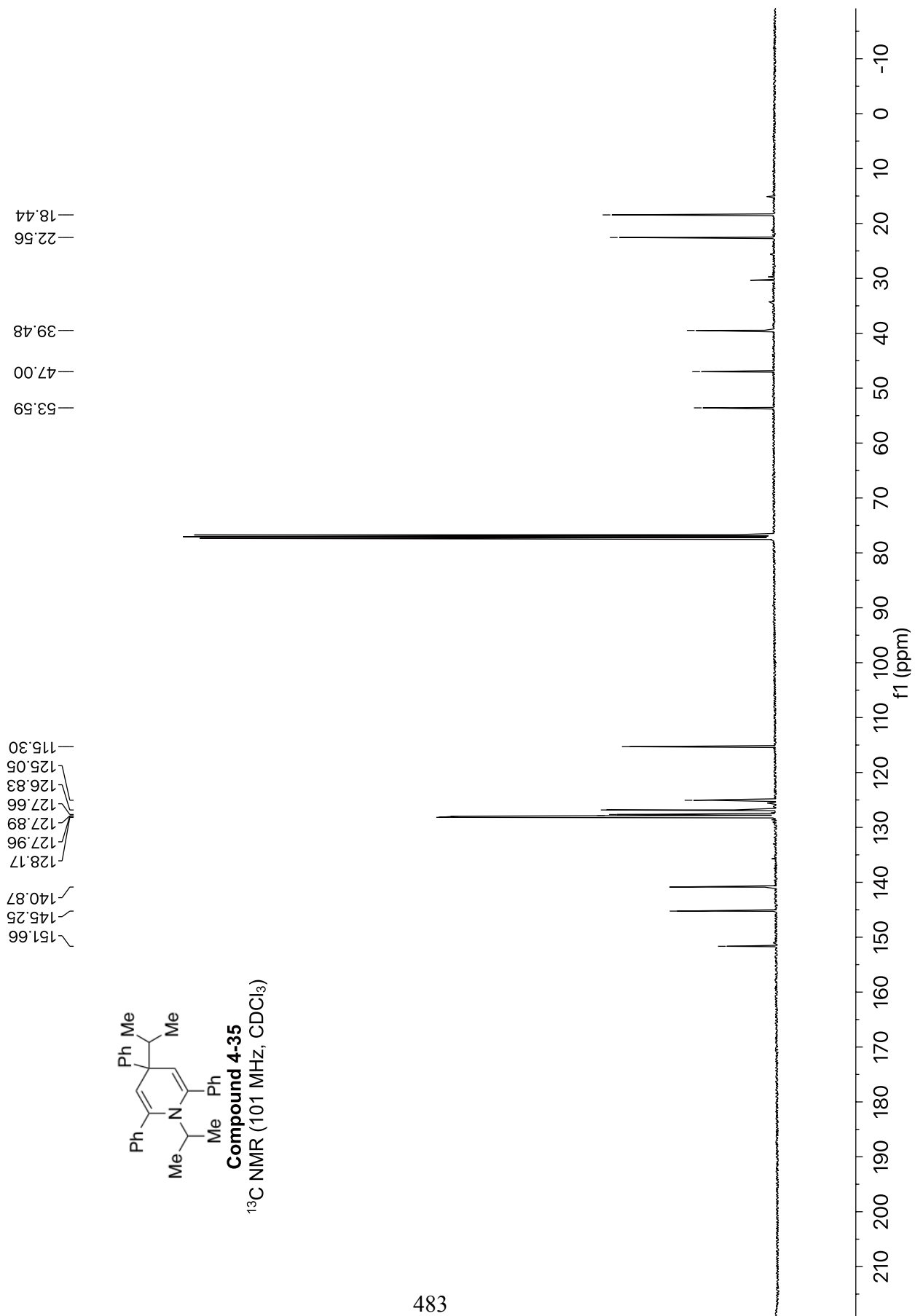


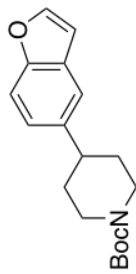




Compound 4-35

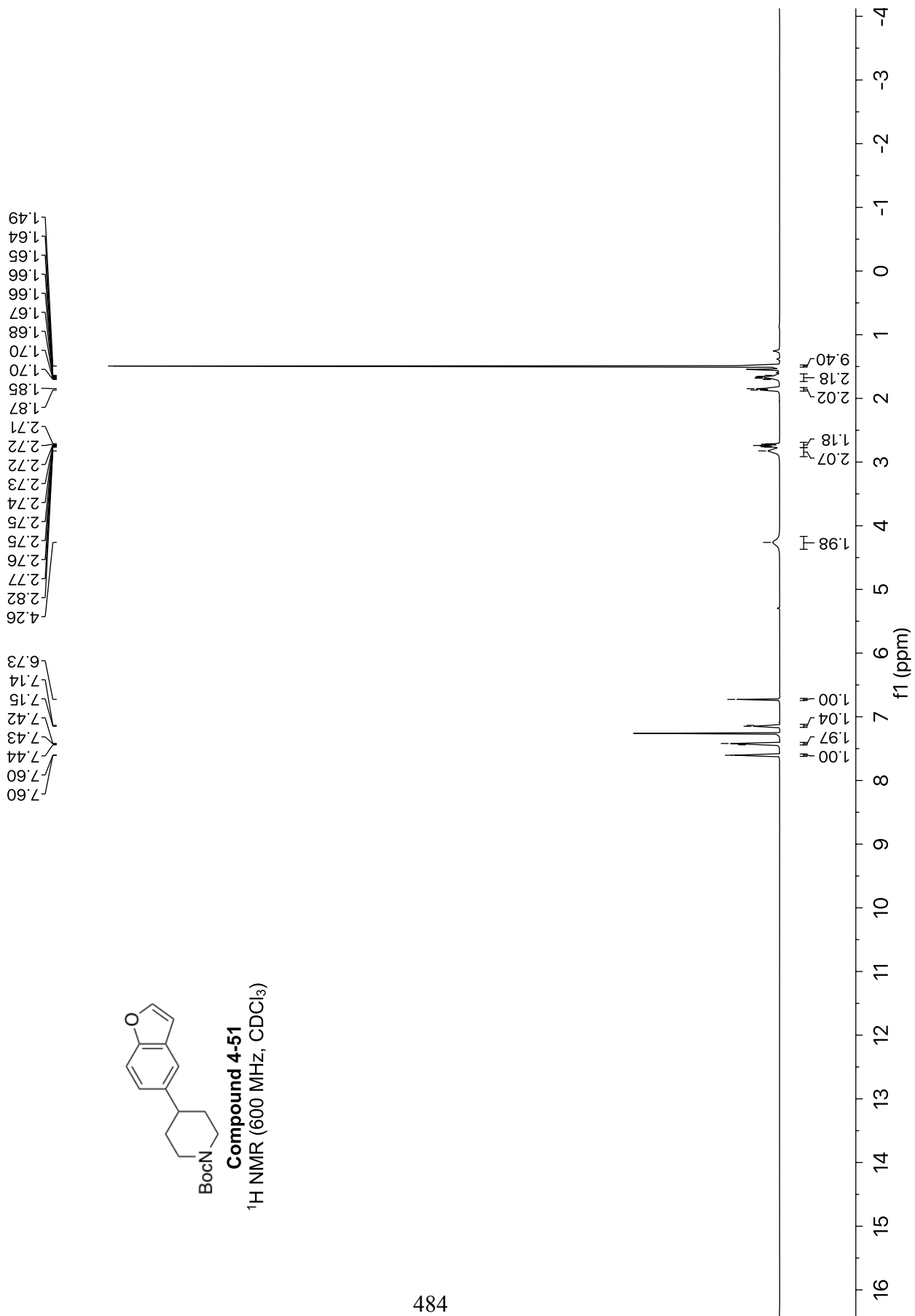
¹³C NMR (101 MHz, CDCl₃)

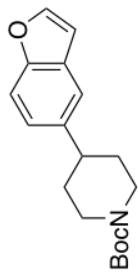




Compound 4-51

¹H NMR (600 MHz, CDCl₃)

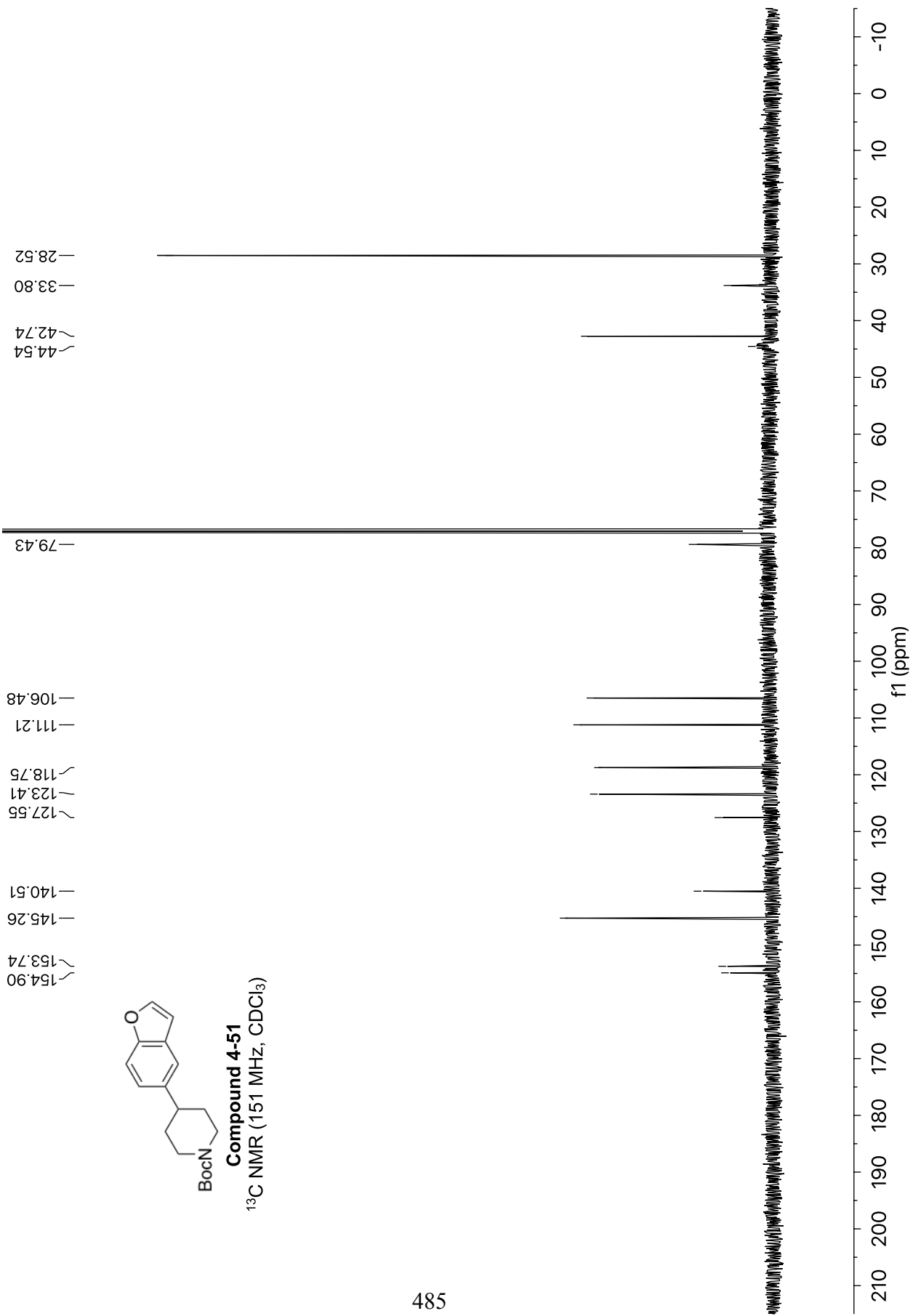


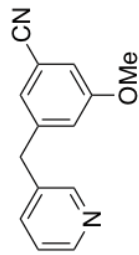


BocN

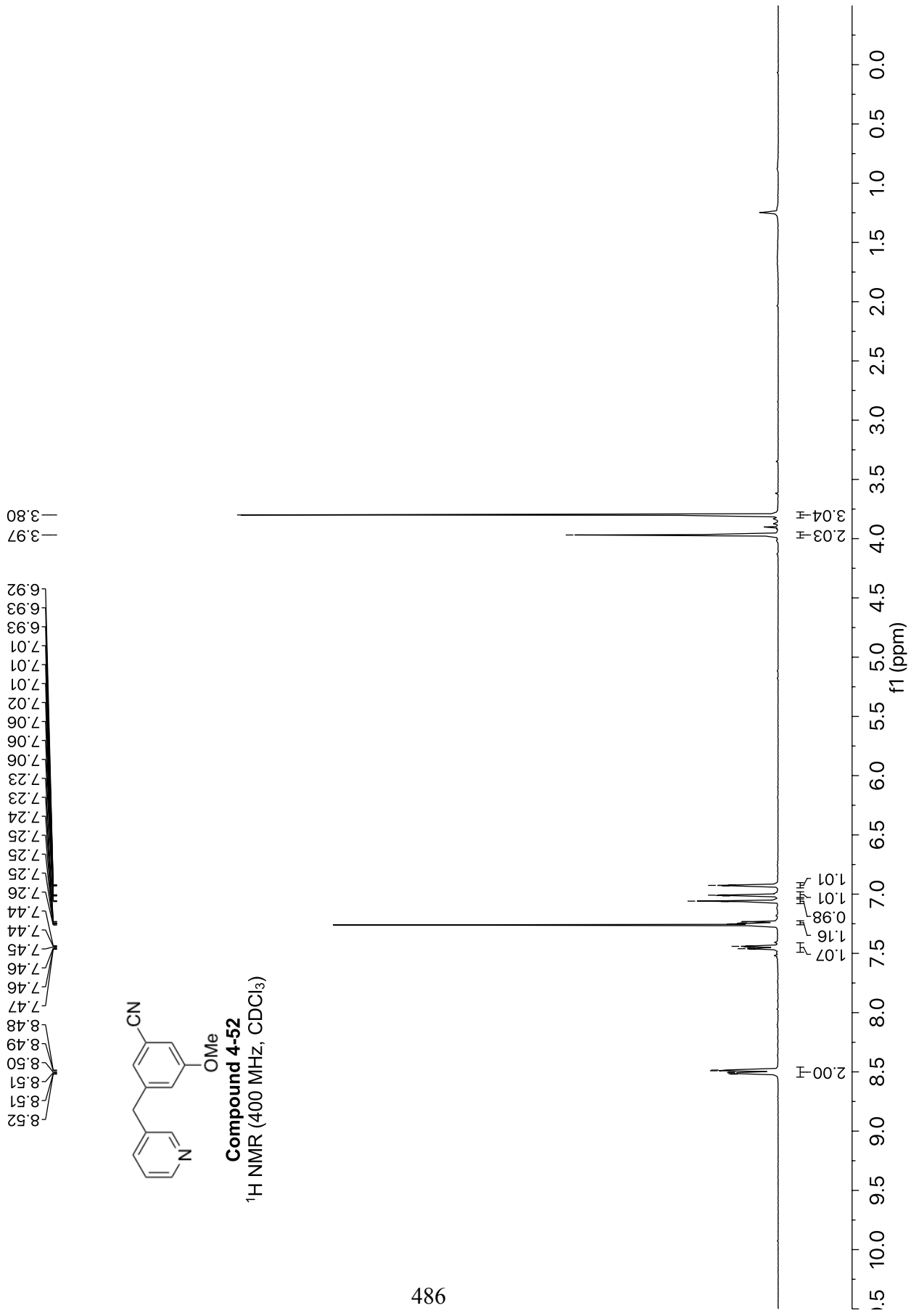
Compound 4-51

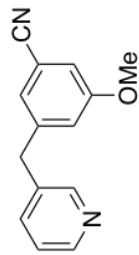
¹³C NMR (151 MHz, CDCl₃)





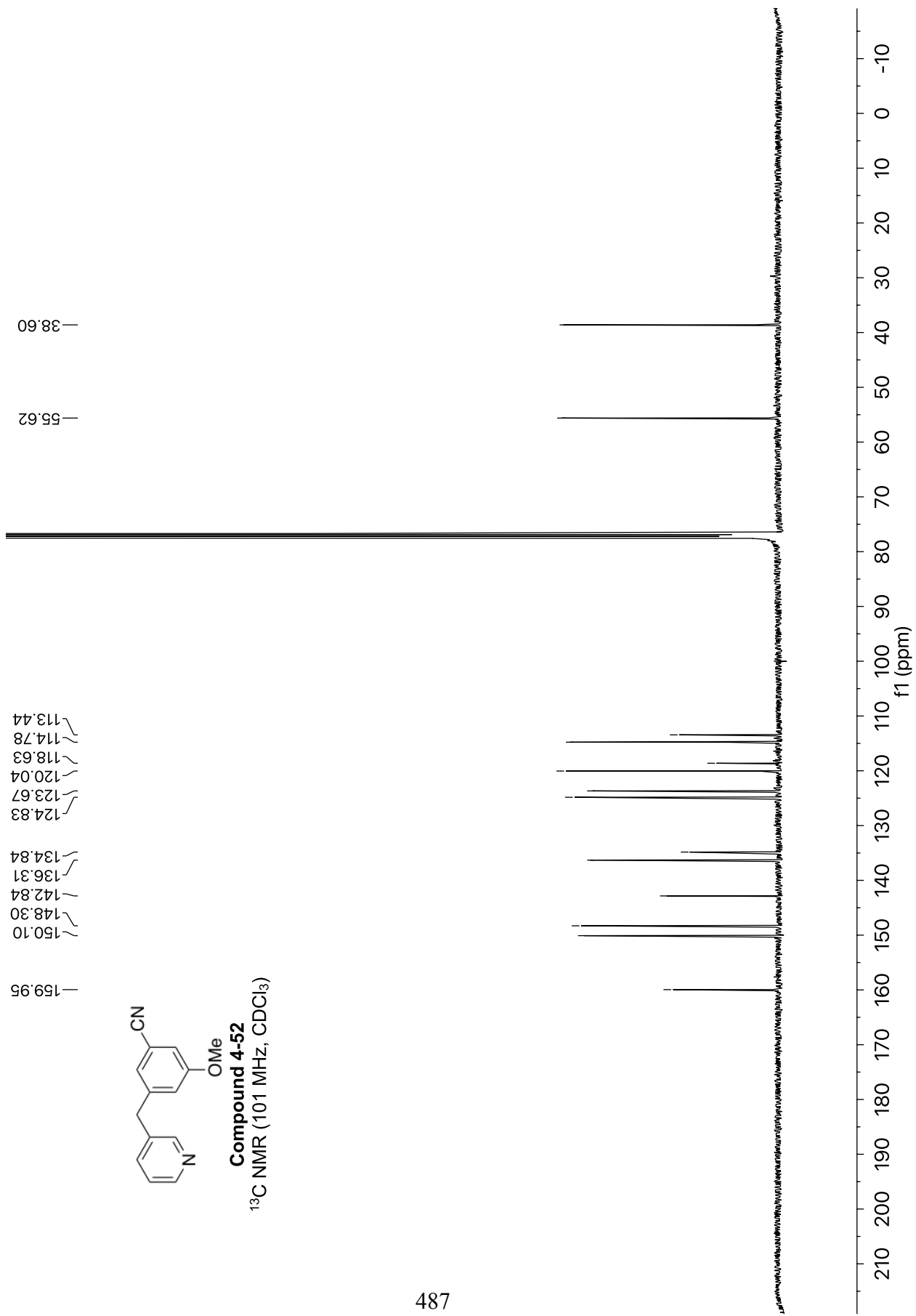
Compound 4-52
¹H NMR (400 MHz, CDCl₃)



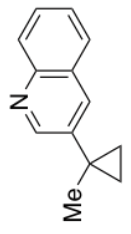


Compound 4-52

¹³C NMR (101 MHz, CDCl₃)

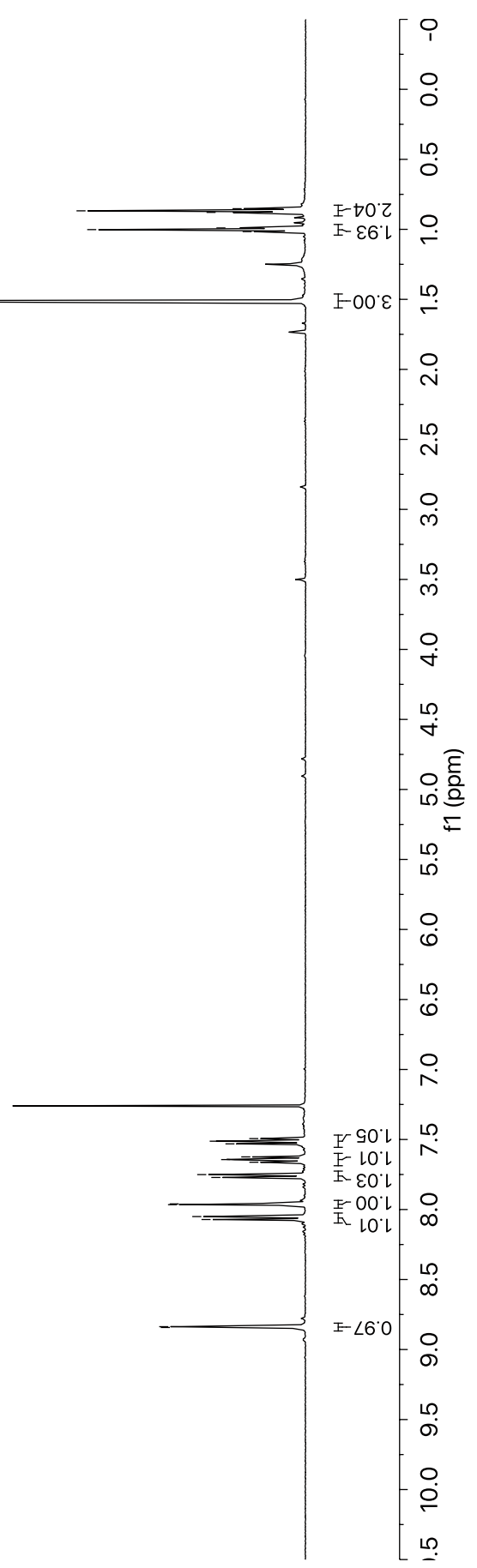


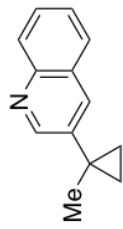
8.84
8.84
8.07
8.05
7.97
7.96
7.77
7.75
7.66
7.64
7.62
7.53
7.51
7.49



Compound 4-53
¹H NMR (400 MHz, CDCl₃)

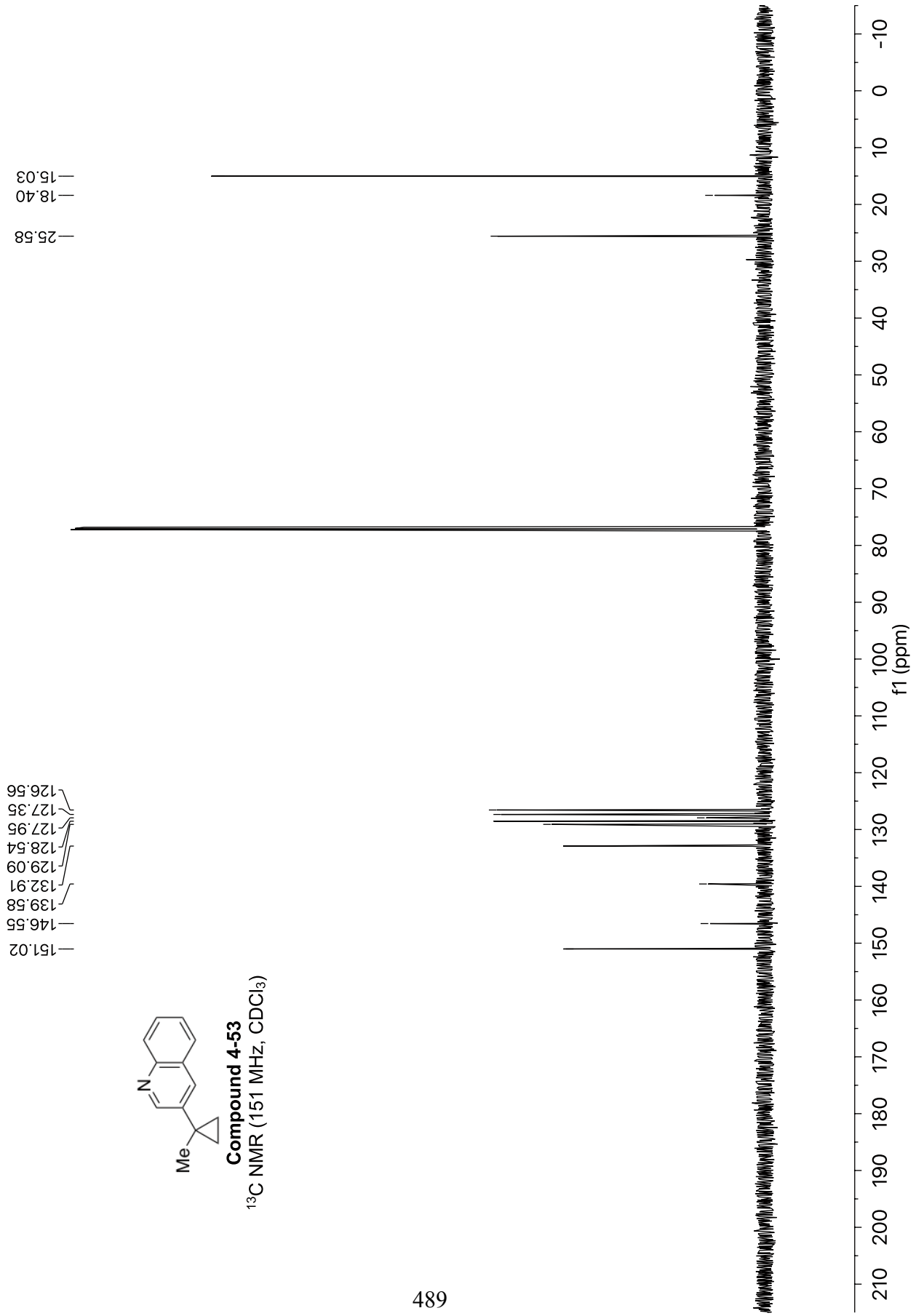
1.51
1.02
1.00
0.99
0.88
0.87
0.85

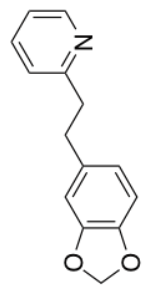
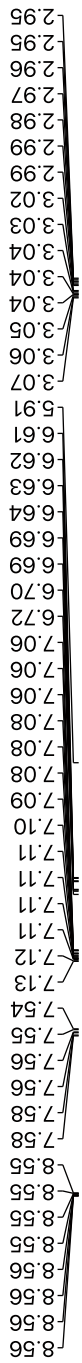




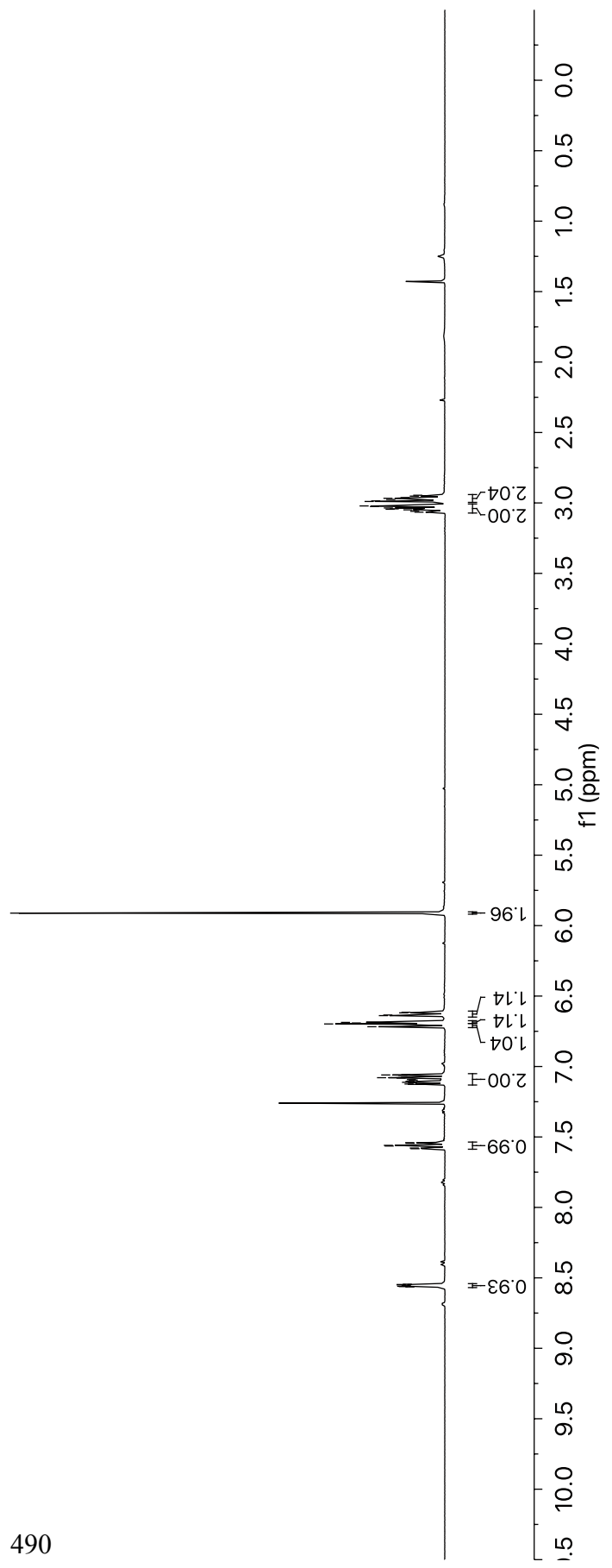
Compound 4-53

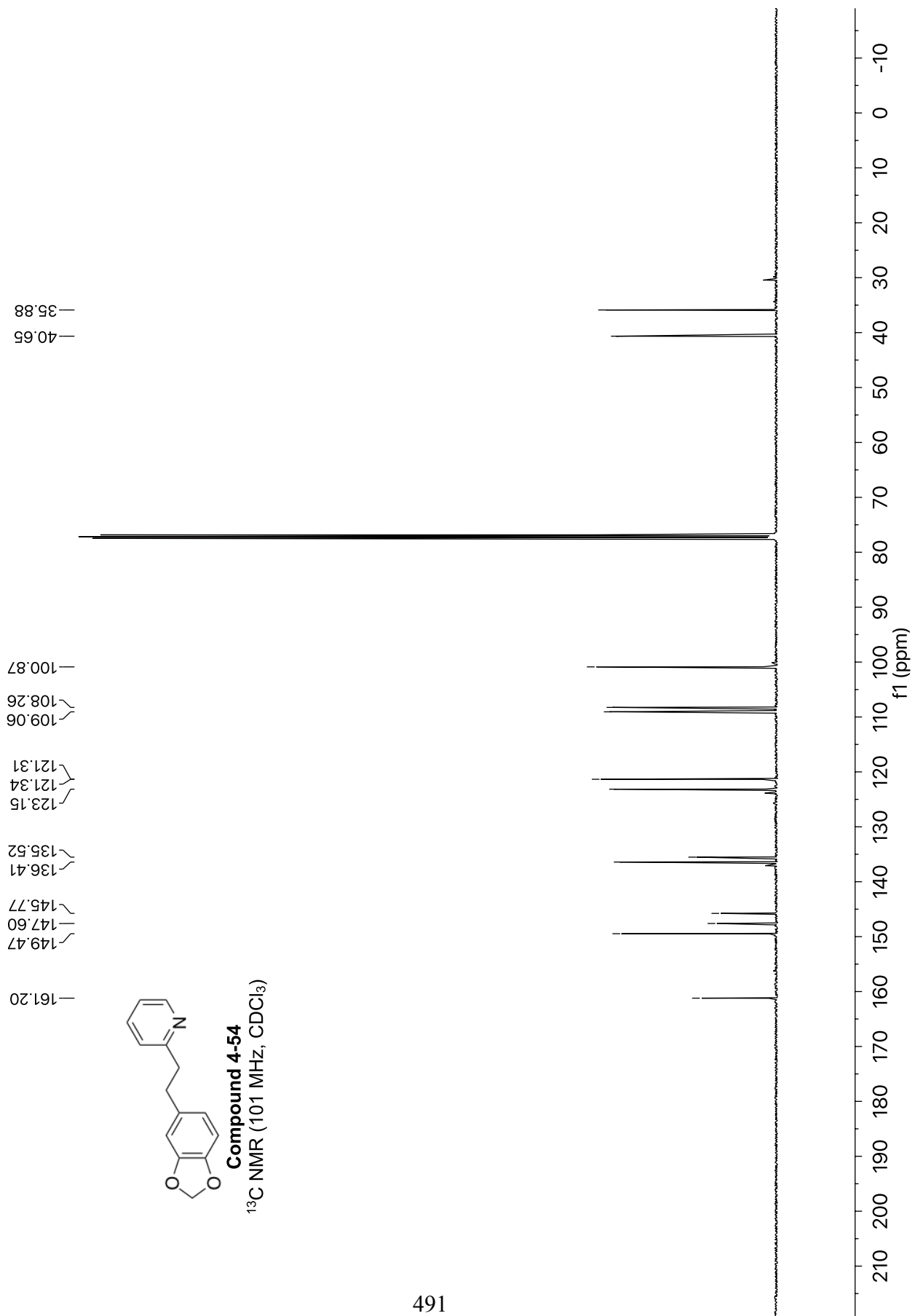
¹³C NMR (151 MHz, CDCl₃)

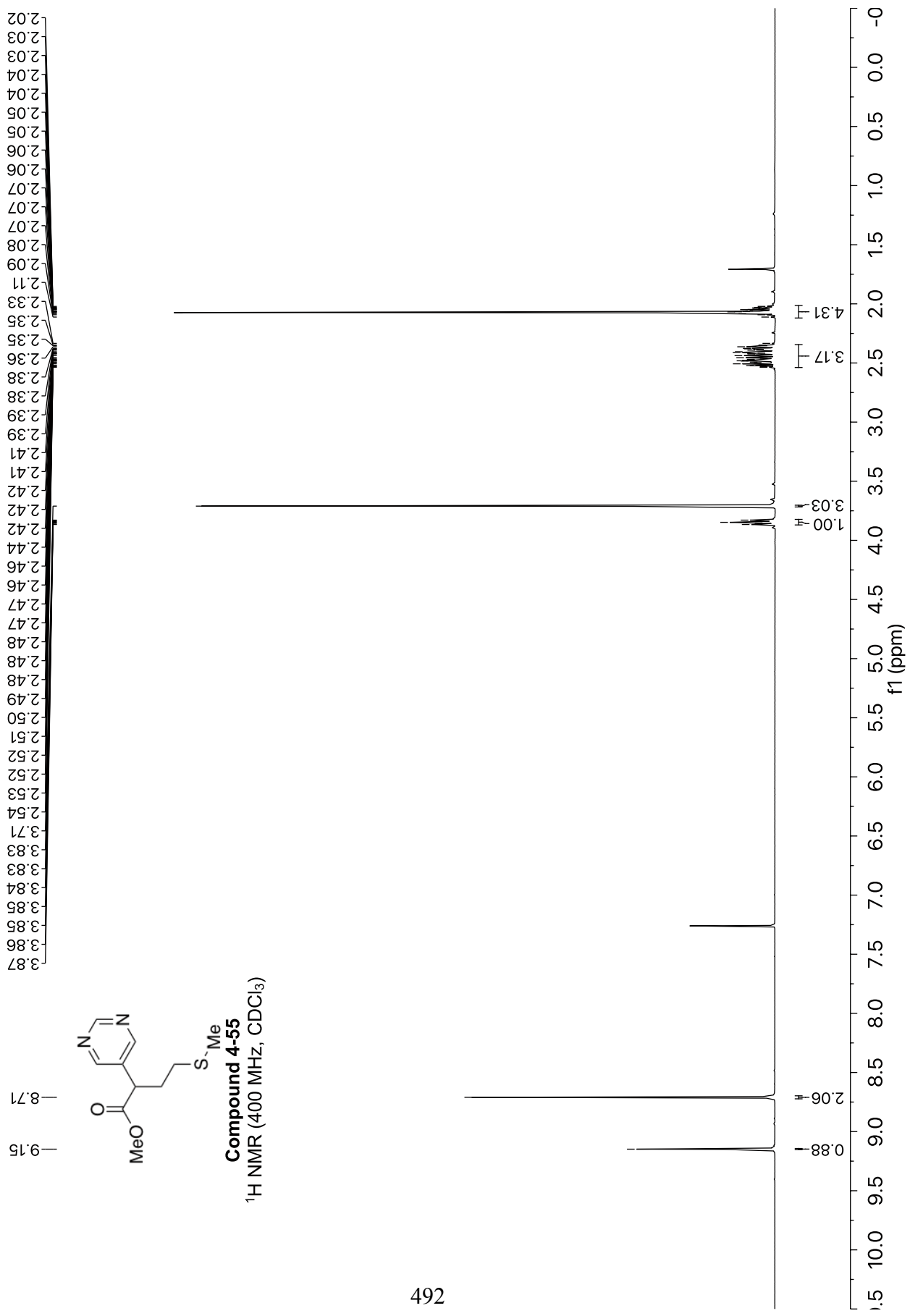


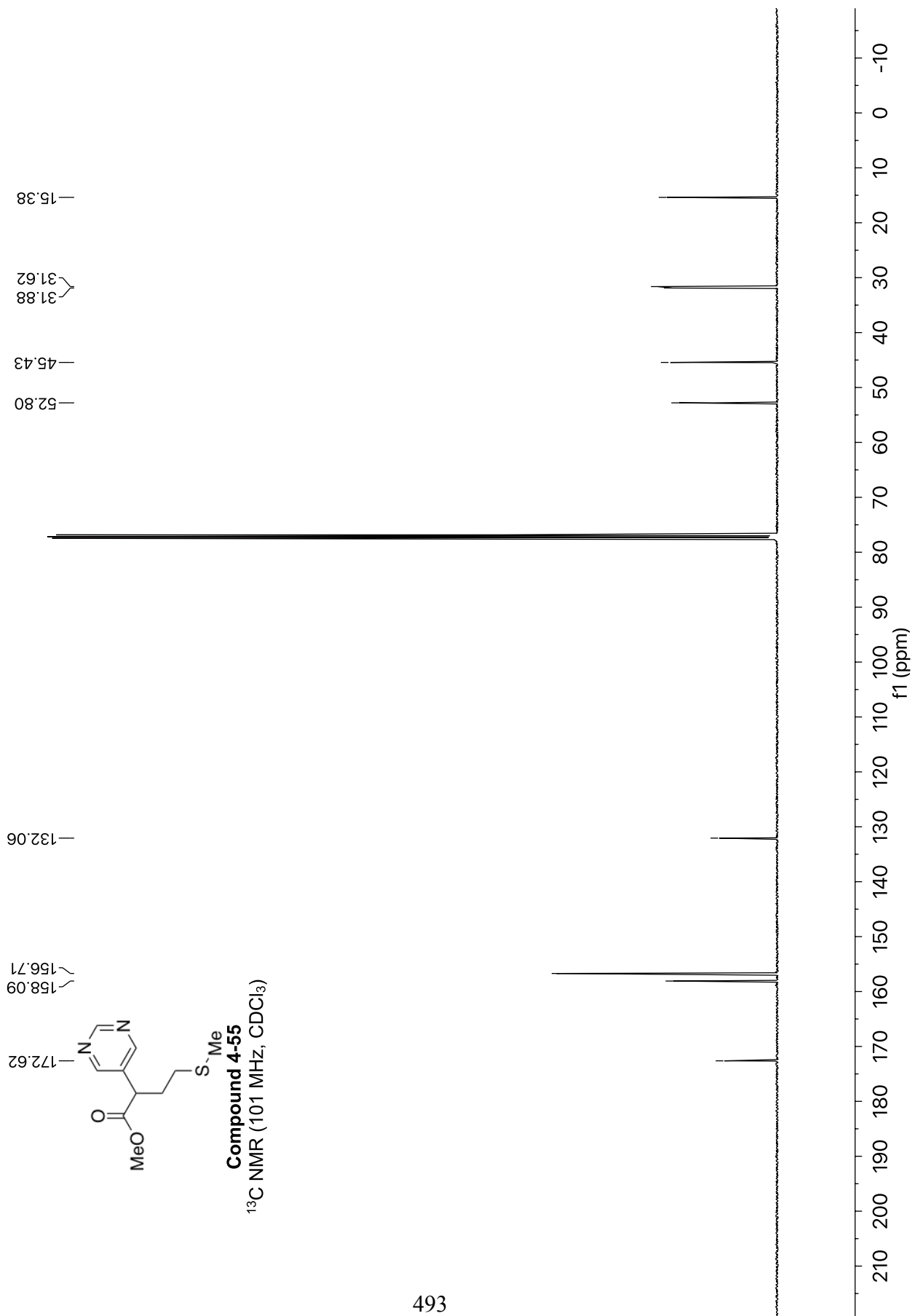


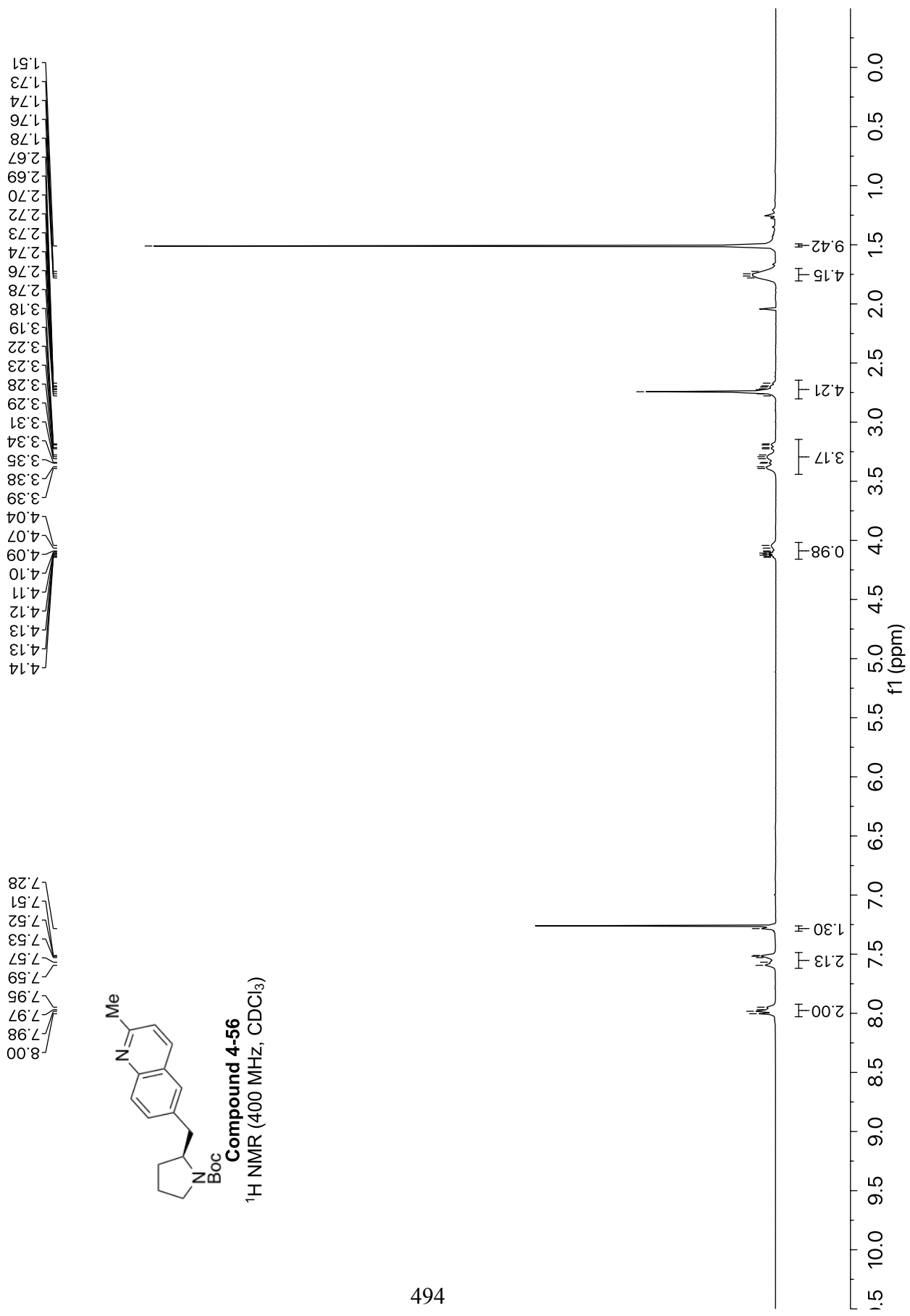
Compound 4-54
¹H NMR (400 MHz, CDCl₃)

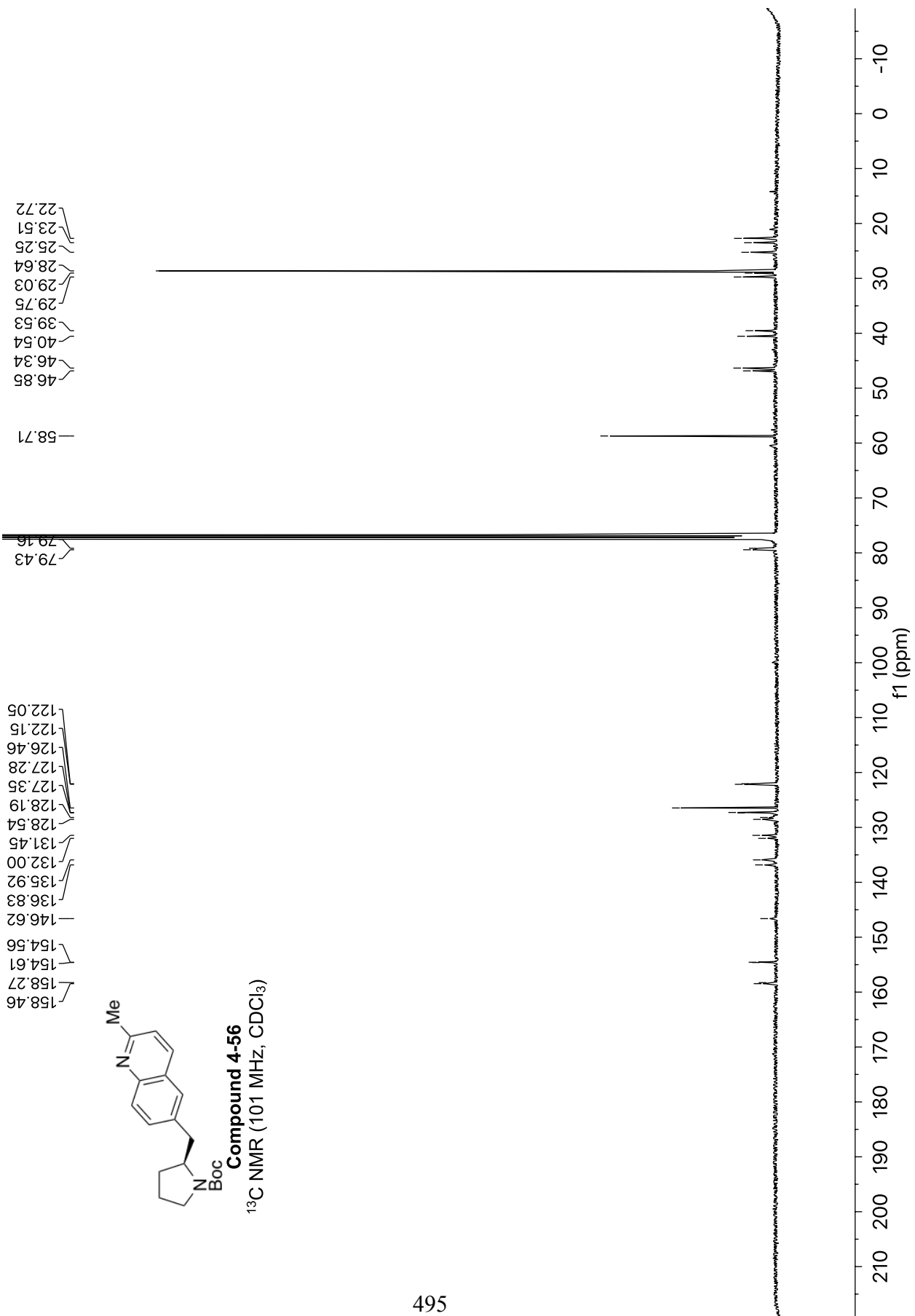


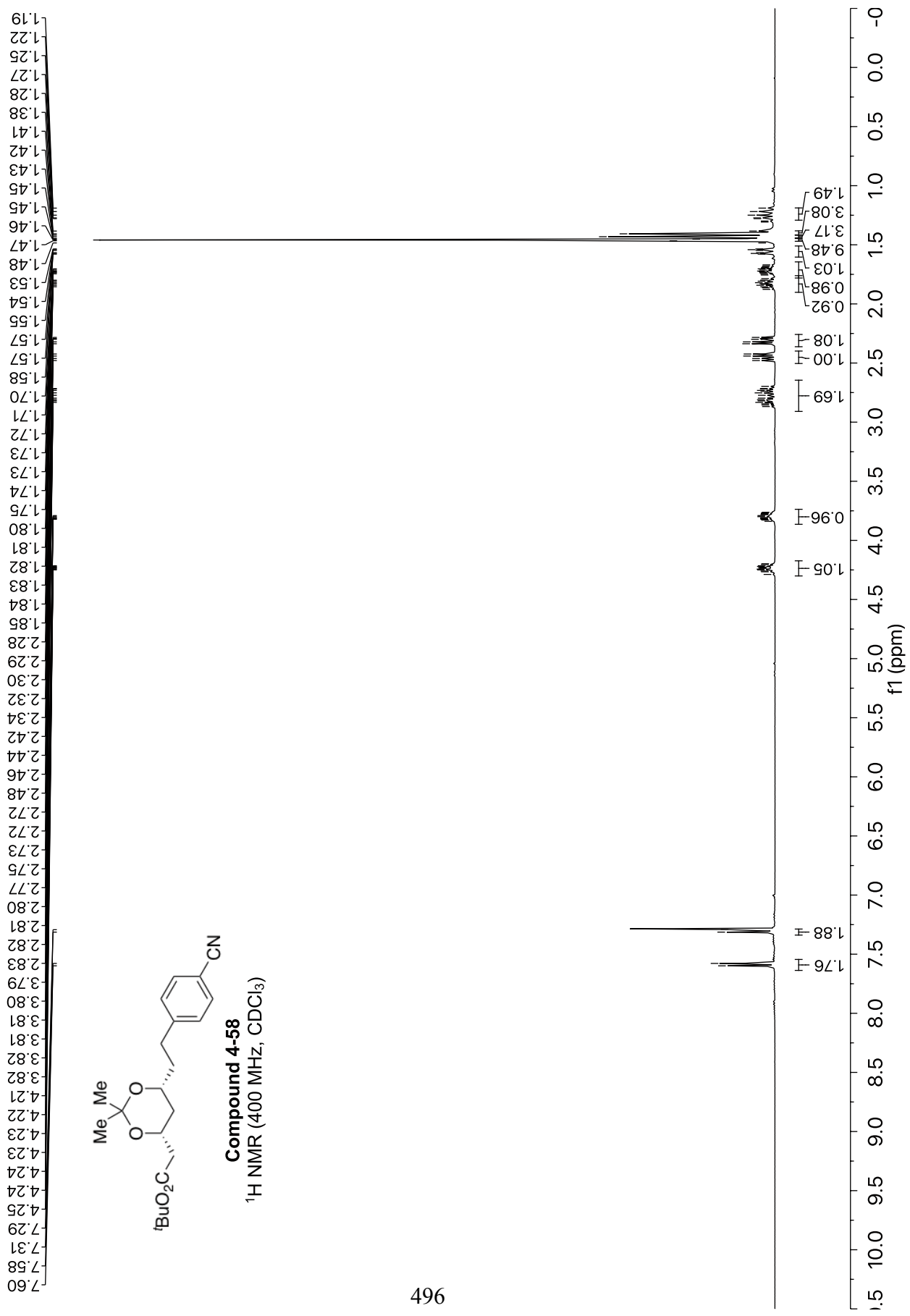


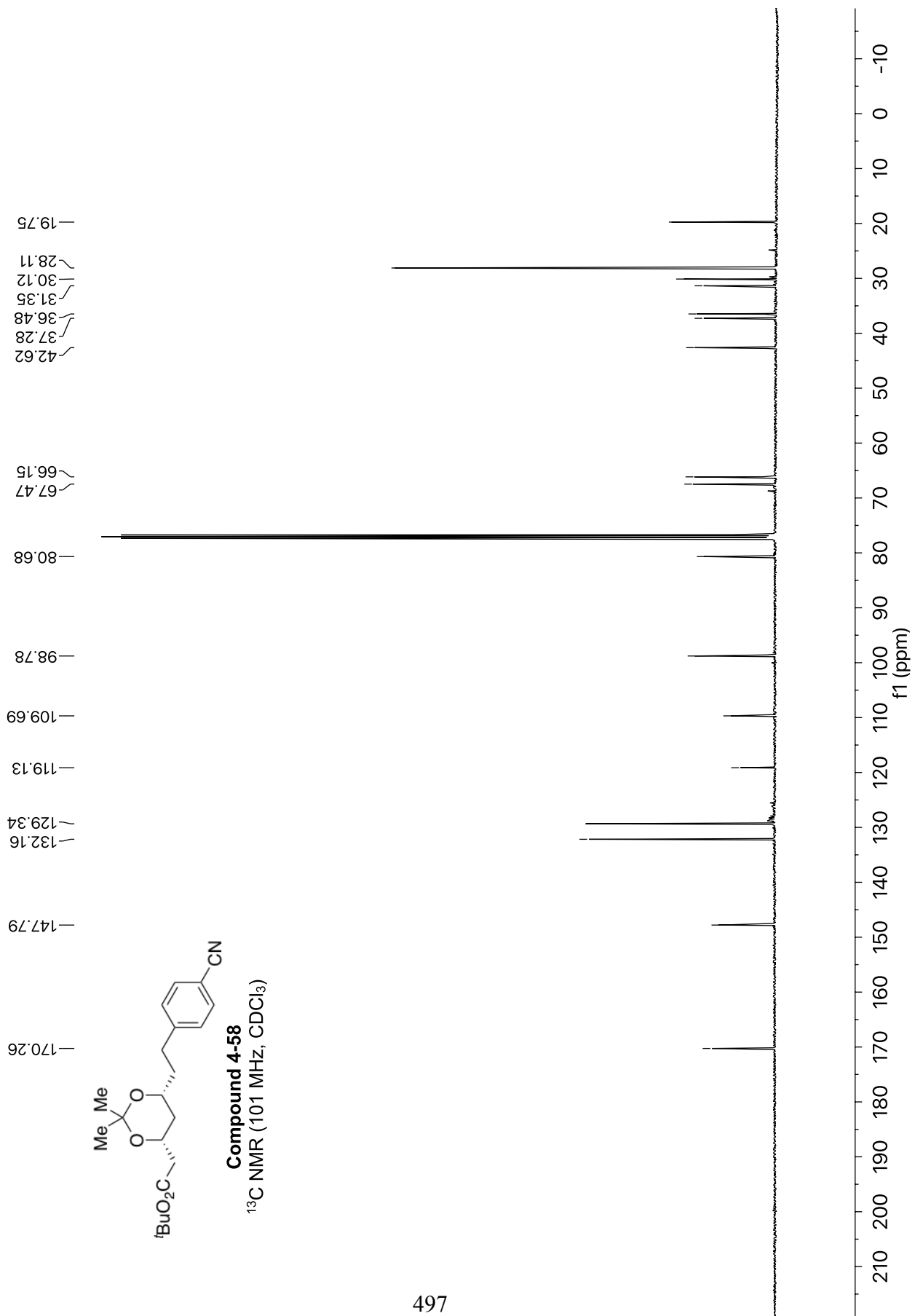


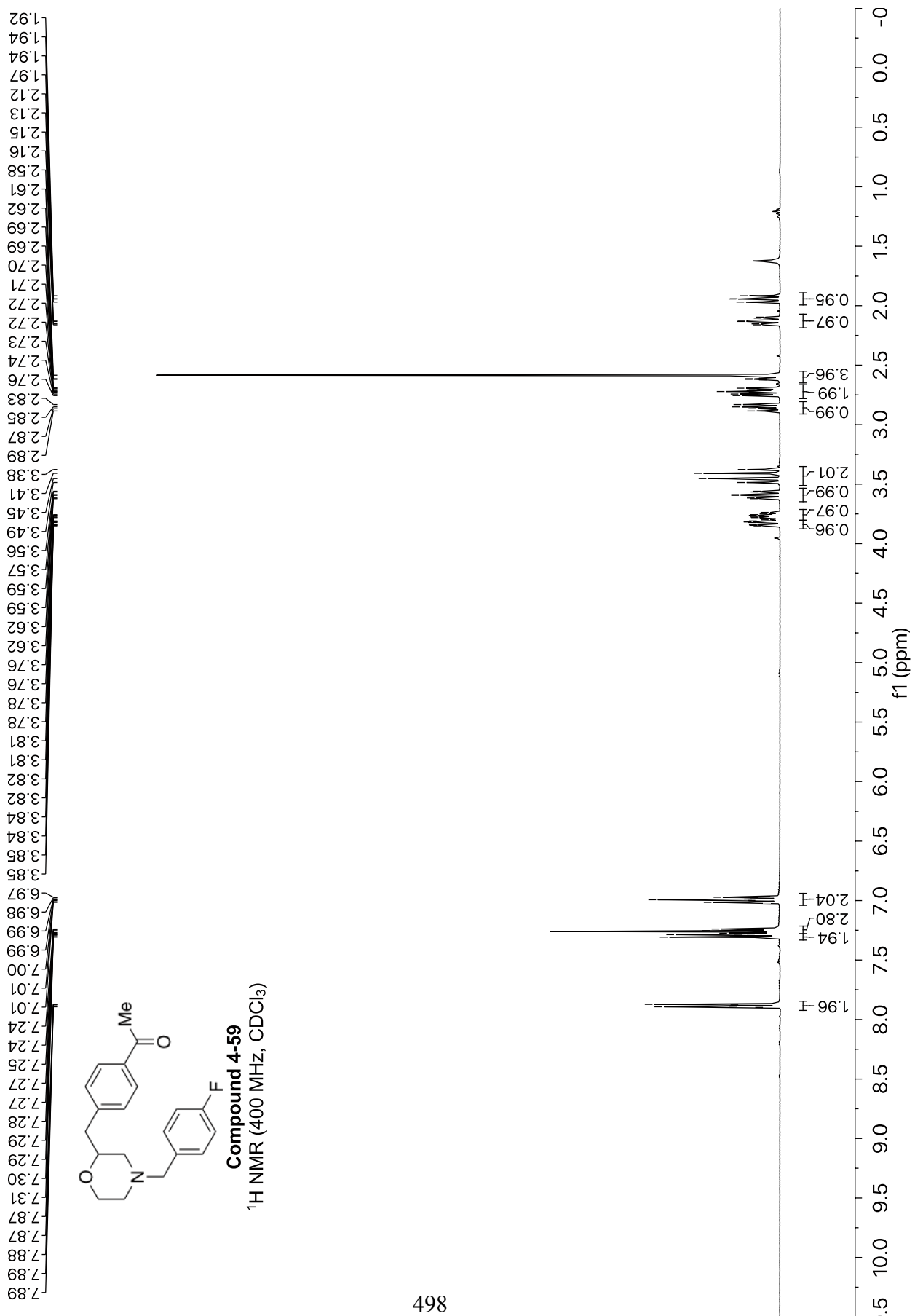


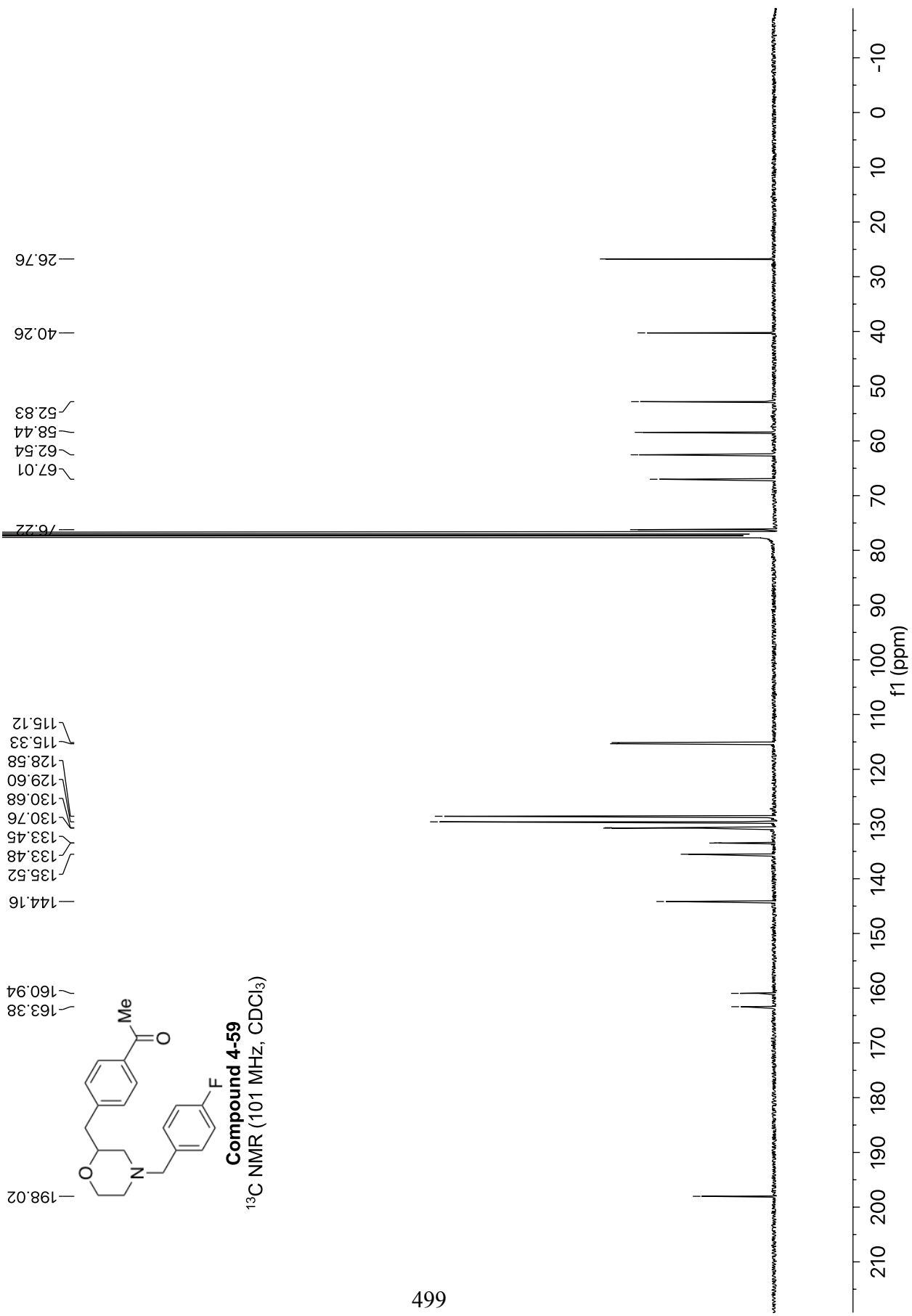


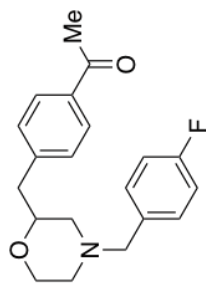










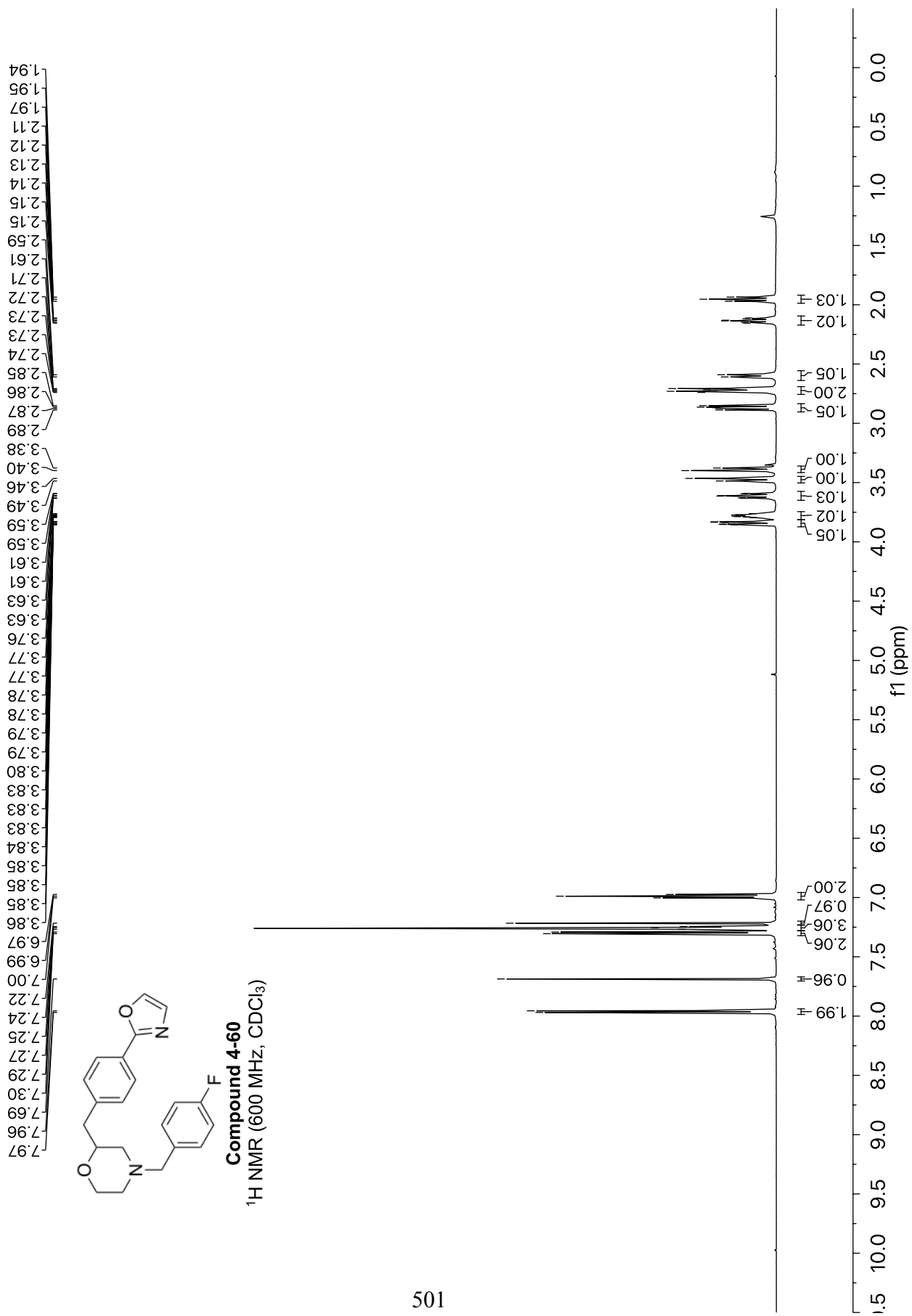


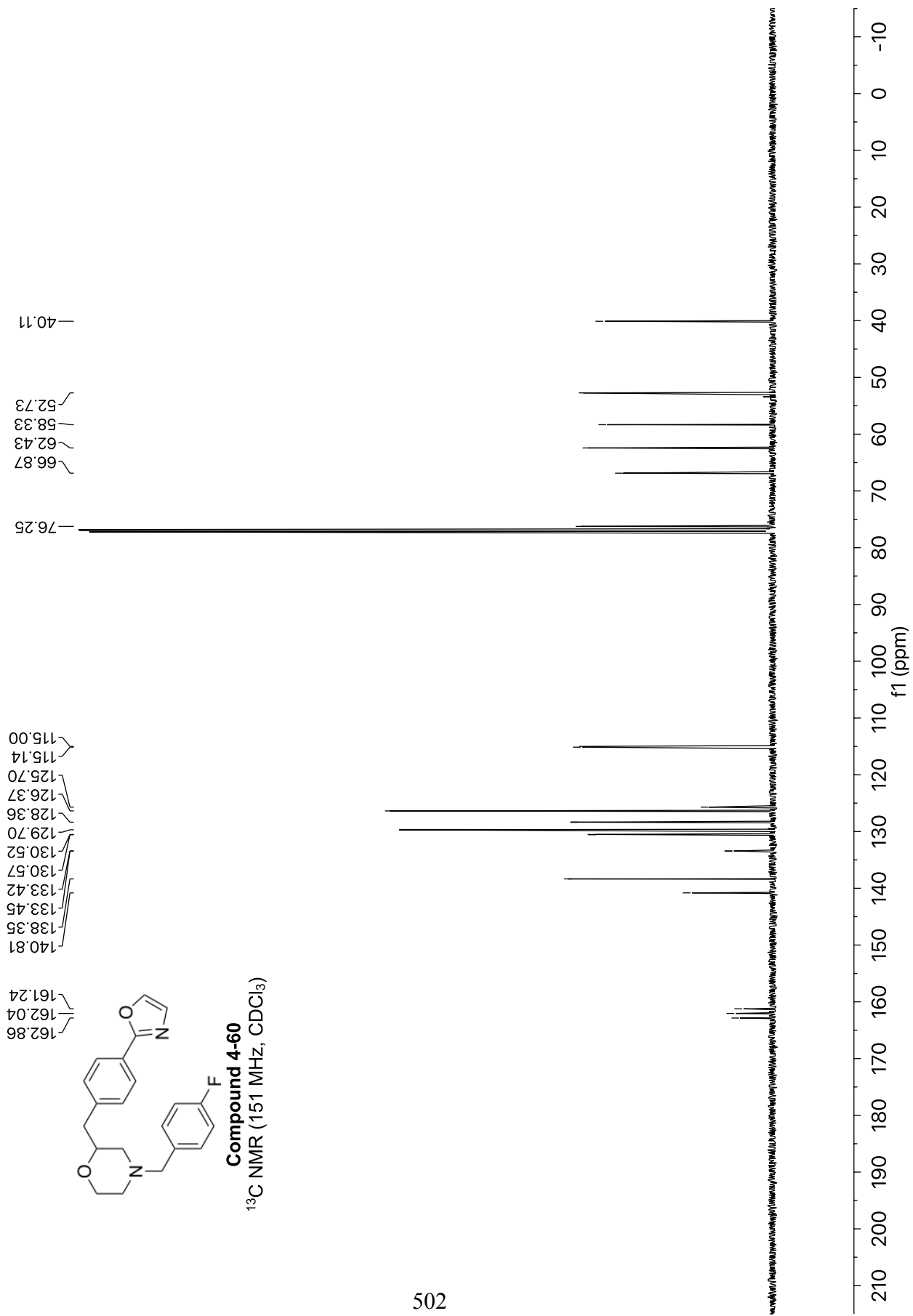
Compound 4-59
¹⁹F NMR (376 MHz, CDCl₃)

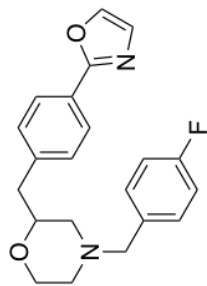
-115.59

-10 -20 -30 -40 -50 -60 -70 -80 -90 -100 -110 -120 -130 -140 -150 -160 -170 -180 -190

f1 (ppm)



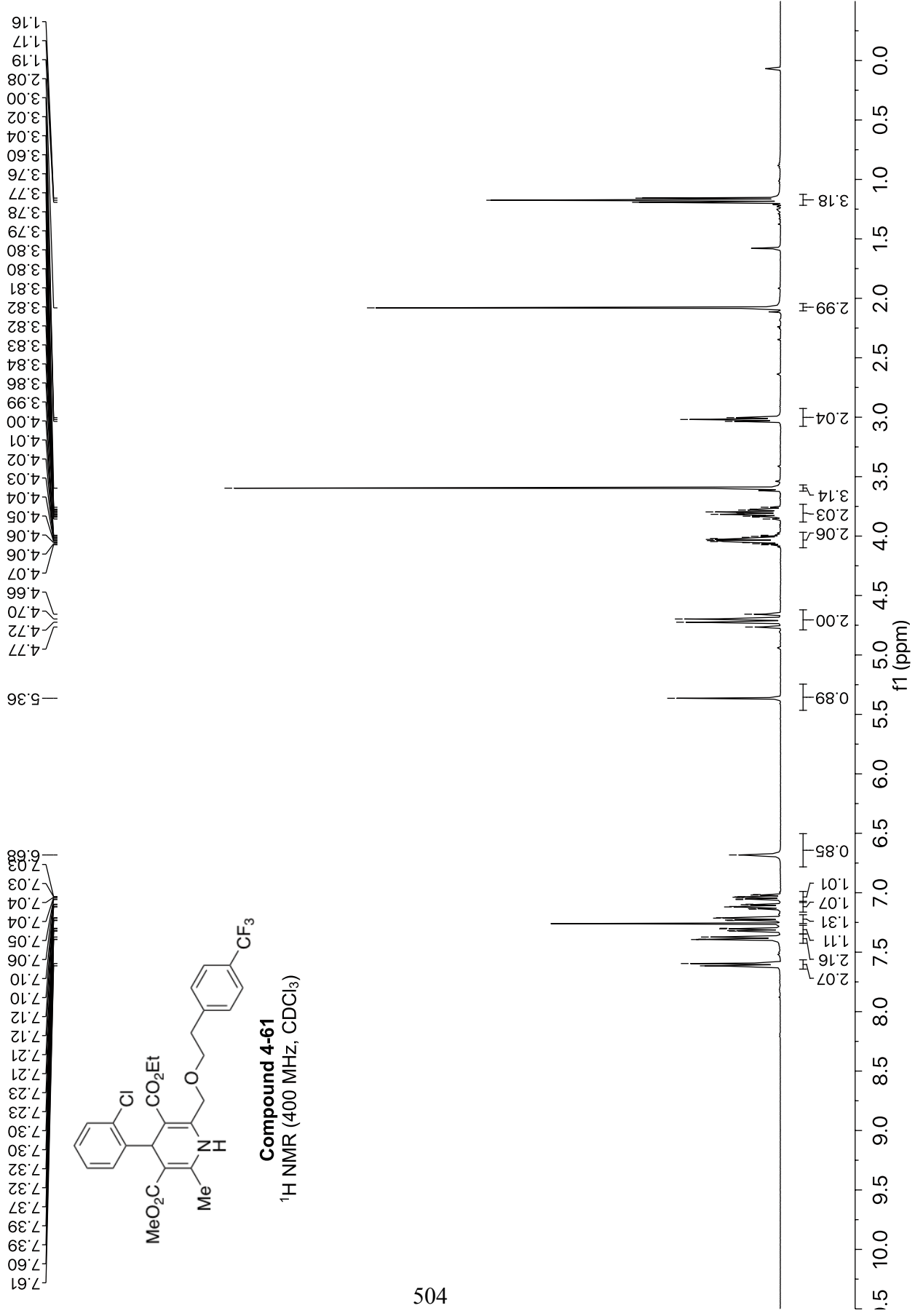


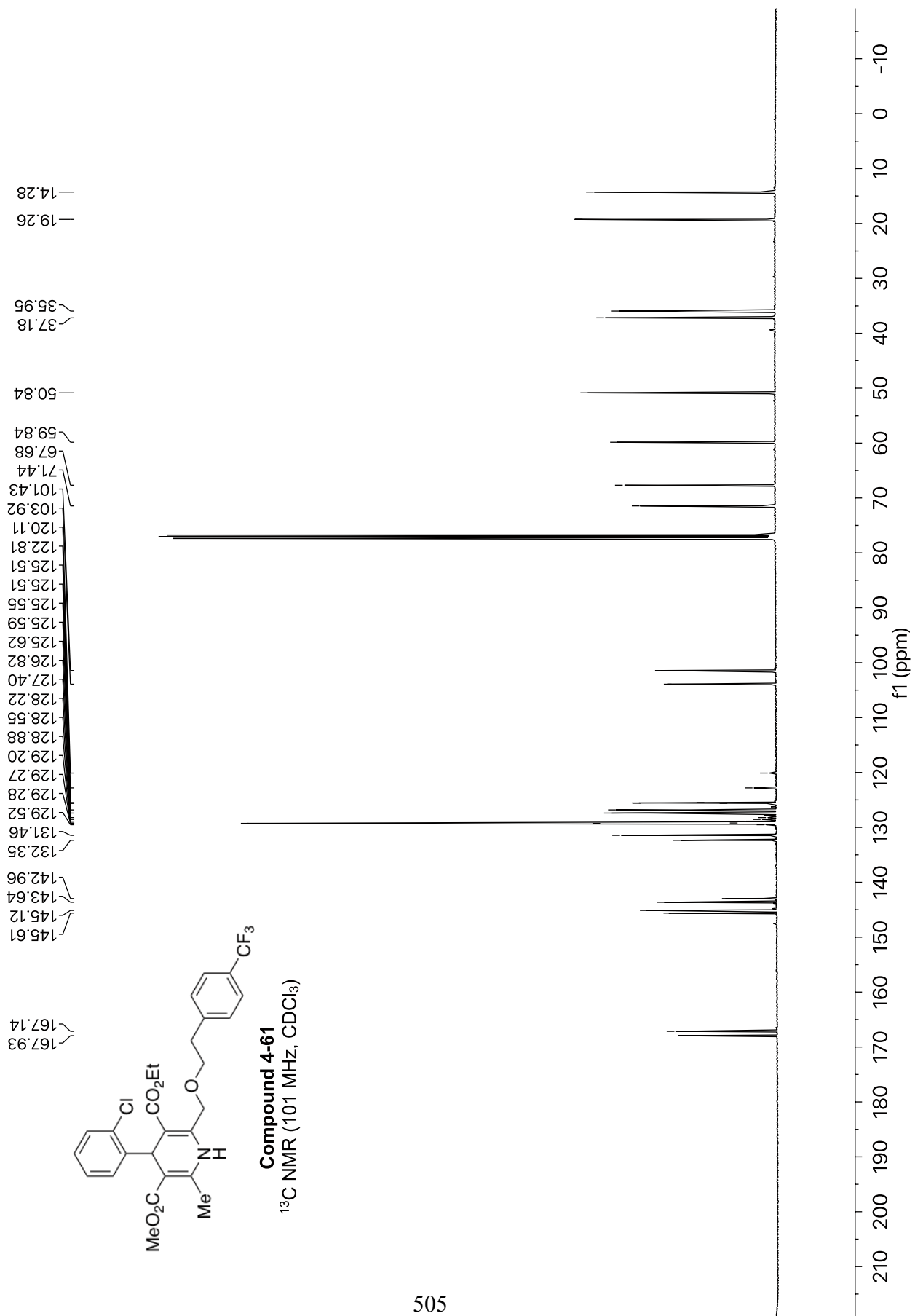


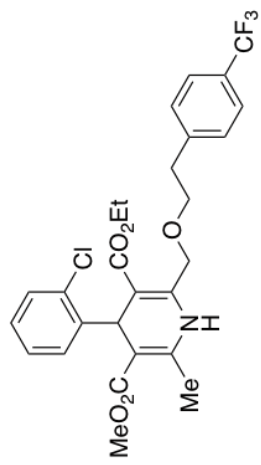
Compound 4-60
¹⁹F NMR (565 MHz, CDCl₃)

--115.72

10 0 -10 -20 -30 -40 -50 -60 -70 -80 -90 -100 -110 -120 -130 -140 -150 -160 -170 -180 -190 -200 -210
f1 (ppm)







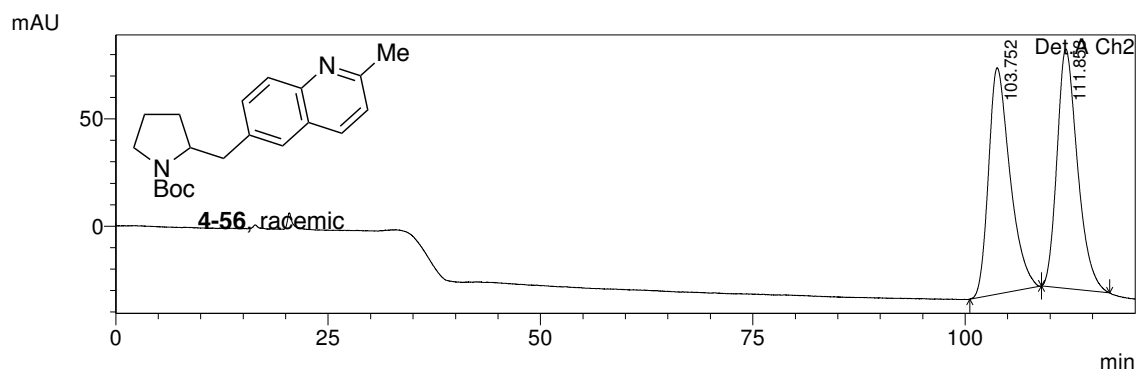
Compound 4-61

¹⁹F NMR (376 MHz, CDCl₃)

—62.43

-10 -20 -30 -40 -50 -60 -70 -80 -90 -100 -110 -120 -130 -140 -150 -160 -170 -180 -190
f1 (ppm)

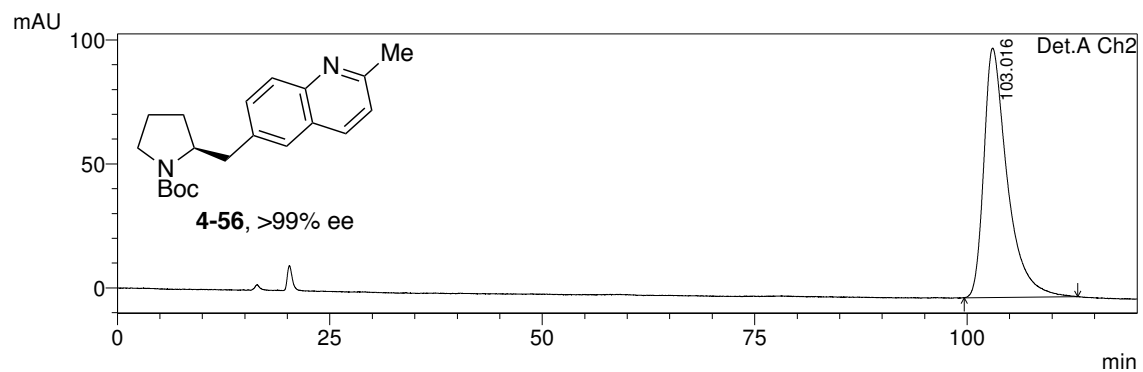
Compound 4-56, racemic (210 nm)



Detector A Ch2 210nm

Peak#	Ret. Time	Area	Height	Area %	Height %
1	103.752	18566299	105683	49.739	48.610
2	111.853	18761296	111728	50.261	51.390
Total		37327594	217412	100.000	100.000

Compound 4-56, >99% ee (210 nm)



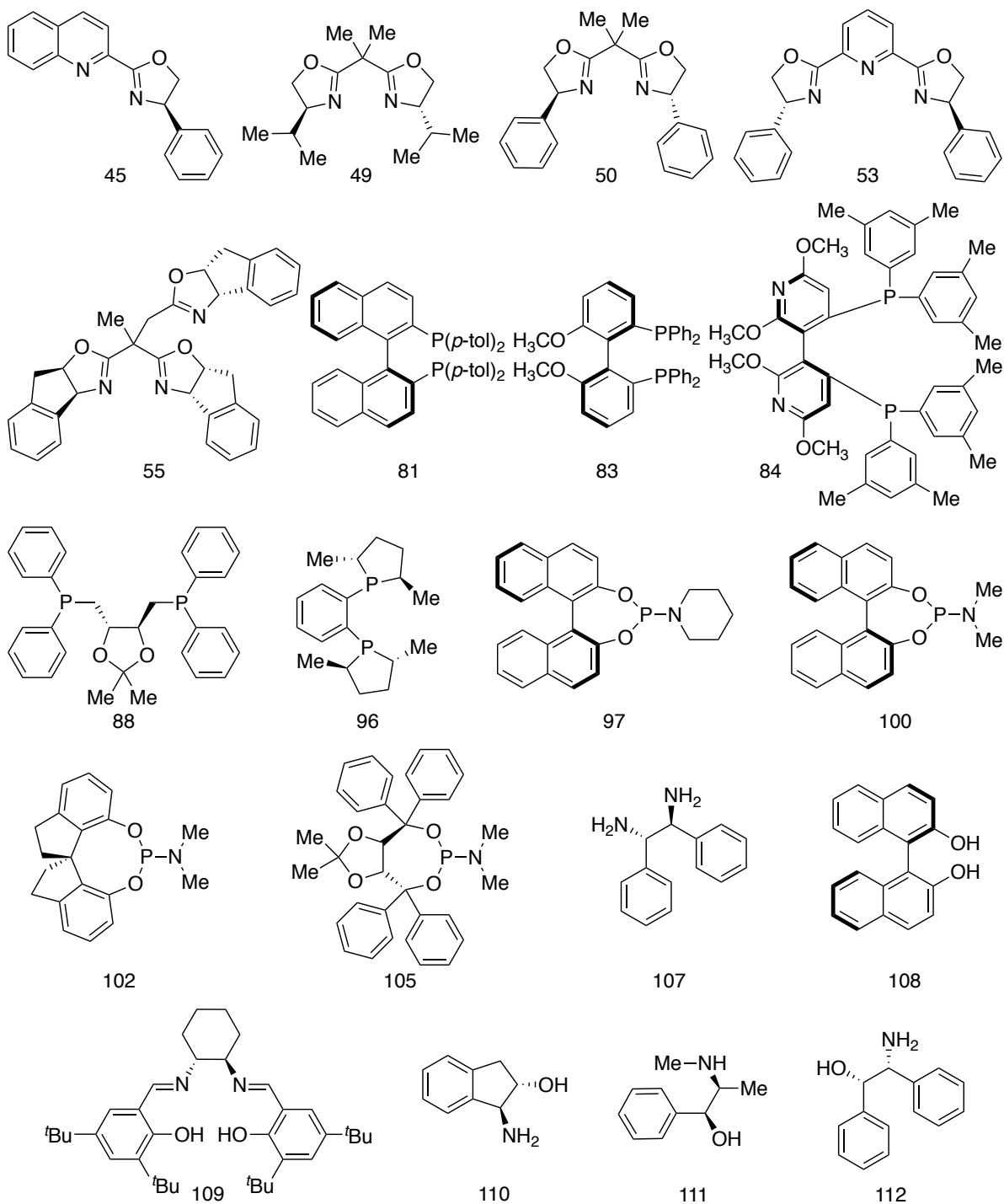
Detector A Ch2 210nm

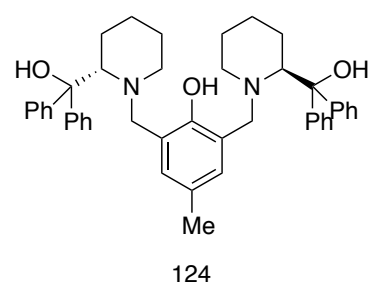
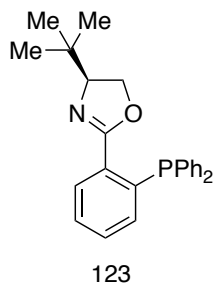
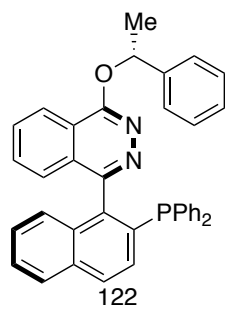
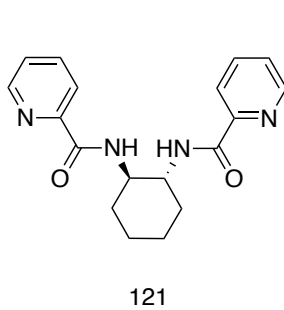
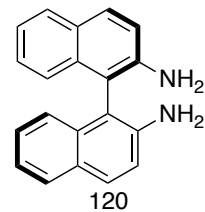
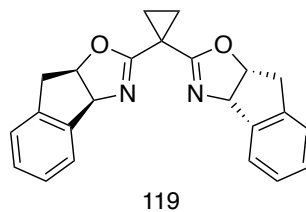
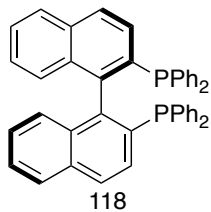
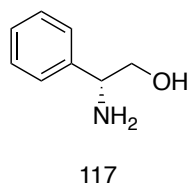
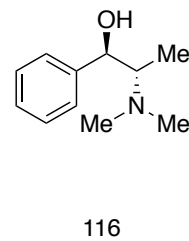
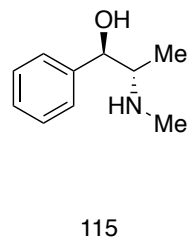
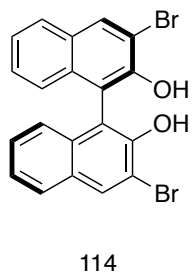
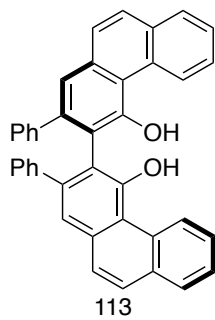
Peak#	Ret. Time	Area	Height	Area %	Height %
1	103.016	19309963	100587	100.000	100.000
Total		19309963	100587	100.000	100.000

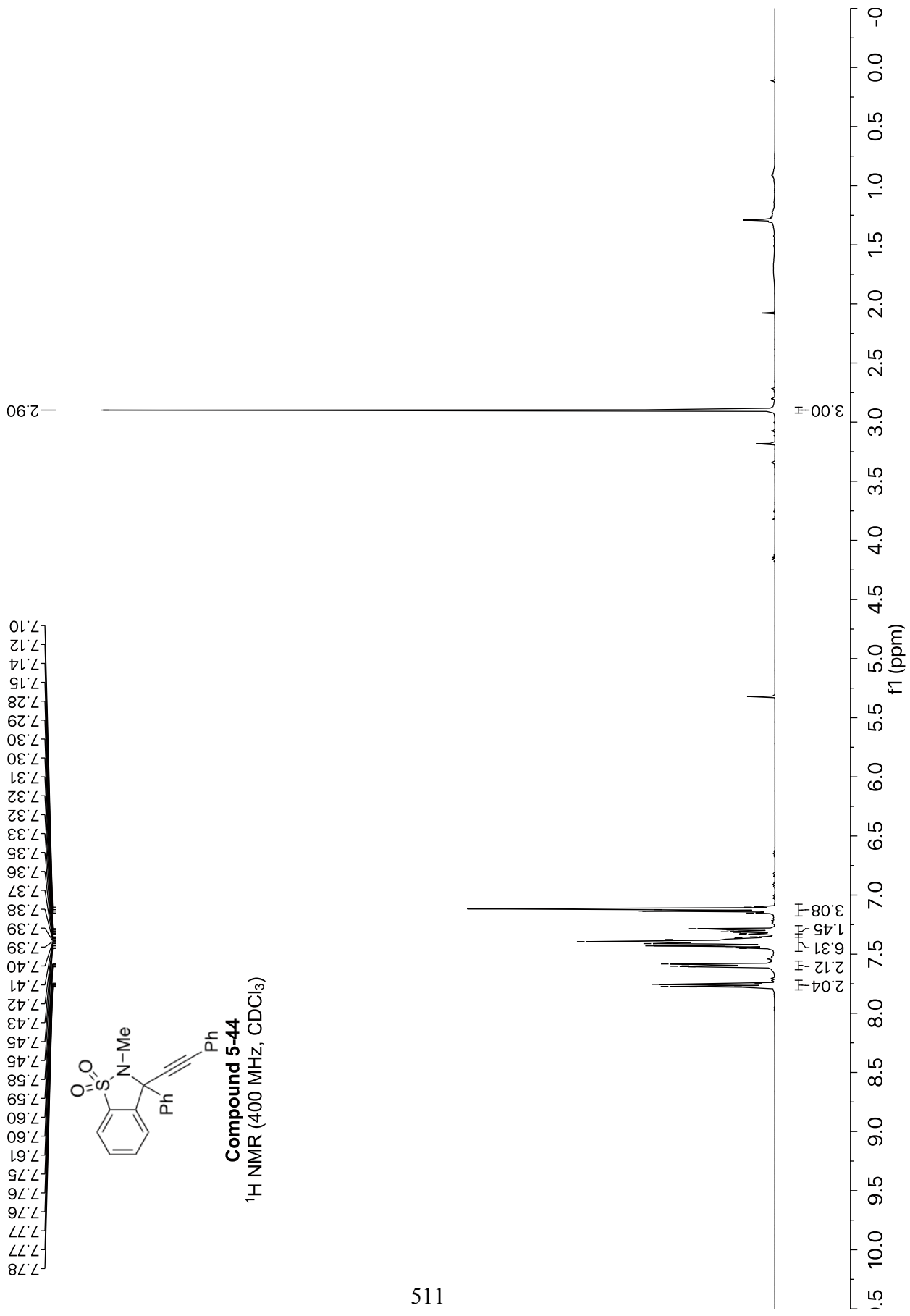
Appendix E

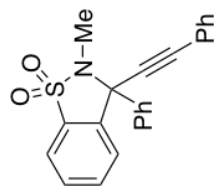
SPECTRAL AND CHROMATOGRAPHY DATA FOR CHAPTER 5

Chiral ligands used in HTE (Scheme 5.13)

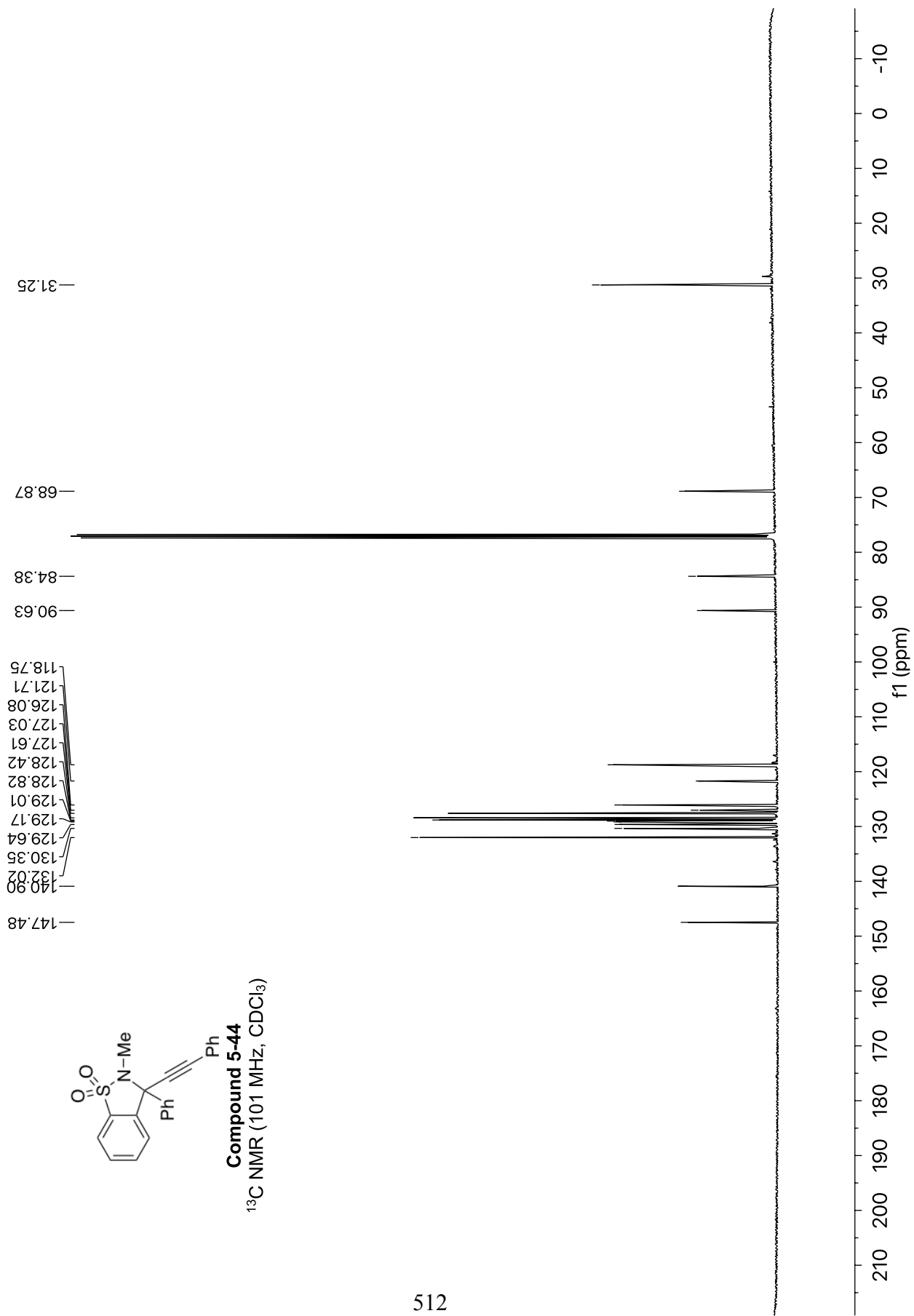


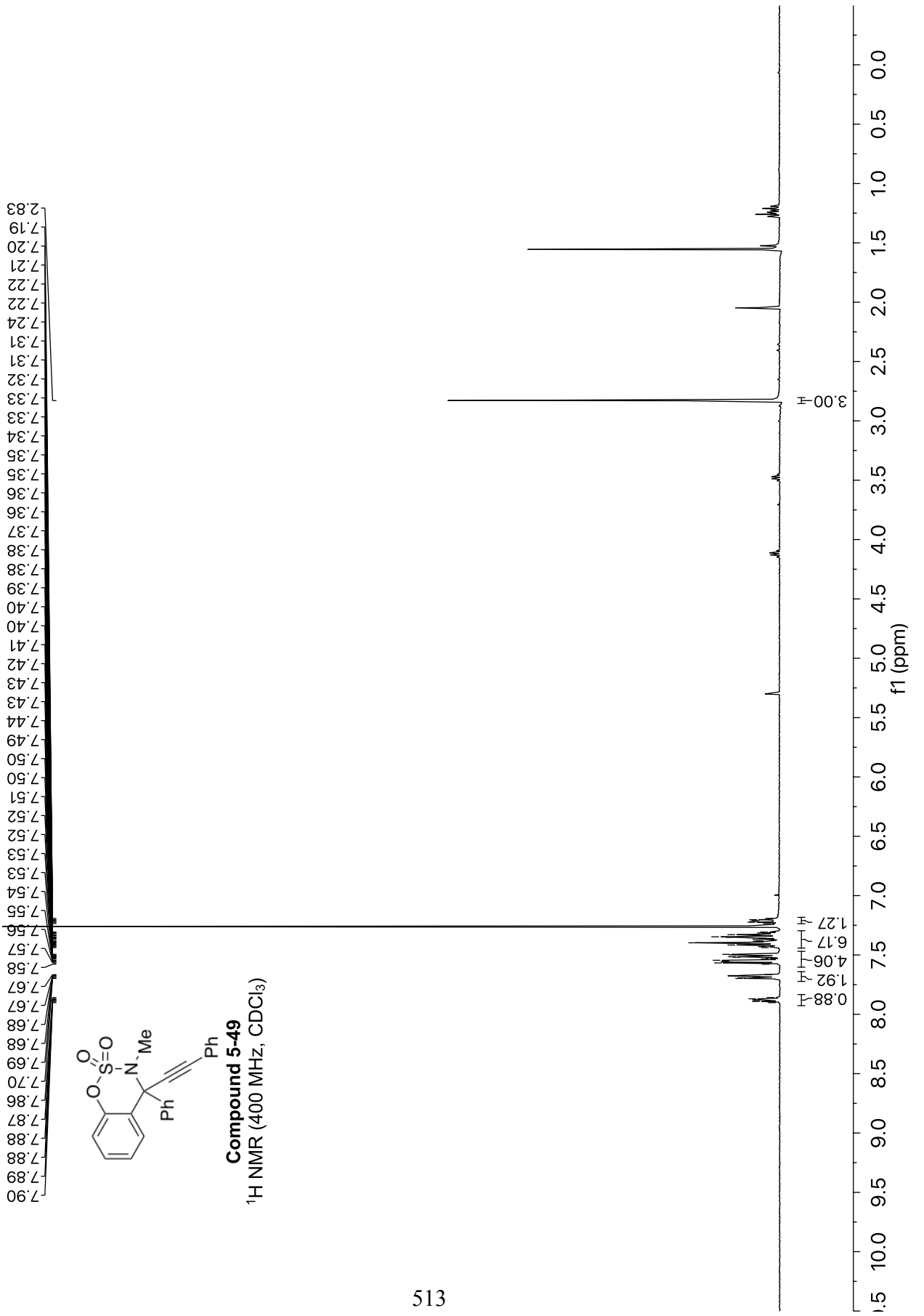


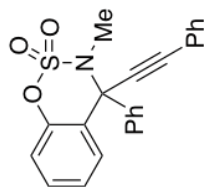




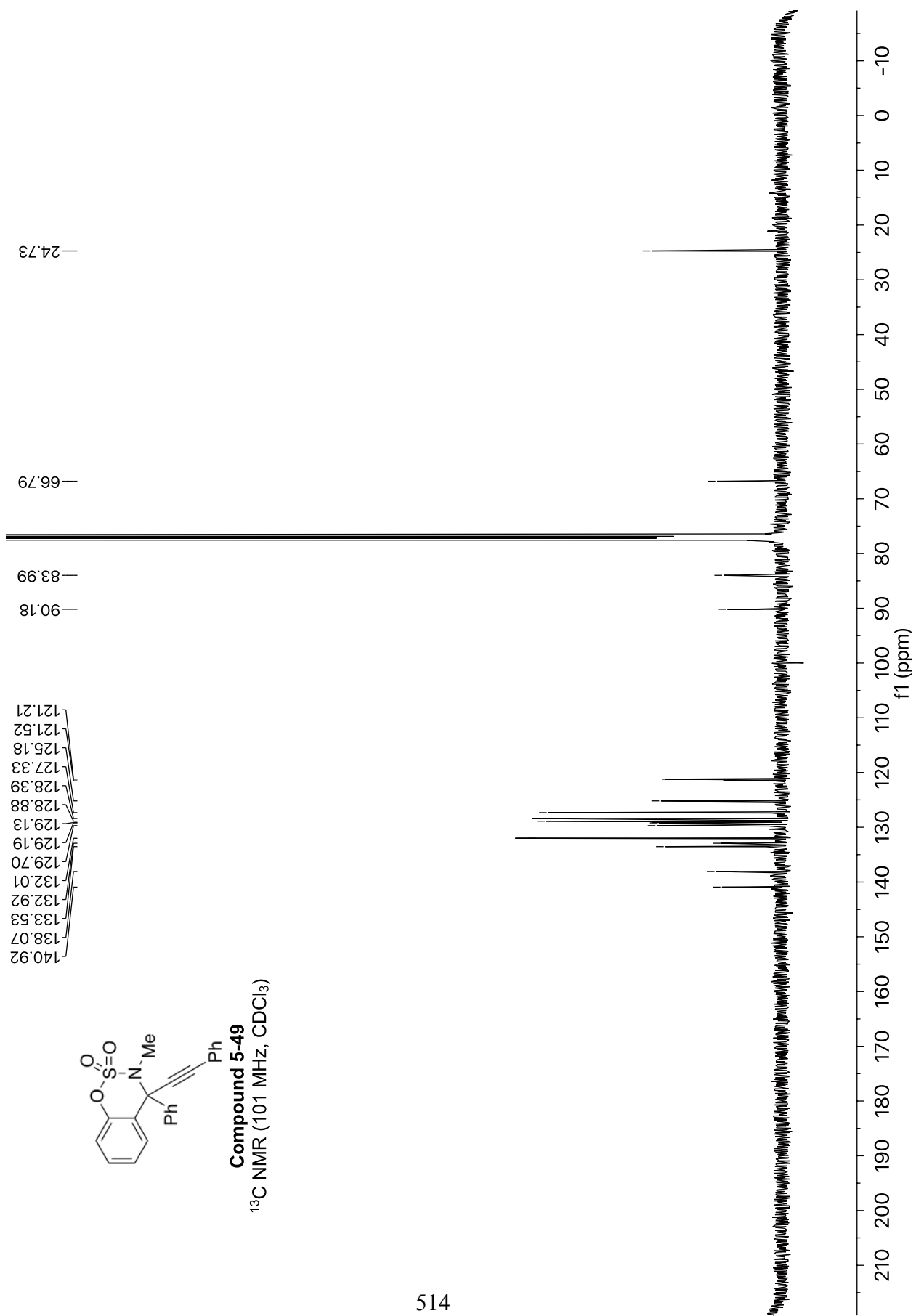
Compound 5-44
¹³C NMR (101 MHz, CDCl₃)

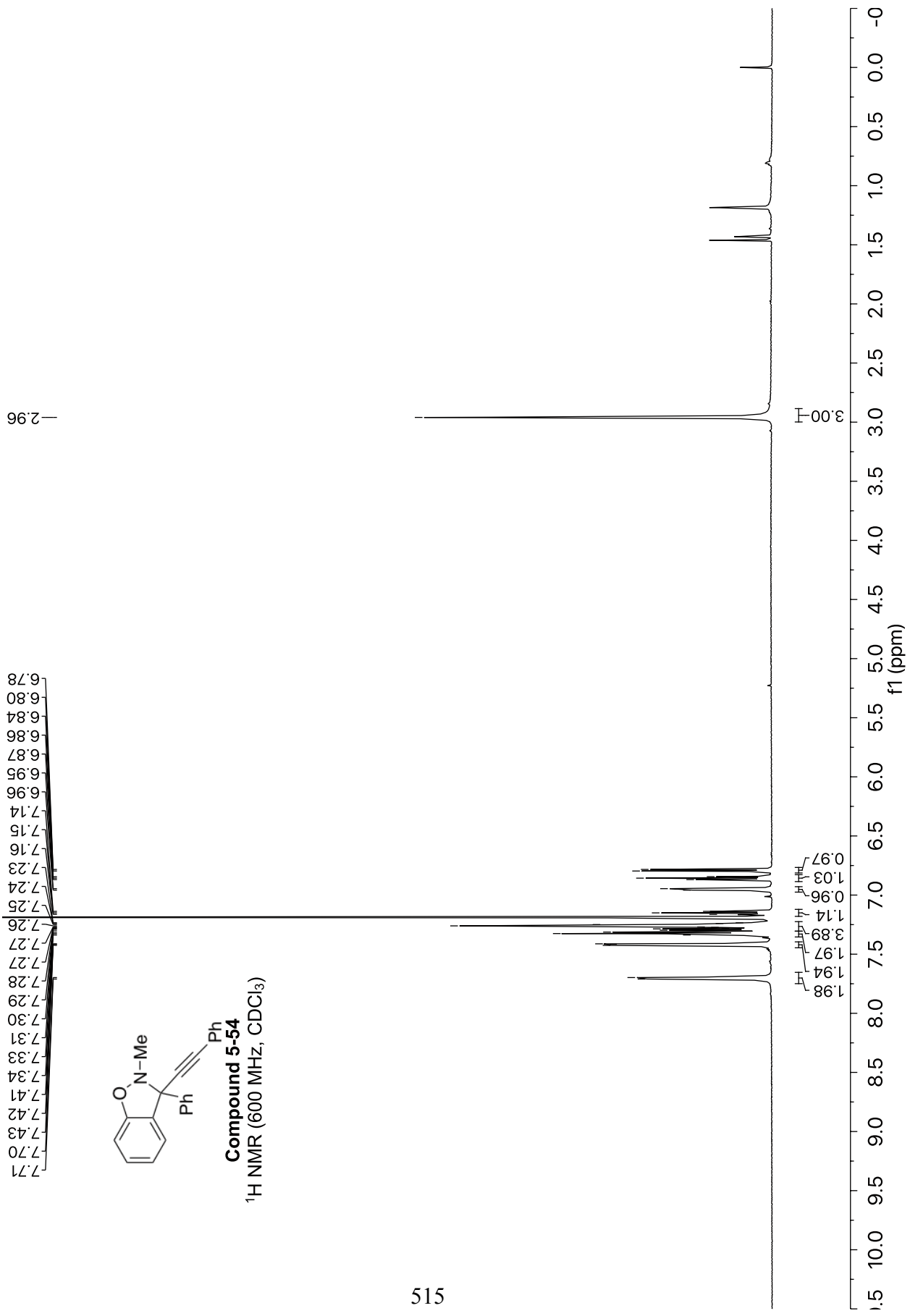




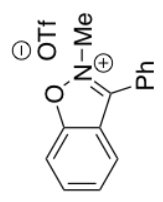


Compound 5-49
 ^{13}C NMR (101 MHz, CDCl_3)





8.08
8.07
8.06
8.06
7.97
7.96
7.96
7.94
7.85
7.84
7.82
7.81
7.80
7.78
7.77
7.75
7.73
7.72
7.71



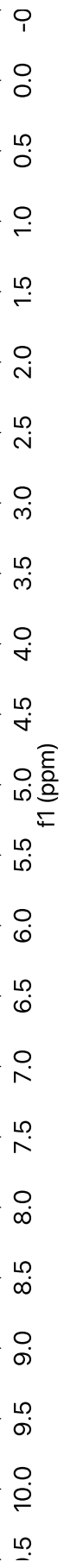
Compound 5-53

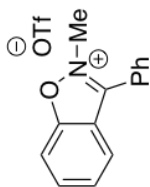
¹H NMR (600 MHz, CDCl₃)

4.60

3.00 H

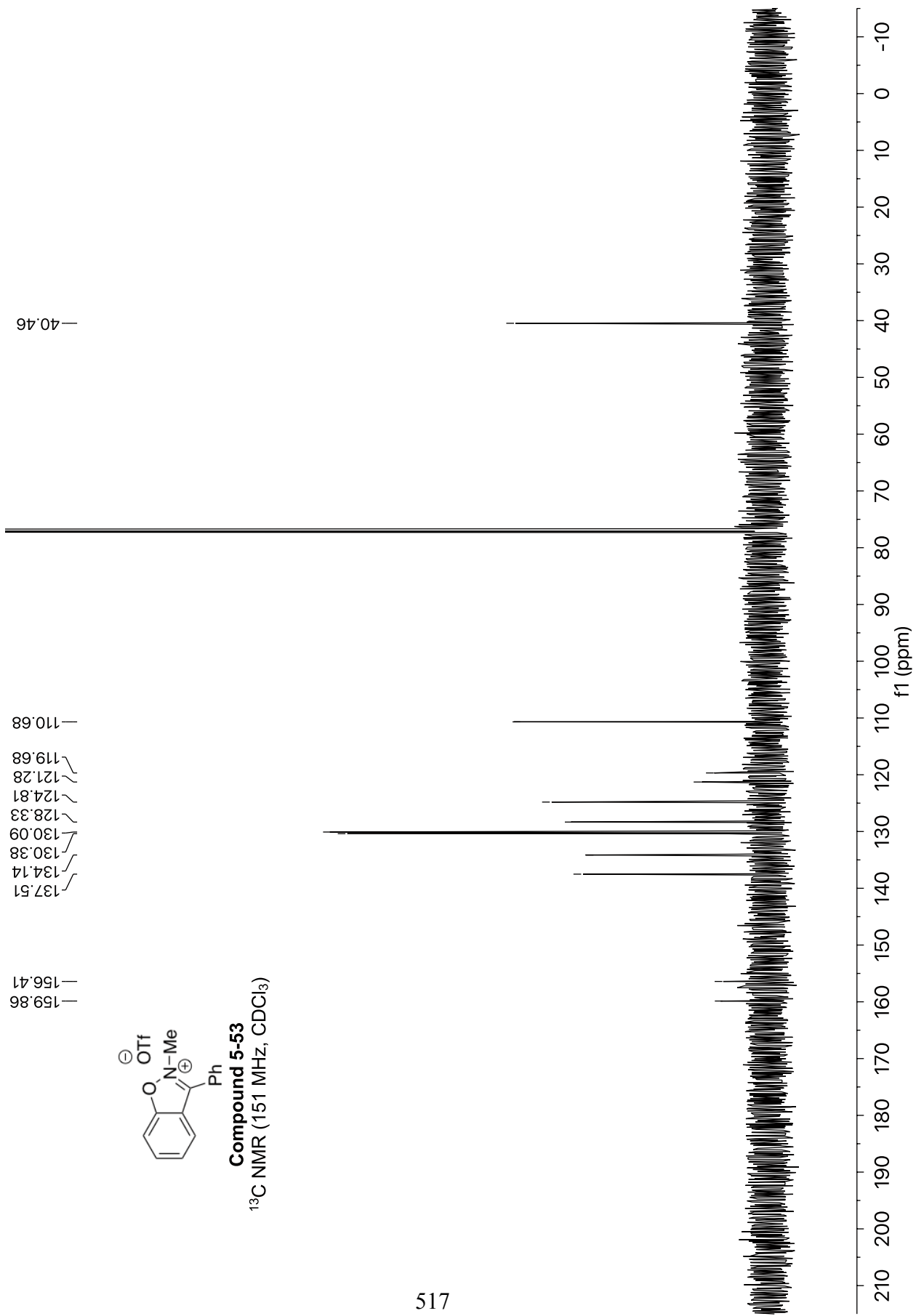
1.04
3.04 H
2.33
2.44
1.09 H

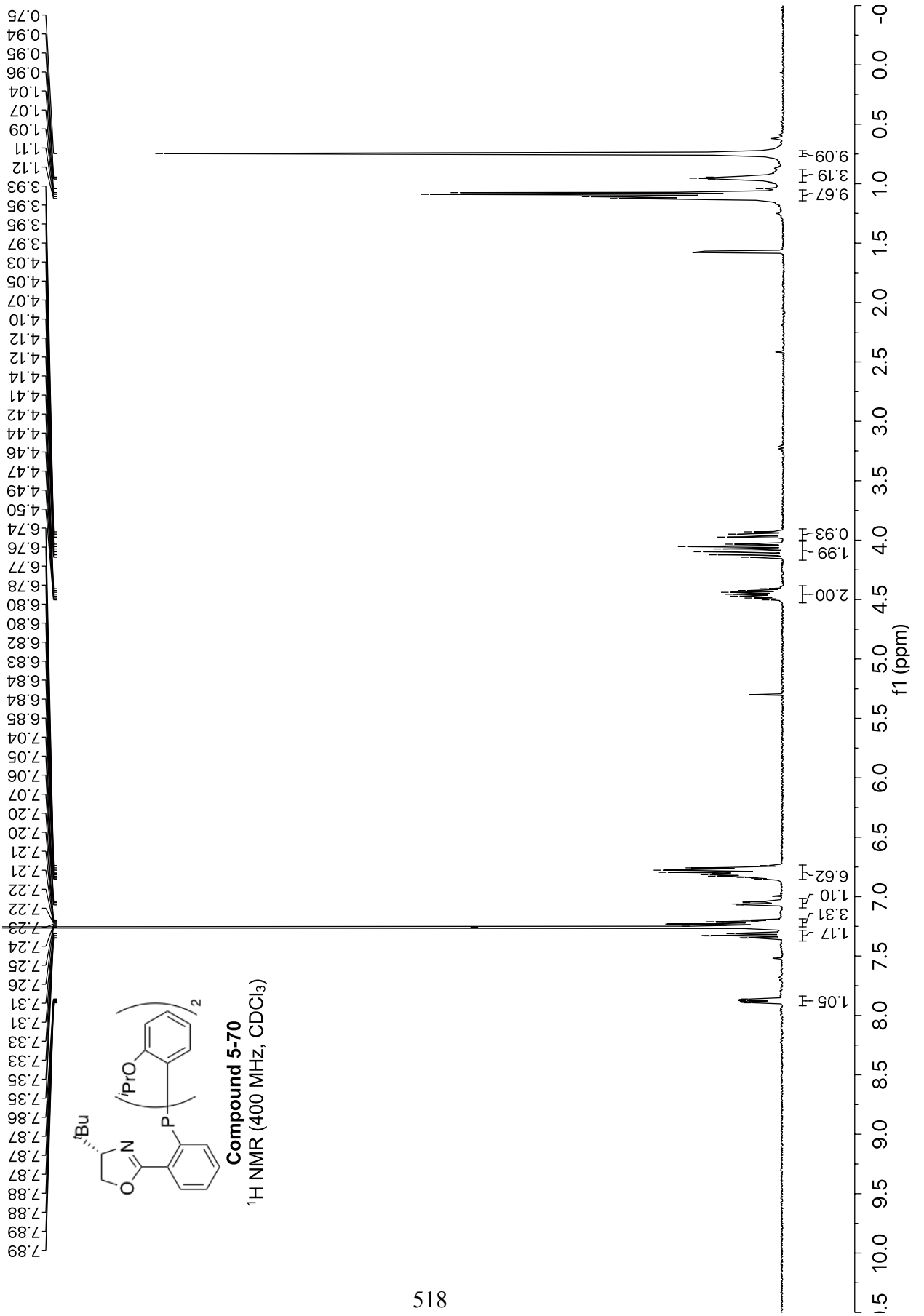


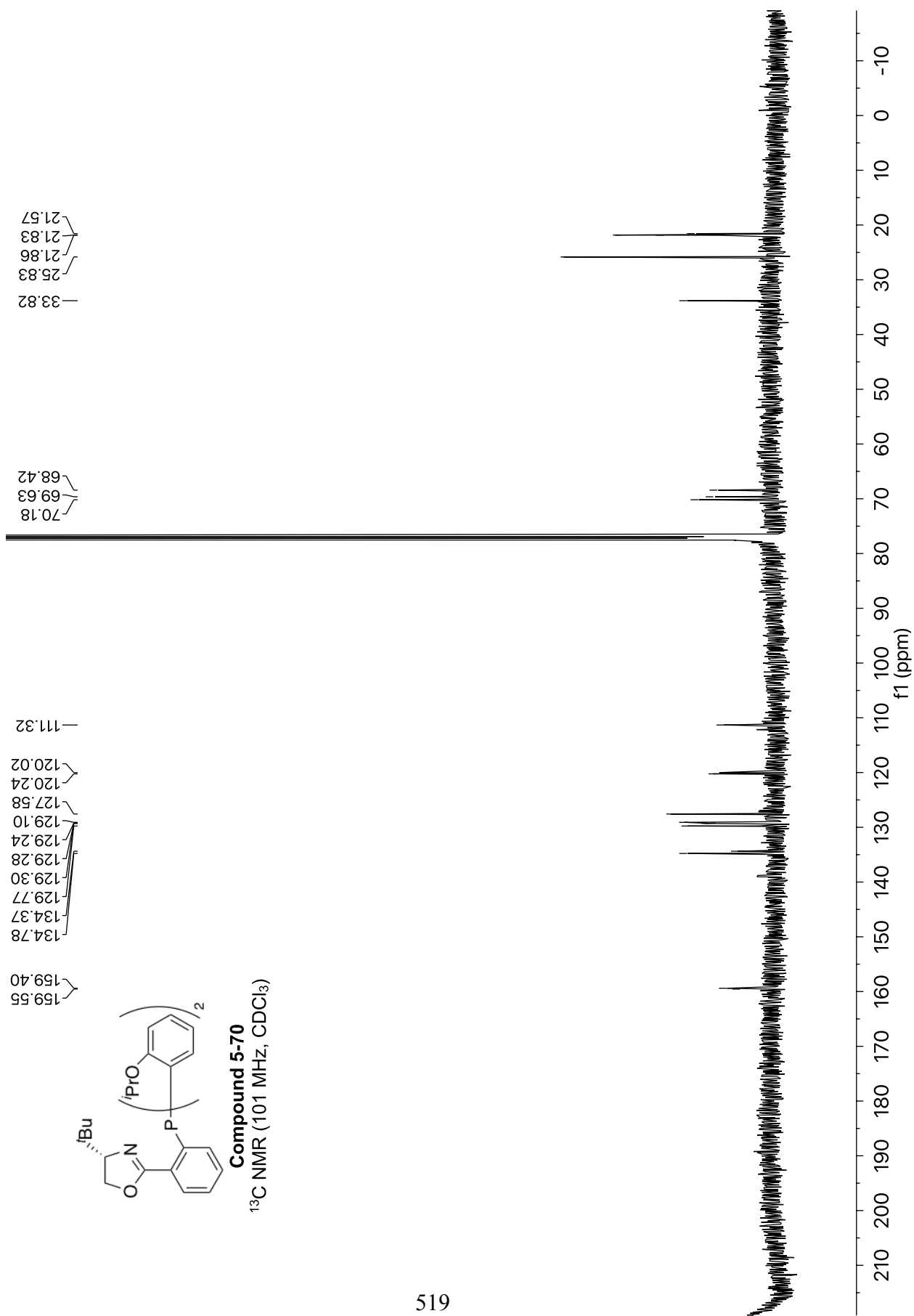


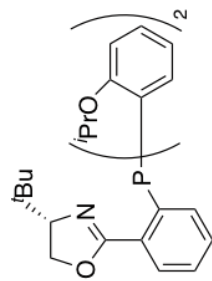
Compound 5-53

¹³C NMR (151 MHz, CDCl₃)



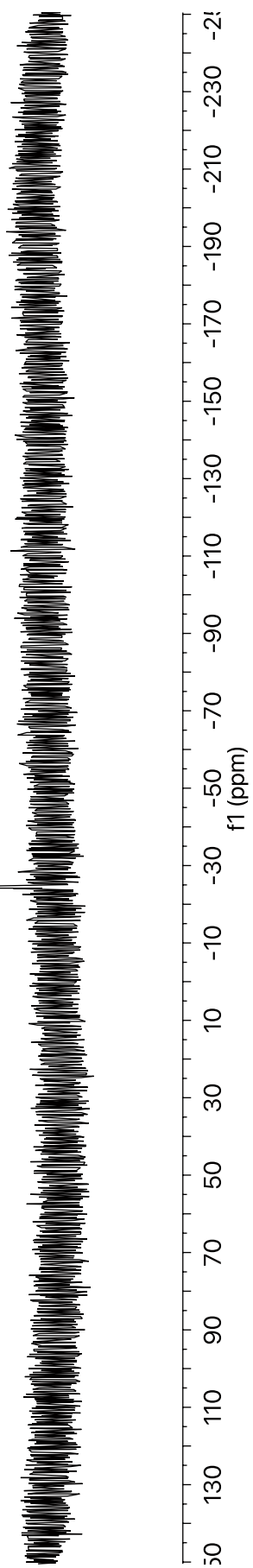






Compound 5-70
 ^{31}P NMR (162 MHz, CDCl_3)

—24.44



Appendix F
PERMISSION LETTERS



Title: Harnessing Alkyl Amines as Electrophiles for Nickel-Catalyzed Cross Couplings via C–N Bond Activation

Author: Corey H. Basch, Jennie Liao, Jianyu Xu, et al

Publication: Journal of the American Chemical Society

Publisher: American Chemical Society

Date: Apr 1, 2017

Copyright © 2017, American Chemical Society

LOGIN

If you're a **copyright.com user**, you can login to RightsLink using your copyright.com credentials.

Already a **RightsLink user** or want to [learn more?](#)

PERMISSION/LICENSE IS GRANTED FOR YOUR ORDER AT NO CHARGE

This type of permission/license, instead of the standard Terms & Conditions, is sent to you because no fee is being charged for your order. Please note the following:

- Permission is granted for your request in both print and electronic formats, and translations.
- If figures and/or tables were requested, they may be adapted or used in part.
- Please print this page for your records and send a copy of it to your publisher/graduate school.
- Appropriate credit for the requested material should be given as follows: "Reprinted (adapted) with permission from (COMPLETE REFERENCE CITATION). Copyright (YEAR) American Chemical Society." Insert appropriate information in place of the capitalized words.
- One-time permission is granted only for the use specified in your request. No additional uses are granted (such as derivative works or other editions). For any other uses, please submit a new request.

BACK

CLOSE WINDOW



Title: Transforming Benzylic Amines into Diarylmethanes: Cross-Couplings of Benzylic Pyridinium Salts via C–N Bond Activation

Author: Jennie Liao, Weiye Guan, Brian P. Boscoe, et al

Publication: Organic Letters

Publisher: American Chemical Society

Date: May 1, 2018

Copyright © 2018, American Chemical Society

LOGIN

If you're a **copyright.com user**, you can login to RightsLink using your copyright.com credentials.

Already a **RightsLink user** or want to [learn more?](#)

PERMISSION/LICENSE IS GRANTED FOR YOUR ORDER AT NO CHARGE

This type of permission/license, instead of the standard Terms & Conditions, is sent to you because no fee is being charged for your order. Please note the following:

- Permission is granted for your request in both print and electronic formats, and translations.
- If figures and/or tables were requested, they may be adapted or used in part.
- Please print this page for your records and send a copy of it to your publisher/graduate school.
- Appropriate credit for the requested material should be given as follows: "Reprinted (adapted) with permission from (COMPLETE REFERENCE CITATION). Copyright (YEAR) American Chemical Society." Insert appropriate information in place of the capitalized words.
- One-time permission is granted only for the use specified in your request. No additional uses are granted (such as derivative works or other editions). For any other uses, please submit a new request.

BACK

CLOSE WINDOW

**GEORG THIEME VERLAG KG LICENSE
TERMS AND CONDITIONS**

Dec 17, 2018

This Agreement between Jennie Liao ("You") and Georg Thieme Verlag KG ("Georg Thieme Verlag KG") consists of your license details and the terms and conditions provided by Georg Thieme Verlag KG and Copyright Clearance Center.

The publisher has provided special terms related to this request that can be found at the end of the Publisher's Terms and Conditions.

License Number	4476470141077
License date	Nov 26, 2018
Licensed Content Publisher	Georg Thieme Verlag KG
Licensed Content Publication	Synthesis
Licensed Content Title	Vinylation of Benzylic Amines via C–N Bond Functionalization of Benzylic Pyridinium Salts
Licensed Content Author	Weiye Guan, Jennie Liao, Mary P. Watson
Licensed Content Date	Jan 1, 2018
Licensed Content Volume	50
Licensed Content Issue	16
Type of Use	Dissertation/Thesis
Requestor type	author of the original Thieme publication
Format	print and electronic
Portion	full article/document
Will you be translating?	no
Distribution quantity	1
Specified additional information	This work will be described in detail in my PhD thesis.
Order reference number	
Title of your dissertation / thesis	Harnessing Alkyl Amines in Nickel-Catalyzed Cross-Couplings Via C–N Bond Activation
Expected completion date	Dec 2018
Estimated size (number of pages)	400
Requestor Location	Jennie Liao 109 King William St NEWARK, DE 19711 United States Attn: Jennie Liao

Publisher Tax ID	DE 147638607
Billing Type	Invoice
Billing Address	Jennie Liao 109 King William St NEWARK, DE 19711 United States Attn: Jennie Liao
Total	0.00 USD
Terms and Conditions	

Terms and Conditions

Introduction

The publisher for this copyrighted material is **Georg Thieme Verlag KG**, in the following referred to as **Publisher**. By clicking "accept" in connection with completing this licensing transaction, you agree that the following terms and conditions apply to this transaction (along with the Billing and Payment terms and conditions established by Copyright Clearance Center, Inc. ("CCC"), at the time that you opened your CCC account and that are available at any time at <<http://myaccount.copyright.com>>).

Limited License

Publisher hereby grants to you a non-exclusive license to use this material. Licenses are for one-time use only with a maximum distribution equal to the number specified in the license. The first instance of republication or reuse granted by this license must be completed within 12 months of the date this license was granted (although copies prepared before the end date may be distributed thereafter).

Licences for reuse in a **dissertation/thesis** are limited to the depositary copies (non-profit and password-protected) that have to be delivered within the university system. Any further use and follow-up publications require separate permission.

If you are **the author requesting full use of your article** in an Institutional Repository, special rules apply. For more detailed information, please check <https://www.thieme.de/de/autorenlounge/Autorenlounge-Zeitschriftenautoren-Autorenrechte-95029.htm>

If you have identified yourself as a signatory to the **STM Permissions Guidelines**, permission is given according to the current version of these Guidelines (<https://www.stm-assoc.org/copyright-legal-affairs/permissions/permissions-guidelines/>).

Geographic Rights: Scope

Licenses may be exercised anywhere in the world.

Altering/Modifying Material: Not Permitted

You may not alter or modify the material in any manner (except that you may use, within the scope of the license granted, one or more excerpts from the copyrighted material, provided that the process of excerpting does not alter the meaning of the material or in any way reflect

negatively on the publisher or any writer of the material), nor may you translate the material into another language.

Reservation of Rights

Publisher reserves all rights not specifically granted in the combination of (i) the license details provided by you and accepted in the course of this licensing transaction, (ii) these terms and conditions and (iii) CCC's Billing and Payment terms and conditions.

License Contingent on Payment

While you may exercise the rights licensed immediately upon issuance of the license at the end of the licensing process for the transaction, provided that you have disclosed complete and accurate details of your proposed use, no license is finally effective unless and until full payment is received from you (either by publisher or by CCC) as provided in CCC's Billing and Payment terms and conditions. If full payment is not received on a timely basis, then any license preliminarily granted shall be deemed automatically revoked and shall be void as if never granted. Further, in the event that you breach any of these terms and conditions or any of CCC's Billing and Payment terms and conditions, the license is automatically revoked and shall be void as if never granted. Use of materials as described in a revoked license, as well as any use of the materials beyond the scope of an unrevoked license, may constitute copyright infringement and publisher reserves the right to take any and all action to protect its copyright in the materials.

Copyright Notice: Disclaimer

Must include the following copyright and permission notice in connection with any reproduction of the licensed material: "© Georg Thieme Verlag KG."

Warranties: None

Publisher makes no representations or warranties with respect to the licensed material and adopts on its own behalf the limitations and disclaimers established by CCC on its behalf in its Billing and Payment terms and conditions for this licensing transaction.

Indemnity

You hereby indemnify and agree to hold harmless publisher and CCC, and their respective officers, directors, employees and agents, from and against any and all claims arising out of your use of the licensed material other than as specifically authorized pursuant to this license.

No Transfer of License

This license is personal to you, but may be assigned or transferred by you to a business associate (or to your employer) if you give prompt written notice of the assignment or transfer to the publisher. No such assignment or transfer shall relieve you of the obligation to pay the designated license fee on a timely basis (although payment by the identified assignee can fulfill your obligation).

No Amendment Except in Writing

This license may not be amended except in a writing signed by both parties (or, in the case of publisher, by CCC on publisher's behalf).

Objection to Contrary Terms

Publisher hereby objects to any terms contained in any purchase order, acknowledgment, check endorsement or other writing prepared by you, which terms are inconsistent with these terms and conditions or CCC's Billing and Payment terms and conditions. These terms and conditions, together with CCC's Billing and Payment terms and conditions (which are incorporated herein), comprise the entire agreement between you and publisher (and CCC) concerning this licensing transaction. In the event of any conflict between your obligations established by these terms and conditions and those established by CCC's Billing and Payment terms and conditions, these terms and conditions shall control.

Jurisdiction:

This license transaction shall be governed by and construed in accordance with the laws of the Federal Republic of Germany. You hereby agree to submit to the jurisdiction of the federal and state courts located in Berlin, Germany for purposes of resolving any disputes that may arise in connection with this licensing transaction.

Special Terms: We grant permission to use this material for the aforesaid publication in printed and electronic form to be stored in the electronic academic repository of the University. The article is to be used in the accepted WORD version without layout. Use of the final PDF version is explicitly excluded. Permission for further rights and for storage in any other repositories is explicitly excluded.

v 1.4

Questions? customer care@copyright.com or +1-855-239-3415 (toll free in the US) or +1-978-646-2777.
